UNIVERSITAT DE BARCELONA

Simple and double conjugates of peptides and oligonucleotides

Jordi Agramunt Pi

Simple and double conjugates of peptides and oligonucleotides

Jordi Agramunt Pi

UNIVERSITAT DE BARCELONA

Simple and double conjugates of peptides and oligonucleotides

Manuscript submitted by:

Jordi Agramunt Pi

Directed and revised by:

Prof. Anna Grandas Sagarra

Universitat de Barcelona

Departament de Química Inorgànica i Orgànica

Secció de Química Orgànica

Programa de Doctorat en Química Orgànica

Universitat de Barcelona, Setembre 2019

Agraïments

M'agradaria començar aquesta tesi agraint-te a tu, lector, el temps que has dedicat a fullejar, llegir o interessar-te pels resultats que bonament he pogut treure i estan aquí compilats.

A continuació voldria agrair a tota la gent que ha passat pels laboratoris 54, 53 i 500. Començant per l'Omar i en Clément qui em van, a la seva manera, posar les pautes del químic que soc avui. Gràcies a tota la gent que ha passat pel grup l'Albert i en Tomeu per ajudar-me sempre que heu pogut, a l'Àlex, Natàlia, Míriam, Carla, Eli, Guillem, Anna, Joaquín, Marina i molts d'altres, gràcies per haver creat un bon ambient de treball.

Vull agrair també als meus alumnes per ensenyar-me a ensenyar. Gràcies a la CRISPR per fer un últim any de tesi més que agradable, per confiar en mi en bolcar els problemes i les emocions. Un somriure teu cada dia és un dels millor regals que he pogut rebre de tu.

Vull agrair en especial a la meva "amiga" (no per voluntat, sinó per tossudesa) Laia. La veritat és que no sé per on començar. Primer perdó, sé que n'hem parlat moltes vegades però una cosa que m'has ensenyat és que el perdó mai és de més. Perdó per fer-te sentir malament en més d'una ocasió. Perdó i gràcies per, no només aguantar-me en els meus pitjors i millors moments, però també ensenyar-me la introspecció i criticar-me constructivament. Estic segur que el viatge a Leeds et serà molt profitós. Gràcies de tot cor.

Del departament voldria agrair al FUT i especialment l'Stuart i la Marina per deixar-me més reactius dels que mai hauria d'haver demanat. Segurament m'heu ajudat a fer una desena part de la tesi. A més voldria agrair l'Aitor per les més d'una conversa sobre la política, menjar i la seva terra, un plaer. A l'Ignasi que se'l ha trobat molt a faltar aquest últim any, gràcies per deixar-me conèixer una mica sobre la teva família. Voldria agrair a en Josep, per les hores i hores i hores que m'has dedicat a ensenyar el nostre amic l'HPLC-MS (el que no està mai calibrat i el vell). A ajudar-me amb el meu Shimadzu i, en general, quan no tenia ni idea del que estava fent amb aparells analítics, sense tu hagués hagut de fer més d'un i de dos pressupostos de reparació extra. Finalment, voldria agrair la colla de químics orgànics. Gràcies al temps i la dedicació invertides a les activitats que heu organitzat.

De fora de la universitat voldria agrair a l'Eduardo per les agradables converses sobre química, pasta i cultura italiana i l'Adrián per engrescar-me a treure l'advanced, aprendre guitarra i, en general, fer una mica el burro. Voldria donar gràcies a l'Ed per les converses de tesi estiuenques i les penes amb els referees. Finalment, als químics de Girona: Toni, Helena, Gina, Anna, Vanessa, Adrià i Judit. Voldria agrair també l'Elena i la Alexia per tot el temps compartit, gràcies per haver-me aguantat en les meves tonteries.

Voldria també agrair a l'Enrique i l'Anna, no només pel tracte professional i personal però també per l'oportunitat d'estar al grup i per confiar en mi quan podrien haver triat qualsevol altre persona. Gràcies de tot cor.

Especialment voldria agrair l'Anna per les innumerables converses de química, biologia, història, art, cultura, política i, entre molts altres temes que hem estat compartint aquests anys. Gràcies per donar-me llibertats de decisió i fer-me créixer no només com a persona sinó també com a científic. En particular, et voldria agrair que em convencessis a acomiadar-me de la meva difunta avia la setmana abans que faltés. És un fet que mai et podré agrair prou.

Finalment voldria agrair la meva família pel suport que sempre m'han donat al llarg de la meva vida. Gràcies als meus pares per inculcar-me l'hàbit de l'esforç i el treball i gràcies a en Joan per ser un referent a seguir.

Aquesta obra està dedicada a la Sra. Catalina Pericay Roure.

INDEX

CHAPTER 1

Introduction

CHAPTER 2

2,2-Disubstituted cyclopent-4-ene-1,3-diones: simple and double conjugations

CHAPTER 3

Retro-1 oligonucleotide conjugates

CHAPTER 4

Oxanorbornene as a novel dienophile for inverse electron-demand Diels-Alder cycloaddition with 1,2,4,5-tetrazines

Conclusions

Experimental part

Resum en català

About the structure of this work

This work is divided into three parts.

The first one contains an introduction to this work and other three chapters explaining the development of two new conjugation methodologies and an exploration of the conjugation of a biologically active molecule. Each of them contains its own reference collection, abbreviations, references and conclusions. Moreover, global conclusions reached during this work are also included at the end.

The second part is the experimental part and contains all the information necessary to reproduce the experiments performed as well as the product characterization. Experiments performed in a given section of the first part can be found in the experimental section with the same name. For clarity, numbering of the experimental sections is the same as in the first part, including the prefix “E.” to each section.

Finally, the third part is a summary of this dissertation in Catalan.

Chapter 1. Introduction

1.1 Biomolecules

Biomolecules are entities present in living organisms ranging from large, complex structures such as nucleic acids, antibodies, carbohydrates or proteins to small and simple like peptides, or fatty acids. Those complex natural entities are usually composed by repeating units and their relevance in metabolic processes is beyond question, for they have all possible function from structural to regulatory, and actively play a role in almost all processes within an organism.

Life is not understood without them and many of those have been proved to be related with disease development and treatment. For example, peptides have made their own spot in the medicinal field with examples such as cyclosporine,[1] somatostatin analogues such as octreotide[2] or polymyxins.[3] In a similar fashion, oligonucleotides can be employed as vaccines,[4] genomic therapy[5] and drug design thanks to their recognition capacity.[6] Another example is taking advantage of antibodies to target specific cells based on cell-specific recognition and binding to an antigen. In particular, delivery of a cytotoxic payload to cancer cells is expected to produce a breakthrough in oncology treatment, offering a way of increasing efficacy and decreasing toxicity in comparison to traditional chemotherapeutic treatments.[7]

1.2 Modifications of biomolecules

Even though biomolecules may be excellent drugs, they usually lack the required pharmacokinetic and pharmacodynamic properties, generally summarized as poor bioavailability. The poor biological stability of natural, unmodified synthetic peptides and oligonucleotides is amongst the principal limitations to their use as drug candidates, being the inherent natural bonds of these biomolecules subjected to digestion by various proteases and nucleases respectively. In order to address this drawback, chemical modifications to increase metabolic stability is virtually obliged.

For this purpose, two main strategies are being used: backbone modification and conjugation. Due to the fact that mainly peptides and oligonucleotides are used in this thesis, both strategies will be primarily discussed in regards to these two biomolecules.

1.2.1 Backbone modification

Backbone modification is one of the most employed strategies to alter the properties of a biomolecule. The main advantage of backbone modification is to avoid altering the recognition motifs usually found in the side-chains of amino acids or in the nitrogenous bases within nucleic acids. Backbone modifications in oligonucleotides and peptides have provided good results in improving the stability towards enzymatic degradation, in the pre-organization of complex structures and also in their activity. The most important modifications will be discussed below in separate sections due to the considerably distinct chemical nature of both polyamides and nucleic acids.

1.2.1.1 Oligonucleotide backbone modification

1.2.1.1.1 Phosphorothioates

The phosphorothioate (PS) backbone modification has been the keystone for contemporary work on oligonucleotide drug design. It replaces one of the non-linking oxygen atoms in the phosphate diester natural moiety with a sulfur atom, distributing the negative charge unsymmetrically and generating two diastereomers (**Figure 1.1**). Although it usually creates a modest reduction in binding affinity, in compensation it provides two important advantages. First, it improves stability to nucleases present in blood and tissues while maintaining solubility in water.[8] Secondly, it promotes protein binding, mainly with albumin and other blood protein thereby hampering renal clearance. The main disadvantage is the significant toxicity associated with said protein-binding capability of PS oligonucleotides.[9]

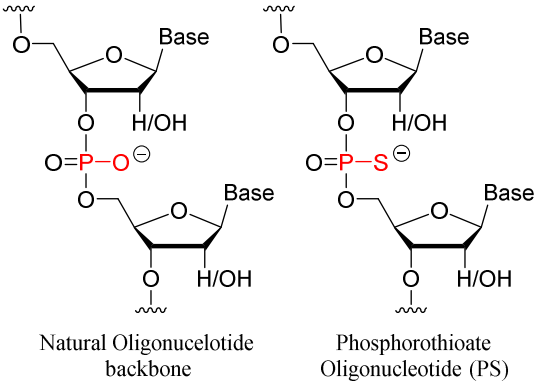

Figure 1.1 Natural and phosphorothioate oligonucleotide backbone.

1.2.1.1.2 Neutral backbones

Among the many alternative chemical approaches to substitute classic oligonucleotide scaffolds, phosphorodiamidate morpholino oligomers (PMOs) seem most promising. PMOs are a class of oligonucleotide derivatives where the ribofuranose ring is replaced with a morpholino ring and the phosphodiester union replaced with a phosphorodiamidate linkage (**Figure 1.2**, left). They have similar stability as DNA:DNA duplexes and are extremely resistant to nucleases. They do not promote RNAse H activity and are used predominantly for translation arrest or for splice switching applications.[10] Their nonionic nature, however seems to impede their delivery into cells, prompting use of complexation with negatively charged DNA or lipids to enhance delivery.

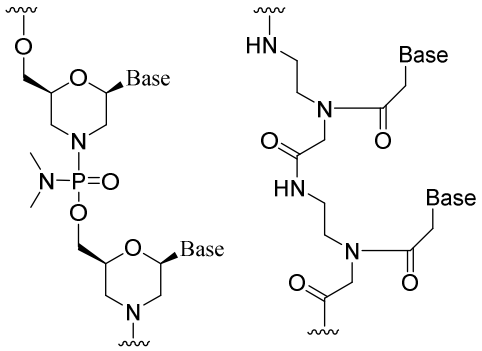

Figure 1.2 Neutral morpholino and PNA backbone analogues.

In the same context, peptide nucleic acids (PNAs) is another type of structure analogous to the natural oligonucleotide scaffold. In the PNA case, the carbohydrate and phosphate backbone is replaced with a polyamide yet maintaining the ability to Watson–Crick base pair with complementary nucleic acids. PNAs were first introduced by Nielsen and Berg in 1991[11] and are based on a (2-aminoethyl)glycine backbone from which the nucleobases are suspended from the glycine nitrogen atom with a methylene carbonyl linker (**Figure 1.2**, right). This backbone was computationally designed to be able to constitute a B-DNA mimic. From a synthetic point of view, the preparation of PNAs is accomplished *via* solid-phase peptide synthesis (SPPS), in a similar fashion as peptides.

Analogously to the PMOs, the lack of a negatively charged backbone give rise to duplexes showing improved thermal stabilities and melting temperatures almost unaffected by ionic strength. On the other hand, they show low solubility in water and low phospholipid membrane permeability making almost impossible to distribute unmodified PNAs through cell membranes.

1.2.1.1.3 Ribose 2' modifications

The furanose sugar in DNA and RNA is replete with electronic effects because of the presence of electron withdrawing oxygen atoms at every carbon (except the 2'-position in DNA) of the five-membered ring. As a result, the furanose ring can adopt a variety of conformations which are represented by the pseudorotation cycle.[12] The two most frequent conformations adopted are depicted in **Figure 1.3** and represent the B-DNA (left) and both RNA and A-DNA (right).

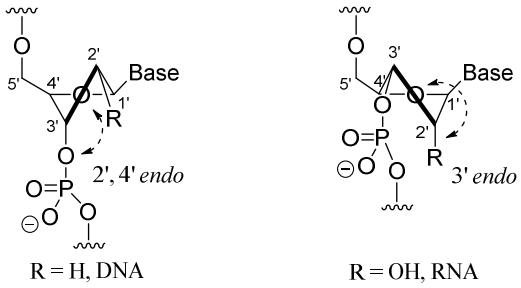

Figure 1.3 Conformationally preferred positions of the furanose rings in DNA and RNA.

Out of all possible modifications at the 2'-position, the most widely used are the 2'-O-Me, 2'-O-(2-methoxyethyl) (MOE) and 2'-fluoro modifications. The great success of these modifications is found in their biophysical properties being similar to the natural ribose. More specifically, they promote "RNA-like" conformation (**Figure 1.3**, right) and considerably increase binding affinity to RNA, providing enhanced nuclease resistance as well as reduced immune stimulation.[13]

1.2.1.1.4 Bridged rings

As discussed, 2'-modified nucleic acid analogues enhance binding affinity for RNA by steering the conformation of the furanose ring into the "RNA-like" C3'-endo sugar pucker. In this context, a locking effect for the furanose ring into this conformation was explored through a covalent tether between the 2'- and the 4'-positions (**Scheme 1.1**).

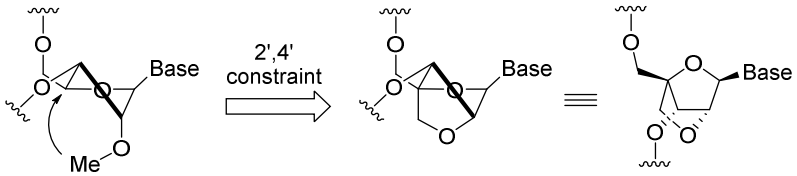

Scheme 1.1 2',4'-Bridged nucleic acids as conformationally restricted 2'-modified nucleic acid analogues.

This strategy led to the identification of locked nucleic acids (LNA) or 2',4'-methyleneoxy bridged nucleic acids which exhibit dramatic increase in RNA binding affinity when incorporated into oligonucleotides and paired with complementary RNA or DNA.

This is just the basis on which medicinal chemists have expanded. Different 2' heteroatom substituents other than oxygen such as sulfur, nitrogen or selenium and even larger six membered rings containing aminooxy, urea, amide or guanidine moieties, just to cite a few, have been extensively explored.[14]

1.2.1.2 Peptide backbone modification

In contrast to small molecules, peptides also display a predictable metabolism and are susceptible to enzymatic degradation and rapid kidney clearance. In a similar fashion to oligonucleotides, modifications, and more specifically of the backbone scaffold, provide increased resistance and specificity towards selected targets. Most common backbone modifications are use of unnatural "D" amino acids, *N*-methylation of amide bonds and, to a lesser extent, use of peptoids (**Figure 1.4**).

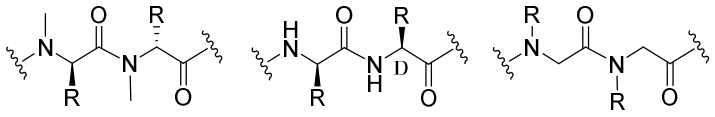

Figure 1.4 Examples of backbone modification of peptides: *N*-methylation, "D" epimers and peptoid analogues.

Peptides incorporating D-amino acids do not present a connectivity alteration but a biologically relevant enantiomeric change. This alteration confers certain resistance against proteases and, in some cases, a boost in activity.[15] *N*-methylation of amide bonds is believed to improve pharmacological properties and is an increasingly employed strategy towards better oral bioavailability.[16]

Even though peptides and peptoids share some similarities such as biocompatibility and the ability to incorporate different functional groups *via* their side-chains, they have significant differences. Unlike peptides, peptoids are completely resistant to proteolysis and therefore advantageous for therapeutic applications where digestion is a major drawback. Moreover, they are characterized for the lack of a chiral center in the polyamide backbone since functional groups are appended from the nitrogen atom instead of the α-carbon. Peptoids are routinely synthesized using the highly flexible monomer haloacetic acid (usually bromoacetic acid) followed by an S_N2 displacement using a primary amine and reacylation to obtain the tertiary amide.[17]

1.2.2 Bioconjugation

Even though backbone modification is widely used for its simplicity and effectiveness it has the limitation of not providing diverse new features to the biomolecule. Another alternative to improve or

provide new or enhanced properties without altering the biomolecule's core structure is the bioconjugation approach.

Bioconjugation is a chemical strategy to produce stable covalent bonds between at least two molecules in which at least one is a biomolecule. In the majority of cases both reactants need derivatization with specific chemical functionalities to react in a controlled and selective manner. Ever since Paul Ehrlich coined the *magic bullet* concept in 1900,[18] much effort has been devoted to the modification of intrinsic fragments of drugs and biomolecules to suffice needs ranging from delivery to specific physiological sites, pharmacokinetics and stability. In this regard, bioconjugation reactions have become an indispensable tool for studying and manipulating biomolecules *in vitro* and *in vivo*.

Ideally, reactions have to meet certain requirements, coined as "click" by Sharpless *et al*. in 2001,[19] for their greatest utility in bioconjugations. The new union should preferably be stable across a broad range of biological environments and should be small in size to minimize steric hindrance and perturbation of natural processes. In addition, the ligation process should proceed with high selectivity and specificity, in aqueous media, be devoid of by-products, quantitative, fast and bioorthogonal in order to avoid interfering with naturally present entities such as metabolites, should the conjugation take place in living systems.

1.3 Modern bioconjugation reactions

1.3.1 Copper(I)-catalyzed alkyne-azide cycloaddition

The Huisgen 1,3-dipolar cycloaddition reaction of organic azides and alkynes to yield triazoles[20,21] has gained considerable attention in recent years due to the introduction in 2001 of Cu(I) catalysis by Tornøe and Meldal and Sharpless, leading to a major improvement in both rate and regioselectivity of the reaction.[22] The basis for the unique properties and rate enhancement for triazole formation under Cu(I) catalyst are found in the high ΔG of the reaction in combination with the low dipole character of the reactants in contrast to the non-catalyzed thermal reaction, which possesses a considerable activation barrier.

The great success of the Cu(I) catalyzed alkyne-azide (CuAAC) reaction is rooted in the fact that it is virtually quantitative, very sturdy, extensive and orthogonal, suitable for both biomolecular ligation and tagging. Moreover, the formed triazole linkage is essentially chemically inert to a plethora of reaction conditions such as oxidation, reduction or hydrolysis. These fertile conditions led to a myriad of applications in many contexts ranging from material science, polymer chemistry or conjugation applications of biomolecules.

The reaction mechanism has been a controversial issue and since the first proposal by Sharpless and co-workers many attempts to establish a definitive reaction pathway have been made. Recent studies point to a mechanism involving copper binuclear complexes. It essentially involves the formation of Cu(I) acetylide and subsequent coordination of a second copper atom *via* the acetylide π-orbitals (see **Scheme 1.2**). This complex is supposed to react with the azide to generate a bis(copper)triazole, which upon acidolysis, yields the final product and regenerate the active binuclear copper acetylide.

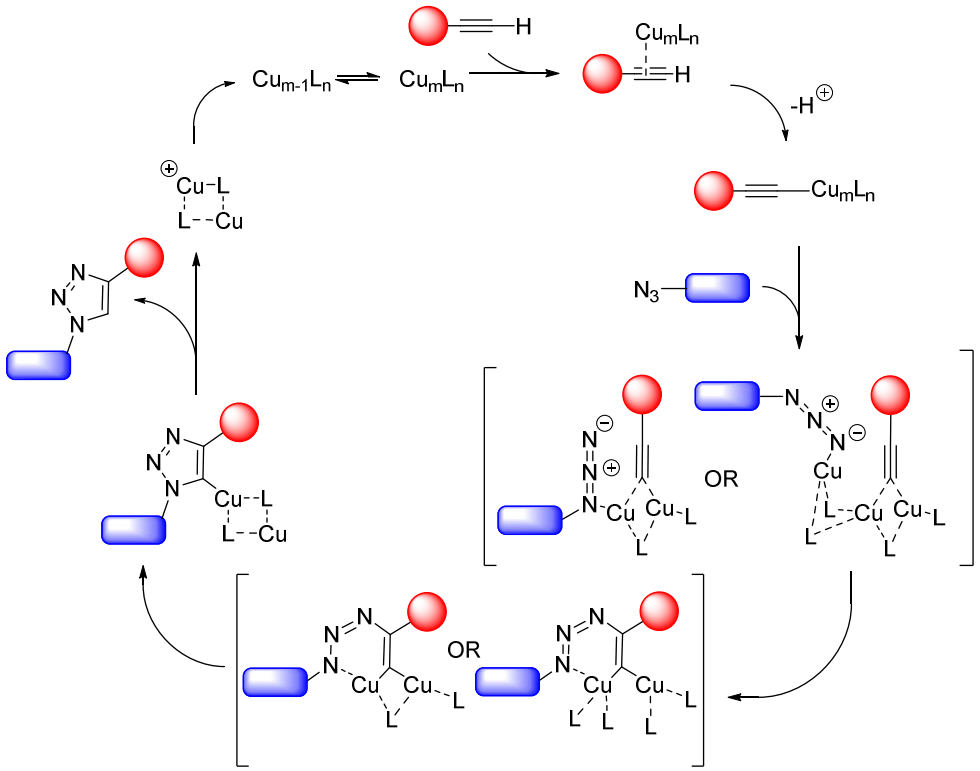

Scheme 1.2 Outline of a plausible mechanism for the Cu(I) catalyzed reaction between organic azides and terminal alkynes postulated by Sharpless and co-workers.[23]

Formation of triazoles from azides and terminal alkynes under catalysis by Cu(I) can be performed under a wide variety of conditions with almost any source of solvated Cu(I), provided that the reactants are maintained in solution and the Cu(I) is not removed by disproportion or oxidation to Cu(II). The most important factor seems to be the maintaining of high concentrations of Cu(I) at all times during the reaction, that is why the use of a Cu(II) source with an addition of a large excess of sacrificial reducing agent has been one of the preferred methodologies for this purpose.

1.3.1.1 CuAAC in nucleic acids and proteins

CuAAC has been used in several different ways to append different moieties to either a fully deprotected[24] or resin-linked[25] oligonucleotides. The prevalent method uses aqueous $CuSO_4$ and sodium ascorbate (NaAsc) as a sacrificial reducing agent and various additives such as complexing agents. The most important modifications using the CuAAC are labeling at either the 5' or internal positions in the oligonucleotide scaffold, which provides the means to monitor distribution and binding intracellularly and allows the investigation of interactions. The most straightforward alternative is the chemical phosphitylation of a terminal alkyne and appending it at the 5' position of a growing oligonucleotide strand (**Scheme 1.3**).

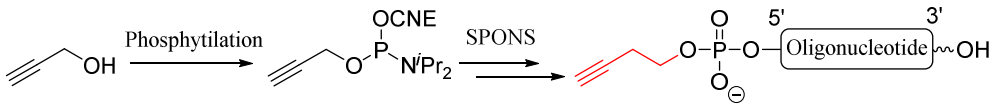

Scheme 1.3 5' Modification with an alkyne functionality of an oligonucleotide *via* phosphoramidite chemistry.

That being said, nucleosides containing a terminal alkyne functionality have also been prepared and these building blocks incorporated into DNA strands.[26] The preferred positions to attach an alkyne at

the nucleoside moiety are the 5-position of the pyrimidine system (**1.1**), the 7-position in the 7-deazapurine system (**1.2**) and the 2'-position at the ribose scaffold (**1.3**, **Figure 1.5**). The phosphate diester backbone may also be modified using diester-phosphoramidate linkages bearing propargylamine.

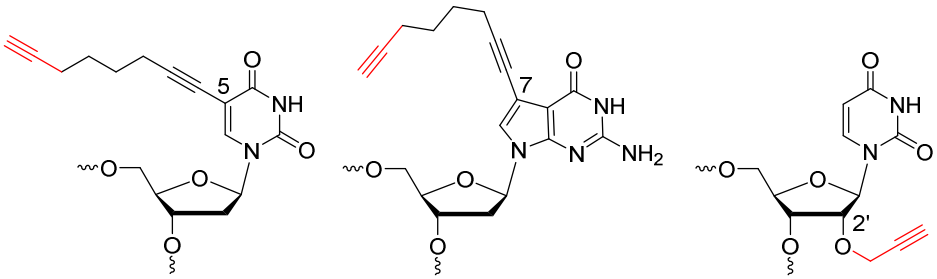

1.1 **1.2** **1.3**

Figure 1.5 Example of alkyne-modified nucleosides as building blocks for postsynthetic modification by CuAAC with azide-tagged labels.

Although CuAAC chemistry is currently broadly applied it seems to be limited to reactions where the alkynyl groups are part of the oligonucleotide and the azide on the other reactant, but not *vice versa*.[27] It was assumed that azides in nucleic acids could not withstand the chemical conditions employed during automated oligonucleotide synthesis, especially presence of the phosphite triester intermediate. To deal with this setback there have been several described proposals. One is the synthesis of an RNA building block bearing a 2'-azido group (**1.4**) that can be introduced into a growing oligonucleotide strand during solid phase synthesis by applying the phosphate diester method for this critical coupling step as, proven by Fauster *et al.*[28] and Aigner *et al.*[29] In a similar fashion, the azide moiety can be introduced *in situ* at the 5 position of 2'-deoxyuridine unit in a pre-synthesized oligonucleotide (**1.5**) by means of the halogenated precursor and a nucleophilic aromatic substitution.[30] Another possibility, is using a 7-deazaguanosine triphosphate bearing an azide group at the 7 position (**1.6**) and inserting it with the aid of DNA-polymerases.[31] More recently, it was found that azides and the phosphoramidite functionality are compatible with each other under a characteristic set of synthetic conditions (**1.7**, **Figure 1.6**). With this phosphoramidite, azide-bearing oligonucleotides were prepared *via* standard solid-phase synthesis and provided a full postsynthetic click functionality.[32]

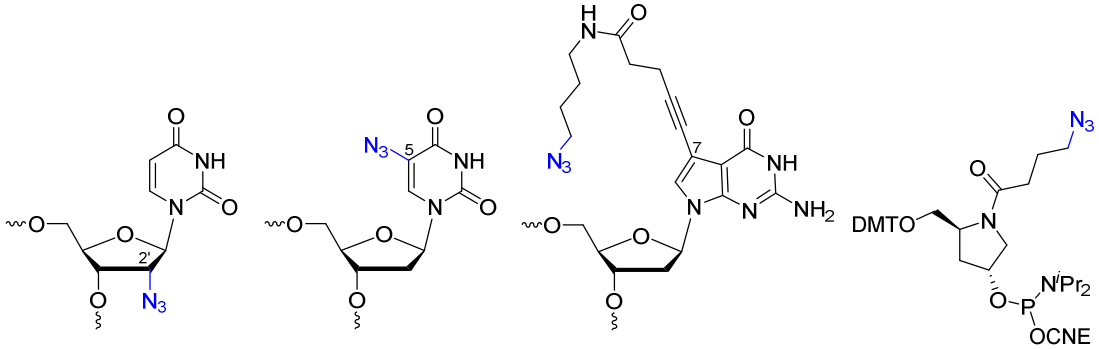

1.4 **1.5** **1.6** **1.7**

Figure 1.6 Examples of azide-modified building blocks for postsynthetic modification by CuAAC with ethynyl-tagged labels.

In the protein field problems can arise in two general circumstances. First, one of the substrates may contain groups that strongly bind copper ions.[33] This is potentially problematic because bound metal may be unavailable for the CuAAC catalysis and may cause protein precipitation. Secondly, the azide or alkyne group within the biomolecule may be sterically hindered or inaccessible to the catalyst and the coupling partner. Such cases are more difficult to both diagnose and treat. Secondly, additives such as reducing agents and complexing agents have to be carefully selected not only to prevent undesirable

by-products as in the case of ascorbate which can lead to formation of dehydroascorbate, diketoglutonate and glyoxal and causing protein adduct formation, crosslinking and precipitation.[34] A vital detail regarding azides and proteins is the possible reduction of the azide moiety in the presence of free thiols rendering the whole scheme suboptimal.

For the introduction of either azides or alkynes into proteins, chemical handles can be incorporated through metabolic insertion,[35] unnatural amino acid mutagenesis systems,[36,37] by activity-based incorporations and chemically *via* SPPS. As an example, newly expressed proteins were labeled inside both *E. coli* and mammalian cells by metabolic incorporation of alkyne-bearing unnatural amino acids like homopropargylglycine or ethynylphenylalanine detecting them by means of *in situ* fluorescence generation.[38,39] Lastly, site-specific incorporation of chemical handles is usually achieved by making use of the unnatural amino acid mutagenesis system and an orthogonal aminoacyl-tRNA synthetase.[40]

Despite the broad applicability and versatility of this type of postsynthetic modifications, there are only few examples in which CuAAC labeling has been clearly accomplished in living cells, and these are only with proteins and not with nucleic acids.[41,42] The use of copper catalysis *in vivo* is highly problematic, due to the strong cytotoxicity of copper ions mainly resulting from the formation of reactive oxygen species (ROS).[43] Even traces of copper ion impurities from the post-synthetic labeling can continuously generate ROS in the presence of molecular oxygen until the reducing agent is consumed. An excess of ROS may degrade delicate biomolecules to varying extent and can potentially interfere with chemical or biological applications of bioconjugates in living cells. As a countermeasure for this drawback, previously cited ligands such as TBTA (**1.8**) or BTTES (**1.9**) have been used to enhance catalytic activity, stabilize Cu(I) oxidation state and prevent, to a great extent but not completely, oxidation of amino acid residues such as free cysteines[44] and histidines[45] in proteins (**Figure 1.7**). For this reason, despite its great advantages, the CuAAC chemistry has been gradually set aside in biological applications in favor of modern approaches.

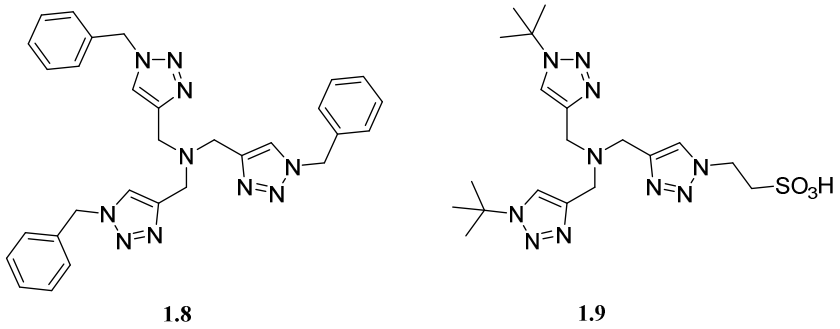

1.8 **1.9**

Figure 1.7 TBTA (**1.8**) and BTTES (**1.9**) respectively, commonly used as Cu(I) ligands in CuAAC for bioconjugation.

1.3.2 Strain-promoted cycloadditions

Cycloadditions are classified as ideal bioconjugation reactions because of tunable electronics and their intrinsic selectivity. Metal-free azide-alkyne reactions, in addition to other few modern cycloadditions are now being referred as “copper-free” click chemistries.[46,47]

1.3.2.1 Strain-promoted azide-alkyne cycloaddition (SPAAC)

One of the main drawbacks for the suitable utilization of the uncatalyzed version of the azide-alkyne cycloaddition is the high energetic activation barrier associated. To increase the rate of the reaction

without the need of a metal catalyst, researchers looked at ring-strain as a way to overcome the sluggish reactivity of alkynes with azides. In these studies, it was found that cyclooctynes react with phenyl azides vigorously. A logical explanation for the fast and spontaneous reaction of cycloalkynes with phenyl azides lies in the highly favorable enthalpic release of ring-strain, by going from a highly energetic strained ring with a bond angle for the sp-hybridized carbons in cyclooctynes ~160º (**1.11**, **Figure 1.8**)[48] to a fused ring system with favorable bond angle for the sp^2-hybridized carbon atoms ~120º in the resulting triazole (**1.12**, **Figure 1.8**).

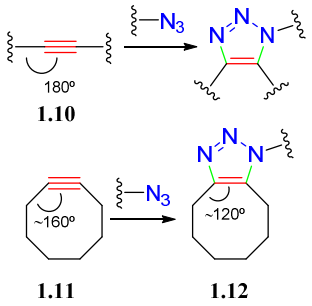

Figure 1.8 Comparison of angles in linear alkynes (**1.10**), cyclooctyne (**1.11**) and bicyclic triazole (**1.12**).

The first example of strain-promoted cycloaddition was described by Bertozzi's group in 2004[49] and it consisted in the cycloaddition of an azide with a strained alkyne, such as cyclooctyne.

Strain-promoted alkyne-azide cycloadditions (SPAAC) with cyclooctynes are convenient for bioconjugation since no additional reagents are required, stable conjugation products are formed and the reaction is devoid of by-products. It was reasoned that attachment of a suitable functional handle to the cyclooctyne moiety would enable a great deal of reaction tuning. And, while first applications of SPAAC rapidly found their way outside the field of metabolic labeling, it also became quickly apparent that the relatively slow reaction kinetics required large excesses of reagents, long incubation times, and led to relatively little target conjugate. In fact, early uses of metabolic labeling of azido-modified living cells were less efficient than the traceless Staudinger ligation (see below, **Section 1.3.6.2**).[50]

In general, two classes of cyclooctynes can be recognized: the earliest aliphatic cyclooctynes and dibenzoannulated cyclooctynes, named DIBOs (**1.16**, **Figure 9**). The first DIBO suitable for conjugation was developed by Ning *et. al.*[51] and steered the field towards the discovery of more reactive probes. It is commonly understood that the enhanced reactivity of DIBOs is due to an increase in ring strain imparted by the multiple sp^2-hybradized carbons. The latter phenomenon can also account for the reactivity order **1.17** > **1.18** > **1.16**, given that the number of sp^2-hybridized atoms in the ring decreases from 6 to 4 respectively. The analogue **1.17** is in fact an interesting example of the needed fine balancing between reactivity and stability that comes along with the development of cyclooctyne probes. That is because it displays a reaction rate constant of nearly 1 M s^{-1}, but unfortunately is inherently unstable and decomposes.

Besides rate constants, which are typically determined employing organic co-solvents like MeOH or ACN, other factors are also important to take into account regarding cyclooctynes. For instance, as commented, benzoannulation has shown to be beneficial for cyclooctyne reactivity, but inevitably it also leads to a concomitant enhance in steric interactions and lipophilicity, which is typically not beneficial in aqueous media.

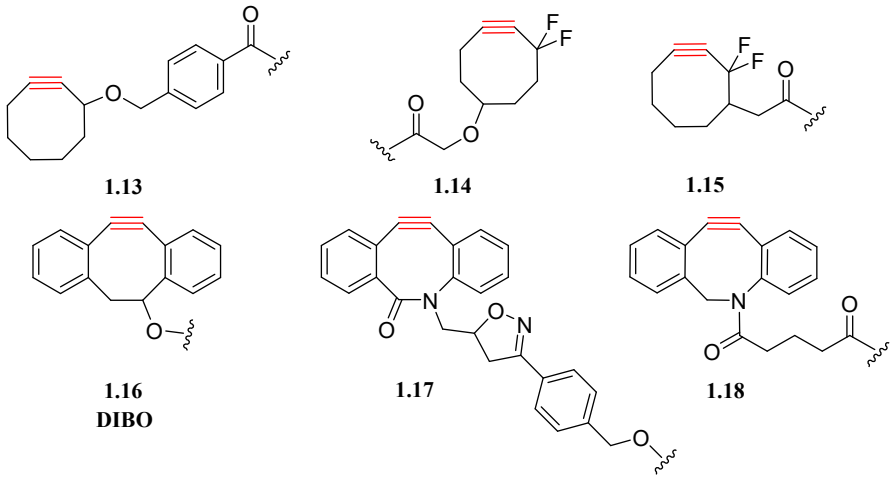

Figure 1.9 Structure of cyclooctyne (top) and dibenzocyclooctyne (down) derivatives used in SPAAC reactions.

As commented, significant effort has been devoted over the years to the development of more reactive cyclooctynes, even though, only scant investigations have been focused on the increase of SPAAC rates by modulation of the remaining component, the azide. In fact, the vast majority of reported applications of SPAAC are based on reactions with simple aliphatic azides. One reason why aromatic azides are generally avoided for SPAAC may lie in a report that *p*-azidophenylalanine exhibits sevenfold lower reactivity than that of the corresponding aliphatic azidomethyl analogue.[52] In addition, measurement of reaction rates of aromatic azides are hardly influenced by changing the electronic nature of substituents and may provide further evidence to avoid aromatic azides for SPAAC.[53] Other studies report a reactivity enhancement upon introduction of electron-withdrawing halogen substituents on DIBOs all of which suggest that the SPAAC mechanism primarily proceeds *via* $HOMO_{azide}$—$LUMO_{cyclooctyne}$ interaction also hinting that electron-rich azides are preferred.

Several examples illustrating the advantages of SPAAC for the functionalization of proteins and nucleic acids have emerged. For instance, Yin group has relied on SPAAC for the labeling of *Escherichia coli* bacteriophage M13[54] and van Delft P. *et al.* have successfully conjugated cyclooctyne-containing RNA to oligopeptides and oligosaccharides[55] proving the compatibility of this strategy with a wide range of biomolecules.

1.3.2.2 Strain-promoted nitrile-oxide-alkyne cycloaddition (SPNAC)

The adoption of dipoles other than azides has progressed click chemistry beyond the triazole conjugation tool. Recent studies on the relative reactivities of nitrile oxides, nitrones and diazocarbonyl derivatives as alternatives to the azide dipole in reaction with cyclooctynes suggest inferior kinetics, respective to azides, for diazocarbonyl-containing compounds and superior for strain-promoted nitrone-alkyne and nitrile-oxide-alkyne cycloaddition (SPNAC).

The isoxazole cycloadduct resulting from the SPNAC reaction, much like the triazole nucleus, is an important class of heterocycle. One of the potential issues with the nitrile-oxide dipole is instability due to dimerization or entrapment by environmental nucleophiles.[56] This problematic is minimized by *in situ* generation and careful selection of reacting partner. The benefits of SPNAC range from the ease and variety of procedures available for dipole formation from oxime substrates by direct or indirect oxidative methods or from nitro precursors in the presence of aryl isocyanates.[57] In regards to the isoxazole heterocycle, despite its status as a rather stable aromatic moiety, it can yield a variety of

functionalities that can potentially be valuable in subsequent manipulations,[58] and it is recurrent in many natural and synthetic bioactive compounds including ibotenic acid[59] or valdecoxib.[60]

From a synthetic point of view, nitrile-oxides and nitrones are commonly generated by the elimination of HCl from hydroximoyl chlorides (**1.20**) in the presence of a base such as NEt_3 (**Scheme 1.4**). Hydroximoyl chlorides (**1.20**) can be prepared from the corresponding oxime (**1.19**) and an electrophilic chlorine-containing source such as *N*-chlorosuccinimide (NCS), NaOCl or Cl_2.[61]

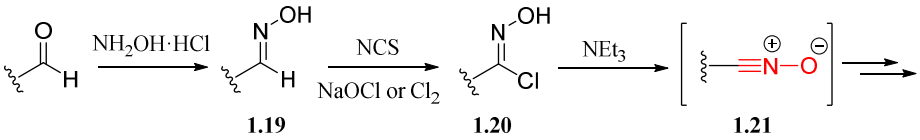

Scheme 1.4 Most common procedure for nitrile-oxide generation.

One of the first examples of strain-promoted nitrile-oxide cycloaddition did not involve an alkyne but a norbornene-modified DNA substrates.[62] The strained alkene, introduced into a growing DNA strand by way of a modified deoxyribo-uridine phosphoramidite, was subjected to cycloaddition with a variety of nitrile oxides generated *in situ* as previously commented (**Scheme 1.5**).

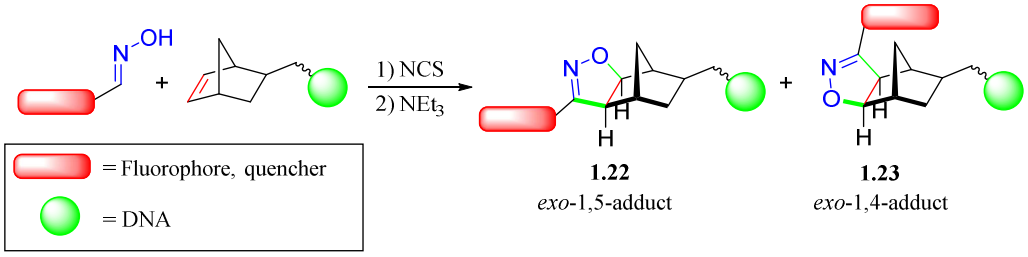

Scheme 1.5 Strain-promoted cycloaddition between norbornene and nitrile oxide.

Since their discovery, strain-promoted cycloadditions have been quickly adopted for synthesis of peptide and oligonucleotide conjugates. Two groups synthesized various ^{18}F-labeled peptides[63] and oligonucleotides[64] for PET molecular imaging and diagnosis. These examples exhibit the amenability of these types of click reactions to label peptides and oligonucleotides without major sequence-specific interferences such as cysteine, arginine or the nucleobases. However, there is still demand for improvements in strain-promoted cycloadditions as even with state-of-the-art cyclooctynes these reactions proceed slower than common CuAAC and other copper-free reactions such as the inverse electron-demand Diels-Alder cycloaddition.

The high size and hydrophobicity of cyclooctyne substrates prevents them from reacting efficiently in locally hampered environments such as enzymatic active sites. Despite this, a bright future lies ahead for cyclooctynes and, although cross-reactivity of the more reactive cyclooctynes with thiols excludes full bioorthogonality,[65] cycloadditions are possible with a much broader range of small dipoles such as azides, nitrones, nitrile oxides and diazo compounds. Furthermore, synthetic access to cyclooctynes can be straightforward and several of them have become commercially available, further expanding their accessibility.

1.3.3 Diels-Alder cycloadditions

The Diels-Alder (DA) cycloaddition is named after the scientists Otto Paul Hermann Diels and Kurt Alder. They first described it in 1928, for which they were awarded the Nobel Prize in Chemistry in 1950. It is the [4+2] cycloaddition reaction between a conjugated diene and a substituted alkene also termed dienophile to yield a substituted cyclohexene. The DA reaction is governed by orbital symmetry

considerations (it is a [4πS+2πS] cycloaddition) which show that the reaction proceeds through suprafacial/suprafacial interactions of a 4π electron system with a 2π electron system. The "click" like characteristics of the DA reaction make it easy to use for a wide array of designs and synthesis, varying from total synthesis,[66] material science[67] or polymer synthesis.[68] It is thermally reversible meaning that the resulting cycloadduct can undergo a reverse reaction when the temperature reaches a level favorable for reverse reaction (retro-Diels-Alder, rDA). That being said, in the biological context, degradation of the biomolecule is expected prior to the thermal reversion, thus, rDA is usually not taken into account.

In the context of bioconjugation, the DA cycloaddition offers encouraging potential due to the fact that one of the paramount dienophiles in DA reactions is the maleimide moiety because of its electron-deficient and sterically unhindered π-system. As a result, maleimides are one of the most commonly used dienophiles in DA reactions[69,70] and still represent one of the most versatile building blocks available for "click" reactions (see **Section 1.3.7.1**). On the other hand, because of synthetic ease of the diene counterpart, these reactions typically rely on substituted furans[71] and electron-rich 2,4-hexadiene derivatives.[72] The advantage of the latter is the system imposed preorganization of the diene conformation into the s-cis form.

The reaction may proceed quantitatively under equimolar conditions from a wide variety of starting materials in a variety of reported kinetics. In this regard, several factors are to be taken into account, being the three most remarkable: steric hindrance,[73] electronic properties[74] and solvent effects.[75] From these elements, the most convenient for bioconjugation is the solvent effect, and specially the use of water, since it greatly enhances the DA kinetics in comparison to organic solvents. An example of this approach was demonstrated by Marchán *et al*. employing a diene-derivatized oligonucleotide (**1.24**) and reacting it with maleimido-containing peptides[72] (**1.25**, **Scheme 1.6**).

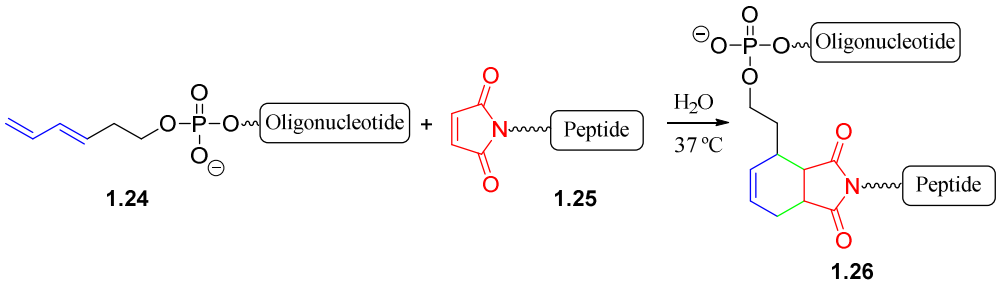

Scheme 1.6 Example of bioconjugation of oligonucleotides and peptides *via* DA reaction.

In a similar fashion, Read de Alaniz and co-workers utilized the DA cycloaddition to obtain vedotin, where an antibody is conjugated to a maleimide-containing auristatin derivative[76] vcMMAE, (**1.27**, **Figure 1.10**).

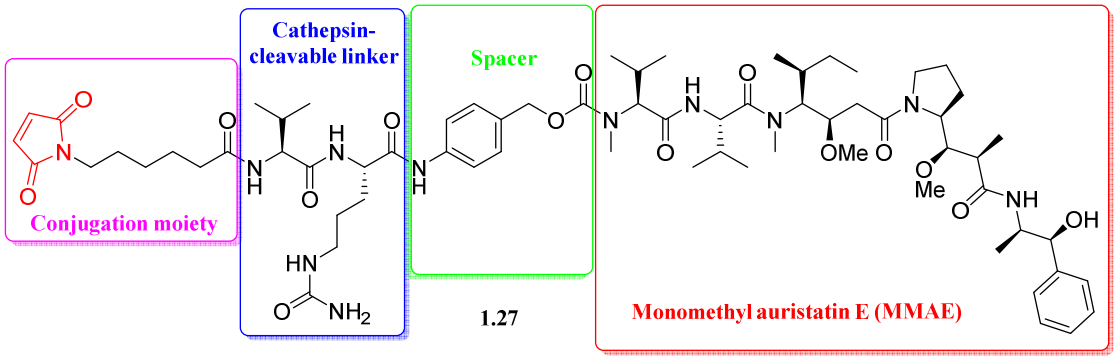

Figure 1.10 Maleimidocaproyl-valine-citrulline-*p*-aminobenzyloxy-carbonyl-monomethyl-auristatin-E (**1.27**) structure.

In their study, they made use of several diene-containing trastuzumab derivatives[77] (tAB) (**1.27-1.32**, **Figure 1.11**) to conjugate through a DA reaction. They found that the reactivity of the furan analogue (**1.28**) with the maleimide was sluggish under antibody conjugation conditions, which prompted them to explore more reactive dienes such as cyclopentadiene (**1.29**), which possesses the best kinetic profile. Yet, it has the detriment of coexisting as an interconverting mixture of 1- and 2-cyclopentadiene isomers through a [1,5]-hydride shift.[78] To avoid this shortcoming, they used stable derivatives (**1.30-1.32**) maintaining a similar reactivity performance.

Aside from the furan-derivatized tAB, which turned out to react restrictively slow, the other diene-maleimide cycloaddition rates yielded nearly quantitative conversion in a time framework of hours with equimolar amounts of dienes and maleimides. Overall, the found DA rates are comparable to that of other commonly used ligation strategies such as strain-promoted azide-alkyne cycloaddition (see **Table 1.1**, **Section 1.4**).

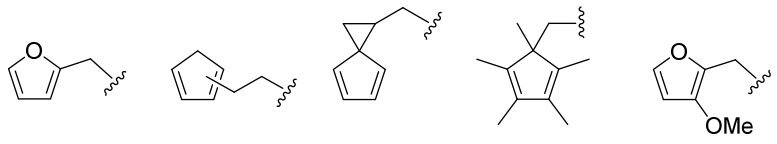

1.28 **1.29** **1.30** **1.31** **1.32**

Figure 1.11 Dienophiles utilized in the tAB-vcMMAE conjugation.

These examples demonstrate the usefulness of the DA reaction for bioconjugation purposes even though they are scarce. A possible explanation is the overall low kinetics associated with the reaction and the limited protocols for the incorporation of both the diene and dienophile moieties into the biomolecule scaffold, proving to be below the desirable standards specially for *in vivo* applications.

1.3.4 Inverse electron-demand Diels-Alder cycloadditions

As already discussed, reactions deemed useful for conjugation need to meet certain criteria such as high selectivity over other potential reactive functional groups present on biomolecules, having the capability to proceed in aqueous media at near physiological pH or fast reaction kinetics at room temperature (or up to 37 ºC) using low reactant concentration. However, within the current toolbox of bioconjugation reactions there is none yet able to meet all the cited criteria simultaneously and thus, specific labelling of biomolecules in their native environment using chemical reactions is still a challenging task.

Amongst all bioorthogonal reactions developed to date, the [4+2] cycloaddition of 3,6-disubsituted 1,2,4,5-tetrazines (Tz) and various dienophiles, which is a case of inverse electron-demand Diels-Alder (IEDDA) reaction, is the one that satisfied most of the above listed criteria necessary for use in applications such as ^{18}F,[79] protein[80]or nucleotide labeling[81] and cancer imaging.[82] As discussed in the previous section, in the normal Diels-Alder reaction conditions, an electron-rich diene reacts with an electron-poor dienophile. In contrast, in an IEDDA setting, an electron-rich dienophile, either alkene or alkyne, reacts with an electron-poor diene such as a Tz.

This reaction proceeds *via* the 1,4-addition of the diene system of the tetrazine (**1.33**) to the appropriate alkene (**1.34**), yielding a highly strained bicyclic intermediate (**1.35**) which evolves in a rDA fashion losing 1 equiv. of molecular nitrogen. This, yields a 4,5-dihydropyridazine (**1.36**) which either isomerizes to the more stable 1,4-dihydro isomer (**1.37**) or is oxidized to afford pyridazine derivatives (**1.38**, **Scheme 7**). This last step is usually carried out employing oxidants such as *in situ* generated HNO_2, milder alternatives such as DDQ[83] or PIDA[84] or atmospheric oxygen in some instances.[85]

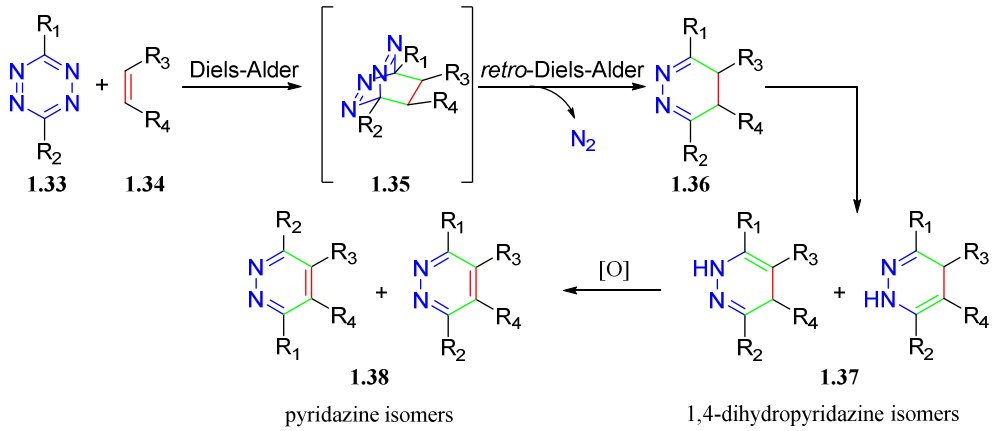

Scheme 1.7 Proposed mechanism for the IEDDA reaction.

The ability of tetrazines to react with unsaturated compounds was first revealed in 1959 by Lindsey *et. al.*[86] yet, over recent years, the IEDDA reaction has emerged as an important tool for probing the mechanism and function of bioactive molecules in living systems. For such applications, rate constants are of critical importance as very fast kinetics are required for labeling cellular constituents involved in processes that occur on biological time scales. Another beneficial aspect of using tetrazines as coupling partners is the usual increase in fluorescence observed after the reaction, resulting in a "turn-on system" useful for cell imaging applications.

The IEDDA reaction kinetics is ruled by the energy gap between the corresponding HOMO and LUMO of the reactants. In particular, any pair of diene/dienophile with a smaller $HOMO_{dienophile}$–$LUMO_{diene}$ energy difference will react faster in IEDDA conditions. For instance, tetrazines attached to electron withdrawing groups (EWGs) such as carboxylate or 6-pyrimidyl present faster kinetics than tetrazines bearing electron donating groups such methoxy or methyl moieties.[87,88]

In the dienophile counterpart, electron-rich substituents are preferred to achieve faster kinetics and in the vast majority of cases, olefinic reactants surpass acetylenic ones in terms of reaction rates. Strain effect is another important aspect in reactivity. Independently from the electronic effect of the dienophile substituents, ring strain plays the most important role in the IEDDA reaction rate by raising the energy of the $HOMO_{dienophile}$. Sauer *et al.* described the reaction kinetics between various tetrazines and a number of dienophiles and quantitatively demonstrated that the rate constant increases with increasing ring strain according the order depicted in **Figure 1.12**,[89] and demonstrating the greater impact of the dienophile features compared to those of tetrazines in tuning the IEDDA kinetics.

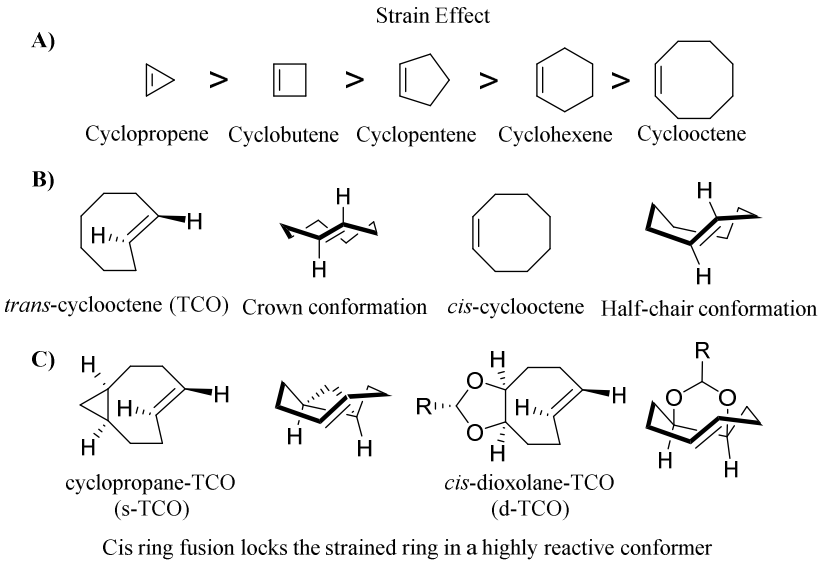

Figure 1.12 Influence of the strain effect on the IEEDA reaction. A) Degree of ring strain along a series of cyclic alkenes. Similar strain effect are also observed for cyclo-enamines and cyclic enol ethers.[90] B) The crown conformation of *trans*-cyclooctene (TCO) makes it 7 orders of magnitude more reactive than *cis*-cyclooctene towards 3,6-bismethoxycabonyl-1,2,4,5-tetrazine and 3,6-bistrufluoromethyl-1,2,4,5-tetrazine.[89] C) *Via* ring fusion, the crown conformation was further locked, resulting in rate enhancement in comparison to TCO.

Stereochemistry is another aspect recently explored regarding the tuning of IEDDA kinetics of different strained dienophiles. The axial isomer of a functionalized TCO was found to be more reactive than the corresponding equatorial isomer by 1.1 kcal mol^{-1} (~ 4×, **Figure 1.13,** A).[91] In a similar fashion, the *exo* isomer of norbornene reacts with tetrazines 3 times faster than the *endo* counterpart (**Figure 1.13**, B).[92] The same trend is observed for syn-d-TCO that has a slightly higher rate constant (1.2×) compared with the anti-diastereomer (**Figure 1.13**, C).[93]

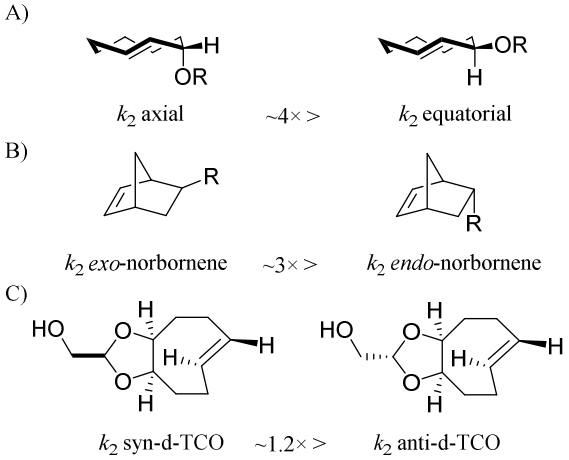

Figure 1.13 Effect of stereochemistry the reactivity of isomers of TCO (A), norbornene (B) and d-TCO (C).

Steric hinderance is also a paramount aspect concerning the IEDDA kinetics. In regards to the Tz diene, a hydrogen substituent at either the 3- o 6-position increases reactivity by lowering the overall bulkiness of the reactive site. For instance, several research groups have reported that *mono* substituted Tzs participate in IEDDA reactions with faster kinetics than *di*-substituted Tzs even the ones bearing strong EWGs.[94] Similarly to the DA reaction, the use of protic polar solvents, and specifically water, has proven beneficial for IEDDA. This advantageous effect is attributed to the stabilized interactions

between the activated complex and water but also to an enhanced hydrophobic interaction between cycloaddends, which is facilitated in water.[95]

There is only a handful suitable dienophiles described in the literature that readily react with Tzs (**Figure 1.14**). The three mainly used IEDDA dienophiles in bioconjugation are norbornenes (**1.39**), *trans*-cyclooctene (TCO, **1.40**) and 1-methylcyclopropene (mCP, **1.41**) derivatives. From these three options, both the TCO and mCP are preferred for *in vivo* and *in vitro* application since they exhibit greater kinetics. On the other hand, norbornene is useful due to its synthetic accessibility, stability and relatively small molecular size.[96,97]

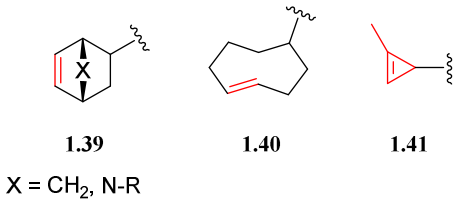

Figure 1.14 Most common dienophiles used in IEDDA reaction.

In this context, the use of 7-substituted norbornenes with Tzs has only recently been reported. Fujii and co-workers described the use of 7-azanorbornene derivatives which can be prepared by Diels-Alder reaction between an alkyne and pyrrole (**Scheme 1.8**).[98]

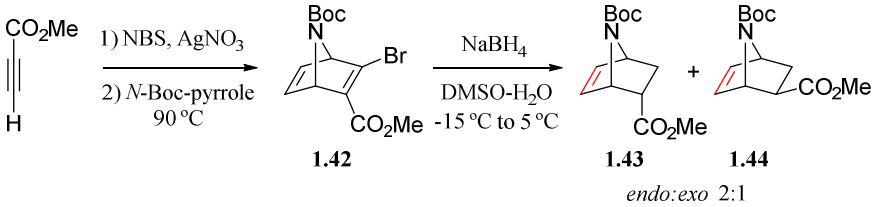

Scheme 1.8 Synthetic approach by Fujii and co-workers to obtain 7-azanorbornenes.

TCO was first prepared as a mixture of *cis/trans*-cyclooctenes *via* Hoffman elimination of trimethylcyclooctyl ammonium iodide.[99] Several stereospecific methods for preparing TCO from *cis*-cyclooctene have also been described.[100] However, a limitation of such protocols is that multistep synthesis is required to invert the alkene stereochemistry. In this context, the photochemical isomerization of *cis*-cyclooctene to the *trans* isomer represents a direct methodology for the synthesis of TCO. Studies by Inoue expanded the scope and understanding of the photoisomerization, which is typically run under singlet state conditions.[101] That said, while the photochemical procedure is effective for the preparation of the parent hydrocarbon, the photochemical synthesis of functionalized TCOs has been limited by low *trans*/*cis* ratios under preparative useful conditions due to the photodegradation of the TCO adduct. Fox and co-workers, elegantly improved the practicality of the photochemical protocol by means of metal complexation of the *trans*-isomer.[102]

Cyclopropenes are usually accessed from TMS-protected propynes *via* rhodium catalyzed cyclopropenation with diazo compounds. **Scheme 1.9** depicts two of the alternatives which may furnish either carbamate- or amide-containing reagents (**1.47** and **1.49**, respectively).[103–105]

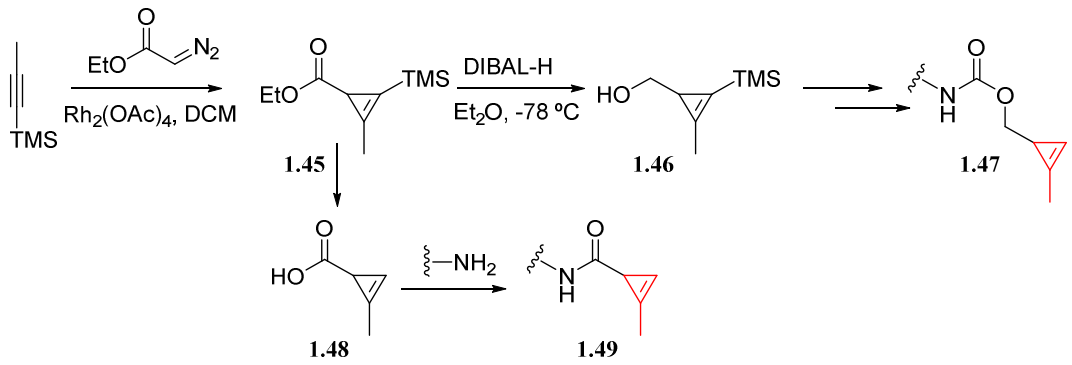

Scheme 1.9 Synthetic route for the preparation of methylcyclopropene derivatives.

Even though cyclopropene-involving IEEDA reactions are markedly slower than other tetrazine-based ligations (~4-5 order of magnitude slower than those of some TCOs[87]), they are advantageous due to the smaller linker size, proving to be the best suited for biological applications. The use of methylcylocpropenes in protein inhibition yields minimal loss in their native biological structure[106] in comparison to the bulkier TCO counterpart.

Due to the display of high selectivity, uniquely fast kinetics and catalyst-free nature of the IEEDA reaction, it has been established during the last decade as the state-of-the-art approach for selective modification of proteins in living cells and notably *in vivo*.[107–109] There is already literature supporting tetrazine decaging reactions as an emergent tool for the study of protein functions[110] and bioorthogonal drug activation.[111,112] Moreover, by carefully choosing the tetrazine-dienophile pair, two parallel IEDDA reactions, mutually orthogonal with each other, can be performed by exploiting different relative reaction rates.[113]

On the other hand, despite recent developments being promising, a number of essential challenges must be addressed in the future in order to fully take advantage of this strategy for bioconjugation. Ligations usually involve relatively large reactive groups (TCOs), leading to greater chances of perturbing native biological processes. Moreover, the hydrophobicity associated with larger reporting groups could also be a detriment in certain situations. To avoid this, an unmet challenge is the development of small, reactive and hydrophilic dienophiles that possess high stability and permeability to accomplish fast and selective labelling with minimal off-target effects. In this context, the highly inconvenient synthesis of, not only the dienophile, but also the tetrazine core combined with their limited commercial availability is still restraining the IEDDA from becoming a widely spread tool.

1.3.5 Light-triggered dipolar cycloadditions

As soon as chemists make a new molecule, they immediately subject it to many different frequencies of light while trying to work out its structure (for example, X-ray, NMR or UV-Vis spectroscopy). While it is clear that we can use light to characterize molecules and materials it is not as straightforward to answer whether we can use it to produce them.

Light is very useful in chemical reactions, not only because it provides the energy needed to drive uphill processes, but also because the photogenerated molecular excited states can undergo chemical processes that are otherwise unthinkable in ground states. Taking advantage of photochemistry enables access to a powerful toolkit for a wide array of chemical transformations which are indeed unique. The efficacy of light in affecting chemical transformations is due to electrons lying in molecular orbitals within molecules entering into excited states upon the absorption of photons.

A clear and intriguing example of such complex chemical processes is photosynthesis. It smoothly occurs in plants and is based on the efficient utilization of sunlight energy and its transformation into chemical energy. This process involves a series of photoinduced electron transfer processes that result in products that are essential components of fueling life on Earth. Nonetheless, we are yet far from completely mastering and mimicking this complex and efficient process.

In the context of bioconjugation, several reactions have been exploited through the years to decorate biomolecules using light[114] and the most prominent will be briefly discussed.

1.3.5.1 Tetrazole ligation

In the late 1960s, Huisgen and co-workers described the first photoinduced 1,3-dipolar cycloaddition between 2,5-diphenyl tetrazole (**1.50**) and methyl crotonate (**1.52**) in benzene.[115] In this seminal study, a medium-pressure mercury lamp was used and led to the formation of a pair of regioisomeric pyrazolines (**1.53** and **1.54**) in a 3:1 ratio. Based on the stereochemistry of the observed products, a concerted reaction mechanism was proposed in which, upon photoirradiation 2,5-diphenyltetrazole (**1.50**) undergoes an effortless cycloreversion reaction to extrude nitrogen and generate *in situ* a nitrile-imine dipole (**1.51**) which then reacts with the crotonate dipolarophile in a concerted manner to afford the pyrazoline cycloadducts (**1.53** and **1.54**, **Scheme 1.10**). The photolysis of 2,5-diaryltetrazoles is extremely efficient under 290 nm UV irradiation with a quantum yield in the range of 0.5-0.9, with electronic properties of the substituents having minimal effect.[116] Despite this, remarkable rate acceleration was observed when the cycloaddition reaction was performed in aqueous media.[117]

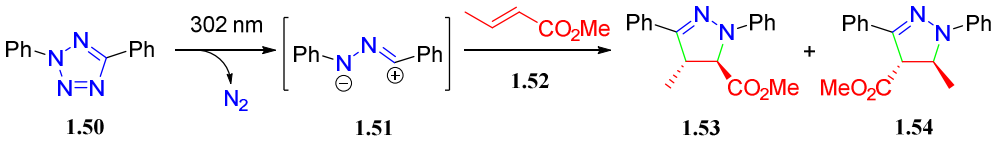

Scheme 1.10 Proposed mechanism for the tetrazole photoclick 1,3-dipolar cycloaddition.

Over the years and in an endeavor to tune the photoactivation wavelength towards the long-wavelength region of the electromagnetic spectrum, great synthetic efforts has been done to modify the reagents with the appropriate substituents and take advantage of this reaction for biological applications. As a representative example, a fumarate-docetaxel conjugate was prepared by attaching *mono*-isopropyl fumarate amide at position 10 of docetaxel (**1.55**, **Figure 1.15**) in conjunction with a naphthalene-derivatize tetrazole and used to image proteins in Chinese hamster ovary cells by means of this photoclick ligation.[118]

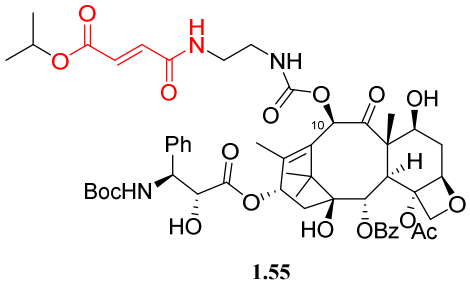

Figure 1.15 Docetaxel analogue containing an isopropyl fumarate moiety.

Not long after, Arndt *et al.* also took advantage of the tetrazole-photoclick ligation to post-synthetically modify nucleic acids.[119] They made use of an uridine phosphoramidite derivative containing a tetrazole moiety at the 5-position (**1.56**) and, after standard SPONS, the resulting DNA strand (**1.57**) was

photoclicked at 365 nm with a maleimide-derivatized cyanine dye (**1.58**) in order to obtain a DNA-dye conjugate (**1.59**, **Scheme 1.11**).

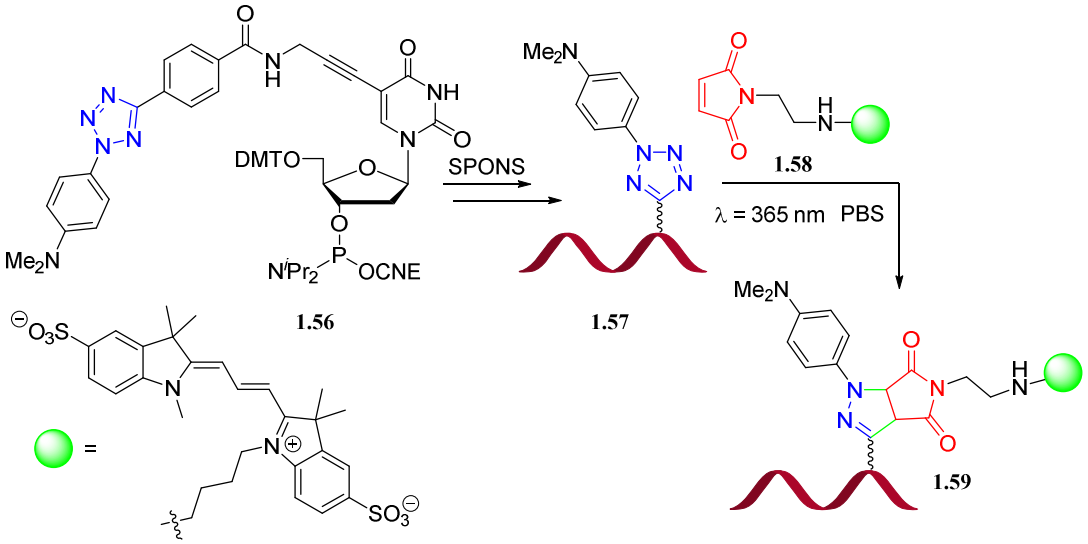

Scheme 1.11 Synthesis of a tetrazole-modified DNA building block (**1.56**) and photoclick reaction of the tetrazole-containing DNA analogue (**1.57**) with a maleimido-dye (**1.58**) to render the desired conjugate (**1.59**).

1.3.9.2 Azirine ligation

It has been long known that highly reactive nitrile ylides (**1.61**) can be generated photochemically *via* ring-opening of 2*H*-azirines (**1.60**), and that these nitrile ylides react spontaneously with electron-deficient alkene dipolarophiles to produce Δ^1-pyrrolines[120] (**1.62**, **Scheme 1.12**). The azirine-mediated cycloaddition reaction is compatible with protic solvents including water,[121] but requires irradiation at UV wavelengths. In an experiment carried out using a handheld UV lamp (room temperature, 2 h), reactions were found to be highly regioselective since only two diastereomers (**1.62**) were observed by NMR spectra with an *endo*/*exo* ratio of roughly 1:1. The authors ascertained that while azirines bearing EDGs did not yield any cycloaddition, nitro-containing ones afforded cleanly the cycloadduct with great yields, indicating that the presence of EWGs is crucial for nitrile-ylide (**1.60**) stabilization (**1.62**, **Scheme 1.12**) in aqueous medium.[122]

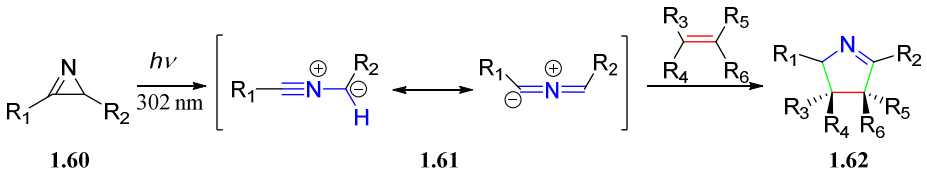

Scheme 1.12 Azirine-alkene dipolar cycloaddition proposed mechanism.

In a similar fashion as the tetrazole-involving reaction, obtaining a photoreactive compound that can undergo ligation by visible light is a desirable feature for biological application in order to avoid toxic UV irradiation. To address this issue, Meuller *et. al.*[123] conceived a two-fragment molecule in which one would be responsible for the absorption of light at the desired wavelength region and the other fragment responsible for efficiently generating the reactive species. For this, a 2*H*-azirine moiety containing pyrene (**1.63**), a visible-light-absorbing chromophore, provided an elegant solution to the challenge (**Scheme 1.13**). The pyrene core is not only crucial for light absorption but is incorporated

into the cycloadducts' carbon framework, thereby providing additional desirable features such as a built-in fluorescent marker or anchor for π-π stacking.

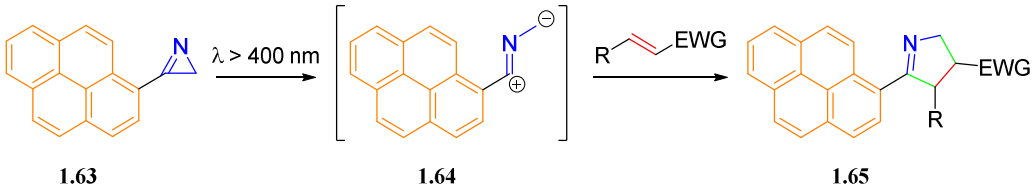

1.63 **1.64** **1.65**

Scheme 1.13 General reaction scheme for azirine-pyrene based visible-light-induced cycloaddition reaction.

Compared to other bioorthogonal reactions, the major advantage of photoclick chemistry is its light inducibility: the use of light confers a spatiotemporal control over the reaction initiation in living systems. Taking that into account, development of reactions with exceptional selectivity and high triggering wavelengths still remains of paramount importance. To date, the majority of the established photoinduced ligation reactions require UV light, have low tissue penetration and can cause unwanted photochemical transformations such as thymine dimerization and subsequent DNA damage.[124,125] Additionally, challenges such as shadows or uneven penetration of light into the tissue have been only partially solved with modern techniques.[126,127]

Furthermore, there still remain many important goals such as extending the wavelength coverage for activation to the visible and infrared light and improving absorption properties and orthogonal activation.

1.3.6 Staudinger ligation

The Staudinger reaction, discovered and named after Hermann Staudinger, is the chemical reaction of an azide with a phosphine or phosphite producing an iminophosphorane intermediate that, upon hydrolysis yields a phosphine oxide and an amine. The Staudinger ligation is a modification of the classical Staudinger reaction where an electrophilic trap is placed on the triaryl phosphine, which yields an "aza-ylide" intermediate that rearranges to produce an amide linkage in aqueous media.

1.3.6.1 Non-traceless Staudinger ligation

In 2000 Bertozzi and co-workers introduced the bio-orthogonal Staudinger ligation,[50] known ever since as the non-traceless azide–phosphine ligation. This reaction is performed with a special substrate: an ortho-phosphinic benzoic acid derivative (**1.66**, **Scheme 1.14**) that, upon reacting with an azide-containing moiety (**1.67**), furnishes an aza-ylide (**1.68**) that extrudes molecular nitrogen in a similar fashion as the classical Staudinger reaction. Thereafter, an internal rearrangement yields an oxazaphosphetane (**1.69**) intermediate which, in aqueous media, spontaneously decomposes into the desired amide (**1.70**), incorporating the phosphine oxide within the benzene scaffold.

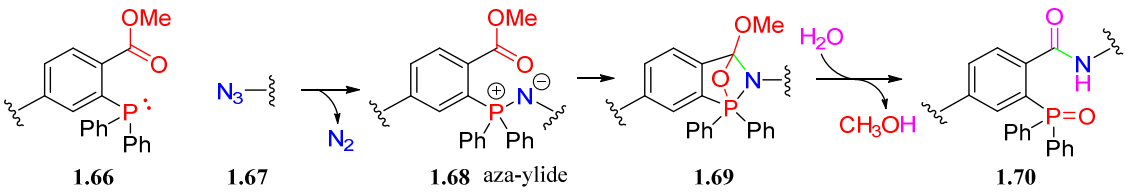

Scheme 1.14 Non-traceless Staudinger reaction of an *ortho*-phosphine benzoic acid derivative.

From a practical standpoint, the more basic and nucleophilic phosphines react faster, however it should be noted that very basic aliphatic phosphines are more prone to oxidation, limiting their use in biological systems.[128]

1.3.6.2 Traceless Staudinger ligation

Shortly after the description of the non-traceless Staudinger ligation, a new method, the so-called "traceless Staudinger ligation" was developed simultaneously by Bertozzi *et al.*[129] and Raines *et al.*[130]

In this methodology, the phosphine oxide (**1.76**) is excluded from the target molecule (**1.77**) during amide formation (**Scheme 1.15**), in contrast to the result of the non-traceless procedure. The mechanism follows a similar path as the non-traceless reaction. Starting from the acyl-substituted arylphosphine (**1.71**), reaction with the azide moiety (**1.72**) yields the "aza-ylide" intermediate (**1.73**) which further reacts with the carbonyl group, trapping the negatively charged nitrogen atom and yields an amidophosphonium salt (**1.75**). Subsequent hydrolysis produces the phosphine oxide (**1.76**) and free amide (**1.77**) as two separate entities.

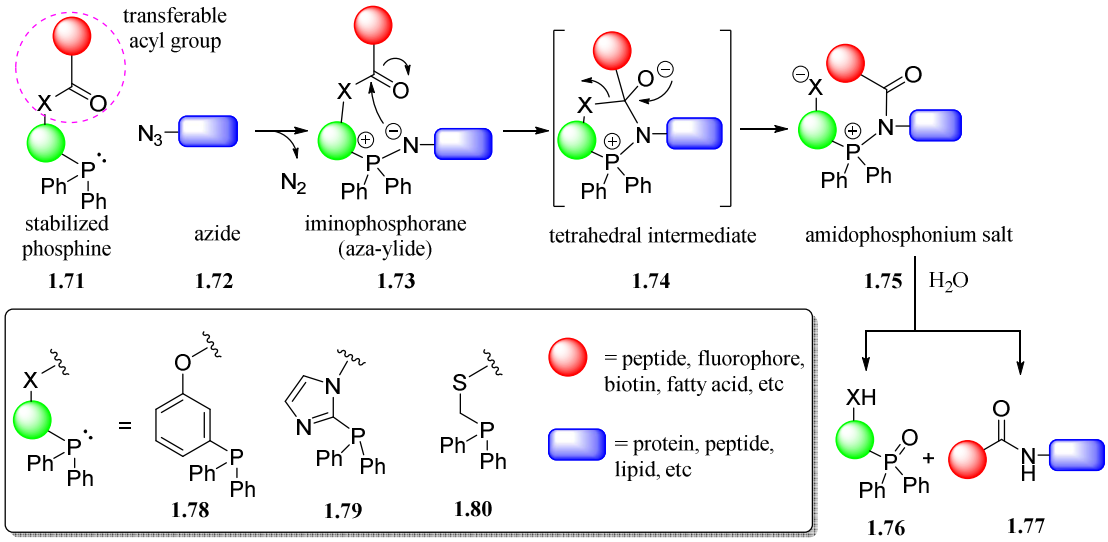

Scheme 1.15 The ''traceless'' Staudinger ligation as reported by Raines and Bertozzi.[129–131]

For *in vivo* experiments, in which the addition of the probe as well as the labelling itself takes place inside a living cell, ligations based on the Staudinger reaction perform advantageously when compared to the classical copper-catalyzed "click" reactions because they avoid the usage of toxic copper salts, even though the reaction itself proceeds slower and often does not run to full conversion.[132] The main drawbacks of the Staudinger ligation are the poor solubility and susceptibility to oxidation of classical phosphines in aqueous media, rendering the overall strategy suboptimal for biological applications, which is still a concern to date.[133] Further work should aim at the design and preparation of phosphine

linkers that are entirely stable towards oxidation for intramolecular acylation in the absence of an organic cosolvent.

1.3.7 Thia-Michael ligation

C─S bonds are common units for a large number of chemicals including pharmaceuticals,[134] bioactive natural products,[135] food additives[136] and polymers.[137] The paramount importance of organosulfur compounds in both chemistry and biology has provided a major impetus for the development of efficient methods for their construction and handling. Within this setting, the thia-Michael addition reaction has distinguished itself as a powerful and widely used tool for the synthesis of organosulfur compounds, especially, in the context of bioconjugation.[138] The utility of this reaction has been exemplified in the synthesis of an array of useful compounds that are associated with drug-delivery processes, polymer chemistry or pharmaceuticals.

The thia-Michael addition is a robust, highly efficient condensation that evolves with high reaction rates under mild conditions and is usually orthogonal to other reactions. It has been described as a class of 1,4-conjugate addition, in which a sulfur-containing nucleophile, coined the "Michael donor", attacks the electrophilic β-carbon atom of an electron-poor enone, the "Michael acceptor", either in the presence of a catalyst or catalyst-free to afford highly selectively thia-Michael adducts.

The rate and yield enhancement observed in aqueous environment can be rationalized by an ambiphilic dual-activation role of the water molecule.[139] That is, not only promoting the electrophilicity of the β-carbon of the α,β-unsaturated carbonyl moiety (**1.81**) but also by H-bond formation between the oxygen atom of water and the sulfhydryl hydrogen (**1.82**), which seems to increase the nucleophilicity of the sulfur atom of the thiol (**Scheme 1.16**).

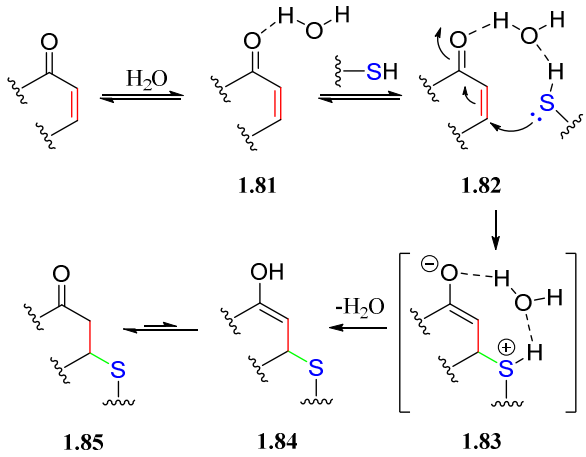

Scheme 1.16 Proposed water-assisted thia-Michael addition reaction mechanism.

It is worth remining that thiols are present in natural products,[138] biomolecules[140] and synthetic precursors.[141] One the other hand, the fact that maleimides are available from commercial sources as maleimido-derivatized tags or drugs makes this one of the most straightforward bioconjugation reaction to implement in the current toolbox.

1.3.7.1 Maleimides as Michael acceptors

Since their first use in bioconjugation more than 50 years ago, maleimides have become privileged chemical partners for the site-selective modification of a wide array of compounds such as proteins,[142] oligonucleotides,[143] or more recently, antibodies.[144] Within this latter framework, only two antibody-

drug conjugates have been approved by the FDA for cancer treatment: Adcetris (brentuximab vedotin)[145,146] and Kadcyla (trastuzumab emtansine)[147,148] both of which contain a sulfenyl-succinimide linkage in their structure.

Maleimides (**1.86**, **Scheme 1.17**) are known for readily reacting with functionalities that are naturally part of biomolecules, such as thiols or amino groups present in cysteine or lysine and ornithine residues, respectively. Michael additions on maleimides have been shown to be highly specific for thiols at a pH ranging between 6.5 and 7.5 in comparison to ε-amino group present in every lysine residue, which are protonated under these conditions.[149] The sulfenyl-succinimide linkage (**1.87**) resulting from the reaction between maleimides and thiols is known to be hydrolytically unstable and can undergo thiol exchange *via* a retro-Michael process (**1.88**). This last undesirable side-reaction is of particular interest when the thia-Michael reaction is to be performed (or the adduct used) *in vivo*, since endogenous thiols such as human serum albumin or glutathione (GSH) may end up replacing the thiol. On the other hand, this exchange is easily avoided by hydrolysis of the thia-Michael adducts into the corresponding succinamic acids (**1.89** and **1.90**), which are resistant to thiol-exchange transformations.

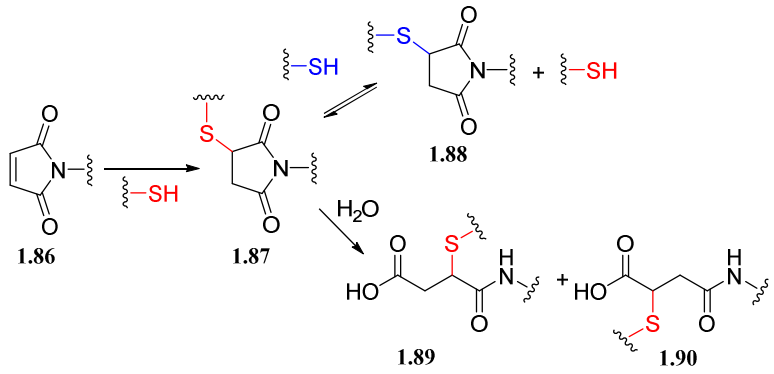

Scheme 1.17 Main side reactions of the sulfenyl-succinimide linkage.

In order to approach the stability problem, and more specifically to lessen the impact of the retro-Michael pathway on sulfenyl-succinimide linkages, novel maleimide scaffolds are being developed. *N*-aryl maleimides were found to be suitable Michael acceptors for their capability of providing more stable thiol-based bioconjugates (after hydrolysis).[150] Replacing the *N*-alkyl substituent with a phenyl group led to an impactful 100-fold increase in the rate of hydrolysis to the corresponding thio-substituted succinamic acid and thus, an improvement in stability of the conjugate compared to those incorporating slowly hydrolyzing sulfenyl-succinimides. Nevertheless, the balance between the rate of Michael addition and hydrolysis of sulfenyl-succinimides and maleimides should also be taken in consideration, as an up to 50% decrease in conjugation efficiency was also observed in early studies with *N*-aryl maleimides that were exposed to physiological buffer prior to conjugation.[150]

Fontaine *et. al.* studied the rates of ring-opening hydrolysis and thiol exchange of a range of *N*-substituted thioether succinimides formed by maleimide-thiol conjugation, suggesting that conjugates made with electron-withdrawing maleimides can be purposefully hydrolyzed rapidly *in vitro* to ensure *in vivo* stability.[151]

1.3.7.2 Maleimide derivatives

With the aim of increasing the stability of thia-Michael adducts, Baker and co-workers introduced bromomaleimides (**1.91**) as a new class of tunable Michael acceptors capable of rapidly reacting with cysteines (**1.92**).[152] The main advantages regarding bromomaleimides in comparison to classical maleimides are the remarkable chemoselectivity towards thiol function over nitrogen alkylation,

superior stability of the end conjugate and, in some contexts, the possibility of selective regeneration of the cysteine residue through DTT or TCEP reduction (**Scheme 1.18**). On the other hand, thiomaleimides can still behave as Michael acceptors allowing for an additional functionalization even though the first Michael addition is considerably faster than the second thiol insertion. This provides a reliable methodology for one-pot sequential dual functionalizations.[153]

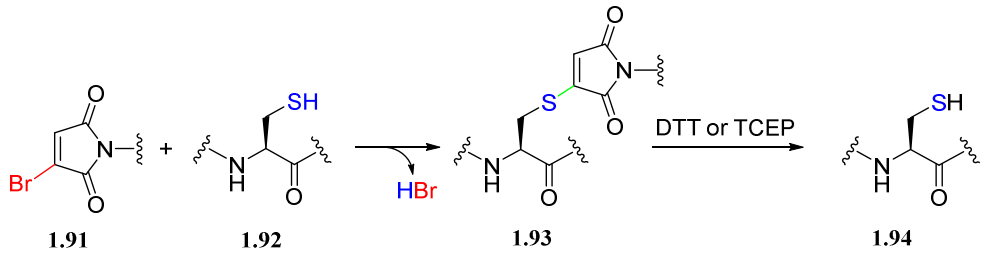

Scheme 1.18 Proposed outcome for the reaction of a cysteine residue with a bromomaleimde and reversal of the process.

Similarly, dibromomaleimides also allow for the addition of two nucleophiles, and can yield bioconjugates that can be reverted upon the addition of thiol reagents such as glutathione (GSH) or β-mercaptoethanol (β-ME). Another investigated utilization of dibromomaleimides is the modification of natural disulfide linkages through a debridging and rebridging strategy. Brocchini *et. al.* highlighted the potential of modifying disulfides *via* bridging reagents that retain structure and function of the target protein.[154] To proof this, they made use of the endogenous peptide hormone somatostatin (**1.95**), a 14-amino acid peptide containing a disulfide bridge. Treatment with TCEP yielded the reduced form (**1.96**), which upon addition of 1.1 equiv. of a fluorescein-derivatized dibromomaleimide (**1.97**) led to complete conversion to a bridged somatostatin derivative (**1.98**). Moreover, treatment of fluorescein-derivatized somatostatin analog (**1.98**) with β-ME led to complete reversion to the reduced form (**1.96**, **Scheme 1.19**).

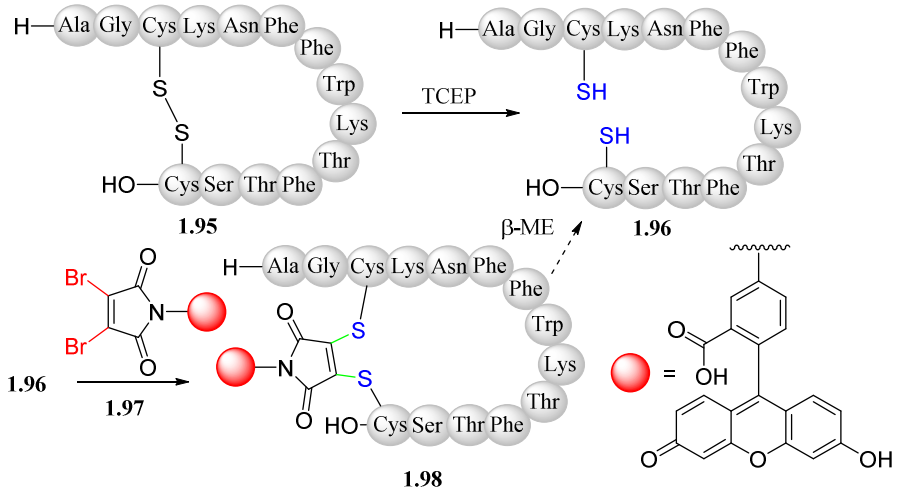

Scheme 1.19 Dibromomaleimide-mediated disulfide rebridging of somatostatin.

As the field of bioconjugation moves towards platforms that are custom-designed and targeted towards highly specific applications, the thia-Michael reaction has stablished a firm foothold among the ever-increasing group of exceptionally effective methodologies in the modern toolbox. Recent advances of several covalently thiol-linked antibodies is the signature example of the powerful nature of the reaction.[7]

Taking into account the limited stability displayed by some adducts (mainly sulfenyl-succinimide and β-mercaptoester) that revert back to the respective parent reagent, throughout the years several groups

focused their research on fine-tuning the scaffolds to enhance stability. This attribute can also be seen as a substantial advantage in the context of controlled drug release field. This continuous reversal of the conjugate adduct to the partner reagents can be exploited when a slow drug release profile is desired.

1.3.8 Thiazolidine ligation

The condensation reaction between aldehydes (**1.99**) and 1,2-aminothiols (**1.100**) to form the thiazolidine (**1.101**) moiety is an interesting bioconjugation tool (**Scheme 1.20**). Reactions involving 1,2-aminothiols are especially interesting because of their natural occurrence and ease of synthetic introduction in proteins and peptides as *N*-terminal cysteines.

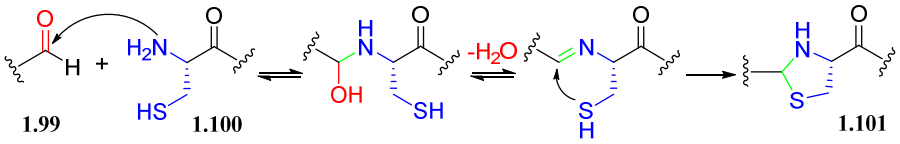

Scheme 1.20 Mechanism for thiazolidine formation.

Over the years, thiazolidine formation has seen some use in the preparation of antibody-drug conjugates,[155] as a protecting group for *N*-terminal cysteines in native chemical ligation[156] and for peptide cyclization.[157] Noteworthy, thiazolidine formation is orthogonal to *N*-acylated cysteines, since thiols react with aldehydes reversibly yielding hemithioacetals (**1.102**, **Scheme 1.21**). This fact implies that the thiazolidine ligation is a platform for the selective derivatization of *N*-terminal cysteines in scaffolds that contain other types of thiols.

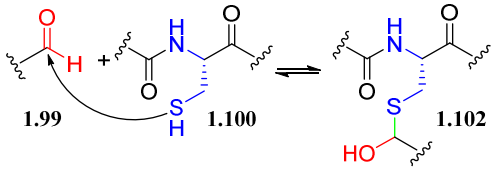

Scheme 1.21 Reversible reaction between *N*-acylated cysteine and aldehydes.

Mechanistically, it is generally accepted that the reaction requires slightly acidic pH, long reaction times[158] and that the thiazolidine adduct is prone to hydrolysis under physiological conditions.[159] Despite this, the overall stability can be modulated by substituent modification.

Preparation of the two reactants is usually straightforward, especially in the peptide or protein framework. *N*-terminal cysteine residues can easily be introduced by SPPS or plasmid expression and the aldehyde counterpart can be obtained by mild oxidation of *N*-terminal serines and threonine residues using periodate, or by incorporation of acetal precursors during SPPS. In the field of oligonucleotides, thiazolidine ligation has been sparingly used. Oretskaya and co-workers synthesized peptide-oligonucleotide conjugates taking advantage of a phosphoramidite bearing a protected 1,2-diol at the 2' position of uridine (**1.103**, **Scheme 1.22**). Introducing this derivative at internal positions of oligonucleotide chains and oxidizing the diol intermediate (**1.104**) under mild conditions rendered the corresponding aldehyde (**1.105**) for conjugation or cross-linking purposes.[160]

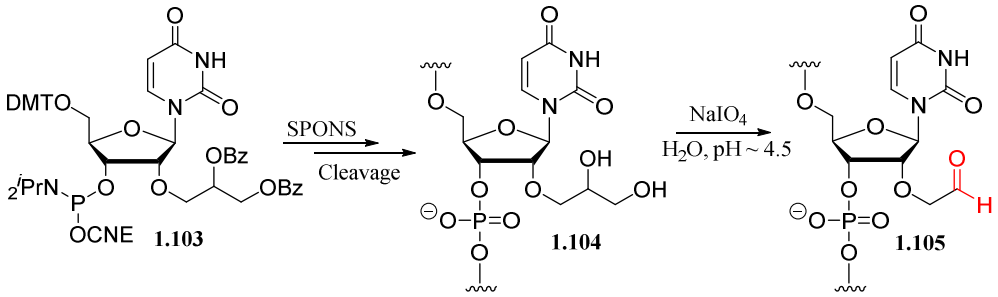

Scheme 1.22 Introduction of 2'-aldehyde uridines *via* periodate oxidative cleavage of 1,2-diols.

Even though thiazolidine ligation is often described as a "click" reaction, it is far from perfection. It cannot be performed *in vitro* or *in vivo*, since the acidic conditions required are neither accessible nor compatible within living systems. Moreover, although it is usually described as a fast, high-yielding reaction, it can take up to four days to achieve completion. Finally, as many others the reaction produces two isomers, which can in principle be separated when low molecular weight adducts are generated.

These reasons, combined with the emergence of other competitors, the has led to little thiazolidine usage in modern bioconjugation schemes.

1.3.9 Oxime and hydrazone ligation

The formation of oximes and hydrazones is commonly used to facilely link biomolecules to various probes. Generally, oximes (**1.108**) and hydrazones (**1.109**) can be easily obtained from the corresponding nucleophile (where the amine is linked to an α-effect-producing atom, that is with lone electron pair) and a carbonyl compound (either an aldehyde or a ketone), with water being the sole byproduct (**Scheme 1.23**).

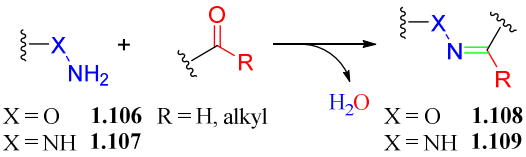

Scheme 1.23 Formation of an oxime (**1.108**) or hydrazone (**1.108**) from an alkoxyamine (**1.106**) or hydrazine (**1.107**) and a carbonyl group, respectively.

These two reactions are considerably older than most of the other bioconjugation reactions. As early as 1882, oximes and their formation were intensively studied by Meyer and Janny.[161,162] Due to its simplicity, the ligation has been used extensively for many purposes such as ^{18}F labeling,[163] derivatization of carbohydrates,[164] and synthesis of protein[165] and oligonucleotide conjugates[166] amongst others. Even though oximes and hydrazones have been known for over 100 years only modern research has focused on their preparation with biological relevance in mind, that is in water and at pH values closer to neutral, since nowadays is common to work with peptides, proteins and nucleic acids as reacting substrates and to carry out reactions not only in solution but also in living systems such as cells.

Oxime and hydrazone formation meet several of the requirements for bioconjugation. The tether is very small in size, consisting only of three non-hydrogen atoms (C=N–X where X = O or NH), and thus constitutes a minimal perturbation to the native biomolecule. The reaction is completely compatible with aqueous environments and displays reasonable rates in the appropriate conditions. The reaction is usually performed under general acid catalysis with a preferred pH ~4.5[167] and is fully reversible. The target conjugates can undergo hydrolysis in aqueous media, becoming linkage stability one of the main

detriments. In this context, pH has also a remarkable effect on the final adduct stability, drastically modulating the half-life span of the desired conjugate.

In regards to bioorthogonality, although the α-effect is hardly found in nature, aldehydes and ketones are common. A significant example is found in the hemiacetal form of every carbohydrate, which is in equilibrium with its respective carbonyl compound, thus making it amenable to reactions with α-nucleophiles.[168] Furthermore, numerous aldehydes and ketones are generated through normal and pathogenic metabolism[169] and specific conditions such as oxidative stress are prone to trigger the production of a variety of aldehydes.[170] Although oxime and hydrazone formation is not strictly bioorthogonal, it can be effectively bioorthogonal if highly reactive electrophiles and aldehydes/ketones are only present at low concentration.

The rates of hydrazone and oxime formation have been widely regarded as slow compared with modern biofunctionalization chemistries such as strain-promoted cycloaddition reactions (see below). However, due to recent studies, new mechanistic insight into substrate reactivity and catalysis has led to identification of reactant features that considerably enhance kinetics. Moreover, most natural products have a readily oxidizable alcohol group, a carboxylic acid susceptible to reduction or directly a keto (and less commonly, aldehyde) moiety. The main drawback of working with aldehydes is the ease of oxidation. This detriment has been partially solved with the use of aldehydes bearing trapping groups nearby, resulting in stable conjugates and, in some cases, with very rapid formation rates.

1.3.9.1 Functionalization of biomolecules with alkoxyamines, hydrazide and hydrazine moieties

The ease of introduction of precursors, reaction and overall applicability has produced a wide range of bioconjugation examples in the literature.[171] The introduction of α-nucleophiles into biomolecules is usually limited to synthetic nucleic acids[172] and peptides.[173] Regarding peptides, the hydrazide moiety can easily be formed by cleaving the respective solid support from the Wang resin with hydrazine (**1.111**, **Scheme 1.24**).[174] Alternatively, the peptidyl hydrazide **1.110** can be obtained directly from the corresponding supports **1.112**[175] or **1.113**[176] either photolytically or under acidic conditions, respectively.

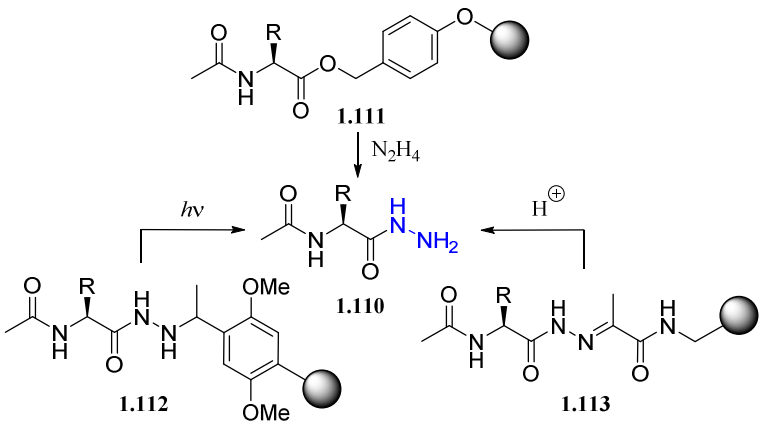

Scheme 1.24 Synthesis of hydrazide-modified peptides (**1.110**) *via* cleavage of resins **1.111-1.113**.

One the other hand, *N*-terminal derivatized peptides can be obtained using *N,N,N'*-tris(boc)hydrazinoacetic acid (**1.114**),[177] *N*-Boc-protected 2-(aminooxy)acetic acid (**1.115**) and 2-(1-ethoxyethylideneaminooxy)acetic acid (**1.116**)[178] for the last coupling step (**Figure 1.16**). Moreover, unnatural amino acids have been synthesized to generate peptides with internal α-nucleophiles.[179,180]

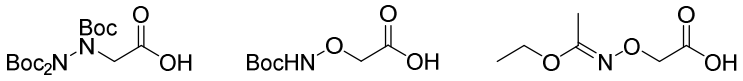

1.114 **1.115** **1.116**

Figure 1.16 Example of Boc-protected hydrazine- and aminoxy- containing carboxylic acids.

1.3.9.2 Functionalization of biomolecules with aldehyde or ketone moieties

Most biomolecules can be readily functionalized with aldehyde or ketone moieties.[181] An old but still widely used methodology for the functionalization of biomolecules with aldehyde groups is the oxidative cleavage of vicinal diols with sodium periodate (**Scheme 1.25**).[182]

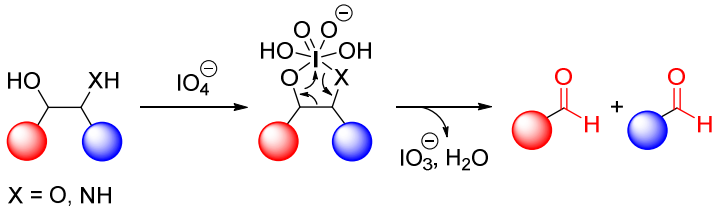

Scheme 1.25 Periodate-mediated oxidative cleavage of vicinal diols or 1,2-aminoalcohols.

This strategy has been used for the easy and selective introduction of aldehyde groups in peptides containing *N*-terminal serine or threonine residues[183] or as an extension, unnatural amino acids[184,185]

In the oligonucleotide counterpart, aside from the classical periodate-mediated aldehyde formation at either 5', 3' or internal position other strategies have been employed. The most common alternative is making use stable formyl-containing nucleoside derivatives and incorporation either enzymatically by means of the triphosphate derivative (**1.117**)[172] or by phosphoramidite chemistry (**1.118**, **Figure 1.17**) *via* SPONS.[186]

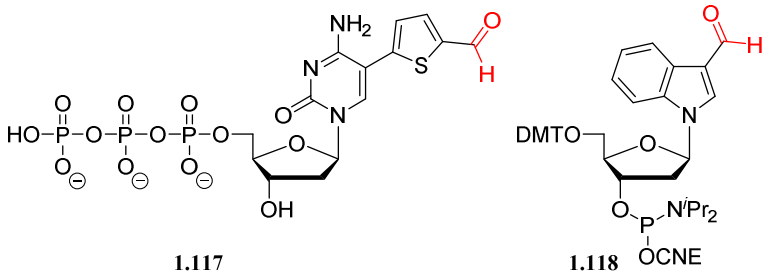

1.117 **1.118**

Figure 1.17 Examples of formyl-containing nucleoside derivatives.

Despite this, in modern bioconjugation techniques, the oxime and hydrazone ligation is being overshadowed by other methodologies, usually exploiting strain-promotion such as in SPAAC or IEDDA reactions (see **1.3.2** and **1.3.4** respectively).

1.4 Comparison between the different bioconjugation methodologies here described

It is true that, among the several conjugation strategies here discussed, several stand out due to their ease, wide applications and overall usefulness. In order to complete the picture to this fact, a brief comparison between all described bioconjugation methodologies will be provided below in **Table 1.1**.

In regards to the rate constant, it is important to keep in mind that the working concentrations of solutions of large molecules are dramatically lower than those typically encountered in classical organic and medicinal chemistry, that is in small molecule reactions. For example, while a 1 mg mL^{-1} solution of a 300 Da drug intermediate has a concentration of 3.3 mM, which is considered to be extremely dilute for a typical organic transformation, the same 1 mg mL^{-1} solution of a 150 kDa is only 6.6 μM. Stoichiometric conjugation reactions of large molecules typically operate in the micromolar regime, necessitating second-order rate constants above 1 $M^{-1}s^{-1}$ for acceptable conversion and larger than 10 $M^{-1}s^{-1}$ for complete conversions. That is why the most advantageous reactions in regards to kinetics are the IEDDA, the Michael-addition and CuAAC, followed by the photoclick cycloadditions.

Reaction	Rate constant ($M^{-1}s^{-1}$)	Chemoselectivity	Comments
CuAAC	~ 10–100 [187]	+	· Stoichiometric amount of Cu(I) necessary and cysteines prone to oxidation by copper traces
SPAAC	~ 10^{-2}–1 [188]	+	· Steric hinderance due to large alkyne dienophiles. Also, possible reactions of strained alkynes with thiols
SPNAC	~ 1–60 [188]	+	· Poor stability of reactive species · Possible reactions with thiols
DA	~ 10^{-2}–10^{-1} [95]	+	· Partially incompatible with thiols
IEEDA	~ 1–10^{6} [189]	+	· Poor stability of tetrazines · Difficult synthesis of reacting partners
Photoclick	~ 10–60 [190]	+	· Use of highly energetic light
Staudinger	~ 10^{-3} [191]	–	· Not chemoselective · Phosphine prone to oxidation
Thia-Michael	~ 700 [192]	+	· Poor stability of *N*-aryl substituted maleimide and ligation products
Oxime and hydrazone ligation	~ 10^{-4}–10^{3} [193]	+	· Poor stability of oxyamine and ligation product

Table 1.1 Examples of bioconjugation reactions, and comments on the problems associated.

1.5 Abbreviations

ΔG	Gibbs free energy
Ac	Acetyl
ACN	Acetonitrile
Bn	Benzyl
Boc	*tert*-Butyloxycarbonyl
BTTES	Bis(*tert*-butyltriazoly)ethylsulfonic acid
Bz	Benzoyl
CNE	2-Cyanoethyl
CuAAC	Copper(I)-catalyzed azide-alkyne cycloaddition
DA	Diels-Alder cycloaddition
DCM	Dichloromethane
DDQ	2,3-Dichloro-5,6-dicyano-1,4-benzoquinone
DIBAL-H	Diisobutylaluminium hydride
DIBO	Dibenzoannulated cyclooctynes
DMSO	Dimethyl sulfoxide
DMT	4,4'-Dimethoxytrityl
DNA	Deoxyribonucleic acid
d-TCO	*cis*-Dioxolane-*trans*-Cyclooctene
DTT	Dithiothreitol
EDG	Electron donating group
Et	Ethyl
Et_2O	Diethyl ether
EWG	Electron withdrawing group
FDA	Food and drug administration
GSH	Glutathione
H-bond	Hydrogen bond
HOMO	Highest occupied molecular orbital
IEDDA	Inverse electron-demand Diels-Alder cycloaddition
^{i}Pr	Isopropyl
LNA	Locked nucleic acids
LUMO	Lowest unoccupied molecular orbital
mCP	1-Methylcyclopropene
Me	Methyl
MeOH	Methanol
MOE	2-Methyoxyethyl
NaAsc	Sodium ascorbate
NBS	*N*-Bromosuccinimide
NCS	*N*-Chlorosuccinimide
NEt_3	Triethylamine
PBS	Phosphate-buffered saline
PET	Positron emission tomography
Ph	Phenyl

PIDA	(Diacetoxyiodo)benzene
PMO	Phosphorodiamidate morpholino oligomers
PNA	Peptide nucleic acid
PS	Phosphorothioate
rDA	retro-Diels-Alder cycloaddition
RNA	Ribonucleic acid
RNAse H	Ribonuclease H
ROS	Reactive oxygen species
SPAAC	Strain-promoted azide-alkyne cycloaddition
SPNAC	Strain-promoted nitrile-oxide-alkyne cycloaddition
SPONS	Solid-phase oligonucleotide synthesis
SPPS	Solid-phase peptide synthesis
tAB	Trastuzumab monoclonal antibody
TBTA	Tris(benzyltriazolylmethyl)amine
TCEP	Tris(2-carboxyethyl)phosphine
TCO	*trans*-Cyclooctene
TMS	Trimethylsilyl
tRNA	Transfer ribonucleic acid
Tz	1,2,4,5-Tetrazine
UV-Vis	Ultraviolet-visible spectroscopy
vcMMAE	Valine-citrulline-monomethyl-auristatin-E
β-ME	2-Mercaptoethanol

1.6 Bibliography

(1) Soleymani, T.; Vassantachart, J. M.; Wu, J. J. *J. Drugs Dermatol.* **2016**, *15* (3), 293–301.

(2) Figueras, E.; Martins, A.; Borbély, A.; Le Joncour, V.; Cordella, P.; Perego, R.; Modena, D.; Pagani, P.; Esposito, S.; Auciello, G.; et al. *Pharmaceutics* **2019**, *11* (5), 220.

(3) Rabanal, F.; Cajal, Y. *Nat. Prod. Rep.* **2017**, *34* (7), 886–908.

(4) Pardi, N.; Hogan, M. J.; Porter, F. W.; Weissman, D. *Nat. Rev. Drug Discov.* **2018**, *17* (4), 261–279.

(5) Jimenez, V.; Jambrina, C.; Casana, E.; Sacristan, V.; Muñoz, S.; Darriba, S.; Rodó, J.; Mallol, C.; Garcia, M.; León, X.; et al. *EMBO Mol. Med.* **2018**, *10* (8), e8791.

(6) Angelbello, A. J.; Chen, J. L.; Childs-Disney, J. L.; Zhang, P.; Wang, Z. F.; Disney, M. D. *Chem. Rev.* **2018**, *118* (4), 1599–1663.

(7) Beck, A.; Goetsch, L.; Dumontet, C.; Corvaïa, N. *Nat. Rev. Drug Discov.* **2017**, *16* (5), 315–337.

(8) Uhlmann, E.; Peyman, A. *Chem. Rev.* **1990**, *90* (4), 543–584.

(9) Eckstein, F. *Nucleic Acid Ther.* **2014**, *24* (6), 374–387.

(10) Partridge, T. A.; Rosenfeld, J.; Lou, F.; Wilton, S. D.; Lu, Q. L.; Rabinowitz, A.; Alter, J.; Yin, H. *Nat. Med.* **2006**, *12* (2), 175–177.

(11) Nielsen, P.; Egholm, M.; Berg, R.; Buchardt, O. *Science (80-.).* **1991**, *254* (5037), 1497–1500.

(12) Altona, C.; Sundaralingam, M. *J. Am. Chem. Soc.* **1972**, *94* (23), 8205–8212.

(13) Robbins, M.; Judge, A.; Liang, L.; McClintock, K.; Yaworski, E.; MacLachlan, I. *Mol. Ther.* **2007**, *15* (9), 1663–1669.

(14) Wan, W. B.; Seth, P. P. *J. Med. Chem.* **2016**, *59* (21), 9645–9667.

(15) Ren, J.; Zhu, X.; Xu, P.; Li, R.; Fu, Y.; Dong, S.; Zhangsun, D.; Wu, Y.; Luo, S. *Mar. Drugs* **2019**, *17* (3), 142.

(16) Nielsen, D. S.; Shepherd, N. E.; Xu, W.; Lucke, A. J.; Stoermer, M. J.; Fairlie, D. P. *Chem. Rev.* **2017**, *117* (12), 8094–8128.

(17) Zuckermann, R. N.; Kerr, J. M.; Moosf, W. H.; Kent, S. B. H. *J. Am. Chem. Soc.* **1992**, *114* (26), 10646–10647.

(18) Tan, S. Y.; Grimes, S. *Singapore Med. J.* **2010**, *51* (11), 842–843.

(19) Kolb, H. C.; Finn, M. G.; Sharpless, K. B. *Angew. Chemie Int. Ed.* **2001**, *40* (11), 2004–2021.

(20) Huisgen, R. *Pure Appl. Chem.* **1989**, *61* (4), 613–628.

(21) Huisgen, R.; Szeimies, G.; Möbius, L. *Chem. Ber.* **1967**, *100*, 2494–2507.

(22) Tornøe, C. W.; Meldal, M. In *Proc Am Pept Symp*; American Peptide Society and Kluwer Academic Publisher: San Diego, 2001; pp 263–264.

(23) Meldal, M.; Tornoee, C. W. *Chem. Rev.* **2008**, *108* (8), 2952–3015.

(24) El-Sagheer, A. H.; Brown, T. *Chem. Soc. Rev.* **2010**, *39* (4), 1388–1405.

(25) Astakhova, I. K.; Wengel, J. *Chem. - A Eur. J.* **2013**, *19* (3), 1112–1122.

(26) Tolle, F.; Rosenthal, M.; Pfeiffer, F.; Mayer, G. *Bioconjug. Chem.* **2016**, *27* (3), 500–503.

(27) Gramlich, P. M. E.; Wirges, C. T.; Manetto, A.; Carell, T. *Angew. Chemie - Int. Ed.* **2008**, *47* (44), 8350–8358.

(28) Fauster, K.; Hartl, M.; Santner, T.; Aigner, M.; Kreutz, C.; Bister, K.; Ennifar, E.; Micura, R. *ACS Chem. Biol.* **2012**, *7* (3), 581–589.

(29) Aigner, M.; Hartl, M.; Fauster, K.; Steger, J.; Bister, K.; Micura, R. *ChemBioChem* **2011**, *12*, 47–51.

(30) Beyer, C.; Wagenknecht, H. A. *Chem. Commun.* **2010**, *46* (13), 2230–2231.

(31) Weisbrod, S. H.; Marx, A. *Chem. Commun.* **2007**, No. 18, 1828–1830.

(32) Fomich, M. A.; Kvach, M. V.; Navakouski, M. J.; Weise, C.; Baranovsky, A. V.; Korshun, V. A.; Shmanai, V. V. *Org. Lett.* **2014**, *16* (17), 4590–4593.

(33) Inesi, G. *IUBMB Life* **2017**, *69* (4), 211–217.

(34) Shangari, N.; Chan, T. S.; Chan, K.; Wu, S. H.; O'Brien, P. J. *Mol. Nutr. Food Res.* **2007**, *51* (4), 445–455.

(35) Link, A. J.; Vink, M. K.; Tirrell, D. A. *J. Am. Chem. Soc.* **2004**, *126* (34), 10598–10602.

(36) Lin, S.; Zhang, Z.; Xu, H.; Li, L.; Chen, S.; Li, J.; Hao, Z.; Chen, P. R. *J. Am. Chem. Soc.* **2011**, *133* (50), 20581–20587.

(37) Ge, Y.; Fan, X.; Chen, P. R. *Chem. Sci.* **2016**, *7* (12), 7055–7060.

(38) Beatty, K. E.; Liu, J. C.; Xie, F.; Dieterich, D. C.; Schuman, E. M.; Wang, Q.; Tirrell, D. A. *Angew. Chemie - Int. Ed.* **2006**, *45* (44), 7364–7367.

(39) Beatty, K. E.; Xie, F.; Wang, Q.; Tirrell, D. A. *J. Am. Chem. Soc.* **2005**, *127* (41), 14150–14151.

(40) Rajendran, V.; Kalita, P.; Shukla, H.; Kumar, A.; Tripathi, T. *Int. J. Biol. Macromol.* **2018**, *111*, 400–414.

(41) Hong, V.; Steinmetz, N. F.; Manchester, M.; Finn, M. G. *Bioconjugate chem.* **2010**, *21* (10),

1912–1916.

(42) Yang, M.; Li, J.; Chen, P. R. *Chem. Soc. Rev.* **2014**, *43* (18), 6511–6526.

(43) Kennedy, D. C.; McKay, C. S.; Legault, M. C. B.; Danielson, D. C.; Blake, J. A.; Pegoraro, A. F.; Stolow, A.; Mester, Z.; Pezacki, J. P. *J. Am. Chem. Soc.* **2011**, *133* (44), 17993–18001.

(44) Nairn, N. W.; Bariola, P. A.; Graddis, T. J.; VanBrunt, M. P.; Wang, A.; Li, G.; Grabstein, K. *Bioconjug. Chem.* **2015**, *26* (10), 2070–2075.

(45) Hong, V.; Presolski, S. I.; Ma, C.; Finn, M. G. *Angew. Chemie - Int. Ed.* **2009**, *48* (52), 9879–9883.

(46) Henriksson, A.; Friedbacher, G.; Hoffmann, H. *Langmuir* **2011**, *27* (12), 7345–7348.

(47) Remzi Becer, C.; Hoogenboom, R.; Schubert, U. S. *Angew. Chemie - Int. Ed.* **2009**, *48* (27), 4900–4908.

(48) Manova, R.; Vanbeek, T. A.; Zuilhof, H. *Angew. Chemie - Int. Ed.* **2011**, *50* (24), 5428–5430.

(49) Agard, N. J.; Prescher, J. A.; Bertozzi, C. R. *J. Am. Chem. Soc.* **2004**, *126* (46), 15046–15047.

(50) Bertozzi, C. R.; Saxon, E. *Science (80-.).* **2000**, *287* (2000), 2007–2010.

(51) Ning, X.; Guo, J.; Wolfert, M. A.; Boons, G. J. *Angew. Chemie - Int. Ed.* **2008**, *47* (12), 2253–2255.

(52) Zimmerman, E. S.; Heibeck, T. H.; Gill, A.; Li, X.; Murray, C. J.; Madlansacay, M. R.; Tran, C.; Uter, N. T.; Yin, G.; Rivers, P. J.; et al. *Bioconjug. Chem.* **2014**, *25* (2), 351–361.

(53) Khoury, G. A.; Baliban, R. C.; Floudas, C. A. *Sci. Rep.* **2014**, *1*, 1–5.

(54) Zou, Y.; Yin, J. *Bioorganic Med. Chem. Lett.* **2008**, *18* (20), 5664–5667.

(55) Van Delft, P.; Meeuwenoord, N. J.; Hoogendoorn, S.; Dinkelaar, J.; Overkleeft, H. S.; Van Der Marel, G. A.; Filippov, D. V. *Org. Lett.* **2010**, *12* (23), 5486–5489.

(56) Pasinszki, T.; Hajgató, B.; Havasi, B.; Westwood, N. P. C. *Phys. Chem. Chem. Phys.* **2009**, *11* (26), 5263–5272.

(57) Feuer, H. *Nitrile Oxides, Nitrones, and Nitronates in Organic Synthesis : Novel Strategies in Synthesis*; Wiley-Interscience, 2008.

(58) Pinho e Melo, T. *Curr. Org. Chem.* **2005**, *9* (10), 925–958.

(59) Karthick, C.; Nithiyanandan, S.; Essa, M. M.; Guillemin, G. J.; Jayachandran, S. K.; Anusuyadevi, M. *Neurol. Res.* **2018**, *00* (00), 1–12.

(60) Roscales, S.; Bechmann, N.; Weiss, D. H.; Köckerling, M.; Pietzsch, J.; Kniess, T. *Medchemcomm* **2018**, *9* (3), 534–544.

(61) Kirihara, M.; Yamamoto, J.; Noguchi, T.; Hirai, Y. *Tetrahedron Lett.* **2009**, *50* (11), 1180–1183.

(62) Gutsmiedl, K.; Wirges, C. T.; Ehmke, V.; Carell, T. *Org. Lett.* **2009**, *11* (11), 2405–2408.

(63) Lim, S. T.; Kim, E.-M.; Jadhav, V. H.; Lee, S. B.; Jeong, H.-J.; Kim, D. W.; Sachin, K.; Kim, H. L.; Sohn, M.-H. *Bioconjug. Chem.* **2012**, *23* (8), 1680–1686.

(64) Jadhav, S.; Käkelä, M.; Mäkilä, J.; Kiugel, M.; Liljenbäck, H.; Virta, J.; Poijärvi-Virta, P.; Laitala-Leinonen, T.; Kytö, V.; Jalkanen, S.; et al. *Bioconjug. Chem.* **2016**, *27* (2), 391–403.

(65) Tian, H.; Sakmar, T. P.; Huber, T. *Chem. Commun.* **2016**, *52* (31), 5451–5454.

(66) Nicolaou, K. C.; Snyder, S. A.; Montagnon, T.; Vassilikogiannakis, G. *Angew. Chemie Int. Ed.* **2002**, *41* (10), 1668–1698.

(67) Khan, N. I.; Halder, S.; Gunjan, S. B.; Prasad, T. *IOP Conf. Ser. Mater. Sci. Eng.* **2018**, *377* (1).

(68) Hou, I. C. Y.; Hu, Y.; Narita, A.; Müllen, K. *Polym. J.* **2018**, *50* (1), 3–20.

(69) Borsenberger, V.; Howorka, S. *Nucleic Acids Res.* **2009**, *37* (5), 1477–1485.

(70) Li, F.; Li, X.; Zhang, X. *Org. Biomol. Chem.* **2018**, *16* (42), 7871–7877.

(71) Sánchez, A.; Pedroso, E.; Grandas, A. *Org. Lett.* **2011**, *13* (16), 4364–4367.

(72) Marchán, V.; Ortega, S.; Pulido, D.; Pedroso, E.; Grandas, A. *Nucleic Acids Res.* **2006**, *34* (3).

(73) Sauer, J.; Lang, D.; Mielert, A. *Angew. Chemie Int. Ed. English* **1962**, *1* (5), 268–269.

(74) Liu, Q.; Cheng, L. J.; Wang, K. *RSC Adv.* **2017**, *7* (49), 30618–30625.

(75) Pardo, L.; Branchadell, V.; Oliva, A.; Bertrán, J. *J. Mol. Struct.* **1983**, *93*, 255–260.

(76) Sandoval-Sus, J. D.; Brahim, A.; Khan, A.; Raphael, B.; Ansari-Lari, A.; Ruiz, M. *Int. J. Hematol.* **2019**, *109* (5), 622–626.

(77) Invernizzi, M.; Michelotti, A.; Noale, M.; Lopez, G.; Runza, L.; Giroda, M.; Despini, L.; Blundo, C.; Maggi, S.; Gambini, D.; et al. *J. Clin. Med.* **2019**, *8* (2), 138.

(78) Mironov, V. A.; Sobolev, E. V.; Elizarova, A. N. *Tetrahedron* **1963**, *19* (12), 1939–1958.

(79) Liu, S.; Hassink, M.; Selvaraj, R.; Yap, L.-P.; Park, R.; Wang, H.; Chen, X.; Fox, J. M.; Li, Z.; Conti, P. S. *Mol. Imaging* **2013**, *12* (2), 121–128.

(80) Peng, T.; Hang, H. C. *J. Am. Chem. Soc.* **2016**, *138* (43), 14423–14433.

(81) Eggert, F.; Kulikov, K.; Domnick, C.; Leifels, P.; Kath-Schorr, S. *Methods* **2017**, *120*, 17–27.

(82) Keinänen, O.; Fung, K.; Pourat, J.; Jallinoja, V.; Vivier, D.; Pillarsetty, N. K.; Airaksinen, A. J.; Lewis, J. S.; Zeglis, B. M.; Sarparanta, M. *EJNMMI Res.* **2017**, *7* (1), 95.

(83) Oliveira, B. L.; Guo, Z.; Boutureira, O.; Guerreiro, A.; Jiménez-Osés, G.; Bernardes, G. J. L. *Angew. Chemie - Int. Ed.* **2016**, *55* (47), 14683–14687.

(84) Selvaraj, R.; Fox, J. M. *Tetrahedron Lett.* **2014**, *55* (34), 4795–4797.

(85) Li, C.; Ge, H.; Yin, B.; She, M.; Liu, P.; Li, X.; Li, J. *RSC Adv.* **2015**, *5* (16), 12277–12286.

(86) Carboni, R. A.; Lindsey, R. V. *J. Am. Chem. Soc.* **1959**, *81* (16), 4342–4346.

(87) Karver, M. R.; Weissleder, R.; Hilderbrand, S. A. *Bioconjug. Chem.* **2011**, *22* (11), 2263–2270.

(88) Jain, S.; Neumann, K.; Zhang, Y.; Geng, J.; Bradley, M. *Macromolecules* **2016**, *49* (15), 5438–5443.

(89) Thalhammer, F.; Wallfahrer, U.; Sauer, J. *Tetrahedron Lett.* **1990**, *31* (47), 6851–6854.

(90) Sauer, J.; Heldmann, D. K.; Hetzenegger, J.; Krauthan, J.; Sichert, H.; Schuster, J. *European J. Org. Chem.* **1998**, *1998* (12), 2885–2896.

(91) Li, J.; Jia, S.; Chen, P. R. *Nat. Chem. Biol.* **2014**, *10* (12), 1003–1005.

(92) Vrabel, M.; Kölle, P.; Brunner, K. M.; Gattner, M. J.; López-Carrillo, V.; de Vivie-Riedle, R.; Carell, T. *Chem. - A Eur. J.* **2013**, *19* (40), 13309–13312.

(93) Darko, A.; Wallace, S.; Dmitrenko, O.; Machovina, M. M.; Mehl, R. A.; Chin, J. W.; Fox, J. M. *Chem. Sci.* **2014**, *5* (10), 3770–3776.

(94) Balcar, J.; Chrisam, G.; Huber, F. X.; Sauer, J. *Tetrahedron Lett.* **1983**, *24* (14), 1481–1484.

(95) Meijer, A.; Otto, S.; Engberts, J. B. F. N. *J. Org. Chem.* **1998**, *63* (24), 8989–8994.

(96) Lang, K.; Davis, L.; Torres-Kolbus, J.; Chou, C.; Deiters, A.; Chin, J. W. *Nat. Chem.* **2012**, *4* (4), 298–304.

(97) Knall, A. C.; Hollauf, M.; Saf, R.; Slugovc, C. *Org. Biomol. Chem.* **2016**, *14* (45), 10576–10580.

(98) Karaki, F.; Ohgane, K.; Imai, H.; Itoh, K.; Fujii, H. *European J. Org. Chem.* **2017**, *2017* (26), 3815–3829.

(99) Adams, R.; Clarke, H. T.; Conant, J. B.; Kamm, O. *Org. Synth.* **1969**, *49*, 39–43.

(100) Vedejs, E.; Fuchs, P. L. *J. Am. Chem. Soc.* **1971**, *93* (16), 4070–4072.

(101) Tsuneishi, H.; Hakushi, T.; Inoue, Y. *J. Chem. Soc. Perkin Trans. 2* **1996**, *0* (8), 1601.

(102) Royzen, M.; Yap, G. P. A.; Fox, J. M. *J. Am. Chem. Soc.* **2008**, *130* (12), 3760–3761.

(103) Yang, J.; Šečkute, J.; Cole, C. M.; Devaraj, N. K. *Angew. Chemie - Int. Ed.* **2012**, *51* (30), 7476–7479.

(104) Kamber, D. N.; Nazarova, L. A.; Liang, Y.; Lopez, S. A.; Patterson, D. M.; Shih, H. W.; Houk, K. N.; Prescher, J. A. *J. Am. Chem. Soc.* **2013**, *135* (37), 13680–13683.

(105) Patterson, D. M.; Nazarova, L. A.; Xie, B.; Kamber, D. N.; Prescher, J. A. *J. Am. Chem. Soc.* **2012**, *134* (45), 18638–18643.

(106) Li, Z.; Hao, P.; Li, L.; Tan, C. Y. J.; Cheng, X.; Chen, G. Y. J.; Sze, S. K.; Shen, H. M.; Yao, S. Q. *Angew. Chemie - Int. Ed.* **2013**, *52* (33), 8551–8556.

(107) Hong, S.; Carlson, J.; Lee, H.; Weissleder, R. *Adv. Healthc. Mater.* **2016**, *5* (4), 421–426.

(108) Keinänen, O.; Mäkilä, E. M.; Lindgren, R.; Virtanen, H.; Liljenbäck, H.; Oikonen, V.; Sarparanta, M.; Molthoff, C.; Windhorst, A. D.; Roivainen, A.; et al. *ACS Omega* **2017**, *2* (1), 62–69.

(109) Šečkutė, J.; Yang, J.; Devaraj, N. K. *Nucleic Acids Res.* **2013**, *41* (15), e148–e148.

(110) Wu, H.; Alexander, S. C.; Jin, S.; Devaraj, N. K. *J. Am. Chem. Soc.* **2016**, *138* (36), 11429–11432.

(111) Van Der Gracht, A. M. F.; De Geus, M. A. R.; Camps, M. G. M.; Ruckwardt, T. J.; Sarris, A. J. C.; Bremmers, J.; Maurits, E.; Pawlak, J. B.; Posthoorn, M. M.; Bonger, K. M.; et al. *ACS Chem. Biol.* **2018**, *13* (6), 1569–1576.

(112) Khan, I.; Agris, P. F.; Yigit, M. V.; Royzen, M. *Chem. Commun.* **2016**, *52* (36), 6174–6177.

(113) Wang, K.; Sachdeva, A.; Cox, D. J.; Wilf, N. W.; Lang, K.; Wallace, S.; Mehl, R. A.; Chin, J. W. *Nat. Chem.* **2014**, *6* (5), 393–403.

(114) Herner, A.; Lin, Q. *Top. Curr. Chem.* **2016**, *374* (1), 1.

(115) Clovis, J. S.; Eckell, A.; Huisgen, R.; Sustmann, R. *Chem. Ber.* **1967**, *100* (1), 60–70.

(116) Lohse, V.; Leihkauf, P.; Csongar, C.; Tomaschewski, G. *J. für Prakt. Chemie* **1988**, *330* (3), 406–414.

(117) Molteni, G.; Orlandi, M.; Broggini, G. *J. Chem. Soc. Perkin Trans. 1* **2000**, No. 22, 3742–3745.

(118) Yu, Z.; Ohulchanskyy, T. Y.; An, P.; Prasad, P. N.; Lin, Q. *J. Am. Chem. Soc.* **2013**, *135* (45), 16766–16769.

(119) Arndt, S.; Wagenknecht, H. A. *Angew. Chemie - Int. Ed.* **2014**, *53* (52), 14580–14582.

(120) Padwa, A.; Smolanoff, J. *J. Am. Chem. Soc.* **1971**, *93* (2), 548–550.

(121) Lim, R. K. V; Lin, Q. *Chem. Commun.* **2010**, *46* (42), 7993–7995.

(122) Hegarty, A. F.; Eustace, S. J.; Tynan, N. M.; Pham-Tran, N.-N.; Nguyen, M. T. *J. Chem. Soc. Perkin Trans. 2* **2001**, No. 7, 1239–1246.

(123) Mueller, J. O.; Schmidt, F. G.; Blinco, J. P.; Barner-Kowollik, C. *Angew. Chemie Int. Ed.* **2015**, *54* (35), 10284–10288.

(124) Hopkins, S. L.; Siewert, B.; Askes, S. H. C.; Veldhuizen, P.; Zwier, R.; Heger, M.; Bonnet, S. *Photochem. Photobiol. Sci.* **2016**, *15* (5), 644–653.

(125) Setlow, P.; Li, L. *Photochem. Photobiol.* **2015**, *91* (6), 1263–1290.

(126) Vatansever, F.; Hamblin, M. R. *Photonics Lasers Med.* **2012**, *1* (4), 255–266.

(127) Shui, S.; Wang, X.; Chiang, J. Y.; Zheng, L. *Exp. Biol. Med.* **2015**, *240* (10), 1257–1265.

(128) Saxon, E.; Luchansky, S. J.; Hang, H. C.; Yu, C.; Lee, S. C.; Bertozzi, C. R. *J. Am. Chem. Soc.* **2002**, *124* (50), 14893–14902.

(129) Saxon, E.; Armstrong, J. I.; Bertozzi, C. R. *Org. Lett.* **2000**, *2* (14), 2141–2143.

(130) Nilsson, B. L.; Kiessling, L. L.; Raines, R. T. *Org. Lett.* **2000**, *2* (13), 1939–1941.

(131) Soellner, M. B.; Nilsson, B. L.; Raines, R. T. *J. Am. Chem. Soc.* **2006**, *128* (27), 8820–8828.

(132) Agard, N. J.; Baskin, J. M.; Prescher, J. A.; Lo, A.; Bertozzi, C. R. *ACS Chem. Biol.* **2006**, *1* (10), 644–648.

(133) Pötzsch, R.; Fleischmann, S.; Tock, C.; Komber, H.; Voit, B. I. *Macromolecules* **2011**, *44* (9), 3260–3269.

(134) Liu, G.; Link, J. T.; Pei, Z.; Reilly, E. B.; Leitza, S.; Nguyen, B.; Marsh, K. C.; Okasinski, G. F.; Von Geldern, T. W.; Ormes, M.; et al. *J. Med. Chem.* **2000**, *43* (21), 4025–4040.

(135) Dunbar, K. L.; Scharf, D. H.; Litomska, A.; Hertweck, C. *Chem. Rev.* **2017**, *117* (8), 5521–5577.

(136) Yang, D. J.; Chen, B. *J. Agric. Food Chem.* **2009**, *57* (8), 3022–3027.

(137) Alswieleh, A. M.; Cheng, N.; Canton, I.; Ustbas, B.; Xue, X.; Ladmiral, V.; Xia, S.; Ducker, R. E.; El Zubir, O.; Cartron, M. L.; et al. *J. Am. Chem. Soc.* **2014**, *136* (26), 9404–9413.

(138) Jackson, P. A.; Widen, J. C.; Harki, D. A.; Brummond, K. M. *J. Med. Chem.* **2017**, *60* (3), 839–885.

(139) Khatik, G. L.; Kumar, R.; Chakraborti, A. K. *Org. Lett.* **2006**, *8* (11), 2433–2436.

(140) Renault, K.; Fredy, J. W.; Renard, P. Y.; Sabot, C. *Bioconjug. Chem.* **2018**, *29* (8), 2497–2513.

(141) Wadhwa, P.; Kharbanda, A.; Sharma, A. *Asian J. Org. Chem.* **2018**, *7* (4), 634–661.

(142) Veronese, F. M. *Biomaterials* **2001**, *22* (5), 405–417.

(143) Sánchez, A.; Pedroso, E.; Grandas, A. *Org. Biomol. Chem.* **2012**, *10* (42), 8478.

(144) Joubert, N.; Denevault-Sabourin, C.; Bryden, F.; Viaud-Massuard, M. C. *Eur. J. Med. Chem.* **2017**, *142*, 393–415.

(145) Office of the Commissioner. Press Announcements - FDA expands approval of Adcetris for first-line treatment of Stage III or IV classical Hodgkin lymphoma in combination with chemotherapy https://www.fda.gov/NewsEvents/Newsroom/PressAnnouncements/ucm601935.htm (accessed Jan 23, 2019).

(146) Research, C. for D. E. and. Postmarket Drug Safety Information for Patients and Providers - Brentuximab Vedotin (marketed as Adcetris) Information https://www.fda.gov/Drugs/DrugSafety/PostmarketDrugSafetyInformationforPatientsandProviders/ucm287672.htm (accessed Jan 23, 2019).

(147) Verma, S.; Miles, D.; Gianni, L.; Krop, I. E.; Welslau, M.; Baselga, J.; Pegram, M.; Oh, D.-Y.; Diéras, V.; Guardino, E.; et al. *N. Engl. J. Med.* **2012**, *367* (19), 1783–1791.

(148) Press Announcements - FDA approves new treatment for late-stage breast cancer https://wayback.archive-it.org/7993/20170112023904/http://www.fda.gov/NewsEvents/Newsroom/PressAnnouncements/ucm340704.htm (accessed Jan 23, 2019).

(149) Hermanson, G. T. *Bioconjugate Techniques*; Elsevier Academic Press, 2008.

(150) Christie, R. J.; Fleming, R.; Bezabeh, B.; Woods, R.; Mao, S.; Harper, J.; Joseph, A.; Wang, Q.; Xu, Z. Q.; Wu, H.; et al. *J. Control. Release* **2015**, *220*, 660–670.

(151) Fontaine, S. D.; Reid, R.; Robinson, L.; Ashley, G. W.; Santi, D. V. *Bioconjug. Chem.* **2015**, *26* (1), 145–152.

(152) Tedaldi, L. M.; Smith, M. E. B.; Nathani, R. I.; Baker, J. R. *Chem. Commun.* **2009**, No. 43, 6583–6585.

(153) Marculescu, C.; Kossen, H.; Morgan, R. E.; Mayer, P.; Fletcher, S. A.; Tolner, B.; Chester, K. A.; Jones, L. H.; Baker, J. R. *Chem. Commun.* **2014**, *50* (54), 7139–7142.

(154) Brocchini, S.; Godwin, A.; Balan, S.; Choi, J. won; Zloh, M.; Shaunak, S. *Adv. Drug Deliv. Rev.* **2008**, *60* (1), 3–12.

(155) Bernardes, G. J. L.; Steiner, M.; Hartmann, I.; Neri, D.; Casi, G. *Nat. Protoc.* **2013**, *8* (11), 2079–2089.

(156) Jbara, M.; Maity, S. K.; Seenaiah, M.; Brik, A. *J. Am. Chem. Soc.* **2016**, *138* (15), 5069–5075.

(157) Zipperer, A.; Konnerth, M. C.; Laux, C.; Berscheid, A.; Janek, D.; Weidenmaier, C.; Burian, M.; Schilling, N. A.; Slavetinsky, C.; Marschal, M.; et al. *Nature* **2016**, *535* (7613), 511–516.

(158) Faustino, H.; Silva, M. J. S. A.; Veiros, L. F.; Bernardes, G. J. L.; Gois, P. M. P. *Chem. Sci.* **2016**, *7* (8), 5052–5058.

(159) Jbara, M.; Laps, S.; Maity, S. K.; Brik, A. *Chem. - A Eur. J.* **2016**, *22* (42), 14851–14855.

(160) Zatsepin, T. S.; Stetsenko, D. A.; Arzumanov, A. A.; Romanova, E. A.; Gait, M. J.; Oretskaya, T. S. *Bioconjug. Chem.* **2002**, *13* (4), 822–830.

(161) Meyer, V.; Janny, A. *Berichte der Dtsch. Chem. Gesellschaft* **1882**, *15* (1), 1164–1167.

(162) Meyer, V.; Janny, A. *Berichte der Dtsch. Chem. Gesellschaft* **1882**, *15* (1), 1324–1326.

(163) Li, X. G.; Haaparanta, M.; Solin, O. *J. Fluor. Chem.* **2012**, *143*, 49–56.

(164) Lattová, E.; Perreault, H. *Mass Spectrom. Rev.* **2013**, *32* (5), 366–385.

(165) Agten, S. M.; Dawson, P. E.; Hackeng, T. M. *J. Pept. Sci.* **2016**, *22* (5), 271–279.

(166) Flor, A. C.; Williams, J. H.; Blaine, K. M.; Duggan, R. C.; Sperling, A. I.; Schwartz, D. A.; Kron, S. J. *ChemBioChem* **2014**, *15* (2), 267–275.

(167) Agten, S. M.; Suylen, D. P. L.; Hackeng, T. M. *Bioconjug. Chem.* **2016**, *27* (1), 42–46.

(168) Prudden, A. R.; Chinoy, Z. S.; Wolfert, M. A.; Boons, G. J. *Chem. Commun.* **2014**, *50* (54), 7132–7135.

(169) Yuen, L. H.; Saxena, N. S.; Park, H. S.; Weinberg, K.; Kool, E. T. *ACS Chem. Biol.* **2016**, *11* (8), 2312–2319.

(170) Mechanism, A.; Anderson, M. M.; Hazen, S. L.; Hsu, F. F.; Heinecke, J. W. *J. Clin. Invest.* **1997**, *99* (3), 424–432.

(171) Kölmel, D. K.; Kool, E. T. *Chem. Rev.* **2017**, *117* (15), 10358–10376.

(172) Raindlová, V.; Pohl, R.; Šanda, M.; Hocek, M. *Angew. Chemie - Int. Ed.* **2010**, *49* (6), 1064–1066.

(173) Ulrich, S.; Boturyn, D.; Marra, A.; Renaudet, O.; Dumy, P. *Chem. - A Eur. J.* **2014**, *20* (1), 34–41.

(174) Bello, C.; Kikul, F.; Becker, C. F. W. *J. Pept. Sci.* **2015**, *21* (3), 201–207.

(175) Qvortrup, K.; Komnatnyy, V. V.; Nielsen, T. E. *Org. Lett.* **2014**, *16* (18), 4782–4785.

(176) Chelushkin, P. S.; Polyanichko, K. V.; Leko, M. V.; Dorosh, M. Y.; Bruckdorfer, T.; Burov, S. V. *Tetrahedron Lett.* **2015**, *56* (4), 619–622.

(177) Margathe, J. F.; Iturrioz, X.; Regenass, P.; Karpenko, I. A.; Humbert, N.; De Rocquigny, H.; Hibert, M.; Llorens-Cortes, C.; Bonnet, D. *Chem. - A Eur. J.* **2016**, *22* (4), 1399–1405.

(178) Foulard, S.; Rasmussen, M. O.; Razkin, J.; Boturyn, D.; Dumy, P. *J. Org. Chem.* **2008**, *73* (3), 983–991.

(179) Itoh, Y.; Aihara, K.; Mellini, P.; Tojo, T.; Ota, Y.; Tsumoto, H.; Solomon, V. R.; Zhan, P.; Suzuki, M.; Ogasawara, D.; et al. *J. Med. Chem.* **2016**, *59* (4), 1531–1544.

(180) Haney, C. M.; Horne, W. S. *J. Pept. Sci.* **2014**, *20* (2), 108–114.

(181) Spears, R. J.; Fascione, M. A. *Org. Biomol. Chem.* **2016**, *14* (32), 7622–7638.

(182) Sudalai, A.; Khenkin, A.; Neumann, R. *Org. Biomol. Chem.* **2015**, *13* (15), 4374–4394.

(183) Chelius, D.; Shaler, T. A. *Bioconjug. Chem.* **2003**, *14* (1), 205–211.

(184) Haney, C. M.; Loch, M. T.; Horne, W. S. *Chem. Commun.* **2011**, *47* (39), 10915–10917.

(185) Amore, A.; Wals, K.; Koekoek, E.; Hoppes, R.; Toebes, M.; Schumacher, T. N. M.; Rodenko, B.; Ovaa, H. *ChemBioChem* **2013**, *14* (1), 123–131.

(186) Okamoto, A.; Tainaka, K.; Saito, I. *Tetrahedron Lett.* **2002**, *43* (26), 4581–4583.

(187) Presolski, S. I.; Hong, V.; Cho, S.-H.; Finn, M. G. *J. Am. Chem. Soc.* **2010**, *132* (41), 14570–14576.

(188) Dommerholt, J.; Rutjes, F. P. J. T.; van Delft, F. L. *Top. Curr. Chem.* **2016**, *374* (2), 16.

(189) Oliveira, B. L.; Guo, Z.; Bernardes, G. J. L. *Chem. Soc. Rev.* **2017**, *46* (16), 4895–4950.

(190) Yu, Z.; Pan, Y.; Wang, Z.; Wang, J.; Lin, Q. *Angew. Chemie - Int. Ed.* **2012**, *51* (42), 10600–10604.

(191) Van Berkel, S. S.; Van Eldijk, M. B.; Van Hest, J. C. M. *Angew. Chemie - Int. Ed.* **2011**, *50* (38), 8806–8827.

(192) Saito, F.; Noda, H.; Bode, J. W. *ACS Chem. Biol.* **2015**, *10* (4), 1026–1033.

(193) Crisalli, P.; Kool, E. T. *J. Org. Chem.* **2013**, *78* (3), 1184–1189.

Chapter 2. 2,2-Disubstituted cyclopent-4-ene-1,3-diones: simple and double conjugations

2.1 Background

As stated in the first chapter, the thia-Michael ligation (see Chapter 1, **Section 1.3.7**) is one of the most commonly used reactions for bioconjugations being the maleimide moiety the preferred Michael acceptor. It has proven useful due to the extreme specificity of maleimides for thiols, fast reaction times, lack of by-products and its overall water compatibility.[1] Despite its success, the Michael thiol-maleimide reaction is not devoid of problems.[2] The succinimide moiety formed after the reaction has taken place may undergo hydrolysis in aqueous media (**Scheme 1.17**), yielding two different isomers, and the thiol-ether linkage may be reversible in the presence of other thiols. In spite of these undesirable properties, the reaction has been widely applied in the biochemistry field due the natural presence of thiols in biomolecules such as peptides, proteins and antibodies allowing the use of these entities without modification (or after reduction of a disulfide bridge, if required) and avoiding the need to introduce an additional reactive group.[3]

When the conjugates are planned to have a therapeutic application, the desired activity may vary and toxicity increase due to premature cleavage of the drug-linker union, liberating the cytotoxic drug far from the desired targeted tissue.[4] In this regard, and considering the tremendous potential of thiol-maleimide conjugates, the development of methods that prevent thiol exchange is highly desirable.

As discussed previously, one strategy for achieving this goal is to allow conventional *N*-substituted sulfenyl-succinimide adducts to undergo ring hydrolysis to yield thiol-exchange resistant succinamic acids. This is why the development of maleimide derivatives that undergo faster ring hydrolysis to rapidly yield stable conjugates at mild temperatures is of great interest. That being said, the inherent problem of thiol exchange may not be intrinsically negative, as it can be regarded as an alternative for controlled drug release.[5]

The mechanism for thiol exchange depicted in **Scheme 2.1** occurs through the reto-Michael reaction of the conjugate (**2.6**). Regression is firmly influenced by thiol's pK_a; the more acidic the thiol, the easier the conjugate will revert.[6] Moreover, the concentration of other thiols will influence half-lives of Michael-adducts, according to Le Châtelier's principle. In practice, this implies that thiol exchange has to be taken into account virtually exclusively inside cells where concentrations of free thiols such as glutathione (GSH) and cysteines is high enough.

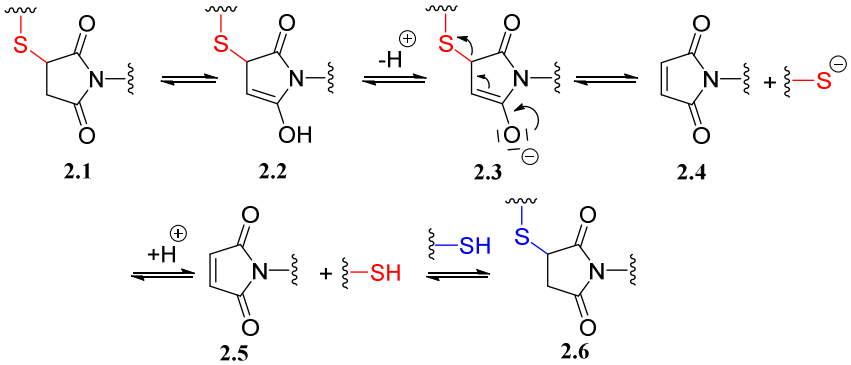

Scheme 2.1 Mechanism of the retro-Michael-type reaction yielding to thiol exchange.

In this regard and as previously discussed in the introduction of this dissertation, a novel approach to promote hydrolysis and thus stabilize the whole conjugate has been found in the use of *N*-aryl-maleimides. The use of such maleimides has proven to greatly increase the rate of hydrolysis of *N*-aryl succinimide linkages into *N*-aryl sulfenyl-succinamic acids. This fact can be rationalized on the basis

of the electronic effect provided by the additional phenyl group, allowing additional delocalization of the nitrogen lone electron pair and thus decreasing the electron density of the carbonyl carbon and rendering it more electrophilic. This facilitates the nucleophilic addition of water and provides a plausible explanation for the observed hydrolysis enhancement. However, it can be troublesome to avoid thiol exchange by taking hydrolysis to completion.[2] Attachment of positive charges to *N*-alkyl substituents can also promote formation of succinamic acids.[7]

To address the problem of maleimide hydrolysis, which yields a mixture of bioconjugates with succinimides and succinamic acids, we decided to explore a more robust non-hydrolysable maleimide analogue, study the stability of the resulting adduct and examine the possibly associated thiol exchange behavior. The idea was to use cyclopent-4-ene-1,3-dione (**2.7**), which can be regarded as a maleimide analogue (**Figure 2.1**).

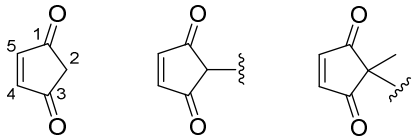

2.7 **2.8** **2.9**

Figure 2.1 Possible structural modifications of the maleimide moiety.

We envisioned that substituting the nitrogen in the maleimide ring by a carbon atom should avoid addition of water to the Michael adduct. However, the 2 position of the mono-alkylated adduct (**2.13**) could pose problems due to its high hydrogen acidity and thus, allow enolization at the α-position giving rise to possible polymerizations or undesired secondary Michael additions. Taking this data into account, we hypothesized that using 2,2-disubstituted cyclopent-4-ene-1,3-diones (CPDs, **2.9**) would be advantageous as it would avoid enolization at the 2 position. Nonetheless, the use of CPDs come at the price of introducing a prochiral position.

2.2 Cyclopentenediones as a click reactant

Omar Brun during his Ph.D. thesis explored the reactivity of CPDs (**2.9**).[8] He observed a characteristic differential behavior of these molecules upon reaction with *N*-terminal cysteines (with the amine free) or *N*-acylated cysteines (**Scheme 2.2**). Internal, acylated cystines, furnished Michael-type adducts (**2.12**) that readily reverted to the starting materials, whilst reaction with non-acylated cysteines at the *N*-terminus of peptides underwent an irreversible, "click-type" reaction that ended up in a bicyclic compound (**2.11**) whose mass was 20 units lower than that of the adduct expected from the thia-Michael reaction (this is why this is compound is referred to as the "M-20" adduct). Formation of the M-20 adduct proceeded within reasonable reactions times, in aqueous environments and under mild conditions and demonstrated excellent selectivity for 1,2-aminothiols.

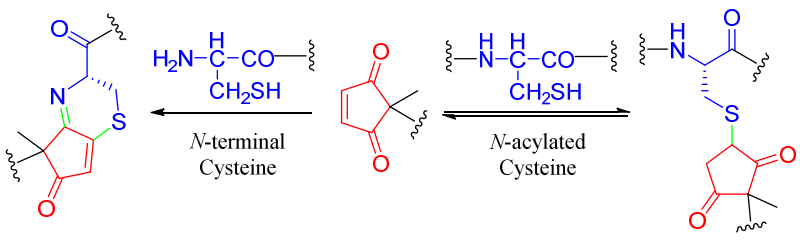

2.11, "M-20" **2.10, CPD** **2.12**

Scheme 2.2 CPD behavior with *N*-acylated and non-acylated cysteines.

Replacement of the nitrogen atom of the maleimide moiety with a carbon entails more electrophilic carbonyl groups in the CPD scaffold due to the lack of electron delocalization of the imide nitrogen atom present in the maleimide ring. This results in a structure overall more predisposed to nucleophilic attacks. As depicted in **Scheme 2.3**, intramolecular imine formation is likely highly favored since it yields a six-membered ring (**2.14**). Formation of this intermediate and subsequent oxidation would displace the equilibrium of the Michael-type addition (**2.13**) into this transitional product and provide an explanation for the observed nearly quantitative conversion.

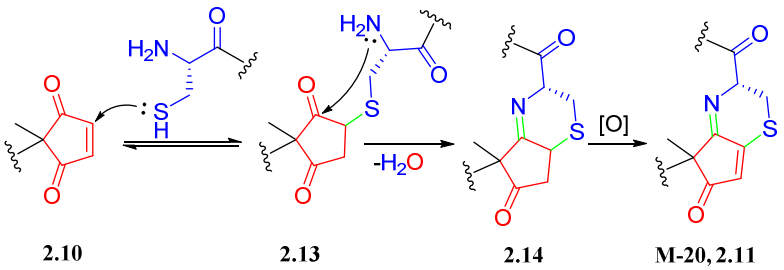

Scheme 2.3 Mechanistic proposal for the CPD-Cys reaction.

Dr. Brun confirmed this behavior utilizing several peptides, observing the formation of a first bicyclic intermediate (**2.14**), which was followed by oxidation yielding the stable M-20 adduct (**2.11**). Due to the CO–C=C–C=N conjugated system the M-20 adduct exhibits a characteristic broad maximum around 330 nm. Moreover, after isolation this adduct was found to be stable under physiological conditions. The Michael-like adduct (**2.13**) was only detected (*via* mass spectrometry) at the very beginning of the reaction in the presence of high thiol concentrations, and attempts to isolate it showed (by HPLC analysis) decomposition into the partner starting materials.

Dr. Brun's work also showed that CPDs do not undergo the Diels-Alder reaction, as observed when reacting a CPD derivative (**2.10**) with a diene (**2.15**) in H_2O at 37 ºC for a week (**Scheme 2.4**). Even after prolonged reaction times, no desired Diels-Alder adduct (**2.16**) could be detected by either NMR or HPLC-MS. This conclusion was further corroborated by analyzing the results of the reaction with several other dienes, such as furan, 2,5-dimethyl furan or ethyl sorbate.

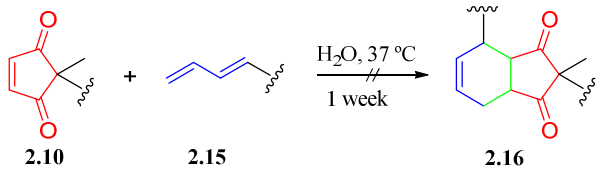

Scheme 2.4 First attempt to run a Diels-Alder reaction between CPD and a diene.

A possible explanation is found in the literature. A communication dealing with the application of CPDs in DA reactions pointed out to the steric hinderance associated with this structure containing two substituents at the 2 position, which actively hampered the DA reaction.[9] This fact was first noticed by Agosta *et. al.*, remarking the sluggishness of CPDs as dienophiles.[10]

2.3 Objectives

The objectives of the work described in this chapter were :

- Utilize 2,2-disubstituted cyclopent-4-en-1,3-diones as maleimide analogues in Michael-type reactions with *N*-terminal cystines to yield conjugates of peptides and oligonucleotides.
- Explore the use of the CPD-Cys addition in conjunction with either thia-Michael addition, CuAAC or oxime formation to produce double conjugates.
- Explore the possibility of using CPDs as tools for derivatization and cyclization of peptides and oligonucleotides in a one-step manner.

2.4 CPD-containing derivatives and building blocks

Since our first intention was to use CPDs for the conjugation of peptide and possibly other polyamides such as peptide nucleic acids (PNAs), one derivative to be made had to include a carboxylic acid to allow for its introduction into the growing polyamide chains by standard SPPS methods. Some CPDs had been previously described containing a three-methylene spacer, and their preparation involved an ozonolysis step.[11] We decided to synthesize a derivative containing instead a two-methylene linker between the carboxylic acid and the five-membered ring, as it was considered long enough to avoid the 2-substituent from sterically hinder attack of the nucleophile to the conjugated double bond of the CPD scaffold. The synthetic scheme for the synthesis of our CPD derivative containing a carboxylic acid (**2.20**, CPD-COOH, **Scheme 2.5**) was straightforward, did not involve reaction with ozone, and had been previously optimized to only require one chromatographic purification step. Starting from commercially available 2-methyl-1,3-cyclopentanedione (**2.17**), reaction with *tert*-butyl acrylate in refluxing NEt_3 overnight rendered the Michael adduct (**2.18**) in 78% yield. Follow-up treatment with TFA furnished the deprotected carboxylic acid form (**2.19**) in a quantitative manner and oxidation of the 4,5-position with $CuCl_2$ as previously described,[12] provided the desired CPD-COOH (**2.20**) derivative in a modest 48 % yield.

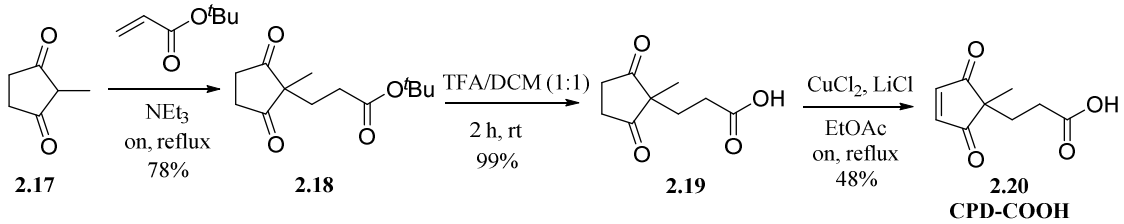

Scheme 2.5 Synthesis of the CPD-COOH (**2.20**) derivative.

Aside from "on-resin" derivatizations, we also intended to obtain reporter groups such as fluorophores or biotin containing the CPD moiety in order to provide the conjugated biomolecule with a fluorescent tag or a biotin for push-pull experiments. Starting from CPD-COOH (**2.20**) analogue, we envisioned attaching a bifunctional linker which might subsequently react with the desired reporter group as depicted in **Scheme 2.6**. First attempts of carboxylic acid activation attempted with a carbodiimide were not successful, only recovering starting material. Subsequently, *N*-hydroxysuccinimide ester formation and subsequent reaction with a nucleophile proved feasible, but the reaction was low yielding and required long reaction times. An improvement in the obtention of the desired amide was accomplished by activation of the carboxylic acid moiety through a mixed anhydride formation with isobutyl

chloroformate (IBCF), and *in situ* reaction with *N*-(Boc-amino)ethylamine linker to render the desired amide (**2.21**) in 76% yield. Finally, quantitative recovery of the amine (**2.22**) was achieved by an acidic treatment with 4 M HCl (in dioxane) at room temperature (**Scheme 2.6**).

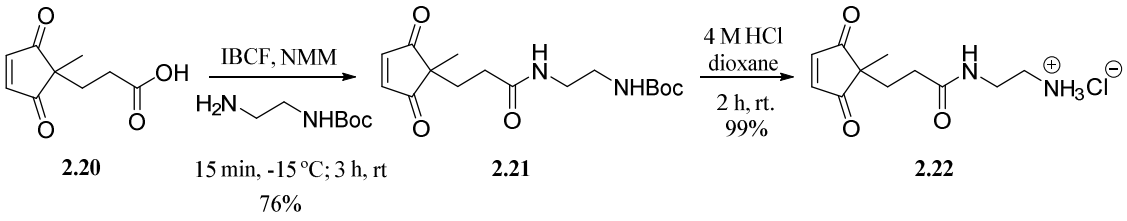

Scheme 2.6 Procedure followed for the obtention of CPD-amine intermediate.

Once we had obtained our valuable intermediate with the appending nucleophilic amine, it had to be derivatized with reporter groups such as D-biotin, which contains a carboxylic acid moiety, or the commercial and readily derivatisable dansyl chloride as depicted in **Scheme 2.7**.

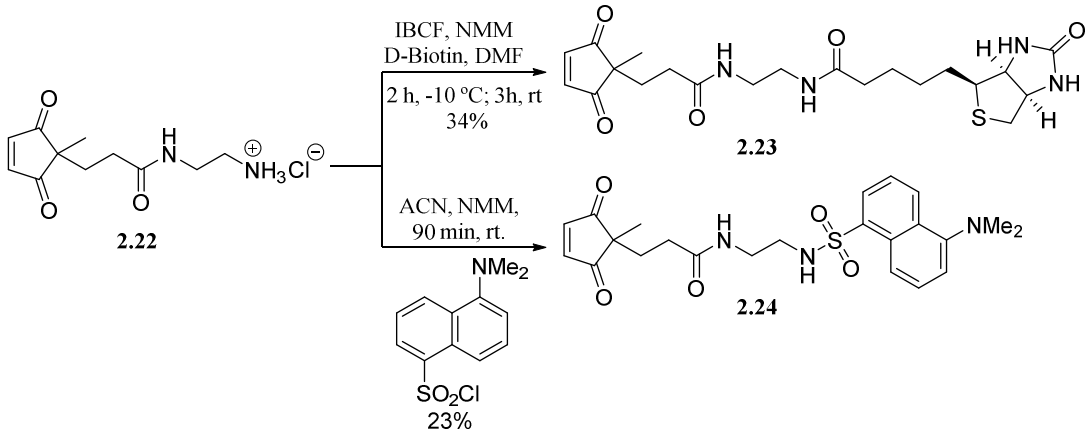

Scheme 2.7 Scheme for the synthesis of dansyl- and biotin-derivatized CPDs.

The first reaction of CPD (**2.22**) with IBCF and biotin was performed in ACN as solvent. TLC analysis showed the formation of a new product. After purification and ^{1}H NMR analysis we reached the conclusion that a side reaction had taken place between mixed anhydride **2.25** and the CPD (**2.22**), yielding the isolated isobutyl carbamate (**2.26**) instead of the desired amide (**2.27**, **Scheme 2.8**).

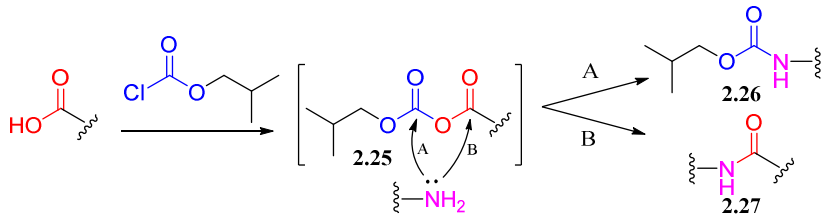

Scheme 2.8 Possible outcomes for the activation of carboxylic acids *via* IBCF.

A plausible explanation for this result was that biotin was sparingly soluble in ACN, resulting in low to none formation of the mixed anhydride reactive intermediate and when the amine (**2.22**) was added, formation of the carbamate with the chloroformate was overwhelmingly favored. Taking this into account, use of DMF instead of ACN and longer preactivation times yielded successfully the CPD-

biotin (**2.23**) analogue. On the dansyl counterpart no major problems were found. It this case, ACN was found to be suitable candidate for the synthesis of the CPD-Dansyl (**2.24**) derivative.

Additionally, a more manageable and doubly methylated CPD was desirable in order to perform reactivity tests with a model compound that would not afford diastereoisomeric mixtures. As depicted in **Scheme 2.9**, synthesis of derivative **2.29** starts with the alkylation of the commercially available 2-metylcyclopentane-1,3-dione (**2.17**) with MeI in basic conditions to provide the dialkylated analogue (**2.28**) as described in the literature[13] with small modifications. For the subsequent transformation into the CPD scaffold, several methodologies had been described in the literature ranging from a photochemical oxidation with a mixture of $CuCl_2$ and LiCl salts,[12] reaction with NBS[13,14] or $CuBr_2$ alone.[15] Our first attempt was the $CuCl_2$ and LiCl route that had previously given positive results in the group (**Scheme 2.5**). First trials with $CuCl_2$ or NBS methodologies were unfruitful and gave complex mixtures. Contrarily to previous experiments, reaction with $CuBr_2$ in anh. MeOH proved useful to convert the dialkylated partner (**2.28**) to the oxidized form (**2.29**) in an excellent 91% yield.

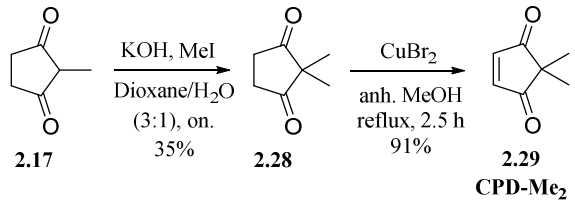

Scheme 2.9 Synthetic route to prepare the 2,2-dimethylated CPD (**2.33**).

CPD-Me_2 (**2.29**) was found to be partially volatile in reduced pressure environments (when we followed described procedures a non-negligible amount of CPD-Me_2 was lost in the rotary evaporator), and decomposed in the freezer. Yet, it remained stable in a refrigerated solution for over a year.

2.5 Conjugates obtained from the CPD-Cys reaction

To complete the work started by Omar Brun with CPDs, we decided to take advantage of the "click-like" reactivity exhibited by CPDs towards *N*-terminal cysteines, firstly using different polyamides as scaffolds. In the second part of this section we will discuss the translation of this methodology to the preparation of oligonucleotide conjugates.

2.5.1 Conjugates of polyamides

Having obtained the CPD-COOH derivative (**2.20**), we started evaluating its reactivity towards reagents and reaction conditions used in SPPS. Firstly, we assessed whether CPDs could be incorporated at the *N*-terminal position of polyamide chains by incubating a small aliquot of CPD-COOH with the standard cleavage and deprotection cocktail (95:2.5:2.5 TFA/TIS/H_2O). HPLC-MS analysis of the crude showed no alteration to the CPD moiety thus, providing evidence that *N*-terminal derivatization of peptides was feasible. In a similar fashion, we envisioned the possibility of utilizing side-chain derivatization of suitable amino acids such as lysine or ornithine to provide another reactive site for the ligation, since occasionally different appending sites yield to differential biological activity.[16] In this latter case, additionally to cleavage and deprotection cocktail, the CPD had to withstand the piperidine treatment

for Fmoc removal. In this regard though, analogously to the maleimide counterpart, the CPD moiety did not resist piperidine treatment, quickly decomposing into a complex mixture, possibly involving aza-Michael aggregates. With all this knowledge we decided to chemically synthesize a fully protected peptide with sequence Gly-Arg-Gly-Ser-Tyr-Glu-Ala-Tyr-Lys (**2.30**) following the procedure outlined in **Scheme 2.10**.

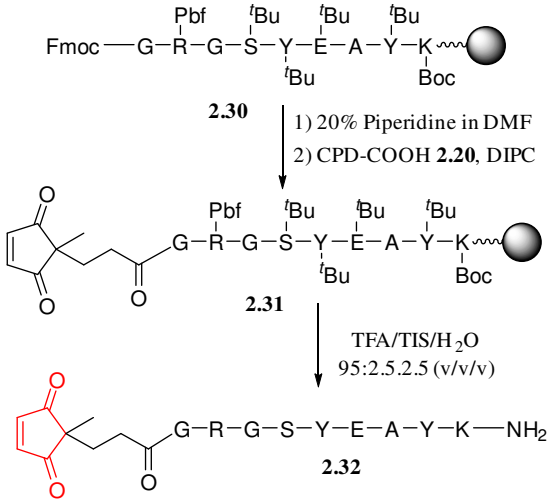

Scheme 2.10 Synthetic scheme for the *N*-terminal derivatization of a peptide with a CPD.

After Fmoc removal, attachment of the CPD moiety at the *N*-terminus was achieved by utilizing standard carbodiimide methodology. Subsequently, acidic cleavage yielded the fully deprotected CPD-peptide, CPD-Gly-Arg-Gly-Ser-Tyr-Glu-Ala-Tyr-Lys-NH_2 (CPD-GRGSYEAYK-NH_2, **2.36**) fairly pure as depicted in **Figure 2.2**.

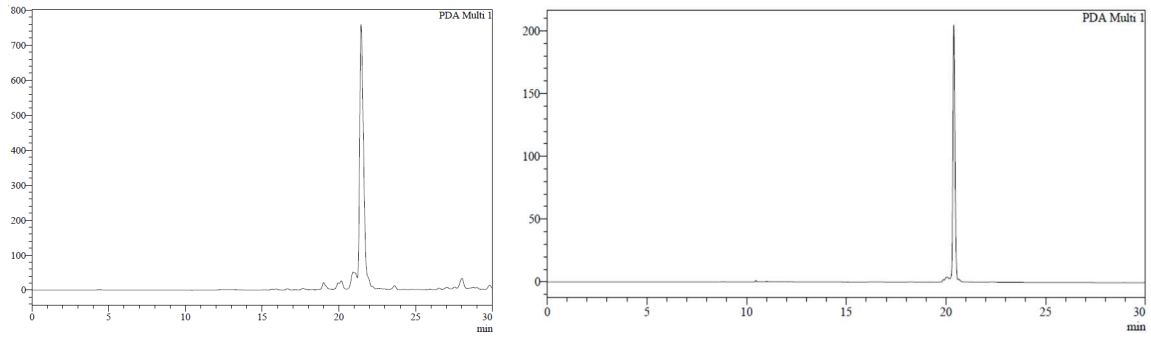

Crude Purified

Figure 2.2 HPLC traces (280) of the crude (left), and purified (right) CPD-derivatized peptide **2.32**.

Following the synthetic procedure described above two other CPD-polyamides were synthesized: first a longer complex peptide, namely CPD-Leu-Val-Pro-Arg-Gly-Ser-Tyr-Lys-Gly-Thr-Ser-Lys-Leu-Asn-Tyr-Leu-NH_2 (**2.33**, CPD-LVPRGSYKGTSKLNYL-NH_2) and then a peptide nucleic acid (PNA) oligonucleotide analogue CPD-catgtcat-Lys-NH_2 (**2.34**, **Figure 2.3**).

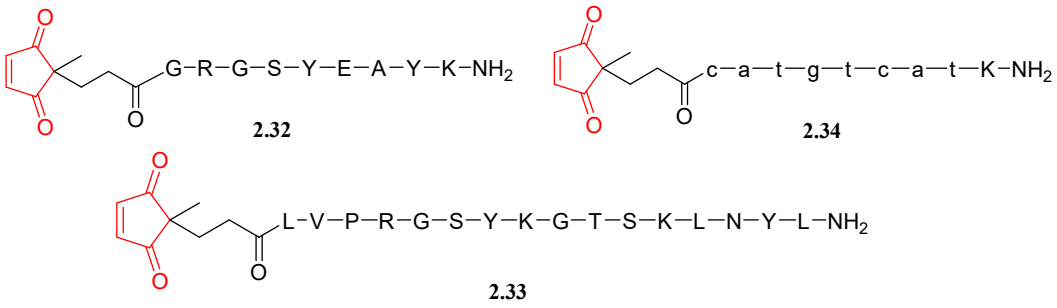

Figure 2.3 CPD-derivatized polyamides obtained.

Following the experimental conjugation procedure optimized by Omar Brun during his Ph.D. thesis, several conjugates were obtained as depicted in **Scheme 2.11**. Conjugation comprised use of either equimolar or little excess of CPD (up to 1.2 equiv.) in aqueous media at 37 ºC for 3 to 4 h. Several 1,2-aminothiol reactants were employed ranging from cysteine (**2.35**) and cysteine methyl ester (**2.36**) as the simplest analogues, to increasingly complex peptides containing an *N*-terminal cysteine (**2.37**, **2.38**). In regards to the CPD counterpart, several analogues were also utilized (**2.20**, **2.23**, **2.24**, **2.29**, **2.34**). Conjugation reaction took place in yields ranging from 70% up to 95% as assessed by HPLC traces.

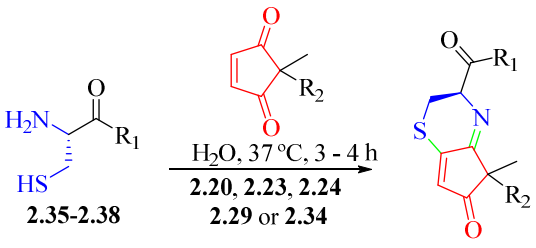

M-20

I) R_1 = OH **2.35**, R_2 = Me **2.29** (**2.39**)
II) R_1 = OMe **2.36**, R_2 = CPD-Dansil **2.24** (**2.40**)
III) R_1 = Tyr-Gly-NH_2 **2.37**, R_2 = Me **2.29** (**2.41**)
IV) R_1 = Ser-Tyr-Ala-Lys-Tyr-Gly-NH_2 **2.38**, R_2 = CPD-COOH **2.20** (**2.42**)
V) R_1 = Ser-Tyr-Ala-Lys-Tyr-Gly-NH_2 **2.38**, R_2 = CPD-Biotin **2.23** (**2.43**)
VI) R_1 = Ser-Tyr-Ala-Lys-Tyr-Gly-NH_2 **2.38**, R_2 = CPD-catgtcatK-NH_2 **2.34** (**2.44**)

Scheme 2.11 CPD-Cys reactions involving several cysteines with the amine free (**2.35**-**2.38**) and CPDs (**2.20**, **2.23**, **2.24**, **2.29**, **2.34**) to furnish M-20 adducts (**2.39**-**2.44**).

In a search for structural elucidation of the M-20 adduct, Dr. Brun reacted methyl cysteinate (**2.36**) with CPD-Me_2 (**2.29**), isolated and characterized the corresponding M-20 adduct by ^{1}H, ^{13}C NMR. Doing a follow-up analysis to further confirm the structure of the M-20 adduct, we synthesized the peptide H-Cys-Tyr-Gly-NH_2 (**2.37**) and reacted it with CPD-Me_2 (**2.29**) to obtain the corresponding M-20 adduct (**2.41**, **Scheme 2.12**). HPLC traces of the crude tripeptide and the final crude adduct are shown in **Figure 2.4**.

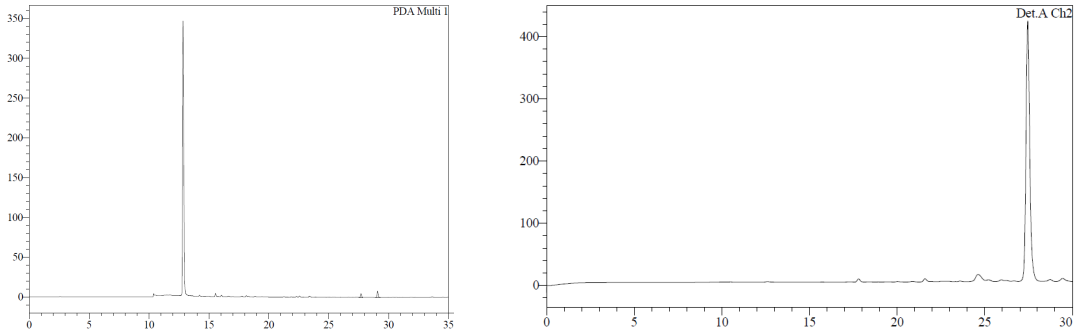

H-CYG-NH_2 (**2.37**) M-20 (H-CYG-NH_2 + CPD-Me_2) (**2.41**)

Figure 2.4 HPLC traces (280 nm) of crude H-CYG-NH_2 after cleavage and deprotection (left), and of the M-20 adduct reaction crude after 3 h time with CPD-Me_2.

We chose a tripeptide containing a tyrosine residue in order to facilitate HPLC purification (tyrosine side chain, phenol, is a chromophore) and NMR analysis (more complex on a larger peptide). On the CPD counterpart, the dimethylated derivative (**2.29**) was employed so as to avoid formation of diastereomeric compounds, as previously commented. Once we obtained the M-20 adduct (**2.41**) we further confirmed its structure by ^{1}H NMR as depicted in **Figure 2.5**.

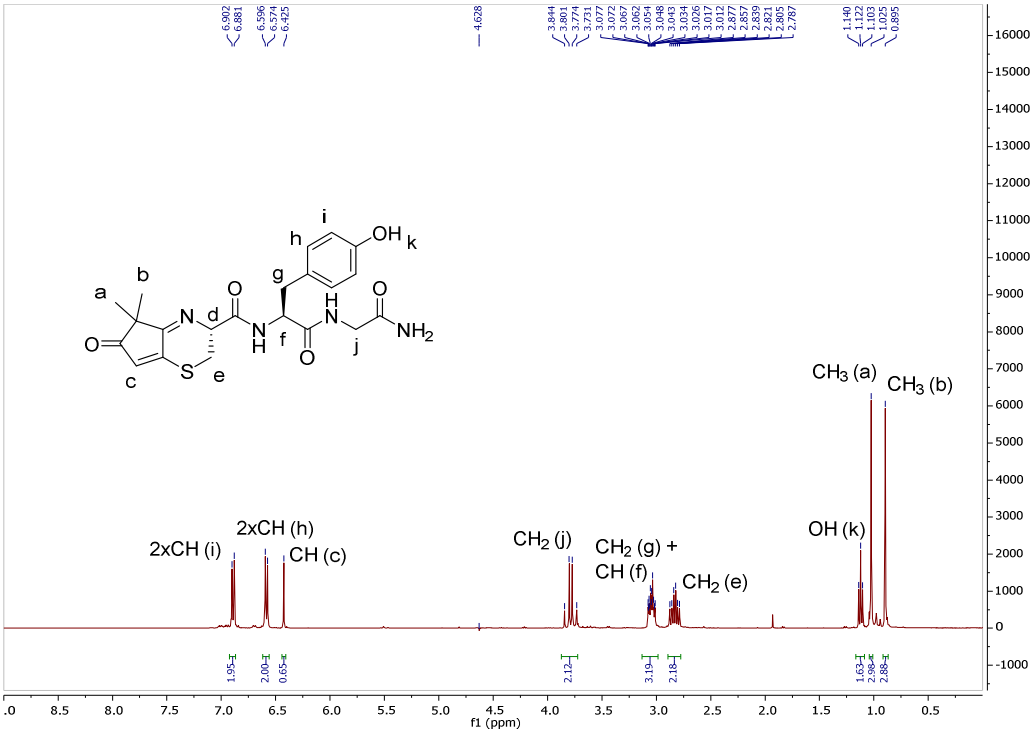

Figure 2.5 ^{1}H NMR (400 MHz) of the M-20 (**2.41**) adduct obtained by reacting H-CYG-NH_2 (**2.37**) and CPD-Me_2 (**2.29**) in D_2O.

2.5.2 Conjugates of oligonucleotides

After the positive results obtained with polyamides, we decided to explore the possibility of preparing conjugates of oligonucleotides using the CPD-Cys reaction. Taking into account where oligonucleotides

are typically modified (on the nucleobases, the phosphates, the 3' terminus or the 5' end), we settled for the 5' position since chemically it is the most readily derivatisable of the groups listed above.

In this instance we had two options for the modification of the 5' end of a fully protected oligonucleotide chain obtained by standard solid-phase assembly: attaching either a CPD or a cysteine residue. The main shortcoming of the first option is the intrinsic instability of the CPD to the final deprotection and cleavage treatment with conc. aq. NH_4OH, in a similar fashion as previously observed with piperidine. On the other hand, in the literature there were described procedures to obtain cysteine amidites.[17,18] Consequently, we opted for the second alternative.

The synthetic route for cysteine phosphoramidites (**Scheme 2.12**) starts from commercially available trityl (Trt, **2.45**) or *tert*-butylthio (S^{t}Bu, **2.46**) thiol-protected cysteine amino acids. They both first have to be derivatized so as to incorporate the hydroxyl group necessary for phosphoramidite preparation. Amide formation with an aminoalcohol was achieved through IBCF activation of the carboxyl group with *trans*-aminocyclohexanol hydrochloride (**2.47**), yielding the expected hydroxyl-containing derivatives (**2.48**, **2.49**) in excellent yields. Subsequently, a phosphitylating agent (**2.50**) was employed to obtain either phosphoramidite derivative (**2.51**, **2.52**) in reasonable yields.

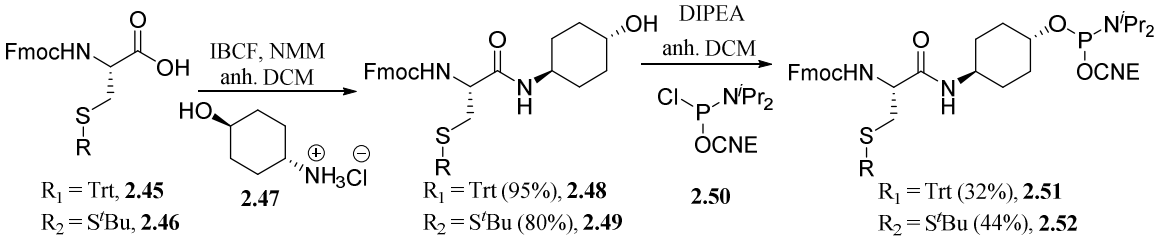

Scheme 2.12 Synthesis of Trt- or S^{t}Bu-protected cysteine amidites.

In order to simplify the synthetic procedure, we explored the possibility of reducing the carboxylic acid of the trityl-protected cysteine (**2.45**) into its hydroxyl counterpart, by treating the activated carboxyl with $NaBH_4$.[19] As seen in **Scheme 2.13** after successful isolation of the cysteinol derivative (**2.53**) in 80% yield, subsequent attempts to phosphitylate the hydroxyl group using the same phosphitylating reagent (**2.50**) proved to be unsuccessful. A possible explanation for this observed phenomenon is the steric hinderance provided by the bulky trityl group, which prevents the hydroxyl from reacting with the phosphine.

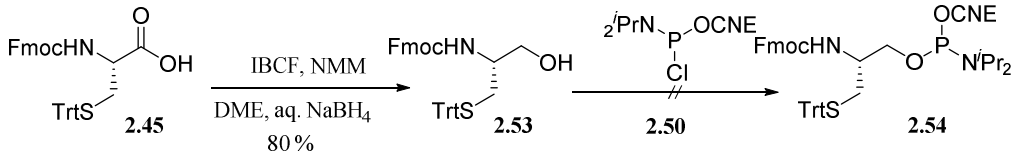

Scheme 2.13 Synthetic route designed for the preparation of an alternative cysteine phosphoramidite derivative.

Cysteine amidites **2.51** and **2.52** had been described to cleanly couple to oligonucleotide chains using standard phosphite triester chemistry. Once we had both cysteine amidites (**2.51**, **2.52**) in our hands, we decided to assess the reproducibility of these results. In a proof-of-concept experiment, we synthesized two deca-2'-deoxythymidine (dT_{10}) oligonucleotides and controlled the coupling yields of both cysteine phosphoramidites by means of deprotection of small aliquots of oligonucleotide-resin and HPLC analysis of the crudes (**Figure 2.6**).

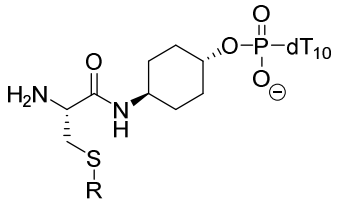

R = Trt (**2.55**); S^{t}Bu (**2.56**)

Figure 2.6 Cysteine-derivatized crude oligonucleotide structures.

To our delight, HPLC traces (254 nm) of both crude oligonucleotides (**2.55** and **2.56**) showed quantitative coupling of both derivatives as depicted in **Figure 2.7**.

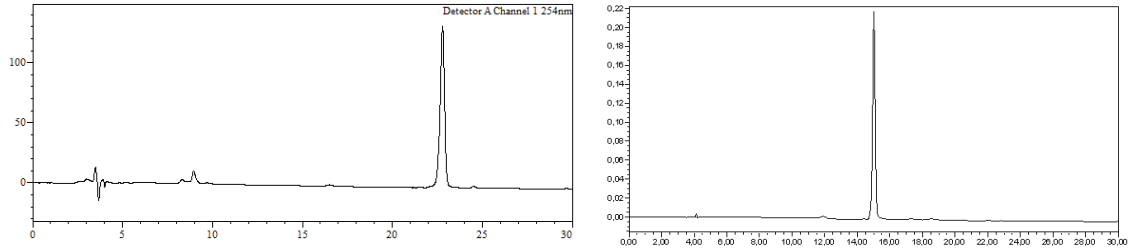

H-Cys(Trt)-dT$_{10}$ (**2.55**) H-Cys(S^{t}Bu)-dT$_{10}$ (**2.56**)

Figure 2.7 HPLC traces (254 nm) of crude H-Cys(Trt)-dT$_{10}$ (**2.55**) and H-Cys(S^{t}Bu)-dT$_{10}$ (**2.56**).

Having both cysteine-protected oligonucleotide derivatives, which were deemed pure enough to be used without further purification, we proceeded differently with the removal of each of the protecting group appending from the sulfur atom following described procedures.[20]

For the S^{t}Bu protected Cys-oligonucleotide (**2.56**), the procedure involved use of a reducing agent in order to deprotect the thiol group. The classical described literature called upon 1,4-dithiothreitol (DTT) as the best suited reducing agent in peptide synthesis.[21] Albeit in our hands, consistent quantitative deprotections could not be achieved, only observing conversions up to 45% as assessed by HPLC after overnight reaction times at room temperature. To overcome this drawback, tris(2-carboxyethyl)phosphine hydrochloride (TCEP), a disulfide reducing agent commonly used in biochemistry and molecular biology was employed instead. Compared to DTT, TCEP has the advantage of being odorless, a more powerful reducing agent, more resistant to air oxidation and efficient over a wider pH range (1.5-9).[22] With this reagent, deprotection yields increased up to 80% as assessed by HPLC analysis of deprotected H-Cys-dT$_{10}$ (**2.57**) crude, thus being the preferred reagent for the deprotection of the S^{t}Bu analogue.

On the other hand, in regards to the trityl-protected analogue (**2.55**), standard peptide acidic deprotection conditions were discarded straight away since the acidic conditions could potentially threaten the structural integrity of the oligonucleotide scaffold. Hence, a milder $AgNO_3$ deprotection methodology was employed.[20] H-Cys(Trt)-dT$_{10}$ (**2.55**) was deprotected by reaction with an aqueous solution of $AgNO_3$ (5 equiv.) for 45 min at 37 ºC, followed by addition of DTT (7 equiv.) for an additional 30 min in order to complex and precipitate Ag^+ ions. In a similar fashion as for the TCEP reaction, this methodology was fairly straightforward and required HPLC purification to remove undesirable DTT and Ag^+ traces. The conclusion of the comparison of deprotection schemes was that neither proved to

be a better way for obtaining H-Cys-dT$_{10}$ (**2.57**) since similar reaction isolation yields were attained as depicted in **Scheme 2.14**.

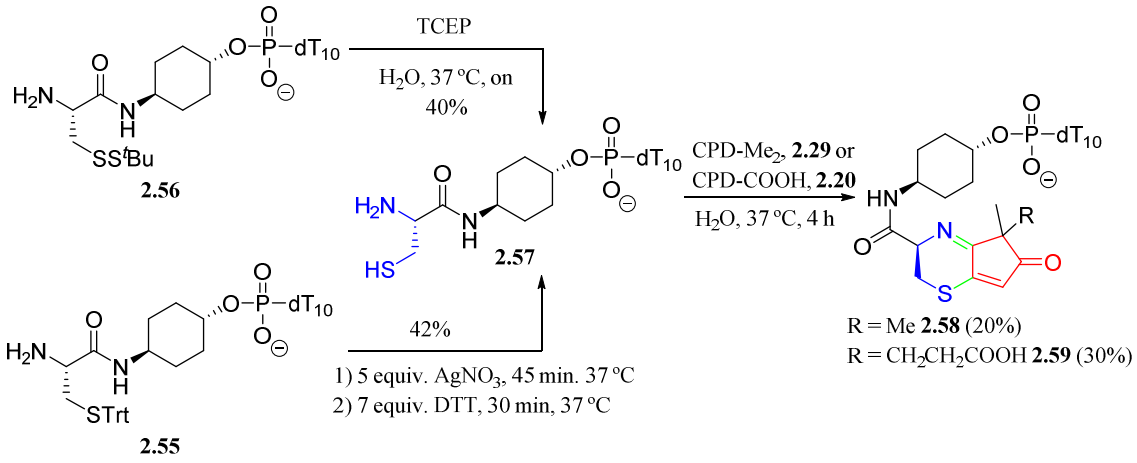

Scheme 2.14 Cysteine-oligonucleotide deprotection conditions and proof-of-concept reaction with CPDs.

Once the common H-Cys-dT$_{10}$ final product (**2.57**) was obtained, we tested whether it would react with CPDs as smoothly as it had been observed in polyamides (as discussed in **Section 2.5.1**). As a proof of concept, we incubated **2.57** (produced from the trityl route) with 1.2 equiv. of CPD-Me$_2$ (**2.29**), for 3 h at 37 ºC in H$_2$O. After observing a new product being formed by HPLC (**Figure 2.8**, left), we confirmed that it also absorbed at the 330 nm channel, in concordance with the spectroscopic observation previously reported for the "M-20" adduct. Its formation was confirmed by purification and MALDI-TOF MS analysis of the isolated product, and its stability assessed by reanalyzing of the isolated conjugate (**2.58**, **Figure 2.8**, right).

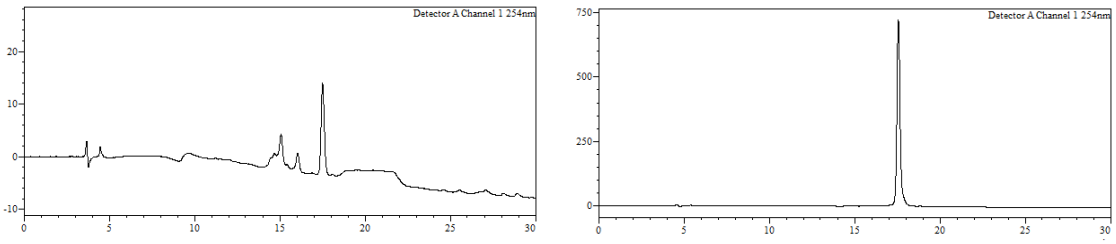

Crude Pure

Figure 2.8 HPLC profiles (254 nm) of the H-Cys-dT$_{10}$ (**2.57**) and CPD-Me$_2$ (**2.29**) reaction (**2.58**), crude (left) and purified conjugate (right).

To further proof that the reaction might also take place cleanly with other CPDs, the CPD-COOH (**2.20**) analogue was subsequently tested. Using the same reaction conditions similar results were obtained, in this instance two new peaks appeared due to the prochiral quaternary carbon present in the CPD moiety (**Figure 2.9**). Again, after isolation and MALDI-TOF MS analysis, formation of conjugate (**2.59**) was confirmed, proving the feasibility of the methodology in the field of oligonucleotide conjugation.

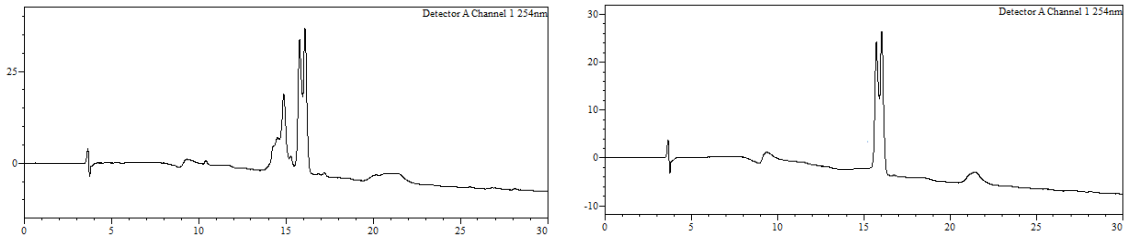

Crude Pure

Figure 2.9 HPLC profiles (254 nm) of H-Cys-dT$_{10}$ (**2.57**) and CPD-COOH (**2.20**) reaction (**2.59**), crude (left) and purified (right).

After these positive results we decided to explore the extent of the CPD-Cys conjugation strategy by making use of CPD-derivatized peptides and react them with H-Cys-oligonucleotides. To do so, we reacted CPD-GRGSYEAYK-NH$_2$ (**2.32**) peptide and H-Cys-dT$_{10}$ (**2.57**) oligonucleotide under identical conditions: 1.2 equiv. of peptide was incubated with H-Cys-dT$_{10}$ (**2.57**) (in this instance coming from the S^{t}Bu route) at 37 ºC for 3 h in H$_2$O. Upon analysis of the crude, though, no reaction seemed to occur, leaving the oligonucleotide nearly unmodified (**Figure 2.10**, left). Since it is known that larger reactants tend to react more sluggishly compared to small molecules, the crude was left reacting overnight in the same reaction conditions. Subsequent HPLC analysis revealed a complex crude (**Figure 2.10**, right). This was the first time that the CPD-Cys reaction did not furnish clean crudes and reacted devoid of problems. The possibility of plausible Michael additions between the CPD and the nucleobases was here discarded, since we were working with deoxythymidine-containing oligonucleotides.

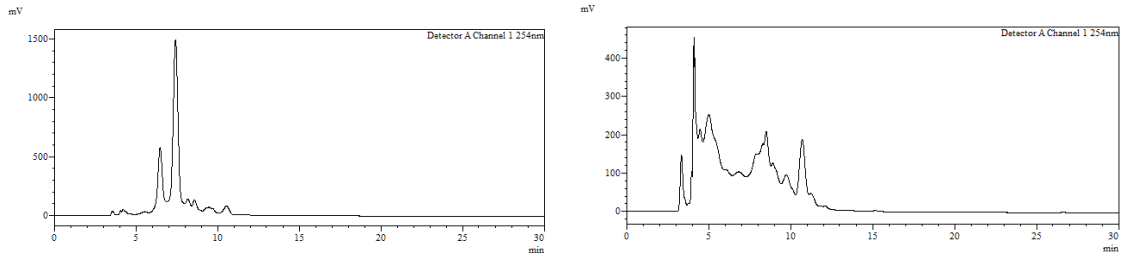

Crude (3 h) Crude (Overnight)

Figure 2.10 HPLC traces (254 nm) of the first attempt of reaction between CPD-GRGSYEAYK-NH$_2$ (**2.32**) and H-Cys-dT$_{10}$ (**2.57**) oligonucleotide at 3 h (left) and overnight (right).

Subsequent isolation and MALDI-TOF MS analysis of the main products in the crude pointed at the formation of an adduct with *m/z* = 1442.2 Da that was different from the value expected for the target conjugate (**Figure 2.11**). Puzzled by this side reaction and considering possible sources of impurities, we surmised that residual TCEP (**M** = 250.2 Da) that might be still present from the previous deprotection step (the H-Cys-dT$_{10}$ used in this experiment had been obtained from H-Cys(S^{t}Bu)-dT$_{10}$, **2.56**) was reacting with the CPD appending from the peptide (**M** = 1192.5 Da). This hypothesis was supported by a report describing that TCEP reacts with maleimides under certain conditions[23] which suggested that TCEP could also react with the CPD.

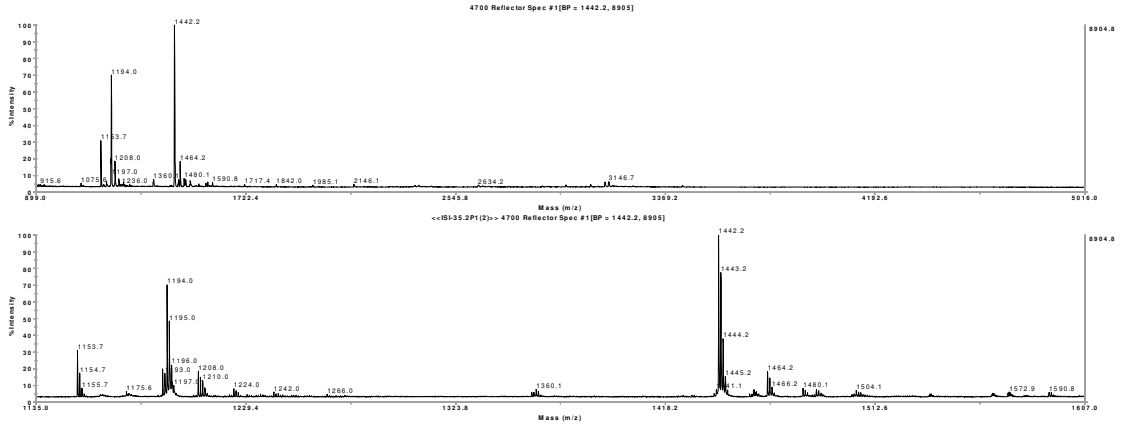

Figure 2.11 MALDI-TOF MS spectrum of the collected side product of the first attempt of conjugation of H-Cys-oligonucleotides with peptides. *m/z* = 1442.2 Da is in accordance with the TCEP-CPD adduct; m/z = 1194.0 Da with the CPD-peptide (**2.32**).

With this possible and plausible explanation for failure to obtain the target conjugate, we decided to carry out an additional purification step after removal of the S^{t}Bu group by size exclusion chromatography (elution through Sephadex™ G-25), in order to further assure that no traces of TCEP would be present in the oligonucleotide reactant. Then, upon performing again the standard conjugation experimental procedure, a different HPLC trace was observed at the 3 h mark (**Figure 2.12**, left), which agreed with previous experimental conjugation results. Formation of the expected conjugate was conclusively validated by MALDI-TOF MS analysis (**Figure 2.12**, *m/z* = 4431.3 Da) proving that the CPD-Cys methodology could satisfactorily be performed also with oligonucleotides and peptides bearing the CPD-moiety.

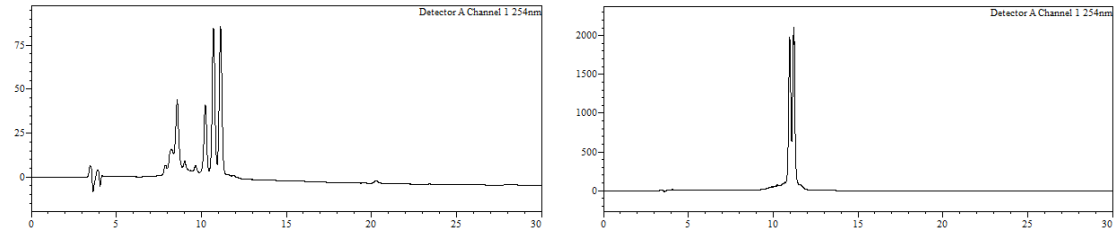

Crude (3 h) Pure

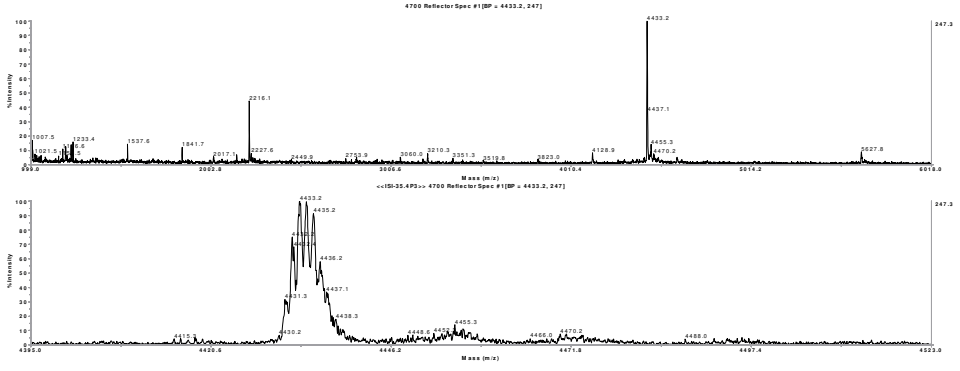

MALDI-TOF MS spectrum

Figure 2.12 HPLC traces (254 nm) of the crude resulting from the reaction between CPD-GRGSYEAYK-NH_2 (**2.32**) and H-Cys-dT_{10} (**2.57**) at 3 h (left), pure (**2.60**, right) and MALDI-TOF MS spectrum of the isolated product.

Afterwards, we decided to explore if there would be any problems with oligonucleotides containing all nucleobases since, so far, we had only assessed the success of the reaction with deoxythymidine-containing oligonucleotides. To answer this question, we synthesized two additional oligonucleotides containing all nucleobases: one 10 nucleotide long with the sequence $d^{5'}$CAGATGTCAC$^{3'}$, and a more complex and longer one containing 21 nucleotides, $d^{5'}$CAGCAGCAGAGTCTTCATCAT$^{3'}$. Both oligonucleotides were assembled using ultra-mild nucleobase protecting groups and appended with both cysteine amidites (**2.51** and **2.52**, **Scheme 2.12**). After cleavage and nucleobase and phosphate protecting group removal, both thiol-protected oligonucleotides (**2.60**, **2.61** for Trt and S^{t}Bu 10-mer analogues and **2.62**, **2.63** for Trt and S^{t}Bu 21-mer) were subjected to the sulfur deprotection schemes as previously discussed for the dT_{10} analogue (**Scheme 2.14**). In this instance, both strategies were found to be compatible with all nucleobases and, as previously stated, no major difference in yield and deprotection ease was found between the two Cys protection approaches. As previously, for the S^{t}Bu deprotection a size exclusion chromatography was performed in addition to HPLC purification.

Once we had both H-Cys-10-mer/21-mer oligonucleotides (**2.64**, **2.65**) each of them was reacted with two CPD-peptides. The first CPD-peptide had already been utilized in previous experiments, CPD-GRGSYEAYK-NH_2 (**2.32**), and the second one had a longer sequence: (CPD-LVPRGSYKGTSKLNYL-NH_2, **2.34**). Both peptides were successfully conjugated to both 10-mer and 21-mer oligonucleotides, which proved the feasibility of the CPD-Cys reaction involving oligonucleotides (**Scheme 2.15**).

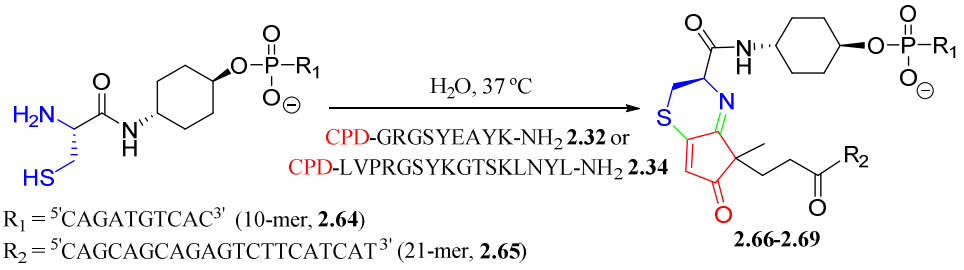

Conjugates

2.66: R_1 = 10-mer, R_2 = GRGSYEAYK-NH_2 (60%)
2.67: R_1 = 10-mer, R_2 = LVPRGSYKGTSKLNYL-NH_2 (20%)
2.68: R_1 = 21-mer, R_2 = GRGSYEAYK-NH_2 (44%)
2.69: R_1 = 21-mer, R_2 = LVPRGSYKGTSKLNYL-NH_2 (33%)

Scheme 2.15 Conjugation reaction involving H-Cys-oligonucleotides (**2.64** or **2.65**) and CPD-derivatized peptides (**2.32**, **2.34**) to yield the M-20 adduct (**2.66**-**2.69**).

As can be seen in the HPLC traces (**Figure 2.13**) of two conjugates (**2.67** and **2.69**, **Scheme 2.15**), the reactions involving both oligonucleotides and peptides were successful, demonstrating once again the wide scope of this methodology to obtain conjugates of not only peptides but also oligonucleotides.

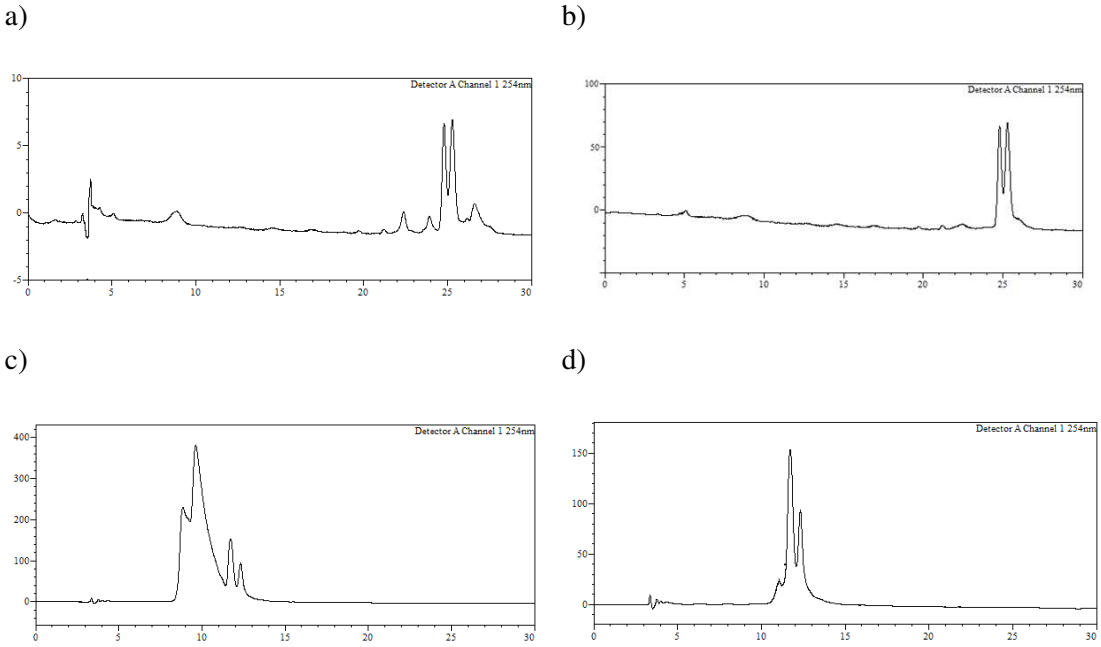

Figure 2.13 HPLC profiles (254 nm) of conjugates **2.67**, crude (a) and purified (b) and **2.69** crude (c) and purified (d).

2.5.3 Concluding remarks

In conclusion, the CPD-Cys conjugation reaction has proven to be an excellent addition to the "click" chemistry toolbox for obtaining conjugates of peptides and oligonucleotides. The unprecedented selectivity of CPDs for 1,2-aminothiols even in the presence of other nucleophiles, lack of by-products and fairly fast kinetics attest for the overall utility of the reaction. More specifically in peptide chemistry, a great deal of versatility is doable due to the ease of introduction of both cysteine and the CPD at the *N*-terminus of a growing peptide chain. Additionally, other polyamides such as PNAs have also been successfully utilized in a similar fashion without any further trouble.

On the oligonucleotide counterpart, a higher degree of commitment is required. Firstly, a cysteine amidite needs to be synthesized since no commercial supply is currently available. Additionally, even though the methodology to deprotect the thiol of cysteine-oligonucleotides is not complex, poor solution stability of the free thiol and overall higher difficulty when employing fully deprotected H-Cys-oligonucleotides, makes it a considerably more challenging endeavor.

2.6 Preparation of doubly conjugated peptide involving one CPD-Cys reaction

As discussed in the introductory chapter of this dissertation, within the field of bioconjugation a considerable number of well-stablished reactions are currently available and many research groups are engaged in developing new methodologies or improving existing one. Within this framework, the topic of multiple derivatizations is still an underexplored issue. Bioconjugations involving more than one

derivatization require the use of at least two "click-type" reactions, either sequentially or simultaneously in order to obtain doubly derivatized biomolecules.[24,25] In both instances there are two possibilities: making use of two distinct reactions, with their intrinsic pros and cons, or a single one performed successively. The latter alternative is often not as attractive since the reactants either need to exhibit different reactivities (by being placed in different environments or because the reactive groups are not identical), or must be shielded with orthogonal protecting groups that will be removed under carefully controlled conditions in order to achieve the desired selectivity.[26]

In this context, we envisioned expanding the repertoire of conjugation possibilities by making use of the already explored CPD-Cys reaction in conjunction with either another Michael addition of thiols, a CuAAC reaction or, less extensively explored, an oxime ligation. Each of the combinations will be discussed below.

2.6.1 Double conjugations involving CPD-Cys and maleimide-thiol reactions

The Michael addition of thiols onto maleimides has been the focus of extensive studies and has been used for a great variety of purposes.[27] As already discussed, it consists in the conjugate addition of a thiol the β-carbon of an α,β-unsaturated carbonyl (or an equivalent reagent such as a nitro, sulfone, etc (see **Section 1.3.7**) rendering a thioether linkage.

Having examined the reactivity of the CPD moiety, (see **Section 2.2**) we wondered whether we could make use of the preferential reaction of CPDs with 1,2-aminothiols to doubly derivatize a two-cysteine containing peptide. The idea was to carry out first the CPD-Cys reaction, followed by the classic Michael addition of a thiol to a maleimide.

2.6.1.1 Background information

In previous proof-of-principle experiments and during his Ph.D. thesis, Omar Brun synthesized two peptides; one containing an *N*-terminal cysteine H-Cys-Ser-Tyr-Ala-Lys-Tyr-Gly-NH_2 (H-CSYAKYG-NH_2, **2.38**) and another with a cysteine in an internal position H-Lys-Tyr-Ala-Tyr-Cys-Gly-NH_2 (H-KYAYCG-NH_2, **2.70**). In his test, he added 1.2 equiv. of a CPD derivative (**2.71**) to a solution containing equimolar concentrations of both peptides and observed the outcome at short and long reaction times by HPLC analysis. At short reaction times, he observed the expected formation of an M-20 adduct (**2.72**) with the H-CSYAKYG-NH_2 peptide, and a small quantity of the Michael-adduct (**2.73**) as a result of the reaction of the CPD with the peptide containing a cysteine in an internal position (H-KYAYCG-NH_2). After longer reaction times, only the expected M-20 adduct (**2.73**) and disulfide peptide **2.74** were present in the crude. After several other trials, he concluded that the selective derivatization of peptides containing *N*-terminal cysteines in the presence of other thiols employing CPDs was feasible.[8] Thus, the possibility for doubly derivatizing mixtures of peptides was made feasible (**Scheme 2.16**).

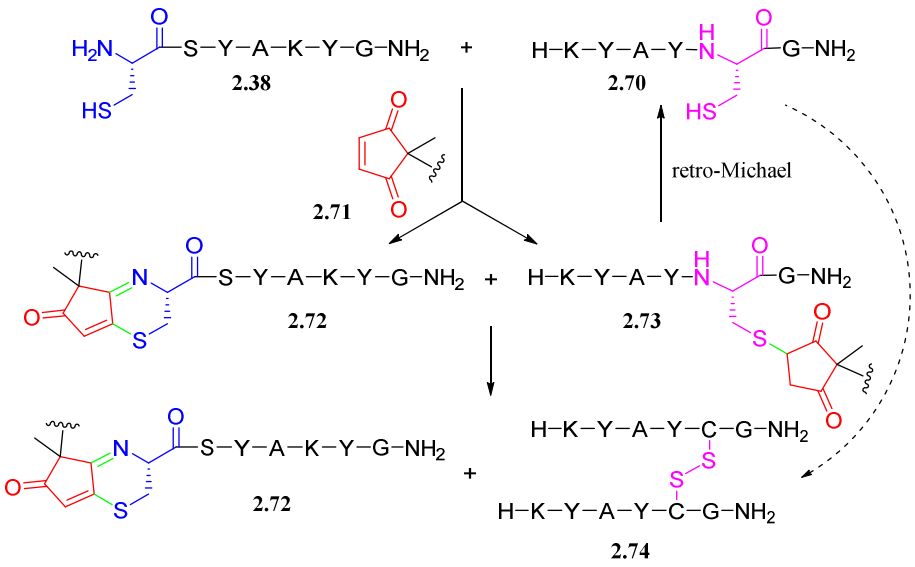

Scheme 2.16 Reaction between a CPD (**2.71**) and two peptides with differently placed cysteines. At short reaction times compounds **2.72** and **2.73** are formed, whereas after a longer incubation time **2.73** reverts to **2.70**, which evolves into **2.74**.

After assessing the preference of CPDs for non-acylated 1,2-aminothiols, we inferred that it could be exploited to prepare a peptide bis-conjugate by using a peptide scaffold containing both an *N*-terminal and internal cysteine. (**2.75**, **Scheme 2.17**) We predicted that if the ratio between peptide and CPD was equimolar (or a little excess of CPD was present), virtually all the CPD would react with the *N*-terminal cysteine, and even though some CPD-internal cysteine adduct (**2.77**) could be formed, the free thiol (**2.76**) would react with the maleimide (**2.78**) and yield the desired doubly derivatized peptide (**2.79**) in a one-pot manner, irrespective of the initial amount of CPD used.

This hypothesis was demonstrated by Dr. Brun in a proof-of-principle experiment carried out with a peptide incorporating two cysteine residues H-Cys-Ser-Try-Ala-Cys-Lys-Try-Gly-NH_2 (CSYACKYG-NH_2, **2.75**), of which one at the *N*-terminus, was reacted first with CPD-COOH (**2.20**) for 30 min and 3-maleimidopropanoic acid (5 equiv., **2.78**) was added afterwards and reacted for an additional hour. The desired model doubly-derivatized peptide (**2.79**) was successfully obtained in a 44% yield.

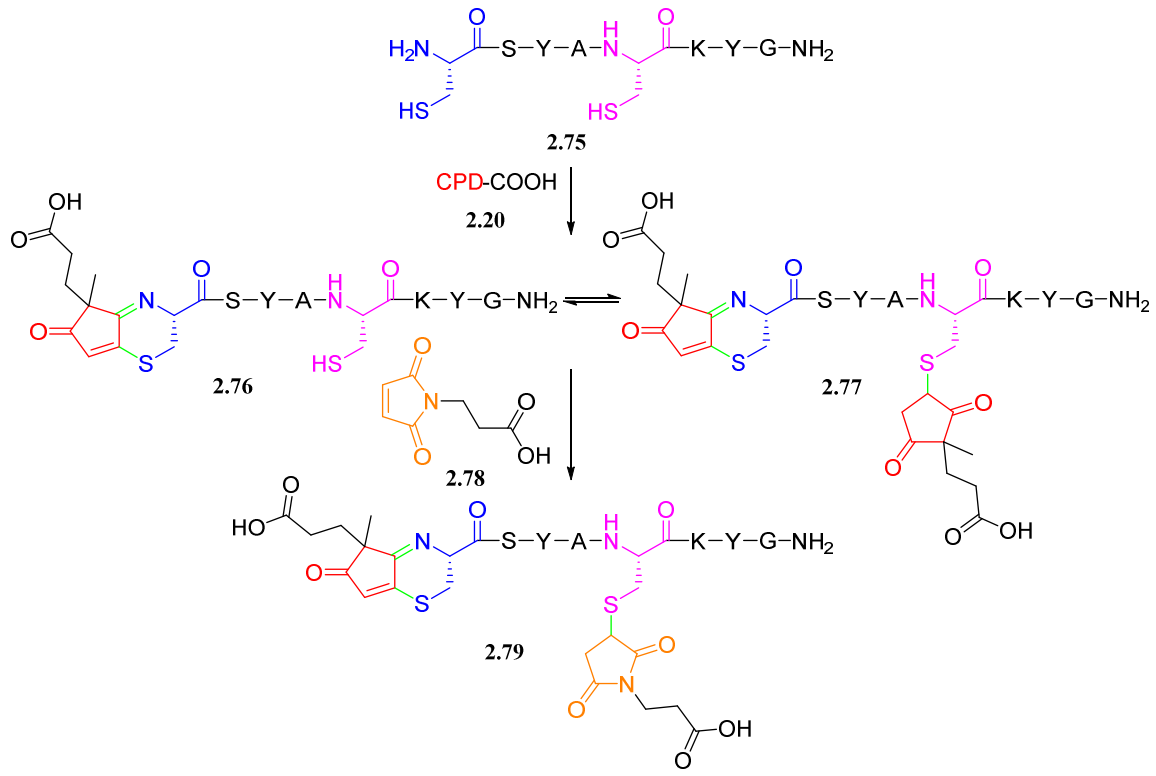

Scheme 2.17 Outline for the regioselective double derivatization of a peptide containing an *N*-terminal and an internal cysteine.

2.6.1.2 Double thiol-based conjugates

In this study we used the peptide H-Cys-Trp-Gly-Arg-Gly-Cys-NH_2 (H-CWGRGC-NH_2, **2.80**), which incorporated residues not present in any of the previous experiments such as tryptophan and arginine. The peptide (**2.80**) was incubated with 1.1 equiv. of CPD-biotin (**2.23**) for 2 h at 37 ºC and, afterwards 3 equiv. of a maleimido-derivatized PNA Mal-gtttc-Lys-NH_2 (**2.78**) was added and reacted for 1 additional hour (**Scheme 2.18**).

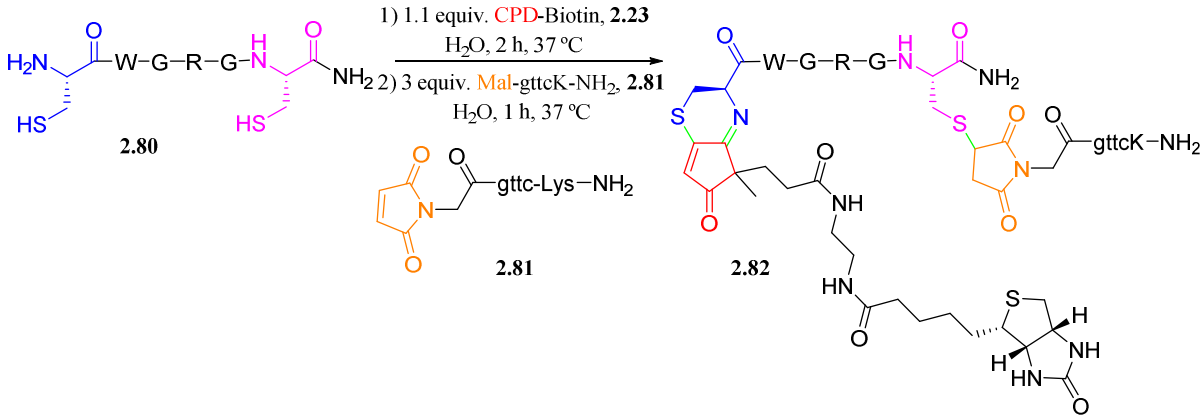

Scheme 2.18 Double derivatization of peptide (**2.80**) with CPD-biotin (**2.23**) and a maleimido derivatized PNA (**2.81**).

The reaction crude at the 2 h mark showed formation of the expected M-20 adduct (data not shown), and after addition of the maleimide-derivatized PNA **2.81** and an additional hour formation of two new peaks was observed (**Figure 2.14**, left). It is worth recalling that the two conjugation reactions generate new stereocenters, and therefore formation of a mixture of stereoisomers is not unexpected. Characterization was carried out after isolation (**Figure 2.14**, right) of the two new compounds by MALDI-TOF MS analysis. The double conjugation process had taken place in good yield (29% isolated target compound).

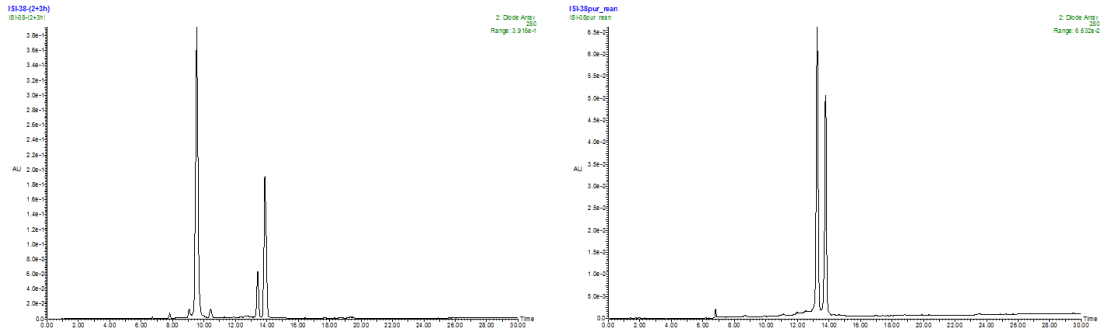

Crude Pure

Figure 2.14 HPLC profiles (280 nm) of double conjugate crude (left) and purified (right).

For further confirmation another similar experiment was carried out, utilizing the same peptide scaffold (**2.80**), a CPD-derivatized PNA (CPD-catgtcat-Lys-NH_2, **2.34**) and a commercially available maleimido-fluorophore (**2.80**, **Scheme 2.19**).

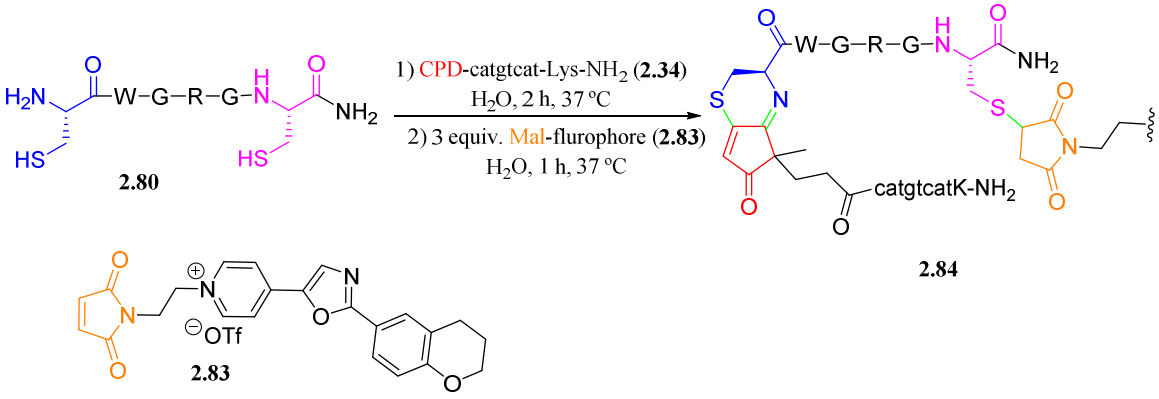

Scheme 2.19 Double derivatization of the H-CWGRGC-NH_2 (**2.80**) peptide with CPD-PNA (**2.34**) and a maleimido-derivatized fluorophore (**2.84**).

As in the previous experiment M-20 formation was quantitatively assessed by HPLC at the 2 h mark and, upon addition of 3 equiv. of maleimido-fluorophore (**2.80**) complete conversion to the target double conjugate (**2.84**) was assessed by HPLC after 1 h (**Figure 2.15**, left). Analogously as before, characterization was carried out by MALDI-TOF MS analysis of the purified double conjugate (**2.84**, **Figure 2.15**, right).

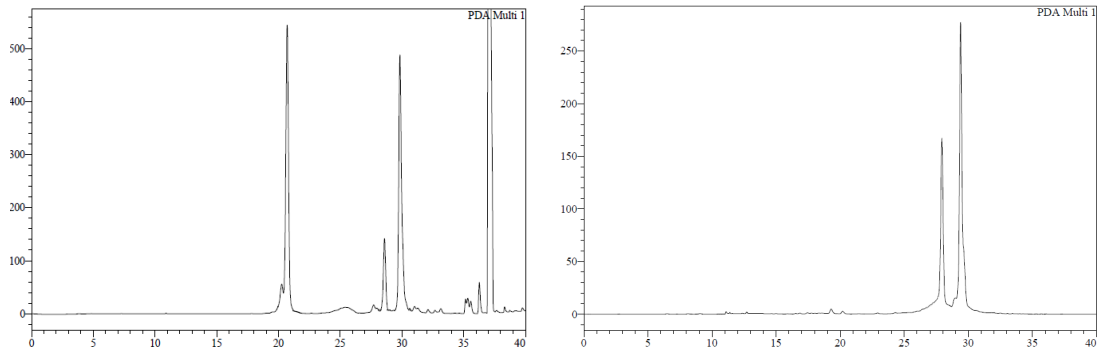

Crude Pure

Figure 2.15 HPLC profiles (254 nm) of double conjugate crude (left) and purified conjugate (right).

2.6.1.3 Concluding remarks

The hypothesis of running double conjugations by means of sequential "click" reactions had proven feasible, complementing the experimental basis conducted by Omar Brun during his Ph.D. thesis. In this work, the CPD-Cys reaction followed by the Michael addition of thiols to maleimides has allowed us to doubly derivatize peptides containing an *N*-terminal and an internal cysteine.

The double conjugation has proved to be feasible in a mild aqueous environment, at physiological pH and temperature and taken place in yields sufficiently high to be regarded as a good approach in the bioconjugation field.

That being said, this approach suffers from some drawbacks. Firstly, the order of the reactions is strictly locked since the CPD-Cys reaction has to precisely be performed in first instance otherwise the maleimide tag would irreversibly react with all available thiol nucleophiles present in the scaffold. Additionally, since we are taking advantage of the maleimide-thiol Michael addition, the resulting adduct has the associated problems of stability in regards to succinimide hydrolysis and possible thiol exchange (see **Section 2.1**). Nonetheless, this strategy has proved to be a straightforward, easy and reliable methodology to obtain double conjugates of peptides.

2.6.2 Double conjugation involving CPD-Cys and CuAAC reactions

After successfully observing the selective double derivatization of cysteines by CPD-Cys and Michael-type reactions, we wondered whether it would fit within the realm of possibility to combine the CPD-Cys reaction with other ligation chemistries. In this instance, we started combining the CPD-Cys reaction with the cycloaddition between an alkyne and an azide catalyzed by Cu(I) (CuAAC), since it is still a widely used click reaction.

2.6.2.1 Background information

In order to carry out double conjugations using CuAAC, either an alkyne functionality or an azide have to be appended from the side chain of an amino acid residue, since either the CPD or the cysteine ought

to be at the *N*-terminus. Another important aspect to consider is the possibility of certain side-reactions taking place. It is known that the azide functionality does not withstand thiols under certain reaction conditions because, thiols may reduce azides[28] and are also known to be prone to oxidation under CuAAC conditions to either disulfides (**2.85**), sulfenic (**2.86**), sulfinic (**2.87**) or cysteic acids (**2.88, Figure 2.16**).[29]

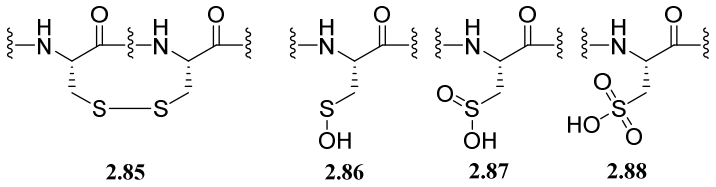

Figure 2.16 Possible oxidation by-products of cysteine residues under CuAAC conditions.

Protection of the cysteine residue could eventually solve this problem, but the whole procedure would imply a higher number of synthetic steps. Yet, this alternative was not within the scope of this research project.

2.6.2.2 Double conjugates of peptides incorporating an alkyne and an *N*-terminal cysteine

With all this information in mind, we envisioned carrying out a lysine modification to incorporate the alkyne moiety within its side chain. As depicted in **Scheme 2.20**, starting from the commercially available Fmoc-Lys-OH (**2.89**) and 4-pentynoic acid (**2.90**), the desired lysine derivative (Fmoc-Lys(Alk)-OH, **2.91**) was obtained by reaction with 4-petnynoic acid, with the carboxyl group previously activated with isobutyl chloroformate as reported before..

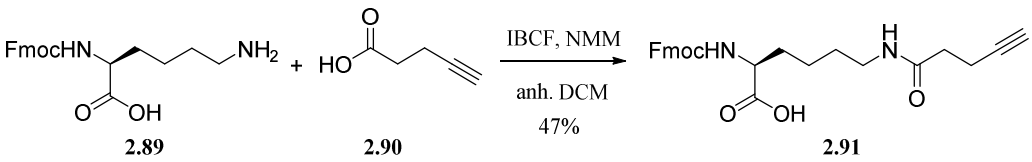

Scheme 2.20 Synthesis of alkyne-containing lysine derivative.

After obtaining the Fmoc-Lys(Alk)-OH monomer, peptide H-Cys-Ser-Tyr-Ala-Lys(Alk)-Ala-Lys-Gly-NH_2 (H-CSYA**K***YG-NH_2 **2.92**, where **K*** is the alkyne-derivatized lysine residue) containing both the alkyne moiety and an *N*-terminal cysteine, was synthesized using standard SPPS conditions. Crude **2.92** showed excellent purity after HPLC analysis (**Figure 2.17**), and was used without further purification.

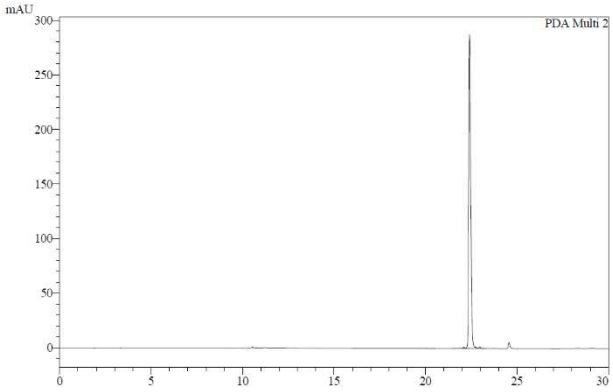

Figure 2.17 HPLC trace (280 nm) of the alkyne-derivatized peptide crude.

Subsequentially, as depicted in **Scheme 2.21**, we investigated if the CPD-Cys reaction could be performed with an alkyne functionality present and, eventually, subsequently reacted with an azide. To test it out, we incubated peptide CSYA**K***YG-NH_2 (**2.92**) with 1.2 equiv. of CPD-COOH (**2.20**), following the same previously described experimental conditions (3 h at 37 ºC).

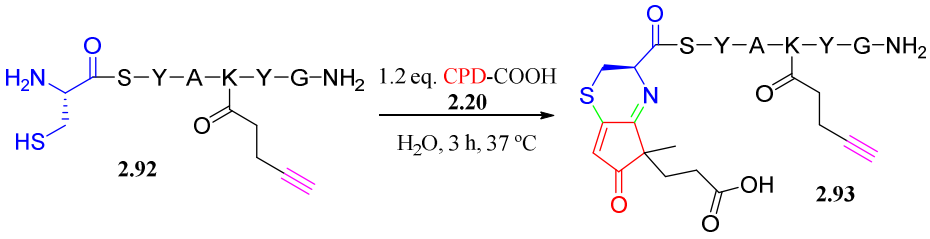

Scheme 2.21 First step in the preparation of a doubly derivatized peptide making use of CPD-Cys and CuAAC reactions.

Gratifyingly, the reaction proceeded cleanly as expected. Success in the ligation (**2.93**) was confirmed by HPLC-MS analysis (**Figure 2.18**).

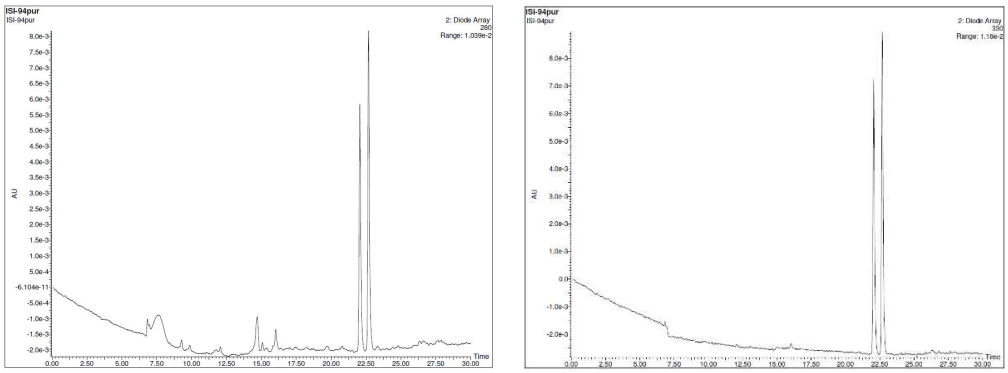

HPLC trace at 280 nm HPLC trace at 330 nm

Figure 2.18 HPLC traces (280 nm, left; 330 nm, right) of the M-20 adduct (**2.93**) resulting from the reaction between H-CSYA**K***YG-NH_2 (**2.92**) and CPD-COOH (**2.20**).

After isolation, the M-20 adduct **2.93** was subjected to reaction with equimolar amounts of $CuSO_4$ and TBTA, an excess of sodium ascorbate (NaAsc, a sacrificial reducing agent that allows the reactive Cu(I) to be obtained) and AZT (**2.94**) in H_2O (**Scheme 2.22**).

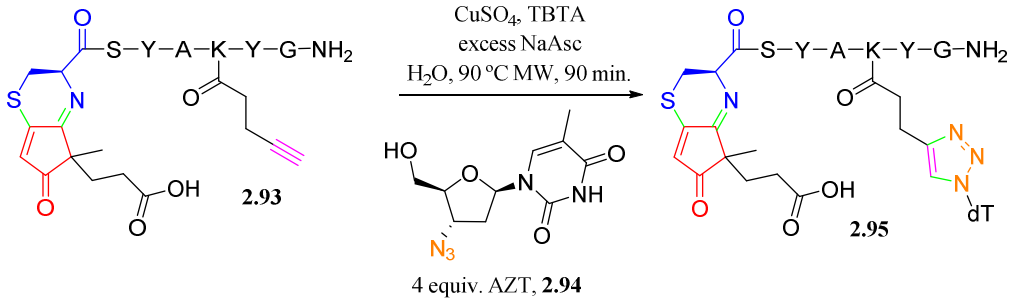

Scheme 2.22 CuAAC reaction between M-20 adduct (**2.93**) and AZT (**2.94**) to obtain doubly derivatized peptide (**2.95**).

In order to conduct the experiment in reasonable conjugation times, a MW oven was employed for this first attempt (heating at 90 ºC for 90 min). HPLC-MS analysis of the reaction crude (**Figure 2.19**) showed clean conversion displaying the expected doubly derivatized product (**2.92**) as assessed by MS.

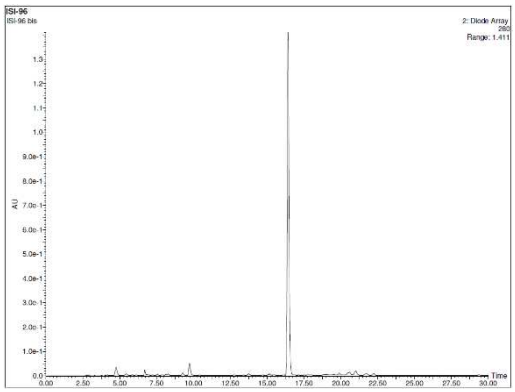

Figure 2.19 HPLC trace (280 nm) of the crude obtained by CuAAC reaction between M-20 adduct (**2.93**) and AZT (**2.94**).

This preliminary experiment suggested that the CuAAC could safely be carried out after the CPD-Cys reaction, implicating that the M-20 adduct formed after the CPD-Cys reaction withstood the CuAAC reaction conditions. Laia Saltor, a bachelor student at that time, was tasked to further confirm and complete this result, for which purpose another peptide was synthesized with sequence H-Cys-Tyr-Asn-Arg-Tyr-Lys(Alk)-Ala-Val-Ser-Leu-NH_2 (H-CYNRY**K***AVSL-NH_2, **2.96**). Both **2.92** and **2.96** were reacted with several CPDs (**2.20**, **2.23**, **2.34**) furnishing the corresponding M-20 adducts (**2.93, 2.97** and **2.98**) in all cases. These adducts were subsequently reacted with either AZT (**2.94**) or an azide-containing PNA (**2.97**) as shown in **Scheme 2.23** in order to obtain the desired double conjugates (**2.95**, **2.100** and **2.101**).

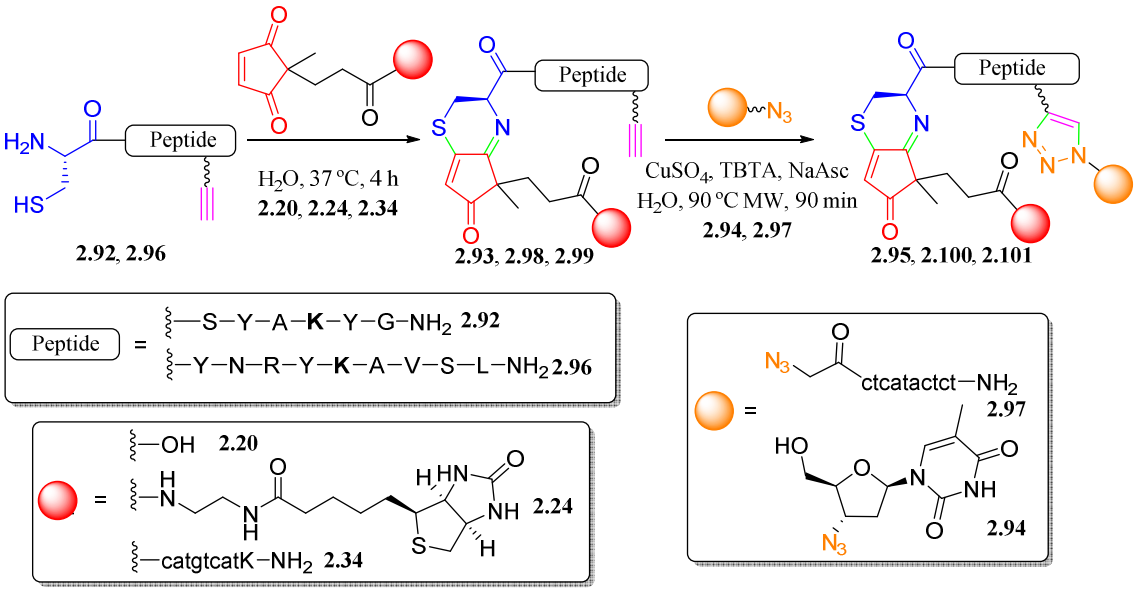

Conjugation Reactions

	CPD-Cys	Simple conjugate	CuAAC	Double conjugate
2.92 + 2.20	→	2.93 + 2.94	→	2.95
2.92 + 2.24	→	2.98 + 2.97	→	2.100
2.96 + 2.34	→	2.99 + 2.94	→	2.101

Scheme 2.23 Synthetic scheme for the obtention of double conjugates from peptides containing *N*-terminal cysteines and alkynes.

Afterwards, we sought to investigate the outcome of altering the order of both reactions, that is to perform first the CuAAC and then the CPD-Cys reaction. As previously stated, free thiols are expected to not withstand the oxidative stress generated by Cu(I) ions. In order to assess whether the orfder of the conjugation reactions could be reversed, we reacted H-CYNRY**K***AVSL-NH_2 (**2.96**) and AZT (**2.94**) in typical CuAAC conditions (**Scheme 2.24**). HPLC-MS analysis of the crude showed a significant amount of 3'-aminodeoxythydimine and quantitative formation of disulfide peptide incorporating two AZT moieties (data not shown) instead of the expected adduct (**2.102**). Detection of "click" adducts was rationalized by the fact that we had used an excess of azide (4 equiv.), and after reduction of the azide to amine the mixture still contained azide that reacted with the alkyne. Therefore, the target **2.102** could only be obtained by using an excess azide (instead of equivalent amount) and subsequent reduction of the disulfide (followed by separation of the reducing agent). Altogether, this double conjugation alternative would be much less straightforward than the previous one.

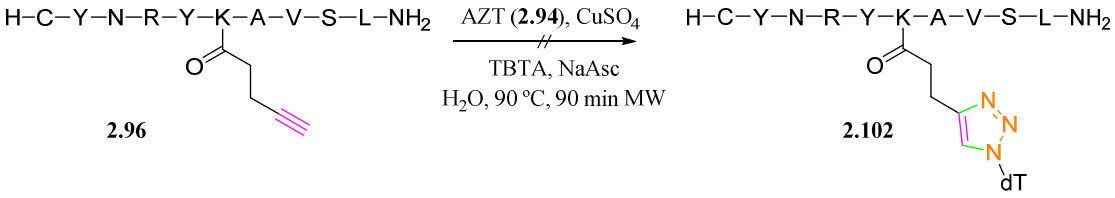

Scheme 2.24 Exploration of the compatibility of the CuAAC reaction with thiol groups.

2.6.2.3 Double conjugates of peptides incorporating and alkyne and a CPD

To formally complete the positive results previously obtained we investigated the double conjugation procedure on peptides with an appending a CPD moiety at the *N*-terminus instead of a cysteine residue. Since the presence of an alkyne on peptides H-CSYA**K***YG-NH_2 (**2.92**) and H-YNR**K***AVSL-NH_2 (**2.96**) had not shown any interference with the CPD-Cys reaction, keeping the same order for the two conjugation reactions, was expected to also work in this case. The sequences used for this study were CPD-Lys-Ala-Lys(Alk)-Ser-Tyr-Gly-Tyr-NH_2 (CPD-KA**K***SYGY-NH_2, **2.103**) and CPD-Tyr-Asn-Arg-Tyr-Lys(Alk)-Ala-Val-Ser-Leu-NH_2 (CPD-YNRY**K***AVSL-NH_2, **2.104**).

Both peptides, were first reacted with another peptide containing an *N*-terminal cysteine (either H-CYG-NH_2, **2.37**, or H-CSYAKYG-NH_2, **2.38**) under the usual CPD-Cys reaction conditions. After isolation of the respective M-20 adducts (**2.105**, **2.106**), a CuAAC reaction with AZT (**2.94**) furnished the two double conjugates (**2.107** and **2.108**, respectively, **Scheme 2.25**).

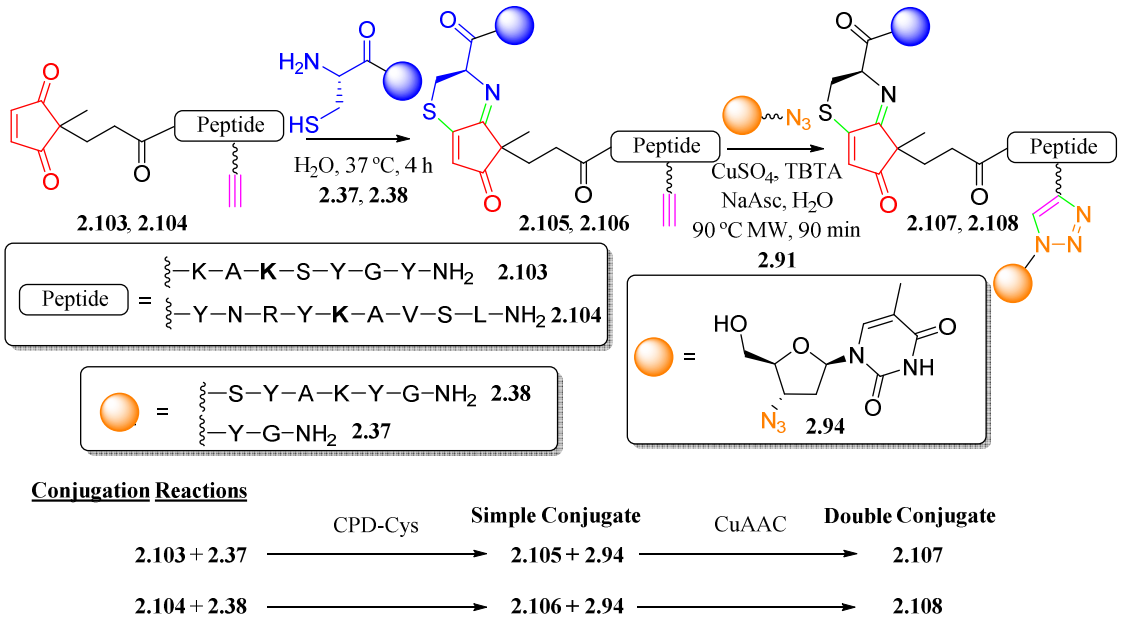

Scheme 2.25 Synthetic scheme for the obtention of double conjugates from peptides containing *N*-terminal CPDs and alkynes.

As previously explained, the CuAAC had to be and was performed after the CPD-Cys reaction. Again, the adduct resulting from the CPD-Cys reaction was perfectly compatible with the CuAAC. To complete the information available, decided to explore the compatibility of CPDs with the CuAAC reaction. For this purpose, we envisioned performing the CuAAC on CPD-YNRY**K***AVSL-NH_2 (**2.103**) with AZT (**2.94**) firstly and, subsequently, the reaction with an *N*-terminal cysteine (**Scheme 2.26**).

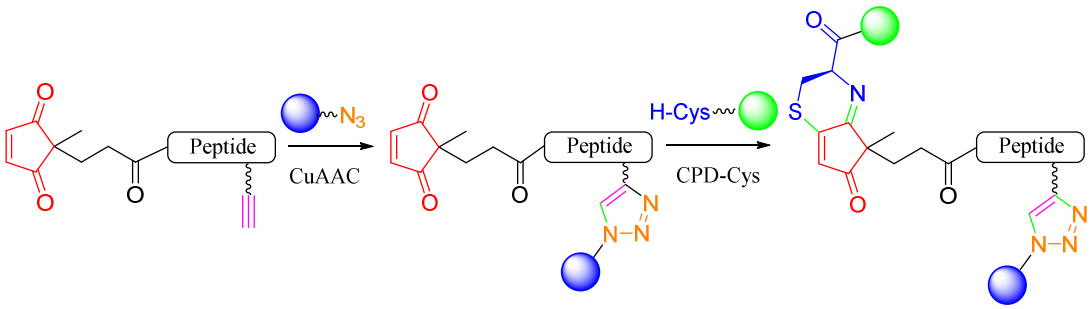

Scheme 2.26 Outline for double conjugations employing the CuAAC followed by the CPD-Cys reaction in peptides containing an *N*-terminal CPD and an alkyne.

Employing the same reaction conditions previously described, the CuAAC reaction between peptide **2.104** and AZT (**2.94**) furnished a complex crude in which the target conjugate was a minor compound that could not be isolated (**Figure 2.20**). This seggested, among other possibilities, some incompatibility between azides and CPDs. Another possibility was that the CPD moiety did not withstand the CuAAC reaction condtions.

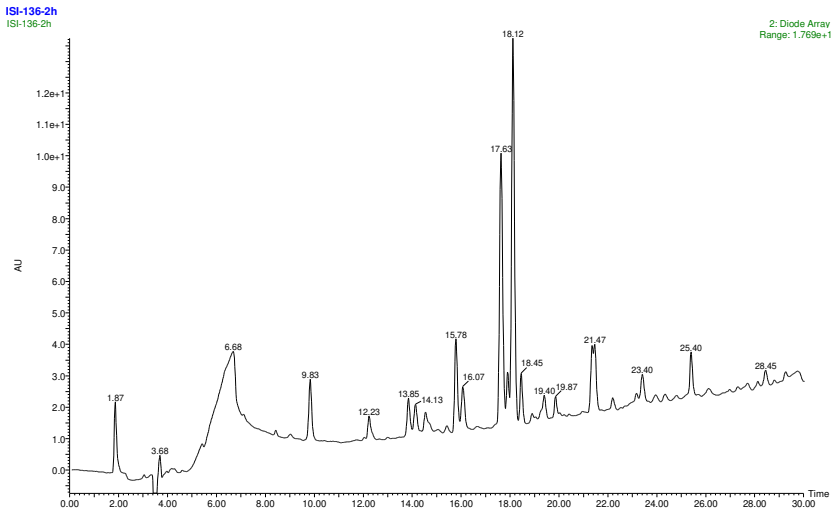

Figure 2.20 HPLC-MS trace (280 nm) of the crude from the reaction between AZT (**2.94**) and CPD-YNR**K***AVSL-NH_2 (**2.104**) under previously utilized CuAAC conditions.

Observing this complex crude, we considered worthwhile to explore the applicability of the reaction involving azides and CPDs. With this goal in mind, we reacted simple and synthetically available CPD-COOH (**2.20**) and AZT (**2.94**) for the identification of the products formed. In a first experiment, equimolar amounts of reactants were incubated in MeOH:H_2O (1:1) at 90 ºC in a MW oven, and the reaction progress was monitored by HPLC-MS at the hour and 3 h marks (**Figure 2.21**).

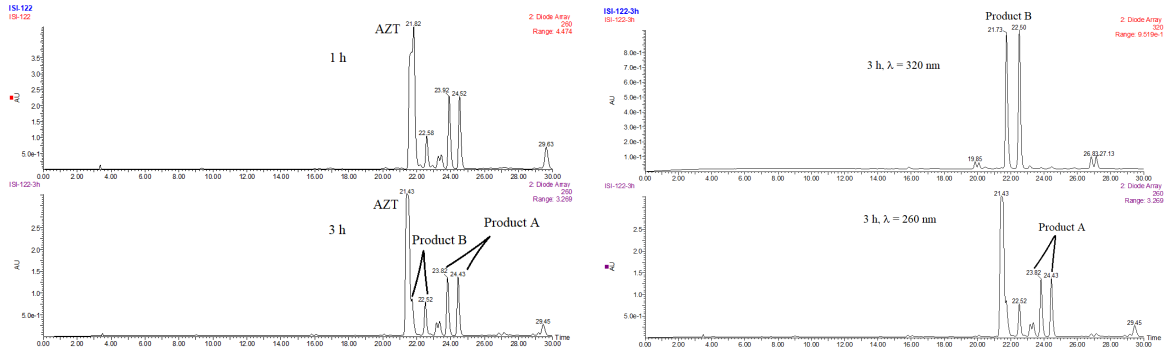

Figure 2.21 HPLC-MS traces (260 nm, left) of the reaction between CPD-COOH (**2.20**) and AZT (**2.94**) at 1 and 3 h mark and HPLC traces (320 nm or 260 nm, right) at the 3 h mark.

At the hour mark, in addition to starting material, the presence of four main products was observed (**Figure 2.21**, left). Of these newly formed products, two showed coinciding masses, and the same happened to the other two, suggesting two pairs of stereoisomeric compounds. One pair of compounds displayed a mass spectrum in agreement with the expected [3+2] cycloaddition reaction (*m/z* = 449.97 Da), whereas the other pair exhibited a mass 28 Da lower, indicating loss of molecular nitrogen (*m/z* = 421.96 Da) (**Figure 2.22**, left). The latter, had an UV-Vis absorption maximum at 320 nm, which suggested a structure similar to that of the CPD (**Figure 2.22**, right).

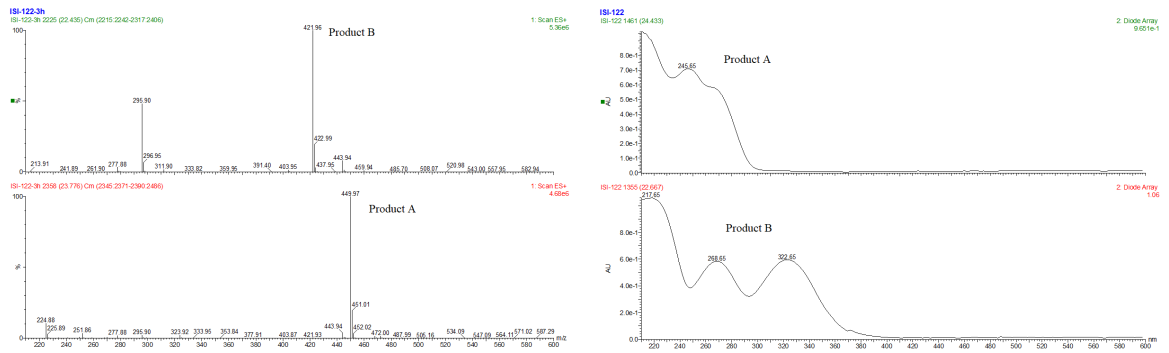

Figure 2.22 MS (left) and UV-Vis spectra (right) of the products composing both set of peaks, respectively.

Observing these results, we sought to investigate the possibility of identifying a set of reaction conditions to yield selectively one of both sets of compounds, and use this reaction as a new conjugation method. In a search for an optimized procedure, we performed a screening of several reaction conditions. Even though it is described in the literature that 1,3-dipolar cycloadditions experience little solvent effect[30] we screened on different solvents and different temperatures and reaction times as shown below in **Table 2.1**. In this instance we conducted the experiments with equimolar amounts of azide and CPD at 1 mM concentrations.

Entry	Solvent	Reaction conditions
1	MeOH	90 ºC, MW, 90 min
2	MeOH	60 ºC, MW, 90 min
3	MeOH	Reflux, on.
4	H_2O	90ºC, MW, 90 min
5	DMF	120 ºC, 3h

Table 2.1 Solvent and great conditions screening for the CPD-Azide reaction.

This little screening showed no differential effect on the reaction kinetics or final yield in the conditions tested, and starting material could still be observed by HPLC in all cases. On the other hand, searching for an improvement of kinetics, we tested a variety of different conditions, here depicted in **Table 2.2**. Addition of TEMPO (to oxidize the possible hydroxyl resulting from the cycloaddition and drive the reaction to completion), a chaotropic agent (LiCl) or Lewis acids[31] including Al^{3+}, Mg^{2+} or Zn^{2+} all were unfruitful to drive the reaction to completion. We tested DBU[32] (entry 14, **Table 2.2**) expecting an effect similar to aniline catalysis in oxime formation[33] but also proving to be unsuccessful and rapidly degrading the CPD moiety. Additionally, different Cu catalysts were also tested with no better results.

Entry	Solvent	Reaction conditions	Additive
1	H_2O	90 ºC, MW, 90 min	TEMPO
2	H_2O	90 ºC, MW, 90 min	H-Cys-OMe
3	H_2O	90 ºC, MW, 60 min	$AlCl_3$
4	H_2O	90 ºC, MW, 90 min	$MgCl_2 \cdot 6H_2O$
5	H_2O	90 ºC, MW, 90 min	LiCl
6	H_2O	90 ºC, MW, 90 min	$MgCl_2$, LiCl
7	H_2O	90 ºC, MW, 60 min	$CuSO_4$, NaAsc, TBTA
8	H_2O	40 ºC, 72 h	$MgCl_2$ + LiCl
9	H_2O	40 ºC, 1 h	DBU
10	H_2O	60 ºC, 1 h	$CuCl_2$, LiCl
11	H_2O	60 ºC, 1 week	Cu (nanopart.), LiCl
12	H_2O	60 ºC, 72 h	Cu (nanopart.), $CuCl_2$, LiCl
13	H_2O	60 ºC, 3 h	$ZnCl_2$

Table 2.2 Other reaction conditions tested for the CPD-azide reaction.

An important fact found with this screening was the impact of heat on the reaction outcome. Overall, higher temperatures favored formation of the denitrogenated compounds and yield more complex mixtures, while milder conditions seemed to promote formation of the cycloadduct but required longer reaction times to be pushed forward. A compromise temperature of 60 ºC was used in subsequent tests, since it seemed to be the best to promote cycloaddition formation and keeping denitrogenation in check, while reaction progress still took place in a reasonable time frame. Nonetheless, still no reaction could be driven to completion even after prolonged times (entry 11 and 12, **Table 2.2**).

Observing these setbacks, we decided to tackle the problem with a different approach and decided to reproduce conditions from a study by Mersbergen *et al*. on 1,3-dipolar cycloaddition of benzonitrile oxide with various dipolarophiles in aqueous solutions.[34] One of their points in the study was to assess the effect of anionic micelles on the cycloaddition kinetics. Sodium dodecyl sulfate (SDS) proved to exert a beneficial effect increasing the second-order rate constant observed above a critical concentration of 8.2 mM, with a linear correlation with higher concentrations. They rationalized this phenomenon by hydrophobic dipole-dipolarophile interactions with the micellar surface, thus reducing the entropic factor of the reaction. On this basis, we investigated the use of SDS in our reaction (100 mM concentration), accompanied by additions of an excess of both reactants (entries 3 and 4, **Table 2.3**). Unfortunately, these conditions did not prove to fully complete the reaction either.

Entry	Solvent	Reaction conditions	Other (SDS 100 mM)
1	H_2O	60 ºC, on	-
2	H_2O	60 ºC, MW, 60 min	-
3	H_2O	60 ºC, 5 h	10 equiv. CPD
4	H_2O	60 ºC, 5 h	10 equiv. AZT

Table 2.3 Results of the CPD-azide reaction using SDS and reactant excesses.

In general, the addition of 100 mM SDS into the reaction mixture seemed to lightly favor the [3+2] cycloaddition, yielding cleaner crudes (as assessed by HPLC), but still no complete consumption of reactants was observed. Another possibility tested was the use of other azides (**2.109**, **2.110, Figure 2.23**) and CPD (**2.111**, **Figure 2.23**) in the optimal reaction conditions of 100 mM SDS, 60 ºC in H_2O.

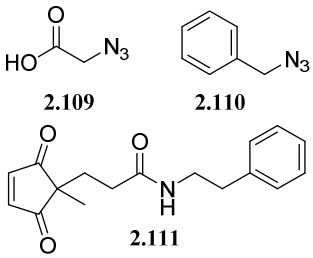

Figure 2.23 Additional organic azides and CPD tested in the CPD-azide reaction assays.

The main idea behind using other azides was to evaluate whether the electronic effect of the benzyl group, (**2.110**) or the decreased steric hinderance when using primary azides (**2.109**) or sodium azide instead of the secondary azide of AZT (**2.94**) had an impact on the evolution of the reaction. None of these reactions occurred with greater success (**Table 2.5**).

Entry	Solvent	Reaction conditions	Azide
1	H_2O	60 ºC, 24 h	Azidoacetic acid (**2.109**)
2	H_2O	90 ºC, 5 h	Azidoacetic acid (**2.109**)
3	H_2O	60 ºC, 24 h	NaN_3
4	H_2O:MeOH (1:1)	60 ºC, 14 h	BnN_3 (**2.110**)
5^{Ψ}	MeOH	60 ºC, 24 h	BnN_3 (**2.110**)

Table 2.2 Additional azides and CPD tested for the CPD-Azide reaction. $^{\Psi}$CPD = **2.111**.

In summary, the reaction could not be driven to completion in any of the tested conditions. None of the solvents or additives examined, other than SDS, proved to be beneficial for the reaction. In regards to temperature, higher temperatures under MW irradiation turned out to be better for the formation of the denitrogenated compound, but also produced a more complex crude. Yet, milder conditions seemed to favor cycloaddition products. Additionally, use of other chemically different azides or excesses of either the CPD or the azide did not seem to substantially influence the reaction outcome. Taking all this data into account, we concluded that even though CPDs react with azides, it seemed not worth pursuing optimization of the reaction conditions for bioconjugation purposes since it did not fulfill most of "click-like" requirements.

2.6.2.4 Structure elucidation of the main products formed upon CPD-azide reaction

It has been long known that azides react with alkenes to furnish Δ^2-triazolines, usually undergoing different transformations including ring expansion and ring contraction.[35,36] This fact provided the initial basis for the analysis of the outcome of the reaction between CPDs and azides.

The main adducts formed upon reacting CPD-COOH and AZT, two pars of stereoisomeric compounds, were purified by HPLC. The target compounds were isolated from the crudes yielding mainly each of the desired pairs. As explained below, from spectroscopic data analysis we concluded that the compounds formed had the structures shown in **Figure 2.24**. In both cases, a mixture of isomers was obtained, since both the monocyclic (**2.112**) and the bicyclic (**2.113**) adducts contain one or two stereocenters, respectively, without defined configurations.

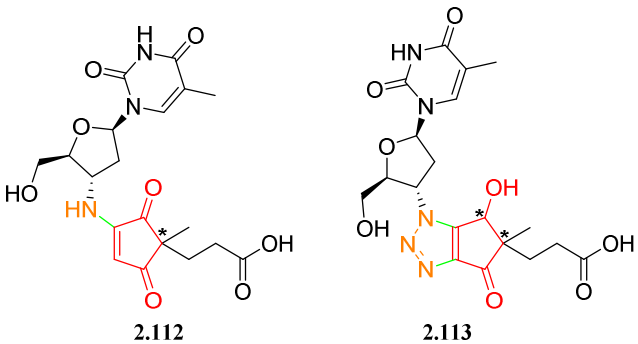

Figure 2.24 Isolated products from reaction between AZT (**2.94**) and CPD-COOH (**2.20**).

2.6.2.4.1 Elucidation of the structure of the products resulting from the cycloaddition (bicycles)

The first pair of compounds analyzed had *m/z* ratios in agreement with the expected adduct after a [3+2] dipolar cycloaddition reaction (*m/z* = 449.97 Da). Upon isolation and characterization by NMR (^{1}H, ^{13}C, HSQC and HMBC), some data did not fit with those expected for a compound simply resulting from a [3+2] cycloaddition. For the [3+2] cycloaddition we expected a Δ^2-triazoline and the coupling between the protons of the bridgehead atoms (**2.114**, **Figure 2.25**) to be observed.

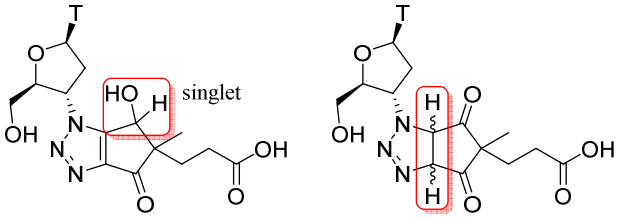

Figure 2.25 Structures and diagnostic coupling of the product expected from a simple [3+2] CPD-azide cycloaddition.

Upon ^{1}H NMR analysis, we observed a singlet with a chemical shift ~5.21 ppm (**Figure 2.26**, left), in clear disagreement with to the multiplicity expected for the bicyclic compound. Moreover, the ^{13}C NMR spectrum (**Figure 2.26**, right) did not provide support either for the triazoline structure due to lack of sp^3 carbons. The HSQC spectrum confirmed the conclusions reached so far

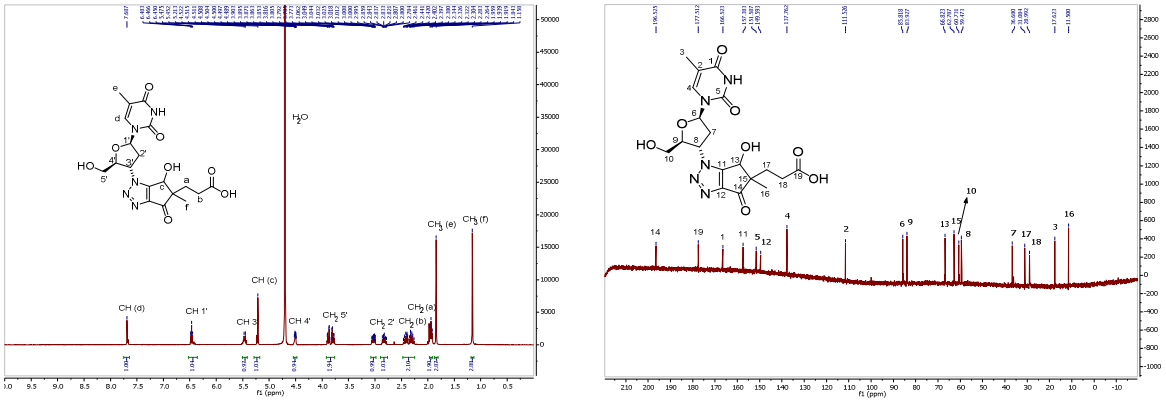

Figure 2.26 Assigned ^{1}H NMR (400 MHz, left) and ^{13}C (101 MHz, right) of the bicyclic adduct in D_2O.

The HMBC spectrum (**Figure 2.27**) shed some light on this puzzling conflict. Upon careful examination, a correlation between the 3' proton (3' at the ^{1}H axis) of the deoxyribose ring and a quaternary carbon of the bicyclic system (C_{T1}, marked in green in the figure) was observed. Moreover, the ~5.21 ppm singlet (CH at the ^{1}H axis) correlated with the first ring-linked methylene of the propanoyl appendage, the quaternary carbon of the CPD moiety (C_q) and two additional quaternary carbons exhibiting chemical shifts different from those of carbonyl groups (C_{T1} and C_{T2}, **Figure 2.27**), providing evidence that we had indeed a triazole structure instead of a triazoline.

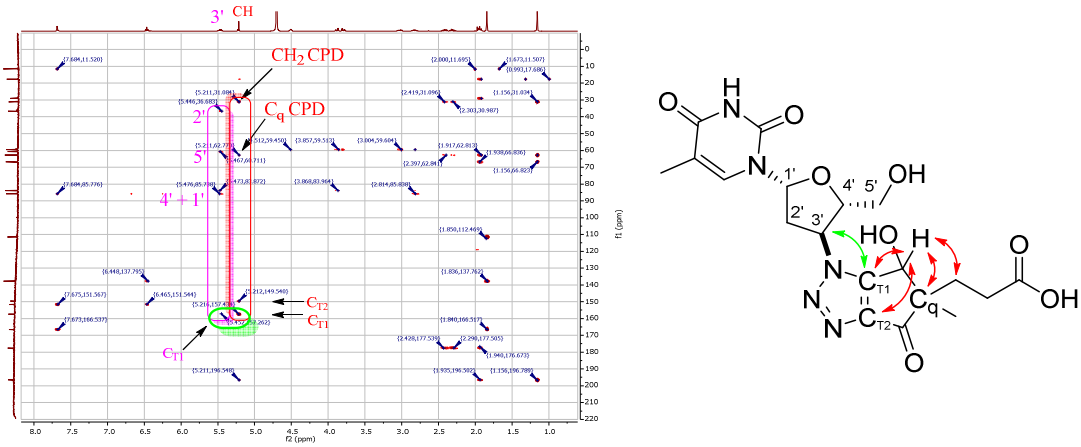

Figure 2.27 Key correlations observed within the HMBC spectrum of the bicyclic adduct in D_2O (^1H-^{13}C 400, 101 MHz, left) shown on the proposed structure (right).

2.6.2.4.2 Elucidation of the structure of the denitrogenated products (monocycle)

In order to gain some insight into the structure of the other adduct, which displayed a mass of 28 Da lower, we proceeded in a similar fashion as previously discussed.

Looking at the NMR spectra of the purified compounds (**Figure 2.28**), two clear differences with the previous spectra were observed. Firstly, the characteristic peak (olefinic CH) of the CPD moiety appeared at ~6.06 ppm, a bit upfield as compared to the chemical shift of the only proton identified in the CPD part of the bicyclic adduct (~5.21 ppm). Secondly, the 3' CH chemical shift value was about ~4.34 ppm, significantly lower than its counterpart (~5.47 ppm). One more the assignments done at this point were confirmed by the HSQC spectrum.

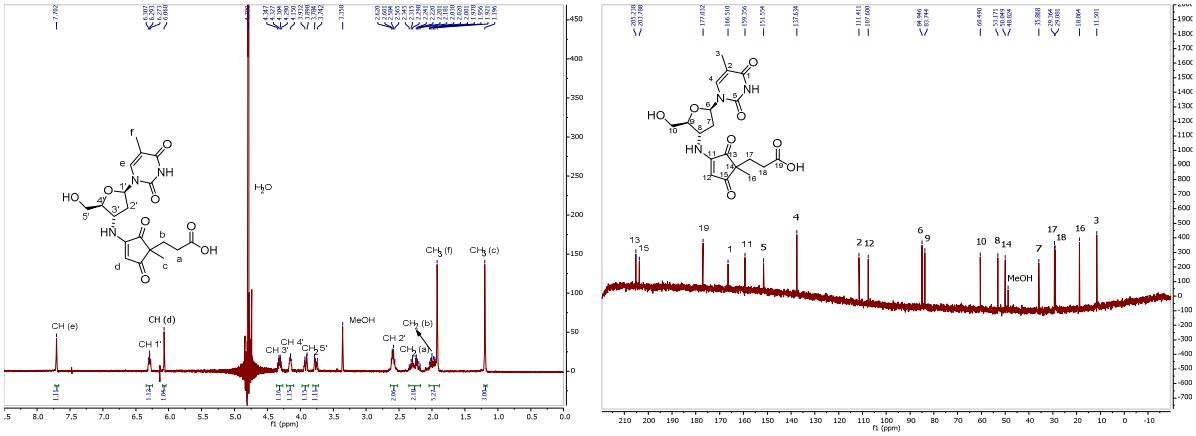

Figure 2.28 ^1H NMR (400 MHz, left) and ^{13}C (101 MHz, right) of the enaminic adduct in D_2O.

Definitive evidence supporting our proposal was observed again within the HMBC spectrum. As it can be seen in **Figure 2.29**, the olefin hydrogen present in the CPD-derived ring (CH at the ^1H axis) correlates with the vicinal quaternary carbon (C_E) and a keto group (C=O), and the quaternary carbon of the same 5-membered ring (C_q). Moreover, the hydrogen linked to the 3' carbon in the deoxyribose ring (3' at the ^1H axis) shows a 3-bond correlation with C_E (marked in green at the HMBC spectrum), providing solid evidence for the proposed structure.

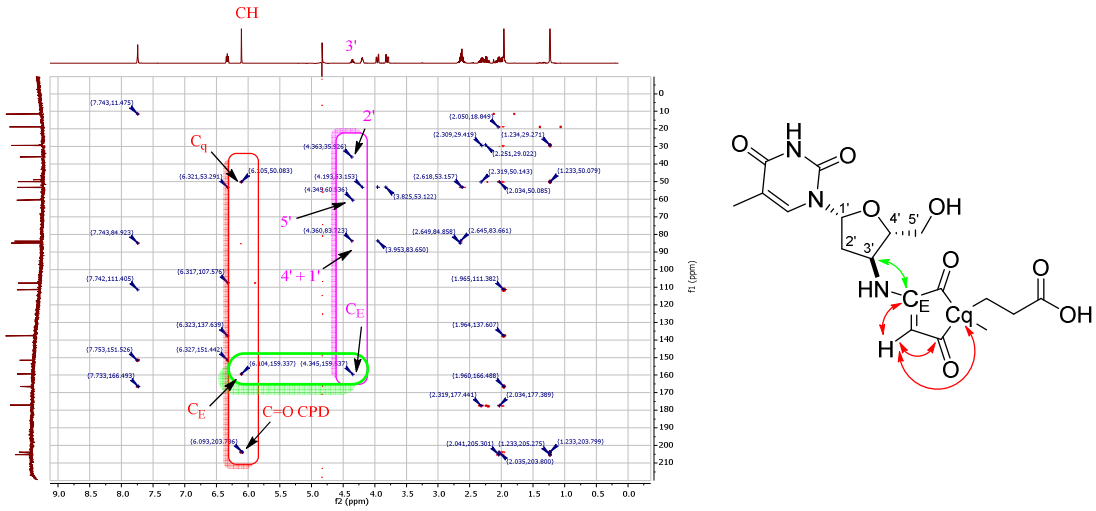

Figure 2.29 HMBC spectrum (left) and key correlations (left) for the identification of the structure of the denitrogenated compounds in D_2O (^1H-^{13}C 400, 101 MHz). On the right, this is shown on the compound structure.

This structure is additionally supported by UV-Vis data, since an absorbance maximum around 320 nm (see **Figure 2.22**) appears at the spectrum of the denitrogenated compounds. This is consistent with three conjugated double bonds in a ring, similarly to the previously studied M-20 adduct.

2.6.2.4.3 Plausible mechanism for the CPD-azide reaction

The 1,3-dipolar cycloaddition between the CPD-moiety and an azide will likely give rise to formation of a di-keto intermediate (**2.114**), which under mild thermic conditions, undergoes a keto-enol tautomerization to yield **2.115** and isomerization to the observed **2.113**. The latter is in all probability driven by aromatic triazole formation. On the other hand, if harsher conditions are employed **2.114** may decompose to give a diazonium intermediate (**2.116**). Loss of nitrogen from this betaine intermediate ends up into an imine derivative (**2.117**) which tautomerizes to the more stable and observed enamine form (**2.112, Scheme 2.27**).

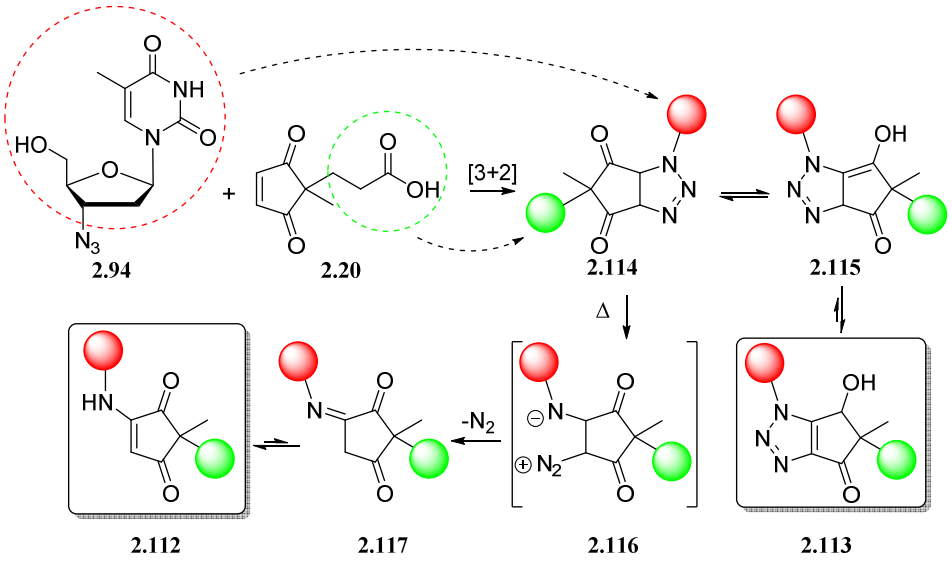

Scheme 2.27 Structures of the main products formed after reacting CPD-COOH (**2.20**, the green ball represents the CH_2CH_2COOH substituent) and AZT (**2.94**, the red ball includes the 2',3'-dideoxyribose and thymine), and plausible steps for the formation of the experimentally observed compounds.

2.6.2.4.4 Concluding remarks

Similarly to the first double conjugation experiments already reported in this chapter, the results described in this section demonstrate that the CPD-Cys and CuAAC reactions can be combined to obtain double conjugates provided that the two reactions are carried out in a precise order. The CPD-Cys reaction must be performed first, and a purification step is required before conduction the CuAAC in order to prevent formation of undesired products by reaction of the azide and possible unreacted CPD. Therefore, this double conjugation alternative is less straight forward than the previously touched which involves two Michael additions (see **Section 2.6.1**).

In conclusion, by carrying-out the CPD-Cys reaction before the CuAAC, polyamides with an appending alkyne and either a CPD or cysteine at the *N*-terminus can undergo two subsequent click conjugation reactions and, therefore, incorporate two new moieties. In addition, closer inspection at the results of he reaction between CPDs and azides, has revealed that they can react and, after having experienced a 1,3-dipolar cycloaddition, yield new compounds incorporating either a triazole ring or an enamine as inferred from spectroscopic evidence. That being said, the CPD-azide reaction could never be driven to completion by any tested means. Thus, it is not a good approach for bioconjugation.

2.6.3 Double conjugation combining the CPD-Cys and oxime formation reactions

As discussed in the introduction of this dissertation, the oxime ligation is achieved by reaction between an α-nucleophile, that is an alkoxyamine, and the carbonyl group of an aldehyde or a ketone. Oxime ligation is believed to provide more stable conjugates respective to hydrazone formation.[37] Another important aspect that tipped the balance in favor of this approach was the ease of the reaction: no catalysis or additional reagents usually are needed in the ligation to provide the desired linkage.

Moreover, the reaction is usually described as high-yielding and biocompatible making it a great candidate for double conjugations.

2.6.3.1 Preliminary reactions with model compounds

The first question to address was whether we could take advantage of the free carbonyl moiety in the "M-20" scaffold (**2.118**, depicted in red) to further react the "M-20" bicycle with a hydroxylamine derivative (**2.119**) in order to perform an oxime ligation (**Scheme 2.28**). The aim was to perform two "click" reactions as previously reported with the CPD-Cys and Michael reactions to furnish double conjugates in a one-pot manner. The reactants in this case would be a CPD, an *N*-terminal cystine and an alkyoxiamine.

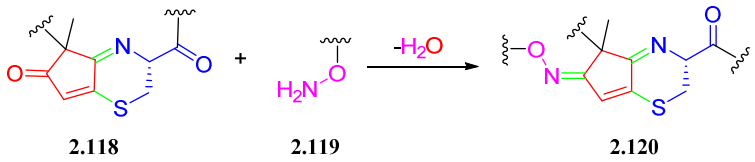

Scheme 2.28 Initially envisioned double conjugation strategy involving CPD-Cys and oxime formation reactions.

Initial screening of reaction conditions involved the use of a model M-20 adduct (**2.121**) and hydroxylamine hydrochloride (**2.122**). Experimental conditions comprised of a one-pot synthesis first reacting CPD-COOH (**2.20**) and H-Cys-OMe (**2.36**) to furnish the M-20 adduct (**2.121**), as observed by HPLC, with a subsequent addition of $NH_2OH{\cdot}HCl$ (**2.122**) as depicted in **Scheme 2.29**. Disappointingly the reaction did not seem to yield positive results, only rendering unaltered "M-20" adduct as observed both by HPLC and MS analysis.

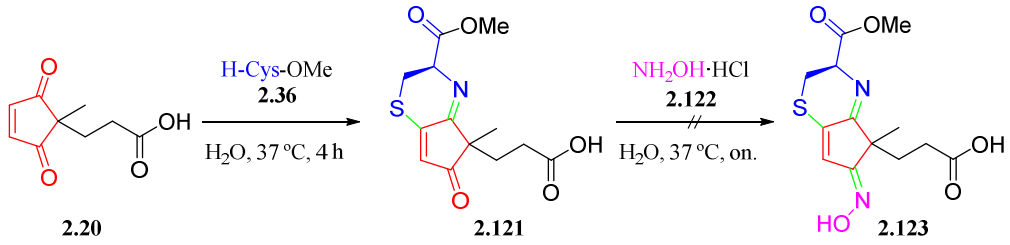

Scheme 2.29 Assessment of the reactivity of the M-20 adduct with hydroxylamine.

After this drawback, we decided to explore whether the CPD moiety would undergo reaction to yield an oxime. To test so, we incubated CPD-COOH (**2.20**) with 5 equiv. of $NH_2OH{\cdot}HCl$ (**2.122**). After overnight reaction at 37 ºC no significant changes were found (data not shown). Classically oximes are formed by refluxing a carbonyl compound with hydroxylamine and pyridine in an alcoholic solution.[38] Therefore, we reacted CPD-COOH (**2.20**) with $NH_2OH{\cdot}HCl$ (**2.122**) in MeOH with 5 equiv. of pyridine at 60 ºC (**Scheme 2.30**). In this instance, the reaction took place, but instead of reacting with one carbonyl group, the double oxime (**2.124**) compound was formed.

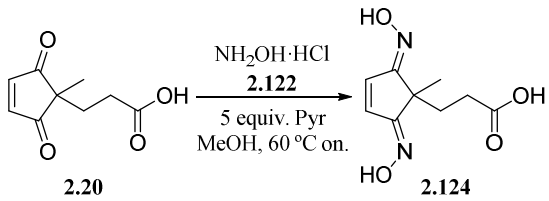

Scheme 2.30 Oxime formation between CPD-COOH (**2.20**) and $NH_2OH·HCl$ (**2.124**) under pyridine catalysis.

In retrospective, this result was somehow expected since two carbonyl moieties are available to undergo reaction with hydroxylamine. The positive point of this experiment was that the CPD only underwent the oxime formation with pyridine catalysis and heating. No conjugate addition was found, thus providing the basis for a double conjugation procedure involving oxime formation on the carbonyl of either the CPD or the M-20 adduct (should conditions for rendering it reactive were found).

2.6.3.2 Assays with doubly functionalized peptides

With these preliminary results, Bence Barna, an Erasmus student at that time, was appointed to synthesize a peptide incorporating a commercially available lysine derivative containing a Boc-protected aminooxy acetyl (AoA) functionality and the CPD moiety, CPD-Tyr-Lys(AoA)-Gly-NH_2 (CPD-YK(AoA)G-NH_2, **2.127**) in hopes of taking advantage of both functionalities for producing double conjugates (**Scheme 2.31**). As previously reported, the CPD moiety was appended at the *N*-terminus by standard SPPS. After acidic treatment to cleave and deprotect the fully protected peptide (**2.125**) a complex mixture was obtained, where products whose mass was 18 Da lower (*m/z* = 585.4 Da) and 26 Da higher (*m/z* = 629.4 Da) that the expected difunctionalized peptide (**2.127**, *m/z* = 603.3 Da) were detected among other side products. Formation of the first undesired product was attributed to intramolecular cyclization, since oxime formation is accompanied by H_2O loss (**2.128**). The other product was identified as resulting from the reaction of the alkyoxyamine group with acetaldehyde traces present in the ACN used for HPLC-MS analysis[39] to yield the corresponding oxime (**2.129**).

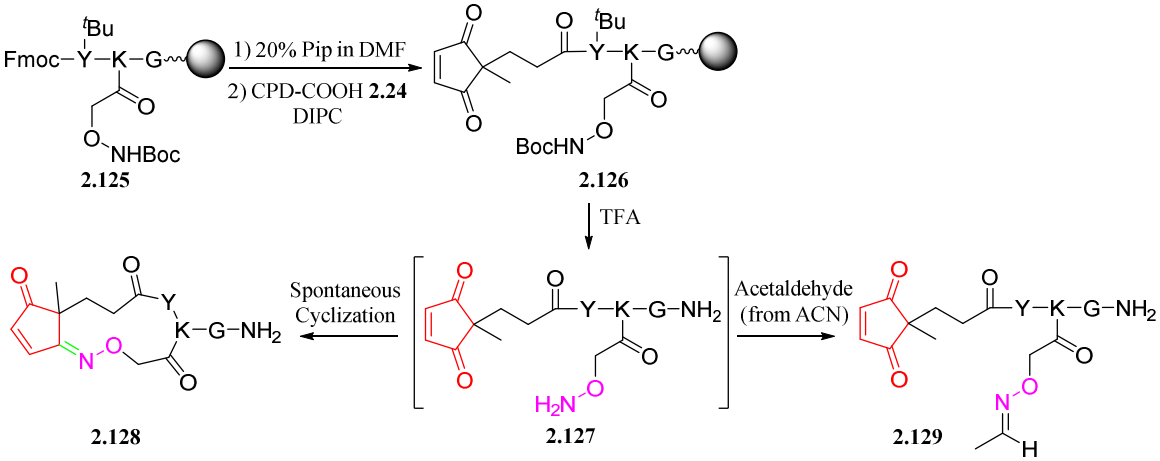

Scheme 2.31 Synthetic scheme for the obtention of peptide derivatized with a CPD and an aminooxy functionality.

Subsequently, another Erasmus student, Rebecca Ginesi was tasked to try and circumvent this shortcoming by synthesizing a peptide containing an *N*-terminal cysteine instead of a CPD (**Scheme**

2.32). The sequence was similar to the previous one, H-Cys-Lys(AoA)-Tyr-Gly-NH_2 (H-CK(AoA)-YK-NH_2, **2.130**). Upon cleavage and deprotection a clean crude was obtained, with a single product (as assessed by HPLC-MS) whose mass was 26 Da higher (*m/z* = 568.4 Da) than expected (*m/z* = 542.2 Da), similarly to the results previously found. Nonetheless, a small aliquot of **2.130** was reacted with vanillin (**2.131**) before any contact with acetonitrile, in order to provide the oxime monoconjugate (**2.132**). After purification, peptide (**2.132**) was reacted with CPD-COOH (**2.20**). The desired double conjugate (**2.133**) could be obtained after this two-step procedure but in low yield.

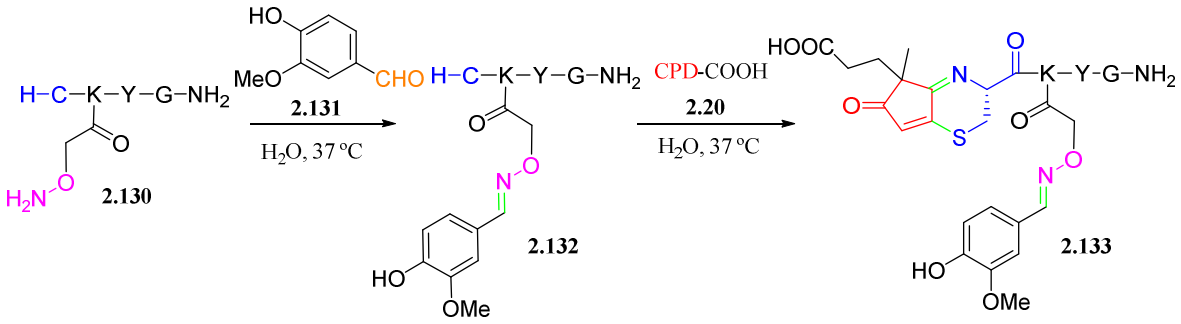

Scheme 2.32 Use of Cys and aminooxy functionalities for double derivatizations of peptides.

Even though this approach turned out to be feasible, simply the fact that alkoxyamine-containing crude peptides cannot be purified using standard elution systems makes it less practical than others. We do not know to what extent may the acetaldehyde traces present in ACN block the alkoxyamine, but even if it is low it is an inconvenience. Additional efforts to improve this approach and make it good enough so as to compete with other already established methodologies were considered unsuitable within the framework of this PhD thesis.

2.7 One-pot derivatization and cyclization involving CPDs

Cyclization of biomolecules is another important backbone modification, commonly employed to increase the stability of "naked" biomolecules towards enzyme-promoted degradation or as a structural preorganization tool in order to enhance the affinity for target motifs.

Cyclic peptides can be found in nature playing very different roles: from human hormones, as oxytocin and somatostatin, to natural venoms such as amanitins[40] and phalloidins[41] (both found in *Amanita Phalloides*). Cyclic peptides have been tested for the regulation of protein-protein interactions, such as preventing amyloid fibrils formation, a process involved in Alzheimer's, Huntington's and Parkinson's disease. An example of a natural cyclic peptide antibiotic are polymyxins, which disrupt the structure of bacterial cell membrane in Gram-negative bacteria.

Cyclic peptides have also found their spot in the antitumor fight. Octreotide is currently used in the treatment of neuroendocrine tumors,[42] and the so-called "RGD peptides" have been used to direct drugs to cancer cells by exploiting recognition of the RGD motif by integrins, which are overexpressed in these cells.[43]

In a similar way, over the past few years, cyclic oligonucleotides have been explored as potential drugs with increased nuclease resistance, as well as exhibiting better recognition properties both for diagnostic and therapeutic applications.[44] That being said, the cyclization of oligonucleotides is not as

straightforward as that of peptides. This fact is evident by looking at the amount of described procedures for peptides in comparison to oligonucleotide cyclization.[45] That is why providing novel methodologies for cyclization and derivatization of oligonucleotides is a sought-after topic.

In this context, given the importance of having good methodologies for peptide and oligonucleotide cyclization, we considered the possibility of exploiting the well-behaving CPD-Cys reaction to cyclize peptides and oligonucleotides.

2.7.1 Background information

Omar Brun, during his Ph.D. thesis, described a methodology for the cyclization and derivatization of peptides utilizing the CPD scaffold.[8,46] The strategy relied on the reaction of a CPD (**2.135**) (either derivatized or not) with a peptide containing two cysteines, of which at least one at the *N*-terminus (**2.134**), in order to sequentially perform a CPD-Cys with the *N*-terminal cysteine and, once the M-20 adduct (**2.136**) was formed, reaction with the other thiol present in the peptide would construct the cyclic adduct (**2.137**) *via* a second Michael addition (**Scheme 2.33**). Since no cyclization was observed during the double CPDC-Cys and Michael conjugate assembly (see **Section 2.6.1**) and given the fact that some additions of thiols to alkenes can be radicalary processes, a radical initiator was added to assist in the second Michael reaction.

Out of the myriad of available reagents, TEMPO was selected as an additive to the reaction for its commercial availability, its known stability and the ability to participate in radicalary oxidative transformations.[47] After several experiments Dr. Brun found out several key parameters to take into account. Foremost, the preferred unnatural "D" configuration of the *N*-terminal cysteine and the use of a chaotropic agent such as Li^+ was found to be beneficial for cyclization rates. On the other hand, the influence of peptide sequence was be taken into consideration since peptides containing an aromatic residue next to the *N*-terminal cysteine were found to cyclize slower.

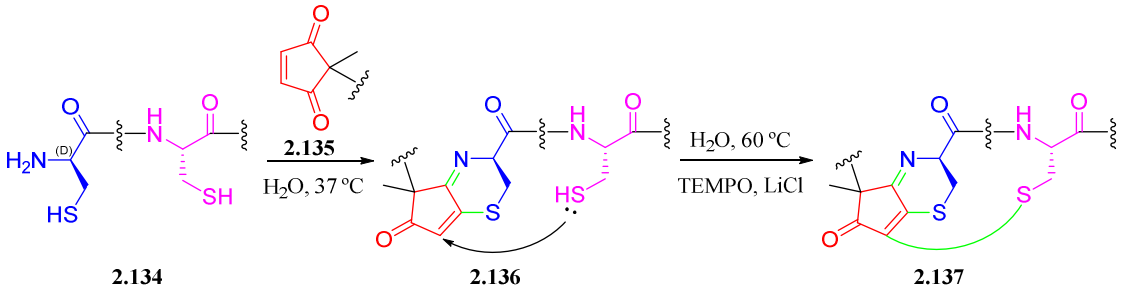

Scheme 2.33 Cyclization of two cystine-containing peptides *via* CPD-Cys reaction.

2.7.2 Peptide cyclization

In order to complete Dr. Brun's work, a peptide with sequence H-(D)Cys-Ser-Lys-Ala-Tyr-Gly-Cys-Tyr-Gly-NH_2 (H-(D)CSKAYGCYG-NH_2, **2.138**) was reacted with CPD-COOH (**2.20**) and once the M-20 adduct was found to be formed (by HPLC analysis), increasing amounts of TEMPO were added following optimized procedures. The desired cyclic compound was satisfactorily obtained (**2.139**, **Scheme 2.34**).

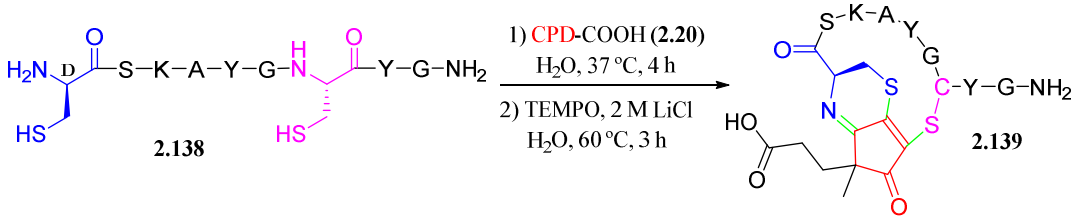

Scheme 2.34 Cyclization of peptide H-(D)CSKAYGCYG-NH_2 (**2.138**) with CPD-COOH (**2.20**).

The conclusion to this brief follow-up study is the reproducibility of Omar Bruns's work to synthesize a larger size cycle than those previously prepared.

2.7.3 Oligonucleotide cyclization

After the success in the cyclization in peptides, we decided to evaluate whether it was possible to transport this methodology to oligonucleotide chemistry, in a similar way as previously discussed with the CPD-Cys reaction (see **Section 2.5.2**). The first concern was whether TEMPO would oxidize the nucleobases.[48,49] In order to assess whether the previously optimized conditions were incompatible with oligonucleotides, a nucleobase-deprotected H-Cys(S^{t}Bu)-21mer oligonucleotide, previously employed in simple conjugations (see **Section 2.5.2**) was incubated with a 2 M aqueous solution of LiCl and increasing amounts of TEMPO (0.2 equiv. every 20 min up to 1 equiv.). This test was carried out utilizing a protected cysteine-oligonucleotide derivative to prevent formation of thiol oxidation by-products such as disulfide, sulfenic, sulfinic or cysteic acids (**Figure 2.16**, **Section 2.6.2**) to be formed, which certainly prove undesirable. To our delight, the oligonucleotide suffered no major alterations even after prolonged reaction times, thus providing a proof that the cyclization could in principle be carried out safely. As depicted in **Scheme 2.35**, a synthetic scheme similar to the one previously utilized for the obtention of the L-cysteine-amidite was followed (**Scheme 2.12**, **Section 2.5.2**) but, in this instance, the "D" enantiomer of cysteine was employed, since it had been was found to be a better promoter of cyclization in the case of peptides (**Scheme 2.34**).

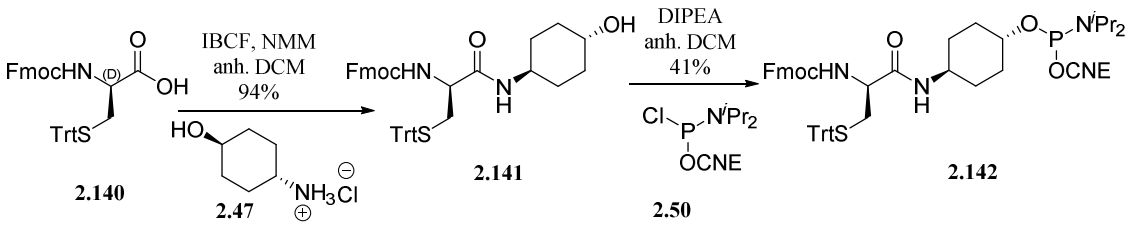

Scheme 2.35 Synthetic scheme for the obtention of the trityl-protected (D)-cysteine amidite.

As depicted in **Scheme 2.36**, a simple and not too long oligonucleotide (dT_{10}) was elongated on a commercially available 3'-thiol modified CPG (**2.143**) using standard SPONS. Subsequently, the previously obtained (D)-cysteine amidite (**2.142**) was incorporated using formerly optimized procedures (see **Section 2.5.2**) in order to obtain the fully protected Fmoc-(D)-Cys(Trt)-$d^{5'}T_{10}{}^{3'}$-SS-CPG oligonucleotide (**2.145**). Following Fmoc removal with 20% piperidine in DMF and oligonucleotide deprotection using conc. aq. NH_4OH at room temperature, an oligonucleotide analogue with the two thiols (that at the 3' end and the Cys side chain) protected (**2.145**) was obtained. Next, the deprotection procedure to remove the trityl group involved use of 5 equiv. of $AgNO_3$ and 7 equiv. of

DTT as complexing agent for the Ag^+ cations. Taking advantage of the DTT step, we proposed a tweak by employing a larger excess (50 equiv.) of DTT to both complex and reduce in a one-step procedure to satisfactorily obtain both deprotected thiols (**2.146**).

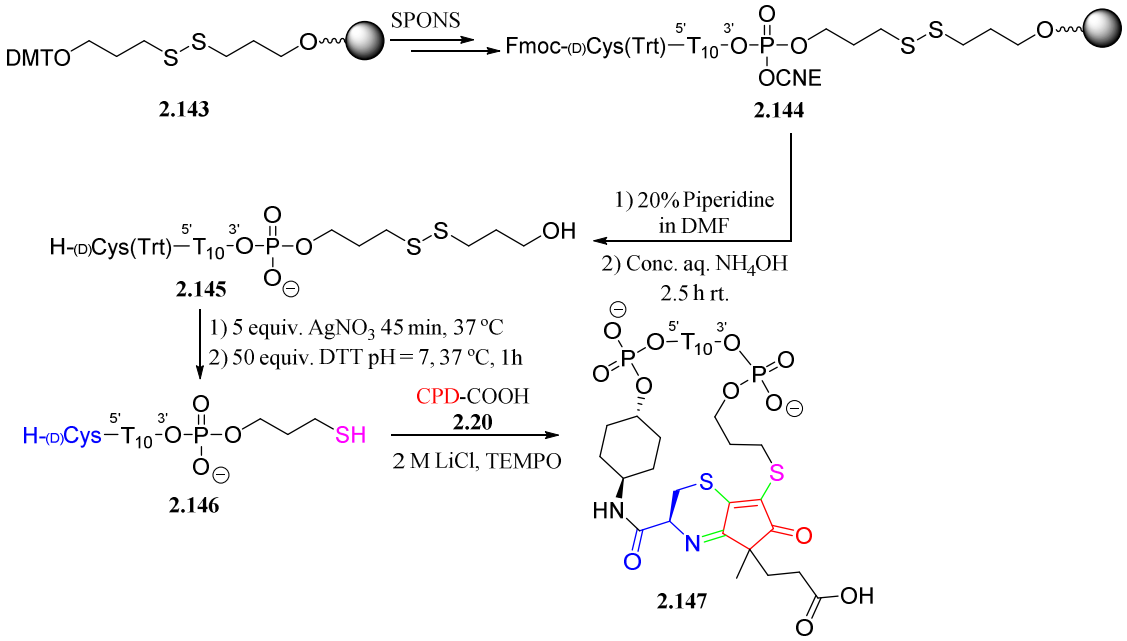

Scheme 2.36 Outline for the obtention of cyclic oligonucleotides *via* CPD-Cys derivatization and cyclization of oligonucleotides incorporating a 3'-thiol and a 5' cysteine.

Upon reaction of the two-thiol containing oligonucleotide (**2.146**) with CPD-COOH (**2.20**) under optimized peptide cyclization conditions a complex crude was obtained as depicted in the HPLC traces shown in **Figure 2.30**. The heterogeneity might have different sources, beginning with the fact that different symmetrical and nonsymmetrical disulfides may be formed upon removal of DTT. Additionally, even though the nucleobases had seemed not be affected by TEMPO, requirement for a larger cyclization time implied that both unprotected thiols might more easily get oxidized. Also, a cycle much larger than those previously assembled was expected to be formed (a 78-membered ring, while the largest peptide cycle obtained so far was 31-membered one).

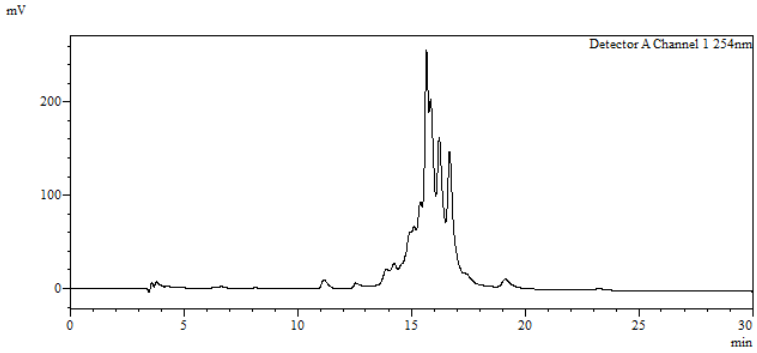

Figure 2.30 HPLC trace (254 nm) of the oligonucleotide cyclization reaction crude after 3 h.

Nonetheless, formation of cyclic diastereomeric oligonucleotides (**2.147**) was confirmed by MALDI-TOF mass spectrometry (found *m/z* = 3572.1; calcd. *m/z* = 3572.5) after isolation as can be seen in **Figure 2.31**.

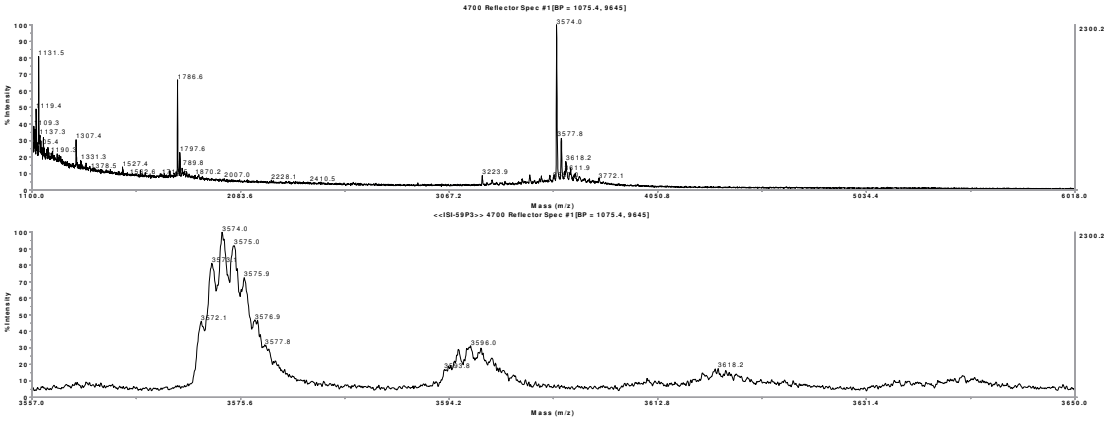

Figure 2.31 MALDI-TOF spectra of the cyclic oligonucleotide adduct.

This first attempt, proved the feasibility of obtaining cyclic oligonucleotides using CPDs, but a simple target product as a cyclic T_{10} was accompanied by many impurities. Additionally, subsequent attempts to reproduce this result were unfruitful. In none of the tested experiments following this initial "success" any cyclic oligonucleotide could be observed, only obtaining complex crudes. Therefore, we decided to abandon this idea and not to pour more efforts onto it.

2.8 Chapter overview

The novel CPD-Cys methodology developed for polyamide conjugates has been formally completed and transferred to oligonucleotide chemistry successfully.

- Adducts generated from the reaction between CPDs and *N*-terminal cysteines are stable and can be used for conjugation.
- Formation of the M-20 adduct can be performed in mild physiological conditions, fairly short times and with minimal side product contamination.
- The synthesis of CPDs linked to peptides or different reporters does not present major problems.

Double conjugates of peptides have been prepared combining the CPD-Cys reaction with several other click reactions.

- CPD-Cys and Michael addition reactions have been exploited to prepare double conjugates of peptides containing two cysteines, one at the *N*-terminus and another at an internal position.
- The CPD-Cys reaction in conjunction with the CuAAC has been explored to prepare double conjugates of peptides. Additionally, the CPDs and azides has been confirmed to react, ascertaining by spectroscopic methods the structure of the two main products formed.
- The feasibility of utilizing the CPD-Cys reaction in conjunction with the oxime ligation, has been checked, but overall it seems impractical because the starting material cannot be analyzed (and likely purified) using standard HPLC conditions.

The procedure stablished by Dr. Brun for one-pot derivatization and cyclization of polyamides with CPDs has been expanded with an additional peptide. Transfer to oligonucleotides have proved unsuccessful.

2.9 Abbreviations

ACN	Acetonitrile
Alk	Alkyne
anh	Anhydrous
AoA	Aminoxyacetyl
aq	Aqueous
AZT	3'-Azidothymidine
CNE	2-Cyanoethyl
CPD	2,2-Disubstituted cyclopent-4-ene-1,3-dione
CPD-COOH	3-(1-Methyl-2,5-dioxocyclopent-3-en-1-yl)propanoic acid
CPD-Me_2	2,2-Dimethylcyclopent-4-ene-1,3-dione
CPG	Controlled Pore Glass
CuAAC	Copper(I)-catalyzed azide-alkyne cycloaddition
Cys	L-Cysteine
DA	Diels-Alder Cycloaddition
Dansyl	5-(Dimethylamino)naphthalene-1-sulfonyl
DBU	1,8-Diazabicyclo[5.4.0]undec-7-ene
DCM	Dichloromethane
DIPC	*N*,*N*'-Diisopropylcarbodiimide
DIPEA	*N*,*N*-Diisopropylethylamine
DME	Dimethoxyethane
DMF	*N,N*-Dimethylformamide
DMT	4,4'-Dimethoxytrityl
DTT	Dithiothreitol
equiv	Equivalents
EtOAc	Ethyl Acetate
Fmoc	Fluorenylmethyloxycarbonyl
Fmoc-Lys(Alk)-OH	N^2-(((9*H*-Fluoren-9-yl)methoxy)carbonyl)-N^6-(pent-4-ynoyl)-L-lysine
HMBC	Heteronuclear Multiple Bond Correlation
HPLC	High performance liquid chromatography
HSQC	Heteronuclear Single Quantum Coherence
IBCF	Isobutyl chloroformate
^{i}Pr	Isopropyl
Lys	L-Lysine
M	Molecular mass
M-20	CPD-Cys addition adduct with a mass 20 Daltons lower
MALDI	Matrix-assisted laser desorption/ionization
MeOH	Methanol
MS	Mass spectrometry
MW	Microwave
NaAsc	Sodium ascorbate
NBS	*N*-Bromosuccinimide
NEt_3	Triethylamine

NMM	*N*-Methylmorpholine
on	Overnight
Pbf	2,2,4,6,7-Pentamethyldihydrobenzofuran-5-sulfonyl
PNA	Peptide nucleic acid
ppm	Part per million
Pyr	Pyridine
rt	Room temperature
SDS	Sodium dodecyl sulfate
SPONS	Solid-phase oligonucleotide synthesis
S^{t}Bu	*tert*-Butylthio
TBTA	Tris(benzyltriazolylmethyl)amine
^{t}Bu	*tert*-Butyl
TCEP	Tris(2-carboxyethyl)phosphine hydrochloride
TEMPO	(2,2,6,6-Tetramethylpiperidin-1-yl)oxyl or (2,2,6,6-tetramethylpiperidin-1-yl)oxidanyl
TFA	Trifluoroacetic acid
TIS	Triisopropylsilane
TOF	Time of flight
Trt	Trityl

2.10 Bibliography

(1) Renault, K.; Fredy, J. W.; Renard, P. Y.; Sabot, C. *Bioconjug. Chem.* **2018**, *29* (8), 2497–2513.

(2) Fontaine, S. D.; Reid, R.; Robinson, L.; Ashley, G. W.; Santi, D. V. *Bioconjug. Chem.* **2015**, *26* (1), 145–152.

(3) Joubert, N.; Denevault-Sabourin, C.; Bryden, F.; Viaud-Massuard, M. C. *Eur. J. Med. Chem.* **2017**, *142*, 393–415.

(4) Tumey, L. N.; Charati, M.; He, T.; Sousa, E.; Ma, D.; Han, X.; Clark, T.; Casavant, J.; Loganzo, F.; Barletta, F.; et al. *Bioconjug. Chem.* **2014**, *25* (10), 1871–1880.

(5) Takeoka, S.; Li, T. *Int. J. Nanomedicine* **2013**, *8*, 3855–3866.

(6) Baldwin, A. D.; Kiick, K. L. *Bioconjug. Chem.* **2011**, *22* (10), 1946–1953.

(7) Lyon, R. P.; Setter, J. R.; Bovee, T. D.; Doronina, S. O.; Hunter, J. H.; Anderson, M. E.; Balasubramanian, C. L.; Duniho, S. M.; Leiske, C. I.; Li, F.; et al. *Nat. Biotechnol.* **2014**, *32* (10), 1059–1062.

(8) Brun Cubero, O. Universitat de Barcelona, 2017.

(9) Liu, P. Y.; Wu, Y. J.; Pye, C. C.; Thornton, P. D.; Poirier, R. A.; Burnell, D. J. *European J. Org. Chem.* **2012**, No. 6, 1186–1194.

(10) Agosta, W. C.; Smith, A. B. *J. Org. Chem.* **1970**, *35* (11), 3856–3860.

(11) Billington, S.; Mann, J.; Quazi, P.; Alexander, R.; Eaton, M. A. W.; Millar, K.; Millican, A. *Tetrahedron* **1991**, *47* (28), 5231–5236.

(12) Kreiser, W.; Wiggermann, A.; Krief, A.; Swinnen, D. *Tetrahedron Lett.* **1996**, *37* (39), 7119–7122.

(13) Agosta, W. C.; Lowrance, W. W. *J. Org. Chem.* **1970**, *35* (11), 3851–3856.

(14) Subramanyam, R.; Bartlett, P. D.; Moltrasio Iglesias, G. Y.; Watson, W. H.; Galloy, J. *J. Org. Chem.* **1982**, *47* (23), 4491–4498.

(15) Manna, M. S.; Mukherjee, S. *J. Am. Chem. Soc.* **2015**, *137* (1), 130–133.

(16) Dhalluin, C.; Ross, A.; Huber, W.; Gerber, P.; Brugger, D.; Gsell, B.; Senn, H. *Bioconjug. Chem.* **2005**, *16* (3), 518–527.

(17) Stetsenko, D. A.; Gait, M. J. *Nucleosides, Nucleotides and Nucleic Acids* **2000**, *19* (10–12), 1751–1764.

(18) Stetsenko, D. A.; Gait, M. J. *J. Org. Chem.* **2000**, *65* (16), 4900–4908.

(19) Sorg, G.; Thern, B.; Mader, O.; Rademann, J.; Jung, G. *J. Pept. Sci.* **2005**, *11* (3), 142–152.

(20) Isidro-Llobet, A.; Álvarez, M.; Albericio, F. *Chem. Rev.* **2009**, *109* (6), 2455–2504.

(21) Postma, T. M.; Giraud, M.; Albericio, F. *Org. Lett.* **2012**, *14* (21), 5468–5471.

(22) Burns, J. A.; Butler, J. C.; Moran, J.; Whitesides, G. M. *J. Org. Chem.* **1991**, *56* (8), 2648–2650.

(23) Kantner, T.; Watts, A. G. *Bioconjug. Chem.* **2016**, *27* (10), 2400–2406.

(24) Huang, N.; Liu, X.; Lei, X.; Dong, T.; Zhou, Y. *Angew. Chemie Int. Ed.* **2016**, *55* (46), 14330–14334.

(25) Reja, R. M.; Sunny, S.; Gopi, H. N. *Org. Lett.* **2017**, *19* (13), 3572–3575.

(26) Werkhoven, P. R.; Van De Langemheen, H.; Van Der Wal, S.; Kruijtzer, J. A. W.; Liskamp, R. M. J. *J. Pept. Sci.* **2014**, *20* (4), 235–239.

(27) Ravasco, J. M. J. M.; Faustino, H.; Trindade, A.; Gois, P. M. P. *Chem. - A Eur. J.* **2018**, 43–59.

(28) Rull-Barrull, J.; D'Halluin, M.; Le Grognec, E.; Felpin, F.-X. *Angew. Chemie Int. Ed.* **2016**, *55* (43), 13549–13552.

(29) Li, S.; Cai, H.; He, J.; Chen, H.; Lam, S.; Cai, T.; Zhu, Z.; Bark, S. J.; Cai, C. *Bioconjug. Chem.* **2016**, *27* (10), 2315–2322.

(30) Huisgen, R.; Geittner, J.; Reissig, H.-U. *Heterocycles* **1978**, *11* (1), 109–120.

(31) Jana, S.; Thomas, J.; Dehaen, W. *J. Org. Chem.* **2016**, *81* (24), 12426–12432.

(32) de Miguel, I.; Herradón, B.; Mann, E. *Adv. Synth. Catal.* **2012**, *354* (9), 1731–1736.

(33) Wang, S.; Gurav, D.; Oommen, O. P.; Varghese, O. P. *Chem. - A Eur. J.* **2015**, *21* (15), 5980–5985.

(34) Van Mersbergen, D.; Wijnen, J. W.; Engberts, J. B. F. N. *J. Org. Chem.* **1998**, *63* (24), 8801–8805.

(35) Huisgen, R. *Angew. Chemie Int. Ed. English* **1963**, *2* (10), 565–598.

(36) L'abbé, G. *Chem. Rev.* **1969**, *69* (3), 345–363.

(37) Kalia, J.; Raines, R. T. *Angew. Chemie - Int. Ed.* **2008**, *47* (39), 7523–7526.

(38) Greene, T. W.; Wuts, P. G. M. *Protective Groups in Organic Synthesis*; John Wiley & Sons, Inc.: New York, USA, 1999.

(39) Forget, D.; Boturyn, D.; Defrancq, E.; Lhomme, J.; Dumy, P. *Chem. - A Eur. J.* **2001**, *7* (18), 3976–3984.

(40) Matinkhoo, K.; Pryyma, A.; Todorovic, M.; Patrick, B. O.; Perrin, D. M. *J. Am. Chem. Soc.* **2018**, *140* (21), 6513–6517.

(41) Bartolami, E.; Basagiannis, D.; Zong, L.; Martinent, R.; Okamoto, Y.; Laurent, Q.; Ward, T. R.; Gonzalez-Gaitan, M.; Sakai, N.; Matile, S. *Chem. - A Eur. J.* **2019**, 1–6.

(42) Relias, V.; Smith, M. H.; Daly, K. P.; Weinstein, B.; Fu, J.; Saif, M. W. *J. Pancreat. Cancer* **2018**, *4* (1), 64–71.

(43) Gandioso, A.; Cano, M.; Massaguer, A.; Marchán, V. *J. Org. Chem.* **2016**, *81* (23), 11556–11564.

(44) Zorzi, A.; Deyle, K.; Heinis, C. *Curr. Opin. Chem. Biol.* **2017**, *38*, 24–29.

(45) Gang, D.; Kim, D. W.; Park, H. S. *Genes (Basel).* **2018**, *9* (11).

(46) Brun, O.; Archibald, L. J.; Agramunt, J.; Pedroso, E.; Grandas, A. *Org. Lett.* **2017**, *19* (5), 992–995.

(47) Okada, T.; Asawa, T.; Sugiyama, Y.; Iwai, T.; Kirihara, M.; Kimura, Y. *Tetrahedron* **2016**, *72* (22), 2818–2827.

(48) Burrows, C. J.; Muller, J. G. *Chem. Rev.* **1998**, *98* (3), 1109–1152.

(49) Cooke, M. S.; Evans, M. D.; Dizdaroglu, M.; Lunec, J. *FASEB J.* **2003**, *17* (10), 1195–1214.

Chapter 3. Retro-1 oligonucleotide conjugates

3.1 Oligonucleotides, more than information.

Genomes hold an extraordinary trove of information concerning development, physiology, medicine and evolution. It was thought that the particular size of it dictated the complexity of the organism. However, when the human genome was sequenced in 2001,[1] it was discovered that humans have similar number of genes compared with 'less complex' organisms it became clear that other cellular processes had a role modulating the complexity of organisms.

In this context, one of the most important cellular process in every living organism is the central dogma of biology. It specifies that, with the exception of retroviruses, genetic information flows from DNA to RNA and, finally, to proteins *via* two sequential steps called transcription and translation, respectively.[2] Transcription is the process by which the information in a strand of DNA is copied into a new molecule of RNA, which is subsequently processed into messenger RNA (mRNA). DNA is responsible for safely and stably storing genetic material in the nuclei of cells as a reference or template. Meanwhile, mRNA is comparable to a copy from a reference book because it carries the same information as the DNA but is not used for long-term storage and can freely exit the nucleus. Importantly, even though mRNA contains the same information, it is not an identical copy of the DNA gene because its sequence is complementary.

By contrast, translation is the process by which a protein is synthesized from the information contained in the mRNA. During translation, an mRNA sequence is read using tRNAs in a set of rules that defines how an mRNA sequence is to be translated into the 20 natural proteinogenic amino acids. Translation occurs at the ribosomes, biological structures composed of several proteins and RNA molecules. The ribosome reads the coding mRNA sequence of the genetic code in a set of three-nucleotide combinations or codons, each of which corresponds with either a specific amino acid or a stop signal. Elongation continues until all of the codons are read and the newly expressed protein is then released. Initially it was tacitly assumed that the coding sequence had to be contiguous, meaning that the codon for one amino acid was immediately adjacent to the codon for the next amino acid in the polypeptide chain. This fact is true in the vast majority of cases in bacteria and their phages but rarely so in eukaryotic genes. In the latter cases, the productive sequence is periodically interrupted by stretches of noncoding sequences.

Many eukaryotic genes are thus mosaic-like arrangements, consisting of blocks of coding sequences separated from each other by blocks of noncoding sequences. The coding sequences are called exons and the intervening sequences, introns (**Scheme 3.1**, top). Typically, the term exon applies to any region retained in a mature RNA, whether or not it is coding. Moreover, their respective sizes may vary, but usually introns are longer than the exons they separate. As a consequence of this alternating pattern, genes bearing noncoding interruptions are often described as "in pieces" or "split". Because of the length and number of introns, the primary transcript (pre-mRNA) can be very long.

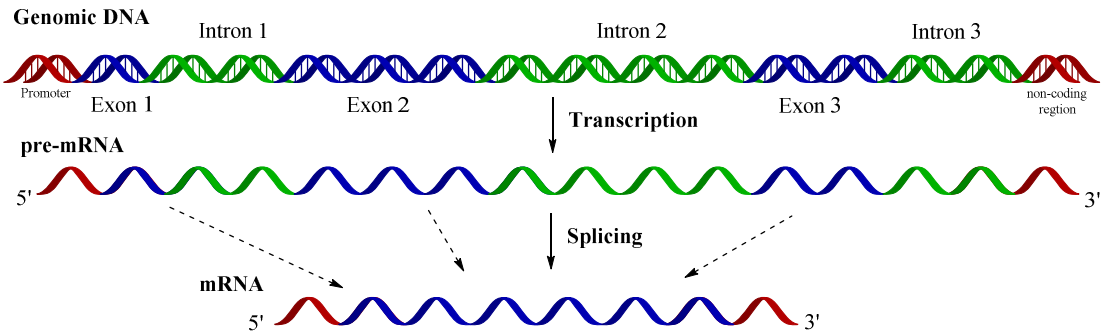

Scheme 3.1 Outline for the splicing process of a gene containing three exons separated by three introns and subsequent transcription into pre-mRNA and mature spliced mRNA.

One of the processes that convert pre-mRNA into mature mRNA is called splicing and must occur with great precision in order to avoid loss, addition or replacement of even a single nucleotide at the site where the exons are joined (**Scheme 3.1**, middle). Lack of precision in splicing would throw the reading frames of exons out of register and downstream codons would be incorrectly selected, thus providing wrong amino acids to be incorporated into the final proteins.

Some pre-mRNAs can be spliced in more than one way, generating diverse mRNAs from a single transcript. This is called alternative splicing and, by this strategy, a gene can give rise to different protein isoform. Alternative splicing protein products are called isoforms and is estimated that up to 75% of the human genes are alternatively spliced. Studies reveal that up to 95% of genes can be alternatively spliced to some degree, indicating that splicing is a common way to generate diversity within a cell.[3]

Even though being the vehicle of transmission of gene information is a key role of RNA, the world of possible functions for RNA inside mammalian cells has not ceased to grow. Over the past decades, novel and unforeseen biological properties have been identified for this molecule and each new discovery has added a new and often surprising layer to biological reaction and function.

3.2 Antisense oligonucleotides as therapeutic agents

In this biological context, tackling disease problems by modifying or controlling the flow of genetic information becomes increasingly difficult, since any new piece of knowledge makes the endeavor more complicated.

Gene therapy may be used to replace mutated genes, but it is not free of problems (the new piece of DNA must reach a precise chromosome, be inserted in the right place, be expressed correctly, etc.). Use of synthetic oligonucleotides as drugs provides an attractive approach to gene therapy. This methodology, much simpler, has been made increasingly accessible and applicable over the years due to several key technologies such as improvements in chemical synthesis and automation[4–6] as well as quick access to sequence information made possible by next generation sequencing technologies.[7]

It was soon clear that the informational nature of oligonucleotide drugs (i.e. drugs designed on the basis of sequence information) held great potential. Researchers were drawn by the promise of rapid and rational design of drugs against virtually any genetic target. However, it has taken more than three decades for these therapies to reach clinical maturity. The use of oligonucleotides (ONs) as therapeutic agents has several beneficial features regarding other alternatives. First, safety: ONs are non-infectious, non-integrating therapeutic tools, implicating that no potential risk of infection or insertional mutagenesis is expected. Additionally, both RNA and DNA are degradable by normal cellular processes and their *in vivo* half-life can be regulated. Secondly, efficacy: as commented in the introductory chapter of this dissertation, modifications make synthetic oligonucleotides more stable and highly applicable. Finally, even though *in vivo* delivery is still a non-well-solved problem, it can be achieved by carrier formulation, allowing rapid uptake and expression in the cytoplasm.[8]

Among the various oligonucleotide-based therapeutic possibilities, several approaches have established themselves as the now preferred for therapeutic applications: small interfering RNAs (siRNAs)[9], antisense oligonucleotides (ASOs)[10] and aptamers.[11] That being said, since the work described in this thesis will be making use of ASOs, this will be the topic of discussion.

ASOs were discovered when Zamecnick and colleagues found that DNA oligonucleotides complementary to the DNA template used for transcription, or antisense, inhibited translation of Rous sarcoma viral proteins.[12] Subsequent studies revealed that some ASOs form DNA-RNA hybrids that recruit RNAse H, resulting in cleavage of the RNA strand (**Scheme 3.2**, A). The cleaved fragments are

then degraded by the cell's RNA surveillance/quality controls system. Alternatively, hybridization to the RNA target without activation RNase H may affect the outcome of translation in other ways, such as steric blockage, which can stall the ribosome and abort protein synthesis, or inhibition of translation by blocking the start site (**Scheme 3.2**, B). Another important mechanism of action of antisense oligonucleotides is induction of changes in splicing, in which case oligonucleotides are said to have splice-switching ability (**Scheme 3.2**, C). The principle behind this last option is the interaction of the ASO with a splice site in a target RNA through Watson-Crick base pairing, hiding it from the splicing machinery and, for instance, causing exons to be skipped during the splicing process. That being said, in all cases, several additional criteria such as suitable delivery through cell membranes, and physiological stability to nucleases are still of paramount importance for these types of drugs in order to be effective.

Chemically speaking, an intron is removed through a series of transesterification reactions in which phosphodiester linkages within the pre-mRNA are broken and new ones are formed. These transesterification reactions are mediated by a molecular machinery called spliceosome, a complex comprised of about 150 proteins and 5 RNAs, being similar in size to a ribosome. The five RNAs are collectively called small nuclear RNAs and the RNA-protein complexes small nuclear ribonuclear proteins (snRNPs). The snRNPs have three roles in splicing: precisely recognizing the 5' splice site and the cleave site, bringing these sites together and catalyzing the cleavage and joining reactions.

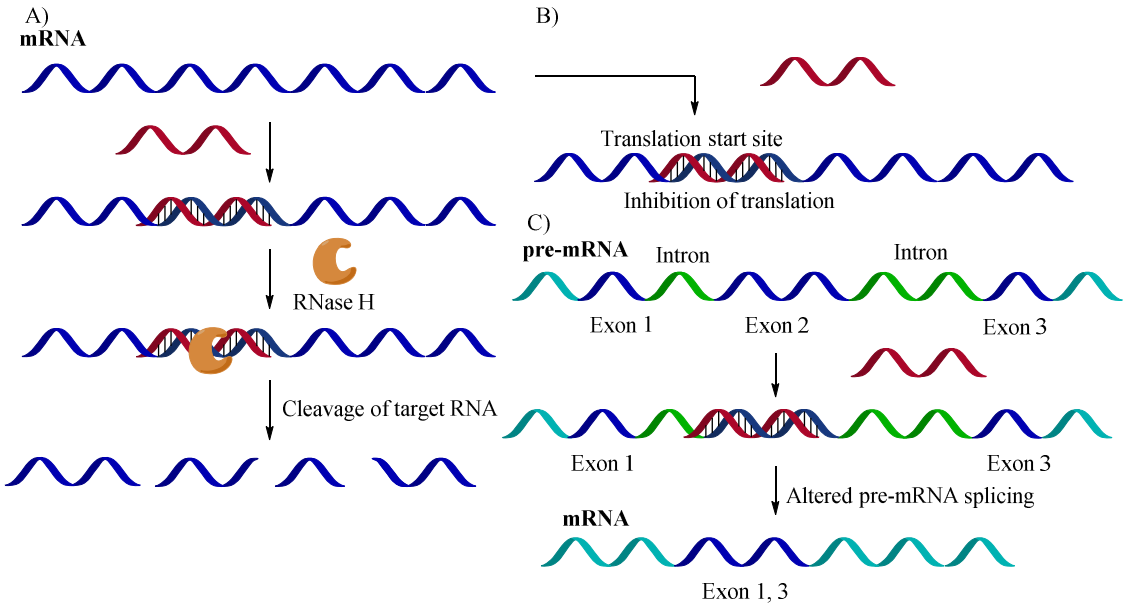

Scheme 3.2 Mechanism of action of antisense oligonucleotides (ASOs). A) ASOs can affect gene expression by recruiting RNase H, resulting in cleavage and degradation of the target RNA. B) ASOs with modifications that prevent recruitment of RNase H can regulate gene expression by sterically blocking the ribosome machinery and hence translation. C) ASOs can target splice sites in pre-mRNAs and thus alter the splicing outcome, thus producing a different mRNA (and a different protein).

Up to date only a handful of oligonucleotide-based drugs have been approved by the FDA, including mipomersen (Kynamro™) an anti-sense oligonucleotide for the treatment of hypercholesterolemia,[13] patisiran (Onapattro™) a double-stranded small-interference RNA encapsulated in a lipid nanoparticle for the treatment of hereditary transthyretin-mediated amyloidosis in adults,[14] or nusinersen (Spinraza™), the first approved treatment for spinal muscular atrophy.[15]

3.3 Molecules enhancing the effect of oligonucleotide drugs

As already stated, amongst all categories of ONs that have evidenced significant therapeutic potential, a key problematic exists in addition to physiological stability, that of low cellular uptake. In order to alleviate these drawbacks, chemical modifications[16,17] have been proposed and have greatly solved the stability problem. Nonetheless, inefficient access of these large, highly polar molecules to their sites of action in the nucleus or cytosol of the desired tissue cell is the biggest detriment to their therapeutic application.[18] To improve tissue penetration, various nanotechnology-based delivery approaches have been designed, and some of them found to be greatly helpful.[19] Other strategies include chemical conjugation to carriers or complexation with cell-penetrating peptides designed to promote endosomal escape,[20] as well as conjugation with ligands to promote receptor-selective cell uptake.[21,22]

Despite these various approaches, the delivery issue still remains a challenge to address. For example, limited distribution as well as associated toxicity with the use of polycationic or lipid moieties as well as polymer nanoparticles[23] have hampered their use in clinical settings. Consequently, it is clear that the discovery of alternative strategies to enhance oligonucleotide access to their intracellular targets will provide a substantial increase to the value of oligonucleotide-based pharmacology and therapeutics.

Some years ago, a group of compounds that profoundly and selectively affected intracellular traffic were described.[24] More specifically, this was the case for two compounds coined Retro-1 (**3.1**) and Retro-2 (**3.2**, **Figure 3.1**). These molecules, were identified from a high throughput screening of small molecules and were found to be able to reduce the harmful action of bacterial and plant toxins. Their means of action is by blocking the retrograde trafficking pathway used by many toxins by interfering with the shuttling between endosomes and the *trans*-Golgi network.

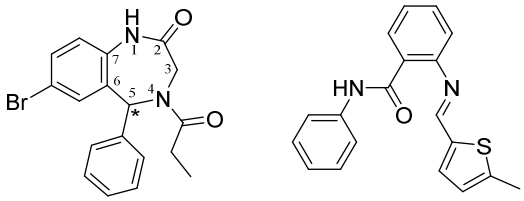

3.1 **Retro-1** **3.2** **Retro-2**

Figure 3.1 Retro-1 and Retro-2 structures.

Upon observing these beneficial properties, R. L. Juliano and co-workers decided to assess whether Retro compounds might be beneficial for the intracellular trafficking of ONs so as to enhance their pharmacological effect.[25] In these studies, they found out that increasing amounts of Retro-1 (**3.1**) progressively enhanced the action of a splice-switching oligonucleotide (SSOs) on a luciferase reporter (Luc) transfected into HeLa cells.

3.4 Objectives

After Prof. Juliano's report on the action of Retro-1 on ASOs,[25] we wondered whether the covalent attachment of antisense oligonucleotides to Retro-1 would be more efficient in enhancing the biological effect of the oligonucleotide drug than the co-administration of the two compounds he described. For this purpose, we decided to prepare Retro-1–oligonucleotide conjugates and, contacted Prof. Juliano for biological evaluation.

In order to assess whether the point from which Retro-1 would link the oligonucleotide, and whether the chemistry used for conjugation had an effect on the oligonucleotide transport into the nucleus, different derivatives of Retro-1 were prepared. These derivatives were conjugated to a splice-switching oligonucleotide and to a control oligonucleotide whose sequence contained the same bases as the biologically active one but in a different order (scrambled oligonucleotide)

3.5 Retro-1-Oligonucleotide conjugates

3.5.1 Design of the Retro-1 derivatives

The chemical structure of Retro-1 has many points in common with that of a benzodiazepine psychoactive drugs such as diazepam[26] (**3.3**), clonazepam[27] (**3.4**) or cinazepam[28] (**3.5**, **Figure 3.2**).

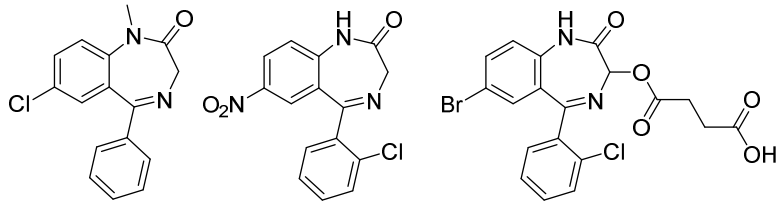

3.3 **Diazepam** **3.4** **Clonazepam** **3.5** **Cinazepam**

Figure 3.2 Commercially available psychoactive drugs based on the benzodiazepine scaffold.

Both entities are composed of two fused rings: a benzene and a 1,4-diazepine, where two carbon atoms of the benzene ring and carbons number 6-7 of the diazepine are bridgehead. Additionally, the diazepine cycle contains a carbonyl functionality at the 2 position and an aromatic ring (phenyl) appending from carbon 5. The main divergence between Retro-1 and classic benzodiazepines is the lack of the double bond between atoms 4 and 5, resulting in a stereocenter at carbon 5 as depicted in **Figure 3.1**.

In order to covalently link the Retro-1 compound with an ON, two main approaches were planned. First, the use of a Retro-1 phosphoramidite derivative suitable to be employed in standard solid-phase oligonucleotide synthesis, and secondly, by means of a bioconjugation reaction in solution. More specifically, either a thiol Michael-addition or a DA cycloaddition with a maleimide appending from the 5' terminus of the ON.

For the first option the Retro-1 had to be modified with a hydroxyl group and, subsequently, prepare the corresponding phosphoramidite functionality. On the other hand, to achieve the conjugation of Retro-1 with oligonucleotides in solution, both reactants had to be modified, in other words, appended with the appropriate moieties that would react chemoselectively with each other in the presence of all the other functional groups.

We envisioned modification of the Retro-1 molecule at two points, carbon 3 and nitrogen 4 of the diazepine ring, as depicted in **Figure 3.3**. We chose two different positions because it is known that the conjugation site may alter both the Retro-1 and oligonucleotide interactions with the target, possibly yielding different results in biological assays.[29]

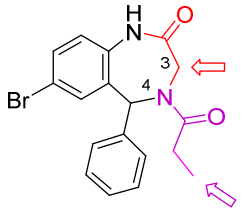

Figure 3.3 Potential link sites to oligonucleotides within the Retro-1 scaffold.

We figured that the most straightforward modification would be changing the acylating reagent of nitrogen 4 (**Figure 3.3**, in purple). The other option was the introduction of a suitable functionality at carbon 3 *via* replacement of the "glycine" residue (that is the N-CH_2-CO unit in the ring) with a trifunctional amino acid such as lysine, glutamic acid or homoserine in order to provide the system with an additional functional group (**Figure 3.3**, in red).

Before synthesizing the Retro-1 derivatives to be used for conjugation, our first objective was to reproduce the Retro-1 synthesis following described procedures[30] not only to obtain partner Retro-1 as a control in subsequent experiments, but also the key intermediate for the synthesis of analogues differently acylated. As depicted in **Scheme 3.3** the synthesis started with commercially available 2-aminobenzophenone (**3.6**), which was reacted with NBS to cleanly furnish the brominated intermediate (**3.7**) in a 97% yield**.** Subsequent acylation with bromoacetyl bromide provided the acylated intermediate (**3.8**) with 84% yield, without the need of chromatographic purification for any of these two steps. A nucleophilic substitution on the bromoacetyl group and cyclization (imine formation) with methanolic ammonia provided the 7-membered benzodiazepine core (**3.9**) in a reasonable 61% yield. Selective imine reduction with $NaBH_3CN$ yielded the free secondary amine (Retro-NH, **3.10**) in a 87% yield. Retro-NH was the precursors of both, Retro-1 (**3.11**) and the *N*-acylated analogs. Finally, acylation with propionyl chloride provided the desired Retro-1 (**3.11**) in a good 83% yield. The overall yield of the whole synthetic scheme was 36% (5 steps).

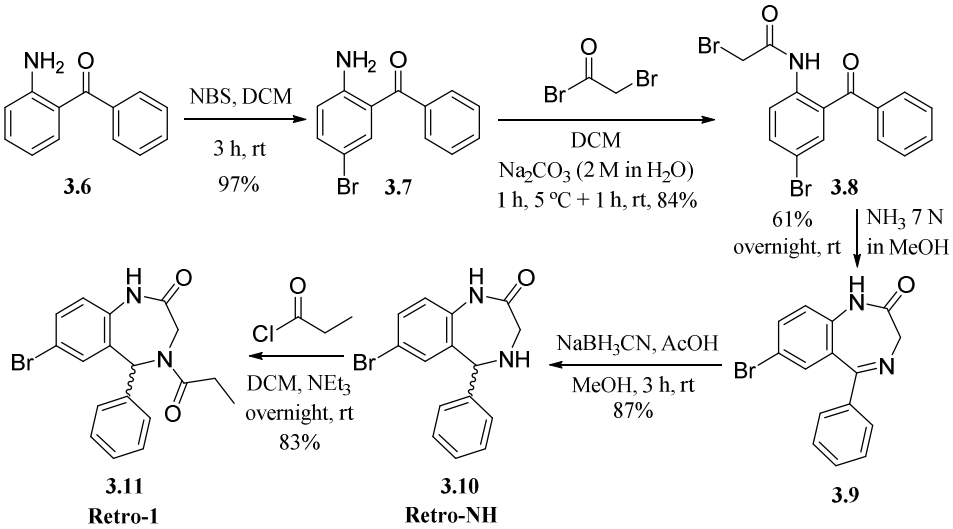

Scheme 3.3 Synthetic scheme for the obtention of Retro-1 as described by Abdelkafi *et al.*[30]

3.5.2 Retro-1 analogs prepared by acylation and further functionalization of the 4 position appendage

The first approach to prepare a hydroxylated analogue was the utilization of lactones, with the idea of obtaining the hydroxyl functionality *via* reaction between the cyclic ester group and the Retro-NH

secondary amine. Subsequent phosphitylation would furnish the desired phosphoramidite (**Scheme 3.4**).

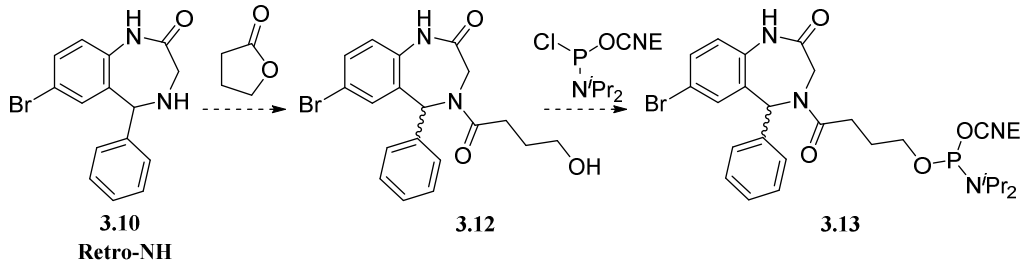

3.10 Retro-NH **3.12** **3.13**

Scheme 3.4 First plan for the synthesis of an *N*-acyl Retro-1 phosphoramidite *via* amine-promoted ring opening of lactones.

Described procedures called upon either protic catalysis,[31] Lewis acid catalysts[32] or thiourea[33] activation. In order to assess whether this option was feasible, we first attempted the ring opening of γ-butyrolactone (**3.14**) and phenylethylamine (**3.15**) with $AlCl_3$ activation under THF reflux as shown in **Scheme 3.5**. The desired hydroxylamide (**3.16**) was isolated in a good 80% yield and characterized by ^{1}H NMR and MS, providing evidence that this option was feasible.

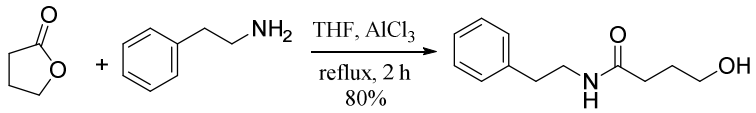

3.14 **3.15** **3.16**

Scheme 3.5 $AlCl_3$ mediated γ-butyrolactone aminolysis.

Subsequently, we decided to test the same reaction conditions with Retro-NH. To our disappointment, the reaction did not seem to progress and only reactants were recovered even after prolonged reaction times as depicted in **Scheme 3.6**.

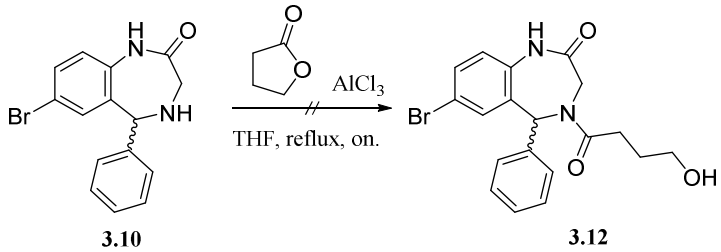

3.10 **3.12**

Scheme 3.6 Attempt of lactone opening *via* aminolysis utilizing the Retro-NH scaffold.

After this initial setback, we tested both acid (HCl) and base (DIPEA) catalysis, but in neither of two cases any progress was observed. A follow-up study of this last approach was the use of *N*-methylimidazole as a nucleophilic catalyst to aid in the ring-opening of the lactone through formation of an acylimidazolium intermediate (**3.19**) as depicted in **Scheme 3.7**.

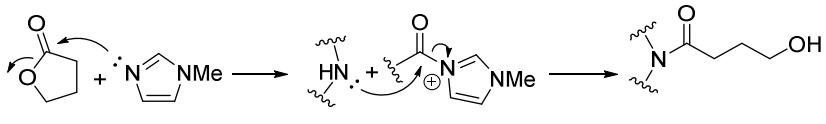

3.14 **3.17** **3.18** **3.19** **3.20**

Scheme 3.7 *N*-Methylimidazole-assisted lactone opening, followed by amide formation.

This last attempt, though, also proved to be ineffective. We surmised that steric hinderance (secondary amine with a substituent on an α carbon) might likely play a non-negligible role in hampering the reaction. We therefore decided to abandon this route and pursue another alternative.

The second option, depicted in **Scheme 3.8**, was attaching a succinyl handle to form an amide and obtain the carboxylic acid derivative (**3.21**). Subsequent reaction with an aminoalcohol (**3.22**) would furnish the desired hydroxylic derivative (**3.23**).

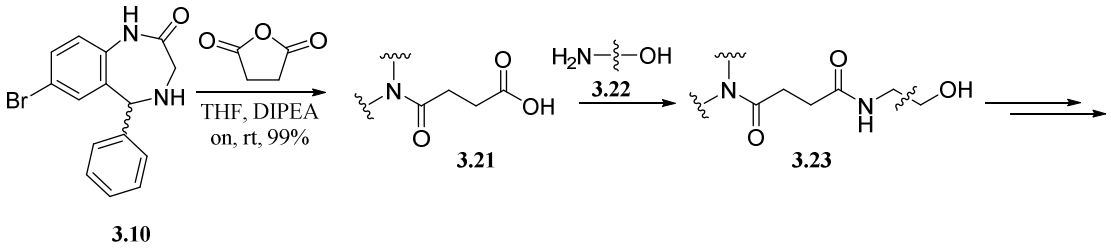

Scheme 3.8 Synthetic scheme for the obtention of a Retro-1 hydroxyl bearing compound *via* reaction with an anhydride and subsequent amide formation.

Starting with the partner Retro-NH (**3.10**) acylation with succinic anhydride provided the carboxylic acid (**3.21**) quantitatively. Subsequent activation of the carboxylic acid, with isobutyl chloroformate and reaction with several aminoalcohols (**3.24-3.26**) proved unsuccessful to obtain the desired Retro-hydroxyl derivatives (**3.27-3.29**) only recovering either starting materials or complex mixtures (**Scheme 3.9**)

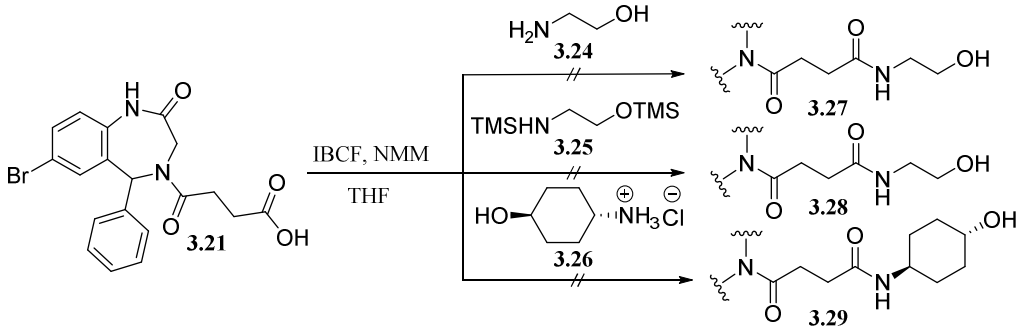

Scheme 3.26 Attempts to form an amide by reacting a carboxyl-derivatized Retro-1 derivative and aminoalcohols.

As depicted in **Scheme 3.10**, another alternative we tested was to reduce the carboxyl group to alcohol, as previously described for several amino acids.[34] Activation of the acid with isobutyl chloroformate, followed by reduction with $NaBH_4$ was not successful for the Retro-1 scaffold. Hence, we switched to carbodiimide and HOBt activation,[35] obtaining equally negative results.

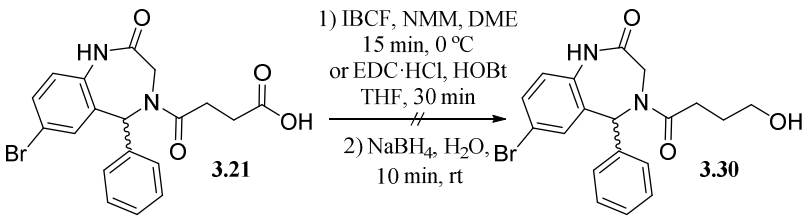

Scheme 3.10 Attempts to reduce the carboxyl group of **3.21**.

Observing these negative results, we decided to pursue a slightly different and simpler strategy. We pictured employing the aza-Michael addition to obtain the desired hydroxyl derivative, in other words, reacting an aminoalcohol with an acryloyl intermediate as depicted in **Scheme 3.11**. The idea was to

first acylate Retro-NH (**3.10**) with acryloyl chloride (**3.31**) to obtain intermediate **3.32**, and then run an aza-Michael addition with 4-hydroxypiperidine (**3.33**). This would yield the desired hydroxyl derivative **3.34**.

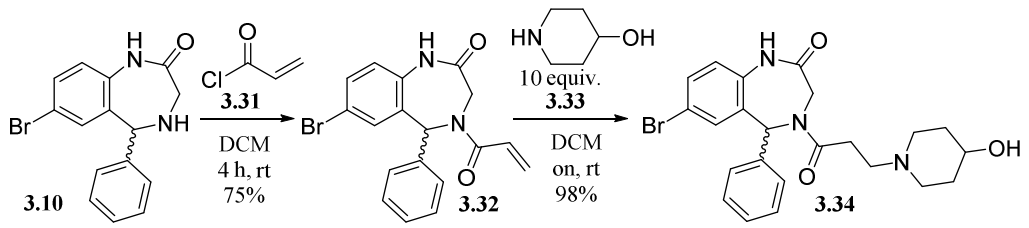

Scheme 3.11 Outline of the synthetic scheme used to obtain the Retro-1 hydroxyl derivative *via* an acryloyl intermediate.

4-Hydroxypiperidine (**3.33**) was selected for the aza-Michael reaction because it is known that the nucleophilicity of secondary cyclic alkyl amines is greater than that of their primary counterparts.[36] Moreover, we anticipated that the tertiary amine formed after the aza-Michael reaction would certainly not cause any problems either in the subsequent phosphitylation reaction or upon attachment to the oligonucleotide-resin. In contrast, the secondary amine resulting from the aza-Michael reaction between the acryloyl group and a primary amine might have been a source of predicaments and in order to avoid these problems, the secondary amine should have been protected.

Once we obtained the hydroxyl derivative **3.34**, the phosphoramidite was synthesized using standard procedures, employing a chlorophosphine and DIPEA as depicted in **Scheme 3.12**. The desired phosphoramidite (**3.35**) was isolated in a modest 42% yield.

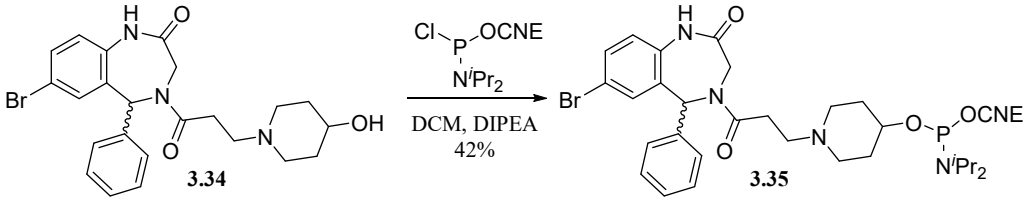

Scheme 3.12 Retro-1-amidite synthesis.

Once we had prepared the amidite derivative, we considered making use of the same methodology to produce a second Retro-1 derivative containing another functionality suitable for bioconjugation in solution.

In this instance, we made use of the previously employed Retro-1 acryloyl derivative (**3.32**) and reacted in an aza-Michael addition as previously, with S-trityl protected cysteamine (**3.36**) to yield the S-trityl protected Retro-1 derivative (**3.37**). Finally, deprotection of the thiol functionality was achieved by acidic treatment with TFA and TIS to quantitatively yield the Retro-SH derivative (**3.38**) as depicted in **Scheme 3.12**.

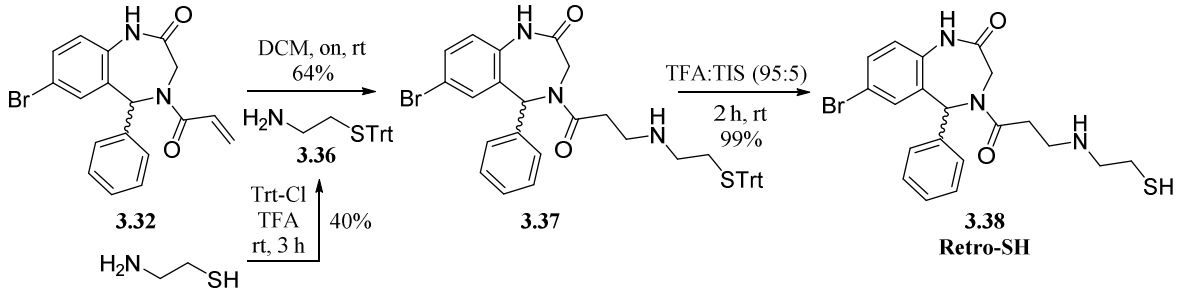

Scheme 3.13 Outline for the synthesis of thiol-containing Retro-1 derivative **3.38** *via* aza-Michael addition and thiol deprotection.

In order to assess the purity of the deprotected Retro-SH derivative, after precipitation and filtration of trityl by-products, an HPLC-MS analysis was performed, confirming the homogeneity (and identity) of the product as depicted in **Figure 3.4**.

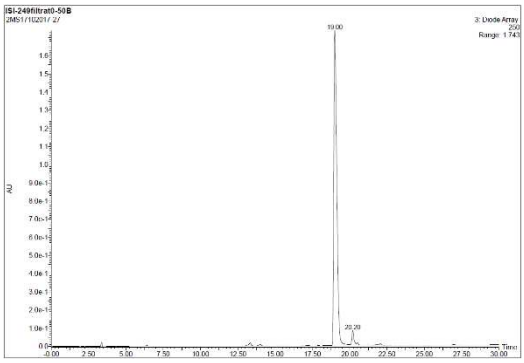

Figure 3.4 HPLC trace of the Retro-SH (**3.38**) derivative after trityl deprotection and filtration.

3.5.3 Retro-1 analogs incorporating L-lysine

As previously touched upon, the manner in which biologically active compounds are linked to a biomolecule might have an influence on the outcome of the biological assay on the compound's behavior both *in vitro* and *in vivo*. Taking this into consideration, we envisioned producing a second linking site to the oligonucleotide within the Retro-1 scaffold, in particular at carbon 3. In this instance, the NH-CH_2-CO segment of the diazepine skeleton, which corresponds to a glycine residue (**Figure 3.3**), was replaced with that of lysine.

As depicted in **Scheme 3.14**, the synthesis started from 5-bromo-2-aminobenzophenone (**3.6**), which instead of reacting with bromoacetyl bromide (**Scheme 3.3**) was be reacted with a lysine derivative with the two amines orthogonally protected. In this case we employed Fmoc-Lys(Boc)-OH to obtain the fully protected acylated intermediate (**3.39**). Then, Fmoc removal and cyclization provided the 7-membered benzodiazepine scaffold (**3.40**). Analogously as for the synthesis of Retro-1 and the two described analogs, imine reduction (**3.41**) rendered the secondary amine and subsequent acylation furnished the Retro-1 core (**3.42**). Finally, Boc removal provided the free amine (**3.43**) appending from the lysine side-chain which could be further transformed into a suitable bioconjugation tool.

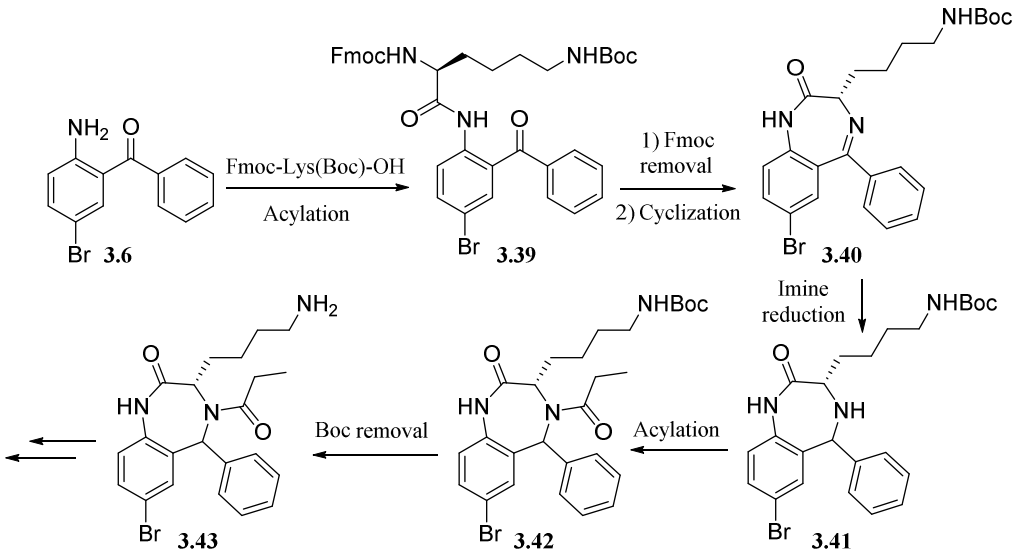

Scheme 3.27 Outline of the planned scheme for the preparation of lysine-containing Retro-1 derivatives.

Since our group is proficient in peptide and oligonucleotide synthesis, the first methodology employed to link the lysine derivative to **3.6** for making an amide was carbodiimide activation of the carboxyl group, using EDC·HCl and HOBt. To our disappointment, this combination seemed not to be a strong enough activation alternative for the reaction with the weakly nucleophilic aniline we were working with. The second round of attempts were carried out using COMU, an uronium salt-based stronger activating agent, also typically used as activating agent in SPPS.[37] Analogously to the first attempt, though, reaction did not proceed and only reactants were recovered. Observing these failures and the previous success with bromoacylation with acyl bromide (**Scheme 3.3**), we decided to try with a classic route, using thionyl chloride for acyl chloride formation, even though we were expecting orthogonality problems due to the acidic conditions of the reaction and the presence of a Boc protecting group. As expected, the reaction proceeded but Boc loss was observed. Thus, this option was not further explored. Another attempted alternative was the use of MSNT, a typical coupling agent in phosphotriester oligonucleotide synthesis, in conjunction with *N*-methylimidazole.[38] In a similar fashion, this strategy did not succeed and so, we decided to explore the mixed anhydride formation.

With this last strategy, the desired acylated product (**3.39**) was isolated in a modest 57% yield. This fact was associated with formation of an isobutyl carbamate side-product, derived from the reaction of the chloroformate and the amine (formation of this type of byproduct has sometimes been observed in difficult couplings). Subsequently, Fmoc removal under basic conditions and intramolecular imine formation provided the 7-membered ring of the benzodiazepine core. Typical Fmoc removal calls for treatment with piperidine, but in this instance, we employed the previously utilized methanolic ammonia solution because this alternative proved useful for the previous diazepine construction and the fact that it is easier to remove ammonia over piperidine. To our delight, after overnight reaction with 7 M ammonia in MeOH, we recovered quantitative amounts of cyclic product (**3.40**) after a silica gel filtration for dibenzofulvene by-products removal (**Scheme 3.15**).

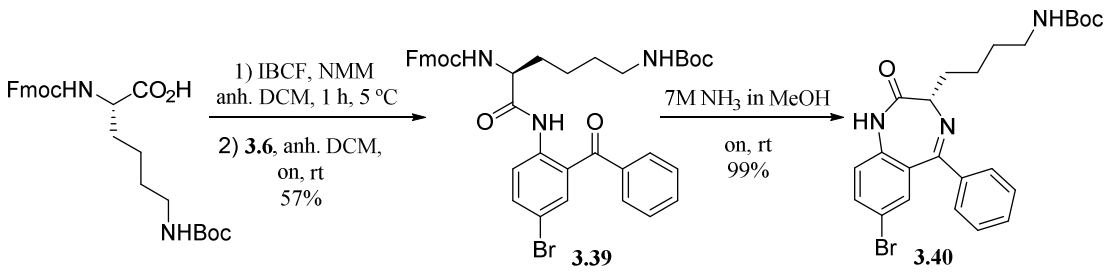

Scheme 3.15 IBCF-mediated acylation of **3.6** to render intermediate (**3.39**) and Fmoc removal and imine cyclization *via* reaction with ammonia to obtain the 7-membered benzodiazepine ring (**3.40**)

As a follow-up optimization of these two-step procedure involving two chromatographic purifications, we tested running the acylation, deprotection and cyclization in a one-pot manner. We applied a tweaked procedure for the chloroformate activation: shorter preactivation and reaction times followed by solvent removal and the same methanolic ammonia conditions for Fmoc removal and cyclization as previously commented. Gratifyingly, the reaction proceeded faster, with only one purification step and with a comparable overall yield (56% vs 55%) (**Scheme 3.16**).

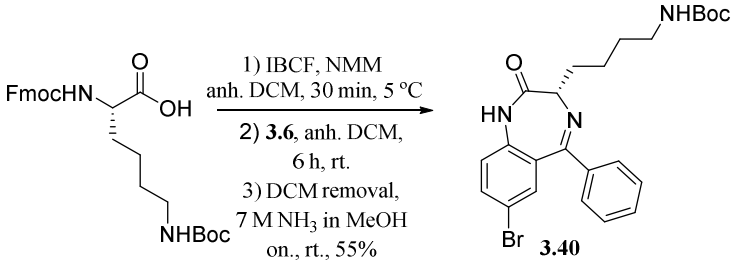

Scheme 3.16 One pot procedure to obtain **3.40** involving the optimized acylation, Fmoc removal and cyclic imine formation procedures.

Once we obtained the cyclic imine intermediate (**3.40**), the same procedure as before for the reduction of the imine to the secondary amine (**3.41**) was followed, employing acidic $NaBH_3CN$ (**Scheme 3.17**). Even though this reaction proceeded smoothly and quantitatively we faced the problem of obtaining a mixture of diastereomeric compounds instead of the enantiomers of the previous Retro-1 synthesis due to the presence of the lysine stereocenter (with defined configuration). That being said, at that point of the work we deemed not worth pouring efforts in their separation. Isolation of diastereomerically pure compounds would be worthwhile if the conjugate were active.

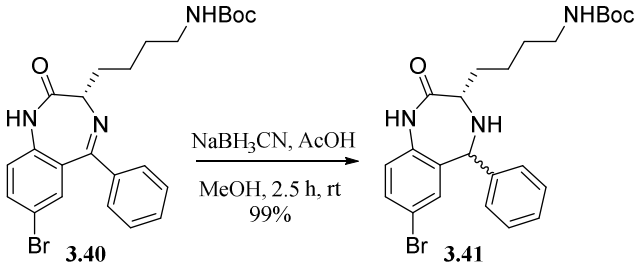

Scheme 3.17 Outline for the selective imine reduction.

Once the secondary amine (**3.41**) was available, we proceeded with the acylation of the amine with propionyl chloride. First attempts provided complex crude mixtures, which was attributed to partial Boc deprotection. This fact, prompted the addition of an organic base in order to quench the *in situ* generated HCl, but this proved also unsuccessful since deprotection products were still observed. In order to circumvent this dilemma, we opted for the use of propionic anhydride which, upon reaction would

provide the target acylated intermediate and propionic acid (pKa ≈ 4.88)[39] instead of HCl. Propionic acid should not remove the Boc group since no deprotection was observed in the previous reduction with $NaBH_3CN$ in the presence of acetic acid (AcOH, pKa ≈ 4.75). In this instance, though, the reaction did not proceed, and only reactants were recovered even after longer reaction times and large excesses of anhydride. This fact was attributed to the increased steric hindrance at N4 and decreased electrophilicity of the anhydride in comparison to the acyl halide (**Scheme 3.18**).

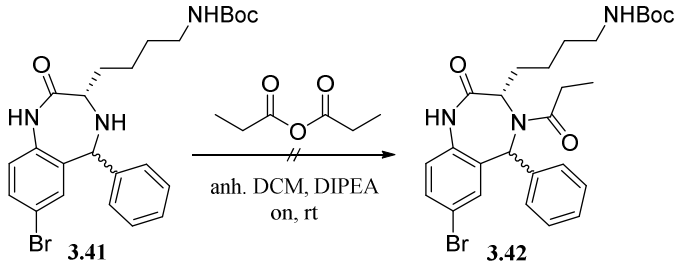

Scheme 3.28 Attempt to acylate the secondary amine using propionic anhydride.

Observing these results, we decided to ignore the acylation step and modify the structure of the planned final product so that instead of having two groups appending from C3 and N4 there would be only one appending from C3. We reasoned that, once the Boc group was removed, the subsequent acylation reaction would be selective for the primary amine over the secondary and not very reactive one. Therefore, we proceeded with Boc removal with an acidic treatment, to obtain the free primary amine of the lysine side chain (**3.43**). This amine was subjected to acylation with a carboxylic acid containing a diene moiety suitable for Diels-Alder cycloaddition (**Scheme 3.19**).

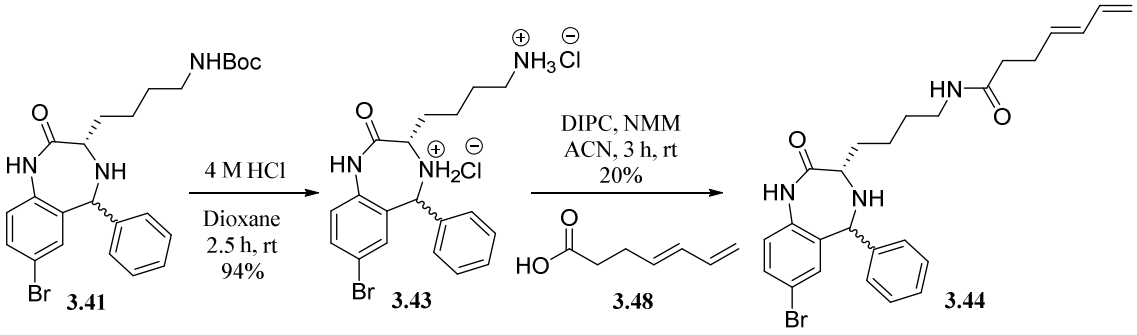

Scheme 3.19 Final steps for the preparation of the diene-modified Retro-1 derivative (**3.44**).

For the synthesis of the diene containing a carboxylic acid, we followed described procedures involving a two-step procedure.[40] A Claisen rearrangement from 1,4-pentadien-3-ol (**3.45**) in triethyl orthoacetate (**3.46**) under propionic acid catalysis yielded the ester diene intermediate (**3.47**) in a moderately good 50% yield. Afterward **3.47** was subjected to basic hydrolysis with LiOH to provide the desired (*E*)-hepta-4,6-dienoic acid in an excellent 99% yield (**3.48**) as depicted in **Scheme 3.20**.

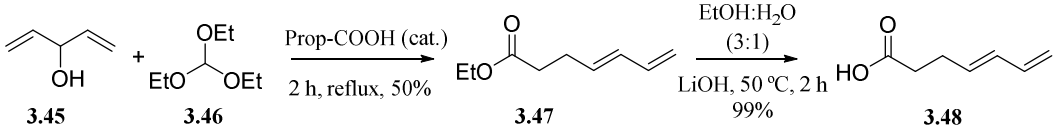

Scheme 3.20 Outline for the obtention of diene-derivatized carboxylic acid.

The reaction involving the Retro-1 analogue (**3.43** and diene derivative **3.48** was carried out using carbodiimide activation with increasing amounts of NMM. Moreover, the reaction was monitored and the products purified by reversed-phase HPLC, not only because the derivative turned out be quite polar

but also by the fact that high purity was imperative for the conjugation step. HPLC purification allowed for the separation of both diastereomers as seen by inspection of the corresponding trace (**Figure 3.5**).

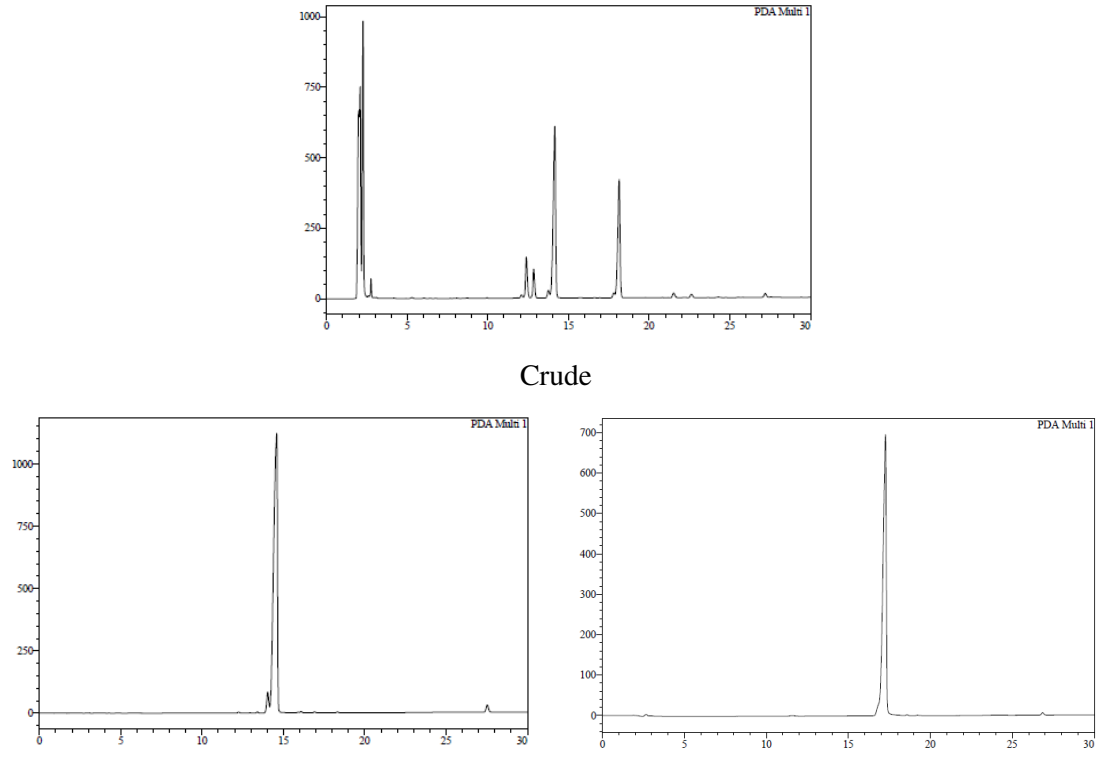

Figure 3.5 HPLC traces (250 nm) of crude **3.44** (top), and purified diastereomeric compounds (bottom).

Additionally, the Retro-1 analog (**3.43**) was also used for reaction with a thiol-containing acid. For this purpose, the thiol group of mercaptoacetic acid (**3.49**) was protected by reaction with trityl chloride under Lewis acid catalysis to render the trityl-protected mercaptoacetic acid[41] (**3.50**) in a fairly good 74% yield. Subsequently, carbodiimide-activated acid (**3.50**) was reacted in a similar fashion as previously with the fully deprotected Retro analogue **3.43** for 3 h to furnish the trityl-protected Retro-1 analog **3.51**.

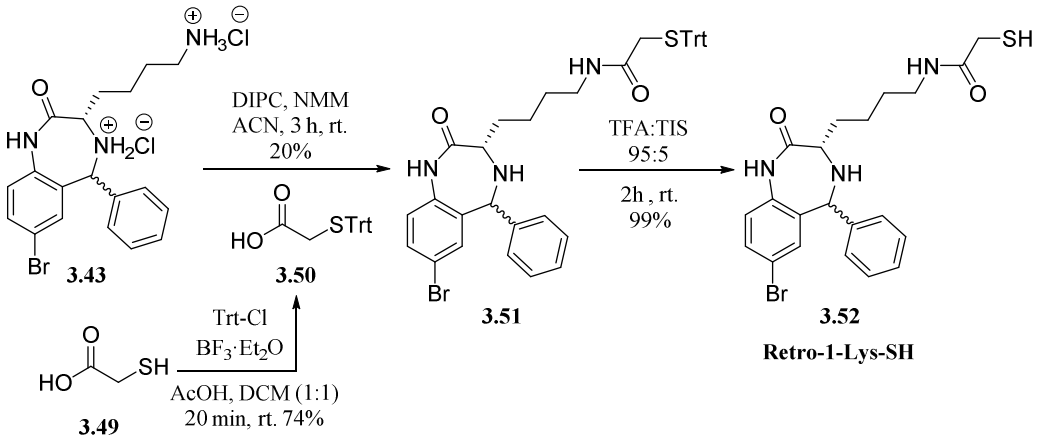

Scheme 3.29 Final steps in the synthesis of the lysine-including, thiol-modified Retro-1 derivative (**3.52**).

Analogously to the diene counterpart, the reaction was monitored and the final product purified by HPLC (**Figure 3.6**). The 2nd peak in the HPLC trace of the first isolated diastereomeric corresponds to the Trt-OH present in the reaction crude. We inferred that this would not be a problem since, after deprotection of the thiol, the trityl-containing compound would be considerably insoluble in water and, thus, simple filtration would allow to get rid of this impurity.

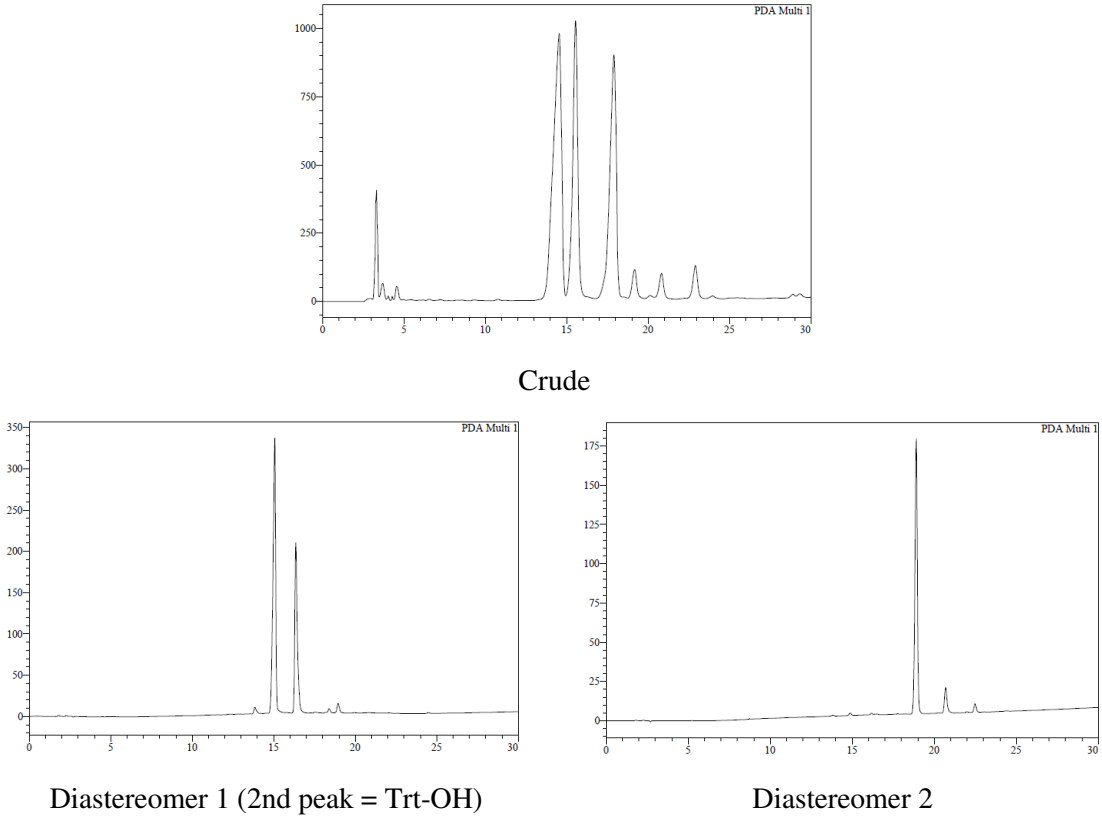

Figure 3.6 HPLC traces (250 nm) of crude **3.51** (top) and purified diastereomeric compounds (bottom).

Finally, acidic treatment with TFA and TIS provided the free thiol group **3.52**. Purification was performed by filtration of the aqueous suspension through a PTFE syringe in order to remove the trityl precipitate. Nonetheless, the purity of compound was assessed by HPLC-MS (**Figure 3.7**).

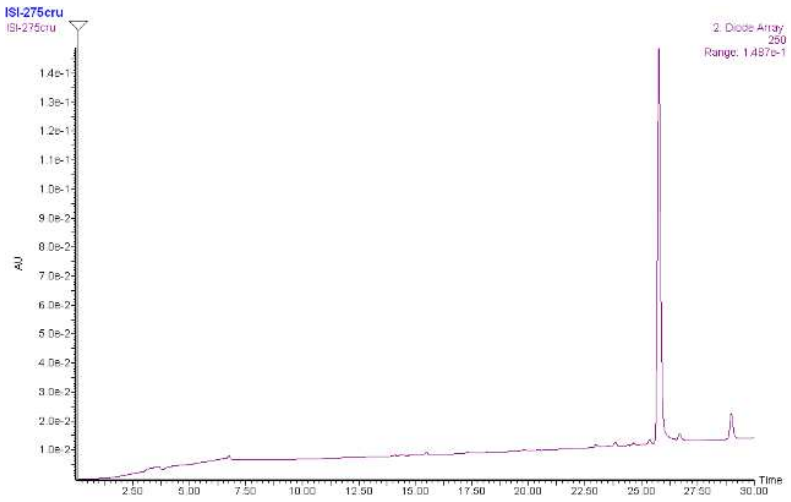

Figure 3.7 HPLC trace (250 nm) of the crude **3.52** after adding water and filtration prior to lyophilization.

3.5.4 Synthesis of Retro-1 oligonucleotide conjugates

3.5.4.1 Preliminary consideration and experiments

As previously discussed, two strategies to obtain the target conjugates were to be tested: union of the Retro-1 moiety to the oligonucleotide *via* a phosphate diester linkage, using a Retro-1 phosphoramidite analog (**3.35**), and solution conjugation using thia-Michael and Diels-Alder reactions. For this purpose, we produced three Retro-1 derivatives, two containing a thiol group (**3.38** and **3.52**) and a third with an appended diene (**3.44**). These three derivatives had to be reacted with a maleimido-oligonucleotide.

Until quite recently, attachment of maleimides to resin-linked oligonucleotides was impractical due to the maleimide instability to the final oligonucleotide deprotection and cleavage conditions, which require concentrated aqueous ammonia. This challenge was solved by Sánchez *et. al.* through the use of 2,5-dimethylfuran as maleimide protecting group, which rendered maleimides suitable for on-resin 5' modification.[42] In their study, they found that among a variety of furans, 2,5-dimethylfran was the best suited maleimide a protecting group. Furthermore, they discovered that the *exo* adduct was stable to conc. aq. NH_4OH, while the *endo* adduct was not. This chemical behavior provided a simple means to purify the *exo* adduct from an *endo*/*exo* mixture before attachment of a protected maleimide to the oligonucleotide-resin. Additionally, of all the three tested furans, 2,5-dimethylfuran required the lowest temperatures for maleimide deprotection through retro-Diels-Alder (rDA) reaction (**Scheme 3.22**). This is a desirable feature since, when working with peptides and oligonucleotides, keeping reaction temperature as low as possible is always desired to prevent their possible degradation.

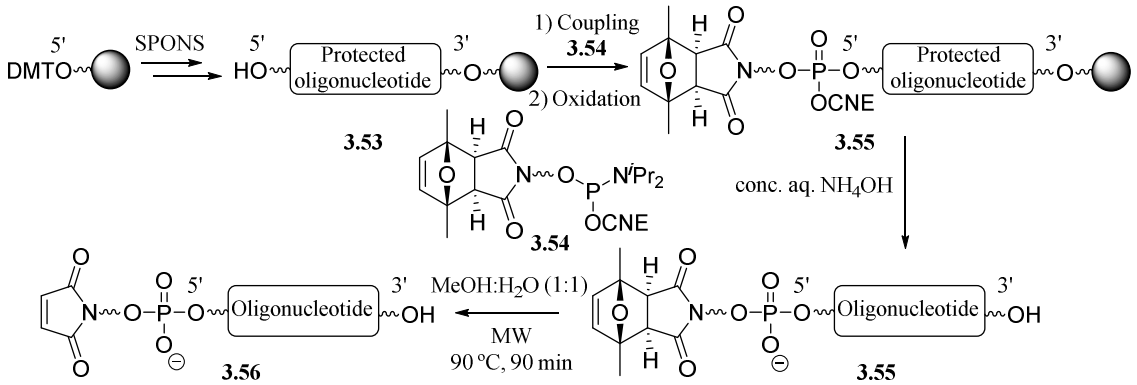

Scheme 3.22 Outline of the synthetic strategy employed for maleimide incorporation into resin-linked oligonucleotides.

In this context, we synthesized the 2,5-dimethylfuran protected maleimide (PMal[Me_2])-phosphoramidite (**3.59**) to be incorporated at the 5' oligonucleotide position as described in the literature. Starting with (2-hydroxyethyl)maleimide (**3.57**), which was available in the laboratory, we reacted it with 2,5-dimethylfuran in anh. ACN overnight at 65 ºC, to yield the appropriate (PMal[Me_2])-hydroxyl derivative as a ~1:4 mixture of *endo:exo* isomers. Treatment with conc. aq. NH_4OH provided the pure *exo* adduct (**3.58**) in a good 74% yield. Finally, the hydroxyl of **3.58** was phosphitylated with the usual chlorophosphine to provide the target phosphoramidite (**3.59**) in an excellent 90% yield (**Scheme 3.23**).

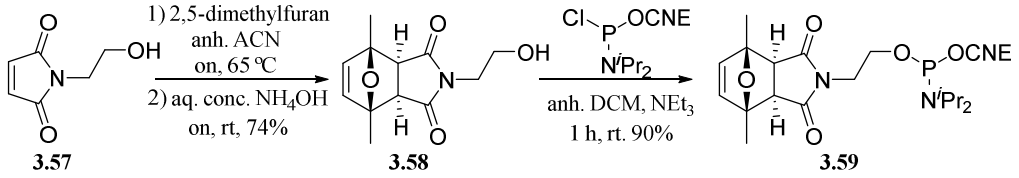

Scheme 3.23 Synthesis scheme for the preparation of the 2,5-dimethylfuran protected maleimide phosphoramidite (**3.59**).

Before starting with the ON synthesis, we performed a control experiment in order to ensure that this methodology would work with the Retro-1 derivatives previously synthesized. We reacted Retro-SH (**3.38**) with the (PMal[Me_2])-hydroxyl compound **3.58** to obtain the corresponding Michael adduct, which was subsequently subjected to the conditions required to remove the maleimide protecting group from the protected maleimido-oligonucleotides (heating for 90 min in a MW oven at 90 ºC in an aqueous methanolic solution, **Scheme 3.24**).

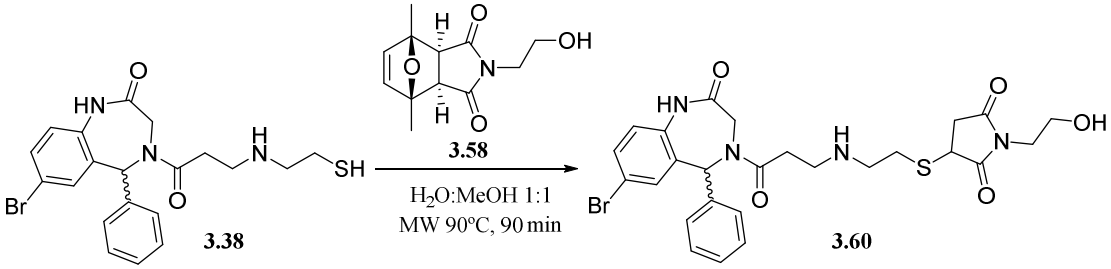

Scheme 3.24 Control experiment to verify that Retro-1 would withstand the conditions that deprotect maleimides.

The reaction was monitored by HPLC-MS at the 90 min mark, confirming nearly quantitative formation of the expected adduct (**3.60**) by MS (*m/z* = 589.3, 591.3; calcd. 589.1, 591.1). This result confirmed the viability of this approach to produce oligonucleotides conjugated with Retro-1 compounds (**Figure 3.8**).

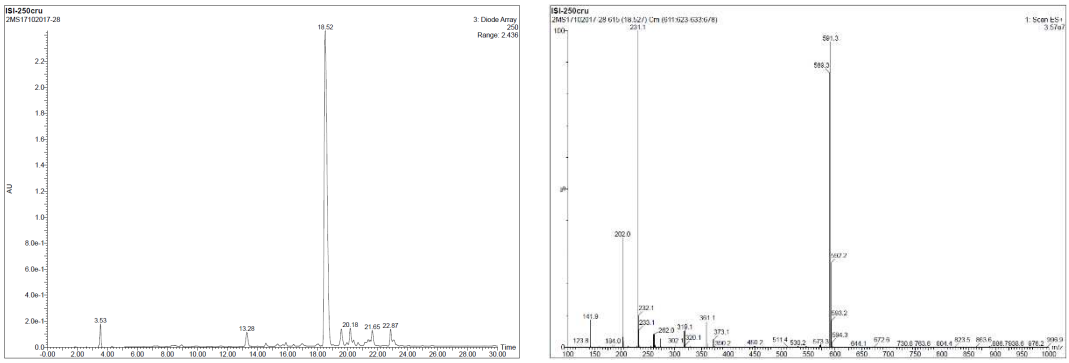

Figure 3.8 HPLC trace (250 nm, left) and MS spectrum (right) of the maleimide deprotection and Michael-addition crude.

3.5.4.2 Oligonucleotide synthesis

Once we had all the reactants ready for coupling to a protected oligonucleotide and conjugation, we just required access to a biologically relevant ON sequence. For our purposes, we assembled the

oligonucleotide coined "623" whose biological relevance was well stablished.[43] In addition, it had been used by the group of Prof. Juliano in biological assays. The 623 oligonucleotide is a 19mer RNA with sequence r[5']GTTATTCTTAGATTGGTGC[3'] containing 2'-OMe ribose modifications and phosphorothioate (PS) linkages instead of the natural phosphates (see **Section 1.2.1.1**). Moreover, it incorporates the unnatural RNA nucleoside ribothymidine (or 5-methyluridine) instead of the natural uridine.

Its biological interest lies in the fact that 623 acts as splice-switcher (SSO, see **Scheme 3.2**, C). Typical experiments involving 623 make use of genetically modified cells, usually melanoma cells, incorporating a luciferase gene[44] with an additional incorrect intron sequence. When present, this intron is not spliced and cells do not produce luciferase. Upon adequate delivery of the SSO 623, the intron is spliced out and the luciferase protein is correctly expressed, thus providing a very sensitive positive readout (luminescence) and proof of ON delivery to the nucleus.

The first route to accomplish the proposed objective involved synthesis of the fully protected modified RNA and attachment of the Retro-1-amidite (**3.35**). Since the Retro-1-amidite was a novel compound, we had to optimize solid-phase coupling conditions. To do so, we elongated a decathymidine (dT_{10}) on CPG, coupled the Retro-1-amidite once (unreacted hydroxyls were not capped) and cleaved a small aliquot in order to assess by HPLC the extent of the single coupling. As depicted in **Figure 3.9**, after one coupling cycle, only partial derivatization (≈35%) of the resin was achieved. Upon observing this we decided to perform a second coupling cycle, again without capping in order to assess whether the conversion extent had improved. Gratifyingly, after the second coupling step, a clean chromatogram (**Figure 3.9**, right) was obtained, demonstrating a high degree of conversion (≈94%) to the protected conjugate Retro-1-dT_{10}-resin oligonucleotide (**3.61**). Thus, this synthetic procedure became the standard one to derivatize ONs with the Retro-1-amidite (**3.35**). As a final proof, we also characterized the construct *via* MALDI-TOF MS analysis and successfully verified formation of the target compound (*m/z* = 3511.0; calcd. 3511.5).

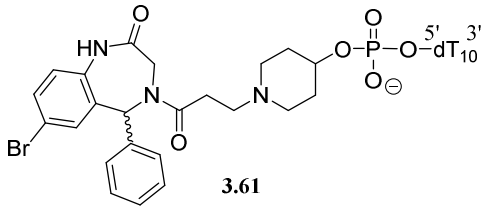

3.61

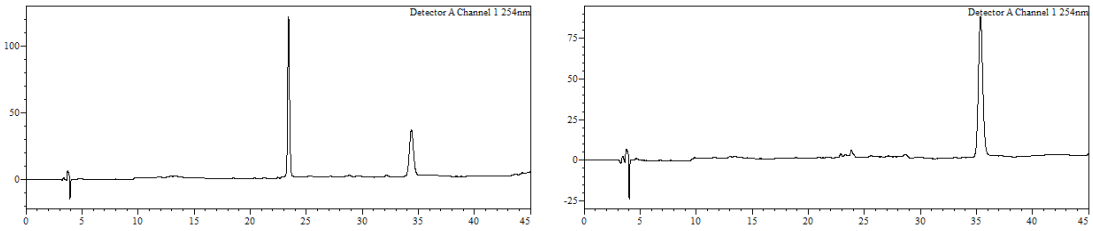

Crude after 1 coupling Crude after 2 Couplings

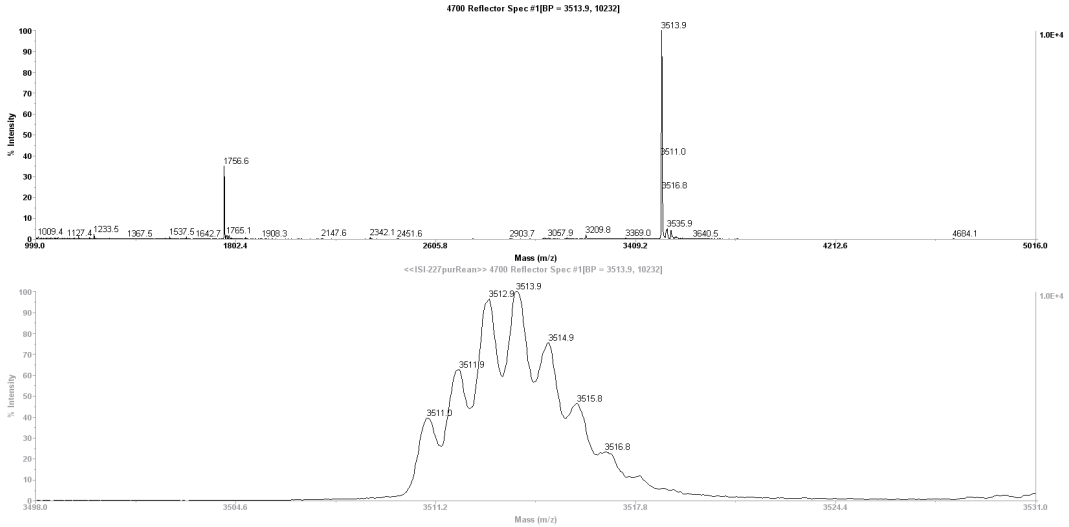

Figure 3.9 Chemical structure of conjugate **3.61** (top), HPLC traces (254 nm) of the crudes obtained after 1 or 2 coupling cycles (middle) and MALDI-TOF MS analysis of the of Retro-1-dT_{10} oligonucleotide (bottom).

After concluding on a successful derivatization of the dT_{10} oligonucleotide, we decided to chemically synthesize the 623 sequence. To do so, we utilized the phosphoramidite derivatives incorporating Ultra-mild nucleobase protecting groups and 2'-OMe derivatized ribose rings, namely rT_{OMe} (**3.62**), $r^{Pac}A_{OMe}$ (**3.63**), $r^{Ac}C_{OMe}$ (**3.64**), and $r^{iPrPac}G_{OMe}$ (**3.65**).

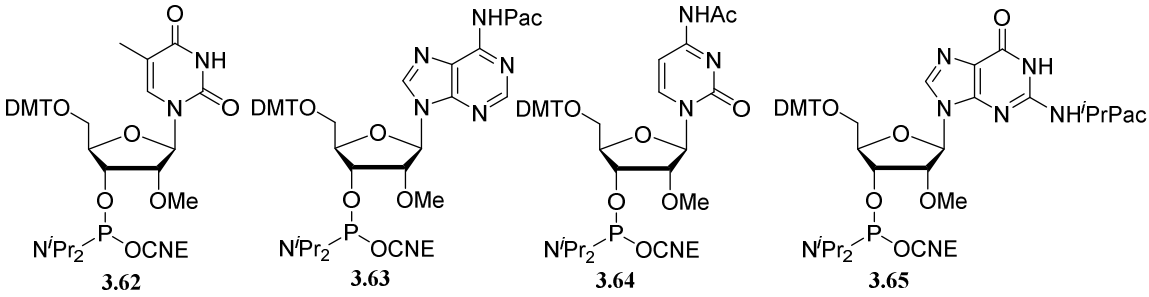

Figure 3.10 Commercially available "ultra-mild" phosphoramidites used.

Additionally, we used 3*H*-1,2-benzodithiol-3-one 1,1-dioxide (Beaucage reagent, **3.66**) as sulfurizing reagent. This reagent is a thiosulfonate introduced by Dr. Serge L. Beaucage as a straightforward sulfurizing agent.[45] Its mode of action relies on the nucleophilic attack by a phosphite triester group (**3.67**) at the sulfenyl sulfur, leading to cleavage of the polarized sulfur-sulfur bond to generate a sulfinate anion (**3.68**). This anion triggers an intramolecular cyclization to complete the sulfur transfer reaction, yielding the desired phosphorothioate linkage (**3.70**, **Scheme 3.25**).

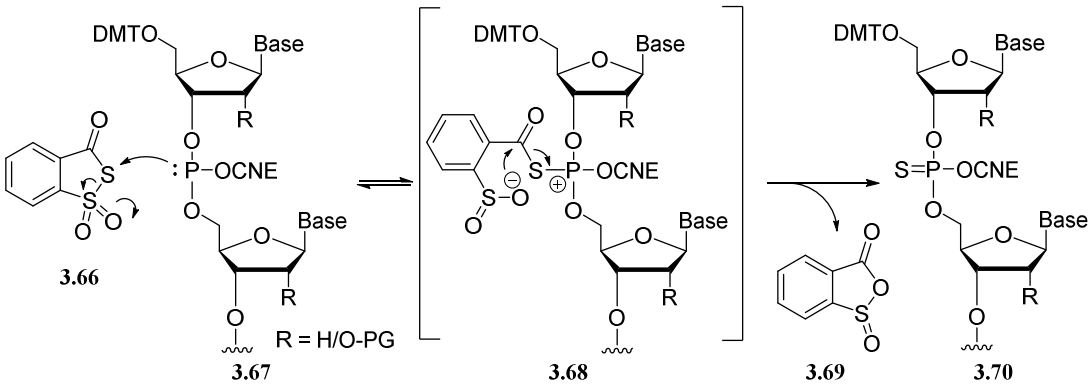

Scheme 3.25 Beaucage reagent-mediated sulfurization of phosphite triester intermediates.

Since the second route for conjugate synthesis had to make use of maleimido-oligonucleotides, it was safer to first corroborate that the (PMal[Me_2])-phosphoramidite (**3.59**) synthesized could be readily attached at the 5'-position of a resin-grown oligonucleotide. As described, the coupling reaction proceeded cleanly and only minor impurities were found in the (PMal[Me_2])-623 (**3.71**) crude as observed in the HPLC trace. To further proof the identity of the product, it was also characterized by MALDI-TOF MS (**Figure 3.11**).

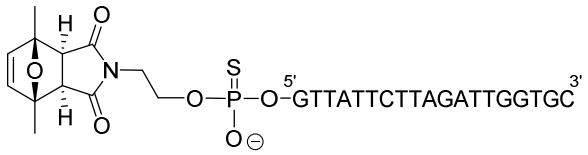

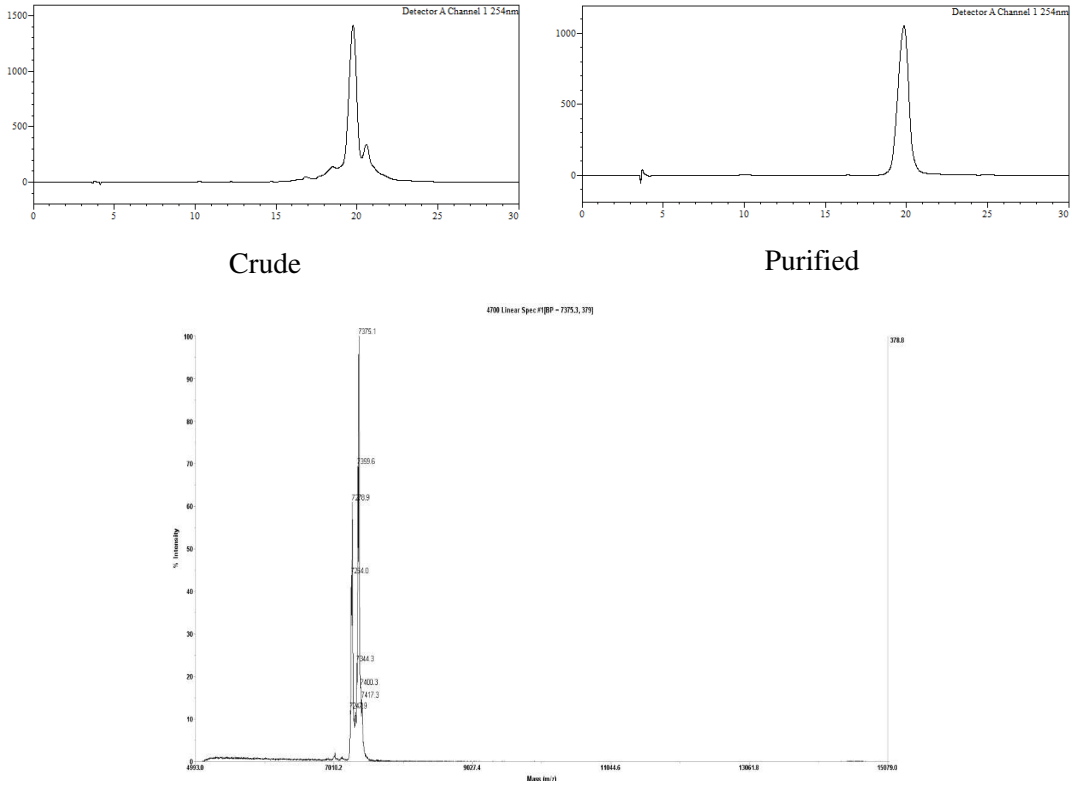

Figure 3.11 Chemical structure (top), HPLC traces (254 nm) of the cleavge crude and purified (middle), and MALDI-TOF MS characterization of the (PMal[Me_2]-623 analogue (**3.71**, bottom). The lowest mass corresponds to the loss of dimethylfuran (-96 Da) under ionization conditions.

In the context of the agreed collaboration, Prof. Rudolph Juliano provided some partner underivatized SSO 623, which was employed to fully characterize the unconjugated oligonucleotide (623) by HPLC and MALDI-TOF MS (**Figure 3.12**).

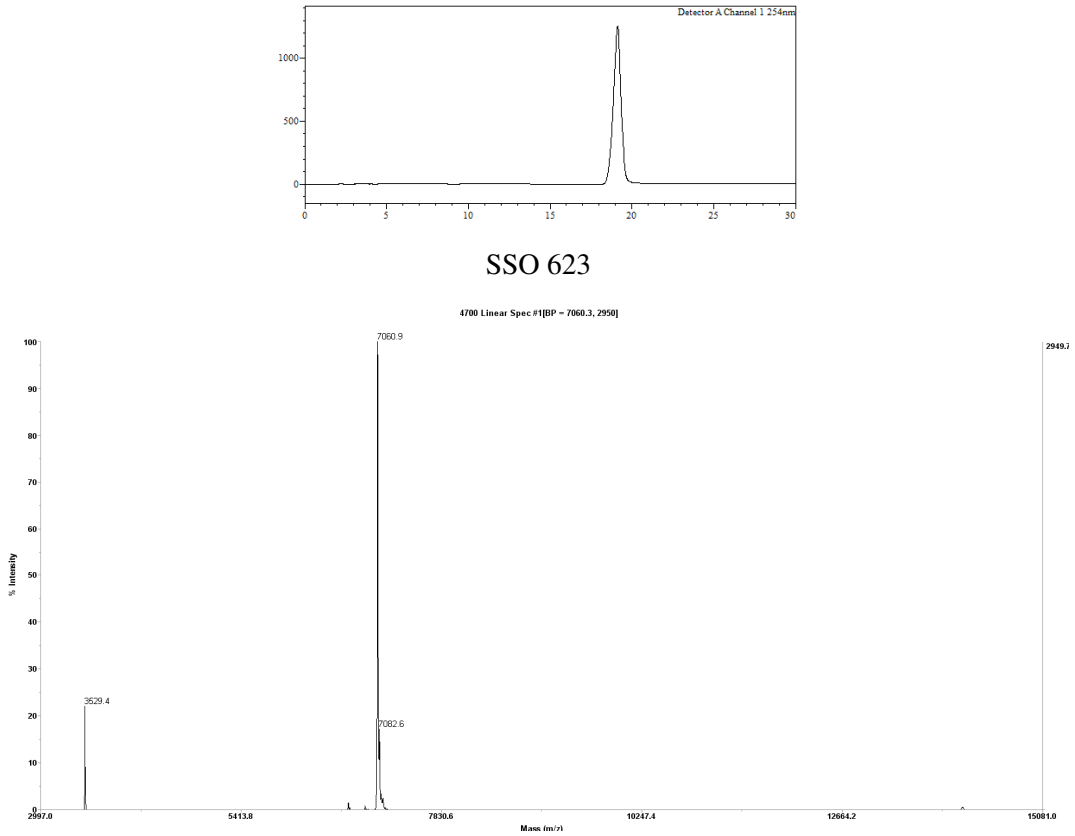

Figure 3.12 HPLC traces (254 nm, top) and MALDI-TOF MS spectrum (bottom) of the 623 oligonucleotide.

In order to biologically test the 623 conjugates, negative controls also had to be produced. Therefore, we envisioned assembling a sequence (called "Scrambled" ON) containing the same nucleobases and backbone modifications, but with the nucleoside order changed ($r^{5'}$TGTGTACTGATGTAGTTATC$^{3'}$). The same synthetic scheme as for the 623 oligonucleotide was employed.

For the underivatized Scrambled version, HPLC analysis of the crude showed an acceptable quality. Nonetheless, after purification identity was confirmed by MALDI-TOF MS (**Figure 3.13**).

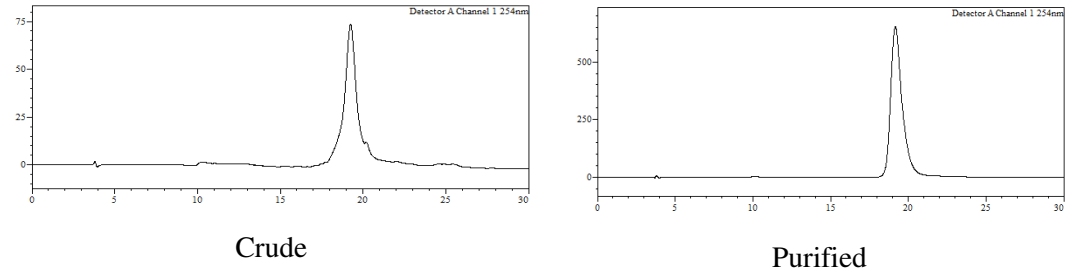

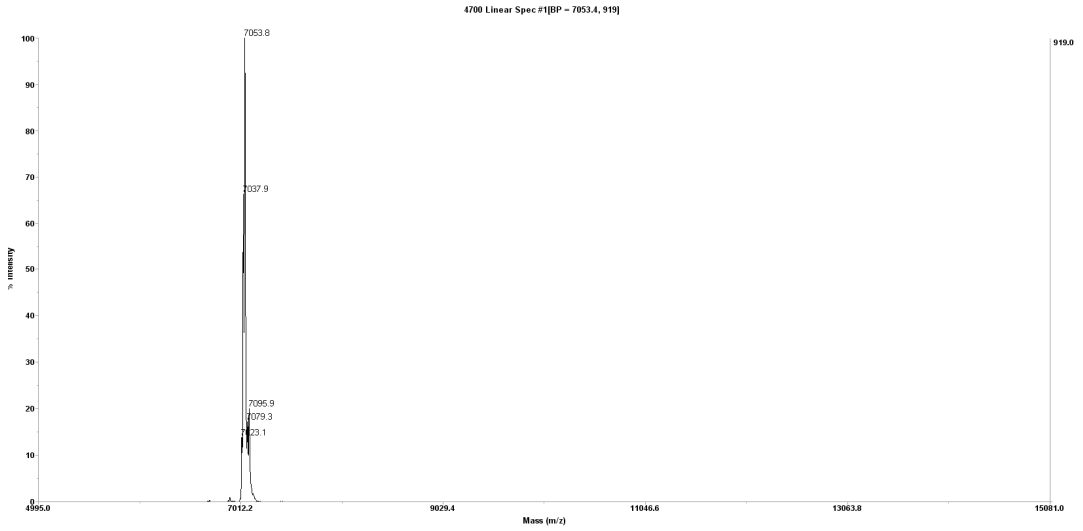

Figure 3.18 HPLC traces (254 nm) of Scrambled ON, crude and purified (top), and MALDI-TOF MS spectrum of the isolated product (bottom).

In summary, both the 623 and the Scrambled oligonucleotides were assembled using the standard phosphite triester methodology, the above described sulfurization procedure, and the 2'-O-Me phosphoramidites whose structure is shown in **Figure 3.10** In both cases, 1 μmol batches of the oligonucleotide-resins were kept fully protected (with the 5' terminal DMT group) awaiting reaction with the Retro-1-amidite (**3.35**), and other 1 μmol batches were elongated with the (PMal[Me_2])-phosphoramidite (**3.59**).

3.5.4.3 Conjugates of oligonucleotide 623

For the synthesis of the first conjugate, the Retro-1-phosphoramidite (**3.35**) was appended *via* a two-coupling cycle to a growing oligonucleotide-resin as previously optimized. Subsequently, conc. aq. NH_4OH treatment for cleavage and deprotection yielded the crude oligonucleotide conjugate (**3.72**), which was analyzed and purified by HPLC (**Figure 3.14**). The isolated oligonucleotide (36%) was also characterized by MALDI-TOF MS.

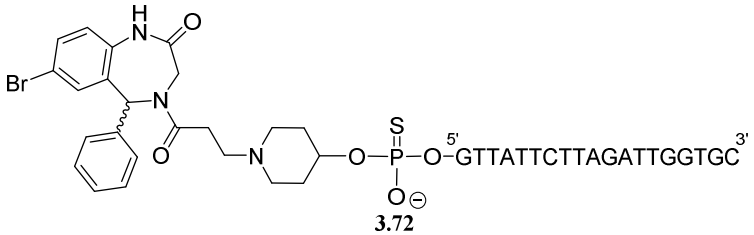

3.72

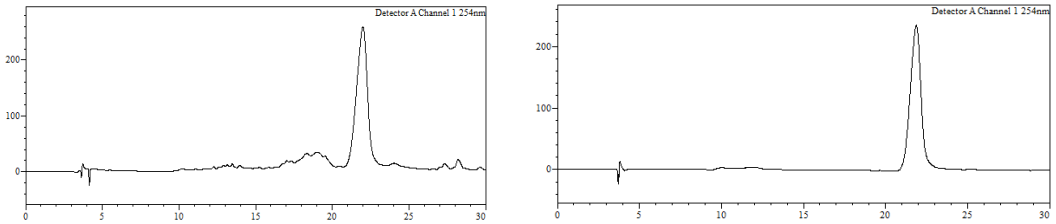

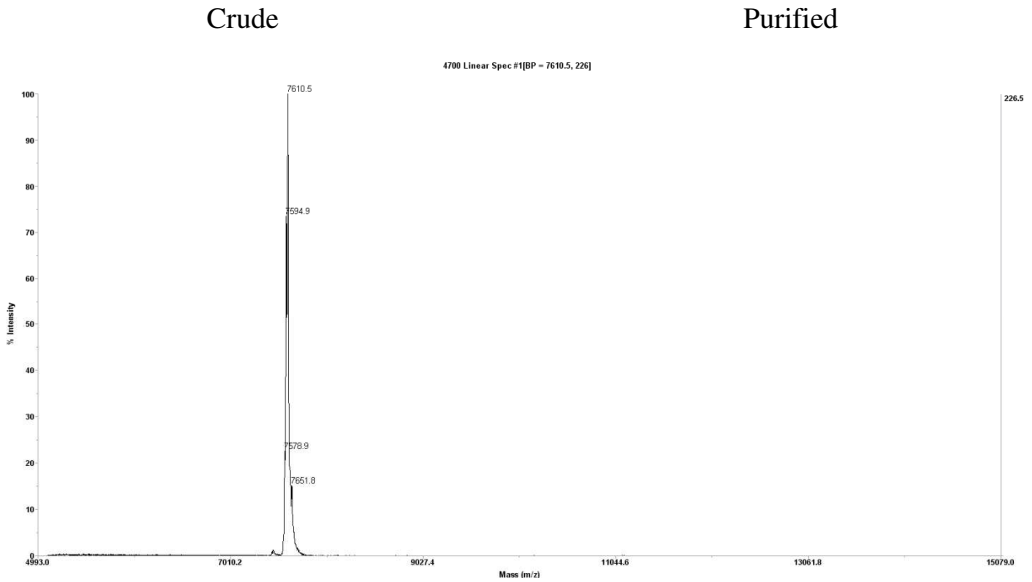

Figure 3.14 Retro-1-623 conjugate chemical structure (**3.72**, top), HPLC traces (254 nm) of the crude and purified (middle) and MALDI-TOF MS spectrum (bottom) of isolated conjugate.

Pleased with these good results, we turned to the second rounds of synthesis, in this case involving the (PMal[Me_2])-623 oligonucleotide (**3.71**). Here, a rDA had to be performed first in order to obtain the maleimido-oligonucleotide (**3.73**) and, finally, react it with the appropriate Retro-1 derivative (**3.38**, **3.44** or **3.52**) as depicted in **Scheme 3.26**.

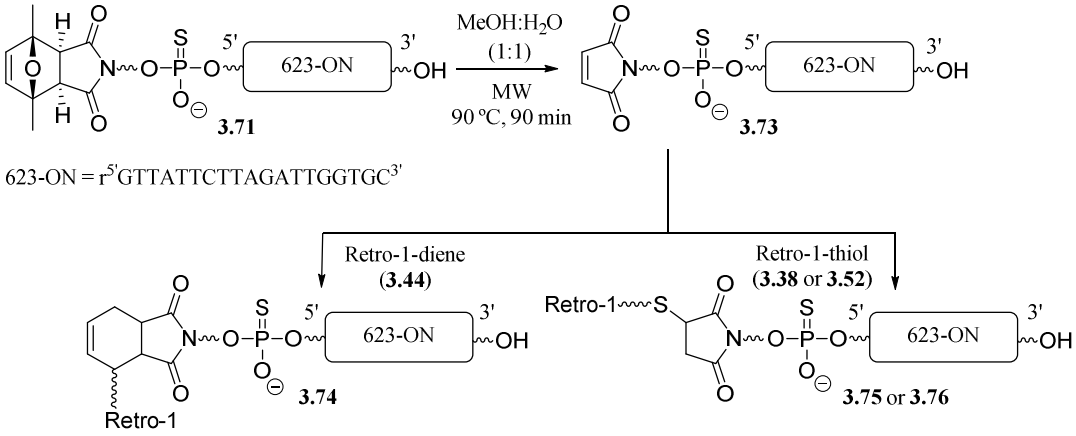

Scheme 3.26 Synthetic outline for the preparation of Retro-1-623 conjugates *via* a Diels-Alder reaction and a thia-Michael addition.

It had been previously observed that the retro-Diels-Alder reaction deprotecting maleimide and the subsequent conjugation reaction (either a diene-maleimide Diels-Alder cycloaddition or a maleimide-thiol Michael-type addition) can be carried out in a one-pot fashion (without purifying the maleimido intermediate) and even simultaneously. In this case, we proceeded with the rDA and subsequent conjugation reaction in a one-pot fashion as described.[42,46] Our initial conjugation attempt was performed with Retro-1-SH (**3.38**), by reacting it with **3.71** in a MeOH:H_2O (1:1) mixture at 90 ºC for 90 min (0.5 mM oligonucleotide concentration). From the crude shown in **Figure 3.15** we purified the major compound, but after MALDI-TOF MS analysis we concluded that it was not the expected conjugate but starting material.

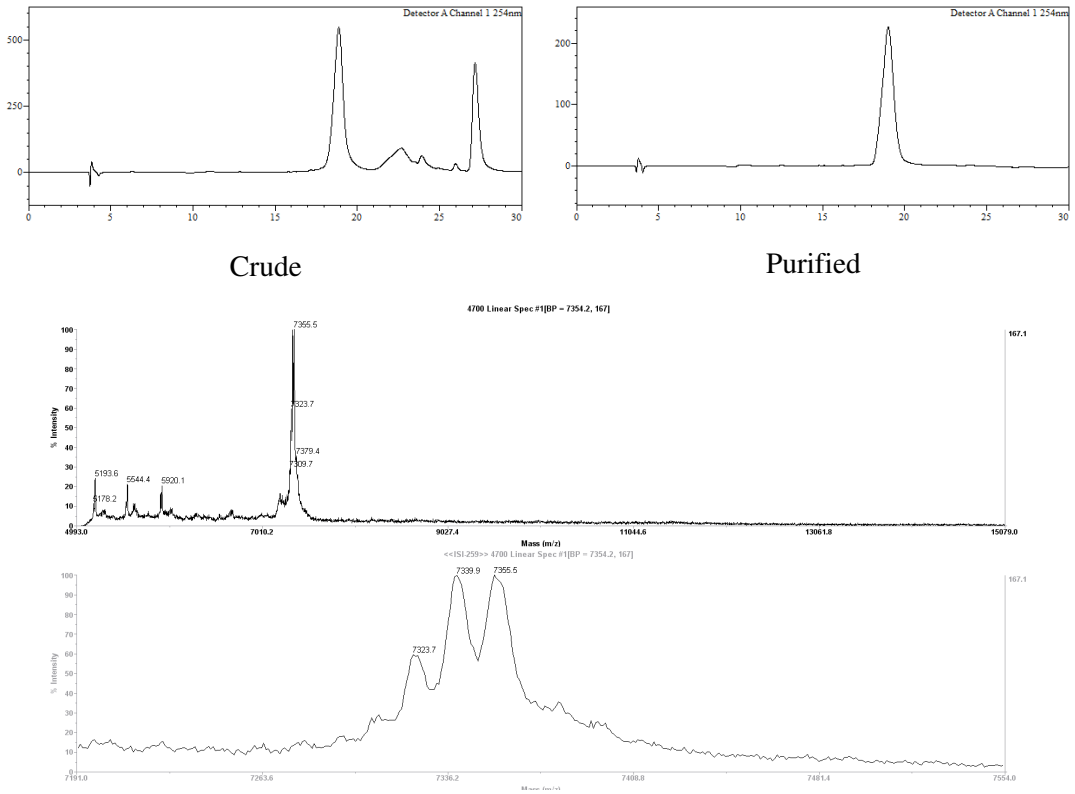

Figure 3.15 HPLC traces (254 nm) of the first attempt of one-pot deprotection and conjugation of a thiol and **3.71** (top), and MALDI-TOF MS characterization of the conjugate (bottom).

Upon careful examination into the described procedures, we found out that protected maleimide concentration was of paramount importance at the deprotection step, and the 0.5 mM concentration previously employed was too high, maleimide deprotection ought to be performed in the 10-200 μM concentration range (**Scheme 3.27**).[47]

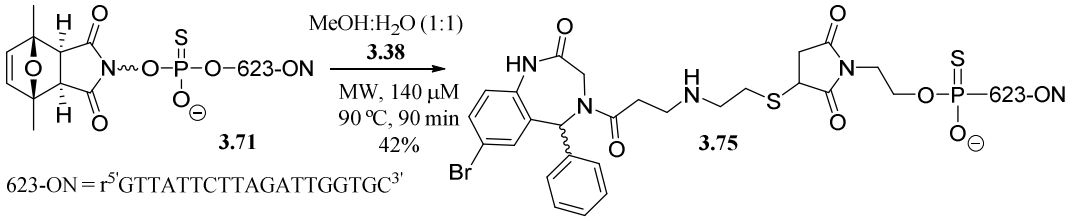

Scheme 3.27 Conjugation reaction of (PMal[Me_2])-623 (**3.71**) and Retro-1-SH (**3.38**).

Therefore, we performed the same reaction but this time using a 140 μM oligonucleotide concentration, and obtained different chromatogram as depicted in **Figure 3.16**. After purification, the final conjugate was characterized by MALDI-TOF MS. It is worth mentioning that having broad peaks is not unexpected, because phosphorothioate ONs are in fact obtained as a mixture of isomers, which very often do not elute as sharp peaks.

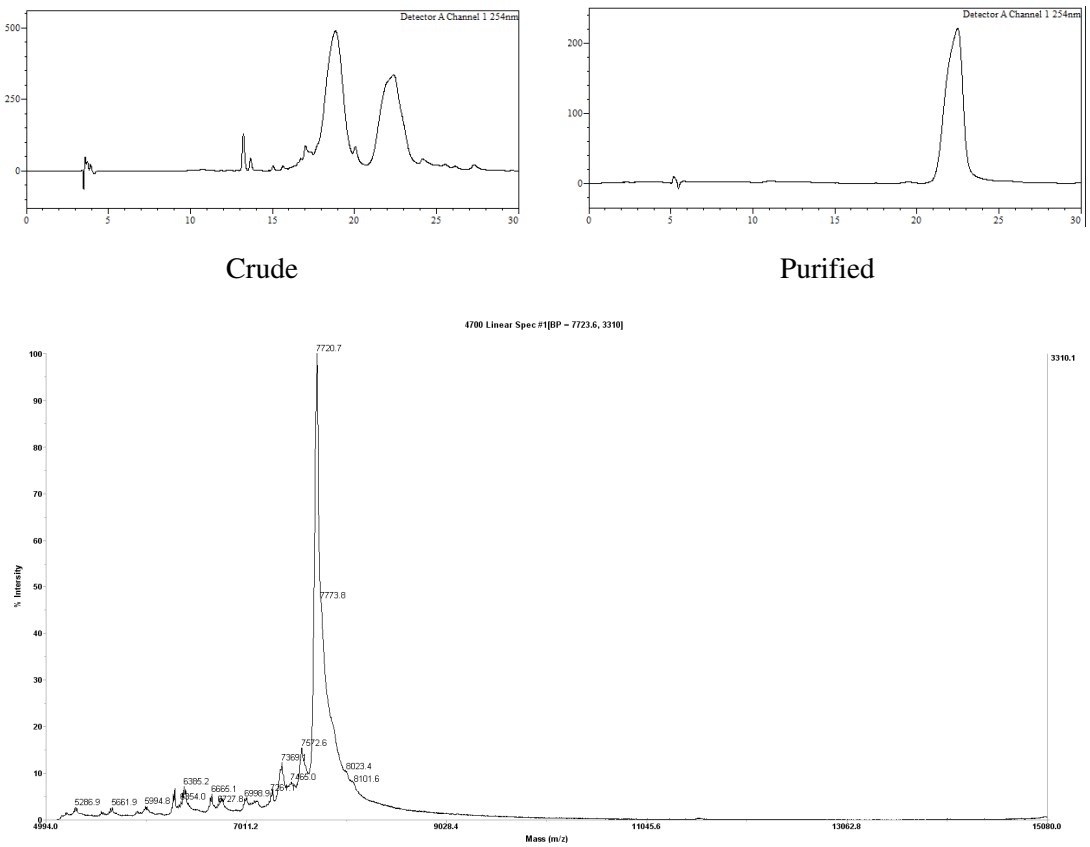

Figure 3.16 HPLC traces (254 nm) of the crude (left) and purified (right) conjugate **3.75** after one-pot maleimide deprotection and conjugation working at 140 μM oligonucleotide concentration (top), and MALDI-TOF MS characterization of the isolated product (bottom).

After the success of the first thiol-maleimide conjugation, we reacted the (PMal[Me_2])-623 oligonucleotide (**3.71**) with the Retro-1-diene (**3.44**) in the optimized maleimide deprotection conditions (40 μM oligonucleotide concentration). After purification, the desired conjugate was isolated in 25% yield (**Scheme 3.28**).

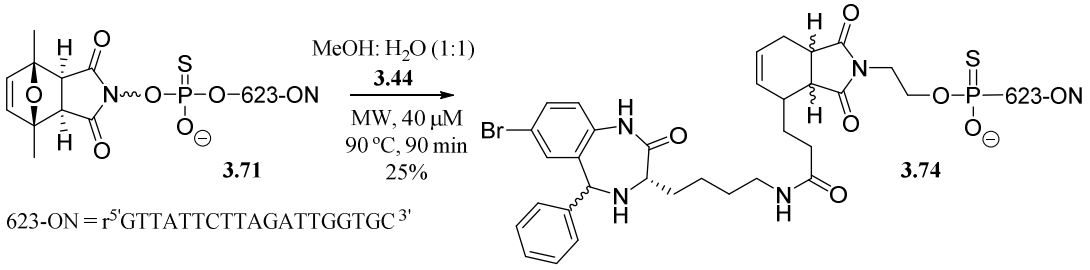

Scheme 3.30 Conjugation reaction of (PMal[Me_2])-623 (**3.71**) and Retro-1-diene (**3.44**).

The reaction also proceeded smoothly in this instance with, no major detriments as demonstrated by the HPLC analysis and MALDI-TOF MS characterization of the target conjugate (**3.74**, **Figure 3.17**).

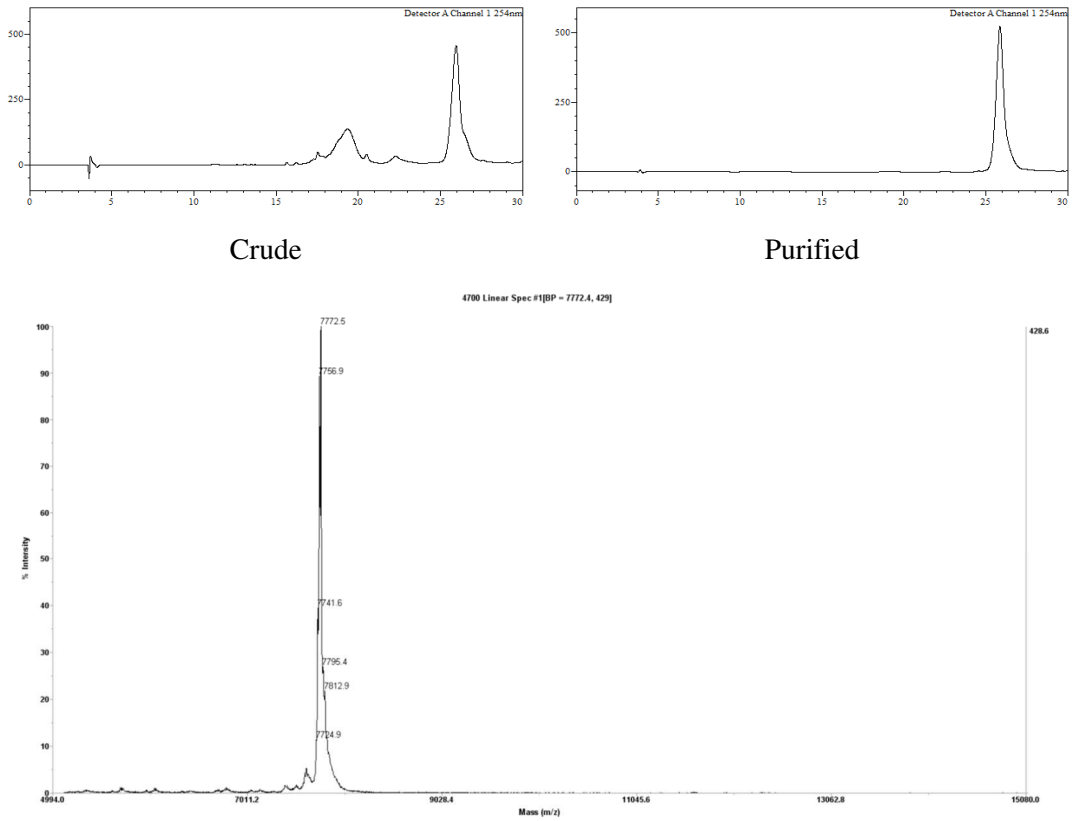

Figure 3.17 HPLC traces (254 nm) of the conjugation reaction between the Retro-1-diene (**3.44**) analogue and (PMal[Me_2])-623 (**3.71**, top), and MALDI-TOF MS characterization of the conjugate (bottom).

Finally, we moved towards the lysine analogue containing a thiol functionality (**3.52**) and reacted it with oligonucleotide **3.71** in a MW oven (40 μM oligonucleotide concentration), for 90 min at 90 ºC (**Scheme 3.29**).

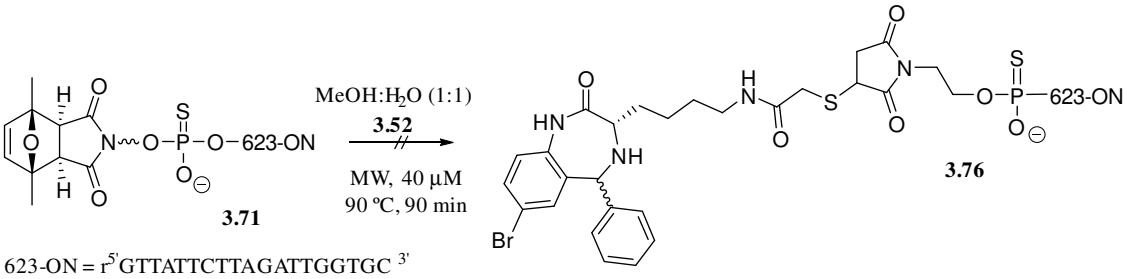

Scheme 3.29 Conjugation attempt of (PMal[Me_2])-623 (**3.71**) and Retro-1-Lys-SH (**3.52**).

In this instance, though, the reaction seemed not to proceed as expected, as seen by HPLC analysis. Nonetheless, we isolated the major compound, but confirmed by MALDI-TOF MS analysis that, the purified major compound was not the target conjugate but an unidentified by-product (**Figure 3.18**).

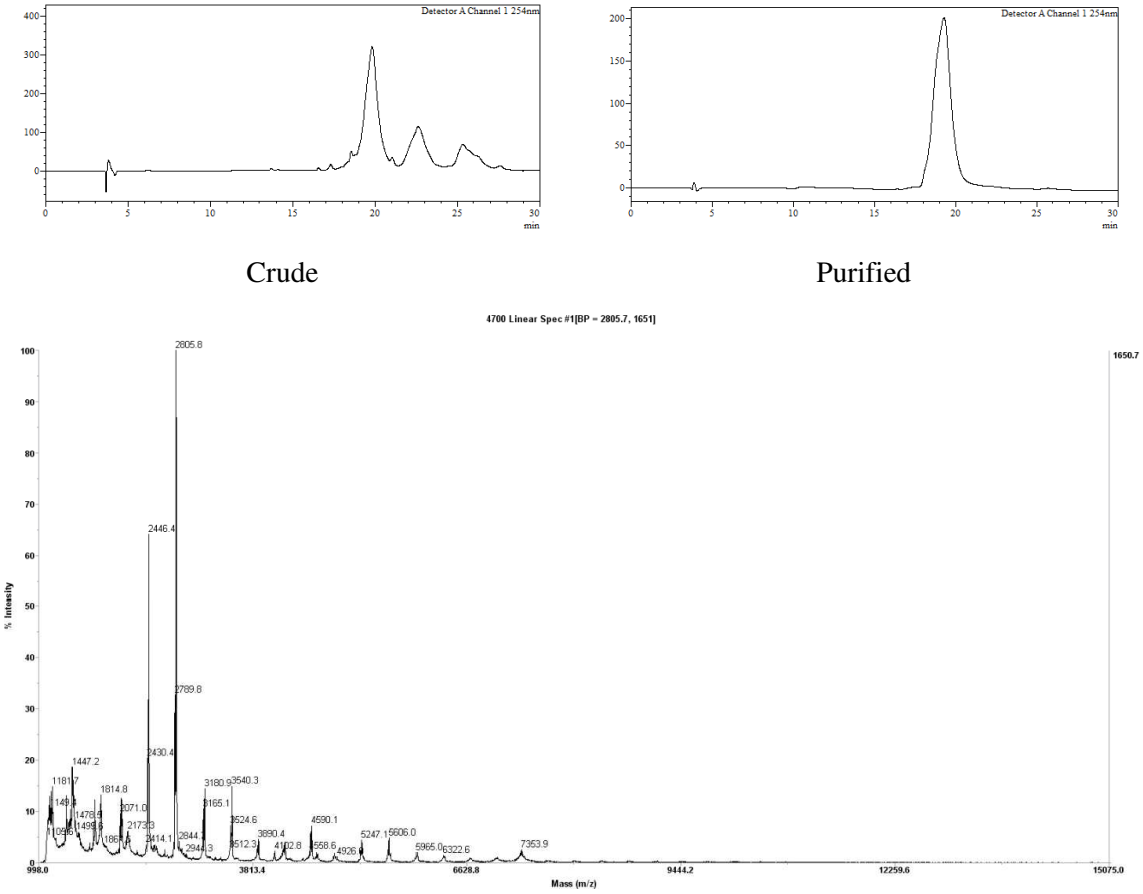

Figure 3.18 HPLC traces (254 nm) of the crude conjugation reaction of Retro-1-Lys-SH (**3.52**) and oligonucleotide **3.71** (top, left) and of the isolated product (top, right), and MALDI-TOF MS spectrum (bottom).

Several additional attempts were done, but all proved to be unsuccessful. The desired conjugate adduct could never be obtained, so we abandoned this route.

3.5.4.4 Conjugates of Scrambled oligonucleotide

With the Scrambled oligonucleotide we proceeded analogously. We firs carried out incorporation of the Retro-1-phosphoramidite (**3.35**) using a double coupling as previously optimized. In this case, though the incorporation was not as successful (**Figure 3.19**). That being said, the overall yield (20%) of pure product (**3.77**) was deemed enough to proceed with biological assays.

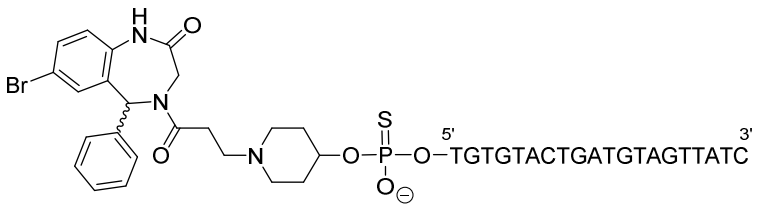

3.77

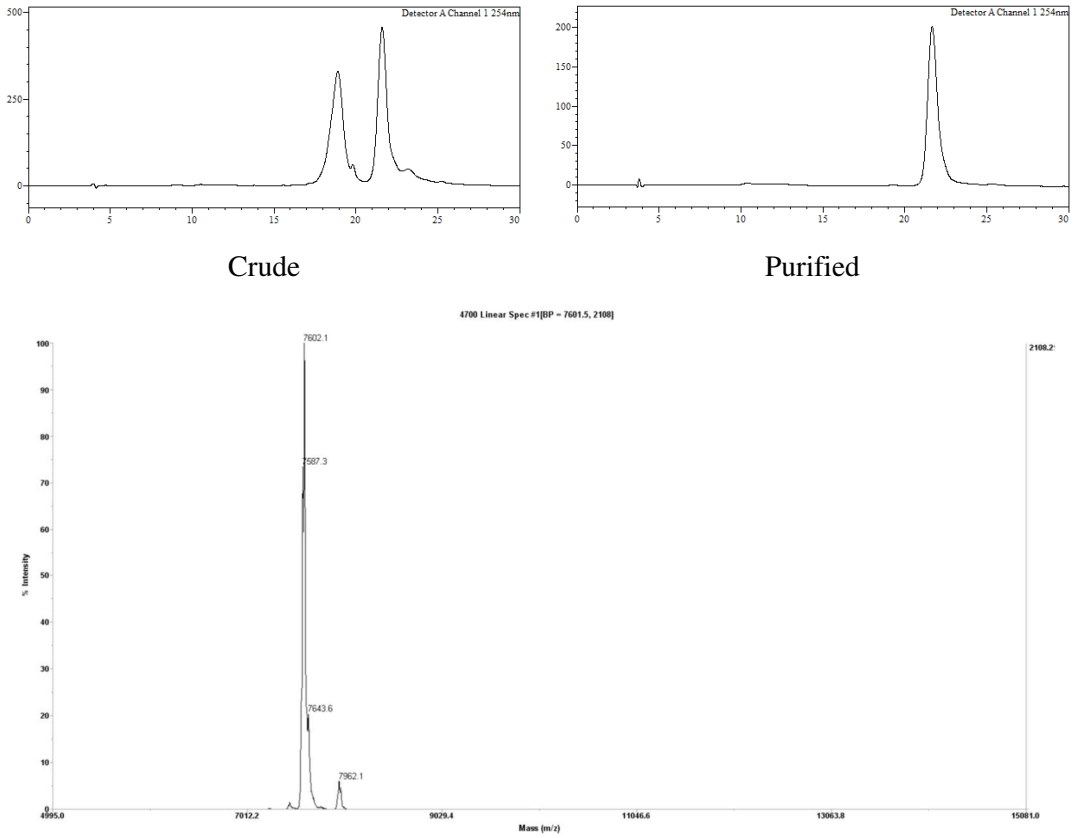

Figure 3.19 Structure of the Retro-1-Scrambled conjugate (**3.77**, top); HPLC traces (254 nm) of the crude and after purification (intermediate segment), and MALDI-TOF MS spectrum of the isolated conjugate (bottom).

In a similar fashion, the diene and thiol conjugates were obtained. That is, after appending the (PMal[Me_2])-phosphoramidite (**3.59**) to the Scrambled oligonucleotide-resin, deprotection with ammonia and purification to yield the 2,5-dimethylfuranprotected maleimide scrambled oligonucleotide (**3.78**). Afterwards, the maleimide was deprotected as previously and reacted with either the Retro-1-diene (**3.44**) or Retro-1 thiols (**3.38** or **3.52**).

In the Retro-1 diene case, the target cycloadduct (**3.79**) was successfully obtained, after purification in 36% yield (**Figure 3.20**).

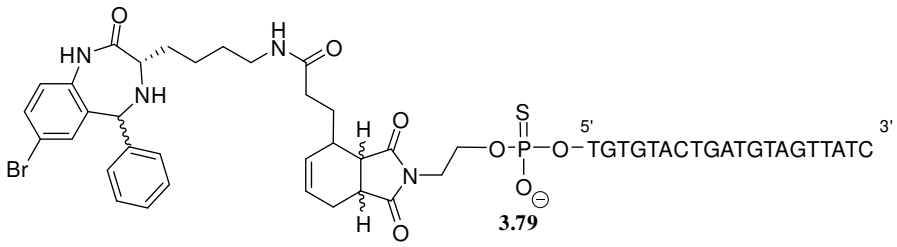

3.79

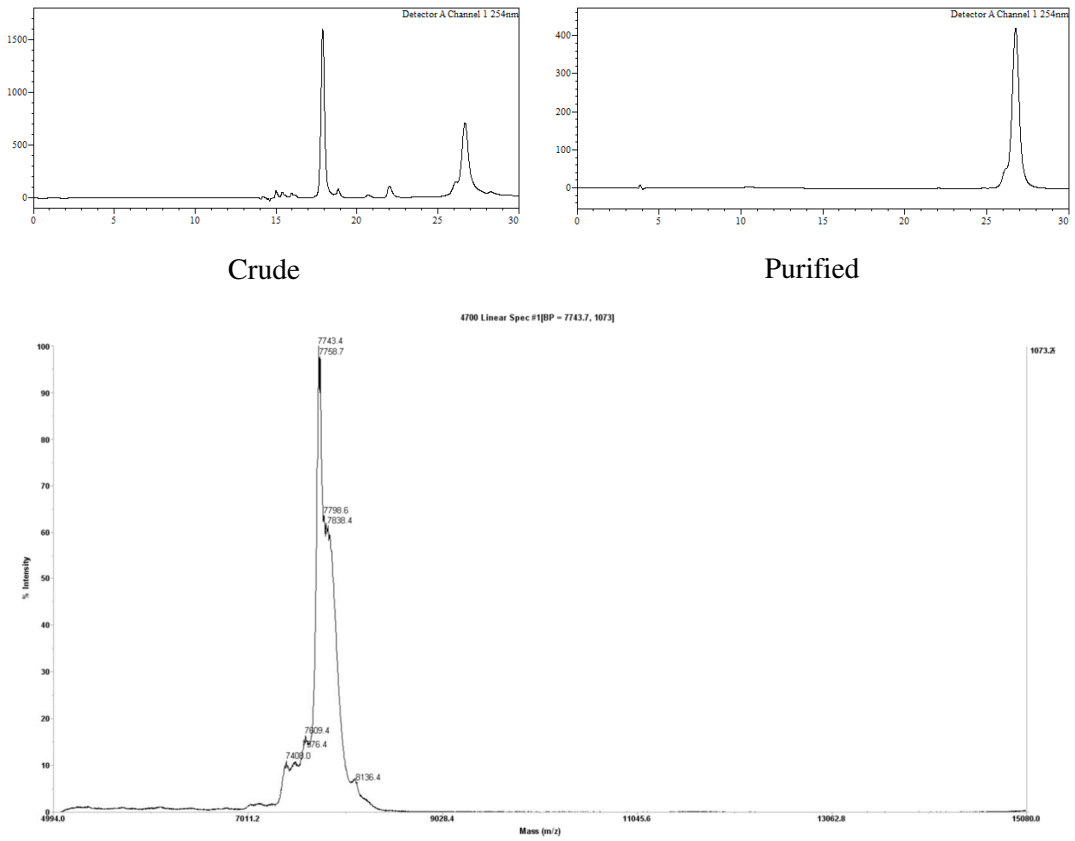

Figure 3.20 Structure of the Retro-1-diene-Scrambled conjugate (**3.79**, top); HPLC traces (254 nm) of crude and pure cycloadduct and MALDI-TOF MS spectrum of the isolated conjugate.

Subsequently, we tackled the reaction of the protected-maleimido Scrambled oligonucleotide with Retro-1-thiol derivatives. Since the conjugation of the Retro-1-Lys-SH analogue (**3.52**) to the (PMal[Me_2])-623 (**3.71**) had previously failed, we decided not to perform it with the Scrambled oligonucleotide.

As to the other thiol-maleimide conjugation, in this instance attempts to reproduce previous positive results (synthesis of conjugate **3.75**) were fruitless. The conjugation reaction between Retro-1-SH (**3.38**) and the protected-maleimido Scrambled oligonucleotide resulted in a complex mixture from which no desired conjugate could be isolated. Nonetheless, since this conjugate had to be used as a control in biological assays, at this stage of the investigation we deemed not worth to put more effort into synthesizing this conjugate either.

3.6 Biological tests

Assays to determine whether the Retro-1-oligonucleotide conjugates got into the nucleus more easily than the two separate components (which could be assessed on the basis of the effect of the oligonucleotide on the splicing reaction) were performed, as previously indicated, in the laboratory of Prof. Rudolph L. Juliano.

The experiments were carried out employing the HeLa Luc 705 cell line[44] and both the conjugated and unconjugated form of oligonucleotide having the already discussed splice correcting sequence r$^{5'}$GTTATTCTTTAGAATGGTGC$^{3'}$ (623). Moreover, the obtained results were compared to those provided by control oligonucleotides with the inactive sequence r$^{5'}$TGTGTACTGATGTAGTTATC$^{3'}$ (Scrambled).

Figure 3.21 assembles the results obtained with the Retro-1-623 conjugate (**3.72**), the control Retro-1-Scrabled conjugate (**3.77**) and unconjugated SSO-623. As seen in the figure, Retro-1-623 (**3.72**) produced a dose-dependent luciferase induction while the control Retro-1-Scrambled (**3.77**) did not. However, SSO 623 itself also gave rise to a progressive induction of luciferase activity that was somewhat greater than the activity produced by the conjugated 623 oligonucleotide (**3.72**).

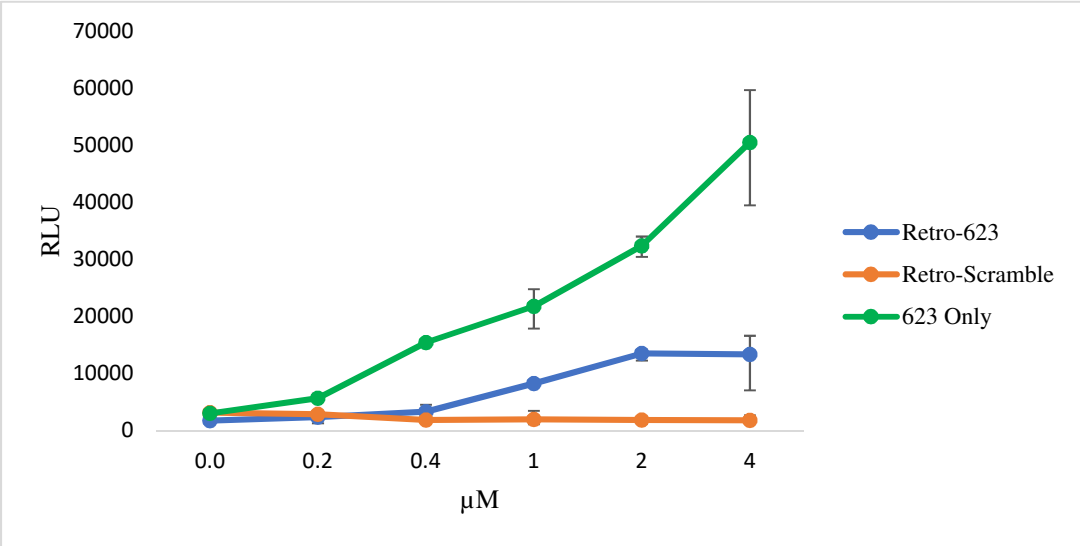

Figure 3.21 HeLa705 cells in complete growth medium were incubated for 16 h with various concentrations of conjugated or unconjugated 623 oligonucleotide. Thereafter the cells were recovered and a luminescence assay was undertaken. RLU = relative luminescence units; n = 3. Means and standard errors are shown. Retro-623 = **3.72**; Retro-Scramble = **3.77**.

This set of experiments demonstrated that coupling of the Retro-1 moiety did not provide an advantage, in terms of potency or efficacy, over the partner SSO 623 itself. Additional conjugates (**3.74**) and (**3.75**) were also examined and neither of these conjugates also displayed an advantage over SSO 623 in the HeLa Luc 705 induction assay (data now shown).

Another experiment was carried out with a different cell line, in this instance, mouse tracheal cells induced with EGFP654. In this experiment, grown cells were treated with Retro-623 conjugate (**3.72**) or unconjugated 623 by either basolateral (BL) of apical (AP) administration (4 µM for 3 h). As can be seen in **Figure 3.22** clear indication of a greater splice-switching efficacy can be observed with the conjugate in comparison to the unmodified 623.

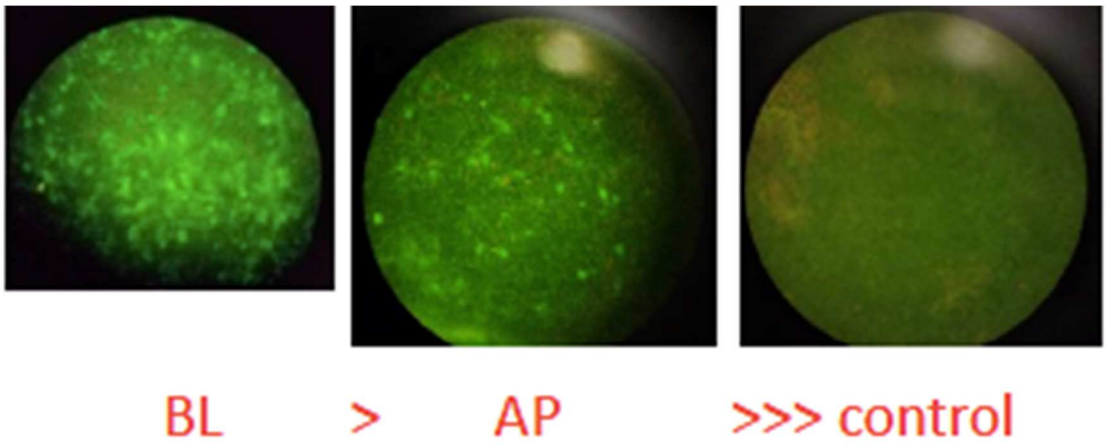

Figure 3.22 Effect of Retro-623 on induction of EGFP654 in Mouse Tracheal Cells. Images show day 7 EGFP expression from basolateral (left) and apical (center) administration or the unconjugated control (right).

In summary, conjugation of the Retro moiety to a splice switching oligonucleotide did not provide a major enhancement of splice correction activity in the widely used HeLa Luc 705 reporter system. It is unclear why the conjugated displayed slightly lower activity than the unmodified ON. A hypothesis could be that the presence of the bulky Retro group might affect either cell uptake or interaction with splicing machinery. On the other hand, with the mouse tracheal cell line, a beneficial improvement clearly took place. This result is not surprising, since examples have been described of substances producing an effect *in vivo* but not *in vitro*. Further work will have to be carried out to really assess whether oligonucleotides conjugated to antisense enhancing compounds hold promise or not.

3.7. Concluding remarks

In this work Retro-1 synthesis has been successfully reproduced. Moreover, several Retro-1 analogues derivatized at two different positions within the diazepine scaffold have been successfully synthesized, one being a phosphoramidite with capabilities for being introduced into a 5' position of a growing oligonucleotide and others incorporating functional groups for conjugation ins solution using click-type reactions. In this context, successful derivatization of a biologically active SSO (623), and a control sequence has been achieved. On-resin bioconjugations and most of the conjugation reactions carried out in solution were successful, allowing for a variety of conjugations to be obtained. Biological studies to assess the splice-switching activity have been carried out, showing that the conjugates were sometimes less potent and sometimes more potent that the unconjugated 623 oligonucleotide.

Testing conjugates of other antisense splice-switching molecules, other site of appendage, different cell lines and even *in vivo* experiments will finally answer the question we tried to answer.

3.8 Abbreviations

Ac	Acetyl
ACN	Acetonitrile
AcOH	Acetic acid
Anh	Anhydrous
AP	Apical administration
Aq	Aqueous
ASO	Antisense oligonucleotide
Beaucage Reagent	3*H*-1,2-Benzodithiol-3-one 1,1-dioxide
BL	Basolateral administration
Boc	*tert*-Butyloxycarbonyl
calcd	Calculated
Cat	Catalytic amount
CNE	2-Cyanoethyl
COMU	(1-Cyano-2-ethoxy-2-oxoethylidenaminooxy)dimethylamino-morpholino-carbenium hexafluorophosphate
conc	Concentrated
Da	Atomic mass unit (Dalton)
DA	Diels-Alder cycloaddition
DCM	Dichloromethane
Diene-COOH	(*E*)-Hepta-4,6-dienoic acid
DIPC	*N*,*N*'-Diisopropylcarbodiimide
DIPEA	*N*,*N*-Diisopropylethylamine
DME	Dimethyoxyethane
DMT	4,4'-Dimethoxytrityl
DNA	Dexyribonucleic acid
EDC·HCl	*N*-(3-Dimethylaminopropyl)-*N*′-ethylcarbodiimide hydrochloride
EGFP	Enhanced green fluorescent protein
Et	Ethyl
EtOH	Ethanol
FDA	Food and Drug Administration (USA)
Fmoc	Fluorenylmethoxycarbonyl
HOBt	Hydroxybenzotriazole
HPLC	High performance liquid chromatography
IBCF	Isobutyl chloroformate
^{i}Pr	Isopropyl
^{i}PrPac	4-Isopropylphenoxyacetyl
Luc	Luciferase reporter
MALDI	Matrix-assisted laser desorption and ionization
Me	Methyl
mRNA	Messenger ribonucleic acid
MS	Mass spectrometry
MSNT	1-(2-Mesitylenesulfonyl)-3-nitro-1*H*-1,2,4-triazole

MW	Microwave
NBS	*N*-Bromosuccinimide
NEt_3	Triethylamine
NMM	*N*-Methylmorpholine
NMR	Nuclear magnetic ressonance
ON	Oligonucleotide
on	Overnight
Pac	Phenoxyacetyl
PG	Protecting group
PMal[Me_2]	*exo*-3,6-Dimethyl-3,6-epoxy-1,2,3,6-tetrahydrophthalimide
PMal[Me_2]-Ol	4-(2-Hydroxyethyl)-1,7-dimethyl-10-oxa-4-aza-tricycle[5.2.1.$0^{2,6}$]dec-8-en-3,5-dione
Prop-COOH	Propionic acid
PS	Phosphorothioate
PTFE	Polytetrafluoroethylene
RLU	Relative luminescence units
RNA	Ribonucleic acid
RNase H	Ribonuclease H
rt	Room temperature
siRNA	Small interfering ribonucleic acid
snRNPs	Small nuclear ribonuclear proteins
SPONS	Solid-phase oligonucleotide synthesis
SPPS	Solid-phase peptide synthesis
SSO	Splice-switching oligonucleotides
TFA	Trifluoroacetic acid
THF	Tetrahydrofuran
TIS	Triisopropylsilane
TMS	Trimethylsilyl
tRNA	Transfer ribonucleic acid
Trt	Trityl

3.9. Bibliography

(1) Lander, E. S. . L.; Birren, L. M. .; Nusbaum, B.; Zody, C.; Baldwin, M. C. .; Devon, J.; Dewar, K.; Doyle, K.; FitzHugh, M.; Funke, W.; et al. *Nature* **2001**, *409* (6822), 860–921.

(2) Crick, F. *Nature* **1970**, *227* (5258), 561–563.

(3) Pan, Q.; Shai, O.; Lee, L. J.; Frey, B. J.; Blencowe, B. J. *Nat. Genet.* **2008**, *40* (12), 1413–1415.

(4) Matteucci, M. D.; Caruthers, M. H. *J. Am. Chem. Soc.* **1981**, *103* (11), 3185–3191.

(5) Beaucage, S. L.; Caruthers, H. M. *Tetrahedron Lett.* **1981**, *22* (20), 1859–1862.

(6) Caruthers, M. H. *J. Biol. Chem.* **2013**, *288* (2), 1420–1427.

(7) Heather, J. M.; Chain, B. *Genomics* **2016**, *107* (1), 1–8.

(8) Guan, S.; Rosenecker, J. *Gene Ther.* **2017**, *24* (3), 133–143.

(9) Suhr, O. B.; Coelho, T.; Buades, J.; Pouget, J.; Conceicao, I.; Berk, J.; Schmidt, H.; Waddington-Cruz, M.; Campistol, J. M.; Bettencourt, B. R.; et al. *Orphanet J. Rare Dis.* **2015**, *10* (1), 109.

(10) Mendell, J. R.; Rodino-Klapac, L. R.; Sahenk, Z.; Roush, K.; Bird, L.; Lowes, L. P.; Alfano, L.; Gomez, A. M.; Lewis, S.; Kota, J.; et al. *Ann. Neurol.* **2013**, *74* (5), 637–647.

(11) Zhang, H.; Ma, Y.; Xie, Y.; An, Y.; Huang, Y.; Zhu, Z.; Yang, C. J. *Sci. Rep.* **2015**, *5* (1), 10099.

(12) Zamecnik, P. C.; Stephenson, M. L. **1978**, *75* (1), 280–284.

(13) Geary, R. S.; Baker, B. F.; Crooke, S. T. *Clin. Pharmacokinet.* **2015**, *54* (2), 133–146.

(14) G. de la Torre, B.; Albericio, F. *Molecules* **2019**, *24* (4), 809.

(15) Stein, C. A.; Castanotto, D. *Mol. Ther.* **2017**, *25* (5), 1069–1075.

(16) Khvorova, A.; Watts, J. K. *Nat. Biotechnol.* **2017**, *35* (3), 238–248.

(17) Sun, Y.; Zhao, Y.; Zhao, X.; Lee, R. J.; Teng, L.; Zhou, C. *Molecules* **2017**, *22* (10), 1724.

(18) Juliano, R. L. *Nucleic Acid Ther.* **2018**, *28* (3), 166–177.

(19) Levins, C. G.; Schroeder, A.; Langer, R.; Cortez, C.; Anderson, D. G. *J. Intern. Med.* **2009**, *267* (1), 9–21.

(20) Konate, K.; Dussot, M.; Aldrian, G.; Vaissière, A.; Viguier, V.; Neira, I. F.; Couillaud, F.; Vivès, E.; Boisguerin, P.; Deshayes, S. *Bioconjug. Chem.* **2019**, *30* (3), 592–603.

(21) Benizri, S.; Gissot, A.; Martin, A.; Vialet, B.; Grinstaff, M. W.; Barthélémy, P. *Bioconjug. Chem.* **2019**, *30* (2), 366–383.

(22) Springer, A. D.; Dowdy, S. F. *Nucleic Acid Ther.* **2018**, *28* (3), 109–118.

(23) Akhtar, S. *Expert Opin. Drug Metab. Toxicol.* **2010**, *6* (11), 1347–1362.

(24) Stechmann, B.; Bai, S.-K.; Gobbo, E.; Lopez, R.; Merer, G.; Pinchard, S.; Panigai, L.; Tenza, D.; Raposo, G.; Beaumelle, B.; et al. *Cell* **2010**, *141* (2), 231–242.

(25) Ming, X.; Carver, K.; Michael Fisher; Romain Noel; Cintrat, J. C.; Gillet, D.; Barbier, J.; Cao, C.; Bauman, J.; Juliano, R. L. *Nucleic Acids Res.* **2013**, *41* (6), 3673–3687.

(26) Calcaterra, N. E.; Barrow, J. C. *ACS Chem. Neurosci.* **2014**, *5* (4), 253–260.

(27) Riss, J.; Cloyd, J.; Gates, J.; Collins, S. *Acta Neurol. Scand.* **2008**, *118* (2), 69–86.

(28) Schukin, S. I.; Zinkovsky, V. G.; Zhuk, O. V. *Pharmacol. Reports* **2011**, *63* (5), 1093–1100.

(29) Monsó, M.; De La Torre, B. G.; Blanco, E.; Moreno, N.; Andreu, D. *Bioconjug. Chem.* **2013**, *24* (4), 578–585.

(30) Abdelkafi, H.; Michau, A.; Clerget, A.; Buisson, D. A.; Johannes, L.; Gillet, D.; Barbier, J.; Cintrat, J. C. *ChemMedChem* **2015**, *10* (7), 1153–1156.

(31) Liu, W.; Xu, D. D.; Repic, O.; Blacklock, T. J. *Tetrahedron Lett.* **2001**, *42* (13), 2439–2441.

(32) Mentzel, M.; Hoffmann, H. M. R. *J. für Prakt. Chemie/Chemiker-Zeitung* **1997**, *339* (1), 517–524.

(33) Bertucci, M. A.; Lee, S. J.; Gagné, M. R. *Chem. Commun.* **2013**, *49* (20), 2055–2057.

(34) Sorg, G.; Thern, B.; Mader, O.; Rademann, J.; Jung, G. *J. Pept. Sci.* **2005**, *11* (3), 142–152.

(35) Morales-Serna, J. A.; García-Ríos, E.; Bernal, J.; Paleo, E.; Gaviño, R.; Cárdenas, J. *Synthesis*

(Stuttg). **2011**, No. 9, 1375–1382.

(36) Brotzel, F.; Ying, C. C.; Mayr, H. *J. Org. Chem.* **2007**, *72* (10), 3679–3688.

(37) El-Faham, A.; Funosas, R. S.; Prohens, R.; Albericio, F. *Chem. - A Eur. J.* **2009**, *15* (37), 9404–9416.

(38) Lönnberg, H. *Beilstein J. Org. Chem.* **2017**, *13*, 1368–1387.

(39) Haynes, W. M. *CRC Handbook of Chemistry and Physics*, 97th ed.; 2016.

(40) Baillie, L. C.; Batsanov, A.; Bearder, J. R.; Whiting, D. a. *J. Chem. Soc. Perkin Trans. 1* **1998**, No. 20, 3471–3478.

(41) Chen, X.; Li, L.; Liu, F.; Liu, B. *Bioorganic Med. Chem. Lett.* **2006**, *16* (21), 5503–5506.

(42) Sánchez, A.; Pedroso, E.; Grandas, A. *Org. Lett.* **2011**, *13* (16), 4364–4367.

(43) Alam, M. R.; Ming, X.; Dixit, V.; Fisher, M.; Chen, X.; Juliano, R. L. *Oligonucleotides* **2010**, *20* (2), 103–109.

(44) Alam, R.; Dixit, V.; Kang, H.; Li, Z. B.; Chen, X.; Trejo, J.; Fisher, M.; Juliano, R. L. *Nucleic Acids Res.* **2008**, *36* (8), 2764–2776.

(45) Iyer, R. P.; Egan, W.; Regan, J. B.; Beaucage, S. L. *J. Am. Chem. Soc.* **1990**, *112* (3), 1253–1254.

(46) Sánchez, A.; Pedroso, E.; Grandas, A. *Chem. Commun.* **2013**, *49* (3), 309–311.

(47) Paris, C.; Brun, O.; Pedroso, E.; Grandas, A. *Molecules* **2015**, *20* (4), 6389–6408.

Chapter 4. Oxanorbornene as a novel dienophile for inverse electron-demand Diels-Alder cycloaddition with 1,2,4,5-tetrazines

4.1 Background

As discussed in the introductory chapter of this dissertation, the IEDDA reaction is one of the currently most utilized bioconjugation tools in order to produce conjugates. Its utility relies on several key points such as its extremely fast kinetics (up to 2000 M s^{-1}), high chemoselectivity, and compatibility with aqueous physiological conditions. In the past, IEDDA reactions have been predominantly used for the preparation of pyridazines, which were further applied as nitrogen donor ligands. In 2008, however, two groups independently discovered that the fast and selective IEDDA reaction of strained olefins and tetrazines can be employed in the field of "click chemistry" fulfilling most of Sharpless' criteria.[1,2] Amongst the expanding repertoire of bioconjugation alternatives, the inverse electron-demanding Diels-Alder (IEDDA) between tetrazines (Tz) and strained dienophiles is attracting significant interest, in particular among scientists interested in *in vitro* and *in vivo* imaging.

The IEDDA is formally a [4+2] Diels-Alder cycloaddition between a diene, primarily a tetrazine, and a dienophile, usually an alkene, to form a six-membered ring. In contrast to the standard DA reaction, the diene ought to be electronically poor and the dienophile rich in order to cleanly react. As previously stated, the electronics of both reactants, but also the intrinsic tension of the alkene (dienophile) and steric hinderance are key factors that play a major role in the kinetics and outcome of the reaction.

Since the vast majority of IEDDA reactions for bioconjugation purposes use the tetrazine scaffold, no major differences can be produced by this reactant aside from electronic and steric hinderance tunings caused by the ring substituents, typically electron-withdrawing groups but sometimes alkyl groups or hydrogen. That being said, on the dienophile counterpart several compounds have been tested ranging from simple electron-rich olefinic compounds such as vinyl-ether[3] (**4.1**), vinyl-boronic acid[4] (**4.2**) or *N*-acylazetines[5] (**4.3**) to the more commonly used olefins *trans*-cyclooctene (TCO, **4.4**), methyl-cyclopropene (mCP, **4.5**) and norbornene (NB, **4.6, Figure 4.1**). These last options are attractive for their enhanced reactivity in comparison to the prior, thus providing a base ground for development of novel dienophiles.

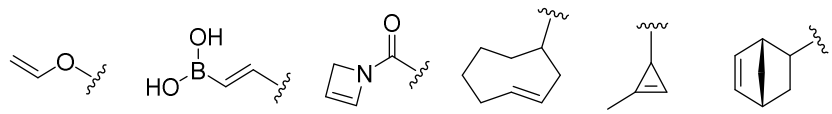

4.1 **4.2** **4.3** **4.4** **4.5** **4.6**

Figure 4.1 Chemical structure of IEDDA dienophiles.

In this context, the search of new dienophiles could greatly improve the utility of the IEDDA reaction for several reasons. Firstly, use of the most reactive dienophile reported to date, TCO, is not straightforward not only because it is difficult to obtain but also to derivatize. Moreover, it suffers from low stability due to facile isomerization to the *cis* counterpart, and its presence may cause a huge steric impact on certain applications where keeping unmodified catalytic sites is of paramount importance, such as enzymatic active sites. In a similar fashion, mCP exhibits similar stability issues and is less reactive but, instead causes a minimal perturbation on the conjugation site. In this framework, NBs offer an ideal compromise between stability and reactivity. Moreover, NBs are being synthetically accessible *via* a DA reaction between cyclopentadiene and acrylic or vinylic derivatives (**Figure 4.2**).

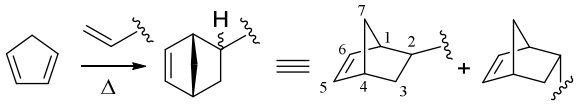

Figure 4.19 Classical norbornene preparation *via* Diels-Alder cycloaddition and numbering of the norbornene atoms (on the *exo* adduct).

The main drawback of norbornene use is the great number of isomer generation at the subsequent IEDDA conjugation reactions due to the unsymmetrical nature of monosubstituted norbornene derivatives (**4.6**). In case enantiopure compounds were require, isolation would likely be not straightforward.

4.2 Objectives

The objectives of this section are the following.

1. Examine 7-oxanorbornenes as IEDDA dienophiles conjugation reactions.
2. Synthesis of 7-oxanorbornene- and tetrazine-derivatized peptides and oligonucleotides.
3. Synthesis of tetrazine-derivatives bearing affinity tags such as GalNAc or biotin and a reporter such as BODIPY.
4. Preparation of peptide and oligonucleotide conjugates using the IEDDA cycloaddition
5. Study of different alternatives to synthesize double conjugates using the IEDDA cycloaddition as one of the conjugation reactions.

4.3 7-Oxanorbornenes as IEDDA dienophiles

4.3.1 Assessment of reactivity

Previous studies conducted in the group had made use of 1,4-dimethyl-7-oxanorbornenes (PMal[Me_2]) where 2,5-dimethyl furan was used as a protecting group of the maleimide moiety in oligonucleotide chemistry (see **Chapter 3**, **Section 3.5.4.1**)[6] as depicted in **Scheme 4.1**. In those studies, Dr. Albert Sánchez tested three different maleimide protecting groups: furan, 2-methylfuran and 2,5-dimethylfuran, and conditions for the subsequent rDA deprotection were examined. During this analysis it was found, in agreement with the letrature,[7] that the ease of rDA directly correlated to the number of methyl groups (k_2 rDA: 2,5-dimethyl > 2-methyl >>> furan). It was also discovered that the *exo* adduct of the 2,5-dimethyl analogue was resistant to conc. aq. NH_4OH, while the *endo* one was not. These facts allow the *exo* adduct of 2,5-dimethylfuran to be used as maleimide protecting group. As a follow-up study, Dr. Elduque *et al*. transferred this methodology to polyamides such as peptides, PNAs or peptoids.[8–10]

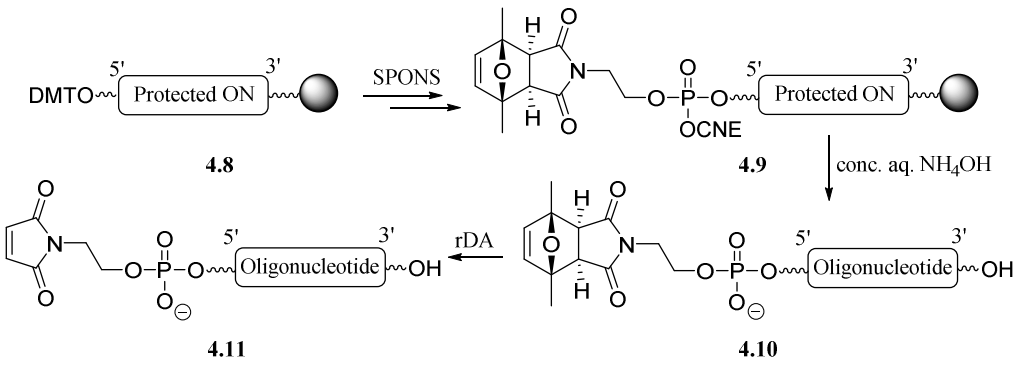

Scheme 4.1 Synthetic scheme for the synthesis of maleimido-derivatized oligonucleotides.

Given the high similarity between 7-oxanorbornenes and norbornenes, (**Figure 4.3**) we envisioned taking advantage of the 7-oxanorbornene (**4.12**) moiety that is produced upon protecting the maleimide moiety with furan to further exploit this structure.

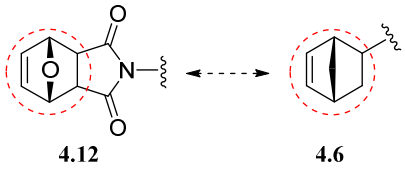

Figure 4.20 7-Oxanorbornene and norbornene structures, the former as part of a furan-protected maleimide.

Previous experiments in the group had already tested whether 2,5-dimethylfuran-protected maleimides (PMal[Me_2]) underwent an IEDDA reaction with commercially available 3,6-di(pyridin-2-yl)-1,2,4,5-tetrazine (2-Pyr_2Tz, **4.14**). As depicted in **Scheme 4.2**, equimolar amounts of carboxyl-derivatized 2,5-dimethylfuran-protected maleimide (PMal[Me_2]-COOH, **4.13**) and 2-Pyr_2Tz (**4.14**) were reacted overnight in an aqueous methanolic solution at room temperature. There were no noticeable changes, only recovering starting materials.

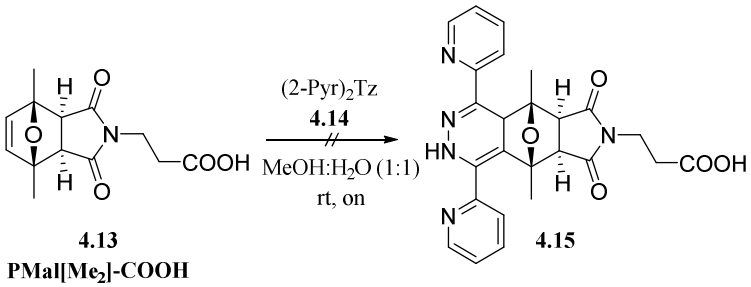

Scheme 4.2 Attempt to react a dimethylfuran-protected maleimide analogue with a tetrazine.

Observing that the structural similarity of furan-protected maleimides (PMal[H_2], **4.12**, **Figure 4.3**) to norbornenes (**4.6**) was even higher than that of dimethylfuran-protected ones, we postulated that the two methyl groups could be sterically interfering with the IEDDA reaction, and that furan-protected maleimides might be suitable dienophiles for IEDDA reactions.

To test this hypothesis, we synthesized the carboxylic acid derivative PMal[H_2]-COOH (**4.20**) as previously described[6] *via* a two-step procedure, starting with maleimide formation from maleic anhydride and β-alanine to yield to corresponding maleimide (**4.18**). A subsequent Diels-Alder reaction with furan provided the PMal[H_2]-COOH (**4.20**) *exo* adduct (stereoisomerically pure after precipitation) as depicted in **Scheme 4.3**. We did not want to work with a mixture of isomeric cycloadducts, and chose

the *exo* one based on our previous findings, namely higher thermal and basic media stability (see above). Other authors have more recently described and confirmed the same relative thermal stability of the two isomers.[11]

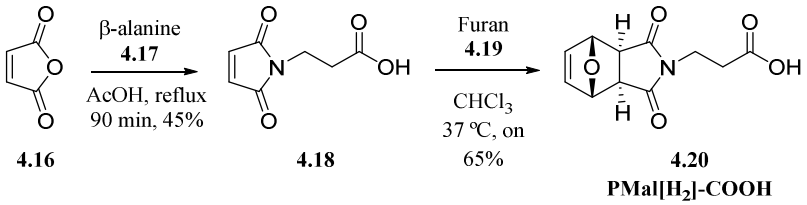

Scheme 4.3 Preparation of the PMal[H_2]-COOH derivative **4.20**.

Once we had obtained PMal[H_2]-COOH (**4.20**), we tested whether this compound underwent an IEDDA reaction with a tetrazine in a similar fashion as norbornene. For this first experiment, we reacted Ph-Tz-Me (**4.21**) (generous gift from the RUBAM research group, CID-CSIC, Barcelona) and PMal[H_2]-COOH, **Scheme 4.4**.

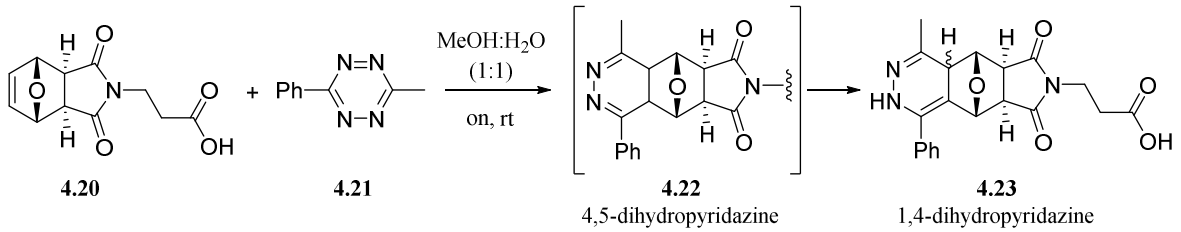

Scheme 4.4 IEDDA reaction between Ph-Tz-Me (**4.21**) and (PMal[H_2]-COOH, **4.20**).

As shown by the HPLC traces, clean conversion to the expected adduct was observed after an overnight reaction under mild conditions and an aqueous solvent (**Figure 4.4**).

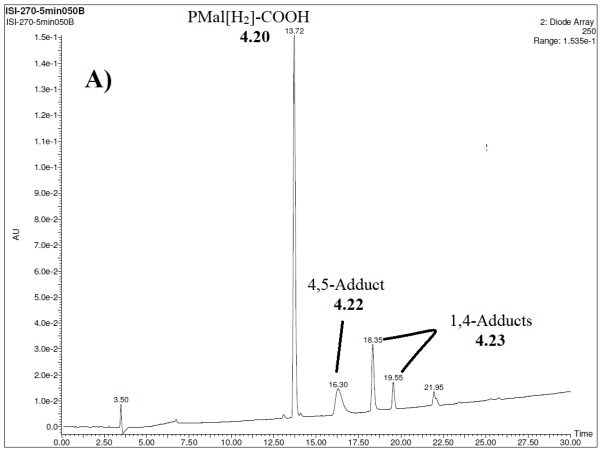

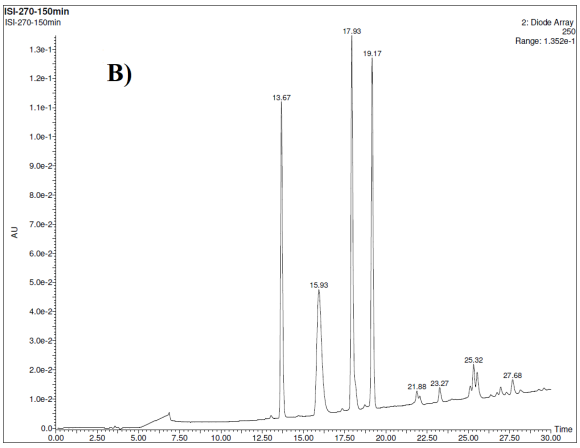

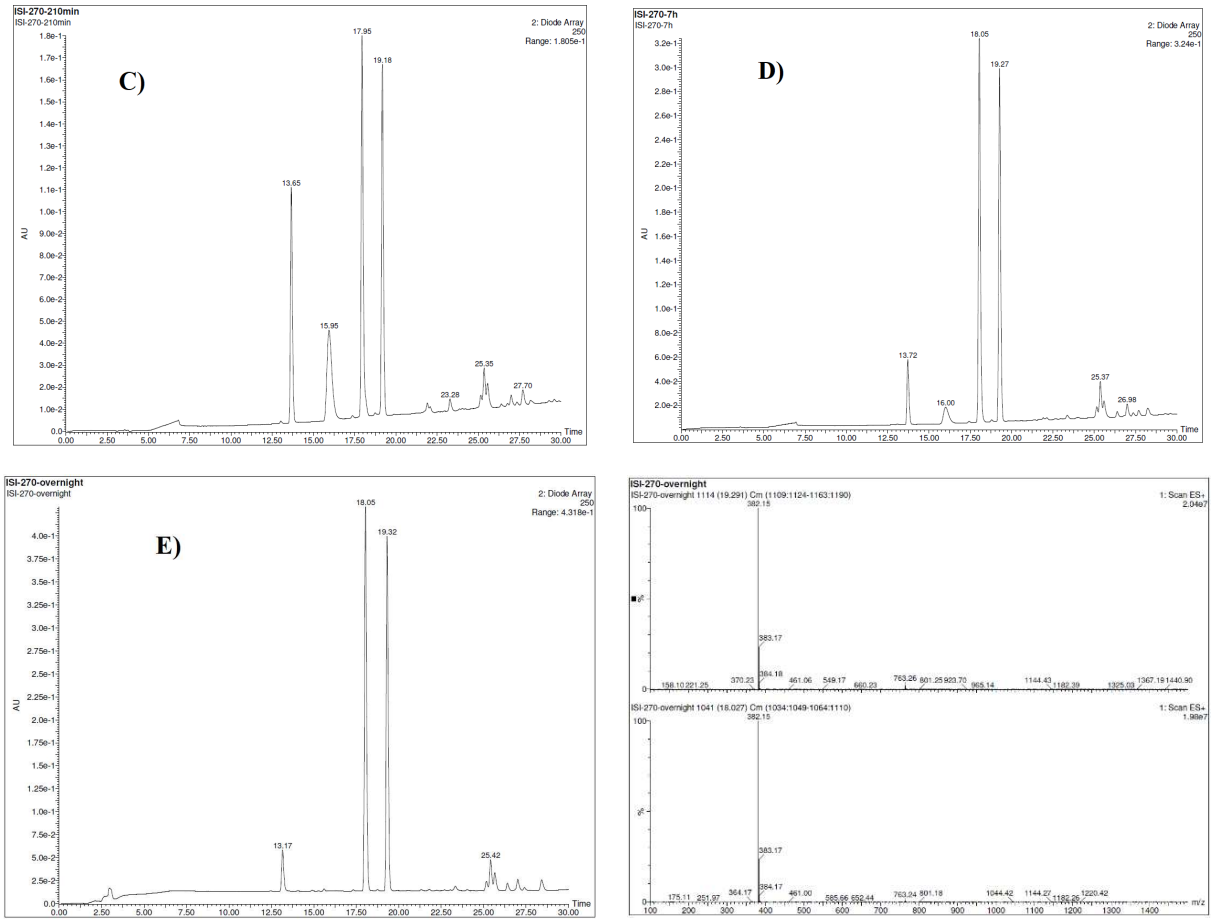

Figure 4.4 HPLC traces (250 nm) of the reaction between PMal[H_2]-COOH (**4.20**) and Ph-Tz-Me (**4.21**) at the 5 min (a), 150 min (b), 250 min (c), 7 h (d) and overnight (e) reaction times, and MS spectrum of the two final adducts, t_R = 18.05 (top) and 19.32 (bottom), respectively.

4.3.2 Incorporation of oxanorbornenes into oligonucleotides and polyamides

Upon observing this positive result, we first wondered whether this type of reactivity could be translated into oligonucleotide chemistry. To do so, we synthesized a PMal[H_2] phosphoramidite following procedures described by Dr. Sánchez.[6] The key reaction was the DA reaction between furan and maleic anhydride in order to selectively obtain exclusively the DA *exo* adduct (**4.24**), which was subsequently reacted with aminoethanol to furnish the hydroxyl derivative (**4.26**) in a moderate 50% yield. Afterwards, phosphitylation with the standard chlorophosphine in the presence of DIPEA provided the desired PMal[H_2] phosphoramidite (**4.27**) in a good 80% isolated yield (**Scheme 4.5**).

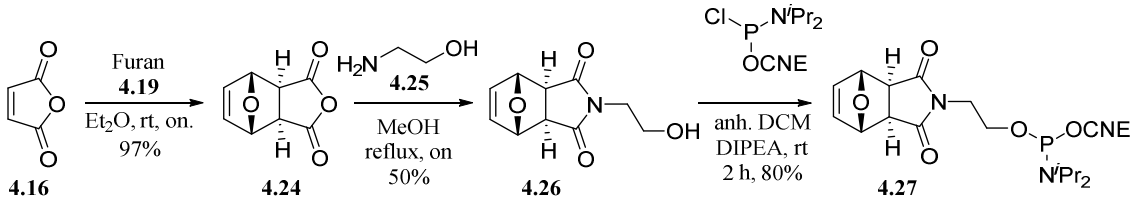

Scheme 4.5 Synthesis of PMal[H_2] phosphoramidite (**4.27**), and assembly of PMal[H_2]-dT_{10} (**4.28**).

Once we obtained the oxanorbornene-containing phosphoramidite, we appended it to the 5' position of a resin-linked dT_{10} oligonucleotide as a proof-of-concept, in order to verify that the oxanorbornene-involving IEDDA reaction could be translated into oligonucleotide chemistry.

After elongation, PMal[H_2] coupling and final deprotection with conc. aq. NH_4OH, the crude was analyzed both by HPLC and MALDI-TOF MS (**Figure 4.5**), and the target compound isolated.

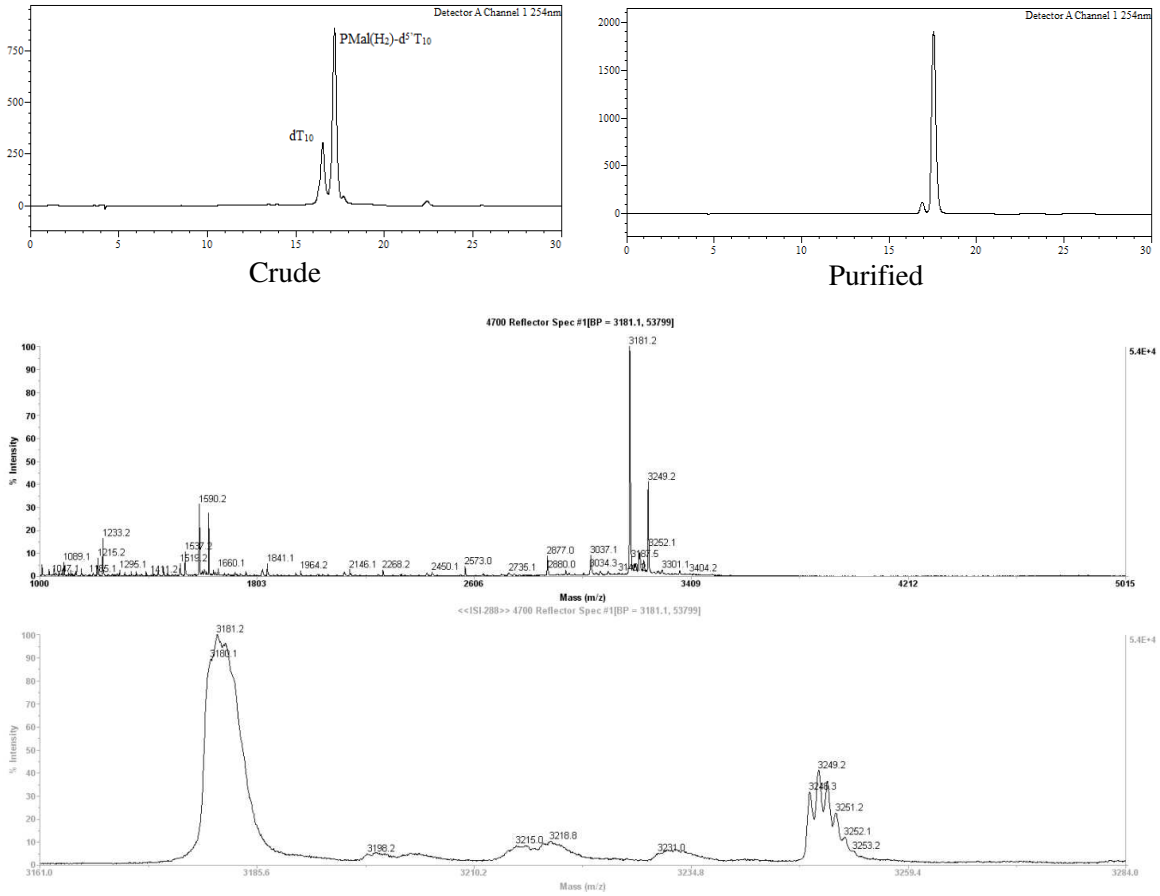

Figure 4.5 HPLC traces (254 nm) and MALDI-TOF MS spectrum of crude 5'-oxanorbornene-derivatized dT_{10} oligonucleotide (*m/z* = 3249: expected mass, *m/z* = 3180 Da corresponds to the loss of furan due to the ionization conditions). The HPLC trace of isolated **4.28** is also shown (top, right).

Once we had this oligonucleotide and before embarking on the assembly of more complex sequences, we tested whether the IEDDA reaction with oxanorbornene-oligonucleotides was feasible. We utilized the same conditions as for the previous assay (see **Scheme 4.4**) but, in this instance, worked with the 2-Pyr_2Tz (**4.14**) tetrazine, which is more reactive than **4.21** due to more favorable electronics (**Scheme 4.6**).

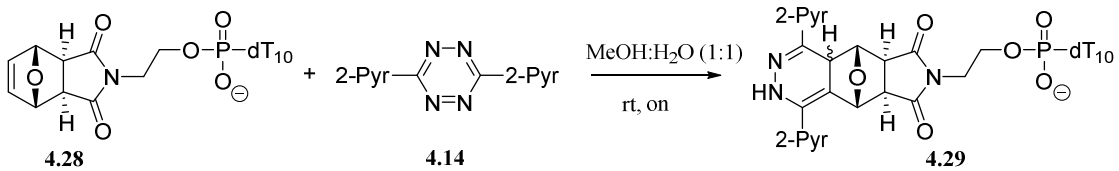

4.28 **4.14** **4.29**

Scheme 4.31 Reaction between oxanorbornene-derivatized oligonucleotide **4.28** and Tz **4.14**.

The reaction was performed using a 0.5 mM oligonucleotide concentration with little excess of the Tz (2 equiv.) overnight. As observed by the HPLC traces, the cycloaddition was nearly quantitative, only

showing little (<5%) partner oligonucleotide. Both collected peaks corresponded to the cycloadduct, as verified by MALDI-TOF MS (**Figure 4.6**).

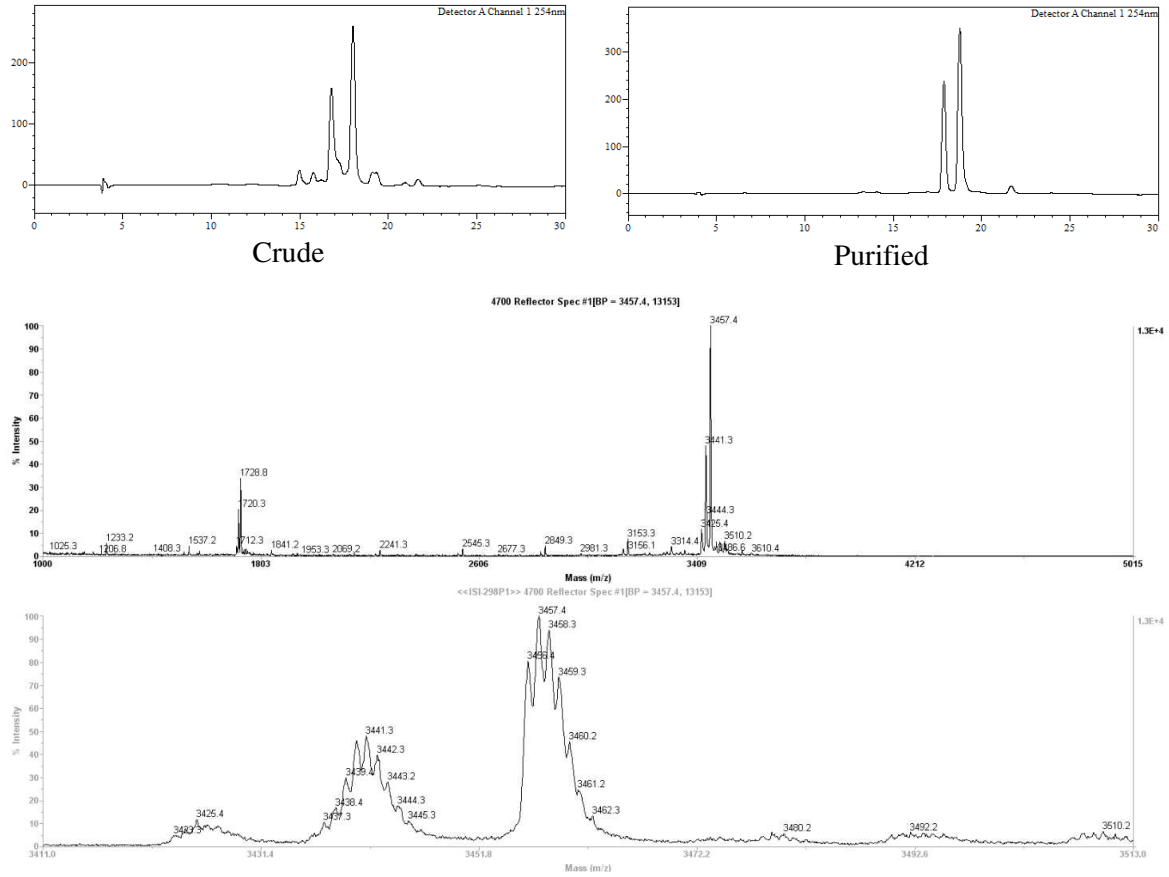

Figure 4.6 Conjugation reaction between **4.28** and **4.14**. HPLC traces (254 nm) of the reaction crude (left) and purified (right) cycloadduct and MALDI-TOF MS spectrum.

After this positive result with the dT_{10} oligonucleotide, we decided to synthesize, utilizing the same oxanorbornene-containing phosphoramidite (**4.27**) an oligonucleotide containing all the nucleobases, namely PMal[H_2]-$^{5'}$dCATGTATCGCATCATCAGT$^{3'}$ (**4.30**, **Figure 4.7**).

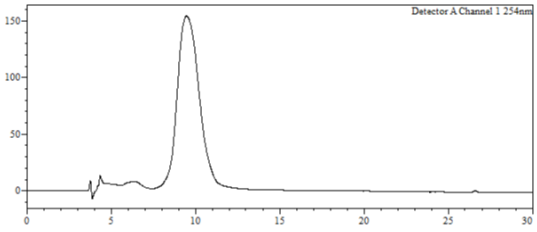

Crude (254 nm)

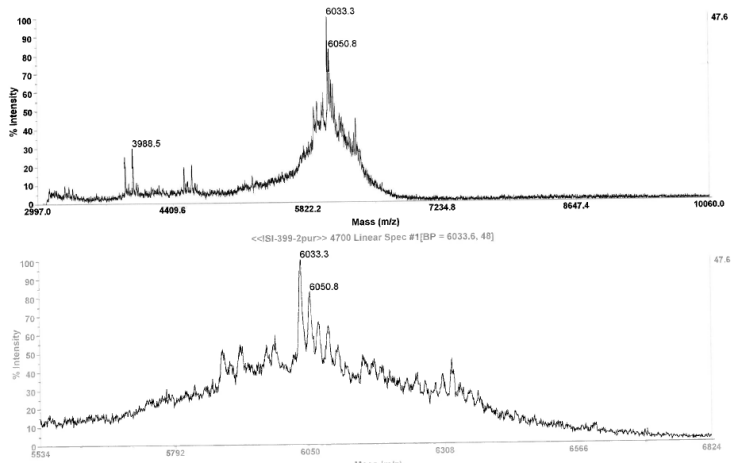

Figure 4.7 HPLC trace (top) and MALDI-TOF MS spectrum (bottom) of the 5' oxanorbornene-derivatized oligonucleotide **4.30**.

To extend the oxanorbornene-involving IEDDA reaction to polyamides we chose a peptide with a well-known cell-penetrating property coined as "TAT" with a polycationic sequence Arg-Lys-Lys-Arg-Arg-Gln-Arg-Arg-Arg-NH_2. In this instance, the oxanorbornene derivative PMal[H_2]-COOH (**4.20**) was introduced after peptide elongation using standard SPPS procedures (**Scheme 4.7**).

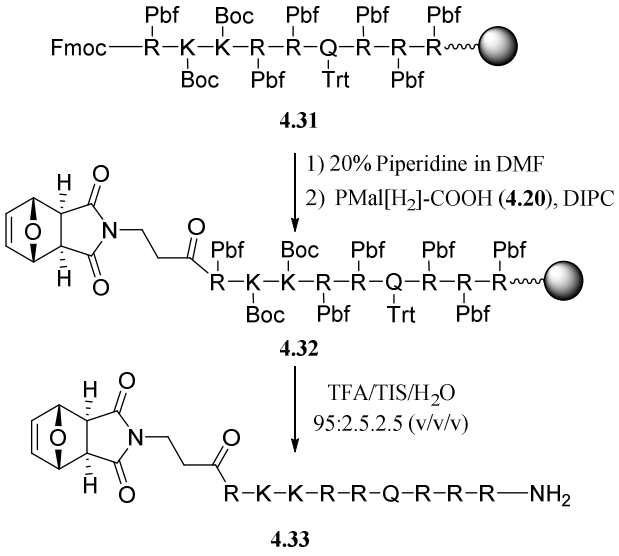

Scheme 4.7 Outline for the derivation of a resin-bound peptide with an oxanorbornene moiety at the *N*-terminal position.

In a similar fashion, the oxanorbornene moiety was appended at the *N*-terminus of a PNA chain (ctcatactct sequence. **4.34**) as usual. The oxanorbornene-PNA was purified by HPLC and characterized by MALDI-TOF MS (**Figure 4.8**).

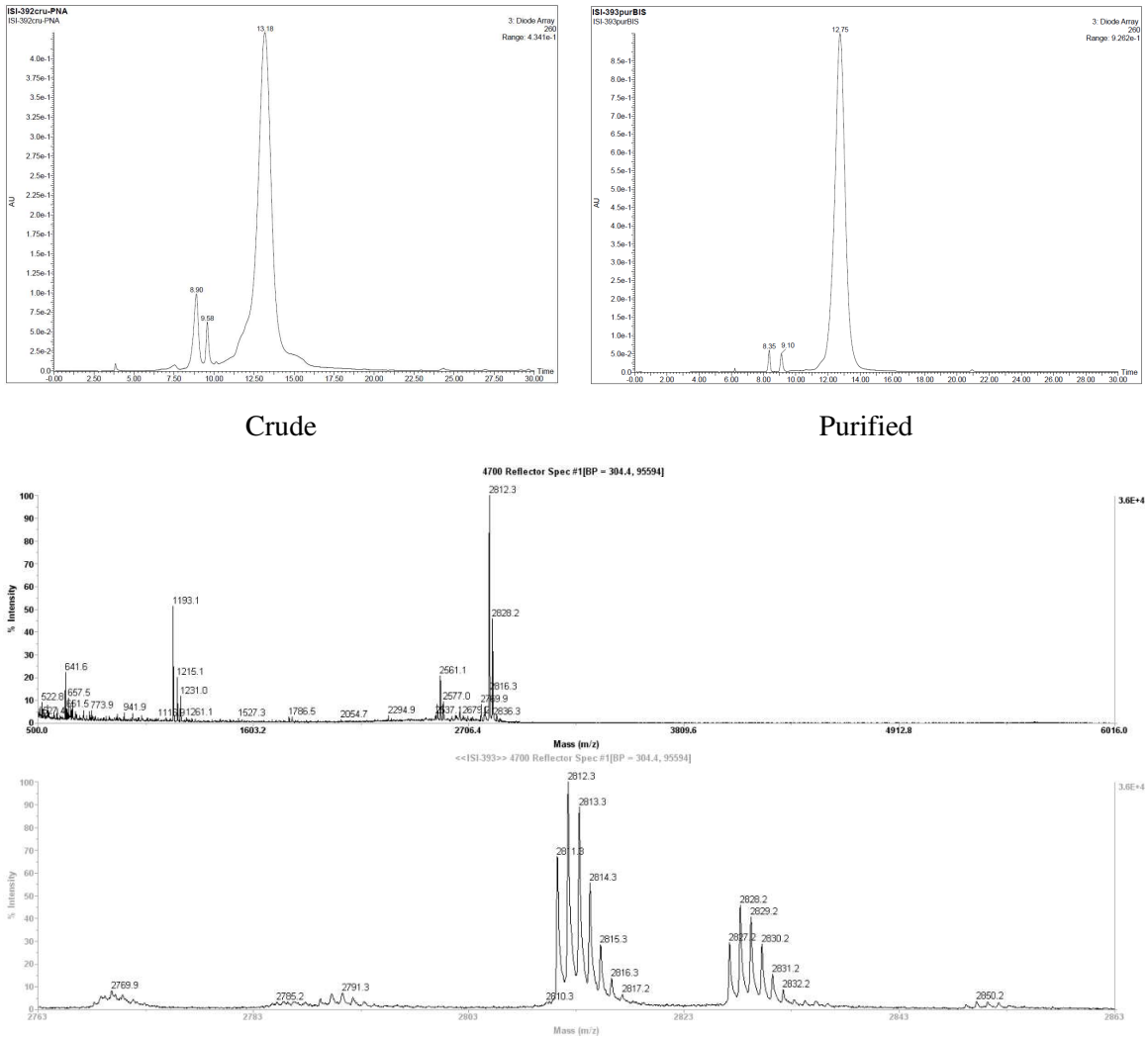

Figure 4.8 HPLC traces (260 nm) of crude and purified (top), and MALDI-TOF MS spectrum (bottom) of the oxanorbornene-derivatized PNA.

4.3.3 Synthesis of tetrazine-containing compounds

4.3.3.1 Synthesis of tetrazines incorporating functional groups for further derivatization

4.3.3.1.1 Formation of the tetrazine core

Tetrazines are typically obtained from dihydrotetrazines, by reacting the appropriate precursors with hydrazine and a subsequent oxidation. Depending on the type of starting materials, hydrazine is often used as the hydrate but sometimes in anhydrous form with THF or ethanol as co-solvents.

The classic method for preparation of tetrazines using Pinner conditions involves reacting imidoesters with hydrazine leading to the formation of amidrazone intermediates, which undergo further reaction with excess of hydrazine and another imidoester to yield dihydrotetrazines. Finally, the desired tetrazine is obtained through oxidation (**Scheme 4.8**, **A**). Another well established, and commonly used method is the condensation of two aryl or alkyl nitriles with hydrazine (**Scheme 4.8**, **B**). This nitrile-based route

is however limited if the aim is to prepare disubstituted asymmetric tetrazines since a statistical mixture of products of difficult purification is obtained. Several strategies to overcome this drawback have been described, and involve the use of a large excess of one of the two nitriles, the addition of sulfur [12,13] or metal catalysts such as nickel or zinc triflates[14] (**Scheme 4.8**, **B**). *N*-Acylhydrazides have been sparingly used as a strategy to overcome the functional group tolerance in classical tetrazine synthesis involving strong oxidation steps. This approach relies on the chlorination of *N*-acylhydrazides with PCl_5 to obtain the 1,2-dichlorohydrazines intermediates that are readily reacted with hydrazine to yield the tetrazine moiety. With this strategy, both symmetric and asymmetric tetrazines bearing both EWGs and aliphatic substituents have been prepared in modest yields.[15]

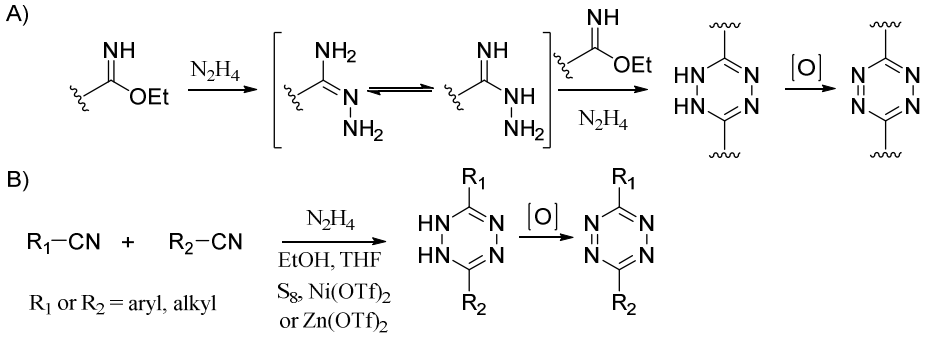

Scheme 4.8 Classic routes for tetrazine synthesis using imidoester (a) and nitriles (b).

The most widely used oxidant in tetrazine synthesis is nitrous gas generated *in situ* from sodium nitrite in acidic media. The typical protocol resembles the preparation of diazonium salts: addition of a $NaNO_2$ solution to an aqueous HCl or glacial acetic acid dihydrotetrazine solution at low temperatures until the oxidation is complete. Other oxidation methods utilizing metal oxides, primarily MnO_2[16] and CrO_3,[17] haven't seen wide application due to excessive toxic waste and poor functional group tolerance. Milder oxidation procedures rely on peroxy acids such as *m*CPBA[18] and Bn_2O_2[19] or quinones such as DDQ.[1] These modern approaches oxidize amino-substituted derivatives where $NaNO_2$ fails. That being said, even though these milder oxidations provide some beneficial aspects, they are not devoid of problems, since the desired product is usually difficult to separate from byproducts generated at this step.

A recent study by Fox *et al.* identified phenyliodine(III) diacetate (PIDA) as an efficient oxidant for dihydrotetrazines that could easily be separated from the by-product iodobenzene. The oxidant is amine-tolerant and useful for synthesizing dialkyl- and diaryl-tetrazines bearing heteroaromatic rings.[20]

From all the available approaches we selected the "cyano approach" (**Scheme 4.8**, **B**) for the synthesis of the tetrazine core. Using this strategy, as described in the literature,[21] we prepared bis-phenyl (**4.35**) and methyl-phenyl (**4.21**) substituted tetrazines using sulfur as catalyst as depicted in **Scheme 4.9**.

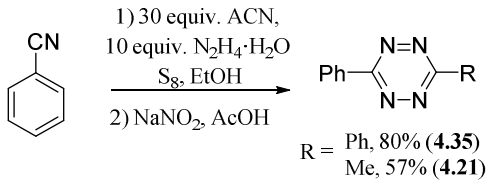

Scheme 4.9 Synthesis of bis-phenyl (**4.35**) and methyl-phenyl (**4.21**) substituted tetrazines.

Following these experiments, we felt the need to expand the number of groups appending from the tetrazines to a wider, more complete biologically relevant repertoire. In this line of work, we envisioned synthesizing tetrazines with appending groups such as *N*-acetylgalactosamine (GalNAc), biotin or a fluorophore such as BODIPY. To fulfill this objective, we required a tetrazine containing a functional group suitable for further derivatization namely a carboxylic acid or amine. The main problematic of

these type of reactions, regardless of the appending functional group, is the desymmetrization of the tetrazine core since mixture of symmetric and asymmetric tetrazines are usually obtained (**Scheme 4.10**).

4.3.3.1.2 Carboxyl-derivatized tetrazines

In this context, first synthetic trials aimed to prepare a carboxyl-containing tetrazine, in particular Pyrim-Tz-COOH (**4.38**, **Scheme 4.10**). These experiments started with *p*-cyanobenzoic acid and 2-cyanopyrimidine essentially following described procedures.[22,23] At the oxidative step, instead of isoamyl nitrite we employed an acidic $NaNO_2$ solution.

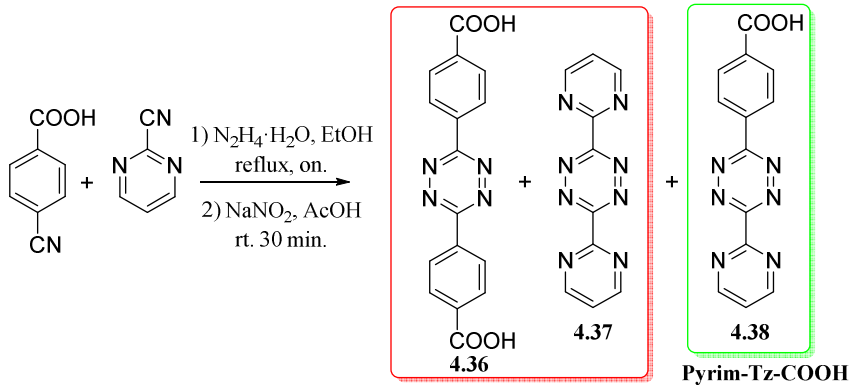

Scheme 4.10 Tetrazine formation by reaction between *p*-cyanobenzoic acid and 2-pyrimidinecarbonitrile to afford the symmetrical tetrazines (**4.36**, **4.37**) in addition to the target compound (**4.38**).

Different attempts to obtain **4.38** gave low yields (≈ 10-20%) of partially pure asymmetric tetrazine, in agreement with reported results for this specific compound. Additionally, in this instance, the poor solubility of Pyrim-Tz-COOH (**4.38**) was an added complication.

Observing the low yields obtained upon formation of the tetrazine core, we performed a small screening of nitriles to react with 4-cyanobenzoic acid, in hopes of finding another carboxyl-containingtetrazine analogue more well-behaved. For this endeavor, we utilized *p*-cyanopyridine and ACN in addition to 2-cyanopyrimidine. In spite of adding S_8 or $NiCl_2$ as catalysts, the reactions took place without success and only yielded complex mixtures in all cases (**Table 4.1**).

Entry	Nitrile 1	Nitrile 2	Conditions	Oxidizing agent
1	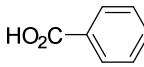	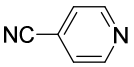	4 equiv. $N_2H_4·H_2O$ (neat)	$NaNO_2$, glacial AcOH
2	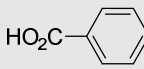	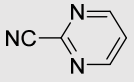	EtOH, 20 equiv. $N_2H_4·H_2O$, 4Å Mol. Siev.	$NaNO_2$, HCl (1M)
3	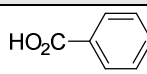	20 equiv. ACN	$NiCl_2 · 6H_2O$, 25 equiv. $N_2H_4·H_2O$	$NaNO_2$, HCl (1M)
4	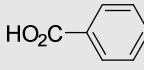	30 equiv. ACN	EtOH, S_8, 20 equiv. $N_2H_4·H_2O$	$NaNO_2$, HCl (1M)

Table 4.1 Screening for tetrazine core synthesis with *p*-cyanobenzoic acid and several cyano-containing compounds.

After all these negative results, we switched back to the starting reaction involving *p*-cyanobenzoic acid and 2-cyanopyrimidine, since it was the only one we had successfully reproduced. The optimization procedure revolved around several items such as the number of equiv. of hydrazine (5, 10, 20 or 40 respectively), use of different co-solvents like EtOH, DMF or toluene, addition of different amounts of sulfur catalyst (0.5, 1, 2 or 4) and different starting amounts of nitrile reagents. Additionally, for the oxidative step we also perform trials with DDQ and PIDA as oxidants, but they proved not beneficial enough to be deemed superior to the acidic $NaNO_2$ solution. This optimization of the reaction conditions led to the use of 20 equiv. of $N_2H_4 \cdot H_2O$ with 2 equiv. of *p*-cyanobenzoic acid and 1 of 2-cyanopyrimidine in EtOH (mixture as concentrated as possible) heating at reflux overnight. Subsequently, solvent removal to dryness, addition of AcOH and dropwise addition of a solution of 4 equiv. of $NaNO_2$ in H_2O until bubbling ceased furnished the desired compound in an overall 90% yield (**Scheme 4.11**).

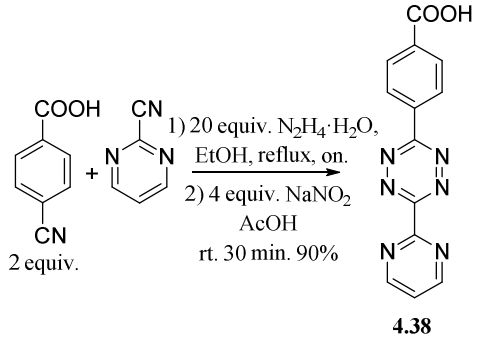

Scheme 4.32 Optimized synthesis of Pyrim-Tz-COOH (**4.38**).

Subsequently, we attempted to further derivatize this valuable intermediate. Initial efforts were focused towards obtaining the activated NHS-ester (**4.39**) using carbodiimide activation of the carboxyl group and DMSO as a solvent.[22] Following this procedure, only starting materials were recovered, even after prolonged reaction times. The second round of attempts aimed to transform the carboxylic acid functionality into an acyl chloride (**4.40**) with thionyl chloride.[23] Unfortunately this alternative also proved unfruitful, only observing complex mixtures (**Scheme 4.12**).

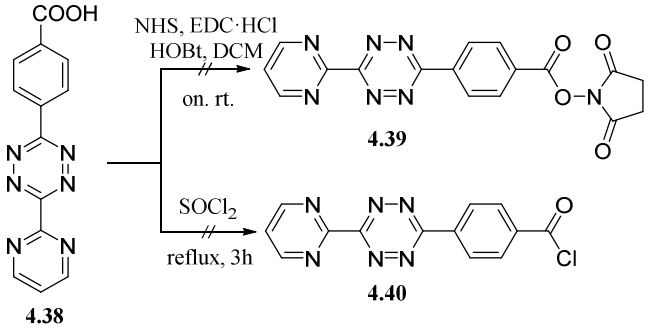

Scheme 4.12 Unfruitful attempts of Pyrim-Tz-COOH activation.

An important fact was observed during all this experimental work, the Pyrim-Tz-COOH (**4.38**) was insoluble in most organic solvents, as already commented, when the carboxylic acid functionality was neutral, that is after acid treatment required for the oxidation to tetrazine. When we explored the possibility of using a base such as NaOH, the compound seemed to solubilize in water but subsequently decomposed (qualitative observation, its color changed). Nonetheless, if an organic base such as NEt_3 or DIPEA was used instead, small amounts of compound were noticed to dissolve. This observation prompted the search for a non-nucleophilic basic solvent culminating in the use of pyridine for subsequent reactions. As depicted in **Scheme 4.13**, when we utilized anh. pyridine as solvent and

activated the carboxyl group of Pyrim-Tz-COOH (**4.38**) with an uronium salt (HATU), reaction with an adequately protected polyethyleneglycol (PEG) linker (**4.41**) afforded the amide in a moderate 56% yield. In this instance we chose the Boc-protected bis-amino PEG (**4.41**) because the addition of PEG units is known to help with aqueous solubility.[24] Finally, we removed the Boc group under acidic treatment, which provided the desired amine **4.43** in 96% yield. Access to amine **4.43** entailed the possibility of further derivatizing the tetrazine with other types of molecules.

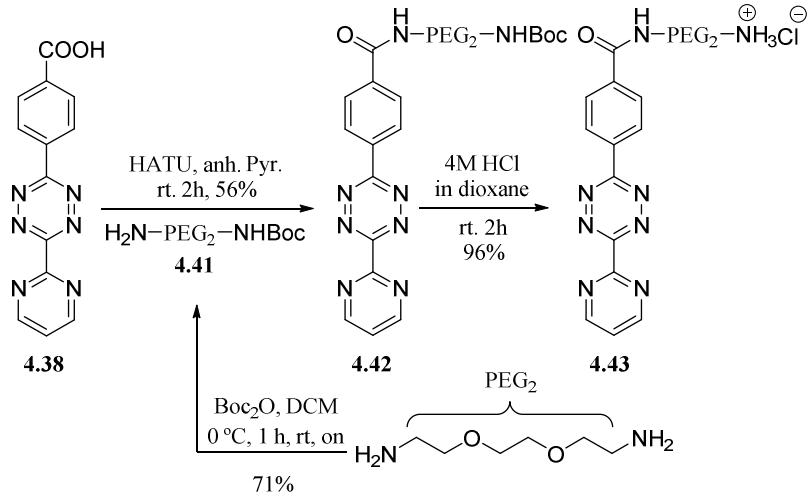

Scheme 4.13 Synthetic outline for the preparation of a pyrimidinyl-derivatized tetrazine with an appending amino functionality (**4.43**).

4.3.3.1.3 Amino-derivatized tetrazines

For the synthesis of amine-containing tetrazines (that is, tetrazines in which the amine is not introduced by derivatization of another functional group, as described above), we started working with *p*-cyanoaniline as depicted in **Table 4.2**.

Entry	Nitrile 1	Nitrile 2	Conditions	Oxidizing agent
1	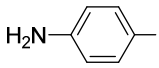	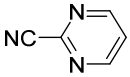	EtOH, S_8, 10 equiv. $N_2H_4 \cdot H_2O$	$NaNO_2$, AcOH
2	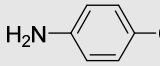	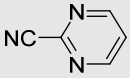	EtOH, 10 equiv. $N_2H_4 \cdot H_2O$	$NaNO_2$, AcOH
3	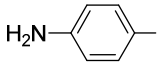	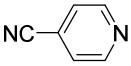	EtOH, S_8, 10 equiv. $N_2H_4 \cdot H_2O$	$NaNO_2$, AcOH
4	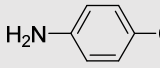	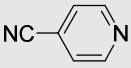	4 equiv. $N_2H_4 \cdot H_2O$ (neat)	DDQ, PhMe
5	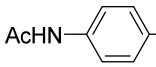	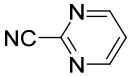	EtOH, 10 equiv. $N_2H_4 \cdot H_2O$	$NaNO_2$, AcOH
6	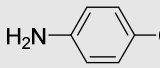	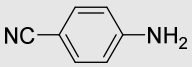	EtOH, S_8, 10 equiv. $N_2H_4 \cdot H_2O$	$NaNO_2$, AcOH

Table 4.2 Screening for tetrazine core synthesis with *p*-cyanoaniline and several cyano-containing compounds.

Reaction conditions similar to the previous ones, addition of S_8 (entry 1 and 3, **Table 4.2**) and different carbonitriles were tested. Nonetheless, we obtained complex mixtures in all cases, which was attributed to formation of diazonium salts and, subsequently, phenolic compounds. To prevent this undesired reaction, we tested a different oxidizing agent DDQ (entry 4, **Table 4.2**), as well as acetylating the partner cyanoaniline, obtaining also similar negative results.

In order to circumvent the poor stability of anilines under acidic $NaNO_2$ oxidative conditions, we envisioned isolating the dihydro-derivative, acylating the aniline and performing a subsequent oxidative step to furnish the tetrazine core as described by K. M. Bonger and co-workers[4] and depicted in **Scheme 4.14**.

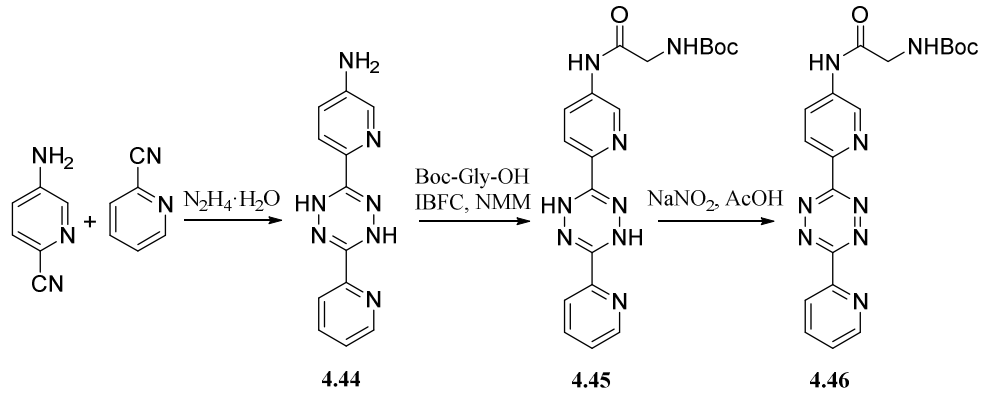

Scheme 4.14 Approach for amine-derivatized tetrazines synthesis *via* dihydro-tetrazine acylation and oxidation, as described by K. M. Bonger and co-workers.[4]

We tested this strategy using *p*-cyanoaniline and *p*-cyanopyridine, but obtained a complex mixture which we were unable to purify (**Scheme 4.15**). In a subsequent test, acylating the crude mixture in a "one-pot" fashion furnished small amounts of impure dihydro-acylated compound. Nonetheless, upon oxidative treatment with aq. acidic $NaNO_2$, the crude was also a complex mixture (as shown by TLC), and we were unable to purify the target *N*-acylated tetrazine.

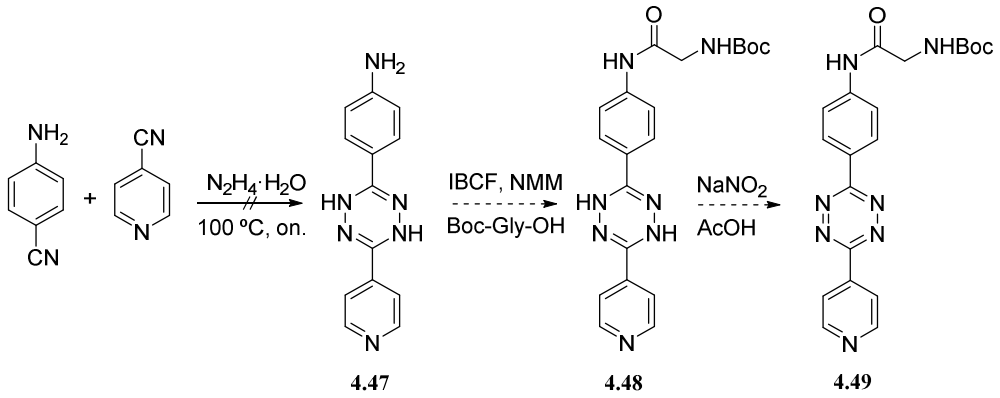

Scheme 4.15 Approach for the preparation of glycine-derivatized tetrazine.

Finally, we switched our efforts towards a less readily reactive tetrazine, that containing a methyl group appending from the tetrazine core instead of a pyrimidine ring. This synthesis started with the commercially available hydrochloride form of 4-cyanobenzylamine and reaction with Boc_2O to obtain the Boc-protected cyano derivative (**4.51**). This step is important for the oxidation step required to construct the tetrazine core since, as previously touched upon, amines do not withstand the oxidative stress caused by HNO_2. Subsequently, tetrazine formation was accomplished *via* $NiCl_2$ catalysis as described by Yang *et al.*[25] furnishing the desired *N*-Boc-protected methyl-bearing tetrazine (**4.52**) in a

good 70% yield. Finally, the desired free amine (**4.53**) was obtained after an acidic treatment that cleanly removed the Boc protection as depicted in **Scheme 4.16**.

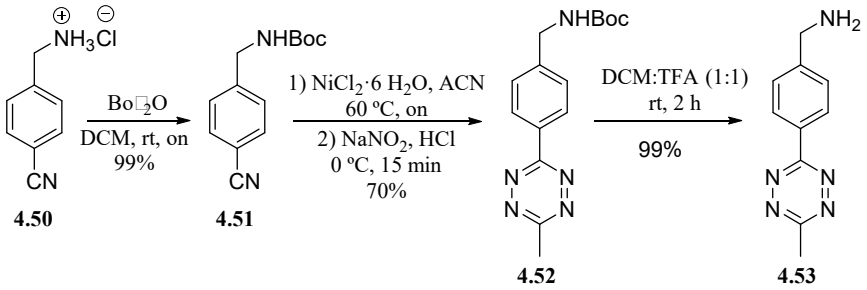

Scheme 4.16 Synthesis of a methyl-substituted tetrazine bearing an amine functionality.

4.3.3.1.4 Solid-phase synthesis of tetrazine-modified peptides

Before tacking the synthesis of the tetrazine derivatives with interest in conjugation reactions cited above (**Section 4.3.1.1**), we sought to investigate the incorporation of the tetrazine core "on-resin". For this endeavor we utilized the previously described pyrimidine-derivatized tetrazine with an appending carboxylic acid functionality (**4.38**). We did not expect any problem with the acidic treatment required for the peptide final cleavage and deprotection step, since tetrazine synthesis requires an acidic treatment. Instead our concerns resided in the structural integrity of the tetrazine when using a reducing silane such as TIS. To our delight, upon addition of TIS into a solution of **4.38**, no reaction was observed, proving feasible to add this tetrazine at the *N*-terminus of a growing peptide. After chain elongation and Fmoc removal with the usual piperidine treatment, we coupled the tetrazine (**4.38**) with small modifications. Usual coupling procedures call upon carbodiimide chemistry such as DIPC (or DCC) and HOBt in DCM/DMF mixtures. In this case, HATU was used for carboxyl activation, we used anh. Pyridine as the reaction solvent, added a 5-fold molar excess of tetrazine (instead of 3-fold), and extended the reaction time (150 min instead of the usual 90 min) to ensure a high degree of coupling. Finally, deprotection and cleavage was performed under usual acidic conditions with the appropriate scavengers as depicted in **Scheme 4.17**.

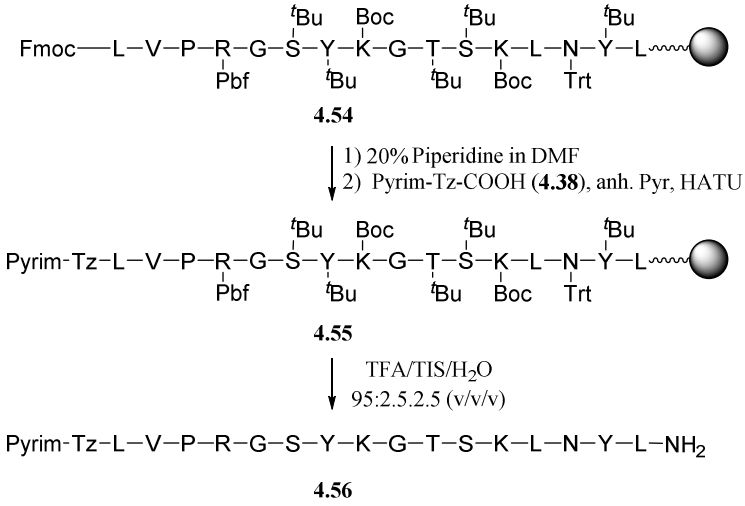

Scheme 4.17 On-resin derivatization of a growing peptide with a tetrazine moiety at the *N*-terminal position.

4.3.3.2 Synthesis of tetrazine-bearing compounds for bioconjugation

4.3.3.2.1 Synthesis of a tetrazine with an appending *N*-acetyl galactosamine (GalNAc) moiety

N-Acetyl-D-galactosamine (GalNAc) is a highly efficient ligand of the asialoglycoprotein receptor (ASGPR), also known as the Ashwell-Morell receptor. The ASGPRs expressed by hepatocytes and facilitates uptake and clearance of circulating glycoproteins with exposed terminal galactose and GalNAc glycans *via* clathrin-mediated endocytosis. The binding affinity of ligands varies from micromolar to low-nanomolar and depends on the number and spatial orientation of the carbohydrate moieties present.[26] GalNAc-melittin-like peptide conjugates have been used for repression of hepatitis B virus RNA, protein and DNA upon coinjection in transgenic mouse models.[27] Recently, GalNAc has also proven as a robust ligand for siRNA-mediated gene silencing through a multivalent GalNAc-siRNA conjugation strategy.[28]

For these reasons we envisioned preparing a GalNAc derivative bearing a tetrazine moiety for eventual tests using IEDDA-prepared conjugates. Synthetically, we followed a strategy that involved the preparation of a carboxylic acid derivative of GalNAc from which the tetrazine core was appended. Starting from the commercially available D-(+)-galactosamine (**4.57**), the first step was the acetylation of all the hydroxyl and amine groups with acetic anhydride in anh. pyridine, which yielded the peracetylated GalNAc (**4.58**) in an excellent 91% yield. Subsequently, TMSOTf-induced oxazoline formation provided exclusively the "α-glycoside" configuration (**4.59**, **Scheme 4.18**) in an exceptional 99% yield.

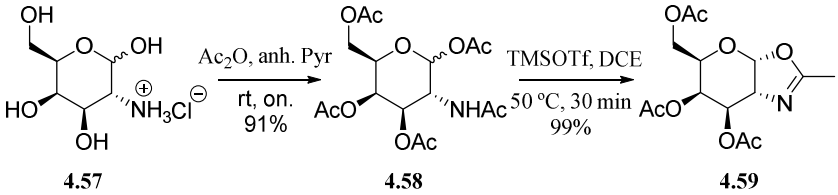

Scheme 4.18 Outline for the GalNAc oxazoline formation.

Mechanistically, oxazoline formation from the GalNAc moiety is based on traditional literature protocols for carbohydrates with some distinct differences due to the presence of the C-2 nitrogen atom. The acetyl-protected anomeric carbon allows the peracetylated GalNAc (**4.58**) to become a suitable glycosyl donor since, after TMSOTf acetyl activation (**4.60**), the formation of an oxocarbenium ion (**4.61**) is readily achieved by elimination of acetic acid, leaving an electrophilic anomeric carbon. Subsequent nucleophilic addition by the oxygen atom of the C-2 trimethylsilyl acetimidate (**4.61**) furnishes the intermediate **4.62** that readily evolves to the observed oxazoline (**4.59**, **Scheme 4.19**)

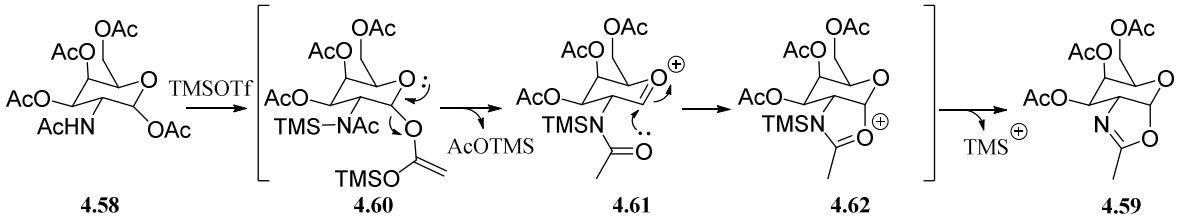

Scheme 4.33 Mechanistic outline for the TMSOTf catalyzed oxazoline formation of peracetylated GalNAc (**4.58**).

This strategy allows for the formation of the *O*-derivatized β-anomer since the subsequent nucleophilic attack takes place from the unhindered position opposite to the leaving group. Described procedures call upon the addition of 5-hexen-1-ol (**4.60**) to obtain the olefinic derivative **4.61** and a subsequent ruthenium-periodate mediated oxidative cleavage to render the desired carboxylic acid functionality (**4.62**, **Scheme 4.20**).[28] In our case, glycosylation proceeded smoothly in a good 79% yield rendering the olefinic derivative, but the last oxidative step was not fruitful, yielding only complex mixtures instead.

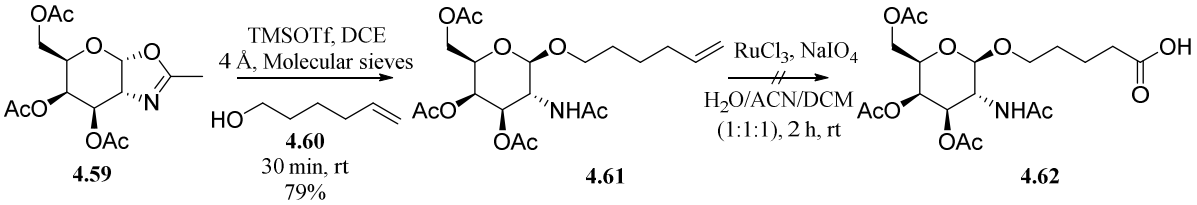

Scheme 4.20 Outline for the carboxylic acid introduction into a GalNAc moiety *via* ruthenium oxidation of a terminal akene.

Observing this negative result, we proceeded with a modification of the synthetic scheme. The main idea was to use an alcohol with a suitably protected carboxylic acid functionality for glycosylation instead of the alkene. For this objective, we synthesized benzyl 4-hydroxybutanoate (**4.63**) following described procedures.[29] The method is based on the nucleophilic ring-opening of γ-butyrolactone and base-catalyzed esterification with benzyl bromide. We could successfully reproduce it and isolate **4.63** in a 64% yield (**Scheme 4.21**).

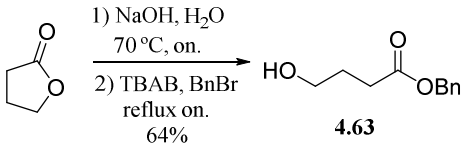

Scheme 4.21 Synthesis of benzyl 4-hydroxybutanoate *via* γ-butyrolactone ring opening and subsequent esterification.

Afterward, we reacted this building block with oxazoline **4.59** employing the same experimental protocol as previously. We obtained compound **4.64**, with a benzyl-protected carboxylic acid, in a moderate 42% yield. Afterwards, removal of the benzyl group *via* Pd-catalyzed hydrogenation provided the desired free carboxylic acid (**4.65**) with an excellent 90% yield (**Scheme 4.22**).

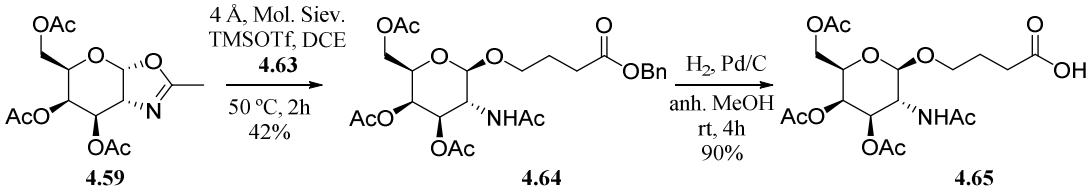

Scheme 4.22 Preparation of a carboxylic acid-derivatized GalNAc moiety.

Subsequently, we coupled the GalNAc-derivatized acid (**4.65**) with Me-Tz-NH_2 (**4.53**) using a carbodiimide, and isolated the fully acetylated GalNAc-tetrazine (**4.66, Scheme 4.23**) in a moderate 34% yield.

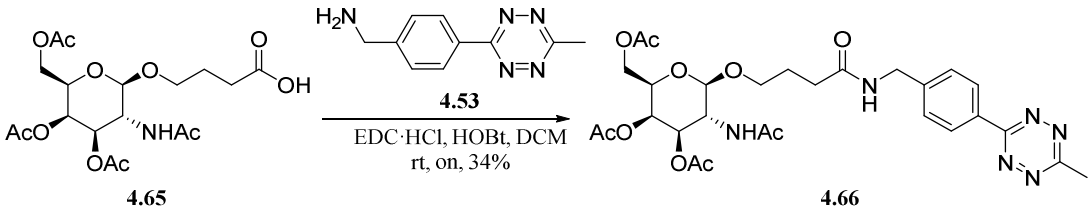

Scheme 4.23 Synthetic scheme for the obtention of carboxylic acid-derivatized GalNAc moiety.

Finally, we treated the peracetylated GalNAc tetrazine (**4.66**) with conc. aq. ammonia overnight to remove all the hydroxyl acetyls, and lyophilized the resulting crude. HPLC analysis showed disappearance of the starting material (**Figure 4.9**), but ESI MS analysis showed no desired compound formation. Instead, the *m/z* ratio of the main peak indicated it was a side product (observed *m/z* = 479.2137 Da; calcd. 491.2249 Da) proving that this last step was unsuitable to be performed on the carbohydrate linked to a tetrazine.

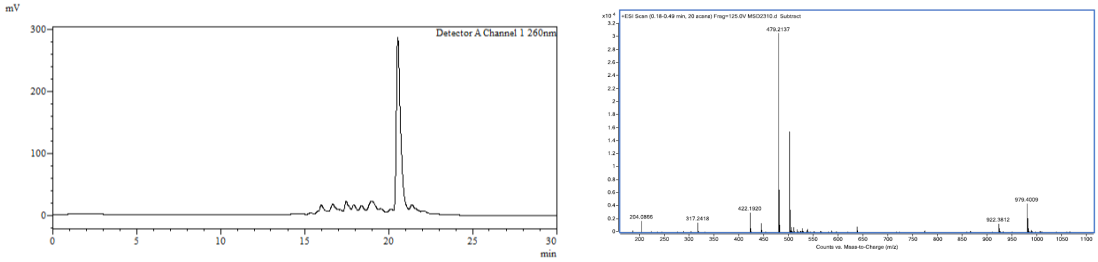

Crude MS Spectrum

Figure 4.9 Deprotection of **4.66**. HPLC trace (260 nm) of lyophilized crude and HRMS (ESI) spectrum of the isolated main product in the crude

Observing this result, we checked the stability of the methy-phenyl-bearing tetrazine (**4.21**) in conc. aq. ammonia and qualitatively observed color change, which pointed out towards instability. Indeed, a mass change was also observed providing evidence that tetrazines were not compatible with hydroxyl deprotection using conc. aq. ammonia. Thus, choosing to first hydrolyze the ester groups (which afforded compound **4.67** in a good 70% yield), followed by attachment of the tetrazine moiety (**4.53**) *via* carbodiimide activation, rendered the desired GalNAc derivative (**4.68**) in 23% yield as depicted in **Scheme 4.24**.

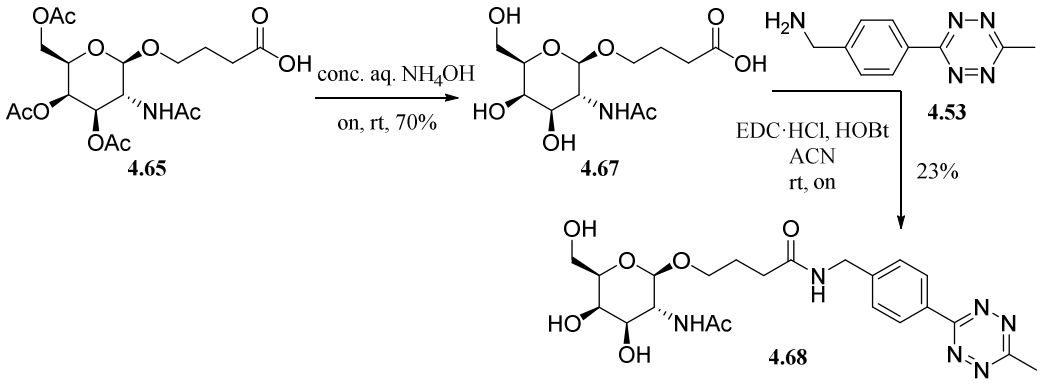

Scheme 4.24 Synthesis of GalNAc tetrazine derivative **4.68**.

4.3.3.2.2 Synthesis of a tetrazine with an appending biotin reporter

In mammals, biotin serves as an essential cofactor for each of the 5 biotin-dependent carboxylases: acetyl-CoA carboxylase 1 & 2, methylcrotonyl-CoA carboxylase, pyruvate carboxylase and propionyl-CoA carboxylase. Zempleni *et al.* suggested that posttranslational biotinylation of histones might play a role in the epigenetic code that regulates DNA transcription. However, subsequent work showed that <0.001% of human histones are biotinylated, suggesting that the abundance is too low to elicit biological effects in vivo.[30] Aside to biological effects, an important biological application of biotin derives from its strong interaction with streptavidin-avidin, allowing for easy affinity purification of biotinylated compounds interacting with immobilized streptavidin.[31]

In this case, since the biologically active D-biotin has a carboxylic acid suitable for amide formation, no additional derivatization was required, and appendage of the tetrazine was straightforward. The biotin carboxylic acid was activated with the uronium salt HATU and added to the pyrimidine-derivatized tetrazine **4.43**, which contained an amine functionality, yielding the tetrazine-derivatized biotin (**4.69**) in 63% isolated yield as depicted in **Scheme 4.25**.

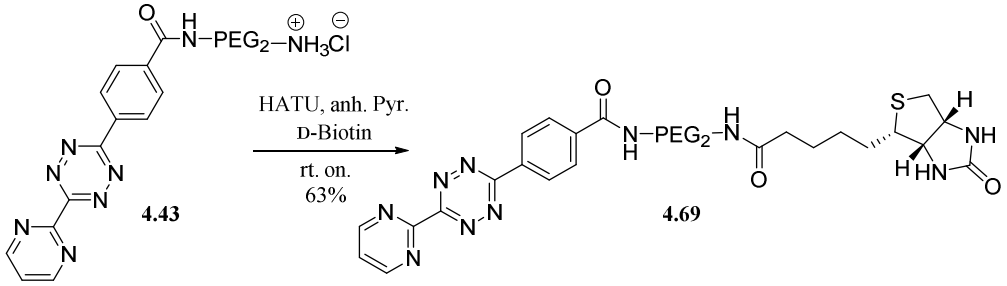

Scheme 4.25 Synthesis of biotin-derivatized tetrazine.

4.3.3.2.3 Synthesis of a tetrazine with an appending BODIPY fluorophore

Fluorescence imaging is a useful technique for a variety of biological applications. Human tissues and cells are made up of several organic molecules that naturally absorb (DNA, collagen, elastin, proteins, NADH, and FAD) and emit (NADH, FAD, proteins and DNA) light in the ultraviolet region.[32] In this context, fluorescent labels can be "free" or attached to other biomolecules, such as antibodies or oligonucleotides, which accumulate in specific organs and allow for imaging in animals and human subjects. Even though technological advances in this field are remarkable, there is a growing realization that imaging events both *in vitro* and *in vivo* by fluorescence is limited by available probes.

4,4-Difluoro-4-bora-3a,4a-diaza-*s*-indacene (BODIPY) dyes are strongly UV-absorbing small molecules that emit relatively sharp fluorescence peaks with high quantum yields. They are relatively insensitive to polarity and pH changes in their environment and reasonably stable in physiological conditions. Moreover, small modifications in their structure enable fine tuning of their fluorescent behavior opening a wide array of possibilities for labelling biomolecules such as proteins[33] and oligonucleotides.[34]

The IUPAC numbering system for BODIPY dyes is different from that used for dipyrromethenes and this fact can lead to confusion. However, the terms α-, β- and meso- are used in just the same way for both systems and thus, are the preferred method (**Figure 4.10**).

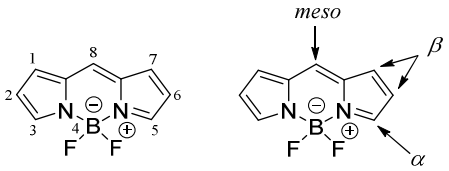

Figure 4.10 BODIPY scaffold IUPAC numbering (left) and alternative nomenclature (right).

meso-Substituted BODIPY dyes tend to be relatively easy to prepare *via* condensation of acyl halides with pyrroles. These transformations involve unstable dipyrromethene hydrochloride salt intermediates (**4.72**), usually not isolated, that are readily reacted with BF_3 under basic media to provide the BODIPY core (**4.73**, **Scheme 4.26**).

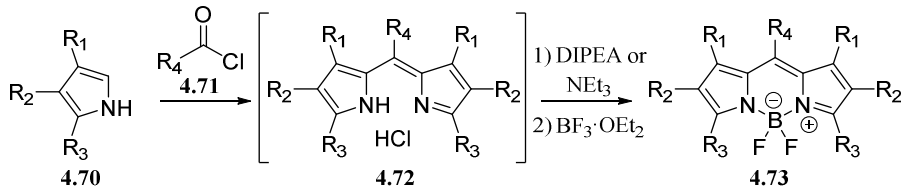

Scheme 4.26 Synthetic outline for the preparation of BODIPY analogues *via* acyl chloride route.

In our case, since the *meso* analogues are described to be best suited for derivatization in terms of synthetic accessability,[35] we pursued this type of structure. The first step was the synthesis of the corresponding acyl chloride. In this case, we chose methyl 4-chloro-4-oxobutanoate (**4.76**) because we deemed good enough a two-methylene linker between the carboxylic acid functionality and the tetrazine core, moreover a longer PEG linker was expected to be appended later on. The synthesis starts with the nucleophilic addition of methanol into succinic anhydride to yield the monoester in a quantitative manner and a subsequent conversion into an acyl chloride using the classic thionyl chloride reagent. Compound **4.76** was isolated in an excellent 95% yield (**Scheme 4.27**).

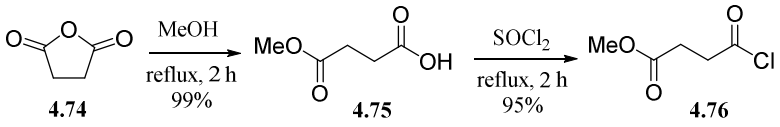

Scheme 4.27 Synthesis of the acyl chloride employed in the construction of the BODIPY scaffold.

Subsequently the key step of BODIPY core construction utilized described procedures.[36] We employed commercially available 2,4-dimethylpyrrole (**4.77**) and reacted it with the previously synthesized acyl chloride overnight in anh. DCM. As previously touched upon, we added DIPEA in order to displace the hydrochloride salt and further reacted the **4.72**-like intermediate with BF_3 to yield the methyl ester-derivatized BODIPY scaffold (**4.78**) in a poor 15% yield. Nonetheless this step is described as being the synthetically challenging one and, since we required a small amount of product, we decided that it was not worth optimizing this step. Subsequently the desired BODIPY-COOH scaffold (**4.79**) was obtained by ester hydrolysis under basic conditions in a fairly good 75% yield (**Scheme 4.28**).

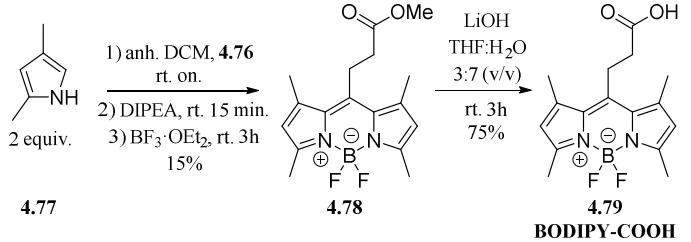

Scheme 4.28 Synthesis of the BODIPY analogue **4.79** *via* the acyl chloride procedure.

The BODIPY derivative (**4.79**) was then reacted with the appropriate tetrazine (**4.43**) in order to furnish the desired tetrazine-BODIPY analogue (**4.80**). In this instance, we chose also the pyrimidyl-containing tetrazine in order to obtain a derivative of the most reactive core, as depicted in **Scheme 4.29**.

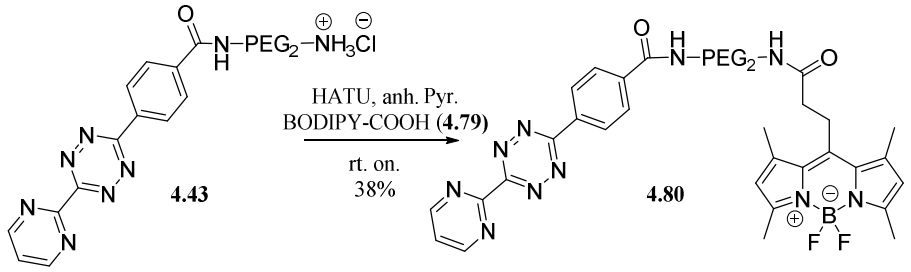

Scheme 4.29 Synthesis of BODIPY-derivatized tetrazine (**4.80**) *via* HATU activation of precursor **4.79**

4.4 Bioconjugation using the IEDDA reaction and an oxanorbornene as a dienophile

After obtaining all desired reactants we performed simple conjugations involving several 7-oxanorbornenes and tetrazines, both with oxanorbornene-polyamides (either peptides or PNA, Scheme **4.34**) and with oxanorbornene-oligonucleotides (**Scheme 4.31**). All conjugation reaction were carried out by reacting the oxanorbornene-containing component (0.5 mM) with small excess (2 equiv.) of tetrazine in a MeOH:H_2O mixture overnight at 37 ºC.

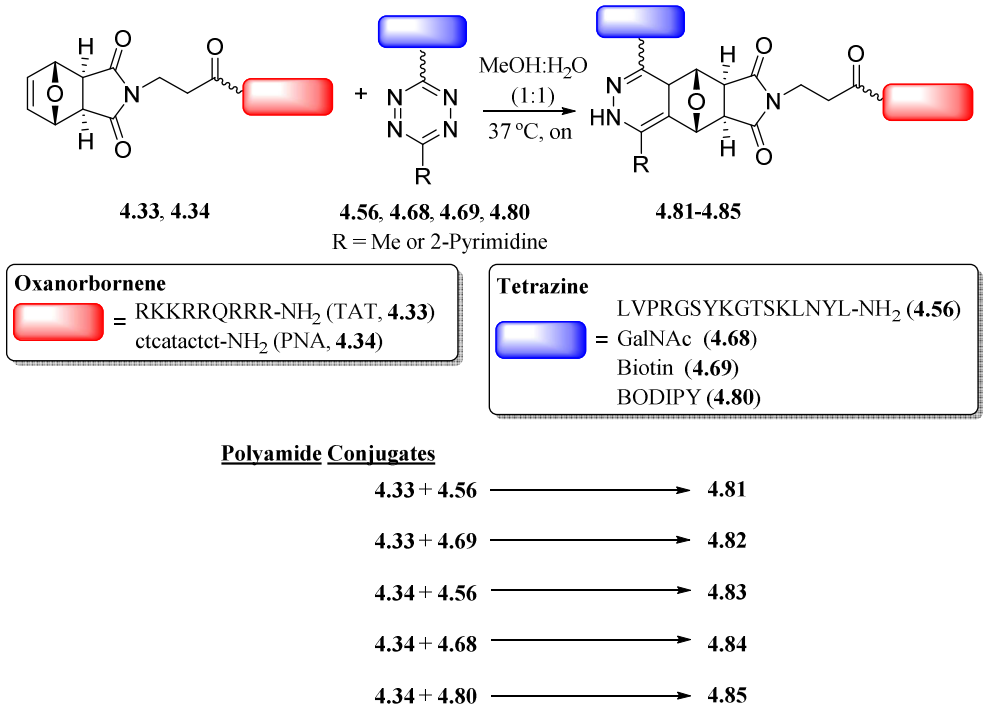

Scheme 4.30 Outline of the IEDDA conjugation reactions between oxanorbornene-containing polyamides and various tetrazines.

As a representative example, HPLC traces of the reaction involving oxanorbornene-containing PNA (**4.33**) and biotin-derivatized tetrazine (**4.69**) is depicted in **Figure 4.11**.

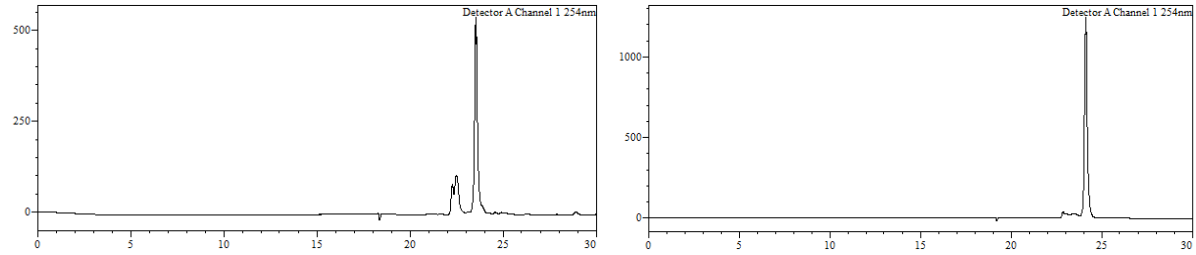

Crude Pure

Figure 4.11 Conjugation reaction involving PMal[H_2]-ctcatactct-NH_2 (**4.34**) and tetrazine-derivatized peptide (Tz-LVPRGSYKGTSKLNYL-NH_2, **4.56**). HPLC traces (254 nm) of the reaction crude (left) and purified conjugate (right).

Analogously, with the oligonucleotide containing all nucleobases and appended with the oxanorbornene moiety at the 5' position (**Scheme 4.5**), we carried out several conjugation reactions as shown in **Scheme 4.31**.

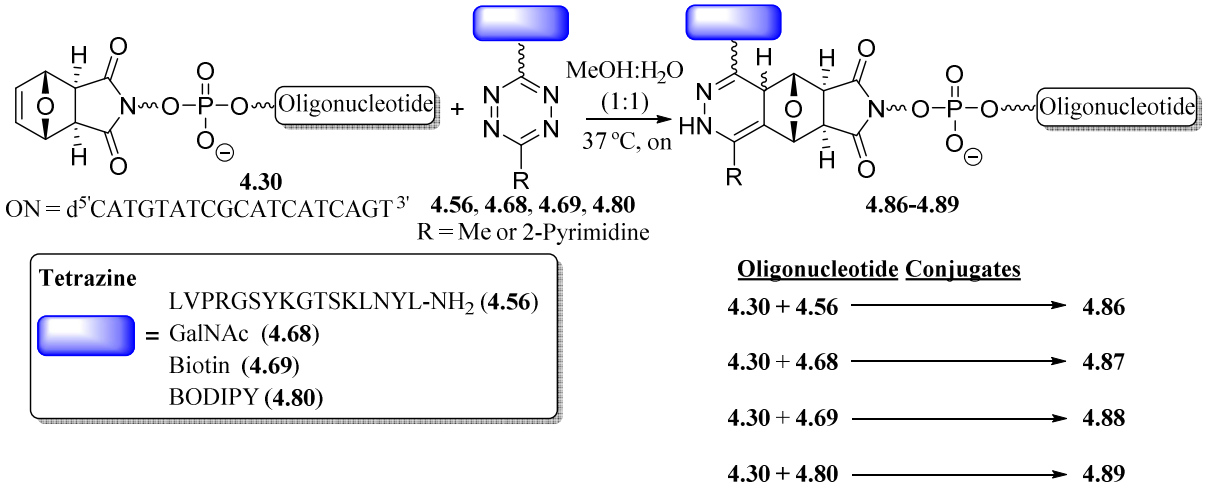

Scheme 4.31 Outline of the IEDDA reaction between an oxanorbornene-containing oligonucleotide

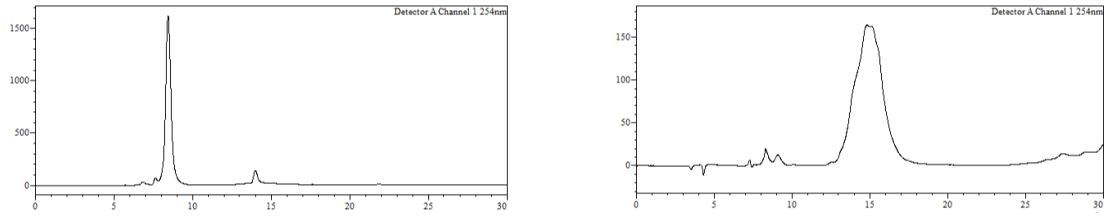

Crude (254 nm) PMal[H_2]-20mer + Tz-GalNAc (**4.87**)

Crude (254 nm) PMal[H_2]-20mer + Tz-BODIPY (**4.89**)

Figure 4.12 HPLC traces (254 nm) of the reaction crude of the conjugation reaction involving PMal[H_2]-oligonucleotide (**4.30**) and tetrazines (**4.87**, left and **4.89**, right).

Observing these positive results both in peptide and oligonucleotide chemistry we concluded that the IEDDA cycloaddition of tetrazines and oxanorbornenes runs smoothly with these two biomolecules. In all cases, good HPLC traces were found and reasonable to high isolation yields were obtained. Moreover, the fact that mild conditions were employed for the conjugation reaction demonstrates that this methodology is indeed biocompatible.

4.5 Preparation of peptide and oligonucleotide double conjugates involving one oxanorbornene-mediated IEDDA reaction

In a similar fashion to the experiments described in the second chapter (**Section 2.6**) of this dissertation, the possibility of synthesizing double conjugates was examined using compounds incorporating two functional groups chosen to react chemoselectively with different reagents. In particular, the set of experiments here described aimed to assess the compatibility of the oxanorbornene-mediated IEDDA conjugation methodology with other conjugation chemistries.

Most of the double conjugation assays were carried out with peptides rather than oligonucleotides. First, because peptides and the corresponding conjugates can normally be analyzed by HPLC-MS which allows information on the nature of the different peaks or components of the mixture to be directly obtained by ESI MS without the need of isolation. This is not possible with oligonucleotides because salt-containing buffered eluents are required for their HPLC analysis, which is not compatible with ESI MS characterization. In the case of oligonucleotide conjugates, the different eluates must be first collected, then lyophilized and finally analyzed by MALDI-TOF MS.

Both peptides and oligonucleotides are easily accessible by solid-phase synthesis. Modifications of peptides or oligonucleotides at the *N*-terminus or the 5' end, respectively to run one of the conjugation reactions involves a fairly similar effort, but the synthesis of derivatives (either a building block or a suitably-modified solid matrix) bearing the functionality required for the other conjugation reaction is more straightforward in the case of peptides.

4.5.1 Double conjugations on a peptide containing an oxanorbornene and a 2,5-dimethylfuran-protected maleimide

4.5.1.1 Preliminary experiments

After the positive results described in the previous section, our interest was to examine the possibility of using as synthetic scaffold a peptide incorporating the two different protected maleimides we have worked with in this thesis. As a first follow-up work we evaluated the feasibility of selectively derivatizing the PMal[H_2] moiety (utilizing the IEDDA reaction) in front of the PMal[Me_2] one, followed by removal of the dimethyl-furan protecting group and another conjugation reaction (either a Diels-Alder cycloaddition or a thia-Michael reaction) with the resulting maleimide. For this purpose, we synthesized a peptide containing both moieties, appending from the *N*-terminus and from a lysine side-chain, respectively. For the preparation of the lysine derivatives, the two respective carboxylic acid derivatives (**4.13** or **4.20**) were reacted with the ε-amine of Fmoc-Lys-OH utilizing the mixed anhydride method which provided the desired lysine derivatives with either the oxanorbornene (**4.90**) or 2,5-dimethyfuran-protected maleimide (**4.91**) in similar yields (≈ 80%) as depicted in **Scheme 4.31**.

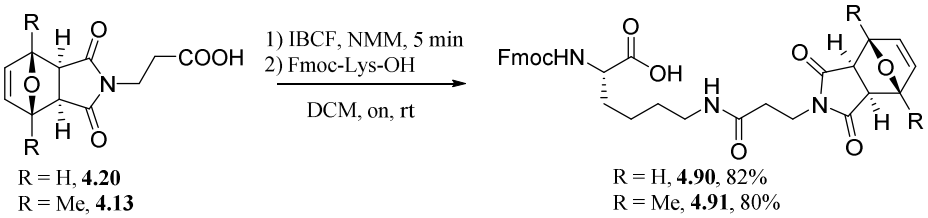

Scheme 4.34 Synthesis of lysine derivatives containing an oxanorbornene (**4.90**) or a 2,5-dimethylfuran-protected maleimide (**4.91**) moiety.

We corroborated that both moieties could be appended into a polyamide and withstand SPPS in accordance to the literature[9] as seen upon inspection of the HPLC trace of the cleavage crude (**Figure 4.13**) of a peptide with sequence PMal[H_2]-Asn-Tyr-Ala-Lys(PMal[Me_2])-Ala-Arg-Lys-Val-NH_2 (**4.92**).

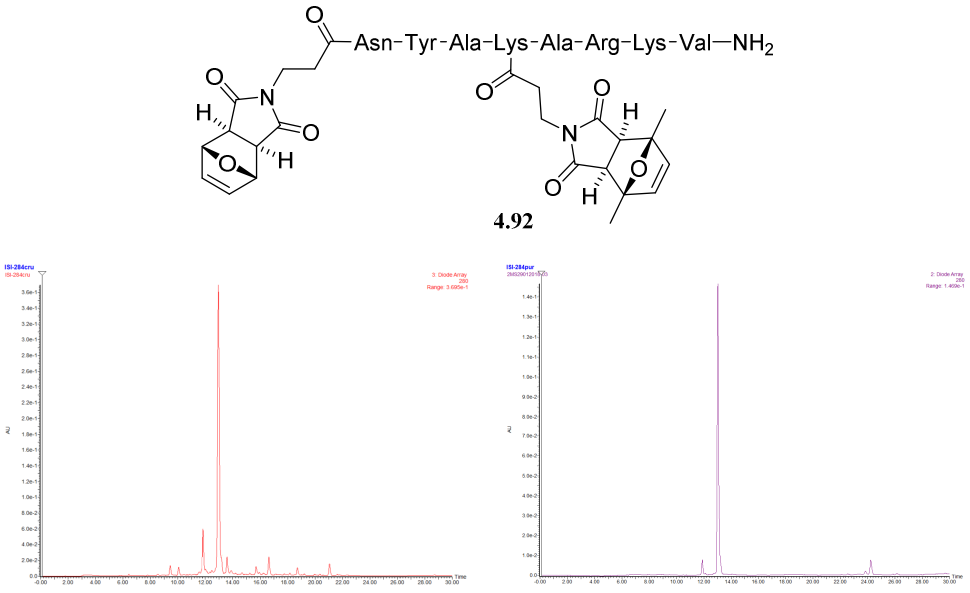

Figure 4.13 Structure of the doubly-derivatized peptide and HPLC traces (280 nm) of the synthesis crude (left) and the purified product (right).

We first tested the feasibility of running the retro-Diels-Alder reaction that yields free maleimides from 2,5-dimethylfuran-protected moieties in front of the furan-protected ones. In case this worked, it would be possible to obtain a double conjugate by first reacting the free maleimide with either a diene or a thiol, and then the remaining oxanorbornene with a tetrazine.

To answer this question, an aqueous methanolic solution of the two maleimides, one protected with 2,5-dimethylfuran (**4.93**) and the other with furan (**4.20**) was heated at 90, 80 or 70 ºC for 45 min in a MW oven (**Scheme 4.33**). HPLC-MS analysis of the resulting crudes showed, as expected, higher rates for the removal of 2,5-dimethylfuran in regards to furan as inferred from the relative 3-maleimido propionic acid (**4.18**) and *N*-(2-hydroxyethyl)maleimide (**4.94**) ratios. Consequently, these data indicated that selective dimethylfuran removal was not quantitatively achievable without affecting the oxanorbornene under any of the tested conditions, since non-negligible amounts of furan-removal were observed in the conditions that quantitatively removed 2,5-dimethylfuran. Of the three temperatures tested, heating at 70 ºC for 45 min minimized the retro-Diels-Alder reaction on furan-protected maleimide, although only 80% 2,5-dimethylfuran was removed from the corresponding protected maleimide.

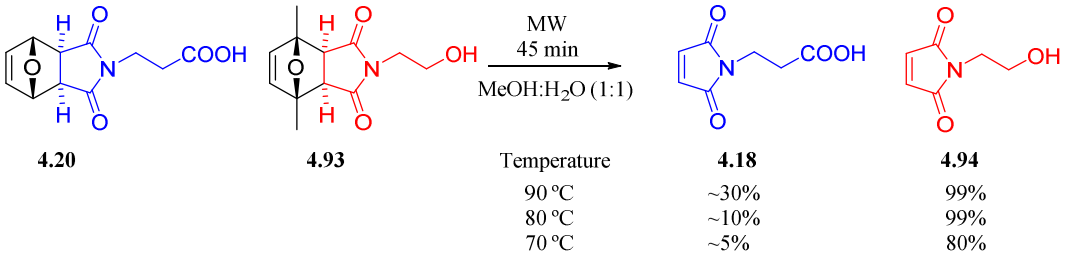

Scheme 4.33 Relative ratios of compounds **4.18** and **4.94** (HPLC analysis) after heating equimolar mixtures of **4.20** and **4.93** at different temperatures.

We next asked whether it would be possible to proceed the other way around, that is carrying out first the IEDDA reaction, then deprotecting the other maleimide and using it for conjugation. It is worth reminding here that we had previously observed that tetrazines do react with oxanorbornenes (or furan-protected maleimides) but not with 2,5-dimethylfuran-protected maleimides (see **Schemes 4.2** and **4.4**). To test so, we incubated peptide **4.92** with 4 equiv. of $(2\text{-Pyr})_2$Tz (**4.14**) in the usual methanolic aqueous solution, at room temperature, and monitored the reaction progress by HPLC-MS. As depicted in **Scheme 4.34**, HPLC traces at different reaction times showed progressive consumption of peptide **4.93** (marked with a star), which evolved into the desired IEDDA adduct (marked with a circle).

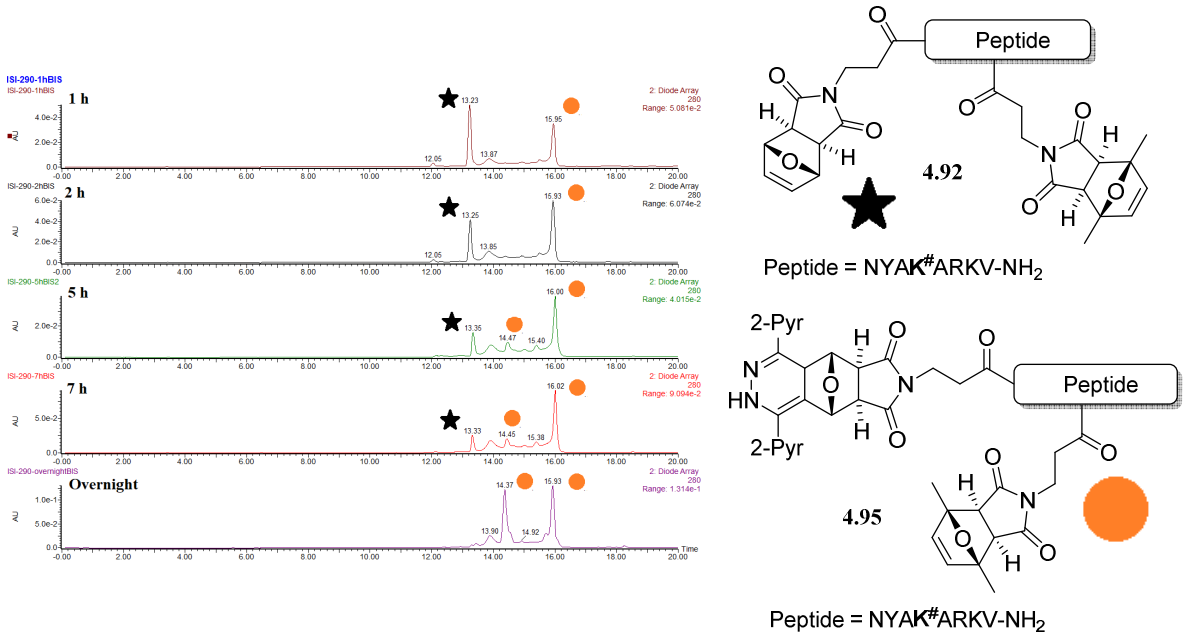

Scheme 4.34 Left: HPLC traces (280 nm) of the crude resulting from the reaction between $(2\text{-Pyr})_2$Tz (**4.14**) and the peptide incorporating furan and 2,5-dimethylfuran-protected maleimides (**4.92**) at different reaction times. Right: simplified structures of partner peptide showing the two differently protected maleimides (black star) and of the target adduct (orange circle). $\mathbf{K^{\#}}$ = 2,5-dimethylfuran-protected 4-maleimidopropionyl lysine derivative.

This experiment was not only consistent with previous data regarding the orthogonality of the oxanorbornene-tetrazine reaction, but also reinforced them by confirming that PMal[Me_2] does not react with tetrazines. In addition, it provided a basis for double conjugations on peptide scaffolds appended with oxanorbornenes and dimethyl-substituted oxanorbornenes (PMal[H_2] and PMal[Me_2], respectively).

4.5.1.2 Double conjugations involving IEDDA and Michael-type addition reactions

First attempts of double conjugations were carried out by simultaneously reacting peptide **4.92**, (2-Pyr)$_2$Tz (**4.14**) and a thiol, namely a peptide containing an internal cystine (H-GYCAS-NH$_2$ **4.96**) with MeOH:H$_2$O (1:1) as a solvent and under MW irradiation at 70 ºC for 45 min, using the heating conditions that minimized furan retro-Diels-Alder (see above and **Scheme 4.35**). In this instance, the reaction crude was a complex mixture where the desired target adduct was a minor product (HPLC-MS), in addition to formation of cysteine disulfide adduct amongst other by-products.

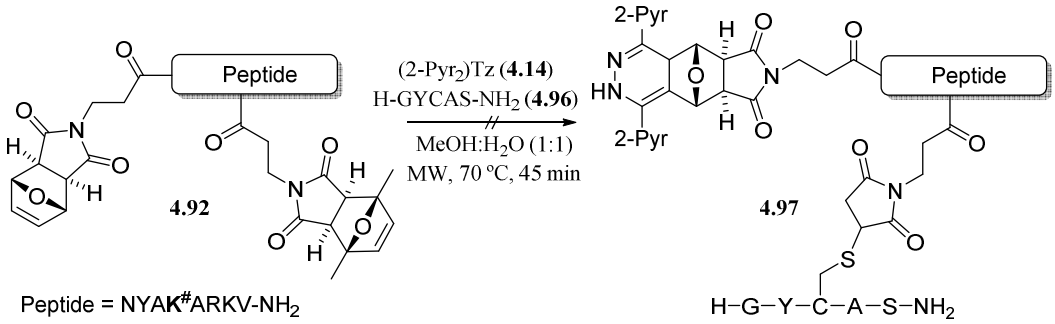

Scheme 4.35 Simultaneous attempt of double conjugation on peptide **4.92**, using with (2-Pyr)$_2$Tz (**4.14**) and peptide H-GYCAS-NH$_2$ (**4.96**). **K$^{\#}$ =** 2,5-dimethylfuran-protected 4-maleimidopropionyl lysine derivative. (**4.91**).

A follow-up experiment of this attempt was running both reactions sequentially in a one-pot manner. That is, doing first the IEDDA reaction (since we knew that tetrazine would exclusively react with the oxanorbornene moiety) and, subsequently and without purification, adding a thiol and heating the reaction mixture (MW irradiation at 90 ºC for 90 min) to promote 2,5-dimethylfuran removal and conjugation with the thiol as depicted in **Scheme 4.36**. In this instance, no Michael-adduct was detected either, but also a complex crude containing the IEDDA adduct among many impurities.

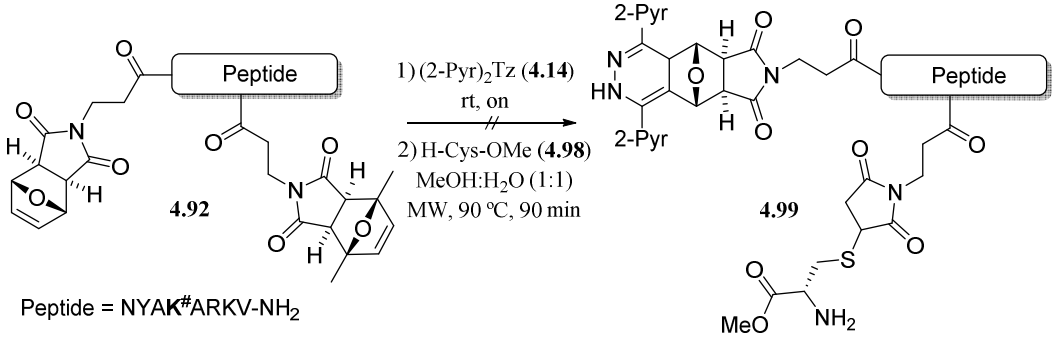

Scheme 4.36 Sequential "one-pot" double conjugation of peptide **4.92** with (2-Pyr)$_2$Tz and methyl cysteinate (**4.98**). **K$^{\#}$ =** 2,5-dimethylfuran-protected maleimide lysine derivative (**4.91**).

Different inferences could be drawn from these results. One might be that the IEDDA adduct does not withstand the heating conditions typically used to remove dimethylfuran from the dimethylfuran-protected maleimides. It could also be possible that heating in the presence of a free thiol harms the IEDDA adduct. In any case, this proved not to be a viable alternative for double conjugations involving oxanorbornene-mediated IEDDA reactions.

4.5.1.3 Double conjugations involving IEDDA and Diels-Alder cycloaddition reactions

Utilizing the same doubly-derivatized peptide **4.92** as starting material, we tried to switch the second click reaction to the Diels-Alder cycloaddition hoping that dienes would not damage the IEDDA cycloadduct.

As depicted in **Scheme 4.37**, an initial attempt of double conjugation with a tetrazine and a diene was carried out by simultaneously reacting peptide **4.92** with 4 equiv. of (2-Pyr)$_2$Tz (**4.14**) and Diene-COOH (**3.48**, see chapter 3, **Scheme 3.20**) under MW irradiation at 90 ºC for 90 min. Similarly, to previously found results with thiols, removal of dimethylfuran and partial deprotection of the furan-protected maleimide was observed. Additionally, Diels-Alder reaction with all free maleimides was encountered. Finally, a compound whose mass suggested formation of an adduct between the tetrazine and the diene was detected, giving reasons to believe that an IEDDA reaction between the tetrazine and one of the double bonds of the diene was taking place.

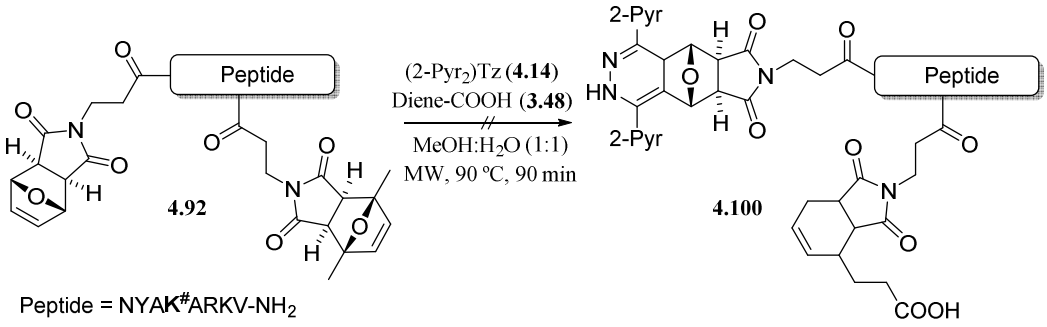

Scheme 4.35 Attempt to simultaneously deprotect the maleimide appending from the lysine side-chain, and obtaining peptide **4.100** double conjugate by MW heating in the presence of (2-Pyr)$_2$Tz (**4.14**) and diene-COOH (**3.48**). **K$^{\#}$ =** 2,5-dimethylfuran-protected maleimide lysine derivative (**4.91**).

The second round of attempts was performed using the sequential one-pot strategy. That is first doing the IEDDA reaction with 2 equiv. of (2-Pyr)$_2$Tz, and afterwards, without purification, adding a larger excess (4 equiv.) of diene-COOH (**4.98**) and heating as depicted in **Scheme 4.38**.

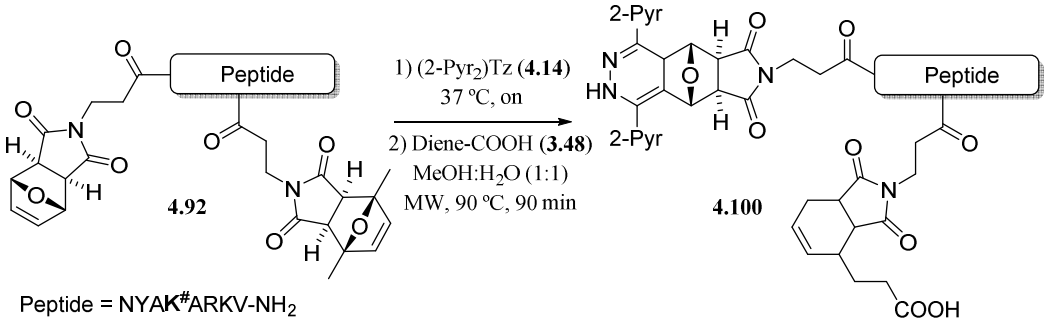

Scheme 4.38 Sequential "one-pot" double conjugation of peptide **4.92** with (2-Pyr)$_2$Tz (**4.14**) and diene-COOH (**3.48**). **K$^{\#}$ =** 2,5-dimethylfuran-protected maleimide lysine derivative (**4.91**).

This strategy was based on the previously observed partial deprotection of PMal[H$_2$] under the conditions required to remove the 2,5-dimethylfuran protecting group, in which the diene-tetrazine IEDDA reaction could have been taking place. Unexpectedly, as can be seen in **Figure 4.14**, HPLC analysis of the reaction crude showed formation of the target doubly derivatized adduct with a mass 18 Da lower than expected (*m/z* found 1633.5, *m/z* calcd. For the double conjugate 1651.7 Da). Some of the tetrazine was also consumed in an IEDDA reaction with the diene.

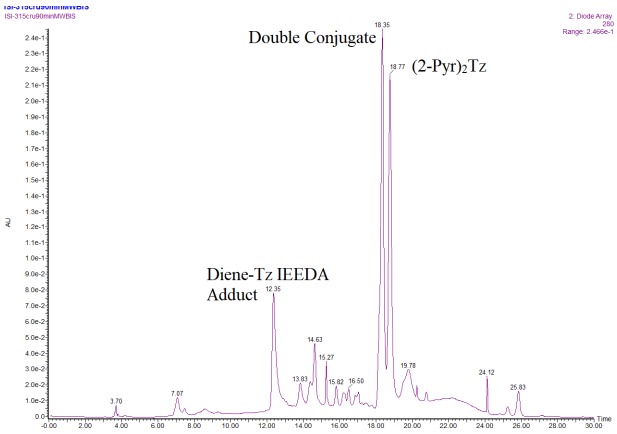

Figure 4.14 HPLC trace (280 nm) of the crude resulting from the reaction depicted in **Scheme 4.38**.

This result was encouraging because the double conjugate was the main product in the crude, yet discouraging because the compound formed was not exactly our target but a double conjugate that seemed to have lost one water molecule. Such behavior had never been observed in any of the experiments performed to obtain "simple" conjugates (see **Section 4.4**).

In order to make sure that this fairly good result could be reproduced, we synthesized a diene-derivatized fluorophore (dansyl) to use another reactant for Diels-Alder reaction instead of the model diene-COOH derivative (**3.48**). As depicted in **Scheme 4.39**, synthesis of such analogue started by reacting commercially available dansyl chloride (**4.101**) with *tert*-butyl (2-aminoethyl)carbamate in DCM to provide the Boc-protected dansyl analogue (**4.102**) in 82% yield. Subsequently, an acidic treatment quantitatively provided the free amine (**4.103**).

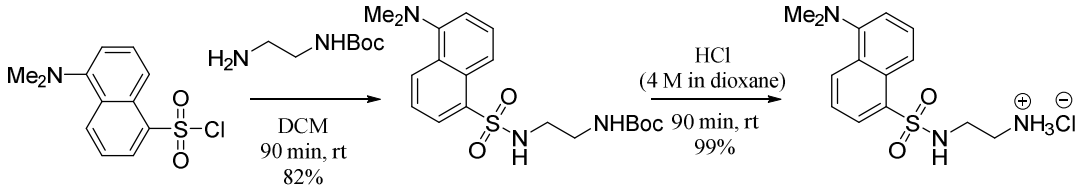

Scheme 4.39 Outline for the synthesis of amine-derivatized dansyl fluorophore.

The first synthetic attempt to obtain the target diene-dansyl derivative was performed *via* EDC·HCl and HOBt-mediated activation of diene-COOH (**3.48**). Nonetheless, this strategy proved to be ineffective due to the low conversions and long reaction times required. Therefore, we switched to the mixed anhydride activation method, *via* reaction with isobutyl chloroformate in the presence of a base, which rendered the desired diene-derivatized dansyl analogue (**4.104**) in a good 82% yield (**Scheme 4.40**).

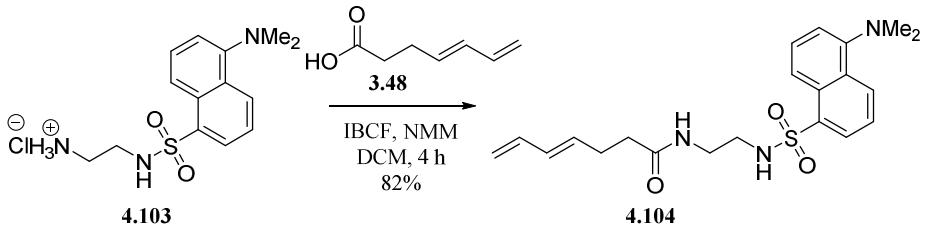

Scheme 4.40 Synthesis of the diene-containing dansyl derivative.

With the dansyl-derivatized diene (**4.104**) in hand, another double conjugation assay was carried out following the same conditions, as depicted in **Scheme 4.41**.

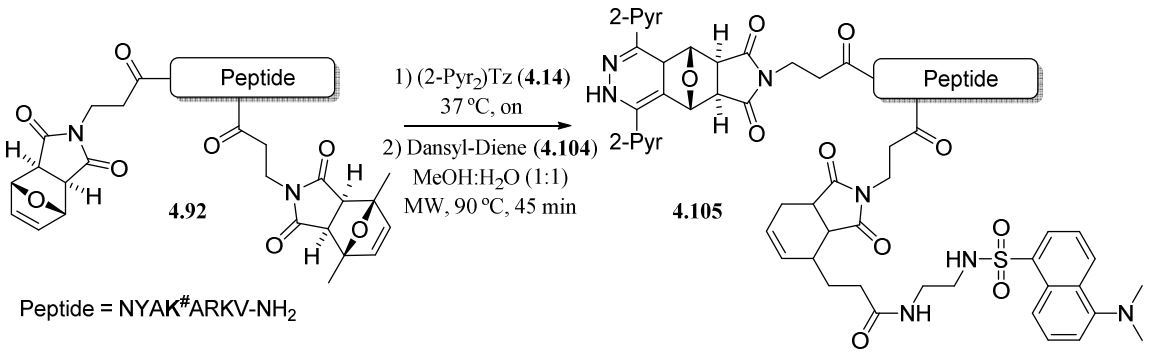

Scheme 4.41 Sequential "one-pot" double conjugation of peptide **4.92** with $(2\text{-Pyr})_2$Tz and diene-dansyl (**4.104**). **K# =** 2,5-dimethylfuran-protected maleimide lysine derivative (**4.91**).

Analogously to the previous attempt with diene-COOH (**4.98**), HPLC analysis of the reaction crude (**Figure 4.15**) showed, in addition to formation of the target double conjugate, another peak whose mass was in agreement with the double conjugation adduct -18 Da (found 1634.0 Da, calcd. 1651.8 Da). The presence of dansyl moiety was also verified by 350 nm UV absorption (**Figure 4.15**, right).

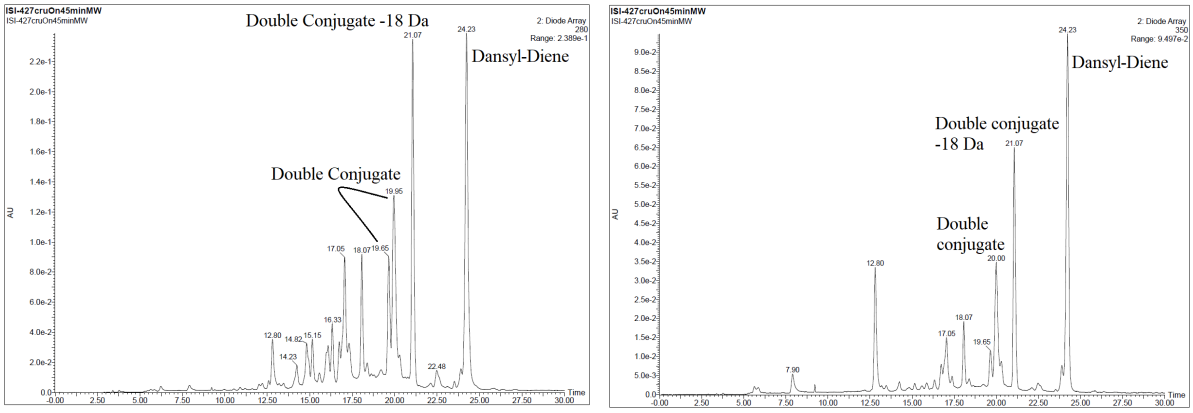

UV trace (280 nm) UV trace (350 nm)

Figure 4.15 HPLC traces (280 nm, left and 350 nm, right) of the reaction crude resulting from a double conjugation assay between peptide **4.92**, $(2\text{-Pyr})_2$Tz (**4.14**) and diene-dansyl (**4.104**).

4.5.1.4 Concluding Remarks

In summary, it is not possible to selectively eliminate dimethylfuran from peptides incorporating both 2,5-dimethylfuran- and furan-protected maleimides, since partial furan removal is always observed. All of the double conjugation experiments here described have further confirmed that tetrazines selective react with 7-oxanorbornenes and not with 1,4-dimethyl-7-oxanorbornenes. Reaction between tetrazines and one of the double bonds of conjugated dienes has also been observed to take place upon heating.

Attempts to simultaneously perform the IEDDA cycloaddition between a tetrazines and an oxanorbornene, the retro-Diels-Alder reaction that liberates a maleimide from 2,5-dimethylfuran, and either a Michael-type thiol addition to the free maleimide or a Diels-Alder reaction with a diene have proved to be unfeasible. In follow-up experiments, sequential one-pot approaches where the IEDDA reaction was performed first and afterwards the rDA and the Michael-type reaction proved unfruitful yielding complex mixtures. However, the one-pot alternative did work when maleimide deprotection was accompanied by reaction with a diene, even though formation of a double conjugate with a mass 18 Da lower than the expected one was also observed.

4.5.2 Double conjugations on a peptide containing an oxanorbornene and a maleimide

The second alternative we thought worth examining involved a peptide containing a maleimide and an oxanorbornene moiety. The fact that the heating step required to remove 2,5-dimethylfuran seemed to yield crude complexity prompted us to replace the protected maleimide with a free maleimide. The peptide sequence selected for this round of experiments was inspired by that of biologically active peptide luteinizing hormone-releasing hormone (LHRH). Natural LHRH peptide sequence is Glp-His-Trp-Ser-Try-Gly-Leu-Arg-Pro-Gly-NH_2 and its biological function is the mediation of gonadotropin secretion from the anterior pituitary, stimulating both luteinizing hormone and follicle-stimulating hormone release. These hormones are involved in controlling male and female reproduction, inducing the production of oestrogens and progestogens in the female and of androgens in male.

In our case, the *N*-terminal pyroglutamic acid was replaced with 3-maleimidopropionic acid, and the 6th residue (Gly) with the synthetic oxanorbornene-derivatized lysine as shown in **Figure 4.16** (top). It is worth mentioning that the acidic treatment that removes all permanent protecting groups after solid-phase peptide assembly yields, as observed in the HPLC traces, two major products (**Figure 4.16**, bottom). MS analysis revealed presence of a carbamic acid (N^{In}-COOH) tryptophan peptide (which are typically formed from the *N*-Boc-protected indole). It has been described that it slowly decarboxylates to furnish the unmodified tryptophan.[37]

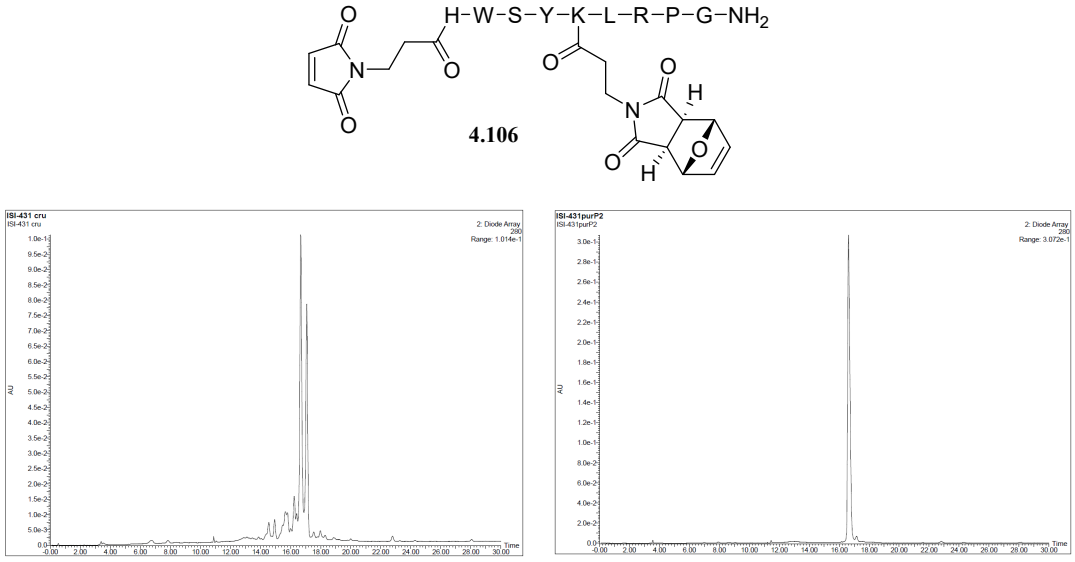

Crude Pure

Figure 4.16 Structure (top) and HPLC traces (280 nm, bottom) of the crude and purified peptide **4.106**. $t_R \approx 17$ min = N^{In}-COOH tryptophan peptide.

Previous experiments with 2,5-dimethylprotected maleimides (**Section 4.5.1**) pointed towards the orthogonality of maleimides respective to tetrazines. Although this is reasonable because both are electron-poor reagents, and thus should not undergo a cycloaddition reaction, we tested whether they reacted or not. For this purpose, we incubated peptide **4.106** with 2 equiv. of 2-Pyr_2Tz (**4.14**) in the usual IEDDA conditions (overnight, 37 ºC) and analyzed the crude mixture by HPLC. This showed formation of the expected simple conjugate even after long reaction times, providing evidence that indeed the reaction was taking place exclusively with the oxanorbornene moiety and not with the maleimide.

With these results in hand, we first proceeded with double conjugations involving reactions with tetrazines and dienes. In this instance, we made use of dansyl-derivatized diene (**4.98**) and (2-Pyr)$_2$Tz (**4.14**) and carried out the two conjugation reactions simultaneously (**Scheme 4.42**).

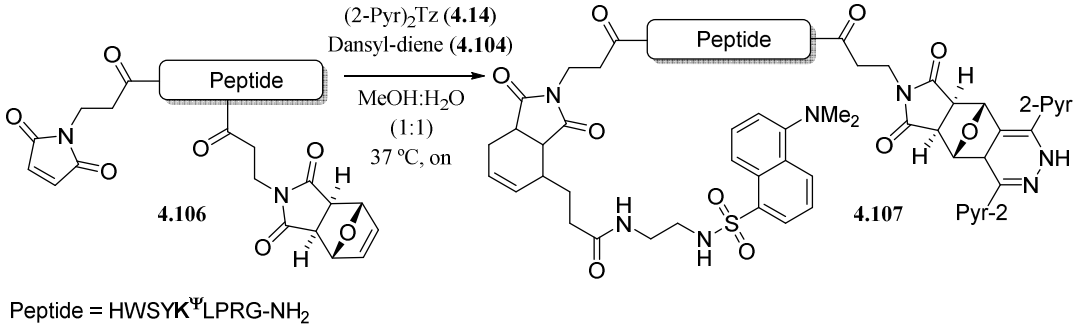

Peptide = HWSYK$^{\Psi}$LPRG-NH$_2$

Scheme 4.42 Simultaneous double conjugation of peptide **4.106** with (2-Pyr)$_2$Tz (**4.14**) and diene-dansyl (**4.104**). **K$^{\Psi}$ =** oxanorbornene-containing lysine derivative (**4.91**).

As can be observed in the HPLC trace (**Figure 4.17**) after overnight reaction conditions, the starting peptide was still present, along with IEDDA adduct, indicating that, to our surprise, the DA reaction wasn't taking place or was much slower than the IEDDA counterpart. Additionally, another adduct whose mass was 18 Da lower than the one expected for the "IEDDA conjugate" was also observed, hinting towards the possibility that formation of the -18 Da adduct was not induced by MW but by the reaction conditions.

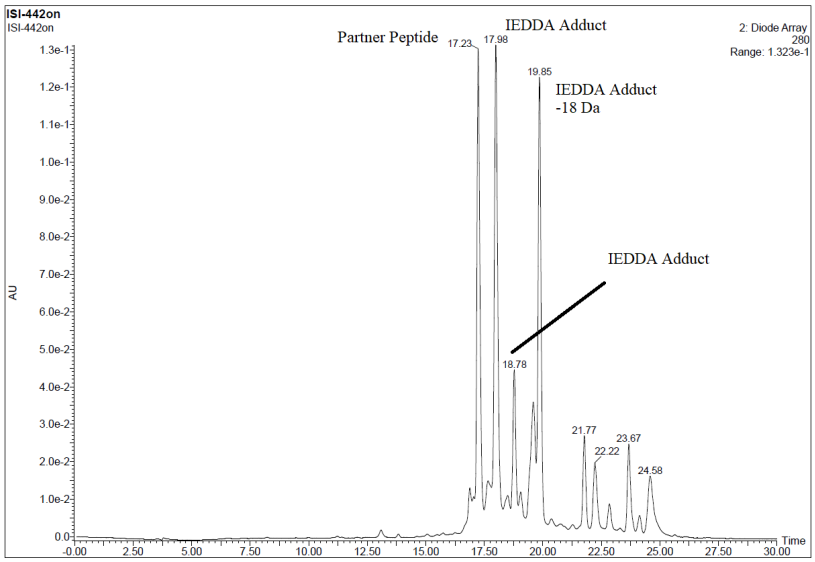

Figure 4.17 HPLC trace (280 nm) of the crude resulting from reaction between peptide (**4.106**), (2-Pyr)$_2$Tz (**4.14**) and diene-dansyl (**4.104**).

Observing the partial success (no DA reaction), we hypothesized that maybe the diene was reacting with the tetrazine. It had been observed in previous trials using MW irradiation but not at room temperature. We therefore proceeded to run the reactions consecutively, first the DA and then the IEDDA, with isolation of the Diels-Alder adduct (**Scheme 4.43**).

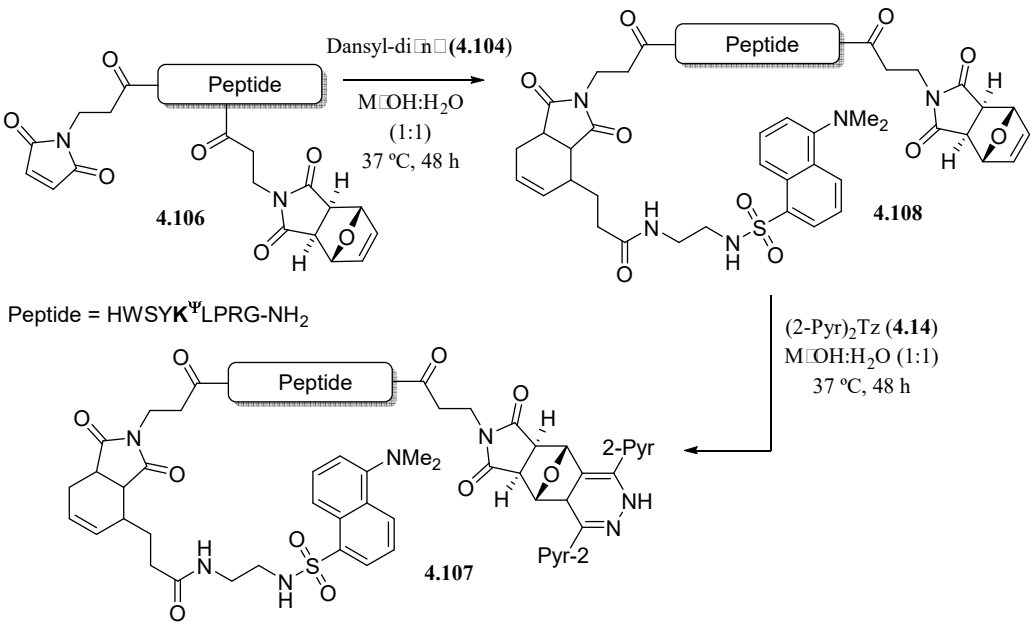

Scheme 4.43 Preparation of double conjugate **4.107** by reacting peptide **4.106** first with diene-dansyl **4.104** and, after purification, with $(2\text{-Pyr})_2$Tz (**4.14**). $\mathbf{K^{\Psi}}$ **=** oxanorbornene-containing lysine derivative (**4.91**).

As can be inferred from the HPLC traces of the Diels-Alder reaction crude (**Figure 4.18**, left), the reaction proceeded cleanly but slowly. This might be due to the fact that it was not carried out in water, which is the most accelerating medium but in a 1:1 MeOH:H_2O mixture (**4.104** is not soluble in water). Although it was not complete yet, after 48 h the reaction was stopped and the crude purified. Afterwards, the Diels-Alder adduct (**4.108**) was reacted with $(2\text{-Pyr})_2$Tz (**4.14**). HPLC analysis showed a crude that seemed to be cleaner than the one obtained previously, from which we could isolate both the double conjugate target but, also the -18 Da product (**Figure 4.18**, right). This result evidenced that this by-product is associated to the IEDDA reaction rather than to MW irradiation.

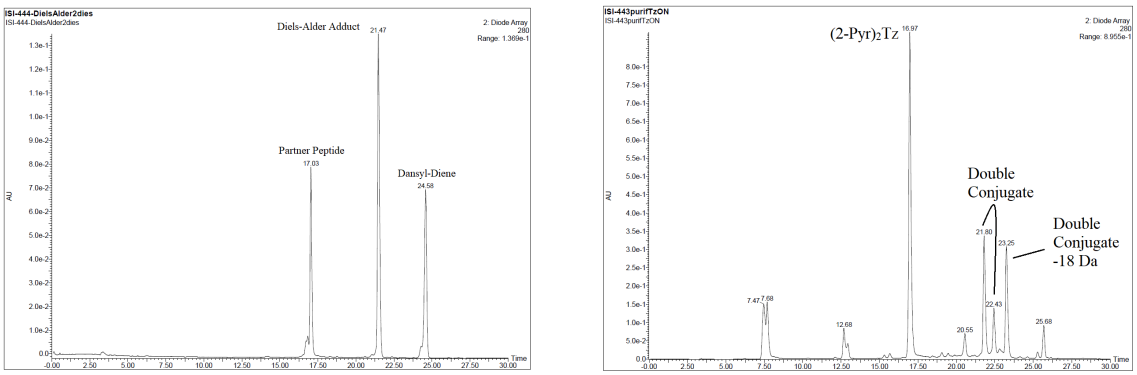

Diels-Alder crude (48 h, 280 nm) IEDDA crude (on, 280 nm)

Figure 4.18 HPLC traces (280 nm) of the crudes obtained after reacting peptide **4.106** with diene-dansyl (**4.104**, left), and of the resulting IEDDA adduct with $(2\text{-Pyr})_2$Tz (right).

In a subsequent experiment, we performed the IEDDA reaction on the peptide scaffold with $(2\text{-Pyr})_2$Tz (**4.14**), and monitored (HPLC) the reaction outcome at 24, 48 and 72 h (**Figure 4.19**). As can be seen, at the 24 h mark, the reaction seemed to be completed since no peptide starting material was detected. Additionally, the expected two IEDDA adducts are observed in conjunction with the now usual 3rd with a mass 18 Da lower. More interestingly, the IEDDA adducts seem to evolve towards the M-18 Da

product over time, giving reasons to believe that the 1,4-dihydropyridazines resulting from the IEDDA reaction are not fully stable adducts.

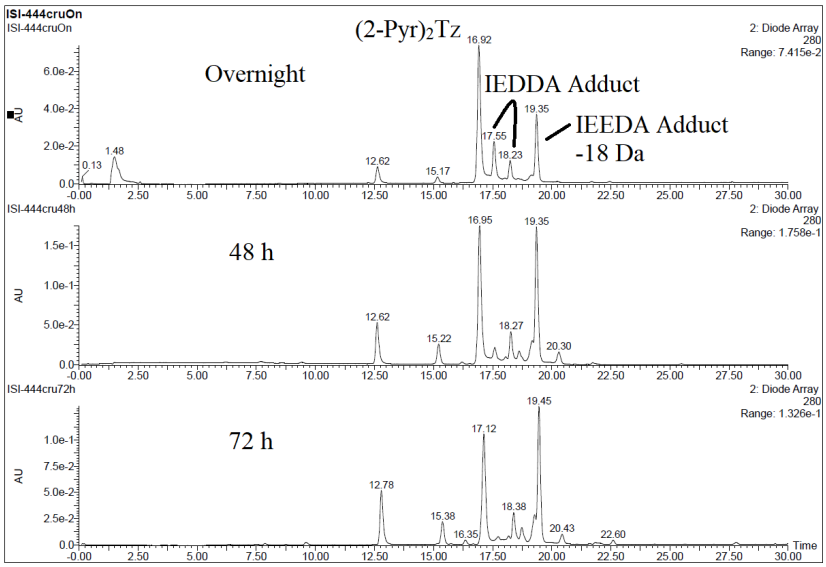

Figure 4.19 HPLC traces (280 nm) of the monitorization of the reaction between (2-Pyr)$_2$Tz (**4.14**) and peptide **4.108** at 24, 48 and 72 h.

Formation of this new produc has not been observed in any of the experiments carried out to prepared simple conjugates making use of an IEDA reaction. At this point, the reaction between oxanorbornene-PNA (**4.34**) and tetrazine (**4.14**) was repeated, and in contrast with preceding results formation of the adduct with a mass 18 units lower was observed (data not shown). Both reagents involved in this assay are the same previously used oxanorbornene-PNA and model bis-(2-pyridyl)tetrazine, which suggest that differences in reaction outcome might be due to differences in the reaction medium.

A plausible explanation to this phenomenon is depicted in **Scheme 4.44**. In short, an electronic reorganization driven by hydrogen caption promotes bridge opening to give an alcohol that may undergo dehydration, yielding a highly conjugated adduct. Formation of the -18 Da product from the mixture of isomers that result from the IEDDA reaction is associated with loss of a chiral center, which is consisten with a reduction in number of isomers (so far, only one – 18 Da compound has been detected in all cases).

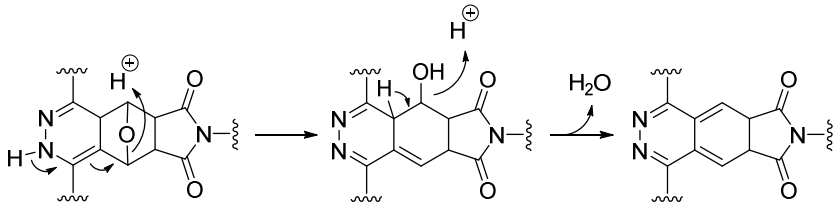

Scheme 4.44 Proposed plausible mechanism for the observed -18 Da mass loss in double conjugation experiments.

To recapitulate, these experiments have first corroborated that maleimides do not react with tetrazines. As to the possibility of preparing double conjugates from peptides incorporating a free maleimide and an oxanorbornene, we have verified that the DA and the IEDDA reactions cannot be performed simultaneously due to reaction of the diene group with the tetrazine (even at room temperature). Nonetheless this problem can be easily circumvented by carrying out a stepwise reaction procedure. By first reacting the maleimide group with the diene and, subsequently and after purification, treating the resulting adduct with a tetrazine the target double conjugate can be obtained.

4.5.3 Double conjugations on a scaffold containing an oxanorbornene and a thiol

In our third approach, we aimed to assess the possibility of combining the IEDDA reaction with a reaction involving a thiol, either with a maleimide or a with a cyclopentenedione (CPD). Hence, we first searched for a scaffold suitable to undergo these two reactions. In this case we selected a peptide inspired in oxytocin because it incorporates two cysteines, one of them being at the *N*-terminal position, which would be suitable for both the Michael-type and the CPD-Cys reactions (see chapter 2, **Section 2.2**).

Natural oxytocin is a disulfide-mediated cyclic peptide with sequence H-Cys-Tyr-Ile-Gln-Asn-Cys-Pro-Leu-Gly-NH_2 that is responsible for many biological functions including uterine contractions and modulation of hypothalamic-pituitary-adrenal axis activity. Oxytocin regulates a myriad of social behaviors and sexual arousals amongst others. Since reaction with the CPD required an *N*-terminal cysteine, we decided to introduce the oxanorbornene substituting the internal cysteine (6^{th} residue) by the previously utilized oxanorbornene-derivatized lysine (**Figure 4.20**).

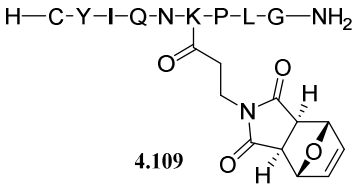

Figure 4.20 Chemical structure of the oxytocin analogue used for thiol and oxanorbornene-involving double conjugation experiments.

In addition to peptide **4.109**, to test this combination of conjugation reactions two additional peptides (**Figure 4.21**) containing both an oxanorbornene and an internal cysteine (prepared by Cristina Moya during her Master thesis) were employed. In this case, the oxanorbornene was attached to the *N*-terminus. The sequence of these two peptides is PMal[H_2]-Lys-Ser-Trp-Ala-Cys-Gly-NH_2 (PMal[H_2]-KSWACG-NH_2, **4.110**) and PMal[H_2]-Arg-Tyr-Thr-Ala-Cys-Gly-NH_2 (PMal[H_2]-RYTACG-NH_2, **4.111**)

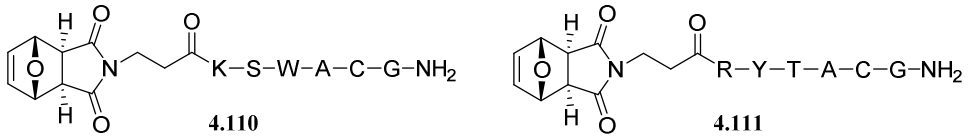

Figure 4.21 Peptides containing an oxanorbornene and an internal cysteine prepared by C. Moya.

4.5.3.1 Double conjugations involving CPD-Cys and IEDDA reactions

Firstly, we tested whether the CPD moiety could undergo an IEDDA reaction by reacting a tetrazine with CPD-COOH (**4.112**) as depicted in **Scheme 4.45**. More specifically, we reacted 2 equiv. of tetrazine **4.21** with CPD-COOH in an aqueous methanolic solution, and analyzed the outcome by HPLC. Even after prolonged reaction times, the mixture did not seem to evolve into any new product, only detecting by-products derived from slow decomposition of the tetrazine moiety.

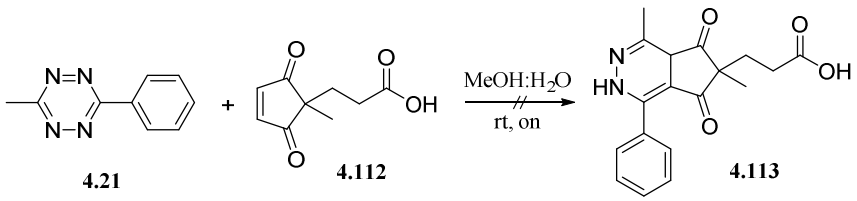

Scheme 4.45 Assay of IEDDA reaction between a tetrazines and a CPD.

The negative outcome of this experiment meant that the double conjugations we were envisioning could be performed simultaneously without the need of an intermediate purification step. As depicted in **Scheme 4.46**, we tested this hypothesis by reacting **4.109** with a small excess (2 equiv.) of CPD-COOH and (2-Pyr)$_2$Tz (**4.14**) at 37 ºC in a methanolic aqueous solution overnight.

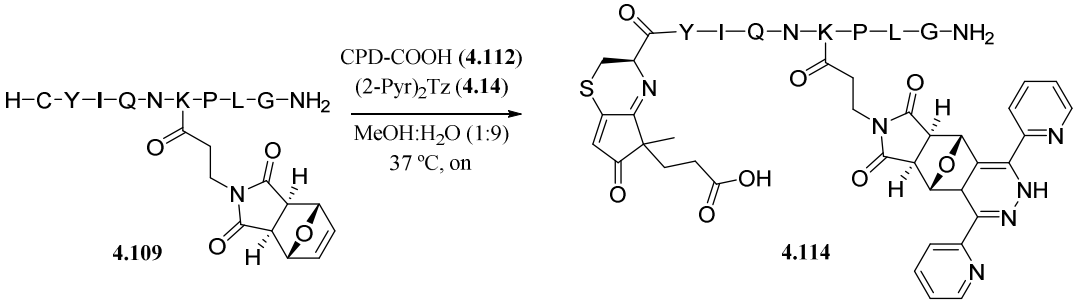

Scheme 4.46 Reaction conditions for the double derivation of peptide **4.109** by means of a CPD-Cys reaction and an IEDDA cycloaddition.

As can be observed analyzing the crude by HPLC (**Figure 4.22**), this double conjugation was feasible, but we again observed formation of the -18 Da adduct. The quality of the crude was quite good, suggesting that a small optimization effort could likely furnish the target conjugate in better yield. In this regard, sequential addition of the reagents, first the CPD and afterwards the 2-Pyr$_2$Tz could provide better results, since it has been shown to yield cleaner crudes in previous experiments.

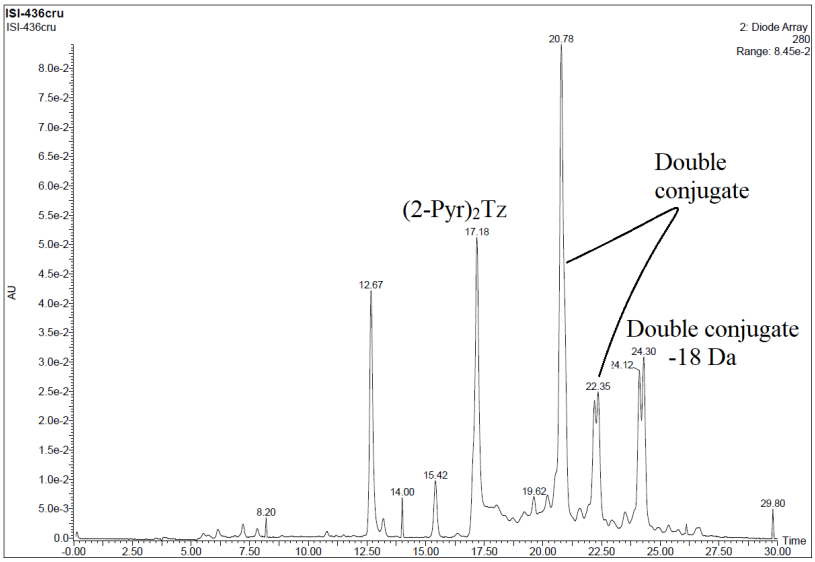

Figure 4.22 HPLC trace (280 nm) of the CPD-Cys and IEDDA reaction crude.

These results demonstrate that tetrazines do not react with cyclopentenediones (CPDs) even after long reaction times. Moreover, we have successfully produced double conjugates utilizing in conjunction both the CPD-Cys and IEDDA reactions.

4.5.3.2 Double conjugations involving thia-Michael and IEDDA reactions

In parallel, using the same peptide scaffold (**4.109**), we tested the double conjugation combination involving Michael-type and IEDDA reactions, carried out simultaneously. As can be seen in **Scheme 4.47**, in this case we employed 2 equiv. of both an *N*-terminal derivatized maleimido-PNA (**4.115**), and $(2\text{-Pyr})_2$Tz (**4.14**), and the mixture was reacted overnight in an aqueous methanolic solution.

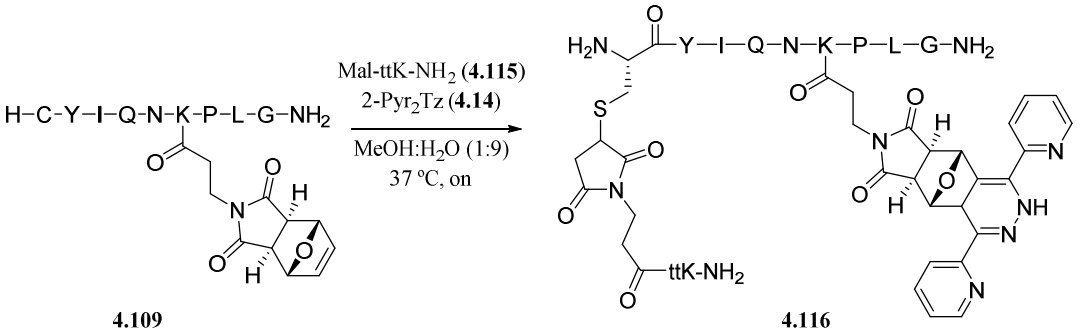

Scheme 4.47 Reaction between peptide **4.109**, a maleimido-derivatized PNA (**4.115**) and $(2\text{-Pyr})_2$Tz (**4.14**).

As can be observed from HPLC analysis (**Figure 4.23**), the double conjugation took place successfully, since the desired adducts were present in the crude. In this instance, we purified and reanalyzed the double conjugation adduct with 18 Da lower, verifying its stability after being collected and lyophilized (**Figure 4.23**, right).

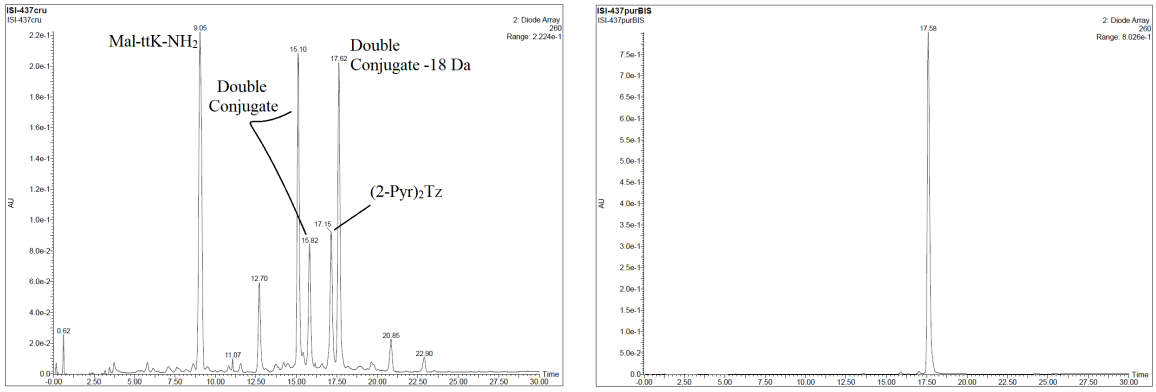

Figure 4.21 HPLC traces (260 nm) of crude (left) and pure (right) doubly derivatized peptide 18 Da lower.

These experiments corroborated the feasibility of combining a thiol and an oxanorbornene in the same scaffold (here, peptide) to obtain the corresponding double conjugate.

4.5.3.3 Double conjugations involving S_NAr and IEDDA reactions

4.5.3.3.1 Preliminary experiments and peptide derivatization

Several groups have reported that 3,6-dichloro-1,2,4,5-tetrazine (Cl_2Tz) can undergo two successive nucleophilic aromatic substitutions with a variety of nucleophiles, such as thiols, amines and alcohols, to form doubly substituted tetrazines. This chemistry has been exploited to form double sugar-peptide

conjugates,[38] for the reversibly disulfide stapling of peptide and protein motifs after reduction of a disulfide,[39] and labeling of proteins under mild conditions.[40]

On this basis, Cristina Moya, a master student in the group at that time, was tasked with the preparation of a thio-substituted chlorotetrazine incorporating a reporter group, with the idea of obtaining conjugates of cyclic peptides incorporating one cysteine residue and an oxanorbornenes (**Scheme 4.48**). The aim was to perform first a S_NAr Cys-chlorotetrazine reaction to attach the label, (which is described to take place extremely fast), and a successive IEDDA reaction with the oxanorbornene in order to cyclize and derivatize in one step.

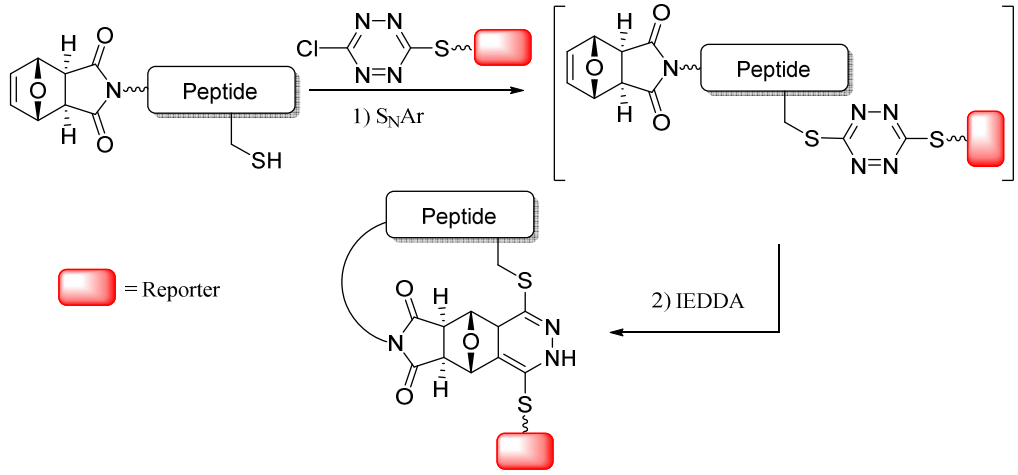

Scheme 4.48 Outline for the planned synthesis of labeled, cyclic peptides utilizing S_NAr and intramolecular IEDDA reaction.

To test this hypothesis, the first step was to synthesize a chlorotetrazine derivative containing a dansyl group. As depicted in **Scheme 4.49**, synthesis started with trityl protection of commercially available cysteamine hydrochloride (**4.117**). Reaction of cysteamine with trityl chloride in acidic conditions rendered the thiol-protected cysteamine analogue (**4.118**) in 40% yield. Subsequent reaction with dansyl chloride provided the *S*-trityl protected dansyl derivative (**4.109**) in 71% yield. Finally, trityl removal with an acidic treatment provided the free thiol (**4.120**) which was reacted with Cl_2Tz to provide the desired chlorotetrazine-dansyl derivative (dansyl-Tz-Cl, **4.121**) in 55% yield.

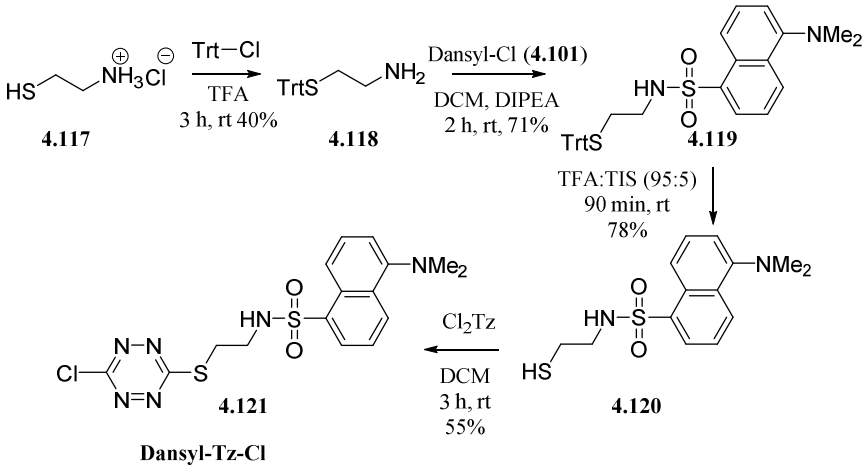

Scheme 4.49 Synthesis of a dansyl-derivatized chlorotetrazine analogue (**4.121**).

Once the desired chlorotetrazine analogue was obtained, first cyclization attempts were performed by reacting peptide PMal[H_2]-KSWACG-NH_2 (**4.110**) with little excess (1.2 equiv.) of dansyl-Tz-Cl (**4.121**, **Scheme 4.50**) and the reaction was monitored by HPLC-MS after 5 min, 2 h, 5 h and overnight.

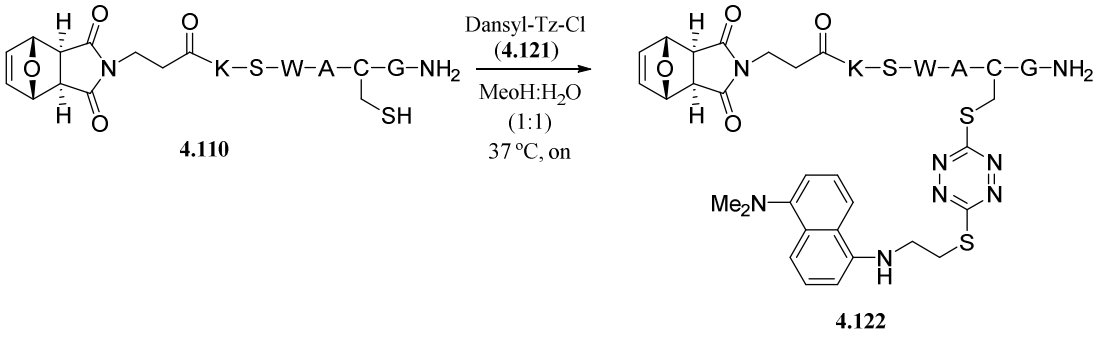

Scheme 4.50 Reaction of peptide PMal[H_2]-KSWACG-NH_2 (**4.110**) with dansyl-Tz-Cl (**4.121**)

It can be observed in the HPLC traces (**Figure 4.24**) that an extremely fast and clean S_NAr took place, as inferred by from MS analysis (*m/z* found 1257.6, calcd. 1257.4) and the product seemed not to evolve even after prolonged reaction times to the desired cyclic adduct (*m/z* 28 Da lower due to nitrogen loss at the IEDDA reaction).

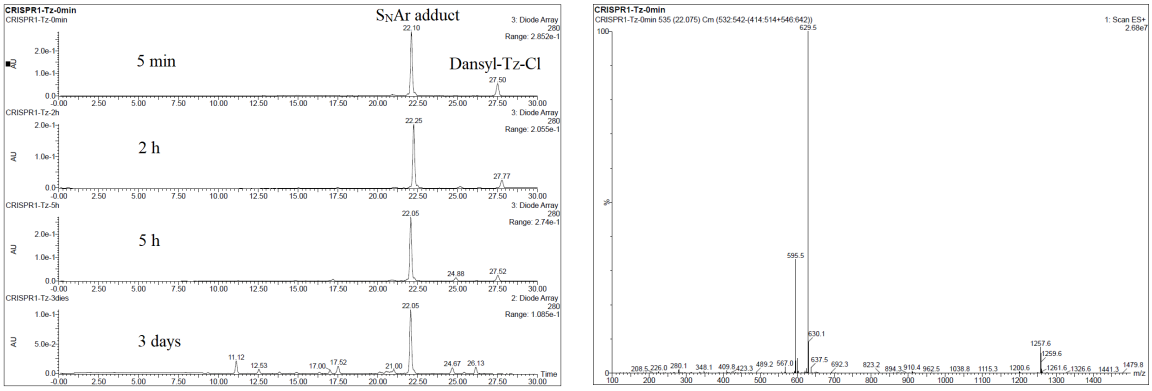

Figure 4.24 Reaction between peptide **4.110** and dansyl-Tz-Cl (**4.121**). HPLC traces (280 nm) of the reaction crude at 5 min, 2 h, 3h and 3 days (left), and ESI MS spectrum of the major product (right).

These results indicated that cyclization (that is, the IEDDA reaction) was not taking place, but they did not explain whether this fact was due to the specific peptide sequence structure (not prone to cyclization) or because the bis-thiosubstituted tetrazine did not undergo an IEDDA reaction with the oxanorbornene moiety. We knew from the literature that bis-thiosubstituted tetrazines do react with cyclooctynes,[40] but nothing was known about their reactivity with 7-oxanorbornenes.

For the first inquiry, we used two different peptides, **4.111**, and the oxytocin analogue **4.109** previously used. For peptide **4.111** similar results were found, obtaining the S_NAr adduct quantitatively after 5 min of reaction (**Figure 4.25**) and no further evolution to the cyclic adduct, even after prolonged times.

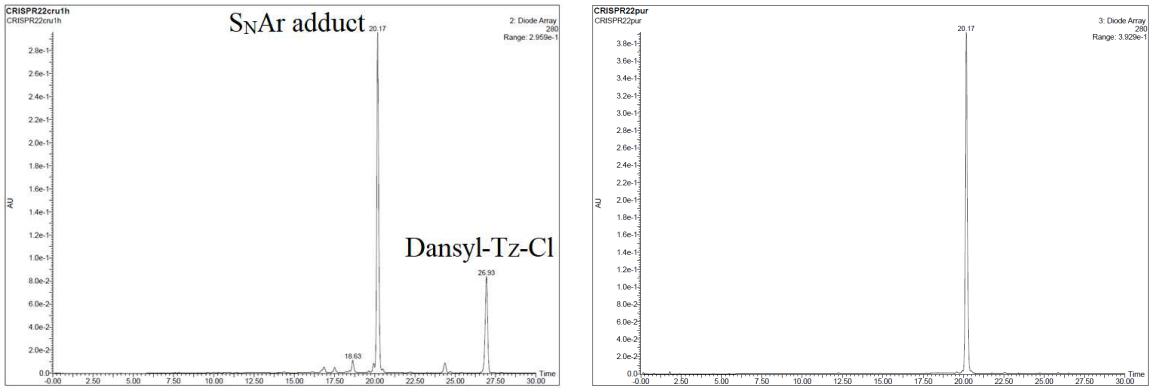

Figure 4.25 HPLC traces (280 nm) of the reaction crude (left) and pure adduct (right) obtained by reaction between peptide **4.111** and dansyl-Tz-Cl (**4.121**).

Then, we reacted peptide **4.109** in a similar fashion. However, in this instance, we obtained a more complex crude, in which there was a mixture of two compounds with a mass in accordance with that expected for a monosubstituted adduct, and a third whose mass fitted with that of a doubly substituted compound, in addition to an unidentified impurity (**Figure 4.26**)

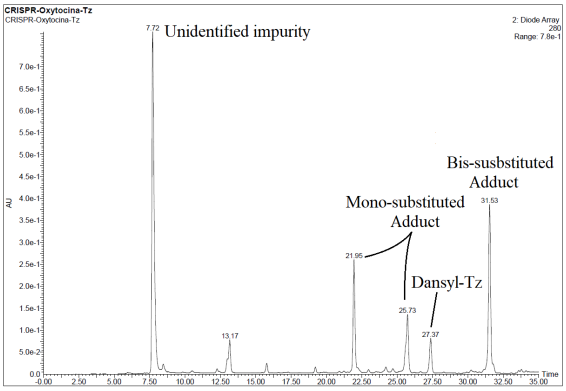

Figure 4.26 HPLC trace (280 nm) of the reaction crude (1 h) resulting from reaction of peptide (**4.109**) with dansyl-Tz-Cl (**4.121**).

The presence of two monosubstituted adducts can be rationalized as follows: First S_NAr would take place between the chlorotetrazine and the thiol (the *N*-terminal amine is less nucleophilic and thus, less prone to react), rendering one of the monoadducts (**4.124**, **Scheme 4.50**). This compound can undergo intramolecular reaction with the *N*-terminal amine, furnishing a new tetrazine (**4.126**). This *N,S*-disubstituted tetrazine is more stable, as described in the literature.[41] In the proposed mechanism a series of two reactions, of which the second is favored by the formation of 5-membered ring intermediate (**4.125**), ends up yielding the more stable "aza" adduct (**4.126**) as depicted in **Scheme 4.51**. The product resulting from these S_NAr reactions (**4.126**) exhibits a free thiol, which can again react with another thiol moiety, furnishing the product with two appending dansyl groups (**4.127**). Consequently, in order to ensure that only one product is obtained (in other words, that the chlorotetrazine reacts solely with the cysteine thiol and only one label is incorporated), when conjugation is to be carried out with peptides including *N*-terminal cystines it is advisable to keep the *N*-terminus protected or to block it (by acylation, for instance).

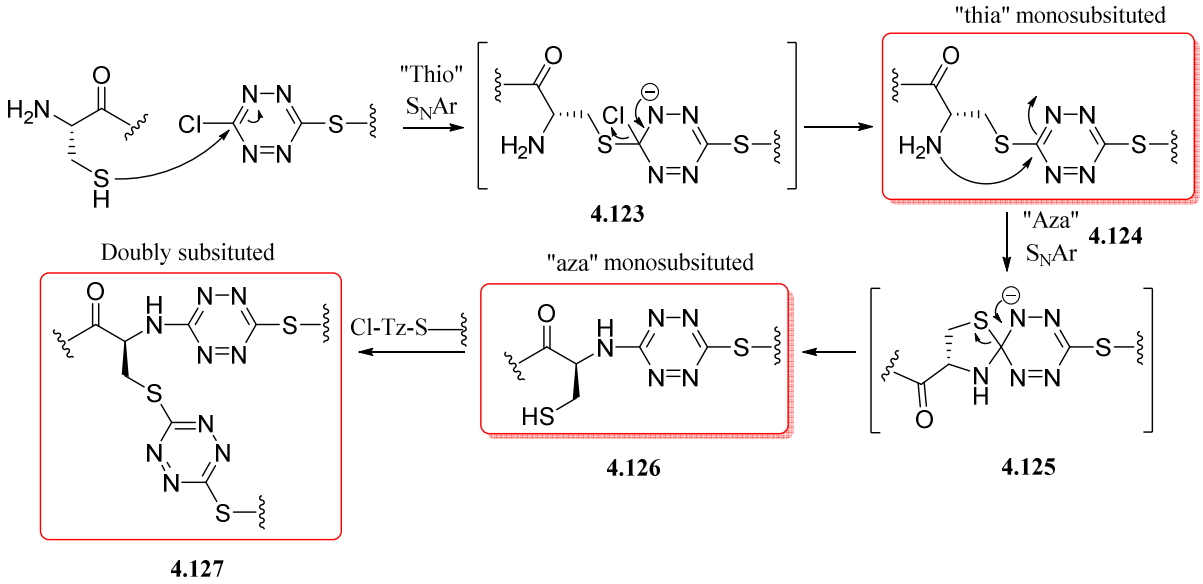

Scheme 4.51 Mechanism proposed for the formation of dithia- and thia,aza-tetrazine monoadducts of peptide **4.109**, and formation of doubly substituted adduct.

Aside from this latter case, which is particular because cysteine's amine was free, and observing the similar results obtained with the three peptides, we decided to further confirm that bis-thiolsubstituted tetrazines do not react with oxanorbornenes. To do so, we synthesized a bis-methyl thioglycolate tetrazine as depicted in **Scheme 4.52**.

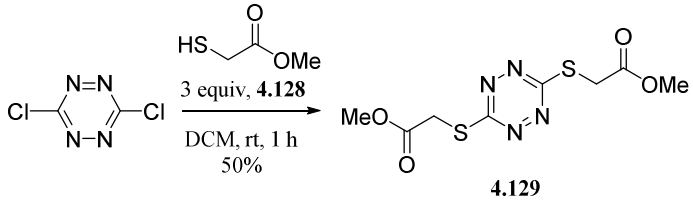

Scheme 4.52 Synthesis of a 1,2,4,5-tetrazine with two thiol groups.

Subsequently, we reacted this molecule (**4.129**) with PMal[H_2]-COOH under typical IEDDA conditions. HPLC-MS analysis of the crude revealed the presence of only starting material, even after prolonged reaction times, confirming that oxanorbornenes and di-thiosubstituted tetrazines do not react.

4.5.3.3.2 SNAr reactions with 5'-mercaptooligonucleotides

Before exploring the possibility of double conjugations, we resolved to take advantage of the exceptionally fast and clean SNAr reaction to produce monoconjugates of not only peptides but also oligonucleotides (which, to date, have not been described). For this purpose, we assembled two oligonucleotide chains, dT_{10} and another containing all nucleobases with sequence: $d^{5'}$CAGTCATGTT$^{3'}$. Subsequently, we reacted a commercially available trityl-protected thiol phosphoramidite with the 5' end, and after the oxidation step, removed all of the permanent protecting groups under standard conc. aq. NH_4OH conditions as depicted in **Scheme 4.53**.

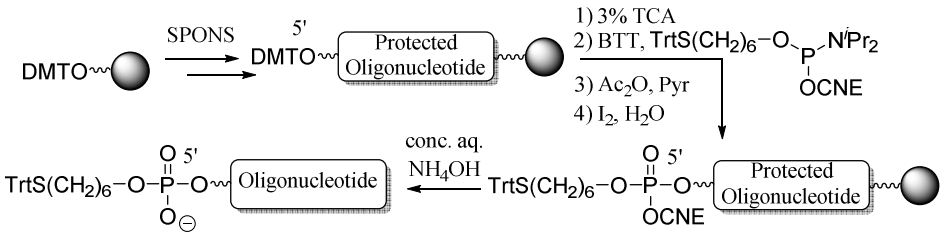

Oligonucleotide = dT_{10} (**4.130**)
$d^{5'}CAGTCATGTT^{3'}$ (**4.131**)

Scheme 4.53 Synthesis of 5' thiol-modified oligonucleotides.

As can be observed at the HPLC traces of both oligonucleotide crudes (**Figure 4.27**) and subsequent analysis by MALDI-TOF MS, incorporation of the thiol phosphoramidite was successful in both cases, obtaining clean conversions to the desired trityl-derivatized oligonucleotide (non-derivatized oligonucleotides elute before, data now shown).

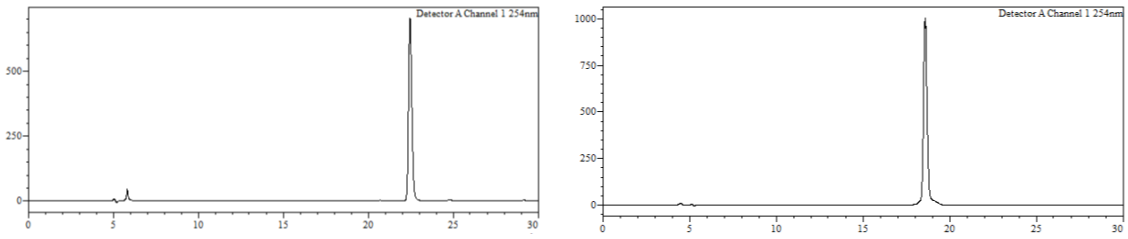

TrtS-dT_{10} (**4.130**) TrtS-$d^{5'}CAGTCATGTT^{3'}$ (**4.131**)

Figure 4.27 HPLC traces (254 nm) of crude S-trityl modified dT_{10} (**4.130**, left) and $d^{5'}CAGTCATGTT^{3'}$ (**4.131**, right) oligonucleotides.

Afterwards, we removed the trityl moiety by reaction with Ag^+ and a subsequent DTT ion complexation as previously described for cysteine-derivatized oligonucleotide (**Scheme 4.54**).[37]

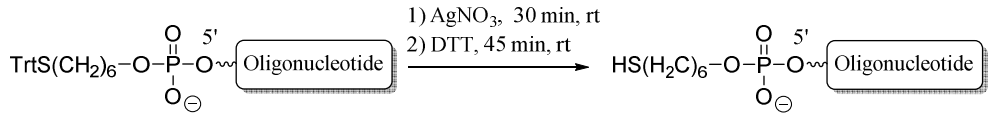

Oligonucleotide = dT_{10} (**4.130**) / $d^{5'}CAGTCATGTT^{3'}$ (**4.131**)

Oligonucleotide = dT_{10} (**4.132**) / $d^{5'}CAGTCATGTT^{3'}$ (**4.133**)

Scheme 4.54 $AgNO_3$ mediated trityl removal of a 5' thiol-derivatized oligonucleotide.

In this instance, HPLC analysis of both oligonucleotides (**Figure 4.28**) showed clean and complete conversions after the DTT complexation step. Nonetheless, we purified by HPLC both oligonucleotides since residual DTT traces could interfere by competing with the chlorotetrazine in the next synthetic step.

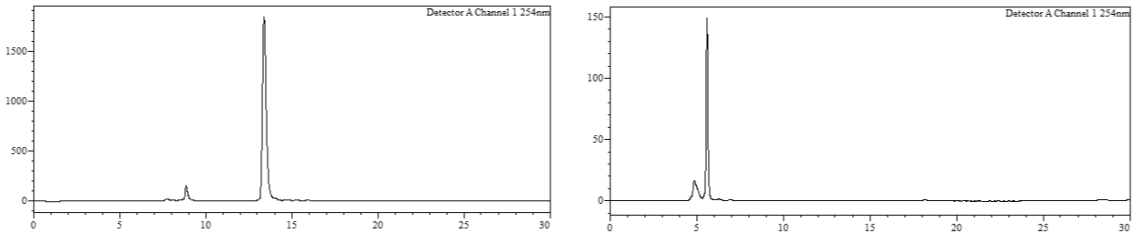

HS-dT$_{10}$ (**4.132**) HS-d$^{5'}$CAGTCATGTT$^{3'}$ (**4.133**)

Figure 4.28 HPLC traces (254 nm) of crude thiol-derivatized oligonucleotides (**4.132**, left) and (**4.133**, right).

Once we had obtained 5' free thiol oligonucleotides, we reacted each of them with dansyl-Tz-Cl (**4.121**) in a similar fashion as with the peptide counterparts (**Scheme 4.55**).

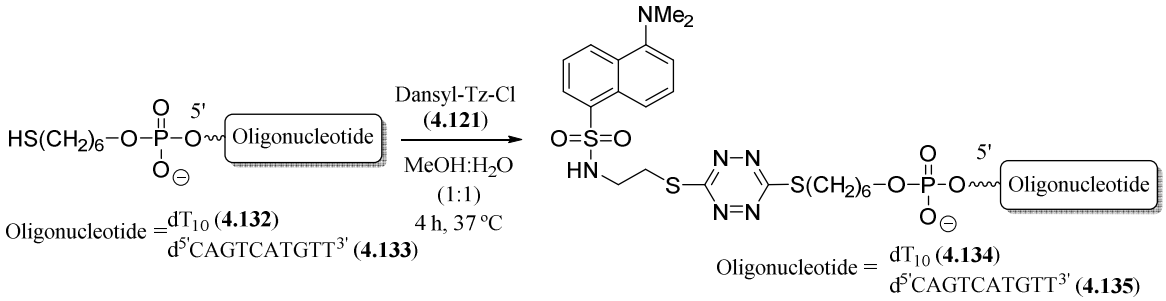

Scheme 4.55 Conjugation reactions involving 5' thiol-modified oligonucleotides and a dansyl-derivatized chlorotetrazine.

Utilizing 1.2 equiv. of dansyl-Tz-Cl (**4.121**) provided partial derivatization of oligonucleotide HS-dT$_{10}$ (**4.132**) even after prolonging the reaction time. Upon optimizing the reaction conditions, we found that addition of a total of 2.2 equiv. of dansyl-Tz-Cl (**4.121**) and 4 h at 37 ºC provided the target conjugate satisfactorily as depicted in **Figure 4.29**.

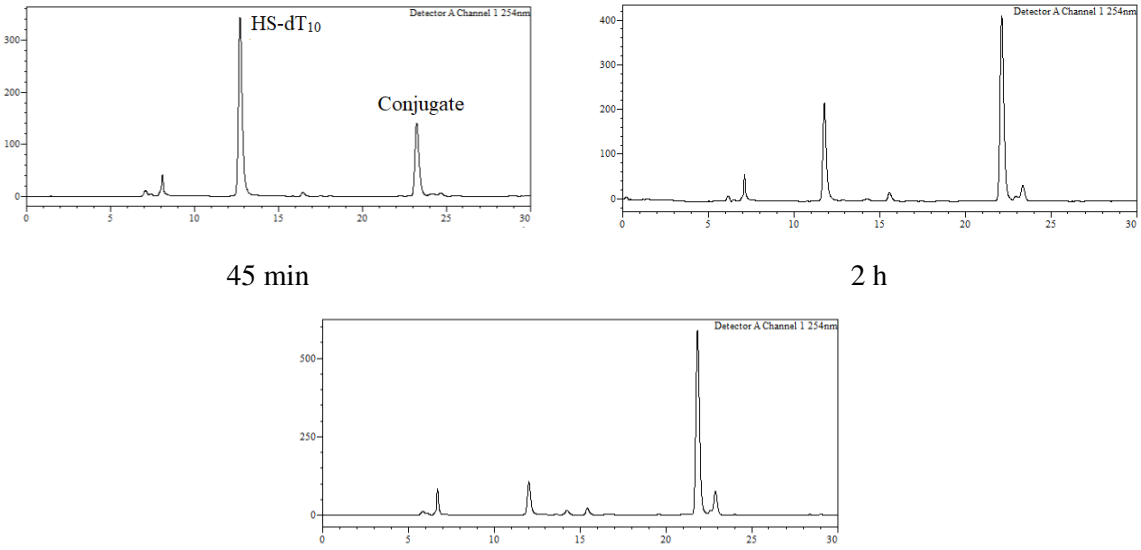

45 min 2 h

4 h

Figure 4.29 HPLC traces (254 nm) of the crude resulting from the reaction between HS-dT$_{10}$ oligonucleotide (**4.132**) and dansyl-Tz-Cl (**4.121**) after 45 min, 2 h and 4 h.

For oligonucleotide **4.133**, a similar approach was taken with similar results. Reaction with 2.2 equiv. of dansyl-Tz-Cl (**4.133**) for 4 h at 37 ºC provided the desired target conjugate (**4.135**) as a major product as seen by HPLC analysis (**Figure 4.30**). These results proved that this strategy satisfactorily provides oligonucleotide conjugates.

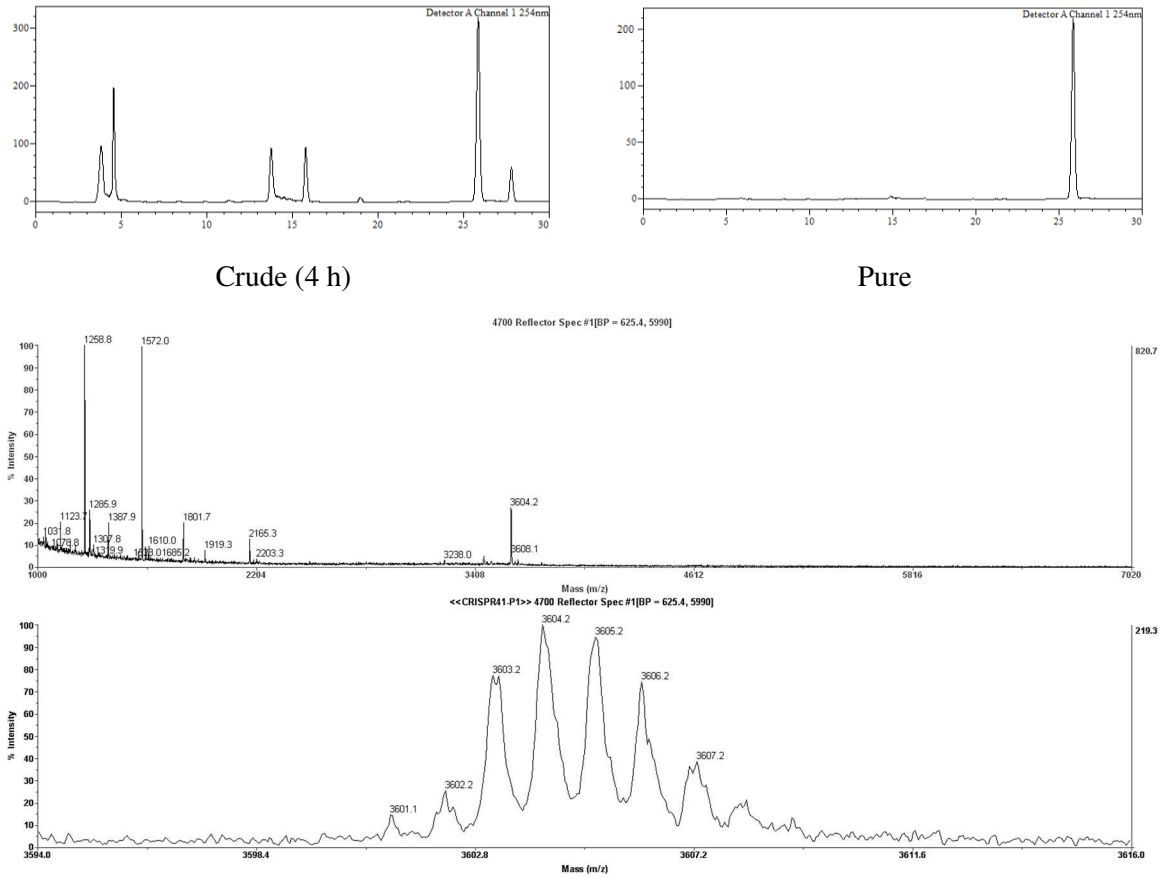

Figure 4.30 HPLC traces (254 nm) of crude and purified **4.135** (top) and MALDI-TOF MS spectrum of the isolated conjugate (bottom).

4.5.3.3.3 Double conjugations combining S_NAr and IEDDA reactions

Section 4.5.3.3.1 has been closed by concluding that 3,6-dithiotetrazines do not react with 7-oxanobornenes, in contrast with tetrazines differently substituted. On the basis of this finding, paired with the excellent kinetics of S_NAr found in peptides, we envisioned performing double conjugations by making use of chlorotetrazines for S_NAr reactions and the previously prepared aryl-substituted tetrazines bearing different reporter groups for IEDDA cycloadditions. The fact that the two reactions are mutually exclusive also prompted us to evaluate the possibility of running them simultaneously, as depicted in **Scheme 4.56**.

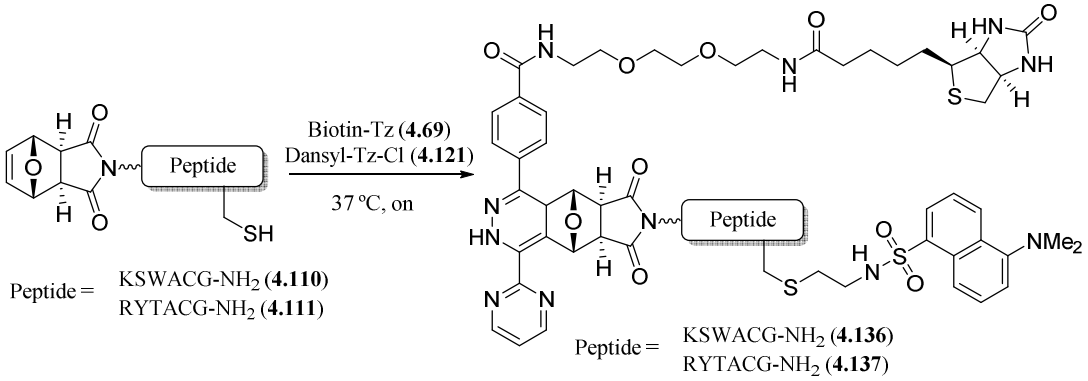

Scheme 4.56 Double conjugations involving S_NAr and IEDDA reactions with chlorotetrazines and aryl-substituted tetrazines, respectively, using peptides **4.110** and **4.111** as starting materials.

We put to test this hypothesis by reacting peptide PMal[H_2]-KSWACG-NH_2 (**4.110**) with a little excess (1.2 equiv.) of dansyl-Tz-Cl (**4.121**) and 2 equiv. of biotin-derivatized tetrazine (**4.69**) at 37 ºC overnight. As observed in the HPLC-MS analysis (**Figure 4.31**), the double conjugation experiment was successful. The double conjugate was formed, but there could be observed a major product whose mass was 18 Da lower, as in all the IEDDA-involving double conjugation attempts carried out.

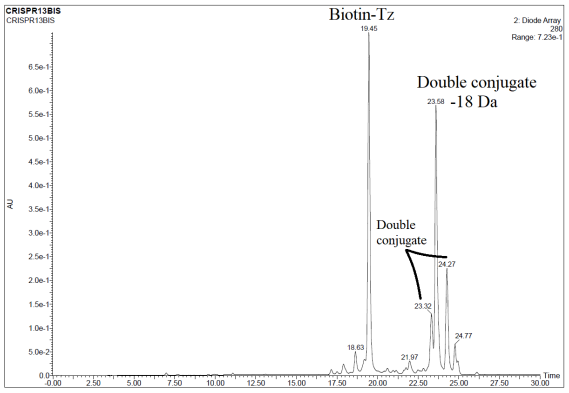

Figure 4.31 HPLC trace (280 nm) of the crude obtained by reaction between PMal[H_2]-KSWACG-NH_2 (**4.110**), biotin-containing tetrazine (**4.69**) and dansyl-derivatized chlorotetrazine (**4.121**).

Analogously, we performed the same double derivatization procedure with the other peptide (PMal[H_2]-RYTACG-NH_2, **4.111**) using the same reaction conditions. In this instance, as can be seen in the HPLC-MS trace (**Figure 4.32**), a similar crude was detected, where both double conjugation adducts in conjunction with another one with a mass 18 Da lower were present.

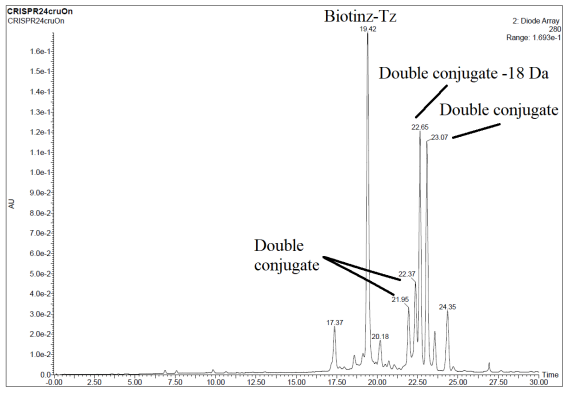

Figure 4.32 HPLC traces (280 nm) of the crude obtained by reaction between PMal[H_2]-RYTACG-NH_2 (**4.111**), biotin-containing tetrazine (**4.69**) and dansyl-derivatized chlorotetrazine (**4.121**).

These results corroborate that combining S_NAr and IEDDA reactions to synthesize double conjugates of peptides is indeed a good alternative. The sum of the areas of all peaks corresponding to double conjugates (including those with a mass lower than expected) gives a very favorable balance for this methodology.

As explained above, in principle it is easier to test new procedures with peptides than with oligonucleotides. Yet, we wanted to extend this chemistry to oligonucleotides. Oligonucleotides chains can be modified at either of the two ends or at an internal position. 3'-Modification requires access to a suitably-derivatized solid support, and internal modifications to the phosphoramidite of a modified nucleoside (this is likely the synthetically most complex alternative). A custom-made phosphoramidite is also required for 5' modification, but this is the most straightforward point to derivatize. One advantage is that after chain elongation it is possible to control the quality of the resin-linked oligonucleotide by retiring a small aliquot and analyzing the crude (HPLC) after deprotection with conc. aq. ammonia. Decision as to attach or not the additional moiety or functional group can be made at that point, with no need to waste a precious compound if the synthesis has not proceeded smoothly. Moreover, the same phosphoramidite can be attached to any oligonucleotide, regardless of sequence or backbone modification.

With these ideas in mind, we envisioned obtaining a cysteine phosphoramidite derivative, similar to that described in chapter 2 of this dissertation (see chapter 2, **Section 2.5.2**), containing an oxanorbornene in addition to the thiol. The starting material was commercially available Fmoc-Cys(Trt)-OH, whose carboxyl group was first derivatized by reaction with isobutyl chloroformate and *trans*-aminocyclohexanol to yield the desired amide and a free hydroxyl group (**2.40**, **Scheme 4.57**) in an excellent 95% yield. This compound was subsequently treated with piperidine to remove the Fmoc group and obtain the desired free amine (**4.138**) in a quantitative manner. Afterwards, addition of PMal[H_2]-COOH was accomplished also by mixed anhydride activation in a moderate 47% yield, and the target phosphoramidite (**4.140**) was obtained after phosphitylation of the hydroxylated precursor **4.139** by treatment with the usual chlorophosphine in 73% yield as depicted in **Scheme 4.57**.

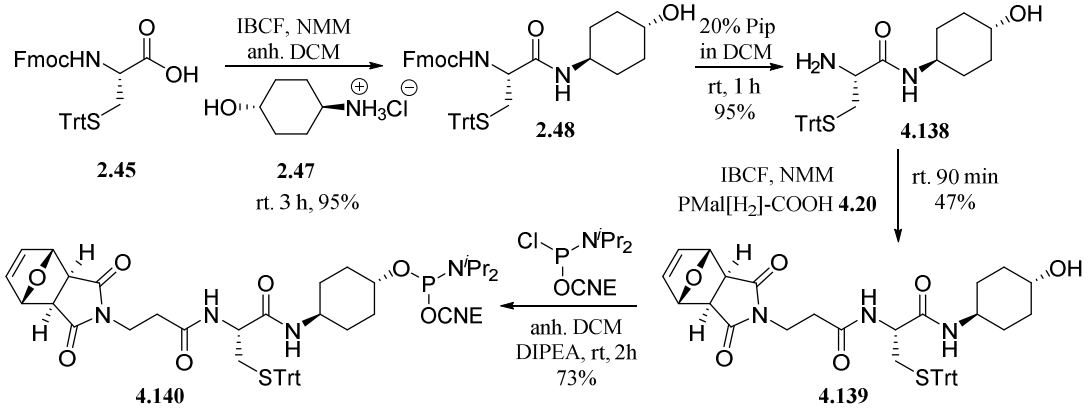

Scheme 4.57 Preparation of an oxanorbornene-containing cystine phosphoramidite derivative.

Making use of this cysteine amidite (**4.140**) we prepared an oligonucleotide containing the oxanorbornene and the protected thiol at the 5' position (**4.141**, **Figure 4.33**) by standard SPONS methodology.

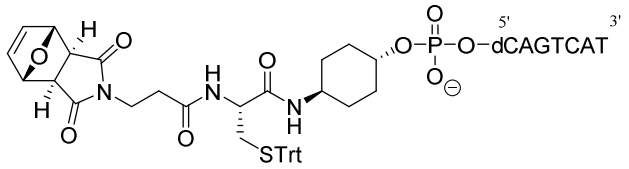

4.141

Figure 4.22 Chemical structure of PMal[H_2]-Cys(Trt)-derivatized oligonucleotide (**4.141**).

Afterwards, we removed the trityl from the thiol group through the usual Ag^+ and DTT treatment to cleanly provide the free thiol (**4.142**) in 70%, as depicted in **Scheme 4.58**.

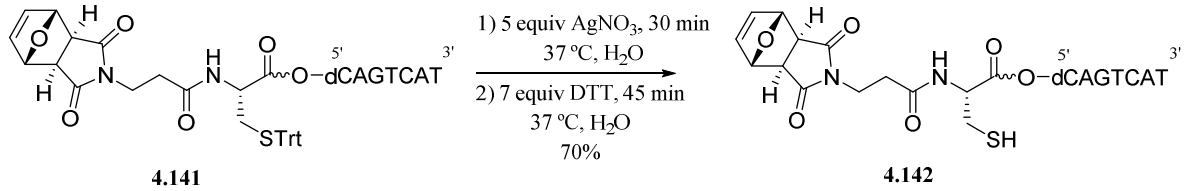

4.141 **4.142**

Scheme 4.58 Trityl removal of oxanorbornene-cysteine derivatized oligonucleotide (**4.142**).

Once we had the desired oligonucleotide appended with an oxanorbornene and a thiol, we proceeded with the double conjugations. In this instance, we utilized the previously synthesized tetrazine-containing peptide (Tz-LVPRGSYKGTSKLNYL-NH_2, **4.56**) and dansyl-derivatized chlorotetrazine (**4.121**, **Scheme 4.59**).

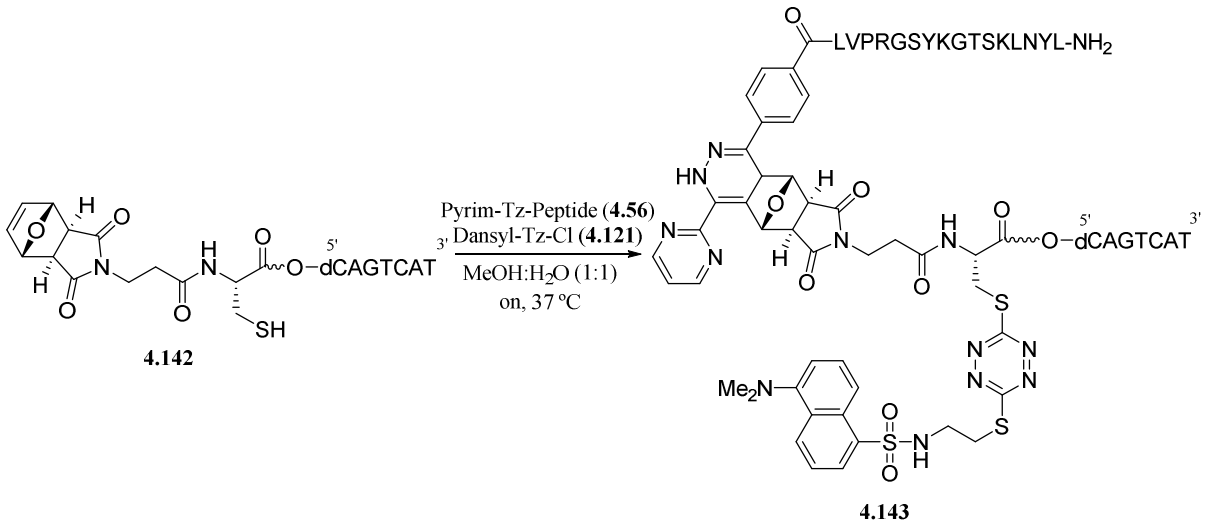

4.142 **4.143**

Scheme 4.59 Double derivatization of an oligonucleotide containing an oxanorbornene and a thiol by simultaneous reaction with a tetrazine and a chlorotetrazine.

4.5.3.3.4 Concluding remarks

In this part of work, we have exploited the classical S_NAr reaction by reacting chlorotetrazines with thiols and thiophosphates. Simple conjugates of peptides and oligonucleotides have been prepared using this reaction, within minutes or hours respectively. Moreover, the displayed non-reactive nature of oxanorbornenes towards dithiosubstituted tetrazines has enabled to produce double conjugates combining the IEDDA and S_NAr reactions both from peptide and oligonucleotide scaffolds.

This alternative seems to be the one of the most promising among those studied in this work. In the case of peptides, it only requires preparation of the carboxyl-derivatized oxanorbornene, since the thiol is a part of a natural residue that can be incorporated into the peptide sequence if required. In the case of oligonucleotides, the oxanorbornene-containing phosphoramidite is one of the necessary compounds if simple monoconjugates are synthesized using the IEDDA cycloaddition. In case S_NAr is the conjugation reaction, commercially available materials, not particularly expensive can be used to prepared thiol-derivatized oligonucleotides suitable for reaction with a chlorotetrazine in order to produce monoconjugates. Finally, double conjugations on oligonucleotides can be carried out making use of the phosphitylated oxanorbornene, *S*-Trt cysteine derivative **4.143**, by combining S_NAr and IEDDA reactions.

4.5.4 Double conjugations on a scaffold containing an oxanorbornene and a diene

It is not possible to obtain diene-derivatized peptides without postsynthetic modifications, because 1,3-dienes do not withstand the acidic conditions (90-95% TFA and scavengers) that remove permanent protecting groups after on-resin assembly using standard methodology (that is, with the Fmoc/^{t}Bu chemical strategy).

For oligonucleotide double conjugate formation combining the IEDDA and DA cycloadditions, we contemplated two possibilities. First of all, synthesizing a suitably-derivatized CPG support, which would enable to append an oxanorbornene (or a diene) to the 3' end, and a diene-phosphoramidite (or the oxanorbornene amidite described above). This would allow oligonucleotide double conjugates to be obtained. The second strategy was the synthesis of the phosphoramidite derivative of an amino acid (see previous section) containing both groups for the modification of the 5'-position of an oligonucleotide.

In this context, Laia Saltor, during her Master's thesis, was tasked to produce a suitable oxanorbornene-derivative to be appended to a LCAA CPG to give access to 3' oxanorbornene-modified oligonucleotides. As depicted in **Scheme 4.60**, the synthesis started by reacting PMal[H_2]-COOH (**4.20**) with serinol *via* carbodiimide-mediated activation in the presence of pentafluorophenol. The oxanorbornene-containing, bis-hydroxylated derivative (**4.144**) was successfully isolated in 70% yield. Subsequently, protection of a single hydroxyl functionality was achieved by reaction with DMT-Cl in anh. pyr, and **4.145** isolated in a modest 20% yield. Finally, ester formation from the mono-protected derivative was performed by opening the succinic anhydride ring under *N,N*-dimethylaminopyridine (DMAP) catalysis, rendered the target compound (**4.146**) in 32% yield.

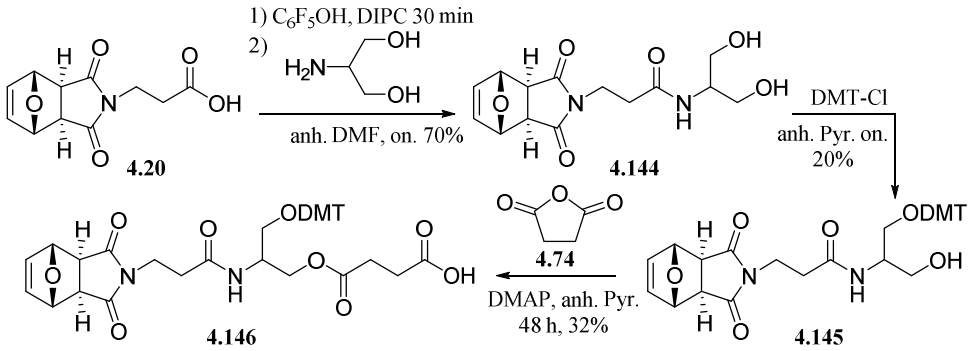

Scheme 4.60 Synthesis of an oxanorbornene-containing derivative suitable for attachment to CPG beads.

Once we had obtained the desired DMT-protected, oxanorbornene-containing hemuisuccinate we made use of standard carbodiimide chemistry to couple it to commercially available long chain aminoalkyl (LCAA) CPG beads as depicted in **Scheme 4.61**.

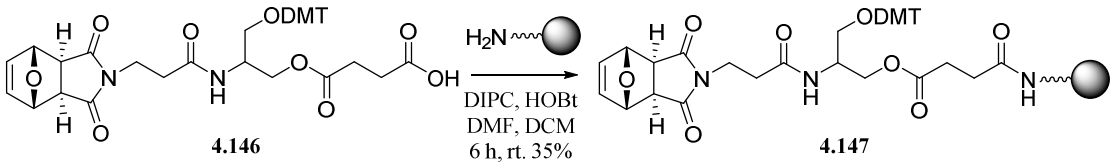

Scheme 4.61 Carbodiimide-mediated coupling of the oxanorbornene-containing serinol derivative **4.147** to CPG for oligonucleotide synthesis.

Since our plans were to perform double conjugations both at the 5' and 3' positions of an oligonucleotide, we opted for the use of a previously described diene phosphoramidite to modify the 5' end. As depicted in **Scheme 4.62**, starting from previously employed ethyl (*E*)-hepta-4,6-dienoate (**3.47**, see chapter 2)[42] we performed a reduction of the ester group with by $LiAlH_4$ that afforded the target alcohol (**4.148**) in a 80% recovery. Afterwards, usual phosphitylation with chloro(2-cyanoethhoxy)diisoproylaminophosphine in the presence of a base provided the desired phosphoramidite (**4.149**) in 45% yield.

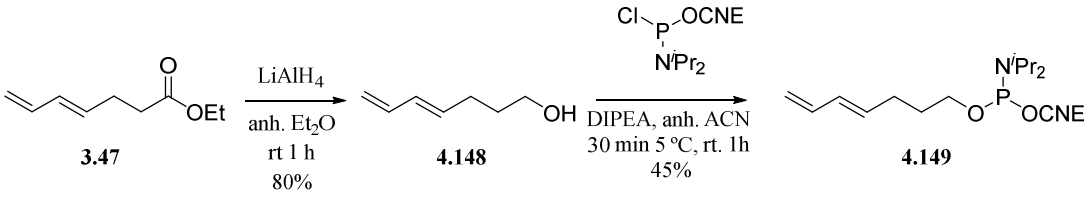

Scheme 4.36 Scheme for the synthesis of a diene-containing phosphoramidite derivative.

Having all the desired reagents and the oxanorbornene-derivatized resin, we elongated a 2'-deoxy-nonathymidine oligonucleotide on resin **4.150** and derivatized the 5' position with the diene phosphoramidite (**4.149**) using BTT as activator. The doubly derivatized target ON (**4.152**) was obtained after cleavage and deprotection with conc. aq. NH_4OH (**Scheme 4.63**).

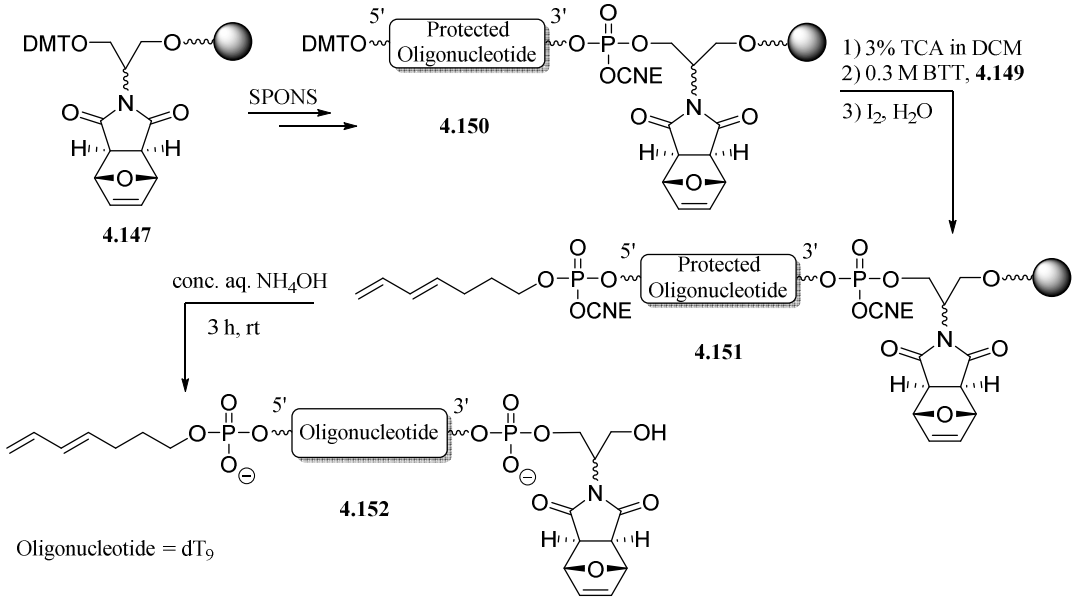

Scheme 4.63 Preparation of 5' diene- and 3' oxanorbornene-modified oligonucleotide dT_9.

Following this synthetic plan, we successfully prepared a dT_9 with a diene at the 5' position and the oxanorbornene moiety at the 3' position (seen the HPLC trace of the analogue (**Figure 4.34**).

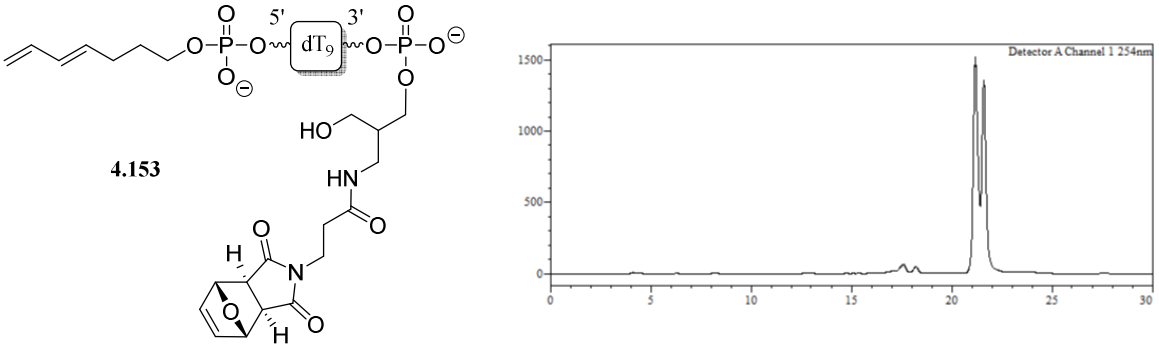

Figure 4.34 Chemical structure (left) and HPLC trace (254 nm, right) of pure, doubly-derivatized oligonucleotide **4.153**.

Subsequently, the doubly-derivatized oligonucleotide was subjected to the usual simultaneous conjugation procedures utilizing proof-of-concept compounds: *N*-(2-hydroxyethyl)maleimide and (2-Pyr)$_2$Tz (**4.14**, 2-fold molar excess of each one) at room temperature overnight in methanol/water solution (**Scheme 4.64**).

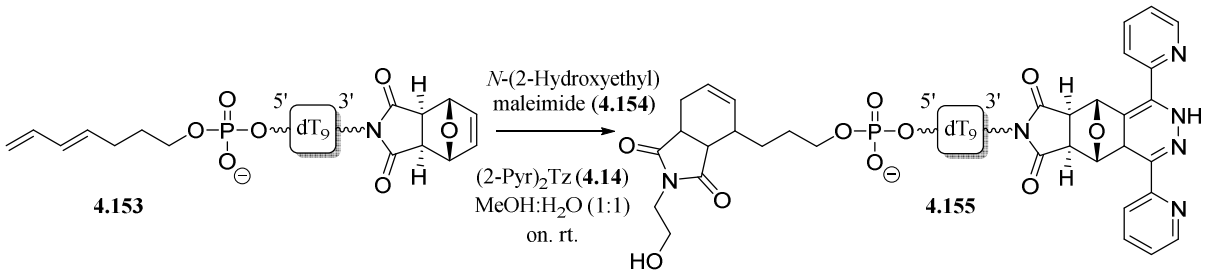

Scheme 4.64 Double conjugation of a diene and oxanorbornene-containing oligonucleotide by reaction with a maleimide and a tetrazine.

As can be observed by HPLC analysis (**Figure 4.35**), a complex mixture was obtained. One impurity plausibly accompanying the target product could derive from reaction of diene-moiety with tetrazines, as reported previously. Hence, this fact prompted us to utilize a consecutive approach instead of the one (simultaneous reactions), used in this trial.

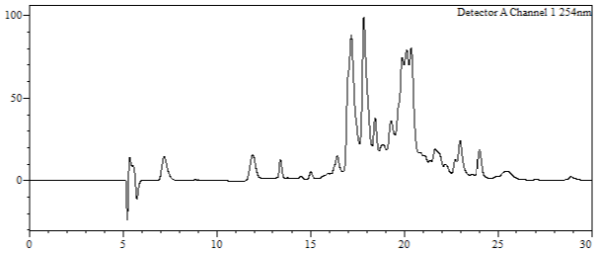

Figure 4.35 HPLC trace (254 nm) of the crude resulting from the simultaneous reaction between **4.153**, **4.154** and (2-Pyr)$_2$Tz (**4.14**).

In the second assay, we utilized the same doubly derivatized oligonucleotide (**4.153**), a peptide containing an *N*-terminal maleimide (Mal-LVPRGSYKGTSKLNYL-NH_2, **4.156**) and the one-pot procedure as shown in **Scheme 4.65**. We first performed the DA reaction in an aqueous media, since water is known to accelerate the DA reaction kinetics, at 37 ºC for 5 h and, subsequently but without

any intermediate purification step, we added Pyrim-Tz-Biotin (**4.69**) and left the mixture react for an additional 12 h.

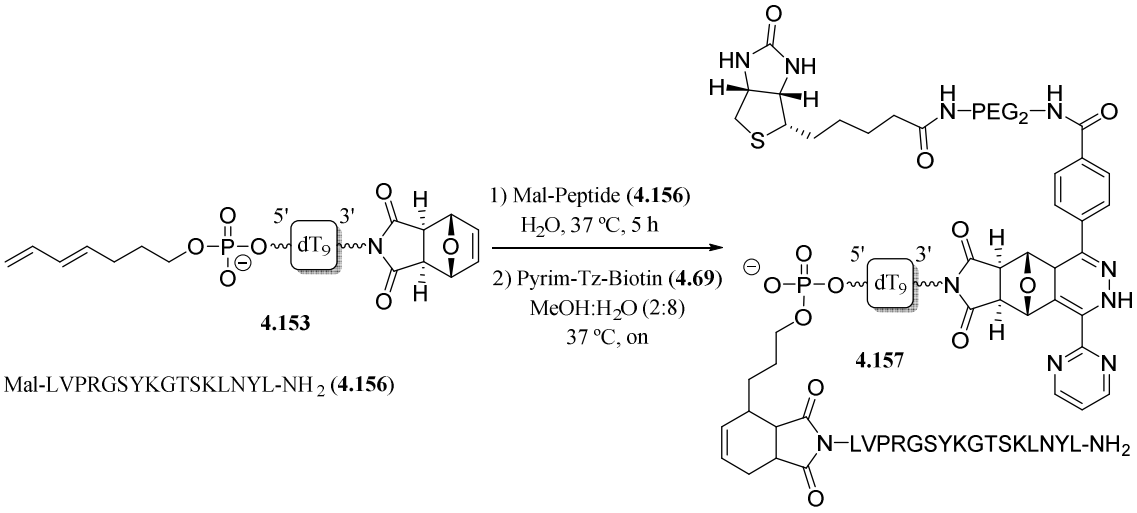

Scheme 4.65 Preparation of double conjugate **4.157** from a DA reaction between oligonucleotide (**4.153**) and a maleimido-derivatized peptide **4.156**, and subsequent reaction with the biotin-bearing tetrazine (**4.69**).

As can be seen in **Figure 4.36**, HPLC traces show complete conversion to the DA adduct (characterized to be the target compound by MALDI-TOF MS, *m/z* found 5159.3, mass calcd. 5179.6), at the 5 h mark. Subsequently, double conjugation was confirmed by HPLC analysis of the crude after the overnight IEDDA reaction, isolation and MALDI-TOF MS analysis of the purified compound.

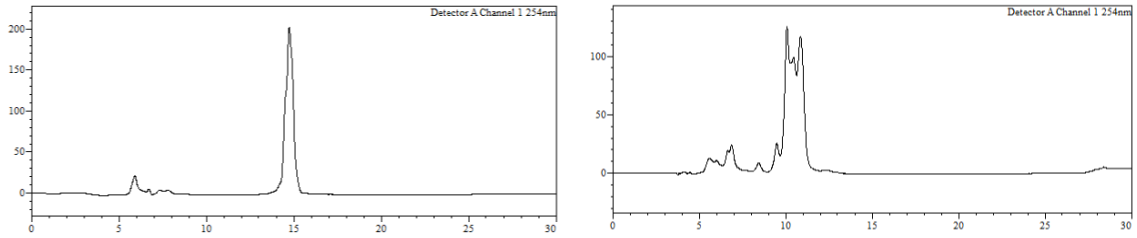

First conjugation crude (5 h)

Crude after the second conjugation (overnight)

Figure 4.36 HPLC traces (254 nm) of crude obtained after Diels-Alder reaction between **4.153** and peptide **4.156** (left), and of the double conjugation crude obtained after addition of tetrazine **4.69** and overnight reaction (right). The 18 Da lower adduct is also detected.

This strategy seems overall positive. That being said, several points need to be taken into account. The diene is strictly tied to on-resin derivatization of oligonucleotides and not peptides due to lack of stability in the acidic cleavage and deprotection conditions that typically follow SPPS. Additionally, the order of both reactions has to be strictly controlled, since performing the double conjugation in parallel seems troublesome, likely because of undesired reaction between the tetrazine and the diene.

Nonetheless, aside from these setbacks, the conjugation strategy seems fruitful and desired double conjugates can be cleanly obtained using this method.

4.6 Acronyms

2-Pyr$_2$Tz	3,6-Di(pyridin-2-yl)-1,2,4,5-tetrazine
Ac	Acetyl
Ac$_2$O	Acetic anhydride
ACN	Acetonitrile
AcOH	Acetic acid
anh	Anhydrous
aq	Aqueous
Bn	Benzyl
Bn$_2$O$_2$	Benzoyl peroxide
BnBr	Benzyl bromide
Boc	*tert*-Butyloxycarbonyl
Boc$_2$O	Di-*tert*-butyl dicarbonate
BODIPY	4,4-Difluoro-4-bora-3a,4a-diaza-*s*-indacene
BTT	5-(Benzylthio)-1*H*-tetrazole
Bz	Benzoyl
Cl$_2$Tz	3,6-Dichloro-1,2,4,5tetrazine
CNE	2-Cyanoethyl
CoA	Coenzyme A
conc	Concentrated
CPD-COOH	3-(1-Methyl-2,5-dioxocyclopent-3-en-1-yl)propanoic acid
CPG	Controlled pore glass
CuAAC	Copper(I)-catalyzed azide-alkyne cycloaddition
Da	Atomic mass unit (Dalton)
Dansyl-Diene	(*E*)-*N*-(2-((5-(Dimethylamino)naphthalene)-1-sulfonamido)ethyl)hepta-4,6-dienamide
Dansyl-Tz-Cl	*N*-(2-((6-Chloro-1,2,4,5-tetrazin-3-yl)thio)ethyl)-5-(dimethylamino)naphthalene-1-sulfonamide
DCC	*N,N*'-Dicyclohexylcarbodiimide
DCE	1,2-Dichloroethane
DCM	Dichloromethane
DDQ	2,3-Dichloro-5,6-dicyano-1,4-benzoquinone
Diene-COOH	(*E*)-hepta-4,6-dienoic acid
DIPC	*N,N*'-Diisopropylcarbodiimide
DIPEA	*N,N*-Diisopropylethylamine
DMAP	4-Dimethylaminopyridine
DMF	*N,N*-Dimethylformamide
DMSO	Dimethyl sulfoxide
DMT	4,4'-Dimethoxytrityl
DNA	Deoxtribonucleic acid
DTT	Dithiothreitol
EDC·HCl	*N*-(3-Dimethylaminopropyl)-*N*′-ethylcarbodiimide hydrochloride
EDG	Electron donating groups
equiv	Equivalents

ESI	Electrospray ionization
Et_2O	Diethyl ether
EtOH	Ethanol
EWG	Electron withdrawing group
FAD	Flavin adenine dinucleotide
Fmoc	Fluorenylmethyloxycarbonyl
GalNAc	*N*-Acetylgalactosamine
HATU	1-[Bis(dimethylamino)methylene]-1*H*-1,2,3-triazolo[4,5-*b*]pyridinium 3-oxide hexafluorophosphate
H-Cys-OMe	Methyl L-cysteinate
HOBt	Hydroxybenzotriazole
HPLC	High performance liquid chromatography
HRMS	High resolution mass spectometry
IBCF	Isobutyl chloroformate
IEDDA	Inverse electron-demand Diels-Alder
^{i}Pr	Isopropyl
LCAA	Long chain aminoalkyl
LHRH	Luteinizing hormone-releasing hormone
m/z	Mass to charge ratio
MALDI	Matrix-assisted laser desorption and ionization
mCP	Methyl-cyclopropene
***m*CPBA**	*meta*-Chloroperoxybenzoic acid
Me	Methyl
MeOH	Methanol
MS	Mass spectrometry
MW	Microwave
NADH	Nicotinamide adenine dinucleotide
NB	Norbornene
NEt_3	Triethylamine
NHS	*N*-Hydroxysuccinimide
NMM	*N*-methylmorpholine
on	Overnight
ON	Oligonucleotide
Pbf	2,2,4,6,7-Pentamethyldihydrobenzofuran-5-sulfonyl
PCl_5	Phosphorus pentachloride
Pd/C	Palladium on carbon
PEG	Polyethyleneglycol
Ph	Phenyl
PhMe	Toluene
PIDA	(Diacetoxyiodo)benzene
Pip	Piperidine
PMal[H_2]	*exo*-3,6-Epoxy-1,2,3,6-tetrahydrophthalimide
PMal[Me_2]	*exo*-3,6-Dimethyl-3,6-epoxy-1,2,3,6-tetrahydrophthalimide
PNA	Peptide nucleic acid
Pyr	Pyridine

Pyrim-Tz-COOH	4-(6-(Pyrimidin-2-yl)-1,2,4,5-tetrazin-3-yl)benzoic acid
rDA	retro-Diels Alder reaction
rt	Room temperature
S_NAr	Nucleophilic aromatic substitution
$SOCl_2$	Thionyl chloride
SPAAC	Strain-promoted azide-alkyne cycloaddition
SPONS	Solid-phase oligonucleotide synthesis
SPPS	Solid-phase peptide synthesis
TBAB	tetra-*n*-Butylammonium bromide
^{t}Bu	tert-Butyl
TCA	Trichloroacetic acid
TCO	*trans*-Cyclooctene
Tf	Triflate
TFA	Trifuoroacetic acid
THF	Tetrahydrofuran
TIS	Triisopropylsilane
TMS	Trimethylsilyl
TMSOTf	Trimethylsilyl trifluoromethanesulfonate
TOF	Time of flight
t_R	Retention time
Trt	Trityl
Tz	1,2,4,5-Tetrazine
UV	Ultraviolet

4.7 Bibliography

(1) Blackman, M. L.; Royzen, M.; Fox, J. M. *J. Am. Chem. Soc.* **2008**, *130*, 13518–13519.

(2) Devaraj, N. K.; Weissleder, R.; Hilderbrand, S. A. *Bioconjug. Chem.* **2008**, *19* (12), 2297–2299.

(3) Staderini, M.; Gambardella, A.; Lilienkampf, A.; Bradley, M. *Org. Lett.* **2018**, *20* (17 mM), 3170–3173.

(4) Eising, S.; Lelivelt, F.; Bonger, K. M. *Angew. Chemie - Int. Ed.* **2016**, *55* (40), 12243–12247.

(5) Engelsma, S. B.; Willems, L. I.; Van Paaschen, C. E.; Van Kasteren, S. I.; Van Der Marel, G. A.; Overkleeft, H. S.; Filippov, D. V. *Org. Lett.* **2014**, *16* (10), 2744–2747.

(6) Sánchez, A.; Pedroso, E.; Grandas, A. *Org. Lett.* **2011**, *13* (16), 4364–4367.

(7) Lu, Z.; Weber, R.; Twieg, R. J. *Tetrahedron Lett.* **2006**, *47* (40), 7213–7217.

(8) Elduque, X.; Pedroso, E.; Grandas, A. *Org. Lett.* **2013**, *15* (8), 2038–2041.

(9) Elduque, X.; Sánchez, A.; Sharma, K.; Pedroso, E.; Grandas, A. *Bioconjug. Chem.* **2013**, *24* (5), 832–839.

(10) Elduque, X.; Pedroso, E.; Grandas, A. *J. Org. Chem.* **2014**, *79* (7), 2843–2853.

(11) Discekici, E. H.; St. Amant, A. H.; Nguyen, S. N.; Lee, I.-H.; Hawker, C. J.; Read de Alaniz, J.

J. Am. Chem. Soc. **2018**, *140* (15), 5009–5013.

(12) Audebert, P.; Sadki, S.; Miomandre, F.; Clavier, G.; Vernieres, M. C.; Saoud, M.; Hapiot, P. *New J. Chem.* **2004**, *28* (3), 387–392.

(13) Li, C.; Ge, H.; Yin, B.; She, M.; Liu, P.; Li, X.; Li, J. *RSC Adv.* **2015**, *5* (16), 12277–12286.

(14) Alge, D. L.; Donohue, D. F.; Anseth, K. S. *Tetrahedron Lett.* **2013**, *54* (41), 5639–5641.

(15) Wang, D.; Chen, W.; Zheng, Y.; Dai, C.; Wang, L.; Wang, B. *Heterocycl. Commun.* **2013**, *19* (3), 171–177.

(16) Skwarczynski, M.; Noguchi, M.; Hirota, S.; Sohma, Y.; Kimura, T.; Hayashi, Y.; Kiso, Y. *Bioorganic Med. Chem. Lett.* **2006**, *16* (17), 4492–4496.

(17) Sauer, J.; Pabst, G. R.; Holland, U.; Kim, H. S.; Loebbecke, S. *European J. Org. Chem.* **2001**, No. 4, 697–706.

(18) Pican, S.; Lapinte, V.; Pilard, J. F.; Pasquinet, E.; Beller, L.; Fontaine, L.; Poullain, D. *Synlett* **2009**, *6* (5), 0731–0734.

(19) Selvaraj, R.; Fox, J. M. *Tetrahedron Lett.* **2014**, No. 34, 4795–4797.

(20) Selvaraj, R.; Fox, J. M. *Tetrahedron Lett.* **2014**, *55* (34), 4795–4797.

(21) Polezhaev, A. V.; Maciulis, N. A.; Chen, C. H.; Pink, M.; Lord, R. L.; Caulton, K. G. *Chem. - A Eur. J.* **2016**, *22* (39), 13985–13998.

(22) Beckmann, H. S. G.; Niederwieser, A.; Wiessler, M.; Wittmann, V. *Chem. - A Eur. J.* **2012**, *18* (21), 6548–6554.

(23) Chen, W.; Wang, D.; Dai, C.; Hamelberg, D.; Wang, B. *Chem. Commun.* **2012**, *48* (12), 1736–1738.

(24) Silva, T. D.; Arantes, V. T.; Resende, J. A. L. C.; Speziali, N. L.; De Oliveira, R. B.; Vianna-Soares, C. D. *Drug Dev. Ind. Pharm.* **2010**, *36* (11), 1348–1355.

(25) Yang, J.; Karver, M. R.; Li, W.; Sahu, S.; Devaraj, N. K. *Angew. Chemie* **2012**, *124* (21), 5312–5315.

(26) Khorev, O.; Stokmaier, D.; Schwardt, O.; Cutting, B.; Ernst, B. *Bioorganic Med. Chem.* **2008**, *16* (9), 5216–5231.

(27) Wooddell, C. I.; Rozema, D. B.; Hossbach, M.; John, M.; Hamilton, H. L.; Chu, Q.; Hegge, J. O.; Klein, J. J.; Wakefield, D. H.; Oropeza, C. E.; et al. *Mol. Ther.* **2013**, *21* (5), 973–985.

(28) Nair, J. K.; Willoughby, J. L. S.; Chan, A.; Charisse, K.; Alam, M. R.; Wang, Q.; Hoekstra, M.; Kandasamy, P.; Kelin, A. V.; Milstein, S.; et al. *J. Am. Chem. Soc.* **2014**, *136* (49), 16958–16961.

(29) Weber, A. E.; Halgren, T. A.; Doyle, J. J.; Lynch, R. J.; Siegl, P. K. S.; Parsons, W. H.; Greenlee, W. J.; Patchett, A. A. *J. Med. Chem.* **1991**, *34* (9), 2692–2701.

(30) Zempleni, J.; Wijeratne, S. S. K.; Hassan, Y. I. *BioFactors* **2009**, *35* (1), 36–46.

(31) Dundas, C. M.; Demonte, D.; Park, S. *Appl. Microbiol. Biotechnol.* **2013**, *97* (21), 9343–9353.

(32) Liu, T.-M.; Conde, J.; Lipiński, T.; Bednarkiewicz, A.; Huang, C.-C. *NPG Asia Mater.* **2016**, *8* (8), 1–25.

(33) Ono, M.; Watanabe, H.; Ikehata, Y.; Ding, N.; Yoshimura, M.; Sano, K. **2017**, No. June 2016, 3337.

(34) Deore, P. S.; Soldatov, D. V.; Manderville, R. A. *Sci. Rep.* **2018**, *8* (1), 16874.

(35) Loudet, A.; Burgess, K. *Chem. Rev.* **2007**, *107* (11), 4891–4932.

(36) Pakhomov, A. A.; Kononevich, Y. N.; Stukalova, M. V.; Svidchenko, E. A.; Surin, N. M.; Cherkaev, G. V.; Shchegolikhina, O. I.; Martynov, V. I.; Muzafarov, A. M. *Tetrahedron Lett.* **2016**, *57* (9), 979–982.

(37) Isidro-Llobet, A.; Álvarez, M.; Albericio, F. *Chem. Rev.* **2009**, *109* (6), 2455–2504.

(38) Venkateswara Rao, B.; Dhokale, S.; Rajamohanan, P. R.; Hotha, S. *Chem. Commun.* **2013**, *49* (92), 10808–10810.

(39) Brown, S. P.; Smith, A. B. *J. Am. Chem. Soc.* **2015**, *137* (12), 4034–4037.

(40) Canovas, C.; Moreau, M.; Bernhard, C.; Oudot, A.; Guillemin, M.; Denat, F.; Goncalves, V. *Angew. Chemie - Int. Ed.* **2018**, *57* (33), 10646–10650.

(41) Andrade-Acuña, D.; Santos, J. G.; Tiznado, W.; Cañete, Á.; Aliaga, M. E. *J. Phys. Org. Chem.* **2014**, *27* (8), 670–675.

(42) Baillie, L. C.; Batsanov, A.; Bearder, J. R.; Whiting, D. a. *J. Chem. Soc. Perkin Trans. 1* **1998**, No. 20, 3471–3478.

Conclusions

1) The experiments carried out in this work have confirmed that the reaction of 2,2-disubstituted cylopent-4-ene-1,3-diones (CPDs), which can be regarded as non-hydrolyzable analogs of maleimides, with cysteines affords stable bicyclic adducts that result from a thia-Michael addition, a cyclization and oxidation. CPD derivatives incorporating a carboxyl group can be on-resin linked to peptides and peptide nucleic acids (PNAs) to produce CPD-polyamides, or derivatized so as to include biotin or dansyl groups that are suitable for the preparation of conjugates. All of these compounds have furnished the expected conjugate by reaction with polyamides (peptides, PNAs) incorporating an *N*-terminal cysteine.

2) CPD-oligonucleotides cannot be prepared because CPDs do not withstand the treatment with conc. aq. ammonia that deprotects the oligonucleotide after chain elongation. Yet, conjugates of oligonucleotides making use of the CPD-Cys reaction can be successfully obtained by using Cys-derivatized oligonucleotides. For this purpose, phosphoramidite derivatives of *S*-trityl or *S*-S-*tert*-butyl cysteine have been synthesized and attached to the 5' end of resin-linked oligonucleotides. The two thiol protecting groups have performed equally well when preparing the desired conjugates.

3) Peptide chains with two cysteine residues, of which one at the *N*-terminus, can be doubly derivatized in a one-pot procedure by first reacting the peptide with a CPD-containing compound, which allows to selectively tag the *N*-terminal cysteine, and subsequent addition of a maleimide-containing molecule to give a thia-Michael reaction with the internal thiol.

4) Double conjugates can also be synthesized from peptides containing either a cysteine or a CPD at the *N*-terminus and an alkyne appending from a lysine residue. In this case it is mandatory to perform the CPD-Cys reaction in first instance, and then a Cu(I)-catalyzed azide-alkyne cycloaddition. A follow-up study has led us to conclude that CPDs react with azides, and give rise to two stable adducts whose structure has been elucidated. It has not been possible to find conditions to drive to completion the reaction that furnishes either of these two compounds, thus excluding the possibility of developing a new conjugation strategy.

5) The two carbonyl groups of the CPD moiety react with alkoxyamines to yield oximes, while the carbonyl of the CPD-Cys adduct does not. The possibility of preparing double conjugates from peptides incorporating either a cysteine or a CPD at the *N*-terminus and an oxyamine appending from a lysine residue has been explored with little success. In addition to formation of fairly complex mixtures upon conjugation, it has been found that the alkoxyamine group readily reacts with traces of acetaldehyde present in acetonitrile, which is the solvent typically used in the isolation and analysis of peptide conjugates. Hence, although double conjugation using this strategy is feasible it is impractical.

6) Peptides containing an *N*-terminal and an internal cysteine can be cyclized by reaction with CPDs. In case the latter incorporates an affinity or tagging unit (biotin or fluorophore) both cyclization and labeling are simultaneously accomplished. Formation of the CPD-Cys adduct (which takes place in first instance) is followed by a second Michael-type addition of the internal thiol to this adduct and finally, by oxidation to yield a conjugated system with an absorption maximum around 370 nm. Attempts to translate this methodology into oligonucleotides have been successful only once, but irreproducible in all subsequent experiments.

7) The compound Retro-1 has been successfully obtained utilizing described procedures. By introducing small changes in the synthesis scheme, derivatives incorporating either a thiol, a diene or a phosphoramidite have been synthesized and used for the preparation of Retro-1-oligonucleotide conjugates. The phosphoramidite has been directly attached to resin-linked oligonucleotides, one

containing a known splice-switching sequence (referred to as 623) and another with the same nucleosides in a different order (scrambled). The same oligonucleotide sequences, but with an appending maleimide at the 5' end, have been used for thia-Michael- and Diels-Alder-mediated conjugation reactions with the other Retro-1 derivatives.

8) Splice-switching assays have been carried out at the laboratory of Prof. R. L. Juliano utilizing the HeLa Luc 705 cell line or mouse tracheal cells induced with EGFP654. In the first instance, assays with the conjugates have shown no major improvement in comparison with the unconjugated 623 or co-administration of Retro-1 and 623. On the other hand, utilizing the mouse tracheal cells, a major benefit has been observed with the Retro-1-623 conjugate in comparison with the unconjugated version of the 623 oligonucleotide.

9) 7-Oxanorbornenes (*exo* adducts, obtained from the furan-maleimide reaction) have proved to be useful dienophiles in inverse electron-demand Diels-Alder (IEDDA) cycloadditions in conjunction with 3,6-disbustituted-1,2,4,5-tetrazines (Tz). The reaction takes place cleanly and smoothly at 37 ºC in aqueous media (preferably water alone) using a 2-fold molar excess of the tetrazine moiety, and is driven to completion after overnight stirring.

10) Oxanorbornene derivatives suitable for introduction at the *N*-terminus or internal polyamide (peptide and PNA) positions, and 5' and 3' of oligonucleotide ends have been prepared and incorporated in their planned positions. Tetrazines bearing reporter groups such as BODIPY or affinity tags like biotin or GalNAc have been synthesized as well. Additionally, the tetrazine group has been appended at the *N*-terminus of a growing peptide chain utilizing solid-phase procedures, which have been optimized. With all these compounds, simple conjugates of peptides, PNAs and oligonucleotides have been prepared successfully utilizing the mild reaction conditions described above.

11) Different alternatives for double conjugation involving at least one oxanorbornene-Tz IEDDA reaction have been examined. Aside from their suitability for the double derivatization of peptides and oligonucleotides (discussed in the conclusions that follow), these assays have shown that alkyl or aryl 3,6-disubstituted 1,2,4,5-tetrazines do neither react with 1,4-dimethyl-7-oxanorbornenes (that is, with 2,5-dimethylfuran-protected maleimides), nor with CPDs or maleimides. Yet, they react with 1,3-dienes. It has also been found that 1,2,4,5-tetrazines with alkylsulfanyl groups at the 3 and 6 positions do not react with 7-oxanorbornenes.

12) Attempts to derivatize peptides incorporating 1,4-dimethyl-7-oxanorbornenes and 7-oxanorbornenes have shown that it is not possible to remove the more labile maleimide protecting group (2,5-dimethylfuran) leaving unaltered the 7-oxanorbornene moiety (or furan-protected maleimide) since, to some extent, furan removal has always been observed. Assays aiming at synthesizing double conjugates by first running the IEDDA reaction then deprotecting the maleimide and reacting it with either a thiol or a diene, have either furnished complex crudes or been relatively successful, respectively.

13) In case the peptide scaffold incorporates an oxanorbornene and a free maleimide, double conjugation has been best achieved by first reacting the peptide with a 1,3-diene, followed by isolation of the intermediate monoconjugate, and final reaction with a tetrazine. Replacing the Diels-Alder cycloaddition with a thia-Michael reaction is also an acceptable alternative.

14) Peptides including a thiol (*N*-terminal or internal cysteine) in addition to the oxanorbornene have allowed the IEDDA reaction to be combined with either CPD-Cys or thia-Michael reactions (the former requires a Cys residue at the *N*-terminus). Interestingly, in both cases the two conjugation reactions can be carried out simultaneously.

15) The same type of scaffold has been used to combine the IEDDA cycloaddition with a S_NAr. In this case the S_NAr has been performed first, by reacting the free thiol with a chloro-1,2,4,5-tetrazine linked to either a dansyl fluorophore or to an oligonucleotide. This is an extremely quick reaction, so that the second reagent (the tetrazine 3,6-disubstituted with alkyl or aryl rings) can be added almost immediately. In case the thiol is the side chain of an *N*-terminal cysteine, its reaction with a chlorotetrazine is followed by a rearrangement that yields the *N*-substituted tetrazine and liberates the thiol, which can undergo a second S_NAr reaction.

16) The S_NAr-IEDDA combination has also been extended to oligonucleotides. For this purpose, it has been necessary to synthesize an *S*-trityl-protected cysteine building block with the amine linked to a 7-oxanorbornene and the carboxyl derivatized so as to allow for the incorporation of a phosphoramidite group. Double conjugation of these Cys-oligonucleotides requires a much longer reaction time for the S_NAr reaction (*ca.* 4 h).

17) Finally, the DA-IEDDA combination has been tested with an oligonucleotide containing an oxanorbornene at the 3' end and a 1,3-diene at the 5' end. A one-pot procedure in which the DA cycloaddition (with a maleimide) is followed by the IEDDA reaction (with a tetrazine) has successfully furnished the target double conjugate.

Experimental section: Materials and methods

E.M.M.1 Reagents and solvents

Synthesis of oligomers

Fmoc-protected amino acids used for the synthesis of peptides were obtained from Novabiochem or Iris Biotech, Fmoc-protected PNA monomers from Link Technologies and commercial phosphoramidites from Glen Research or Link technologies. Regarding solid supports, NovaSyn TGR resin was obtained from Novabiochem, TentaGel R Ram from Rapp and Rink amide MBHA from Merck. Polymer and CPG supports from Glen Research or Link Technologies. All solution and solvents employed for the synthesis of oligonucleotides were purchased from Glen Research or Link Technologies. DIPC, COMU and HATU were from Sigma-Aldrich. HOBt from Iris Biotech. Piperidine and NMP were from Sigma-Aldrich, acetic anhydride from Scharlau and DMF from Carlo Erba. TFA and TIS were from Sigma-Aldrich and concentrated aqueous ammonia from Merck.

Synthesis of small organic molecules

Reagents employed for the synthesis of small organic molecules were purchased from different suppliers (Sigma-Aldrich, Fluka, Alfa Aesar, Acros, etc) and employed without further purified. Salts and other common products usually employed in the work-up were from Panreac.

Annhydrous solvents

DCM: Distilled from CaH_2 and stored under Ar atmosphere over CaH_2

DMF: Utilizing 4 Å activated molecular sieves.

ACN: Bought anhydrous. Trap Pack was used always to avoid wetting over time.

Buffer Solutions

2 M Triethylammonium acetate (TEAA) pH 7: To prepare 500 mL of this buffer solution, TEA (140 mL) and glacial AcOH (58 mL) were mixed in an ice-cooled Erlenmeyer flask containing 200 mL of Mili-Q water. Magnetic stirring was kept during an hour, the pH was adjusted to 7.0 with either additional TEA or AcOH as required and Milli-Q water was added until the volume was adjusted to 500 mL in a volumetric flask.

E.M.M.2 Chromatographic techniques

Thin layer chromatography (TLC). Thin layer chromatography analysis was done using aluminum foils coated with silica gel (60 F, 0.2 mm, Merck). Different methods and reagents were employed to visualize spots depending on the nature of the analyzed compounds: UV lamp (254 nm), potassium permanganate, p-anisaldehyde, etc.

Column chromatography. Purification by flash column chromatography was carried out using 60 Å CC Chromatogel silica gel (35-70 μm, from SDS) as stationary phase. An appropriate mixture of organic solvents was used as mobile phase.

High performance liquid chromatography (HPLC). Reversed-phase analysis by HPLC was carried out in a Shimadzu (LC-20AD pump, SIL-20A HT Autosampler and SPD-M20A or SPD-20A detector) or Waters 2695 (Separations Module 2695 and PDA detector 2996) instruments. For purification, a semi-preparative HPLC Waters 600 (Controller 600, Detector 2487) was employed.

The HPLC column was chosen depending on the compounds to be analyzed and the elution conditions:

Buffered conditions:

For analysis (A = TEAA 0.1 M in H_2O, B = ACN) a Jupiter C_{18} 300A (250 × 4.6 mm, 10 µm particle size) column from Phenomenex. Elution was carried out with 1 mL/min flow.

For purification (A = TEAA 0.1 M in H_2O, B = ACN) a Jupiter Proteo 90A C_{18} (250 × 10 mm, 10 µm particle size) column from Phenomenex. Elution was carried out with a 3 mL/min flow.

Acidic conditions

For analysis (A = 0.045% (v/v) TFA/H_2O, B = 0.036% (v/v) TFA/ACN) a Jupiter Proteo 90A C_{18} (250 × 4.6 mm, 4 µm particle size) column from Phenomenex. Elution was carried out with a 1 mL/min flow.

For purification (A = 0.1% (v/v) TFA/H_2O, B = 0.1% (v/v) TFA/ACN) a Jupiter Proteo 90A C_{18} (250 × 10 mm, 10 µm particle size) column from Phenomenex. Elution was carried out with a 3 mL/min flow.

E.M.M.3 Spectroscopic techniques

*Matrix-Assisted Laser Desorption/Ionization Time-of-Flight (*MALDI-TOF*)*. Routine experiments were carried out in a 4800 Plus MALDI TOF/TOF from Applied Biosystems (CCiT, UB). Samples were generally prepared by mixing 1 µL of an aqueous solution of the analyte and 1 µL of a mixture 1:1 (v/v) mixture of ammonium citrate (CA) solution (50 mg/mL H_2O) and THAP (10 mg/mL 1:1 ACN/H_2O) for the negative mode and 1 µL of a solution of DHB (10 mg/mL 1:1 ACN/H_2O + 0.1% TFA) for the positive mode.

Different experimental parameters were used depending on the behavior and the molecular weight of the analyte. Reflector mode was employed as a first option because of its accuracy. The linear mode, which is less precise but more sensitive than the reflector mode, was used to analyze molecules with large molecular weights. Depending on the structure of the analyte, positive or negative analysis mode was employed.

conditions: For analysis (A = 0.1% (v/v) formic acid/H_2O, B = 0.1% (v/v) formic acid/ACN) a Jupiter Proteo 90A C_{18} (250 × 4.6 mm, 4 µm particle size) column from Phenomenex. Elution was carried out with a 1 mL/min flow.

Electrospray MS. ESI-MS high resolution experiments for simple organic compound characterization were carried out by the *Unitat d'Espectrometria de Masses* of the CCiT of the UB using an ESI-MS LC/MSD-TOF mass spectrometer from Agilent Technologies.

A Micromass ZQ with a quadrupole detector from Waters, connected to an HPLC Waters 2695, was also used as a self-service instrument. Electrospray samples were prepared by dissolving the analyte in Milli-Q water, methanol or ACN as deemed necessary. Samples were injected using a Reodyne injector or directly from the HPLC to the mass instrument with a 0.2 mL/min constant flow of Milli-Q water,

methanol or ACN (depending on the solvent of the sample). In case chromatographic separation was needed for analysis a 30 min linear gradient of (A = 0.1% (v/v) formic acid/H_2O, B = 0.1% (v/v) formic acid/ACN) was used. Jupiter Proteo 90A C_{18} (250 × 4.6 mm, 4 µm particle size) column from Phenomenex. Elution was carried out with a 1 mL/min flow. In all cases, positive or negative analysis mode was employed depending on the analyte.

Nuclear magnetic resonance

^{1}H , ^{13}C and ^{31}P spectra were recorded in a Varian Mercury-400 spectrometers from the NMR unit of the *Centres Científics i Tecnològics (CCiT)* from *UB*. For sample preparation, between 5-10 mg for ^{1}H, ^{19}F or ^{31}P and 20-30 mg for ^{13}C of sample and 700 µL of the appropriate deuterated solvent was employed. Chemical shifts were either referenced on TMS (δ = 0 ppm) or residual solvent signal.

UV-Vis Spectroscopy

UV-Vis absorption spectra were performed in a Jasco V-550 spectrophotometer interfaced with a computer and equipped with a Jasco Peltier ETC-505T. Hellman Quartz cells with an optic path length of 10 mm were used.

Other instrumentation

Lyophilization of aqueous solutions was accomplished in either a Labconco Freezone 6 or a Christ Alpha 2-4LDplus.

Melting points were measured in a Bibby Stuart Scientific SMP10 instrument.

Suspensions were centrifugated in a 5430R Eppendorf centrifuge.

pH Was measured with a Crison micropH Basic 20 pH-meter.

The microwave oven employed was a Biotage Initiator. For MW-promoted reactions, sealed vials of volumes ranging from 0.2 to 20 mL were used.

E.M.M.4 Oligomeric synthesis

Polyamide (Peptide and PNA) synthesis (**Scheme E.1.1**)

Synthesis Cycle and elongation of the chain:

Polyamide solid-phase synthesis involves receptive cycles composed by several steps:

1.- A **deprotection** of the *N*-terminal amine with a 20% piperidine solution in DMF (2 × 20 mL).

2.- A **coupling** step involving the monomer's carboxylic acid (3 eq.). Activation takes place by reacting the monomer with a coupling agent (DIC, 3 eq.) and HOBt (3 eq.) in the minimum amount of DCM and DMF and reacting for 90 minutes.

The efficiency of the coupling reaction was assessed by the Kaiser's test. In the case it yielded positive, the coupling step was repeated.

3.- A **capping** step of the unreacted amino groups with the capping solution: Ac_2O (6%) and 2,6-lutidine (6%) in NMP (1 × 10 min.).

Between cycle steps, the resin was washed with DMF, MeOH and DCM thoroughly.

Before the final treatment for cleavage and removal of the acid-labile protecting group, the *N*-terminal Fmoc protecting group was remove as explained above.

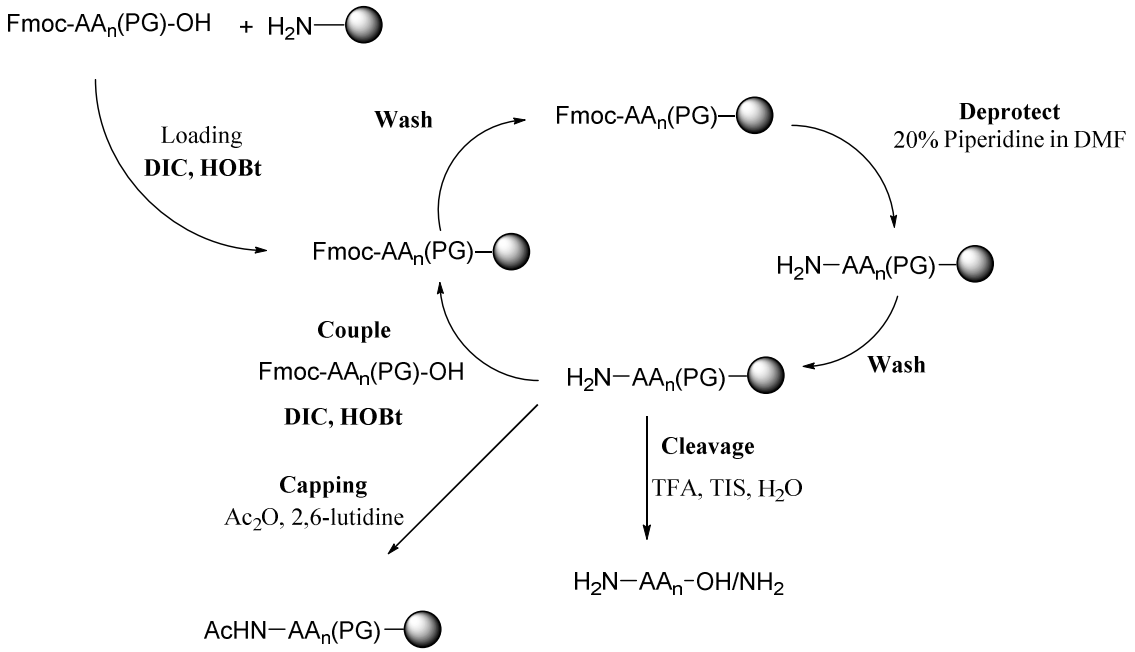

Scheme E.1.1 Schematic representation of a cycle in the polyamide solid-phase synthesis.

Cleavage, deprotection and purification

Polyamide oligomers were generally treated with a mixture of 95:2,5:2,5 (TFA/TIS/H_2O) (v/v/v) for peptides and PNA. If either contained a cysteine residue, the cleavage and deprotection mixture was instead (94:2,5:2,5:1) (v/v/v/v) (TFA/TIS/EDT/H_2O) and reacted for 150 min at room temperature. Then, the reaction mixture was filtered and the resin washed with additional TFA (3 × 1 mL). Filtrates and washings were combined and the TFA removed under a N_2 stream. The polyamide crude was precipitated by the addition of HPLC grade Et_2O. Afterwards, the crude centrifuged and the Et_2O decanted. This procedure was repeated 3 times.

Crude polyamide was analyzed and purified by HPLC. Unless stated, a 30 minutes gradient of eluents using acidic conditions. The purity of oligomers was assessed by analytical HPLC and characterized by HPLC-MS (ESI-MS) or MALDI-TOF.

Kaiser Test. The ninhydrin test is employed to detect the presence of free primary amines. The tests are performed in a small amount of dry resin and treated with 6 drops of reagent A and 2 drops of reagent B (see below.) The suspension is heated to 100 ºC for 3 min. in an oven sand bath. The outcome is determined by its color. If there is a presence of free amines (<1%) the solution becomes blue, positive test, whereas it exhibits colorless or pale yellow, the test is negative and chain elongation can proceed.

Reagent A: A solution containing 40 g of phenol in 10 mL of absolute ethanol and a solution of 2 mL of 10 mM KCN in 100 mL of anh. pyr. are stirred separately with 4 g of Amberlite MB-3 resin (Merck) for 45 minutes, filtered and mixed together.

Reagent B: 2.5 g of ninhydrin are dissolved in 50 mL of absolute ethanol.

Both reagents A and B must be kept in an opaque bottle protected from light.

Determination of the substitution degree of a Fmoc-resin. The resin-linked Fmoc-protected polyamide was treated twice with 1 mL of 20% piperidine in DMF for 10 minutes. Both filtrates and the subsequent washings with DCM were combined in a 10 mL volumetric flask and the solution was brought to volume with additional DCM.

Then, the solution's absorbance was measured at 301 nm determining the absorption maximum of the *N*-(9-flurenylmethyl)piperidine adduct formed during the deprotection step.

The determined quantity (moles) of Fmoc groups, which can be calculated using the Beer-Lambert Law, is equal to the quantity of (mol) of PNA chains attached to the resin

$$n_{PNA}(\mu mole) = \frac{Abs_{301} V \cdot 10^3}{\varepsilon_{301} \cdot l}$$

Where Abs_{301} is the absorbance of the solution at 301 nm, V is the volume (in mL) of the volumetric flask and l is the cell's optic path length (cm).

Polyamide quantification by UV-Vis absorption

In order to calculate the amount of either peptide or peptide PNA, the molar extinction coefficient ($\varepsilon_{polyamide}$) of the oligomer must be known. To obtain the molar extinction coefficient the individual contributions of all the chromophores present in the molecule must be taken into account using the following formula.

$$\varepsilon_{polyamide} = \sum n_i \cdot \varepsilon_{chromophore_i}$$

Where n_i is the number of chromophores present in the polyamide and $\varepsilon_{chromophore}$ is its corresponding molar extinction coefficient.

PNA	Bases	ε_{260}	Amino acid	ε_{280}
	a	13700	**Tryptophan** (W)	5500
	c	6600	**Tyrosine** (Y)	1500
	g	11700	**Cystine** (C)	125
	t	8800		

Table E.1.1 Molar extinction coefficients of the different PNA monomers and amino acids determined at 25 ºC, pH 7.0 and 260 nm and 280 nm respectively.

Oligonucleotide synthesis

The synthesis of all deoxyribonucleic and ribonucleic acids was performed in an automatic 3400 Applied Biosystems synthesized using the standard phophite trimester methodology at the 1 µmol scale. For either DNA or RNA synthesis, standard β-cyanoethyl phophoramidite chemistry with methoxy (OMe) protection of the ribose 2'-hydroxyl group in the RNA case was employed ($^{Pac}rA_{OMe}$, $^{iPr\text{-}Pac}rG_{OMe}$, $^{Ac}rC_{OMe}$, rT_{OMe} and ^{Pac}dA, $^{iPr\text{-}Pac}dG$, ^{Ac}dC, dT monomers purchased from Link Technologies)

Synthesis cycle and elongation of the chain

Each synthetic cycle comprises (**Scheme E.1.2**)

1. A **detritylation** step that unmasks the 5'-hydroxyl group with 3% TCA in DCM for chain elongation.
2. Washings with anh. ACN.
3. A **coupling** step in which the desired nucleoside as phosphoramidite building block (0.1 M in anh. ACN) is activated with by a solution of either tetrazole (in DNA synthesis) or BTT (5-benzylmercapto)1*H*-tetrazole, in RNA synthesis) 0.3 M in anh. ACN, 10 minutes.
4. A **capping** step to acylate any unreacted 5'-hydroxy group to avoid the possibility of obtaining deletion sequences. Two capping solutions are used, namely cap mix solutions A and B containing 1:1:8 Pac_2O/Pyr/THF mixtures (v/v/v) and 16% 1-methylimidazole in THF, respectively.
5. Either an **oxidation** step that converts the phosphite triester (P(III)) into a phosphate triester (P(V)) using a 0.02 M solution of I_2 in H_2O/Pyr/THF or a **sulfurization** step that converts the phosphite triester into a phosphorothioate triester using a 0.05 M solution of Beaucage reagent in anh. ACN.
6. A final washing step and cycle start.

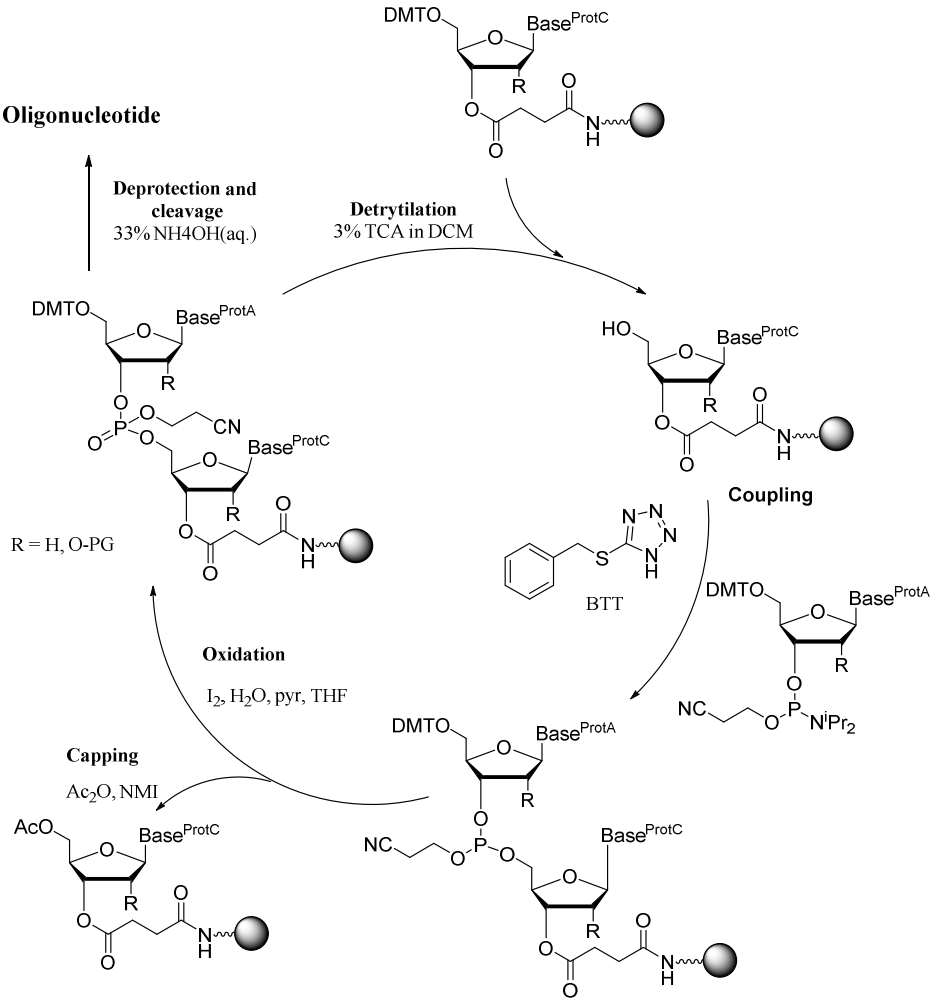

Scheme E.1.2 Oligonucleotide synthesis cycle. TCA (trichloroacetic acid), BTT, Ac_2O, CNE (β-cyanoethyl), ^{i}Pr, Pyr, THF, NMI (*N*-metilimidazole), PG = Protecting group

Manual cleavage, deprotection and purification

After chain elongation, oligonucleotide-grown resin was treated with conc. aq. ammonium hydroxide (32%) at room temperature for 2.5 h in order to remove all protecting groups and cleave. After ammonia removal under reduced pressure, analysis and purification was carried out by HPLC. Characterization was carried out by HPLC and MALDI-TOF.

Oligonucleotide quantification by UV-Vis absorption

Quantification synthesized oligonucleotides was done by measuring the absorbance of a well-known volume solution at 260 nm. The amount of oligonucleotide present in the sample was calculated applying the Beer-Lambert law and expressed in µmol or nmol.

To calculate the amount of oligonucleotide using the Beer-Lambert law, the molar extinction coefficient (ε_{oligo}) of the oligonucleotide must be calculated adding the contribution of the present bases in the oligonucleotide corrected by a factor (f) related to stacking phenomena. This factor is $f = 0.9$ in the case of single-stranded chains and $f = 0.88$ in the case of double-stranded chains.

$$\varepsilon_{oligo} = \sum f \cdot n_i \cdot \varepsilon_{base_i}$$

DNA	Bases	ε_{260}	RNA	Bases	ε_{260}
	A	13700		A	15100
	C	6600		C	11500
	G	11700		G	10100
	T	8600		U	7700

Table E.1.2 Molar extinction coefficients of the different nucleosides determined at 25 ºC, pH 7.0 and 260 nm.

Experimental section: Chapter 2

tert-Butyl-3-(1-methyl-2,5-dioxocyclopentyl)propanoate (2.18)

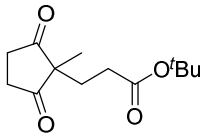

2-Methylcyclopentane-1,3-dione (**2.17**, 1.22 g, 10.90 mmol) and *tert*-butyl acrylate (5.9 mL, 26.8 mmol) were dissolved in NEt_3 (20 mL) and the mixture refluxed overnight. Thereafter, NEt_3 and excess *tert*-butyl acrylate were removed *in vacuo* to render the title compound as a dark brown solid used without further purification (2.50 g, 78%).

mp. 63-64 ºC.

TLC (DCM/AcOH 98:2): R_f = 0.30.

IR (ATR, solid): ν 2980, 1708, 1365, 1294, 1143, 840 cm^{-1}.

^{1}H NMR ($CDCl_3$, 400 MHz): δ 2.87 – 2.70 (m, 4H), 2.20 (t, *J* = 7.5 Hz, 2H), 1.92 (t, *J* = 7.6 Hz, 2H), 1.40 (s, 9H), 1.12 (s, 3H) ppm.

^{13}C NMR ($CDCl_3$, 101 MHz): δ 215.9, 172.3, 81.1, 55.4, 35.0, 30.0, 29.3, 28.2, 19.8 ppm.

ESI-HRMS (positive mode): *m/z* 241.1446 $[M+H]^+$, calcd. for $C_{13}H_{21}O_4$ 241.1434.

3-(1-Methyl-2,5-dioxocyclopentyl)propanoic acid (2.19)

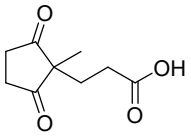

2.18 (1.00 g, 4.16 mmol) was dissolved in TFA/DCM (1:1, 26 mL) and the solution stirred for 2 h at rt. Afterwards, toluene (15 mL) was added to the reaction mixture and dried under vacuum to yield the title compound as a brown solid (760.0 mg, 99%).

mp. 121-122 ºC.

TLC (DCM/EtOAc/AcOH 78:20:2): R_f = 0.35.

IR (ATR, solid): ν 3045, 1697, 1404, 1192 cm^{-1}.

^{1}H NMR (CD_3OD, 400 MHz) δ 2.78 (s, 4H), 2.26 (t, *J* = 8.0 Hz, 2H), 1.89 (t, *J* = 8.0 Hz, 2H), 1.10 (s, 3H) ppm.

^{13}C NMR (CD_3OD, 101 MHz) δ 217.9, 176.4, 56.5, 35.6, 30.2, 29.5, 19.6 ppm.

ESI-HRMS (negative mode): *m/z* 183.0661 $[M-H]^-$, calcd. for $C_9H_{12}O_4$ 183.0663.

3-(1-Methyl-2,5-dioxocyclopent-3-en-1-yl)propanoic acid (2.20 or 4.112)

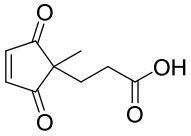

To a solution of **2.19** (500.0 mg, 2.72 mmol) in EtOAc (20 mL), $CuCl_2$ (803.0 mg, 5.98 mmol) and LiCl (253.0 mg, 5.98 mmol) were added and the mixture left refluxing overnight. Afterwards, additional EtOAc was added (20 mL) and the resulting mixture transferred into a separatory funnel. The organic layer was washed with aq. HCl 5% (3 × 40 mL). The organic fraction was dried over anh. $MgSO_4$, filtered and the solvent removed *in vacuo*. The resulting extract was further purified by silica gel column chromatography eluting with an isocratic mixture of DCM/AcOH (98:2). The title compound was obtained as a yellow solid (240.0 mg, 48%).

mp. 82-83 ºC.

TLC (DCM:EtOAc:AcOH 78:20:2): R_f = 0.55.

IR (ATR, solid): ν 3060, 2916, 1693, 1303 cm^{-1}.

^{1}H NMR ($CDCl_3$, 400 MHz) δ 7.25 (s, 2H), 2.33 – 2.24 (m, 2H), 2.01 – 1.93 (m, 2H), 1.18 (s, 3H) ppm.

^{13}C NMR ($CDCl_3$, 101 MHz) δ 206.9, 176.9, 148.1, 49.2, 28.8, 28.5, 18.6 ppm.

ESI-HRMS (negative mode) *m/z* 181.0500 $[M-H]^-$, calcd. for $C_9H_9O_4$ 181.0506.

tert-Butyl (2-(3-(1-methyl-2,5-dioxocyclopent-3-en-1yl)propanamido)ethyl)car-bamate (2.21)

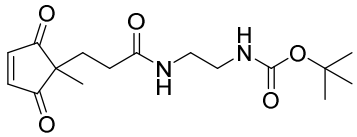

A solution of **2.20** (50 mg, 0.27 mmol) in DCM (1 mL) was cooled to -15 ºC. Subsequently, NMM (30 µL, 0.27 mmol) and IBCF (35 µL, 0.27 mmol) were added. After 10 min, *tert*-butyl (2-aminoethyl)carbamate (48 mg, 0.30 mmol) was added. The suspension was kept at -15 ºC for another 15 min and afterwards was reacted for 3 h at rt. Afterwards, the solvent was removed under reduced pressure, the crude dissolved in EtOAc (20 mL) and washed with H_2O (2 × 10 mL), aq. HCl 5% (2 × 10 mL) and aq. $NaHCO_3$ 5% (2 × 10 mL). The organic layer was dried over anh. $MgSO_4$, filtered and evaporated under reduced pressure to afford the title compound as a yellow solid (67 mg, 76%).

mp. 102-103 ºC.

TLC (DCM/EtOAc/AcOH 78:20:2): R_f = 0.17.

IR (ATR, solid): ν 3368, 3322, 2962, 1697, 1689, 1237 cm^{-1}.

^{1}H NMR ($CDCl_3$, 400 MHz) δ 7.24 (s, 2H,), 6.31 (bs, 1H), 5.05 (bs, 1H,), 3.32 – 3.23 (m, 4H), 2.13 – 2.09 (m, 2H), 1.99 – 1.96 (m, 2H), 1.44 (s, 9H), 1.16 (s, 3H) ppm.

^{13}C NMR ($CDCl_3$, 101 MHz) δ 206.9, 171.8, 156.9, 147.8, 79.8, 49.3, 40.8, 40.1, 31.1, 29.5, 28.4, 18.4 ppm.

ESI-HRMS (positive mode): *m/z* 325.1767 $[M+H]^+$, calcd. for $C_{16}H_{25}N_2O_5$ 325.1758.

N-(2-Aminoethyl)-3-(1-methyl-2,5-dioxocyclopent-3-en-1-yl)propenamide (2.22)

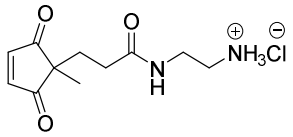

A solution of HCl (4 M in dioxane, 500 µL, 7.39 mmol) was added to a solution of **2.21** (60 mg, 0.18 mmol) in DCM (500 µL) and the mixture stirred at rt for 2 h. Afterwards, the solvent was removed under reduced pressure to afford the title compound as a yellow solid (42 mg, quantitative yield).

mp. 134-136 ºC.

TLC (DCM/EtOAc 1:1): R_f = 0.54.

IR (ATR, solid) ν 3279, 2922, 1693, 1643, 1444 cm^{-1}.

^{1}H NMR (CD_3OD, 400 MHz): δ 7.34 (s, 2H), 3.38 (t, *J* = 8.0 Hz, 2H), 3.02 (t, *J* = 8.0 Hz, 2H), 2.15 – 2.11 (m, 2H), 1.93 – 1.89 (m, 2H), 1.12 (s, 3H) ppm.

^{13}C NMR (CD_3OD, 101 MHz): δ 207.3, 174.4, 148.1, 49.0, 39.5, 36.8, 30.2, 29.1, 17.5 ppm.

ESI-HRMS (positive mode): *m/z* 225.1234 $[M+H]^+$, calcd. for $C_{11}H_{17}N_2O_3$ 225.1234.

N-(2-(3-(1-Methyl-2,5-dioxocyclopent-3-en-1-yl)propanamido)ethyl)- 5-((3a*S*,4*S*,6a*R*)-2-oxohexahydro-1*H*-thieno[3,4-*d*]imidazol-4-yl)pentanamide (2.23)

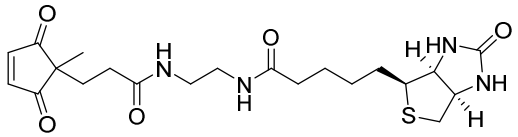

D-Biotin (50 mg, 0.20 mmol) was dissolved in anh. DMF (3 mL) under a N_2 atmosphere and stirred for 30 min at -10 ºC. Once dissolved, NMM (56 µL, 0.51 mmol) and IBCF (27 µL, 0.20 mmol) were added, and the mixture was reacted at -10 ºC for 1 h. Thereafter, a solution of **2.22** (46 mg, 0.20 mmol) in anh. DMF (2 mL) was added, and the mixture stirred for 1 additional h at -10 ºC and at rt for 3 h. Afterwards, the solvent was removed *in vacuo* and the crude was purified by reversed-phase chromatography, using a 10 mL-syringe filled with 2.0 mL of C_{18}-derivatized silica (Vydac). Elution was carried out with a gradient of 8.0 mL of H_2O, 8.0 mL of 1:3 (v/v) MeOH/H_2O and 8.0 mL of 1:1 (v/v) MeOH:H_2O. The title compound was obtained as a yellow solid (28 mg, 34%).

mp. 126-127 ºC.

TLC (DCM/MeOH/AcOH 88:10:2): R_f = 0.23.

IR (ATR, solid): ν 3296, 3199, 2976, 2923, 2415, 1703, 1628, 1138 cm^{-1}.

^{1}H NMR (CD_3OD, 400 MHz) δ 7.38 (s, 2H), 4.53 (dd, *J* = 4.4 Hz, *J* = 7.6 Hz, 1H), 4.35 (dd, *J* = 4.8 Hz, *J* = 8.0 Hz; 1H), 3.26 (m, 4H); 3.26 (m, 1H), 2.96 (dd, *J* = 4.8 Hz, *J* = 12.4 Hz, 1H), 2.74 (d, *J* = 12.8 Hz, 1H), 2.22 (t, *J* = 6.4 Hz, 2H), 2.09 (m, 2H), 1.91 (m, 2H), 1.81 – 1.57 (m, 4H), 1.45 (q, *J* = 7.6 Hz, 2H), 1.15 (s, 3H) ppm.

^{13}C NMR (CD_3OD, 101 MHz) δ 207.3, 174.9, 173.4, 164.7, 148.1, 61.9, 60.2, 55.5, 49.0, 39.7, 38.6, 38.5, 35.4, 30.5, 29.6, 28.3, 28.1, 25.4, 17.5 ppm.

ESI-HRMS (positive mode): *m/z* 451.2015 $[M+H]^+$, calcd. for $C_{21}H_{31}N_4O_5S$ 451.2010.

N-(2-(5-(dimethylamino)naphthalene-1-sulfonamido)ethyl)-3-(1-methyl-2,5-dioxocyclopent-3-en-1-yl)propanamide (2.24)

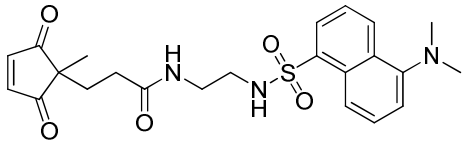

Dansyl chloride (54.6 mg, 0.20 mmol) was added to a solution of **2.22** (50 mg, 0.22 mmol) in anh. ACN (1 mL). Subsequently, NEt_3 (0.5 mL, 3.59 mmol) was added and the mixture left for 3 h stirring at rt. Afterwards, the solvent was removed under reduced pressure, and the resulting residue dissolved in DCM (15 mL), transferred into a separatory funnel and washed with distilled H_2O (3 × 15 mL). The organic layer was extracted with aq. HCl 5% (3 × 15 mL). The acidic aqueous layer was basified to pH 6-7 with aq. $NaHCO_3$ 5% and extracted with DCM (3 × 15 mL). The organic layer was dried over anh. $MgSO_4$, filtered and the solvent removed under vacuum. The title compound was obtained as a yellow solid (21.1 mg, 23% yield).

mp. 128-129 ºC.

TLC (DCM/EtOAc 95:5): R_f = 0.35.

IR (ATR, Solid): ν 3296, 3074, 2918, 2874, 1698, 1641, 1309, 1140, 788, 727, 622 cm^{-1}.

^{1}H NMR ($CDCl_3$, 400 MHz) δ 8.54 (d, *J* = 8.4 Hz, 1H); 8.28 (d, *J* = 8.4 Hz, 1H); 8.22 (d, *J* = 7.2 Hz); 7.58 – 7.50 (m, 2H); 7.20 (s, 2H), 7.19 (d, *J* = 6.8 Hz); 6.04 (t, *J* = 2.4 Hz, 1H); 5.82 (t, *J* = 5.2 Hz, 1H); 3.24 – 3.20 (m, 2H); 3.02 – 2.98 (m, 2H); 2.89 (s, 6H); 2.03 – 1.98 (m, 2H); 1.92 – 1.89 (m, 2H); 1.13 (s, 3H) ppm.

^{13}C NMR ($CDCl_3$, 101 MHz) δ 207.0, 172.20, 152.1, 147.9, 134.4, 130.6, 129.9, 129.6, 129.4, 128.5, 123.2, 118.6, 115.3, 49.3, 45.4, 42.8, 39.5, 30.9, 29.3, 18.4 ppm.

ESI-HRMS (positive mode) *m/z* 458.1730 $[M+H]^+$, M calcd. for $C_{23}H_{29}N_3O_5S$ 458.1744.

2,2-Dimethylcyclopentane-1,3-dione (2.28)

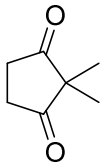

Potassium hydroxide (1.00 g, 17.82 mmol) and iodomethane (2.53 g, 17.82 mmol) were added to a solution of 2-methylcyclopentane-1,3-dione (**2.17**, 2.00 g, 17.82 mmol) in dioxane:water (3:1, 40 mL) and heated to reflux overnight. The reaction mixture was cooled and transferred into a separatory funnel. The aqueous layer was extracted with Et_2O (3 × 30 mL), and the combined organic layers evaporated under reduced pressure. Afterwards, aq. HCl 10% (50 mL) was added to the resulting crude and the mixture heated to boiling for 5 min. Subsequently, an excess amount of aq. $NaHCO_3$ 10% was added to the mixture and allowed to cool down. Finally, the mixture was extracted with DCM (3 × 20 mL). The organic layers were dried over anh. $MgSO_4$, filtered and evaporated under reduced pressure to afford a white solid (801 mg, 35% yield).

mp. 52-53 ºC.

TLC (Hexanes/EtOAc 4:1): R_f = 0.53, dyeing reagent: 100 mg 2,4-dinitrophenyl-hydrazine dissolved in 100 mL EtOH + 1 mL conc. aq. HCl (yellow spot).

IR (ATR, solid): ν 2972, 2923, 2865, 1694, 1689, 1454, 1285 cm^{-1}.

^{1}H NMR ($CDCl_3$, 400 MHz) δ 2.80 (s, 4H), 1.15 (s, 6H) ppm.

^{13}C NMR ($CDCl_3$, 101 MHz) δ 216.5, 57.8, 34.7, 20.4 ppm.

ESI-HRMS (positive mode): *m/z* 127.0758 $[M+H]^+$, calcd. for $C_7H_{11}O_2$ 127.0754.

2,2-Dimethylcyclopent-4-ene-1,3-dione (2.29)

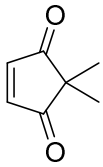

Copper(II) chloride (926.73 mg, 6.97 mmol), lithium chloride (292.82 mg, 6.97 mmol) and **2.28** (400 mg, 3.17 mmol) were dissolved in EtOAc (25 mL), and the mixture refluxed for 17 h at 85 ºC. Once the reaction was complete (as assessed by TLC analysis), H_2O (10 mL) was poured onto the round-bottomed flask, and its content fully transferred into a separatory funnel. The organic layer was further washed with H_2O until the aqueous phase was colorless. Afterwards, the organic layer was dried over anh. $MgSO_4$ and filtered before solvent was removed under reduced pressure. The crude was further purified using silica gel flash column chromatography eluting with hexanes/Et_2O mixtures from 99:1 to 95:5. The title compound was obtained as a yellow oil (85.5 mg, 22%).

TLC (Hexanes/EtOAc 4:1): R_f = 0.60.

IR (ATR, oil): ν 1695, 1290, 1139, 1045, 854 cm^{-1}.

^{1}H NMR ($CDCl_3$, 400 MHz) δ 7.20 (s, 2H), 1.16 (s, 6H) ppm.

^{13}C NMR ($CDCl_3$, 101 MHz) δ 207.7, 147.1, 46.4, 19.6 ppm.

ESI-HRMS (positive mode): the product does not ionize.

CPD-GRGSYEAYK-NH_2 (2.32)

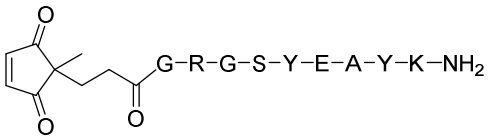

HPLC: purification gradient: 0-40% (21%) B; analysis conditions, 0-40% B, t_R = 21.0 min (**Figure E.2.1**).

MALDI-TOF (positive mode, DHB): *m/z* 1193.5 $[M+H]^+$, M calcd. for $C_{54}H_{77}N_{14}O_{17}$ 1193.6.

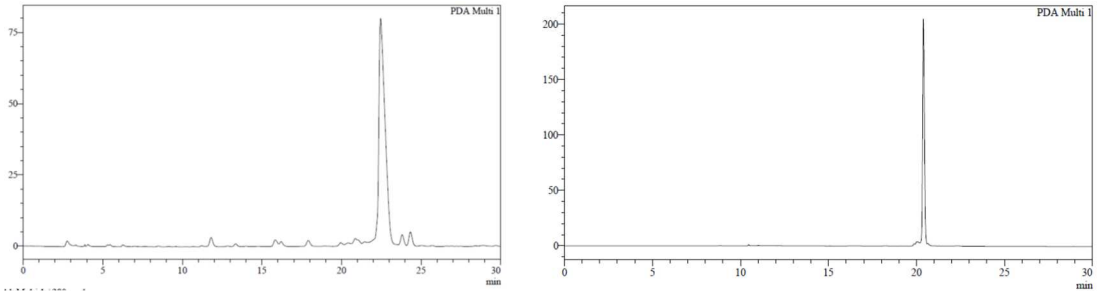

Crude Purified

Figure E.2.1 HPLC traces (280 nm) of crude (left) and purified (right) CPD-derivatized peptide **2.32**.

CPD-catgtcat-K-NH_2 (2.33)

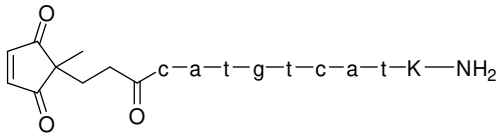

HPLC: purification gradient: 0-40% B (11%); analysis conditions, 0-40% B, t_R = 19.1 min (**Figure E.2.2**).

MALDI-TOF (positive mode, DHB): *m/z* 2452.5 $[M+H]^+$, M calcd. for $C_{101}H_{130}N_{46}O_{29}$ 2451.0.

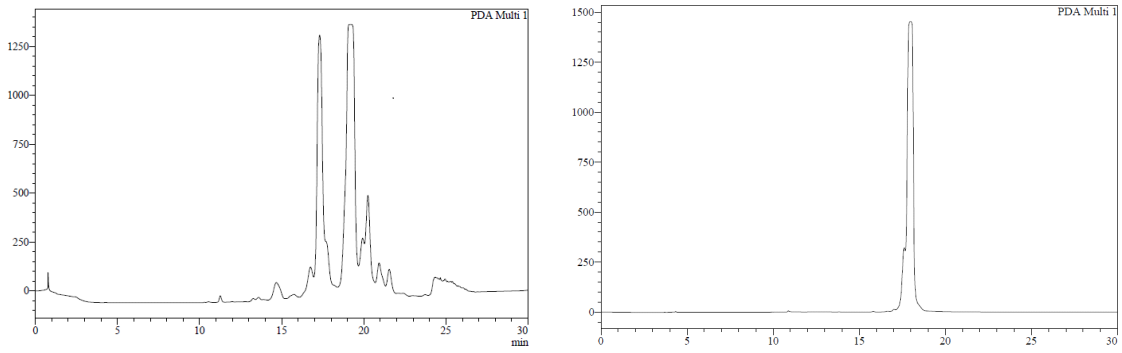

Crude Purified

Figure E.2.2 HPLC traces (260 nm) of crude (left) and purified (right) CPD-derivatized PNA (**2.33**).

CPD-LVPRGSYKGTSKLNYL-NH_2 (2.34) 17% yield

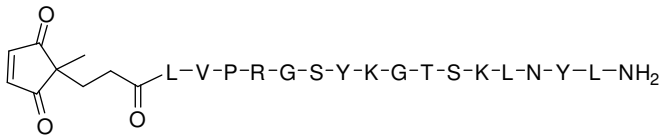

HPLC: purification gradient: 20-40% B; analysis conditions, 25-40% B, t_R = 14.3 min (**Figure E.2.3**).

MALDI-TOF (positive mode, DHB): *m/z* 1959.8 $[M+H]^+$, M calcd. for $C_{91}H_{144}N_{23}O_{25}$ 1959.0.

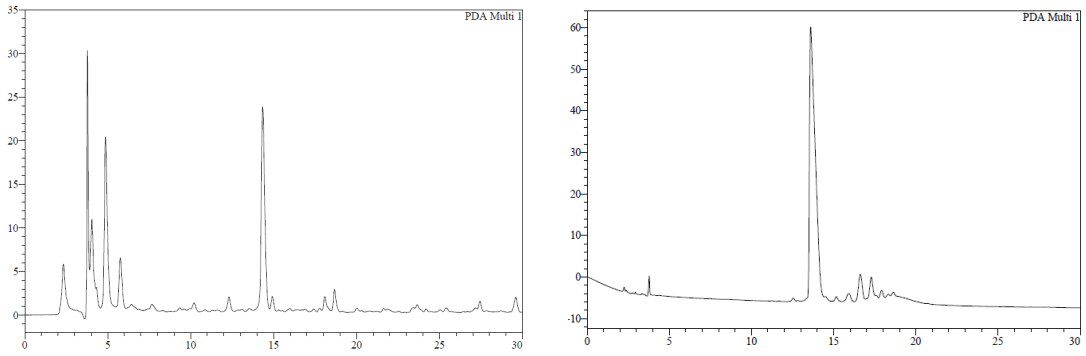

Crude Purified

Figure E.2.3 HPLC traces (280 nm) of crude (left) and purified (right) CPD-derivatized peptide **2.34**.

CPD-Dansil + H-Cys-OMe (2.40)

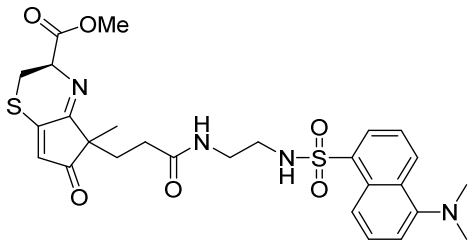

H-Cys-OMe (50 nmol) was reacted with 1.2 equiv of CPD-dansil in water at 37 ºC (0.5 mM peptide concentration). Progress of the reaction was monitored by HPLC-MS (analysis conditions, 0-15% B). The final conjugate (**2.40**) was purified by HPLC (20-70% B) and isolated in 40% yield.

Product characterization:
HPLC: analysis conditions, 20-70% B, t_R = 18.7 and 19.0 min (Figure S20).
HPLC-MS (positive mode): *m/z* 572.8 $[M+H]^+$, M calcd. for $C_{27}H_{32}N_4O_6S_2$ 572.2.

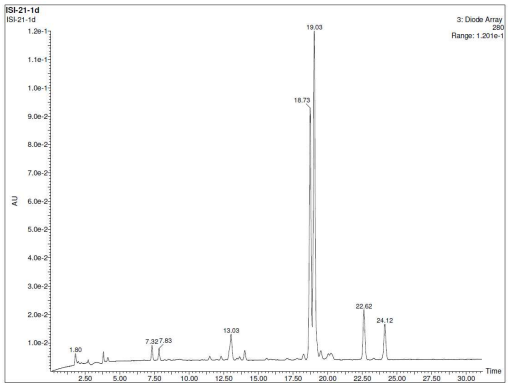

Figure E.2.4 HPLC traces (280 nm) of crude conjugate **2.40**.

H-CYG-NH_2 + CPD-Me_2 (2.41)

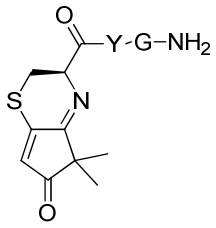

H-Cys-OMe (50 nmol) was reacted with 1.2 equiv of CPD-dansil in water at 37 ºC (0.5 mM peptide concentration). Progress of the reaction was monitored by HPLC-MS (analysis conditions, 0-40% B). The final conjugate (**2.41**) was purified by HPLC (15-40% B) and isolated in 30% yield.

Product characterization:
HPLC: analysis conditions, 15-40% B, t_R = 27.4 min (**Figure E.2.5**).
HPLC-MS (positive mode): *m/z* 572.8 $[M+H]^+$, M calcd. for $C_{27}H_{32}N_4O_6S_2$ 572.2.

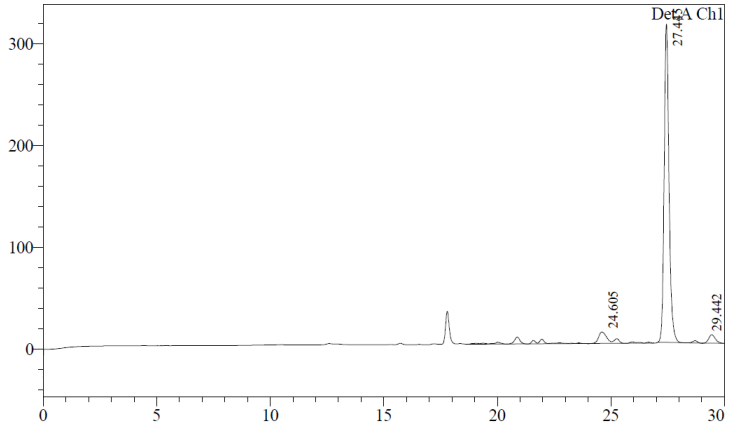

Figure E.2.5 HPLC traces (280 nm) of crude conjugate **2.41**.

H-CSYAKYG-NH_2 + CPD-catgtcat-K-NH_2 (2.44)

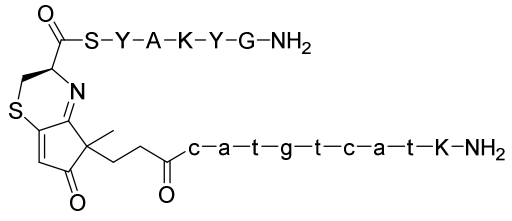

Peptide H-CSYAKYG-NH_2 (**2.38**, 50 nmol) was reacted with 1.2 equiv of CPD-catgtcat-K-NH_2 (**2.34**) in H_2O at 37 ºC (0.5 mM peptide concentration). Progress of the reaction was monitored by HPLC-MS (analysis conditions, 0-15% B, 60 ºC). This reaction seemed to have finished after 2 h (90% conjugation yield, HPLC-based).

The final conjugate (**2.44**) was purified by HPLC (0-30% B, 60 ºC) and isolated in 40% yield.

Product characterization:

HPLC: analysis conditions, 0-15% B, t_R = 26.7 and 27.7 min (**Figure E.2.6**).

MALDI-TOF (positive mode, DHB): *m/z* 3222.4 $[M+H]^+$, M calcd. for $C_{136}H_{178}N_{55}O_{36}$ 3221.3.

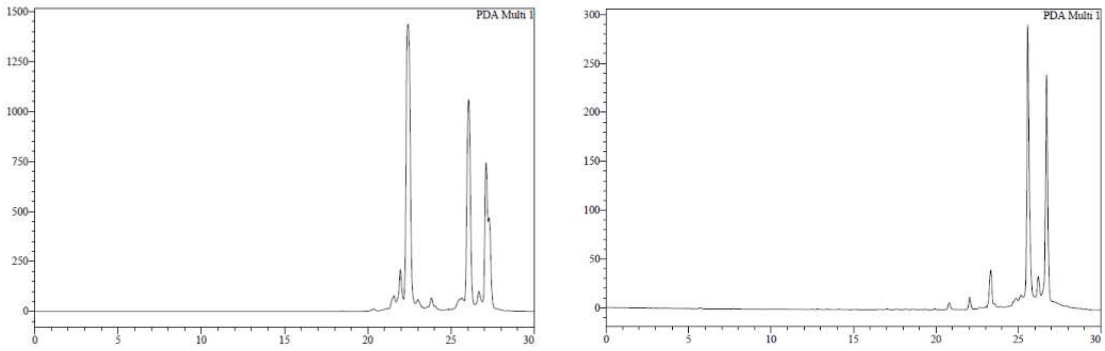

Crude Purified

Figure E.2.6 HPLC traces (260 nm) of crude (left) and purified (right) conjugate **2.34**. Peaks around 22 min in (a) is PNA excess used for conjugation**.**

(9*H*-Fluoren-9-yl)methyl ((*R*)-1-(((1*r*,4*R*)-4-hydroxycyclohexyl)amino)-1-oxo-3-(tritylthio)propan-2-yl)carbamate (2.48)

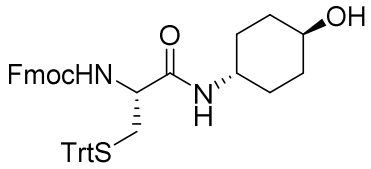

Fmoc-Cys(Trt)-OH (**2.45**, 300 mg, 0.696 mmol) was solved in anh. DCM (10 mL) at low temperature (−10ºC). Subsequently, NMM (168 µL, 1.53 mmol) and IBCF (197 µL, 1.53 mmol) were added under an argon atmosphere. After 30 minutes of preactivaction, a solution of *trans*-4-aminocyclohexanol (**2.47**, 160 mg, 1.392 mmol) in anh. DCM (8 mL) was added. The mixture was left 30 min at −10ºC and then 2 additional hours at rt. Subsequently, the crude was precipitated into 100 mL of hexanes, filtered in a Büchner funnel and washed with H_2O and hexanes successively. If precipitate was left in the mother liquor an additional filtration step would be carried out. Finally, the solid was dissolved in DCM (10 mL), dried over anh. $MgSO_4$, filtered and the solvent removed under reduced pressure to yield the title product as a white solid (451 mg, 95%).

TLC (DCM:MeOH 95:5): R_f= 0.63

MP: 149-152 °C

IR (ATR, Solid): 3290, 1651 cm^{-1}

^{1}H NMR ($CDCl_3$, 400 MHz) δ 7.75 (t, *J* = 6.8 Hz, 2H), 7.56 (d, *J* = 6.5 Hz, 2H), 7.43 – 7.38 (m, 8H), 7.31 – 7.27 (m, 6H), 7.26 – 7.19 (m, 5H), 5.53 (d, *J* = 8.2 Hz, 1H), 5.01 (d, *J* = 7.4 Hz, 1H), 4.37 (d, *J* = 6.7 Hz, 2H), 4.18 (t, *J* = 6.7 Hz, 1H), 3.75 – 3.54 (m, 3H), 2.61 (ddd, *J* = 49.2, 13.1, 6.6 Hz, 2H), 1.99 – 1.86 (m, 4H), 1.42 – 1.29 (m, 2H), 1.19 – 1.06 (m, 2H) ppm.

^{13}C NMR ($CDCl_3$, 101 MHz): δ 169.4, 156.1, 144.5, 143.8, 141.5, 141.4, 128.2, 127.9, 127.2, 127.1, 125.1, 120.2, 69.8, 67.5, 67.1, 47.9, 47.2, 34.1, 33.9, 30.6, 30.5 ppm.

(9*H*-Fluoren-9-yl)methyl ((*R*)-3-(*tert*-butyldisulfanyl)-1-(((1*r*,4*R*)-4-hydroxycyclohexyl)amino)-1-oxopropan-2-yl)carbamate (2.49)

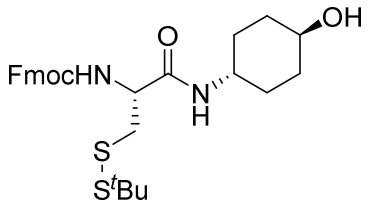

In a round-bottomed flask, Fmoc-Cys(S^{t}Bu)-OH (**2.46**, 300.0 mg, 0.69 mmol) was solved in anh. DCM (10 mL) at −10 ºC and NMM (168 µL, 1.531 mmol) and IBCF (197 µL, 1.53 mmol) were added under an argon atmosphere. After 30 minutes of preactivaction, a solution of *trans*-4-aminocyclohexanol (**2.47**, 160.0 mg, 1.39 mmol) in anh. DCM (8 mL) was added and the reaction left 30 min at −10 ºC and 1 h at rt. Subsequently, the crude was precipitated into 100 mL of hexanes, filtered in a Büchner funnel and washed with distilled H_2O (3 × 30 mL) and hexanes (3 × 30 mL) successively. The mother liquor is filtrated one additional time. The title product as a white solid (498.0 mg, 80%).

^{1}H NMR (DMSO-d$_6$, 400 MHz) δ 7.87 (dd, *J* = 16.3, 7.6 Hz, 3H), 7.73 (d, *J* = 7.4 Hz, 2H), 7.62 (d, *J* = 8.4 Hz, 1H), 7.42 (t, *J* = 7.5 Hz, 2H), 7.32 (t, *J* = 7.4 Hz, 2H), 4.51 (d, *J* = 4.3 Hz, 1H), 4.22 (m, 4H), 3.52 – 3.35 (m, 3H), 3.05 – 2.89 (m, 2H), 1.82 – 1.75 (m, 2H), 1.73 – 1.68 (m, 2H), 1.28 (s, 9H), 1.19 (q, *J* = 11.6, 10.8 Hz, 4H) ppm.

(9*H*-Fluoren-9-yl)methyl ((2*R*)-1-(((1*r*,4*R*)-4-(((2-cyanoethoxy)(diisopropylamino)phosphanyl)oxy)cyclohexyl)amino)-1-oxo-3-(tritylthio)propan-2-yl)carbamate (2.51)

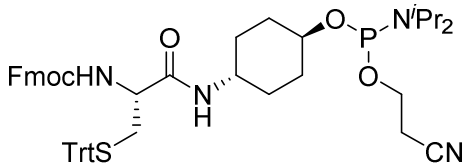

In an ice-cooled round-bottomed flask, **2.48** (481.6 mg, 0.71 mmol) was dissolved in anh. DCM (4 mL) under an argon atmosphere and added DIPEA (369 µL, 2.12 mmol). Afterwards, a solution of chloro(diisopropylamino)-β-cyanoethoxyphosphine (**2.50**, 250 mg, 1.06 mmol) in anh. DCM (1mL) was added dropwise. The mixture was left reacting at low temperature for 1 h and overnight at rt. Once the reaction finished, as assessed by TLC, 0.1 mL of MeOH was added and the solvent removed under low pressure. Subsequently, to the crude was added EtOAc (20 mL), transferred into a separatory funnel and the organic phase washed with aq. sat. $NaHCO_3$ (2 × 20 mL) and brine (2 × 20 mL). The organic layer was dried over anh. $MgSO_4$ and the extract was further purified by silica gel column chromatography eluting with hexanes:EtOAc:NEt_3 mixture from 83:15:2 up to 58:40:2 to afford the title product as a white foam (205 mg, 32%).

^{1}H NMR (CDCl$_3$, 400 MHz): δ 7.73 (t, *J* = 7.0 Hz, 2H), 7.54 (d, *J* = 7.5 Hz, 2H), 7.44 – 7.32 (m, 8H), 7.29 – 7.15 (m, 11H), 5.72 (d, *J* = 7.9 Hz, 1H), 5.18 (d, *J* = 7.5 Hz, 1H), 4.35 (d, *J* = 6.6 Hz, 2H), 4.17 (t, *J* = 7.0 Hz, 1H), 3.83 – 3.52 (m, 6H), 2.73 – 2.52 (m, 4H), 2.00 – 1.83 (m, 3H), 1.54 – 1.39 (m, 2H), 1.25 – 1.11 (m, 16H) ppm.

^{13}C NMR ($CDCl_3$, 101 MHz) δ 169.15, 144.34, 143.63, 141.28, 129.56, 128.07, 127.75, 127.06, 126.90, 124.98, 124.94, 120.00, 117.64, 71.86, 71.68, 67.33, 66.92, 58.20, 58.02, 54.14, 47.57, 47.08, 43.11, 42.99, 34.00, 32.37, 30.36, 24.69, 24.61, 24.50, 24.42, 22.51, 22.39, 20.39, 20.32 ppm.

^{31}P NMR ($CDCl_3$, 162 MHz) δ 145.94 ppm.

ESI-HRMS (positive mode): *m/z*: 905.3815 $[M+Na]^+$, M calcd for $C_{52}H_{59}N_4NaO_5PS$ 905.3836.

(9*H*-Fluoren-9-yl)methyl ((2*R*)-3-(*tert*-butyldisulfanyl)-1-(((1*r*,4*R*)-4-(((cyanomethoxy)(diisopropylamino)phosphanyl)oxy)cyclohexyl)amino)-1-oxopropan-2-yl)carbamate (2.52)

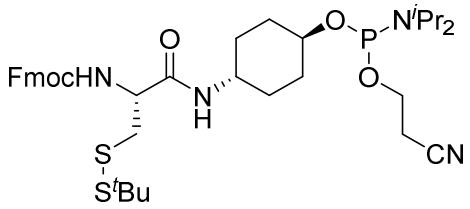

To an ice-cooled solution of **2.49** (372.9 mg, 0.70 mmol) in anh. DCM (10 mL) under an argon atmosphere was added DIPEA (369 µL, 2.12 mmol) and a solution of chloro(diisopropylamino)-β-cyanoethoxyphosphine (**2.50**, 250 mg, 1.059 mmol) in anh. DCM (1mL) dropwise. Afterwards, the mixture was left reacting at low temperature for 1 h and 2 additional more hours at rt. Once the reaction finished, as assessed by TLC, 0.1 mL of MeOH was added and the solvent removed under low pressure. Afterwards, the crude was dissolved in EtOAc (20 mL) and washed with aq. sat. $NaHCO_3$ (2 × 20 mL) and brine (2 × 20 mL). The organic layer was dried over anh. $MgSO_4$, filtered and the solvent removed under vacuum. The extract was further purified by silica gel column chromatography eluting with hexane/EtOAc/NEt_3 mixtures from 83:15:2 to 58:40:2. The title compound was obtained as a white foam (226.2 mg, 44%)

^{1}H NMR (CD_3CN, 400 MHz): δ 7.85 (d, *J* = 8.0 Hz, 2H), 7.70 (d, *J* = 7.5 Hz, 2H), 7.44 (t, J = 8 Hz, 2H), 7.36 (td, *J* = 7.5, 1.2 Hz, 2H), 6.60 (d, *J* = 8.1 Hz, 1H), 6.08 (d, *J* = 8.3 Hz, 1H), 4.44 – 4.22 (m, 4H), 3.84 – 3.55 (m, 6H), 2.65 (t, *J* = 6.0 Hz, 2H), 2.02 – 1.85 (m, 4H), 1.53 – 1.38 (m, 2H), 1.34 (s, 9H), 1.30 – 1.25 (m, 2H), 1.19 (d, *J* = 1.9 Hz, 6H), 1.18 (d, *J* = 1.9 Hz, 6H) ppm.

^{13}C NMR (CD_3CN, 101 MHz): δ 169.28, 156.13, 144.36, 141.43, 138.21, 129.21, 128.51, 128.02, 127.45, 127.42, 125.55, 125.50, 120.30, 118.93, 72.11, 71.94, 66.75, 58.54, 58.35, 54.89, 32.66, 30.07, 29.37, 24.26, 24.19, 24.12, 24.05, 20.37, 20.30 ppm.

^{31}P NMR (CD_3CN, 162 MHz): δ 145.42 ppm.

H-Cys(Trt)-NH-cHex-O-P(O)(O^-)P-O-$^{5'}$dT$_{10}$ (2.55)

dT_{10}-resin was automatically assembled at the 1 µmol-scale using standard phosphoramidite chemistry. For the introduction of **2.51** BTT-mediated coupling (0.1 M solution in anh. ACN, 10 min coupling time) was employed.

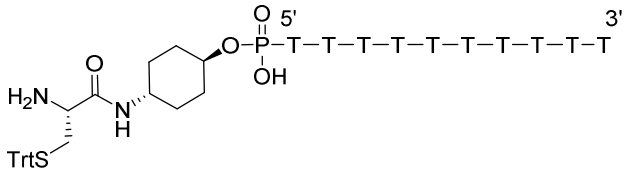

No purification was required (see Figure S22). Yield: 70%.

HPLC: analysis conditions, 10-50%B, t_R = 22.8 min (**Figure E.2.7**).

MALDI-TOF (negative mode, THAP/CA): *m/z* 3498.9 $[M-H]^-$, M calcd. for $C_{128}H_{161}N_{22}O_{72}P_{10}S$ 3499.7.

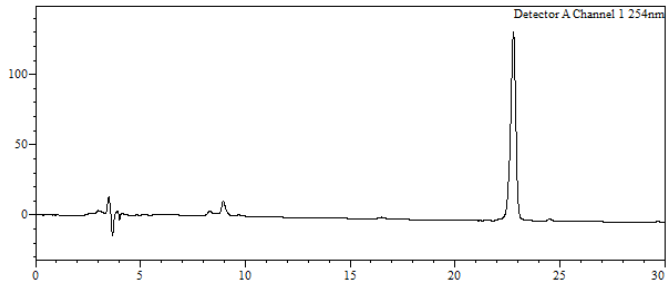

Figure E.2.7 HPLC trace (254 nm) of crude oligonucleotide H-Cys(Trt)-NH-cHex-O-P(O)(O^-)P-O-$^{5'}dT_{10}$.

H-Cys(S^{t}Bu)-NH-cHex-O-P(O)(O^-)P-O-$^{5'}dT_{10}$ (2.56)

dT_{10}-resin was automatically assembled at the 1 µmol-scale using standard phosphoramidite chemistry. For the introduction of **2.52** BTT-mediated coupling (0.1 M solution in anh. ACN, 10 min coupling time) was employed.

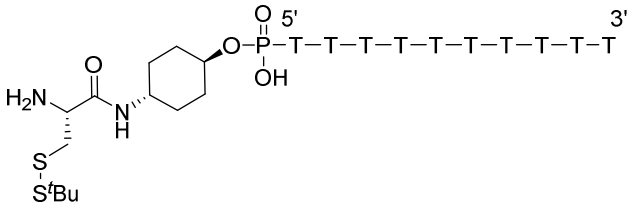

No purification was required (see F**igure E.2.8**). Yield: 80%.

HPLC: analysis conditions, 0-50 % B, t_R = 15.0 min (**Figure E.2.8**).

MALDI-TOF (negative mode, THAP/CA): *m/z* 3345.1 $[M-H]^-$, M calcd. for $C_{113}H_{155}N_{22}O_{72}P_{10}S_2$ 3345.6.

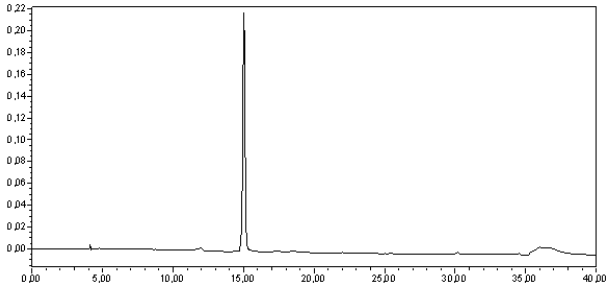

Figure E.2.8 HPLC profile (254 nm) of crude oligonucleotide H-Cys(S^{t}Bu)-NH-cHex-O-P(O)(O$^-$)P-O-$^{5'}$dT$_{10}$.

Cysteine deprotection and Cys-oligonucleotides characterization

Deprotection of Cys(S^{t}Bu)-oligonucleotides:

Cysteine deprotection was carried out by adding TCEP (500 equiv.) and H_2O (400 µL) to the lyophilized oligonucleotide (200 nmol; crude or purified, depending on the quality of the crude). The pH was adjusted to 5 by adding 5% aq NaOH, and the mixture was stirred overnight at 37 °C. Gel filtration of the resulting crude (Sephadex G-25, elution with H_2O, 3 mL/min) allowed most of the excess TCEP to be removed. Finally, the Cys-oligonucleotide was purified by reversed-phase HPLC.

Deprotection of Cys(Trt)-oligonucleotides:

$AgNO_3$ (100 nmol, 10 µL of a 10 mM) was added to a solution of the oligonucleotide (20 nmol) in H_2O (30 µL), and the mixture was reacted for 45 min at 37 °C. Subsequentially, DTT was added (140 nmol, 14 µL, 10 mM solution), and the mixture left to react for an additional 30 min (37 °C). Afterwards centrifugation and decantation, the supernatant was cleaned by gel filtration (Sephadex G-25, elution with H_2O, 3 mL/min) and HPLC purification.

H-Cys-NH-cHex-O-P(O)(O$^-$)P-O-$^{5'}$dT$_{10}$ (2.57)

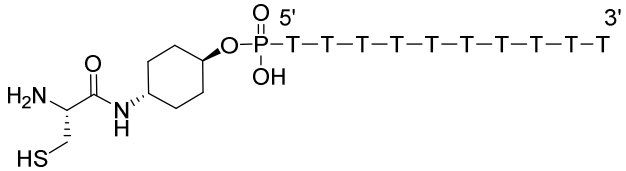

Purification gradient: 0-50% B. Yield: 30%.

HPLC: analysis conditions, 0-50% B, t_R = 16.0 min (**Figure E.2.9**).

MALDI-TOF (negative mode, THAP/CA): *m/z* 3257.2 [M-H]$^-$, M calcd. for $C_{109}H_{147}N_{22}O_{72}P_{10}S$ 3257.6.

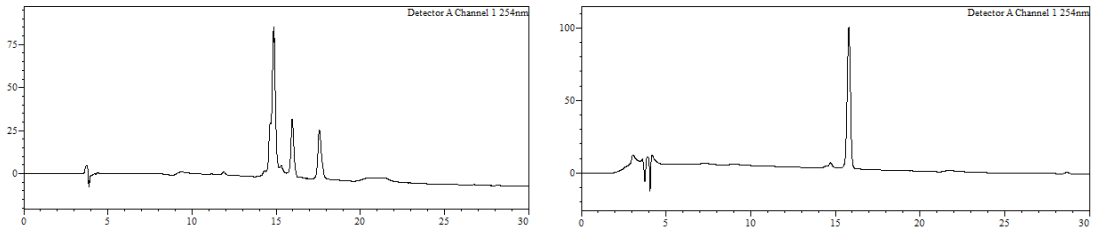

Crude Purified

Figure E.2.9 HPLC profiles (254 nm) of oligonucleotide **2.57**, crude (left) and purified (right).

Synthesis of peptide-oligonucleotide conjugates

A mixture containing Cys-oligonucleotide and CPD-peptide (1.2 equiv.) was prepared (either by mixing solutions of each of the reagents, or by dissolving one reagent and pouring this solution into an eppendorf containing a lyophilized of the other reagent) making the oligonucleotide concentration 0.5 mM. This mixture was reacted at 37 ºC, and the reaction progress was monitored by HPLC. Formation of the conjugate was assessed by the appearance of two new peaks absorbing at 330 nm (absorption maximum of the stable CPD-1,2-aminothiol adduct). The target conjugate was purified by HPLC.

No differences were observed when the conjugation reaction was carried out with Cys-oligonucleotides of different origin, that is, obtained from either Cys(S^{t}Bu)- or Cys(Trt)-oligonucleotides.

H-Cys-dT$_{10}$ + CPD-Me$_2$ (2.58)

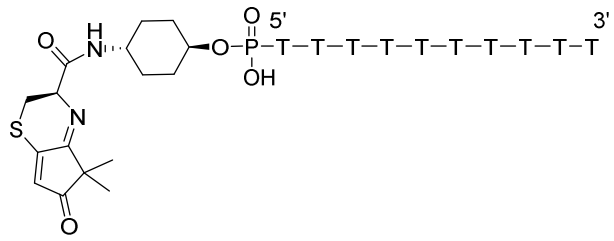

Purification gradient: 0-50% B. Yield: 20%.

HPLC: analysis conditions, 0-50% B, t_R = 17.5 min (**Figure E.2.10**).

MALDI-TOF (negative mode, THAP/CA): *m/z* 3364.8 [M-H]$^-$, M calcd. for $C_{116}H_{151}N_{22}O_{73}P_{10}S$ 3361.6.

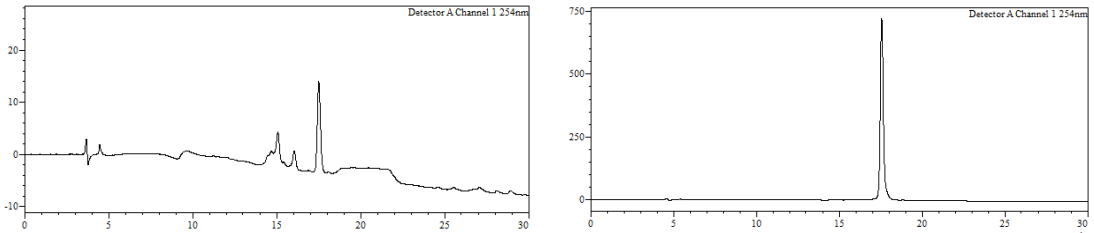

Crude Purified

Figure E.2.10 HPLC profiles (254 nm) of conjugate crude (left) and purified (right).

H-Cys-dT$_{10}$ + CPD-COOH (2.59)

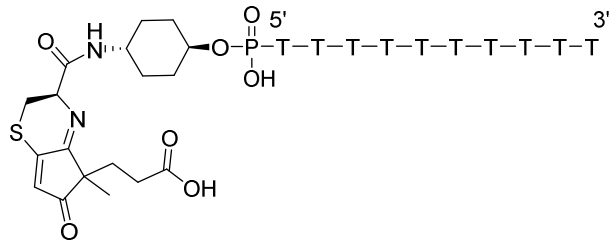

Purification gradient: 0-50% B. Yield: 30%.

HPLC: analysis conditions, 0-50% B, t_R = 15.8 and 16.1 min (**Figure E.2.11**).

MALDI-TOF (negative mode, THAP/CA): *m/z* 3422.1 $[M-H]^-$, M calcd. for $C_{118}H_{153}N_{22}O_{75}P_{10}S$ 3419.6.

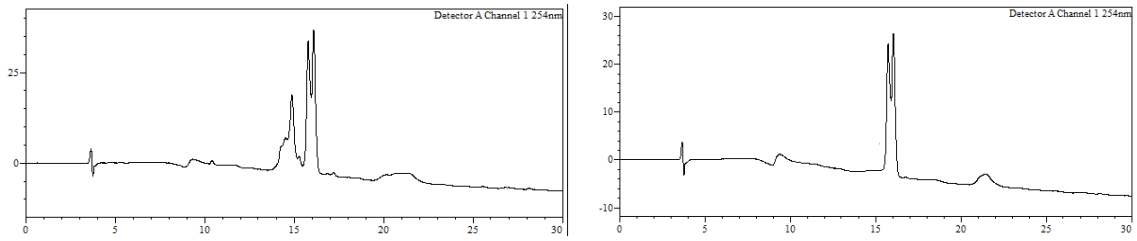

Crude Purified

Figure E.2.11 HPLC profiles (254 nm) of conjugate, crude (left) and purified (right).

H-Cys-dT$_{10}$ + CPD-GRGSYEAYK-NH$_2$ (2.60)

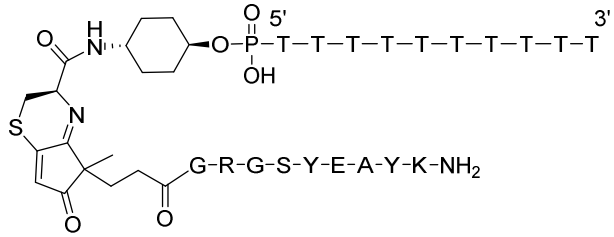

Purification gradient: 10-60% B. Yield: 50%.

HPLC: analysis conditions, 10-60% B, t_R = 11.1 and 11.5 min (**Figure E.2.12**).

MALDI-TOF (negative mode, THAP/CA): *m/z* 4433.2 $[M-H]^-$, M calcd. for $C_{163}H_{219}N_{36}O_{88}P_{10}S$ 4430.1.

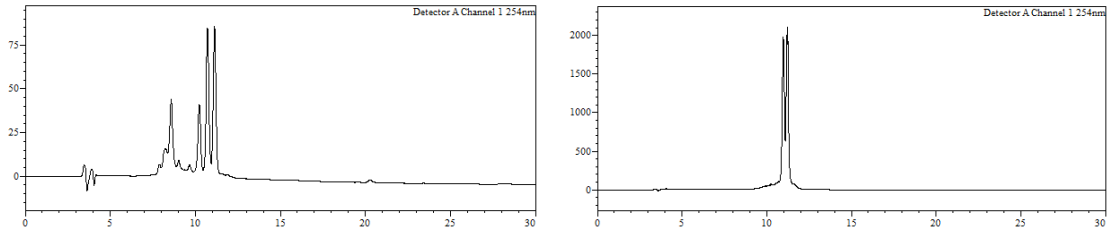

Crude Purified

Figure E.2.12 HPLC profiles (254 nm) of conjugate, crude (left) and purified (right).

H-Cys(Trt)-NH-cHex-O-P(O)(O$^-$)-O-$^{5'}$dCAGATGTCAC (2.61)

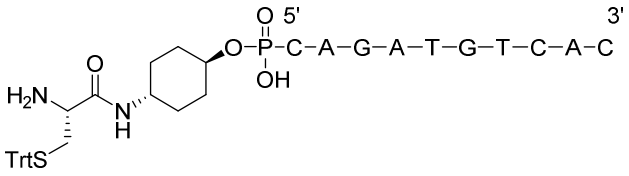

No purification was required (**Figure E.2.13**). Yield: 72%

HPLC: analysis conditions, 10-40% B, t_R = 23.4 min (**Figure E.2.13**).

MALDI-TOF (negative mode, THAP/CA): *m/z* 3531.1 $[M-H]^-$, M calcd. for $C_{125}H_{153}N_{40}O_{61}P_{10}S$ 3531.7.

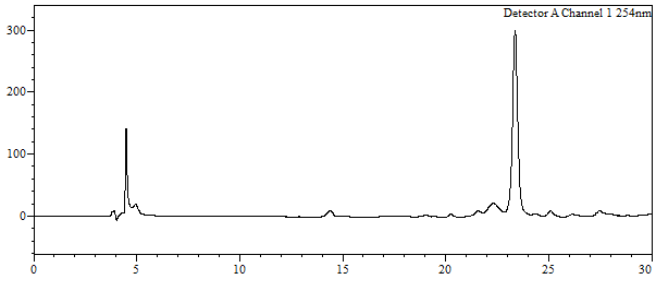

Figure E.2.13 HPLC profile (254 nm) of crude oligonucleotide H-Cys(Trt)-NH-cHex-O-P(O)(O$^-$)P-O-$^{5'}$dCAGATGTCAC.

H-Cys(S^{t}Bu)-NH-cHex-O-P(O)(O$^-$)-O-$^{5'}$dCAGATGTCAC (2.62)

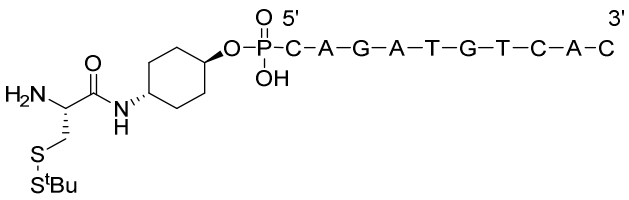

No purification was required (**Figure E.2.14**). Yield: 71%

HPLC: analysis conditions, 10-40% B, t_R = 11.0 min (**Figure E.2.14**)

MALDI-TOF (negative mode, THAP/CA): *m/z* 3375.1 $[M-H]^-$, M calcd. for $C_{110}H_{147}N_{40}O_{61}P_{10}S_2$ 3377.6.

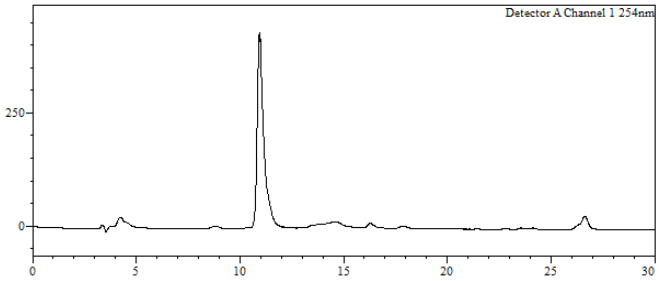

Figure E.2.14 HPLC profile (254 nm) of crude oligonucleotide H-Cys(S^{t}Bu)-NH-cHex-O-P(O)(O$^-$)P-O-$^{5'}$dCAGATGTCAC.

· H-Cys(Trt)-NH-cHex-O-P(O)(O$^-$)-O-$^{5'}$dCAGCAGCAGAGTCTTCATCAT (2.62)

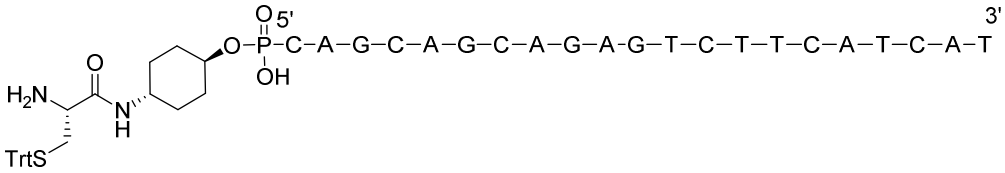

Purification gradient: 10-40% B. Yield: 32%

HPLC: analysis conditions, 10-40% B, t_R = 24.5 min (**Figure E.2.15**)

MALDI-TOF (negative mode, THAP/CA): *m/z* 6905.7 $[M-H]^-$, M calcd. for $C_{232}H_{288}N_{80}O_{127}P_{21}S$ 6908.3.

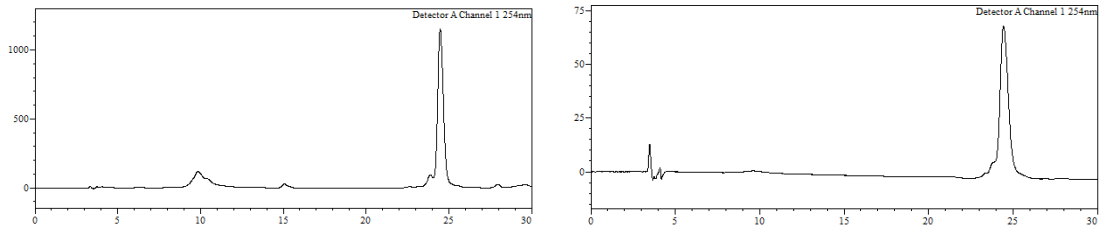

Crude Purified

Figure E.2.15 HPLC profiles (254 nm) of oligonucleotide H-Cys(Trt)-NH-cHex-O-P(O)(O$^-$)P-O-$^{5'}$dCAGCAGCAGAGTCTTCATCAT, crude (left) and purified (right)

H-Cys(S^{t}Bu)-NH-cHex-O-P(O)(O$^-$)-O-$^{5'}$dCAGCAGCAGAGTCTTCATCAT (2.63)

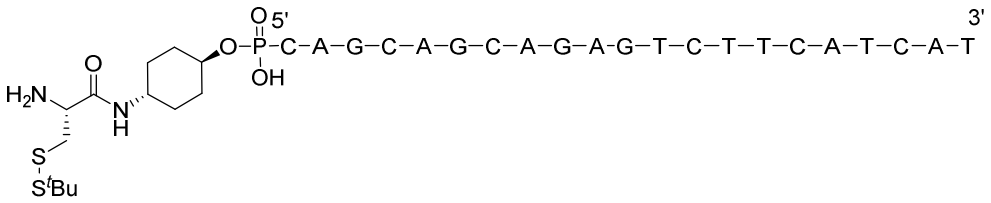

Purification gradient: 10-40% B . Yield: 28%

HPLC: analysis conditions, 10-40% B, t_R = 11.8 min (**Figure E.2.16**).

MALDI-TOF (negative mode, THAP/CA): *m/z* 6753.0 [M-H]$^-$, M calcd. for $C_{217}H_{282}N_{80}O_{127}P_{21}S_2$ 6754.2.

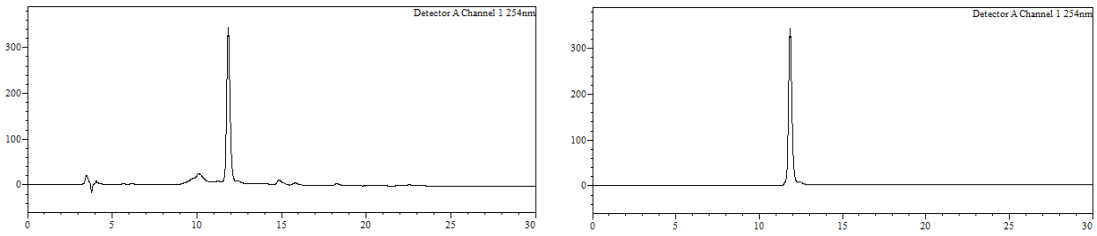

Crude Purified

Figure E.2.16 HPLC profiles (254 nm) of oligonucleotide H-Cys(S^{t}Bu)-NH-cHex-O-P(O)(O$^-$)P-O-$^{5'}$dCAGCAGCAGAGTCTTCATCAT, crude (left) and purified (right).

H-Cys-NH-cHex-O-P(O)(O$^-$)-O-$^{5'}$dCAGATGTCAC (2.64)

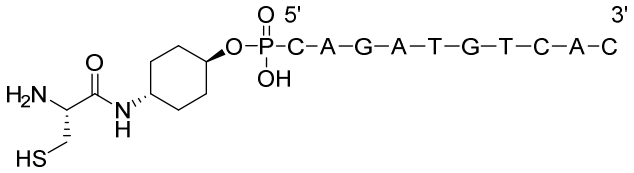

Purification gradient: 0-25% B. Yield: 58%.

HPLC: analysis conditions, 0-25 % B, 60 ºC t_R = 19.8 min (**Figure E.2.17**).

MALDI-TOF (negative mode, THAP/CA): *m/z* 3290.1 [M-H]$^-$, M calcd. for $C_{106}H_{139}N_{40}O_{61}P_{10}S$ 3289.6.

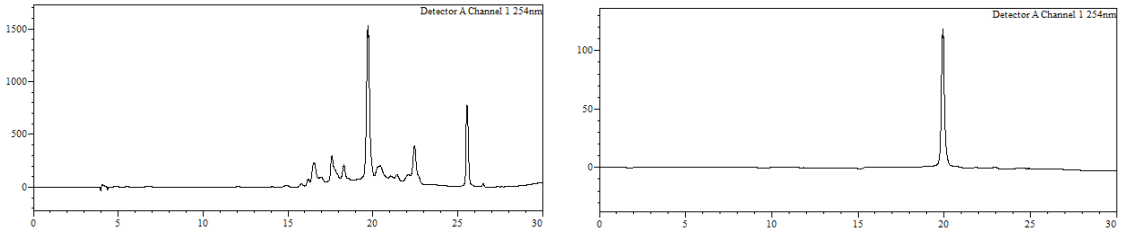

Crude Purified

Figure E.2.17 HPLC profiles (254 nm) of oligonucleotide 30, crude (left) and purified (right).

H-Cys-NH-cHex-O-P(O)(O$^-$)-O-$^{5'}$dCAGCAGCAGAGTCTTCATCAT (2.65)

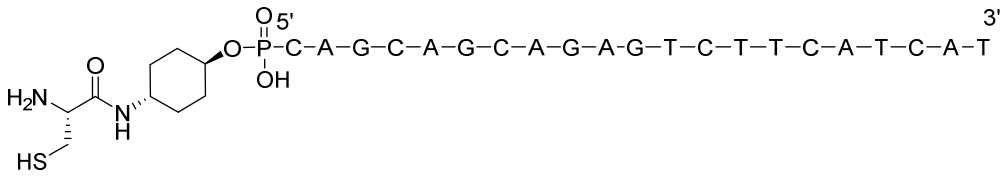

Purification: 0-30% B, 60 ºC. Yield: 50%

HPLC: analysis conditions, 0-30% B, 60 ºC t_R = 22.5 min (**Figure E.2.18**).

MALDI-TOF (negative mode, THAP/CA): *m/z* 6662.3 [M-H]$^-$, M calcd. for $C_{213}H_{274}N_{80}O_{127}P_{21}S$ 6666.2.

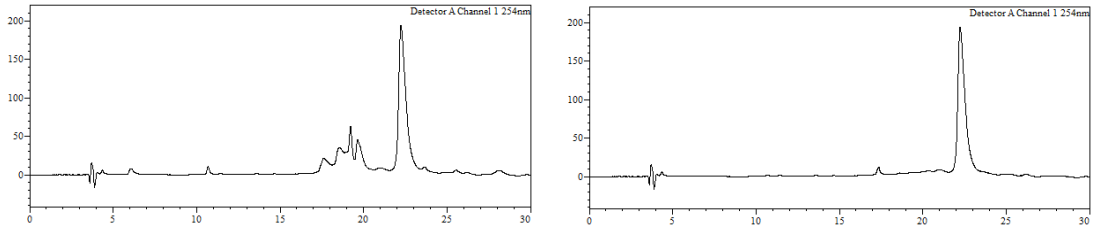

Crude Purified

Figure E.2.18 HPLC profiles (254 nm) of oligonucleotide 31, crude (left) and purified (right).

H-Cys-$^{5'}$dCAGATGTCAC (30) + CPD-GRGSYEAYK-NH$_2$ (2.66)

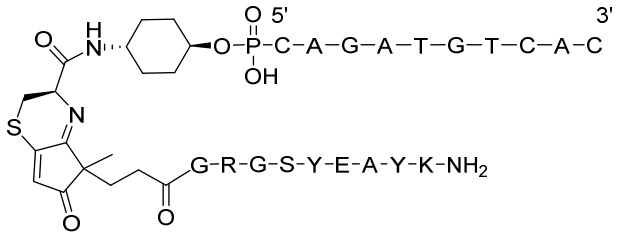

Purification gradient: 5-35% B. Yield: 60%.

HPLC: analysis conditions, 5-35% B, 60 ºC t_R = 23.4 and 24.3 min (**Figure E.2.19**).

MALDI-TOF (negative mode, THAP/CA): *m/z* 4466.4 [M-H]$^-$, M calcd. for $C_{160}H_{211}N_{54}O_{77}P_{10}S$ 4462.1.

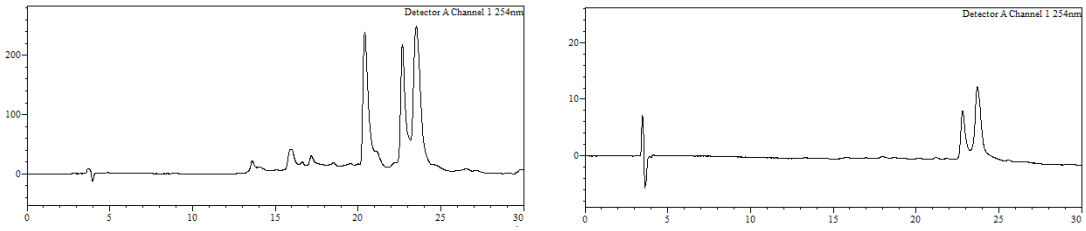

Crude Purified

Figure E.2.19 HPLC profiles (254 nm) of conjugate, crude (left) and purified (right).

H-Cys-$^{5'}$dCAGATGTCAC (30) + CPD-LVPRGSYKGTSKLNYL-NH_2 (2.67)

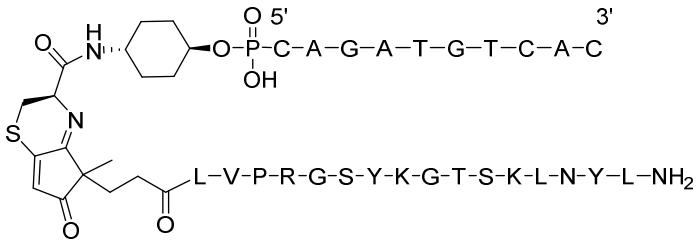

Purification gradient: 30-70% B, 60 ºC. Yield: 20%

HPLC: analysis conditions, 20-50% B, 60 ºC t_R = 24.8 and 25.3 min (**Figure E.2.20**).

MALDI-TOF (negative mode, THAP/CA): *m/z* 5225.1 $[M-H]^-$, M calcd. for $C_{197}H_{278}N_{63}O_{85}P_{10}S$ 5227.6.

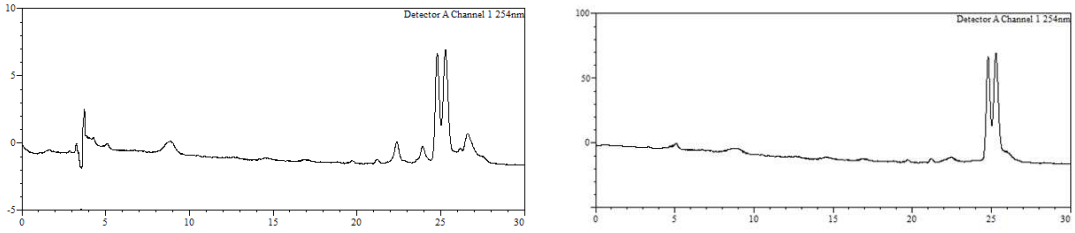

Crude Purified

Figure E.2.20 HPLC profiles (254 nm) of conjugate, crude (left) and purified (right).

H-Cys-$^{5'}$dCAGCAGCAGAGTCTTCATCAT (31) + CPD-GRGSYEAYK-NH_2 (2.68)

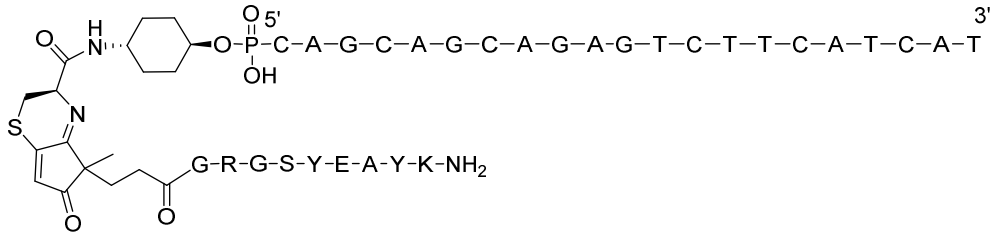

Purification gradient: 10-40% B. Yield: 44%.

HPLC: analysis conditions, 10-40% B, 60 ºC t_R = 11.9 and 12.3 min (**Figure E.2.21**).

MALDI-TOF (negative mode, THAP/CA): *m/z* 7832.4 $[M-H]^-$, M calcd. for $C_{267}H_{346}N_{94}O_{143}P_{21}S$ 7838.7.

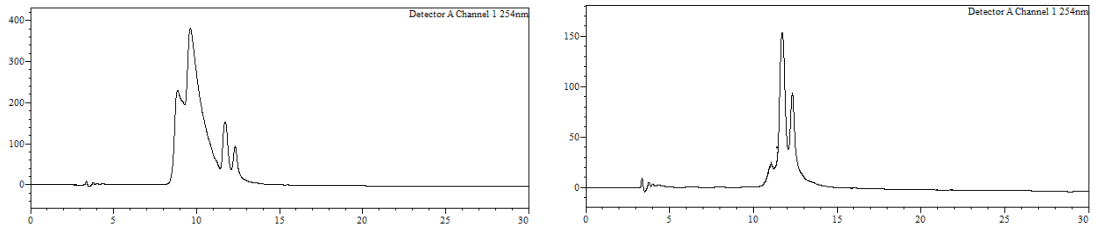

Crude Purified

Figure E.2.21 HPLC profiles (254 nm) of conjugate, crude (left) and purified (right).

H-Cys-$^{5'}$dCAGCAGCAGAGTCTTCATCAT + CPD-LVPRGSYKGTSKLNYL-NH_2 (2.69)

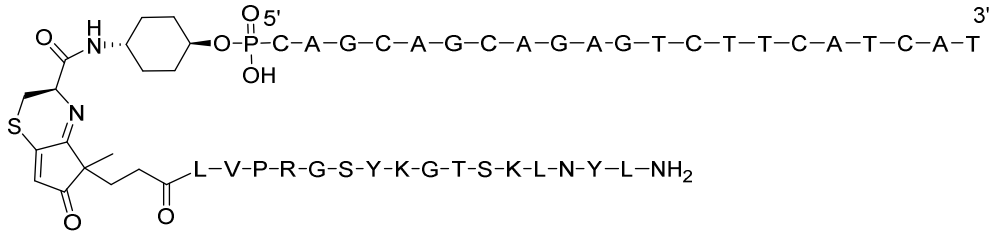

Purification gradient: 30-70% B. Yield: 33%.
HPLC: analysis conditions, 10-40% B, 60 ºC t_R = 20.0 min (**Figure E.2.22**).
MALDI-TOF (negative mode, THAP/CA): *m/z* 8601.3 $[M-H]^-$, M calcd. for $C_{304}H_{413}N_{103}O_{151}P_{21}S$ 8604.2.

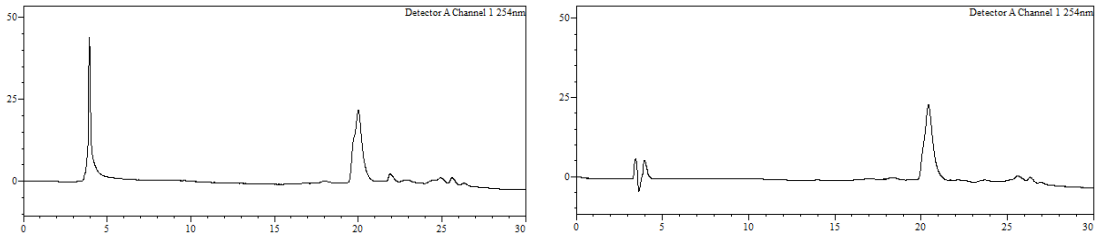

Crude Purified

Figure E.2.22 HPLC profiles (254 nm) of conjugate, crude (left) and purified (right).

Conjugation of H-CWGRGC-NH_2 with CPD-biotin and Mal-gtttcK-NH_2 (2.82)

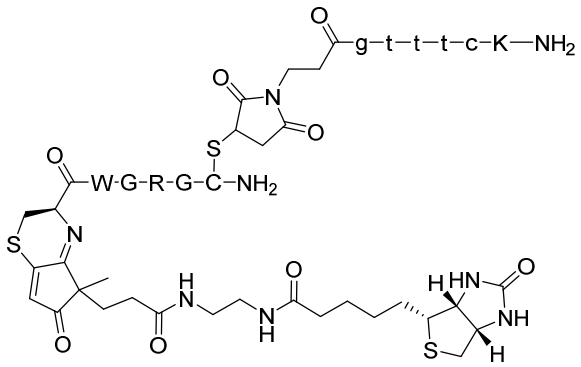

Peptide H-CWGRGC-NH_2 (**2.80**, 50 nmol) was dissolved in water (95 µL) and reacted with CPD-Biotin (**2.23**, 4.46 µL of a 13.45 mM, 60 nmol) at 37 ºC (0.5 mM peptide concentration). Subsequently, Mal-gtttc-NH_2 (**2.81**, 50 µL, 3 mM, 150 nmol) was added and the resulting mixture left reacting for an additional hour. The final conjugate was purified by HPLC and isolated in 29% yield.

Product characterization:

HPLC: analysis conditions, 0-50% B, t_R = 13.4 min and 13.9 min (**Figure E.2.23**).

MALDI-TOF (positive mode, DHB): *m/z* (both products) 2747.6 $[M+H]^+$, M calcd. for $C_{115}H_{155}N_{43}O_{32}S_3$ 2747.1.

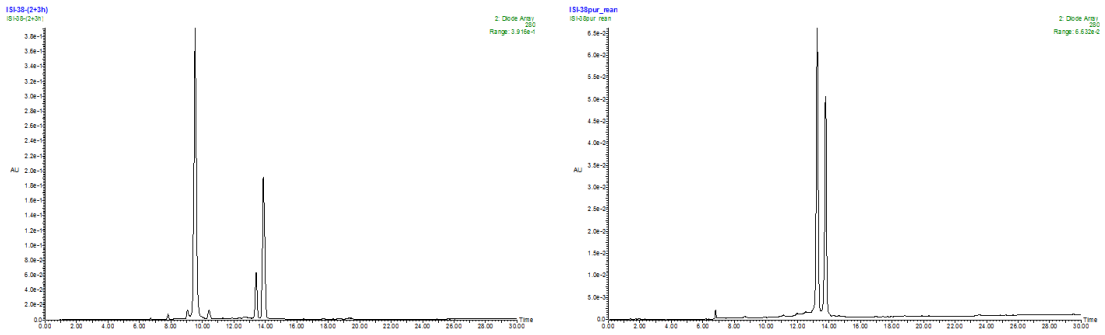

Crude Purified

Figure E.2.23 HPLC profiles (254 nm) of double conjugate crude (left) and purified (right).

Conjugation of H-CWGRGC-NH_2 with CPD-catgtcatK-NH_2 and 1-[2-(maleimido)ethyl]-4-[2-(3,4-dihydro-2*H*-1-benzopyran-6-yl)-5-oxazolyl]pyridinium triflate → Conjugate (2.84)

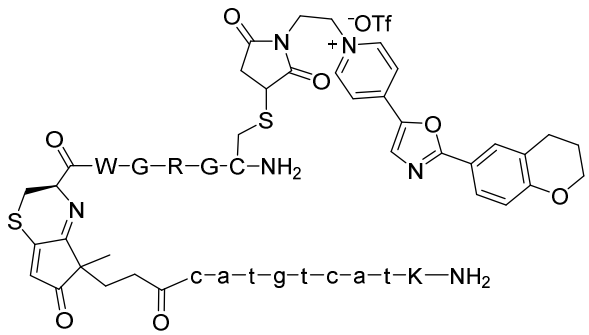

Peptide H-CWGRGC-NH_2 (**2.80**, 50 nmol) was reacted with 1.2 equiv of CPD-catgtcatK-NH_2 (**2.34**, 60 nmol) in MQ-H_2O (100 µL) at 37 ºC (0.5 mM peptide concentration). Subsequently, the maleimido-fluorophore (15 µL, 10 mM, 150 nmol) was added and the mixture left reacting for an additional hour.

The final conjugate was purified by HPLC and isolated in 34% yield.

Product characterization:

HPLC: analysis conditions, 0-30% B, 60 ºC t_R = 28.5 min and 29.8 min (**Figure E.2.24**).

ESI-HRMS (positive mode): *m/z* (both products) 3513.31 $[M+H]^+$, M calcd. for $C_{151}H_{188}N_{60}O_{38}S_2$ 3513.4.

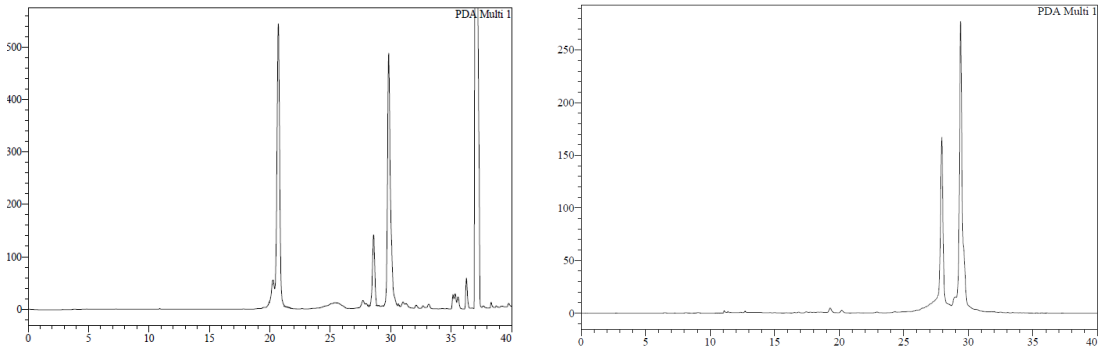

Crude Purified

Figure E.2.24 HPLC profiles (254 nm) of conjugate crude (left) and purified (right).

(*S*)-2-((((9*H*-Fluoren-9-yl)methoxy)carbonyl)amino)-6-(pent-4-ynamido)hexanoic acid (2.91)

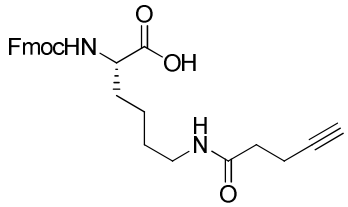

To an ice-cooled solution of 4-pentynoic acid (**2.90**, 87 mg, 0.99 mmol) in anh. DCM (5 mL), NMM (98 µL, 0.89 mmol) and IBCF (115 µL, 0.99 mmol) were added and the mixture left stirring for 20 minutes. Afterwards, a solution of Fmoc-Lys-OH (**2.87**, 300 mg, 0.82 mmol) in anh. DCM (3 mL) was added and the mixture left for 1 hour at low temperature and overnight at rt. Thereafter, the solvent was removed under low pressure, the crude dissolved in EtOAc (20 mL) and transferred into a separatory funnel. The organic phase was washed with aq. HCl 5% (3 × 20 mL) and brine (3 × 20 mL), dried over anh. $MgSO_4$, filtered and the solvent removed under vacuum. The resulting extract was purified by silica gel column chromatography eluting with EtOAc:DCM:AcOH from 68:30:2 up to 98:0:2. The title compound was obtained as a white solid (170 mg, 47%).

TLC (EtOAc/AcOH 98:2) R_f = 0.41

^{1}H NMR ($CDCl_3$, 400 MHz) δ 7.75 (d, *J* = 7.6 Hz, 2H), 7.59 (t, *J* = 6.5 Hz, 2H), 7.38 (t, *J* = 8 Hz, 2H), 7.29 (t, *J* = 7.5 Hz, 2H), 5.95 (t, *J* = 5.6 Hz, 1H), 5.72 (d, *J* = 6.9 Hz, 1H), 4.41 – 4.34 (m, 2H), 4.20 (t, *J* = 7.0 Hz, 1H), 3.27 (td, *J* = 13.9, 13.3, 6.7 Hz, 2H), 2.50 (td, *J* = 7.3, 6.7, 1.8 Hz, 2H), 2.37 (t, *J* = 6.8 Hz, 2H), 2.00 (t, *J* = 2.6 Hz, 1H), 1.95 – 1.85 (m, 2H), 1.58 – 1.51 (m, 2H), 1.47 – 1.38 (m, 2H) ppm.

^{13}C NMR ($CDCl_3$, 101 MHz) δ 177.42, 171.91, 156.33, 143.68, 141.27, 127.71, 127.08, 127.06, 125.10, 119.97, 82.80, 69.68, 67.08, 54.73, 47.12, 39.03, 35.34, 31.68, 28.86, 22.06, 14.96 ppm.

ESI-HRMS (negative mode): *m/z* 447.1933 $[M-H]^-$; M calcd for $C_{26}H_{27}N_2O_5$ 447.1925.

H-CSYAK*YG-NH$_2$ (2.92)

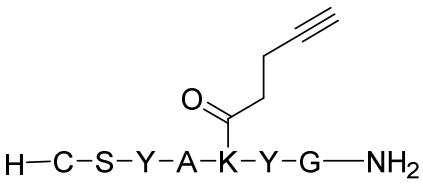

HPLC: analysis conditions, 0-40% B, t_R = 15.7 min (**Figure E.2.25**).
Yield: 20%
HPLC-MS (ESI, positive mode): *m/z* 870.2 $[M+H]^+$, M calcd. for $C_{40}H_{55}N_9O_{11}S$ 869.4

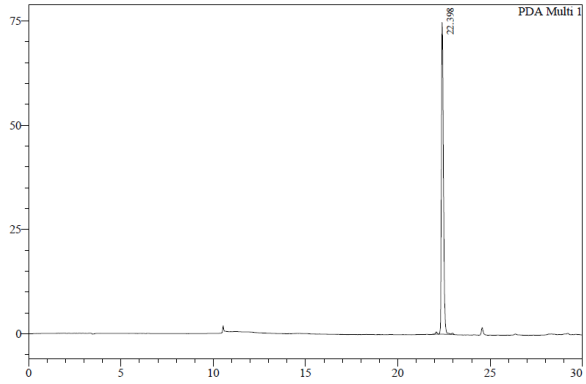

Figure E.2.25 HPLC profiles (280 nm) of crude peptide.

M-20: CPD-COOH + H-CSYAK*YG-NH$_2$ (2.93)

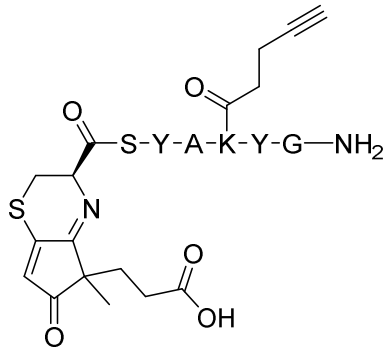

To a solution of peptide H-CSYA**K***YG-NH$_2$ (**2.92**, 400 nmol) in MQ-H$_2$O (752 µL) was added a solution of CPD-COOH (**2.20**, 48 µL, 10 mM, 480 nmol) in MQ-H$_2$O to achieve a final peptide concentration of 0.5 mM. The reaction was left 3 h at 37 ºC, and monitored by HPLC. The conjugate was purified by reversed phase HPLC.

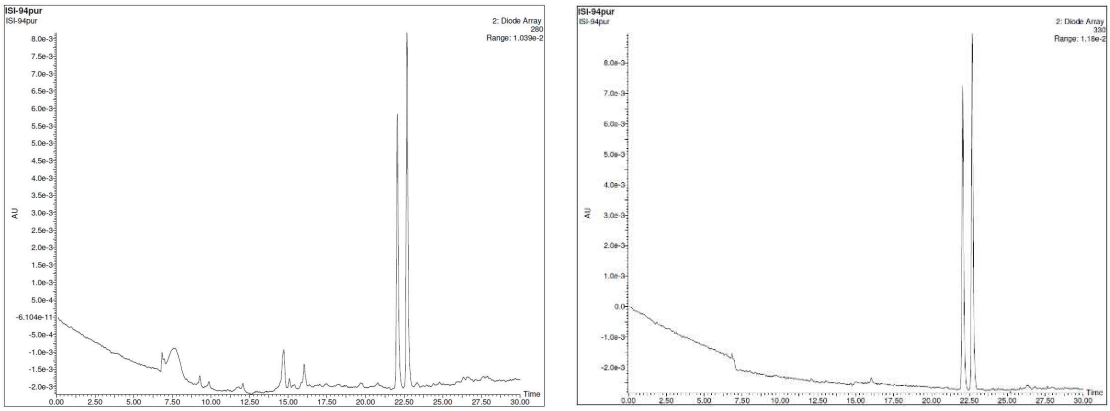

HPLC trace at 280 nm HPLC trace at 330 nm

Figure E.2.26 HPLC profiles (280 nm) of conjugate crude (left) and purified (right).

HPLC-MS: Analysis conditions, 0-50% B, t_R = 22.1 and 22.7 min (**Figure E.2.26**).

Purification gradient: 0-50% B. t_R = 22.1 and 22.6 min Yield: 50%.

HPLC-MS (ESI, positive mode): *m/z* 1032.5 $[M+H]^+$, M calcd. For $C_{49}H_{61}N_9O_{14}S$ 1031.4.

(M-20 CPD-COOH + H-CSYAK*YG-NH2) + AZT (2.95)

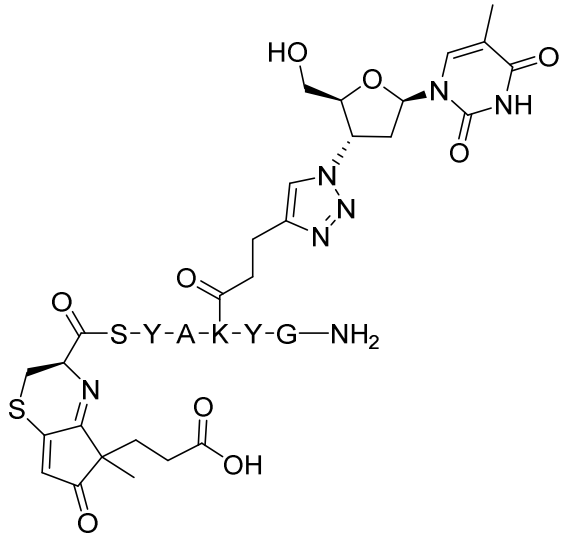

To a solution of conjugate **2.93** (80 nmol) in MQ-H_2O (40 µL) was added $CuSO_4$ (16 µL, 5 mM, 80 nmol) in MQ-H_2O, NaAsc (24 µL, 80 mM, 1920 nmol) in MQ-H_2O, a solution of TBTA (16 µL, 5 mM, 80 nmol) in HPLC-MeOH and a solution of AZT (**2.94**, 64 µL, 5 mM, 320 nmol) in MQ-H_2O to achieve a final conjugate concentration of 0.5 mM. The mixture was reacted in a microwave oven for 1 h at 90 ºC and monitored by HPLC. The conjugate was purified by reversed phase HPLC.

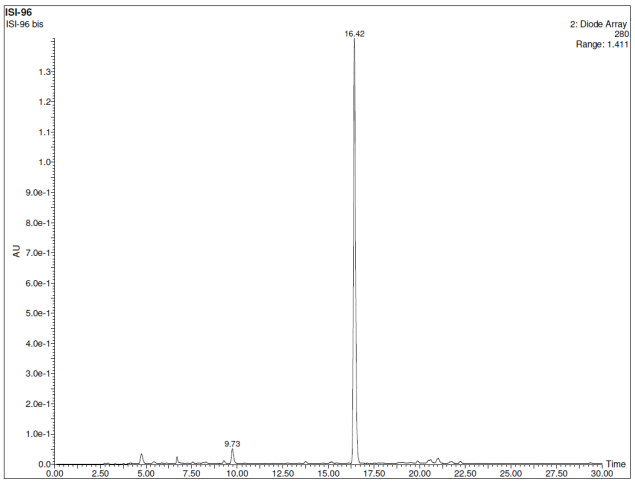

Figure E.2.27 HPLC profiles (280 nm) of crude double conjugate.

HPLC-MS: Analysis conditions, 0-50% B, t_R = 16.4 min (Figure **E.2.27**).

HPLC-MS (ESI, positive mode): *m/z* 1299.3 $[M+H]^+$, M calcd. For $C_{59}H_{74}N_{14}O_8S$ 1298.5.

H-CYNRYK*(Alkyne)AVSL-NH$_2$ (2.96)

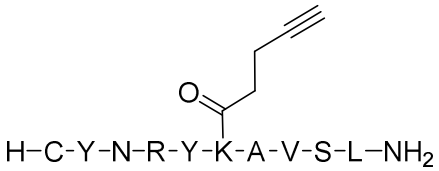

HPLC: analysis conditions, 0-50% B, t_R = 21.4 min.
Purification: 20-60% B t_R = 11.0 min Yield: 20%
HPLC-MS (ESI, positive mode): *m/z* 1295.7 $[M+H]^+$, M calcd. for $C_{59}H_{90}N_{16}O_{15}S$ 1294.7.

N$_3$-ctcatactct-NH$_2$ (2.97)

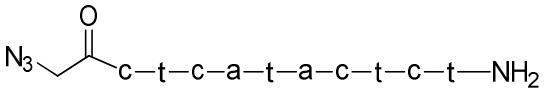

HPLC: analysis conditions, 0-50% B, t_R = 15.3 min
Purification: 5-35% B t_R = 21.0 min Yield: 35%
MALDI-TOF (positive mode, DHB): *m/z* 2716.3 $[M+H]^+$, M calcd. for $C_{108}H_{138}N_{54}O_{33}$ 2719.1.

M-20: CPD-Biotina + H-CSYAK*YG-NH$_2$ (2.98)

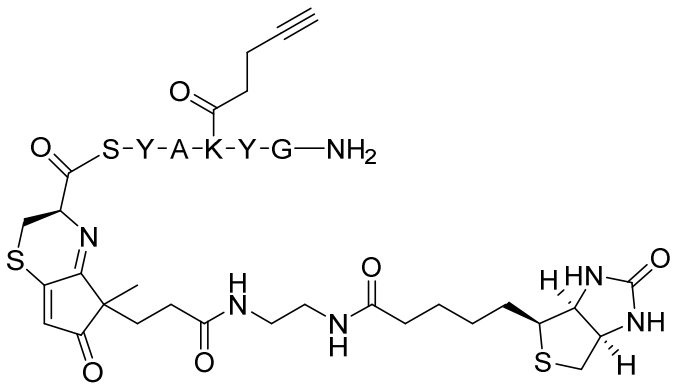

A solution of CPD-Biotin (**2.24**, 33 µL, 13.45 mM, 440 nmol) in MQ-H_2O was added to a peptide solution H-CSYAK*YG-NH$_2$ (**2.92**, 400 nmol) in MQ-H_2O (725 µL) to achieve a final peptide concentration of 0.5 mM. The reaction was left 5 h at 37 ºC, and monitored by HPLC. The conjugate was purified by reversed phase HPLC.

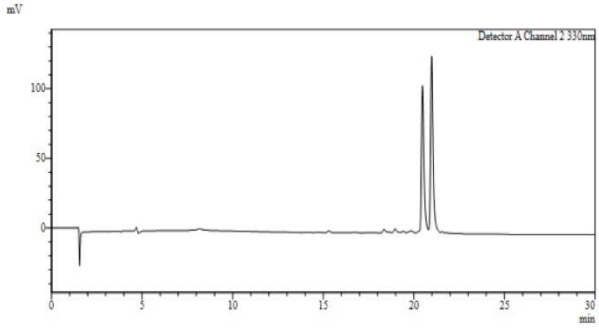

Figure E.2.28 HPLC profiles (280 nm) of crude conjugate.

HPLC-MS: Analysis conditions, 10-50% B, t_R = 20.6 and 21.1 min (Figure **E.2.28)**.

Purification gradient: 10-50% B. t_R = 11.4 and 15.4 min Yield: 30%.

MALDI-TOF (positive mode, DHB): *m/z* 1323.1 $[M+H]^+$, M calcd. For $C_{61}H_{82}N_{13}O_{15}S_2$ 1299.5.

M-20 CPD-catgtcatK-NH2+H-CYNRYK*AVSL-NH2 (2.99)

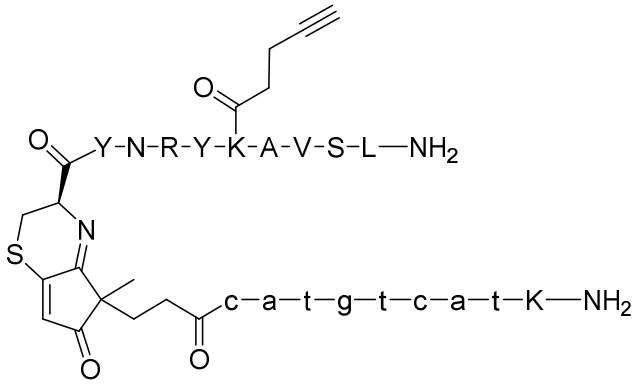

A solution of CPD-c-a-t-g-t-c-a-t-K-NH_2 (**2.34**, 275 µL, 2 mM, 550 nmol) in MQ-H_2O was added to a peptide solution H-CYNRYK*AVSL-NH_2 (**2.96**, 500 nmol) in H_2O (725 µL) to achieve a final peptide concentration of 0.5 mM. The reaction was left 4.5 h at 37 ºC, and monitored by HPLC. The conjugate was purified by reversed phase HPLC.

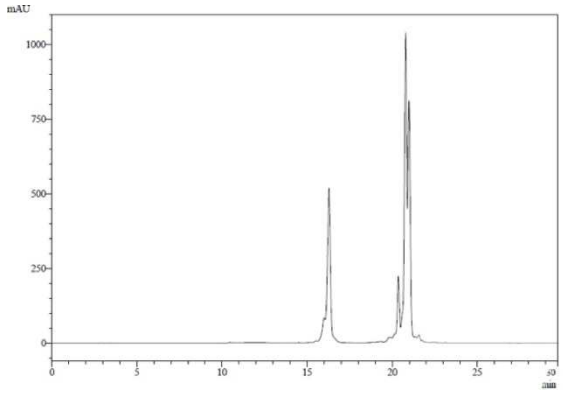

Figure E.2.29 HPLC profiles (280 nm) of crude conjugate.

HPLC-MS: Analysis conditions, 0-50% B, t_R = 20.8 and 21.0 min (Figure **E.2.29**).

Purification gradient: 20-60% B. t_R = 9.7 and 10.2 min Yield: 19%.

MALDI-TOF (positive mode, DHB): *m/z* 3729.9 $[M+H]^+$, M calcd. For $C_{160}H_{216}N_{62}O_{43}S$ 3725.6.

(M-20 CPD-Biotin + H-CSYAK*YG-NH2) + N_3-ctcatactct-NH_2 (2.100)

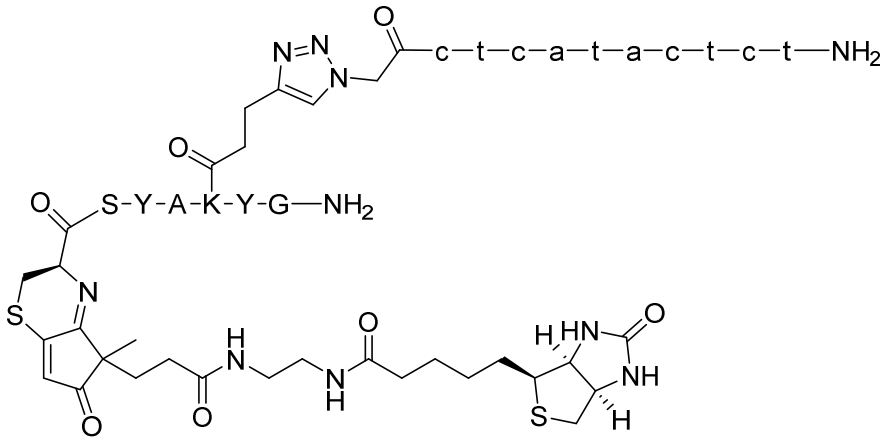

To a solution of conjugate **2.98** (120 nmol) in MQ-H_2O (97 µL) was added $CuSO_4$ (12 µL, 10 mM, 100 nmol) in MQ-H_2O, NaAsc (29 µL, 100 mM, 2880 nmol) in MQ-H_2O, a solution of TBTA (12 µL, 10 mM, 100 nmol) in HPLC-MeOH and a solution of N_3-ctcatactct-NH_2 (**2.97**, 140 nmol) in MQ-H_2O (90 µl) to achieve a final conjugate concentration of 0.5 mM. The mixture was reacted in a microwave oven for 150 min at 60 ºC and monitored by HPLC. The conjugate was purified by reversed phase HPLC.

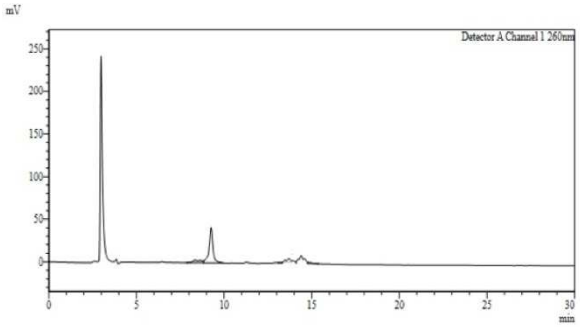

Figure E.2.30 HPLC profiles (260 nm) of crude double conjugate.

HPLC-MS: Analysis conditions, 10-50% B, t_R = 16.7 (Figure **E.2.30**).

Purification gradient: 20-60% B. t_R = 16.7 min Yield: 15%.

MALDI-TOF (positive mode, DHB): *m/z* 4019.4 $[M+H]^+$, M calcd. For $C_{126}H_{219}N_{67}O_{48}S_2$ 4018.6.

(M-20 CPD-catgtcatK-NH2 + H-YNRYK*AVSL-NH2) + AZT (2.101)

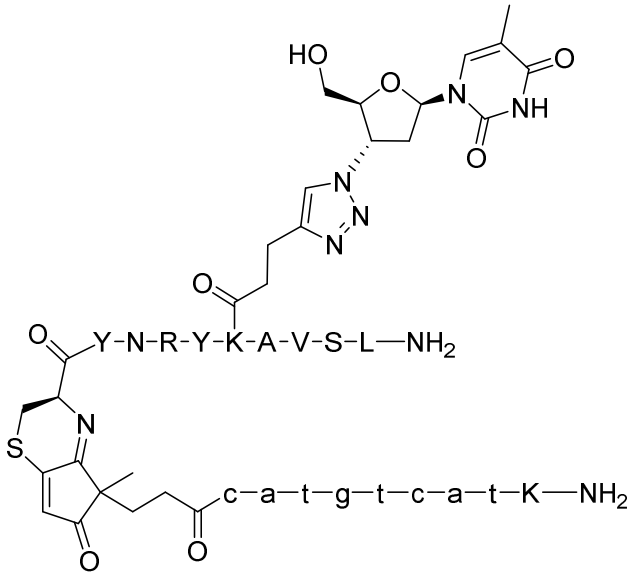

To a solution of conjugate **2.99** (100 nmol) in MQ-H_2O (116 µL) was added $CuSO_4$ (10 µL, 10 mM, 100 nmol) in MQ-H_2O, NaAsc (24 µL, 100 mM, 2400 nmol) in MQ-H_2O, a solution of TBTA (10 µL, 10 mM, 100 nmol) in HPLC-MeOH and a solution of AZT (**2.94**, 40 µL, 10 mM, 400 nmol) in MQ-H_2O to achieve a final conjugate concentration of 0.5 mM. The mixture was reacted in a microwave oven for 1 h at 60 ºC and monitored by HPLC. The conjugate was purified by reversed phase HPLC.

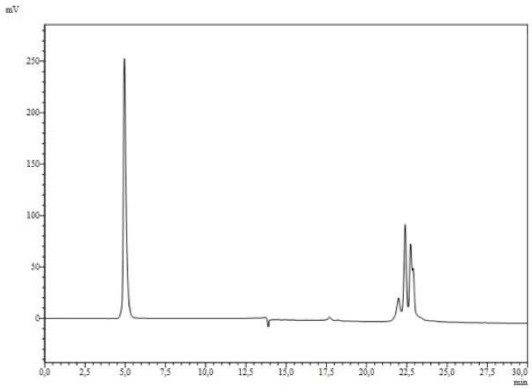

Figure E.2.31 HPLC profiles (260 nm) of crude double conjugate.

HPLC-MS: Analysis conditions, 0-50% B, t_R = 22.4 and 22.9 min (**Figure E.2.31**).

Purification gradient: 20-60% B. t_R = 11.2 and 11.8 min Yield: 19%.

MALDI-TOF (positive mode, DHB): *m/z* 3994.1 $[M+H]^+$, M calcd. For $C_{170}H_{229}N_{67}O_{47}S$ 3992.7.

CPD-KAK(Alkyne)SYGY-NH2 (2.103)

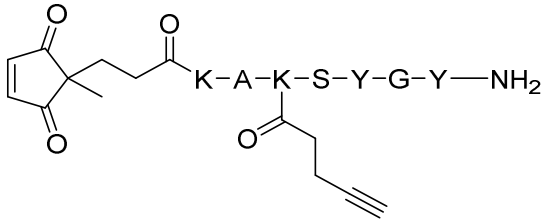

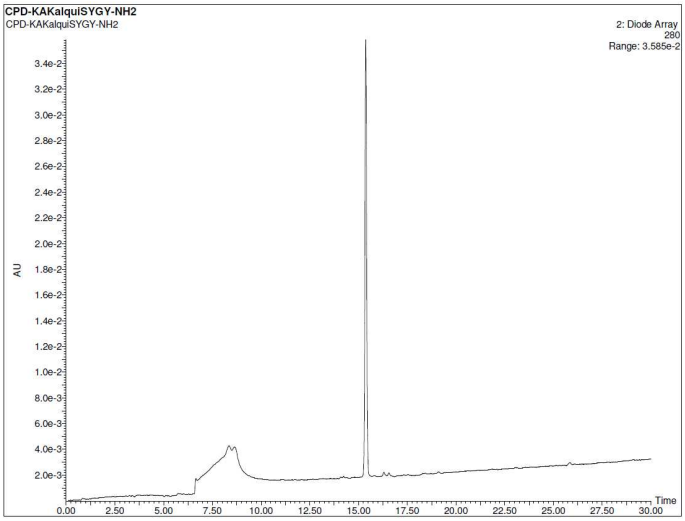

Figure E.2.32 HPLC profiles (260 nm) of crude peptide.

HPLC: analysis conditions, 0-40% B, t_R = 15.6 min (Figure **E.2.32**).
Purification: 5-35% B t_R = 10.0 min Yield: 50%
HPLC-MS (ESI, positive mode): *m/z* 1059.0 $[M+H]^+$, M calcd. for $C_{52}H_{70}N_{10}O_{14}$ 1058.5.

CPD-YNRYK(Alkyne)AVSL-NH2 (2.104)

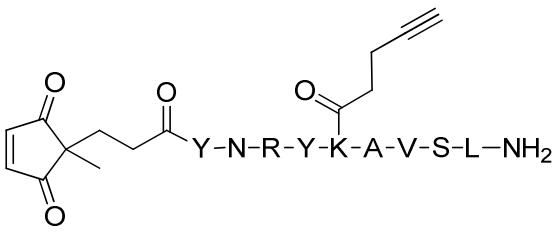

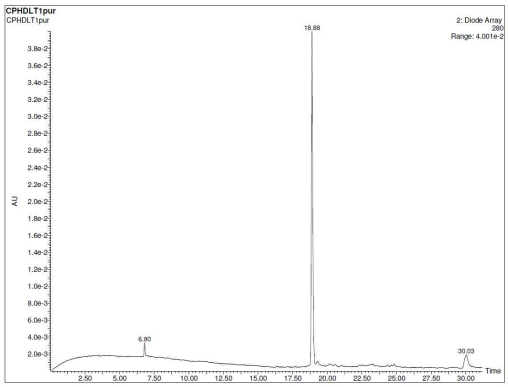

Figure E.2.33 HPLC profiles (260 nm) of crude peptide.

HPLC: analysis conditions, 0-50% B, t_R = 18.8 min (**Figure E.2.33**).
Purification: 20-60% B t_R = 15.3 min Yield: 50%
HPLC-MS (ESI, positive mode): *m/z* 1356.5 $[M+H]^+$, M calcd. for $C_{63}H_{93}N_{15}O_{17}$ 1355.7.

M-20: CPD-KAK*SYGY-NH2+H-CYG-NH2 (2.105)

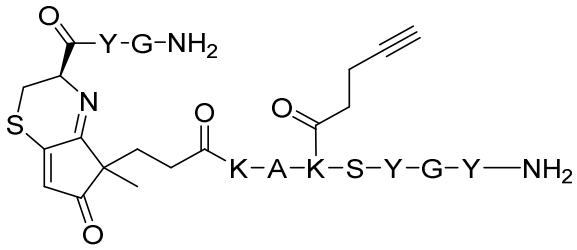

A solution of H-CYG-NH_2 (**2.37**, 50 µL, 10 mM, 500 nmol) in MQ-H_2O was added to a solution of CPD-KA**K***SYGY-NH_2 (**2.103**, 500 nmol) in MQ-H_2O (950 µL) to achieve a final CPD-peptide concentration of 0.5 mM. The reaction was left 3 h at 37 ºC, and monitored by HPLC. The conjugate was purified by reversed phase HPLC.

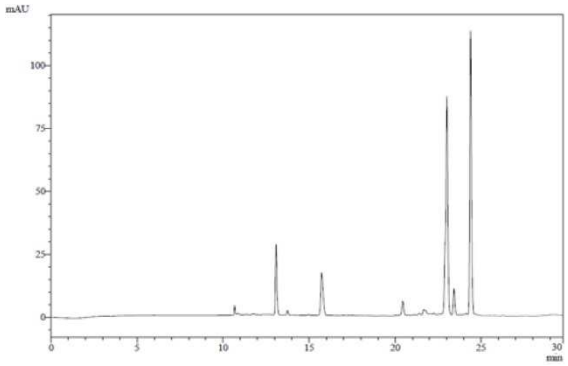

Figure E.2.34 HPLC profiles (280 nm) of crude conjugate.

HPLC-MS: Analysis conditions, 0-50% B, t_R = 22.9 and 24.4 min (Figure **E.2.34**).

Purification gradient: 0-50% B. t_R = 23.1 and 23.6 min Yield: 28%.

MALDI-TOF (positive mode, DHB): *m/z* 1381.3 $[M+H]^+$, M calcd. For $C_{66}H_{87}N_{14}O_{17}S$ 1379.6.

M-20: **CPD-YNRYK*SYGY-NH2+H-CSYAKYG-NH2 (2.106)**

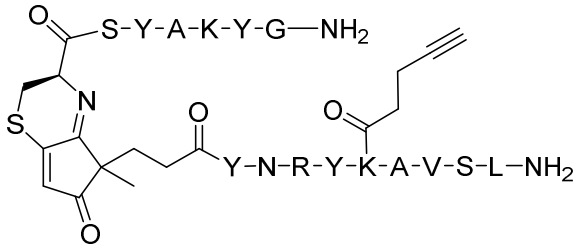

A solution of peptide H-CSYAKYG-NH_2 (**2.38**, 30 µL, 15.4 mM, 455 nmol) in MQ-H_2O was added to a solution of CPD-YNR**K***AVSL-NH_2 (**2.104**, 500 nmol) in H_2O (970 µL) to achieve a final CPD-peptide concentration of 0.5 mM. The reaction was left 3 h at 37 ºC, and monitored by HPLC. The conjugate was purified by reversed phase HPLC.

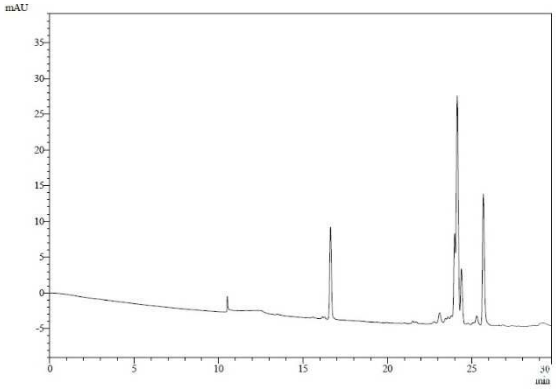

Figure E.2.35 HPLC profiles (280 nm) of crude conjugate.

HPLC-MS: Analysis conditions, 0-50% B, t_R = 23.9 and 24.1 min (**Figure E.2.35**).

Purification gradient: 20-60% B. t_R = 13.2 min Yield: 33%.

MALDI-TOF (positive mode, DHB): *m/z* 2126.4 $[M+H]^+$, M calcd. For $C_{100}H_{140}N_{24}O_{26}S$ 2125.0.

(M-20 CPD-KAK*SYGY-NH2 + H-CYG-NH2) + AZT (2.107)

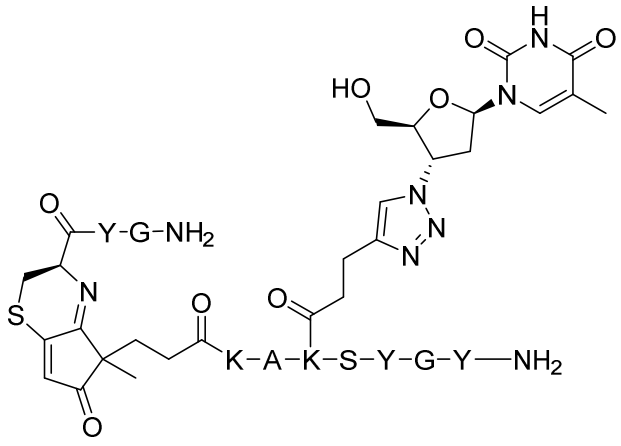

To a solution of conjugate **2.105** (140 nmol) in MQ-H_2O (151 µL) was added $CuSO_4$ (28 µL, 5 mM, 140 nmol) in MQ-H_2O, NaAsc (17 µL, 200 mM, 3400 nmol) in MQ-H_2O, a solution of

TBTA (28 µL, 5 mM, 144 nmol) in HPLC-MeOH/MQ-H_2O (3:2) and a solution of AZT (56 µL, 10 mM, 560 nmol) in MQ-H_2O to achieve a final conjugate concentration of 0.5 mM. The mixture was reacted in a microwave oven for 1 h at 90 ºC and monitored by HPLC. The conjugate was purified by reversed phase HPLC.

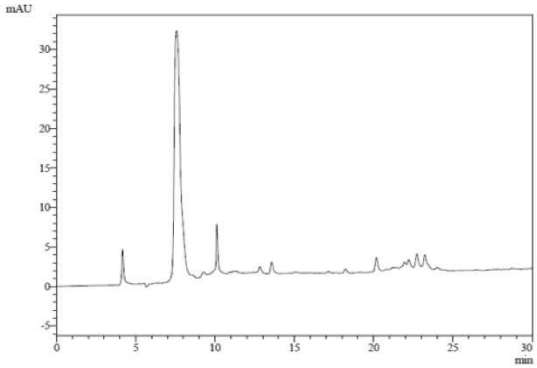

Figure E.2.36 HPLC profiles (260 nm) of crude double conjugate.

HPLC-MS: Analysis conditions, 0-50% B, t_R = 22.6 and 23.6 min (**Figure E.2.36**).

Purification gradient: 0-50% B. t_R = 21.9 and 22.7 min Yield: 17%.

HPLC-MS (ESI, positive mode): *m/z* 1647.1 $[M+H]^+$, M calcd. For $C_{76}H_{99}N_{19}O_{21}S$ 1645.7.

(M-20 CPD-YNRYK*AVSL-NH2 + H-CSYAKYG-NH2) + AZT (2.108)

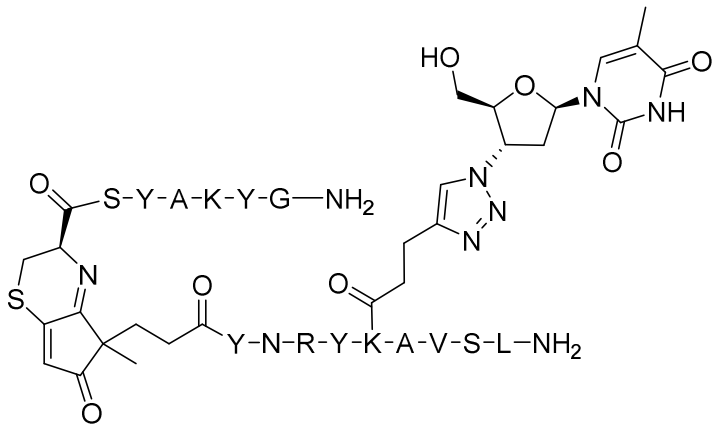

To a solution of conjugate **2.106** (150 nmol) in MQ-H_2O (174 µL) was added $CuSO_4$ (15 µL, 10 mM, 150 nmol) in MQ-H_2O, NaAsc (36 µL, 100 mM, 3600 nmol) in MQ-H_2O, a solution of TBTA (15 µL, 10 mM, 100 nmol) in HPLC-MeOH/MQ-H_2O (3:2) and a solution of AZT (60 µL, 10 mM, 600 nmol) in MQ-H_2O to achieve a final conjugate concentration of 0.5 mM. The mixture was reacted in a microwave oven for 1 h at 60 ºC and monitored by HPLC. The conjugate was purified by reversed phase HPLC.

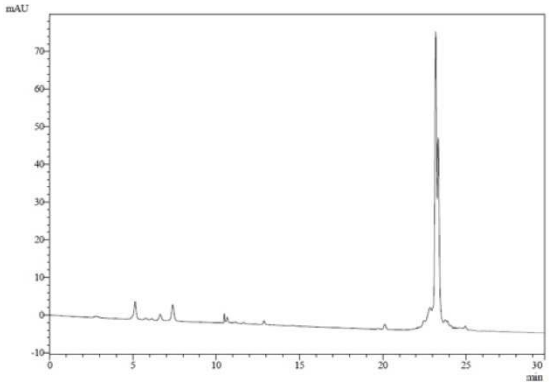

Figure E.2.37 HPLC profiles (260 nm) of crude double conjugate.

HPLC-MS: Analysis conditions, 0-50% B, t_R = 23.1 and 23.2 min (**Figure E.2.37**).

Purification gradient: 20-60% B. t_R = 12.6 and 11.8 min Yield: 67%.

MALDI-TOF (positive mode, DHB): *m/z* 2394.2 $[M+H]^+$, M calcd. For $C_{109}H_{156}N_{29}O_{30}S$ 2392.1.

Azidoacetic acid (2.109)[1]

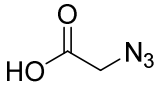

To a solution of NaN_3 (1.00 g, 14.50 mmol) in H_2O (3 mL), bromoacetic acid (943 mg, 7.25 mmol) was added and the solution left stirring overnight at rt. Afterwards, aq. cc. HCl (1 mL) and water (10 mL) were added and the crude transferred to a separatory funnel. The aqueous layer extracted with Et_2O (3 x 15 mL), the combined organic phases were dried over anh. $MgSO_4$, filtered and the solvent removed under low pressure. The title compound was obtained as colourless oil (725 mg, 99%).

^{1}H NMR ($CDCl_3$, 400 MHz) δ 7.11.08 (br. s, 1H), 3.97 (s, 2H) ppm.

^{13}C NMR ($CDCl_3$, 101 MHz) δ 174.53, 50.00 ppm.

Benzylazide (2.110)

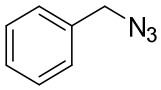

To a solution of NaN_3 (250 mg, 3.85 mmol) in Acetone:H_2O (20 mL; 4:1), benzyl bromide (304 µL, 2.56 mmol) was added and the mixture left overnight at rt. Afterwards, the crude was transferred into a separatory funnel and extracted with DCM (3 × 20 mL). The combined organic phases were dried over anh. $MgSO_4$, filtered and the solvent removed under low pressure to obtain the title compound as colourless oil (340 mg, 99%).

^{1}H NMR ($CDCl_3$, 400 MHz): δ 7.39 - 7.27 (m, 5H), 4.29 (s, 2H) ppm.

^{13}C NMR ($CDCl_3$, 101 MHz): δ 135.5, 129.3, 128.3, 128.2, 54.8 ppm.

3-(1-Methyl-2,5-dioxocyclopent-3-en-1-yl)-*N*-phenethylpropanamide (2.111)

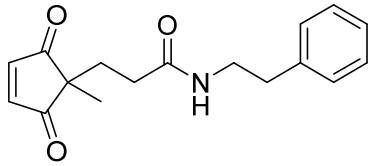

To an ice-cooled solution of **2.20** (200 mg, 1.10 mmol) in anh. DCM (5 mL) was added NMM (161 µL, 1.46 mmol) and IBCF (104 µL, 0.81 mmol). After 10 minutes, 2-phenylethylamine (92 µL, 0.73 mmol) was added the reaction left for 30 min. at low temperature and overnight at room temperature. Afterwards, additional DCM was added (15 mL) and washed with aq. HCl 10% (2 × 10 mL) and aq. sat. $NaHCO_3$ (2 × 10 mL). The organic layer is dried over anh. $MgSO_4$, filtered and the solvent removed under vacuum. The resulting crude was further purified by silica gel column chromatography eluting with DCM/EtOAc mixtures from 100:0 to 70:30. The title compound was obtained as yellow solid (170 mg, 81%).

TLC (DCM:EtOAc 70:30): R_f = 0.35

^{1}H NMR ($CDCl_3$, 400 MHz) δ 7.32 – 7.28 (m, 2H), 7.25 – 7.22 (m, 1H), 7.20 (s, 2H), 7.18 – 7.16 (m, 2H), 5.39 (s br, 1H), 3.47 (td, *J* = 7.0, 5.9 Hz, 2H), 2.78 (t, *J* = 6.9 Hz, 2H), 2.06 – 2.01 (m, 2H), 1.98 – 1.91 (m, 2H), 1.15 (s, 3H).

^{13}C NMR ($CDCl_3$, 101 MHz) δ 206.88, 171.08, 147.79, 138.73, 128.71, 128.64, 126.53, 49.28, 40.55, 35.54, 31.10, 29.52, 18.37.

ESI-HRMS (positive mode): *m/z* 286.1445 $[M+H]^+$, M calcd. for $C_{17}H_{20}NO_3$ 286.1438.

3-(3-(((2*S*,3*S*,5*R*)-2-(hydroxymethyl)-5-(5-methyl-2,4-dioxo-3,4-dihydropyrimidin-1(2*H*)-yl)tetrahydrofuran-3-yl)amino)-1-methyl-2,5-dioxocyclopent-3-en-1-yl)propanoic acid (2.112)

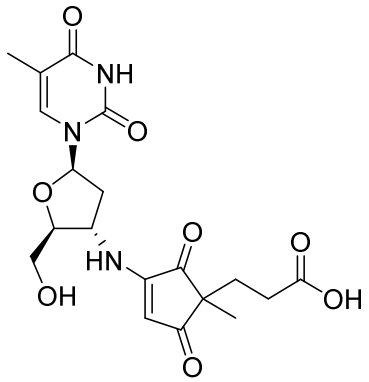

To an aqueous solution of **2.20** (10 mg, 0.054 mmol) in a pressure tube, was added **2.96** (14.6 mg, 0.054 mmol) and the crude left mixing at 90 ºC in a MW over for 4 h. Afterwards the reaction crude was purified by HPLC, collecting the appropriate peaks. The title compound was obtained as a pale yellow powder (3.1 mg, 13%).

^{1}H NMR (D_2O, 400 MHz) δ 7.70 (s, 1H), 6.29 (t, *J* = 5.6 Hz, 1H), 6.06 (s, 1H), 4.31 (dt, *J* = 8.0, 17.2 Hz, 1H), 4.17 – 4.13 (m, 1H), 3.92 (d, *J* = 13.6 Hz, 1H), 3.76 (d, *J* = 16.8 Hz, 1H), 2.63 – 2.56 (m, 2H), 2.37 – 2.17 (m, 2H), 2.06 – 1.94 (m, 2H), 1.92 (s, 3H), 1.19 (s, 3H).

^{13}C NMR (D_2O, 101 MHz) δ 205.2, 203.8, 177.0, 166.5, 159.3, 151.5, 137.6, 111.4, 100.7, 84.9, 83.7, 60.5, 53.1, 50.0, 35.8, 29.3, 29.1, 18.8, 11.5.

ESI-HRMS (negative mode): *m/z*: 420.1414 $[M-H]^+$, M calcd for $C_{19}H_{22}N_3O_8$ 420.1412.

3-(6-hydroxy-1-((2*S*,3*S*,5*R*)-2-(hydroxymethyl)-5-(5-methyl-2,4-dioxo-3,4-dihydropyrimidin-1(2*H*)-yl)tetrahydrofuran-3-yl)-5-methyl-4-oxo-1,4,5,6-tetrahydrocyclopenta[d][1,2,3]triazol-5-yl)propanoic acid (2.113)

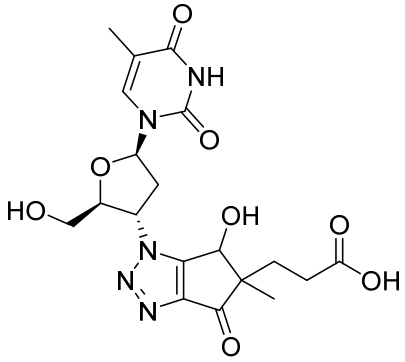

To an aqueous solution of **2.20** (10 mg, 0.054 mmol) in a round-bottomed flask, was added **2.96** (14.6 mg, 0.054 mmol) and the crude left mixing at 60 ºC in for 2 days. Afterwards the reaction crude was purified by HPLC, collecting the appropriate peaks. The title compound was obtained as a pale-yellow powder (6.7 mg, 28%).

^{1}H NMR (D_2O, 400 MHz): δ 7.68 (s, 1H), 6.47 (t, *J* = 6.7 Hz, 1H), 5.50 – 5.43 (m, 1H), 5.21 (s, 1H), 4.54 – 4.48 (m, 1H), 3.93 – 3.75 (m, 2H), 3.08 – 2.98 (m, 1H), 2.88 – 2.77 (m, 1H), 2.47 – 2.25 (m, 2H), 2.00 – 1.89 (m, 2H), 1.84 (s, 3H), 1.15 (s, 3H) ppm.

^{13}C NMR (D_2O, 101 MHz): δ 195.52, 177.51, 166.52, 157.38, 151.58, 149.59, 137.76, 111.52, 85.82, 83.93, 66.82, 62.79, 60.73, 59.47, 36.68, 31.08, 28.99, 17.62, 11.50 ppm.

ESI-HRMS (negative mode): *m/z*: 448.1475 $[M-H]^+$, M calcd for $C_{19}H_{23}N_5O_8$ 448.1474.

Experimental section: Chapter 3

5-Bromo-2-aminobenzophenone (3.7)

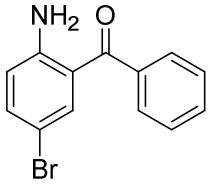

To a solution of 2-aminobenzophenone (**3.6**, 2.00 g, 10.15 mmol) in DCM (60 mL) was added (1.79 g, 10.15 mmol) at 0 ºC. The mixture was stirred at low temperature in an ice bath for 1 h and for an additional 2 h at rt. The mixture was diluted with additional DCM (20 mL) and washed with distilled H_2O (3 × 30 mL). The organic layer was dried over anh. $MgSO_4$, filtered and concentrated under vacuum to afford the title compound as a yellow solid (2.71 g, 97%).

TLC (DCM:hexanes 7:3): R_f = 0.50.

IR (ATR, solid): 3411, 3306, 1563, 1565, 1533, 1457, 1229 cm^{-1}.

^{1}H NMR ($CDCl_3$, 400 MHz) δ 7.65 - 7.61 (m, 2H), 7.59 - 7.53 (m, 2H), 7.51 - 7.46 (m, 2H), 7.36 (dd, *J* = 8.8, 2.4 Hz, 1H), 6.65 (d, *J* = 8.8 Hz, 1H), 6.08 (br s, 2H) ppm.

^{13}C NMR ($CDCl_3$, 101 MHz) δ 197.86, 149.68, 139.26, 136.81, 136.17, 131.51, 129.09, 128.30, 119.42, 118.78, 106.60 ppm.

ESI-HRMS (positive mode): *m/z* 276.0014 / 277.9993 (^{81}Br) $[M+H]^+$; calcd. for $C_{13}H_{11}BrNO$ 276.0019.

N-(2-Benzoyl-4-bromophenyl)-2-bromoacetamide (3.8)

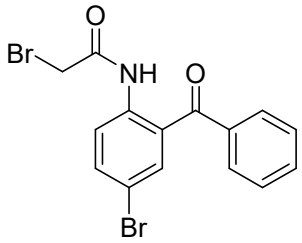

To a solution of 5-bromo-2-aminobenzophenone (**3.7**, 2.71 g, 9.86 mmol) in DCM (60 mL) was added bromoacetyl bromide (11.83 mmol, 1.01 mL) followed by a 2 M aqueous solution of Na_2CO_3 (10 mL) at 0 °C and the mixture stirred 2 h at this temperature. Afterwards, the crude was transferred into a separatory funnel and the organic layer was washed with distilled H_2O (3 × 50 mL), dried over anh. $MgSO_4$, filtered and concentrated under vacuum to yield the title compound as a yellowish solid (3.25 g. 84%).

TLC (DCM): R_f = 0.48.

IR (ATR, solid): 3414, 3309, 2359, 2331, 1682, 1568, 1520, 1223, 1150, 697 cm^{-1}.

^{1}H NMR ($CDCl_3$, 400 MHz) δ 11.31 (s, 1H), 8.52 (d, *J* = 9.6 Hz, 1H), 7.75 – 7.74 (m, 1H), 7.73 – 7.69 (m, 3H), 7.65 (tt, *J* = 1.2 Hz, *J* = 6.8 Hz 1H), 7.55 – 7.51 (m, 2H), 4.01 (s, 2H) ppm.

^{13}C NMR ($CDCl_3$, 101 MHz) δ 197.64, 164.93, 138.36, 137.51, 136.67, 135.48, 133.13, 130.00, 128.59, 125.72, 123.23, 115.68, 29.45 ppm.

ESI-HRMS (positive mode): *m/z* 395.9232 / 397.9207 (^{81}Br) $[M+H]^+$; calcd. for $C_{15}H_{12}Br_2NO_2$ 395.9229.

7-Bromo-1,3-dihydro-5-phenyl-2*H*-1,4-benzodiazepin-2-one (3.9)

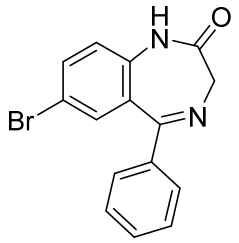

Into an ice-cooled round-bottomed flask, *N*-(2-benzoyl-4-bromophenyl)-2-bromoacetamide (**3.8**, 3.25 g, 8.23 mmol) was weighed and dissolved in a 7 M NH_3 solution (in MeOH, 60 mL), the mixture was stirred for 1 h at low temperature and then allowed to warm up to rt overnight. The crude mixture was concentrated under vacuum to dryness, dissolved in EtOAc (120 mL) and washed with distilled H_2O (3 × 50 mL). The organic layer was dried over anh. $MgSO_4$, filtered and concentrated under vacuum. The crude mixture was purified by flash chromatography eluting with hexanes/EtOAc mixtures from 80:20 to 50:50. The title compound was obtained as a white solid (1.46 g, 57%).

TLC (Hexanes:EtOAc 50:50): R_f = 0.45.

IR (ATR, solid): 3430, 2951, 1680, 1605, 1476, 1381, 1355, 1319, 1285, 1259, 1233, 1193, 1082, 1012, 946, 895 cm^{-1}.

^{1}H NMR ($CDCl_3$, 400 MHz) δ 9.28 (s, 1H), 7.60 (dd, *J* = 8.6, 2.3 Hz, 1H), 7.54 – 7.52 (m, 2H), 7.50 – 7.44 (m, 2H), 7.43 – 7.38 (m, 2H), 7.07 (d, *J* = 8.6 Hz, 1H), 4.33 (s, 2H) ppm.

^{13}C NMR ($CDCl_3$, 101 MHz) δ 171.97, 169.77, 138.74, 137.82, 134.68, 133.63, 130.63, 129.57, 128.86, 128.39, 122.93, 116.26, 56.60 ppm.

ESI-HRMS (positive mode): *m/z* 315.0126 / 317.0109 (^{81}Br) $[M+H]^+$; calcd. for $C_{15}H_{12}BrN_2O$ 315.0128.

7-Bromo-1,3,4,5-tetrahydro-5-phenyl-2*H*-1,4-benzodiazepin-2-one (3.10)

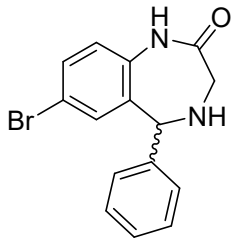

To a solution of **3.9** (500 mg, 1.58 mmol,) in MeOH (15 mL), was added $NaBH_3CN$ (150 mg, 2.37 mmol) followed by AcOH (440 µL, 7.90 mmol,) dropwise. The mixture was stirred at room temperature until complete reduction of the starting material as assessed by TLC (2 h). The mixture was evaporated to dryness under vacuum, dissolved in EtOAc (30 mL) and washed with aq. sat. $NaHCO_3$ (3 × 20 mL) and distilled H_2O (3 × 20 mL). The organic layer was dried over anh. $MgSO_4$, filtered and concentrated under vacuum. The title compound was obtained as a white solid (438 mg, 87%).

TLC (DCM:EtOAc 1:1): R_f = 0.50.

IR (ATR, solid): 3420, 3303, 2359, 2337, 1615, 1555, 1457, 1239, 1147 cm^{-1}.

^{1}H NMR (DMSO-d_6, 400 MHz): δ 9.96 (s, 1H), 7.44-7.26 (m, 6H), 7.06 (d, 1H, *J* = 8.5 Hz), 6.83 (d, 1H, *J* = 2.14 Hz), 5.23 (d, *J* = 4.9 Hz, 1H), 3.68 (br s, 1H), 3.39 (dd, *J* = 15.7 Hz, J = 5.4 Hz, 1H), 3.26 (dd, *J* = 15.7 Hz, J = 8.0 Hz, 1H) ppm.

^{13}C NMR ($CDCl_3$, 101 MHz) δ 173.74, 139.97, 136.06, 135.21, 132.76, 131.36, 128.76, 128.26, 128.13, 122.31, 117.95, 61.85, 50.11 ppm.

ESI-HRMS (positive mode): *m/z* 317.0282 / 319.0260 (^{81}Br) $[M+H]^+$; calcd for $C_{15}H_{14}BrN_2O$ 317.0284.

7-Bromo-1,3,4,5-tetrahydro-4-(1-oxopropyl)-5-phenyl-2*H*-1,4-benzodiazepin-2-one (3.11)

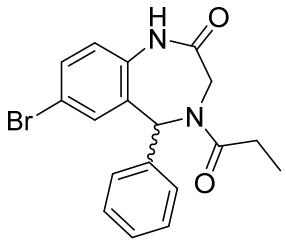

To a solution of **3.10** (250 mg, 0.79 mmol) in DCM (10 mL) was added propionyl chloride (69 µL, 1.02 mmol) followed by NEt_3 (110 µL, 0.79 mmol,). The mixture was stirred at room temperature overnight. Afterwards, aq. sat. $NaHCO_3$ (20 mL) was added, and the aqueous layer was extracted with DCM (3 × 20 mL). The combined organic layers were dried over anh. $MgSO_4$, filtered, and then concentrated under vacuum. The crude mixture was further washed with Et_2O (2 × 15 mL) and centrifuged discarding the organic supernatant. The title compound was obtained as a white solid (245 mg, 83%).

TLC (DCM): R_f = 0.30.

IR (ATR, solid): 3642, 3414, 3300, 2356, 2337, 1555, 1501, 1457, 1315, 1235, 1150, 700 cm^{-1}.

^{1}H NMR ($CDCl_3$, 400 MHz) δ 8.21 and 8.07 (s, 1H), 7.45 – 7.40 (m, 2H), 7.33 - 7.28 (m, 3H), 7.05 – 6.99 (m, 1H), 6.88 and 6.82 (d, *J* = 8.5 Hz, 1H), 7.03 and 6.11 (s, 1H), 4.19 – 3.99 (m, 2H), 2.64 – 2.50 (m, 1H), 2.46 – 2.33 (m, 1H), 1.20 (t, *J* = 7.3 Hz, 2H) ppm.

Diastereomer 1: ^{13}C NMR ($CDCl_3$, 101 MHz) δ 173.27, 170.61, 138.59, 134.74, 134.29, 132.00, 130.39, 128.76, 127.82, 127.10, 122.81, 117.40, 59.22, 48.59, 27.09, 9.13 ppm.

Diastereomer 2: ^{13}C NMR ($CDCl_3$, 101 MHz) δ 173.64, 171.31, 137.45, 135.51, 133.02, 132.56, 130.28, 129.17, 128.43, 128.07, 123.36, 117.01, 63.05, 46.05, 26.65, 9.35 ppm.

ESI-HRMS (positive mode): *m/z* 373.0541 / 375.0526 (^{81}Br) $[M+H]^+$; calcd for $C_{18}H_{18}BrN_2O$ 373.0546.

4-(7-Bromo-2-oxo-5-phenyl-1,2,3,5-tetrahydro-4*H*-benzo[*e*][1,4]diazepin-4-yl)-4-oxobutanoic acid (3.21)

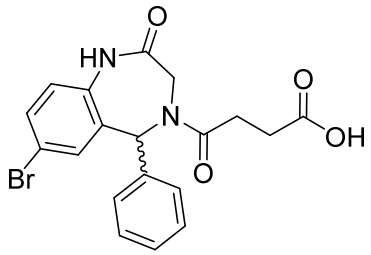

3.10 (200 mg, 0.63 mmol) and succinic anhydride (316.4 mg, 3.16 mmol) were dissolved in THF (10 mL). Subsequently, DIPEA (220 µL, 0.74 mmol) was added and the mixture was reacted overnight at rt. Afterwards, the solvent was removed under low pressure, the crude dissolved in DCM (20 mL) and this solution was washed with aq. HCl 10% (3 × 20 mL). The organic phase was dried over anh. $MgSO_4$, filtered, and the solvent removed under low pressure. The title compound was obtained as a white solid (104 mg, 99%).

TLC (DCM:EtOAc:AcOH 78:20:2): R_f = 0.20.

IR (ATR, solid): 3179, 3065, 2955, 2353, 2331, 1729, 1650, 1631, 1574, 1432, 1182, 691 cm^{-1}.

^{1}H NMR (DMSO-d_6, 400 MHz) δ 12.05 (s. br, 1H), 10.10 and 10.05 (s, 1H), 8.00 and 7.72 (d, *J* = 2.4 Hz, 1H), 7.57 and 7.54 (dd, *J* = 2.4, 10.8 Hz, 1H), 7.36 – 7.24 (m, 3H), 7.07 – 6.93 (m, 3H), 6.71 and 6.49 (s, 1H), 4.31 and 3.86 (d, *J* = 14.9 Hz, 1H), 4.17 and 4.07 (d, *J* = 15.5 Hz, 1H), 2.88 – 2.75 (m, 1H), 2.65 – 2.52 (m, 1H), 2.48 – 2.43 (m, 2H) ppm.

Diasteromer 1: ^{13}C NMR (DMSO-d_6, 101 MHz) δ 174.17, 171.65, 168.83, 139.44, 137.166, 134.03, 132.22, 131.96, 128.82, 127.63, 126.73, 123.95, 116.44, 61.79, 49.62, 29.37 ppm.

Diasteromer 2: ^{13}C NMR (DMSO-d_6, 101 MHz) δ 174.17, 171.044, 168.53, 139.61, 136.98, 134.25, 132.49, 131.96, 129.01, 127.93, 127.08, 124.11, 116.38, 60.19, 49.62, 28.517, 28.236 ppm.

ESI-HRMS (negative mode): *m/z* 415.0310 / 417.0310 (^{81}Br) $[M-H]^-$; calcd. for $C_{19}H_{16}BrN_2O_4$ 415.0299.

7-Bromo-1,3,4,5-tetrahydro-4-(acryloyl)-5-phenyl-2*H*-1,4-benzodiazepin-2-one (3.32)

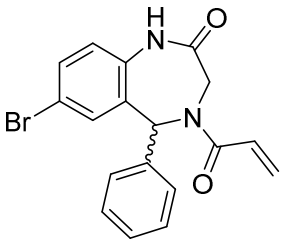

To a suspension of **3.10** (150 mg, 0.47 mmol) in DCM (5 mL) acryloyl chloride (50 µL, 0.62 mmol) was added and the mixture stirred at rt for 3 h. Afterwards, additional DCM (30 mL) was added, and the mixture was washed with distilled H_2O (3 × 20 mL). The organic layer was dried over anh. $MgSO_4$, filtered, and the solvent removed under low pressure. The resulting crude was purified by silica gel flash column chromatography eluting with DCM/EtOAc mixtures from 100:0 to 75:25. The title compound was obtained as a white foam (130 mg, 74%).

TLC (DCM:EtOAc 80:20): R_f = 0.50.

IR (ATR, solid): 3221, 2920, 2359, 2340, 1682, 1647, 15155, 1416, 665 cm^{-1}.

^{1}H NMR ($CDCl_3$, 400 MHz) δ 8.88 and 8.85 (s, 1H), 7.45 (s, 1H), 7.46 and 7.40 (d, *J* = 8.5 Hz, 1H), 7.32 – 7.24 (m, 3H), 7.05 (s, 1H), 7.04 and 6.16 (s, 1H), 6.93 and 6.89 (d, *J* = 8.5 Hz, 1H), 6.61 and 6.54 (dd, *J* = 10.4, 16.4 Hz, 1H), 6.45 and 6.41 (s, 1H), 5.84 – 5.78 (m, 1H), 4.34 – 4.02 (m, 2H) ppm.

Diasteromer 1: ^{13}C NMR ($CDCl_3$, 101 MHz) δ 170.39, 166.04, 138.44, 134.30, 132.09, 130.61, 129.02, 127.93, 126.67, 122.91, 117.43, 59.46, 48.72 ppm.

Diasteromer 2: ^{13}C NMR ($CDCl_3$, 101 MHz) δ 170.39, 166.63, 137.52, 135.52, 134.71, 133.15, 132.73, 130.86, 130.00, 129.06, 128.39, 128.21, 127.08, 126.79, 123.67, 117.55, 63.49, 46.30 ppm.

ESI-HRMS (positive mode): *m/z* 371.0391 / 373.0368 (^{81}Br) $[M+H]^+$; calcd for $C_{18}H_{16}BrN_2O_2$ 371.0390.

7-Bromo-1,3,4,5-tetrahydro-4-[1-oxo-3-(4-hydroxypiperidin-1-yl)propyl]-5-phenyl-2*H*-1,4-benzodiazepin-2-one (3.34)

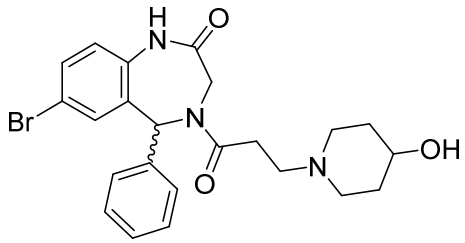

In a round-bottomed flask, **3.32** (100.0 mg, 0.27 mmol) and 4-hydroxypiperidine (**3.33**, 273.1 mg, 2.70 mmol) were weighed, dissolved in DCM (5 mL) and the mixture left overnight at rt. Afterwards, the solvent was removed under reduced pressure, the resulting crude dissolved in EtOAc (40 mL) and washed with distilled H_2O (3 × 20 mL). The organic phase was dried over anh. $MgSO_4$, filtered, and the solvent removed under low pressure. The title compound was obtained as a white solid (125 mg, 98%).

TLC (DCM:EtOAc 50:50): R_f = 0.20.

IR (ATR, solid): 3214, 3119, 2983, 2353, 2334, 1865, 1650, 1558, 1553, 1508, 1239, 783, 666 cm^{-1}.

^{1}H NMR ($CDCl_3$, 400 MHz) δ 8.70 and 8.68 (s, 1H), 7.46 – 7.38 (m, 2H), 7.34 – 7.27 (m, 3H), 7.06 – 7.00 (m, 2H), 6.95 and 6.20 (s, 1H), 6.92 – 6.87 (m, 1H), 4.45 – 3.98 (m, 2H), 3.65 (p, *J* = 4.5 Hz, 1H), 2.80 – 2.54 (m, 6H), 2.20 – 2.12 (m, 2H), 1.87 – 1.79 (m, 4H), 1.57 – 1.47 (m, 1H) ppm.

Diasteromer 1: ^{13}C NMR ($CDCl_3$, 101 MHz) δ 171.64, 170.40, 138.33, 134.86, 134.25, 132.05, 130.34, 129.14, 128.96, 127.74, 122.87, 117.39, 67.49, 63.07, 59.29, 53.75, 51.19, 34.18, 31.60 ppm.

Diasteromer 2: ^{13}C NMR ($CDCl_3$, 101 MHz) δ 171.96, 170.94, 137.60, 135.50, 133.17, 132.60, 130.37, 128.44, 128.10, 127.05, 123.45, 117.19, 67.44, 60.42, 53.82, 51.30, 46.10, 34.19, 31.30 ppm.

ESI-HRMS (positive mode): *m/z* 472.1222 / 474.1205 (^{81}Br) $[M+H]^+$; calcd for $C_{23}H_{27}BrN_3O_3$ 472.1230.

7-Bromo-1,3,4,5-tetrahydro-4-[1-oxo-3-(4-hydroxypiperidin-1-yl)propyl]-5-phenyl-2*H*-1,4-benzodiazepin-2-one, 2-cyanoethyl *N*,*N*-diisopropylphosphoramidite (3.35)

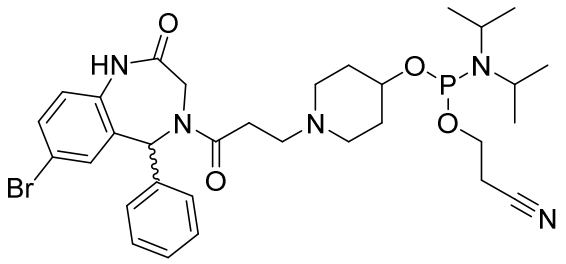

3.34 (453.5 mg, 0.96 mmol) was dissolved in anh. DCM (15 mL) subsequently, anh. DIPEA (310 µL, 2.41 mmol) was added and the mixture was stirred in an ice bath for 5 min under an argon atmosphere. Afterwards, a solution of CECP (250 mg, 1.06 mmol) in anh. DCM (1 mL) was added, and the mixture was reacted at 5 ºC for 30 min. Then, it was left stirring for 6 h at room temperature until complete phosphitylation as shown by TLC. The solvent was removed under low pressure, the crude dissolved in EtOAc (50 mL) and washed with aq. sat. $NaHCO_3$ (3 × 30 mL). The organic phase was dried over anh. $MgSO_4$, filtered, and the solvent removed under low pressure. The resulting crude was further purified by silica gel flash column chromatography eluting with DCM/EtOAc/NEt_3 mixtures from 98:0:2 to 48:50:2. The title compound was obtained as a white foam (272.4 mg, 42%).

TLC (DCM:EtOAc:NEt_3 48:50:2): R_f = 0.50.

^{1}H NMR ($CDCl_3$, 400 MHz) δ 7.90 and 7.86 (s, 1H), 7.48 – 7.40 (m, 2H), 7.33 – 7.27 (m, 3H), 7.05 – 7.01 (m, 2H), 6.95 and 6.22 (s, 1H), 6.88 – 6.80 (m, 1H), 4.44 – 4.00 (m, 2H), 3.90 – 3.71 (m, 3H), 3.65 – 3.45 (m, 2H), 2.80 – 2.56 (m, 8H), 2.38 – 2.23 (m, 2H), 1.93 – 1.79 (m, 2H), 1.76 – 1.60 (m, 2H), 1.27 and 1.17 (dd, *J* = 6.8, 5.5 Hz, 12H) ppm.

^{31}P NMR ($CDCl_3$, 162 MHz,) δ 145.85 ppm.

ESI-HRMS (positive mode): *m/z* 672.2298 / 674.2281 (^{81}Br) $[M+H]^+$; calcd for $C_{32}H_{44}BrN_5O_4P$ 672.2309.

2-(Tritylthio)ethanamine (3.36)

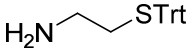

To a solution of 2-aminoethanthiol hydrochloride (1.00 g, 12.98 mmol) in TFA (40 mL) was added trityl chloride (3.61 g, 12.98 mmol) and the mixture stirred for 3 h at rt. Afterwards, the solvent was removed *in vacuo*, the residue diluted in EtOAc (50 mL) and transferred into a separatory funnel. The organic phase was washed with 1 M NaOH (4 × 20 mL), water (20 mL) and aq. sat. $NaHCO_3$ solution (2 × 20 mL). The organic phase was dried over anh. $MgSO_4$, filtered and concentrated under vacuum. The resulting crude was recrystallized with DCM and hexane (1:1, 5 mL) and filtered to give the title compound as a pale yellow solid (1.50 g, 40%).

TLC (hexanes:EtOAc 8:2): R_f = 0.17.

mp. 146─148 ºC.

^{1}H NMR ($CDCl_3$, 400 MHz) δ 7.46 – 7.24 (m, 15H), 2.53 (t, *J* = 6.5 Hz, 2H), 2.31 (t, *J* = 6.5 Hz, 2H)

^{13}C NMR ($CDCl_3$, 101 MHz) δ 144.6, 129.5, 127.9, 126.7, 66.6, 40.4, 34.7 ppm.

ESI-HRMS (positive mode): *m/z* 320.1489 $[M+H]^+$ M calcd. for $C_{21}H_{21}NS$ 320.1467.

7-Bromo-5-phenyl-4-(3-((2-(tritylthio)ethyl)amino)propanoyl)-1,3,4,5-tetrahydro-2*H*-benzo[*e*][1,4]diazepin-2-one (3.37)

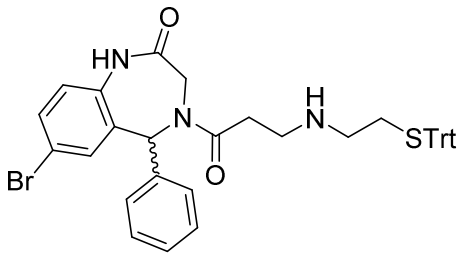

3.32 (370 mg, 0.99 mmol) and **3.36** (1.50 g, 4.49 mmol) were dissolved in DCM (5 mL) and reacted overnight at rt. Afterwards, the solvent was removed under low pressure, and the resulting crude was purified by silica gel flash column chromatography eluting with hexane:EtOAc:MeOH mixtures from 30:70:0 to 0:100:3. The title compound was obtained as a white solid (441 mg, 64%).

TLC (EtOAc:MeOH 97:3): R_f = 0.35.

IR (ATR, solid): 3211, 2926, 1729, 1666, 1664, 1482, 1448, 1368, 1242, 1216, 1188, 1058, 821, 745, 694 cm^{-1}.

^{1}H NMR ($CDCl_3$, 400 MHz) δ 7.44 – 7.40 (m, 9H), 7.30 – 7.18 (m, 14H), 7.03 – 6.99 (m, 1H), 6.90 and 6.11 (s, 1H), 4.42 – 3.96 (m, 2H), 2.80 – 2.66 (m, 2H), 2.60 – 2.45 (m, 3H), 2.41 – 2.31 (m, 3H), 1.87 (br s, 1H) ppm.

Diasteromer 1: ^{13}C NMR ($CDCl_3$, 101 MHz) δ 171.49, 169.75, 145.01, 138.34, 134.80, 134.45, 133.43, 132.28, 130.38, 129.15, 128.00, 127.85, 127.13, 126.80, 122.89, 117.61, 66.71, 63.16, 48.73, 44.67, 41.11, 33.67, 31.86 ppm.

Diasteromer 2: ^{13}C NMR ($CDCl_3$, 101 MHz) δ 171.86, 170.35, 144.90, 137.43, 135.47, 133.43, 132.83, 130.41, 129.33, 128.62, 128.30, 128.04, 127.13, 126.80, 123.40, 117.61, 66.80, 63.16, 48.40, 44.89, 41.11, 33.31, 31.81 ppm.

ESI-HRMS (positive mode): *m/z* 690.1776 / 692.1765 (^{81}Br) $[M+H]^+$; calcd for $C_{39}H_{37}BrN_3O_2S$ 690.1784.

7-Bromo-4-(3-((2-mercaptoethyl)amino)propanoyl)-5-phenyl-1,3,4,5-tetrahydro-2*H*-benzo[*e*][1,4]diazepin-2-one (3.38)

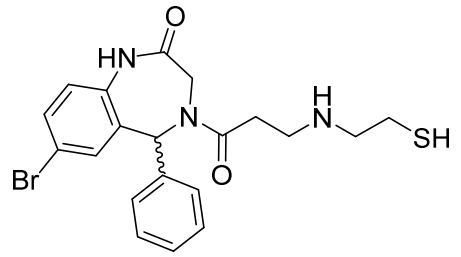

3.37 (20.0 mg, 0.03 mmol) was dissolved in a mixture of TFA:TIS (95:5) and reacted at room temperature for 90 min. Afterwards, the solvent was removed under N_2 stream and the resulting crude dissolved in a mixture MeOH:H_2O (1:1, 2 mL) and filtered through a PTFE syringe filter (0.22 µm), lyophilized and used without further purification.

HPLC (**Figure E.3.1**):
Analysis conditions 0-50 % B (0.1% Formic acid) t_R = 19.0 min.

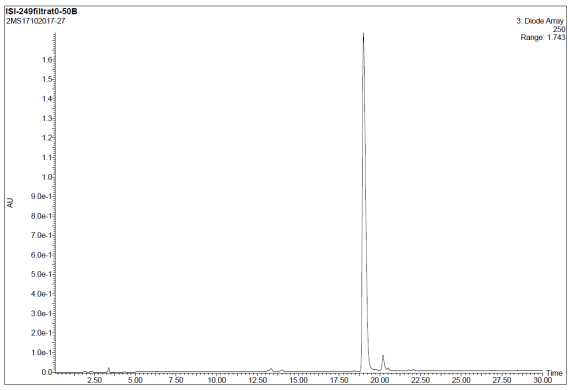

Figure E.3.1 HPLC profiles (250 nm) of deprotection crude.

N-(*N*$^{\alpha}$-Fmoc-*N*$^{\varepsilon}$-Boc-L-lysinyl)-2-amino-5-bromobenzophenone (3.39)

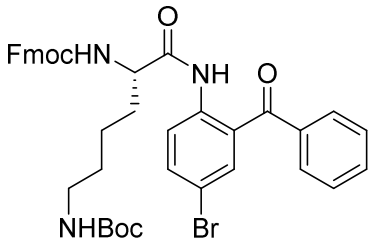

NMM (200 µL, 1.81 mmol) and IBCF (94 µL, 0.72 mmol) were added to a solution of Fmoc-Lys(Boc)-OH (337.1 mg, 0.72 mmol) in anh. DCM (5 mL) and cooled in an ice bath. After 15 minutes, a solution of **3.6** (200.0 mg, 0.72 mmol) in anh. DCM (1 mL) was added and the mixture was stirred for 1 h at 5 ºC and overnight at rt. Afterwards, further DCM was added (15 mL) and the mixture was washed with aq. HCl 10% (2 × 10 mL). The organic phase was dried over anh. $MgSO_4$, filtered and the solvent evaporated under reduced pressure. The resulting crude was purified by silica gel flash column chromatography eluting with DCM/MeOH mixtures from 100:0 to 98:2. The title compound was obtained as a pale white foam (301 mg, 57%).

TLC (DCM:MeOH 95:5): R_f = 0.40.

IR (ATR, solid): 2980, 2905, 2355, 1730, 1658, 1599, 1571, 1497, 1425, 1437, 1391, 1254, 1248, 1173, 1158, 1071, 1043, 757, 744, 694, 533 cm^{-1}.

^{1}H NMR ($CDCl_3$, 400 MHz): δ 8.57 (d, *J* = 8.8 Hz, 1H), 7.85 – 7.52 (m, 9H), 7.46 – 7.23 (m, 7H), 5.95 (br. s, 1H), 4.78 – 4.63 (m, 1H), 4.55 – 4.34 (m, 2H), 4.32 – 4.20 (m, 2H), 3.13 (t, *J* = 8.0 Hz, 2H), 2.02 (m, 2H), 1.93 – 1.78 (m, 2H), 1.77 – 1.50 (m, 2H), 1.45 (s, 9H) ppm.

^{13}C NMR ($CDCl_3$, 101 MHz): δ 197.84, 171.21, 156.47, 156.31, 143.69, 141.23, 138.78, 137.60, 136.75, 135.51, 132.91, 129.94, 128.46, 127.73, 127.66, 127.09, 127.05, 125.47, 125.14, 120.01, 119.89, 115.13, 79.21, 77.48, 77.16, 76.84, 67.44, 56.46, 47.20, 39.77, 31.73, 29.81, 28.47, 22.42 ppm.

ESI-HRMS (positive mode): *m/z* 726.2173 / 728.2161 (^{81}Br) $[M+H]^+$; calcd for $C_{39}H_{41}BrN_3O_6$ 726.2173

tert-Butyl (*S*)-(4-(7-bromo-2-oxo-5-phenyl-2,3-dihydro-1*H*-benzo[*e*][1,4]diazepin-3-yl)butyl)carbamate (3.40)

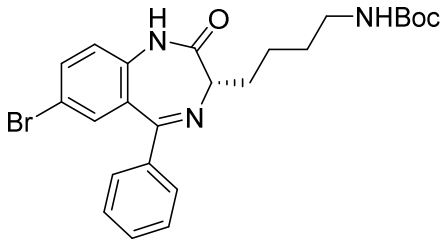

3.39 (150 mg, 0.21 mmol) was dissolved in a 7 M ammonia solution (in MeOH, 3 mL) and reacted at rt overnight. Afterwards, the reaction mixture was taken to dryness and the crude purified by silica gel flash column chromatography eluting with isocratic hexanes/EtOAc mixtures 70:30. The title compound was obtained as a pale yellow solid (104 mg, 99%).

One-Pot Alternative

To an ice-cooled solution of Fmoc-Lys(Boc)-OH (1.87 g, 4.00 mmol) in anh. DCM (15 mL) was added NMM (1.37 mL, 9.09 mmol) and IBCF (0.81 mL, 3.64 mmol). After 10 minutes, a solution of **3.6** (1.00 g, 3.64 mmol) in anh. DCM (2 mL) was added, and the mixture left 30 min at 5 ºC and 5.5 h at rt. Afterwards, the solvent was removed under vacuum to dryness, to the crude added 7 M NH_3 (in MeOH, 40 mL) and the solution left to react overnight at rt. Subsequently, the solvent was removed under vacuum, the resulting crude dissolved in EtOAc (100 mL) and washed with aq. HCl 10% (3 × 30 mL). The organic phase was dried over anh. $MgSO_4$, filtered and the solvent evaporated under vacuum. The crude material was further purified by silica gel flash column chromatography eluting with isocratic hexanes/EtOAc mixtures 70:30. The title compound was obtained as a pale yellow solid (970 mg, 55%).

TLC (Hexanes:EtOAc 1:1): R_f = 0.42.

IR (ATR, solid): 3414, 3309, 2929, 2359, 2337, 1682, 1653, 1508, 1232, 1156, 669 cm^{-1}.

^{1}H NMR ($CDCl_3$, 400 MHz): δ 9.45 (s, 1H), 7.60 (dd, *J* = 8.6, 2.3 Hz, 1H), 7.52 – 7.34 (m, 6H), 7.08 (d, *J* = 8.6 Hz, 1H), 4.63 (s br, 1H), 3.50 (dd, *J* = 8.2, 5.7 Hz, 1H), 3.19 (d, *J* = 7.6 Hz, 2H), 2.32 – 2.14 (m, 2H), 1.69 – 1.56 (m, 2H), 1.44 (s, 11H) ppm.

^{13}C NMR ($CDCl_3$, 101 MHz): δ 172.13, 168.09, 156.03, 138.64, 137.65, 134.57, 133.30, 130.51, 129.67, 129.10, 128.34, 123.04, 116.00, 79.01, 63.22, 40.47, 30.66, 30.00, 28.44, 23.32 ppm.

ESI-HRMS (positive mode): *m/z* 486.1386 / 488.1370 (^{81}Br) $[M+H]^+$; calcd for $C_{24}H_{29}BrN_3O_3$ 486.1387.

7-Bromo-1,3,4,5-tetrahydro-4-[4-(*N*-Boc-amino)butyl]-5-phenyl-2*H*-1,4-benzodiazepin-2-one (3.41)

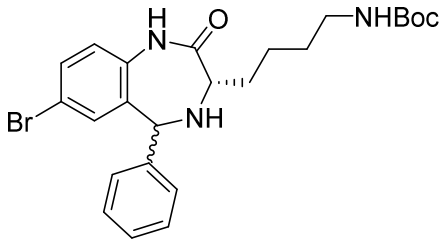

To a solution of **3.40** (800 mg, 1.65 mmol) and $NaBH_3CN$ (155.4 mg, 2.48 mmol) in MeOH (10 mL), AcOH (500 µL, 8.24 mmol) was added, and the mixture was stirred at rt for 2.5 h until complete reduction of the imine as assessed by TLC. Afterwards, the solvent was removed under low pressure, the crude was dissolved in EtOAc (50 mL) and washed with aq. sat. $NaHCO_3$ (2 × 20 mL). The organic layer was dried over anh. $MgSO_4$, filtered and the solvent removed under low pressure. The title compound was obtained as a pale yellow solid (799 mg, 99%).

TLC (Hexanes:EtOAc 1:1): R_f = 0.52.

IR (ATR, solid): 3290, 2967, 2929, 2866, 1663, 1479, 1365, 1245, 1159, 817, 700 cm^{-1}.

^{1}H NMR ($CDCl_3$, 400 MHz): δ 7.99 and 7.67 (s, 1H), 7.45 – 7.27 (m, 5H), 7.13 and 6.76 (d, *J* = 2.3Hz, 1H), 6.89 and 6.80 (d, 8.4 Hz, 1H), 5.34 and 5.24 (s, 1H), 4.56 (br s, 1H), 3.57 and 3.31 (t, *J* = 7.2 Hz, 1H), 3.14 – 3.05 (m, 2H), 1.94 – 1.44 (m, 6H), 1.42 (s, 9H) ppm.

Diastereomer 1: ^{13}C NMR ($CDCl_3$, 101 MHz): δ 175.02, 156.00, 142.23, 139.97, 136.56, 132.23, 128.64, 128.45, 127.19, 122.69, 117.53, 79.06, 63.98, 59.94, 40.29, 31.65, 29.93, 28.41, 23.50 ppm.

Diastereomer 2: ^{13}C NMR ($CDCl_3$, 101 MHz): δ 174.27, 156.00, 142.33, 139.97, 135.88, 131.35, 128.57, 128.20, 127.54, 123.32, 118.88, 79.06, 58.97, 56.14, 40.29 31.65, 30.04, 28.42, 23.21 ppm.

ESI-HRMS (positive mode): *m/z* 488.1559 / 490.1555 (^{81}Br) $[M+H]^+$; calcd for $C_{24}H_{31}BrN_3O_3$ 488.1543.

(*S*)-3-(4-Ammoniobutyl)-7-bromo-2-oxo-5-phenyl-2,3,4,5-tetrahydro-1*H*-benzo[*e*][1,4]diazepin-4-ium chloride (3.43)

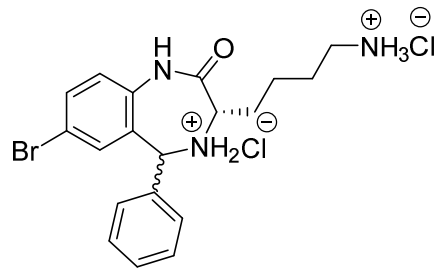

In a 10 mL round-bottom flask, **3.41** (100 mg, 0.21 mmol) dissolved in 4 M HCl (in dioxane, 5 mL) and the reaction mixture was left stirring for 2.5 h at room temperature. Afterwards the solvent was removed under low pressure to afford the title product as a pale yellow solid (94 mg, 99%).

TLC (DCM:MeOH 9:1): R_f = 0.20.

IR (ATR, solid): 3474, 3199, 2911, 2711, 2524, 1704, 1590, 1568, 1479, 1448, 1375, 1315, 1270, 1245, 1131, 998, 916, 827, 697 cm^{-1}

^{1}H NMR (CD_3OD, 400 MHz) δ 7.75 and 7.73 (s, 1H), 7.69 – 7.55 (m, 4H), 7.44 – 7.38 (m, 1H), 7.34 – 7.29 (m, 2H), 7.19 (d, *J* = 8.5 Hz) and 7.09 (d, *J* = 9.2 Hz, 1H), 6.02 and 5.71 (s, 1H), 4.12 (dd, *J* = 9.0, 4.6 Hz) and 3.86 (dd, *J* = 10.5, 3.1 Hz, 1H), 2.99 – 2.89 (m, 2H), 2.32 – 2.10 (m, 1H), 2.00 – 1.80 (m, 1H), 1.71 (h, *J* = 7.3 Hz, 2H), 1.58 – 1.34 (m, 2H) ppm.

Diastereomer 1: ^{13}C NMR ($CDCl_3$, 101 MHz): δ 166.45, 138.28, 135.43, 135.17, 133.98, 130.67, 130.20, 129.58, 130.20, 129.58, 128.34, 125.45, 120.24, 60.83, 57.09, 40.24, 28.13, 27.96, 23.88 ppm.

Diastereomer 2: ^{13}C NMR ($CDCl_3$, 101 MHz): δ 167.82, 136.80, 135.87, 134.92, 133.34, 131.13, 130.35, 129.58, 128.34, 126.16, 119.84, 63.60, 57.38, 40.24, 29.17, 28.05, 23.66 ppm.

ESI-HRMS (positive mode): *m/z* 388.1016 / 390.1000 (^{81}Br) $[M+H]^+$; calcd for $C_{19}H_{23}BrN_3O$ 388.1019.

(*E*)-*N*-(4-((3*S*)-7-Bromo-2-oxo-5-phenyl-4-propionyl-2,3,4,5-tetrahydro-1*H*-benzo[*e*][1,4]diazepin-3-yl)butyl)hepta-4,6-dienamide (3.44)

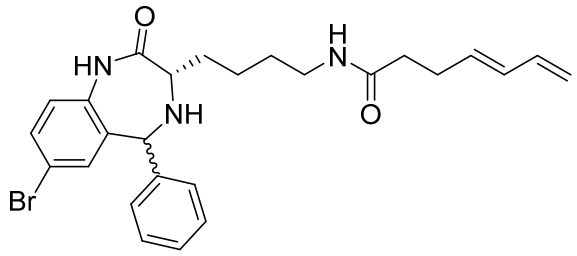

DIPC (61 µL, 0.39 mmol) and NMM (2.6 µL, 0.03 mmol) were added to a solution of **3.48** (49 mg, 0.39 mmol) in HPLC ACN (1 mL) and left stirring for 10 minutes. Afterwards, **3.43** (50.0 mg, 0.13 mmol) and additional NMM (2.6 µL, 0.03 mmol) were poured into the mixture. Additional NMM (2.6 µL, 0.03 mmol) was added after 20 and 40 minutes and the solution stirred up to 2 h at rt. Subsequently, addition ACN was added (4 mL), the crude filtered using a PTFE syringe filter (0.22 µm), purified by HPLC and lyophilized. The title compound was obtained as a white solid (10.7 mg, 20%)

TLC (9:1 EtOAc:MeOH): R_f = 0.10.

^{1}H NMR ($CDCl_3$, 400 MHz) δ 7.65 - 7.53 (m, 4H), 7.42 - 7.28 (m, 4H), 7.16 and 7.04 (d, *J* = 8.5 Hz, 1H), 7.47 and 6.97 (d, *J* = 2.2 Hz, 1H), 6.35 – 6.21 (m, 1H), 6.13 – 6.02 (m, 1H), 5.80 and 5.68 (s, 1H), 5.70 – 5.61 (m, 1H), 5.06 (dd, *J* = 16.9, 1.9 Hz, 1H), 4.92 (dt, *J* = 10.2, 2.2 Hz, 1H), 4.17 – 3.77 (m, 1H), 3.72 (dd, *J* = 10.1, 3.7 Hz, 1H), 3.23 – 3.07 (m, 2H), 2.39 – 2.31 (m, 2H), 2.27 – 2.12 (m, 3H), 1.81 – 1.63 (m, 1H), 1.55 – 1.31 (m, 4H) ppm.

^{13}C NMR ($CDCl_3$, 101 MHz) δ 173.99, 173.93, 136.91, 135.65, 133.59, 132.93, 132.50, 131.86, 129.62, 129.28, 128.67, 127.77, 126.88, 123.98, 118.74, 114.45, 59.34, 55.99, 38.24, 35.25, 29.37, 28.76, 28.34, 22.80 ppm.

ESI-HRMS (positive mode): *m/z* 496.1584 / 498.1573 (^{81}Br) $[M+H]^+$; calcd. for $C_{26}H_{30}BrN_3O_3$ 496.1594.

HPLC analysis (**Figure E.3.2**)
Analysis conditions 30-70 % B (0.1% Formic acid) t_R = 14.3 min and 18.1 min.
Purification 40-80 % B (0.1% Formic acid)

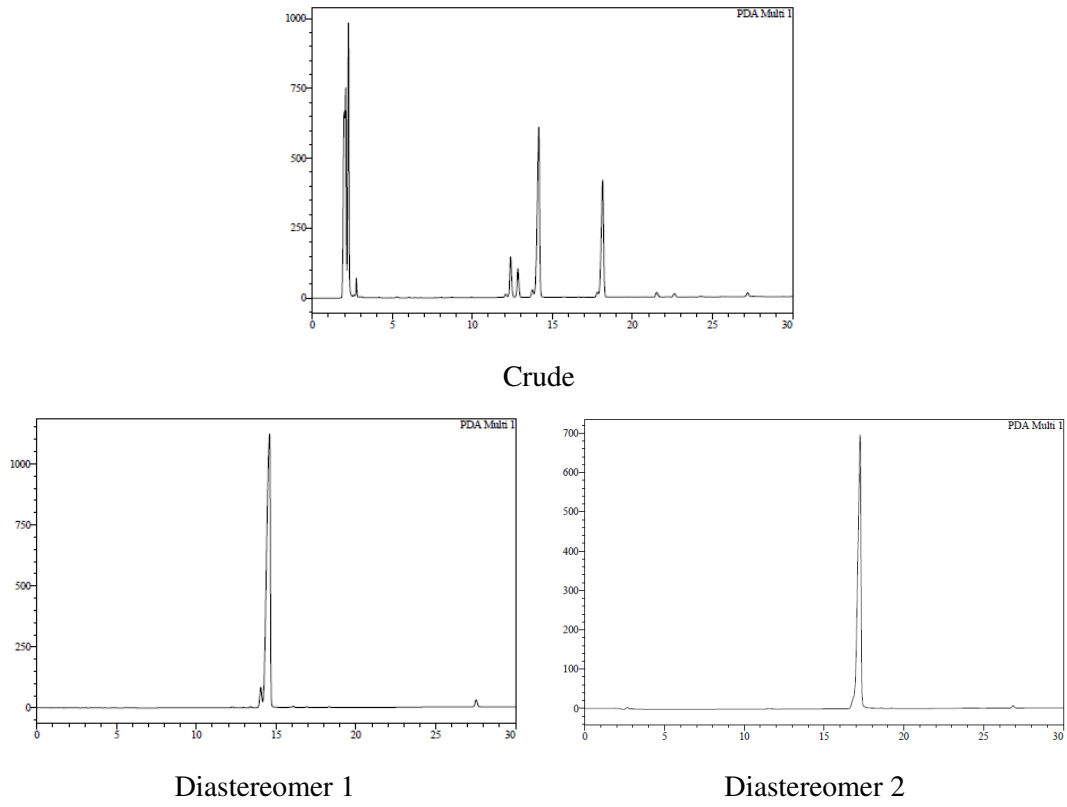

Figure E.3.2 HPLC traces (250 nm) of crude reaction (top) and purified diastereomers (bottom).

Ethyl (*E*)-hepta-4,6-dienoate (3.47)

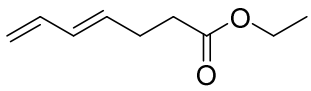

To a solution of 1,4-pentandie-3-ol (**3.45**, 1.15 mL, 11.89 mmol) and triethyl orthoacetate (**3.46**, 17.4 mL, 95.17 mmol) was added propionic acid (90 µL, 1.19 mmol) and the mixture refluxed for 2 h. Afterwards, the ethanol formed was distilled and BHT (40 mg) was added and left an additional hour refluxing. Subsequently the excess solvent is removed under vacuum and the crude was purified by silica gel column chromatography eluting with 100:0 up to 60:40 (hexanes:DCM mixture). The title compound was obtained as a colorless oil (901 mg, 50%).

TLC (Hexanes:DCM 60:40): R_f = 0.30.

^{1}H NMR ($CDCl_3$, 400 MHz): δ 6.29 (dd, *J* = 17.0, 10.3 Hz, 1H), 6.08 (dd, *J* = 15.2, 10.3 Hz, 1H), 5.75 – 5.64 (m, 1H), 5.11 (d, *J* = 16.9 Hz, 1H), 4.99 (d, *J* = 10.1 Hz, 1H), 4.13 (q, *J* = 7.1 Hz, 2H), 2.42 – 2.39 (m, 4H), 1.25 (t, *J* = 7.1 Hz, 3H) ppm.

^{13}C NMR ($CDCl_3$, 101 MHz): δ 172.92, 136.83, 132.64, 131.92, 115.67, 60.35, 33.84, 27.79, 14.23 ppm.

(*E*)-Hepta-4,6-dienoic acid (3.48 or 4.98)

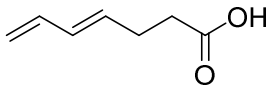

To a solution of ethyl (**3.47**) (901 mg, 5.85 mmol) in EtOH:H_2O (3:1) (90 mL) was added LiOH (702 mg, 29.25 mmol) and heated to 50 ºC for 2 h. Afterwards, EtOH was removed under pressure, the aqueous phase washed with DCM (50 mL) and acidified with aq. HCl 10% (30 mL). The aqueous phase was extracted with DCM (3 × 40 mL), the combined organic phases were dried over anh. $MgSO_4$, filtered and the solvent removed under vacuum. The title compound was obtained as a colorless oil (735 mg, 99%).

^{1}H NMR ($CDCl_3$, 400 MHz) δ 6.29 (m, 1H), 6.11 (dd, *J* = 14.8, 10.4 Hz, 1H), 5.74 – 5.65 (m, 1H), 5.13 (d, *J* = 16.8 Hz, 1H), 4.99 (d, *J* = 10.0 Hz, 1H), 2.50 – 2.42 (m, 4H) ppm.

^{13}C NMR ($CDCl_3$, 101 MHz) δ 179.43, 136.73, 132.14, 132.12, 115.92, 33.59, 27.37 ppm.

2-(Tritylthio)acetic acid (3.50)

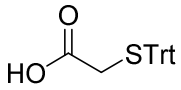

2-Mercaptoacetic acid (**3.49**, 900 µL, 12.97 mmol) was dissolved in a mixture of DCM:AcOH (1:1, 12 mL). Subsequently, trityl chloride (2.87g, 12.97 mmol) and $BF_3{\cdot}Et_2O$ (2 mL, 33.82 mmol) were added and the solution left stirring for 20 min at rt. Afterwards, the solvent was removed under vacuum and distilled H_2O (10 mL) was added to the residue. The resulting precipitate was filtered and washed with both H_2O and ACN. The title compound was obtained as a white solid (3.20 g, 74%).

^{1}H NMR ($CDCl_3$, 400 MHz) δ 7.46 – 7.24 (m, 15H), 3.06 (s, 2H) ppm.

^{13}C NMR ($CDCl_3$, 101 MHz) δ 175.82, 143.85, 129.50, 128.12, 127.02, 67.27, 34.50 ppm.

(*S*)-*N*-(4-(7-Bromo-2-oxo-5-phenyl-2,3,4,5-tetrahydro-1*H*-benzo[*e*][1,4]diazepin-3-yl)butyl)-2-(tritylthio)acetamide (3.51)

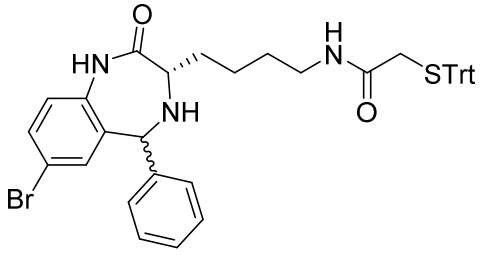

DIPC (61 µL, 0.39 mmol) and NMM (28 µL, 0.26 mmol) were added to a solution of **3.50** (130 mg, 0.39 mmol) in HPLC ACN (1 mL) and left stirring for 10 minutes. Afterwards, **3.43** (50 mg, 0.13 mmol) were poured into the mixture and the solution stirred up to 2 h at room temperature. Subsequently,

addition ACN was added (4 mL), the crude filtered using a PTFE syringe filter (0.22 µm) and purified by HPLC. The title compound was obtained as a white solid (18.3 mg, 20%)

ESI-HRMS (positive mode): *m/z* 704.1927 / 706.1916 (^{81}Br) $[M+H]^+$; calcd. for $C_{40}H_{38}BrN_3O_2S$ 704.1941.

Chromatogram

HPLC:
Analysis conditions 50-100 % B (0.1% Formic acid) t_R = 14.3 min and 18.1 min. (**E.3.3**)
Purification 60-100 % B (0.1% Formic acid)

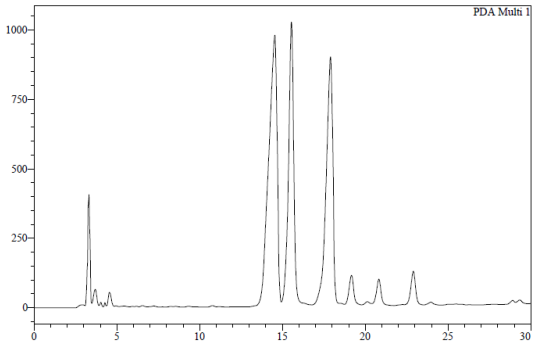

Crude

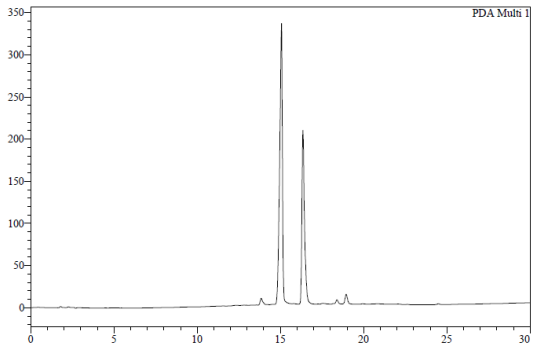

Diastereomer 1

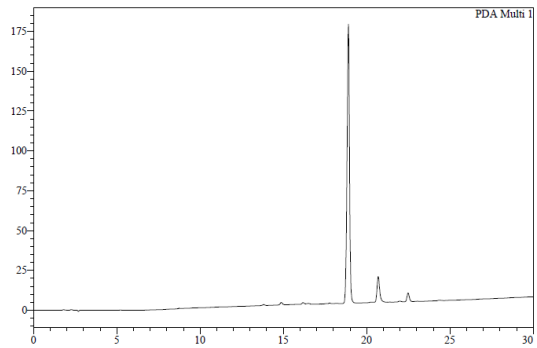

Diastereomer 2

Figure E.3.3 HPLC traces (250 nm) of crude reaction (top) and purified diastereomers (bottom).

(*S*)-*N*-(4-(7-bromo-2-oxo-5-phenyl-2,3,4,5-tetrahydro-1*H*-benzo[*e*][1,4]diazepin-3-yl)butyl)-2-mercaptoacetamide (3.52)

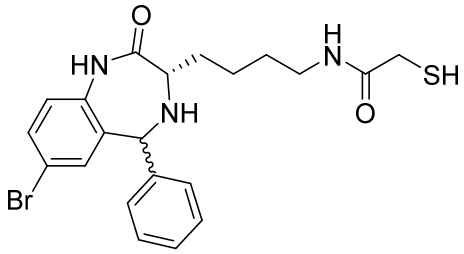

3.51 (5.0 mg, 0.007 mmol) was dissolved in a mixture of TFA:TIS (95:5, 1 mL) and reacted at room temperature for 90 min. Afterwards, the solvent was removed under N_2 stream, the resulting crude dissolved in a mixture H_2O:MeOH (1:1, 2 mL), filtered through a PTFE syringe filter (0.22 µm), lyophilized and used without further purification.

HPLC analysis (**Figure E.3.4**)
Analysis conditions 0-50 % B (0.1% Formic acid) t_R = 25.8 min.

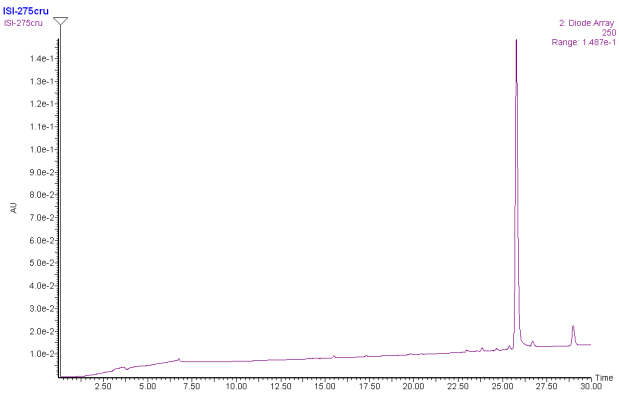

Figure E.3.4 HPLC traces (250 nm) of the deprotection crude reaction.

4-(2-Hydroxyethyl)-1,7-dimethyl-10-oxa-4-azatricyclo[5.2.1.$0^{2,6}$]dec-8-en-3,5-dione, *exo* isomer (3.58)

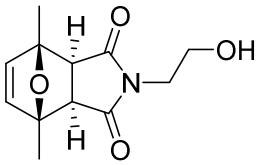

To a solution of *N*-(2-hydroxyethyl)maleimide (**3.57**, 1.00 g, 7.09 mmol) in anh. ACN (10 mL) was added 2,5-dimethylfuran (3.80 mL, 35.45 mmol) and the mixture left reacting overnight at 65 ºC under an argon atmosphere. Afterwards, the solvent was removed under reduced pressure and the resulting oil was treated with 32 % conc. aq. ammonia (40 mL) and the mixture left overnight at rt. Subsequently, ammonia was removed under reduced pressure followed by the addition of brine (20 mL) and aq. HCl 10% (10 mL). The solution was transferred to a separatory funnel and the aqueous layer extracted with DCM (3 × 20 mL). The combined organic phases were dried over anh. $MgSO_4$, filtered and the solvent removed under vacuum. The title compound was obtained as a dark yellow oil (1.24 g, 74%).

^{1}H NMR ($CDCl_3$, 400 MHz): δ 6.31 (s, 2H), 3.75 (t, *J* = 4.3 Hz, 2H), 3.70 (t, *J* = 4.3 Hz, 2H), 2.86 (s, 2H), 1.70 (s, 6H) ppm.

^{13}C NMR ($CDCl_3$, 101 MHz): δ 175.32, 140.80, 87.67, 60.24, 52.50, 41.56, 15.83 ppm.

2-Cyanoethyl (2-((3a*R*,7a*S*)-4,7-dimethyl-1,3-dioxo-1,3,3a,4,7,7a-hexahydro-2*H*-4,7-epoxyisoindol-2-yl)ethyl) (3.59)

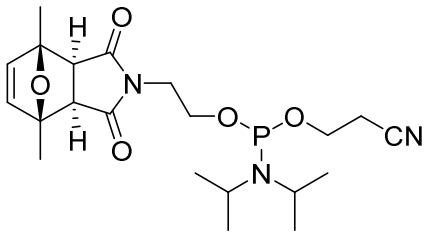

To a solution of **3.58** (250 mg, 1.05 mmol) in DCM (1 mL), NEt_3 (730 µL, 5.23 mmol) was added. Afterwards, a solution of CECP (250 mg, 1.06 mmol) in anh. DCM (1 mL) was added, and the mixture was reacted at room temperature for 1 h. Subsequently, additional DCM (10 mL) were added and the mixture transferred into a separatory funnel. The organic layer was washed with aq. $NaHCO_3$ sat. (2 × 10 mL), dried over anh. $MgSO_4$, filtered and the solvent removed under vacuum. The crude was further purified by silica gel column chromatography eluting with 95:5 (DCM:NEt_3 mixture). The title compound was obtained as a pale-yellow oil (417 mg, 90%).

TLC (DCM:NEt_3 95:5): R_f = 0.60.

^{1}H NMR ($CDCl_3$, 400 MHz) δ 6.29 (s, 2H), 3.85 – 3.47 (m, 8H), 2.85 – 2.80 (m, 2H), 2.62 (m, 2H), 1.69 (s, 6H), 1.14 (dd, *J* = 8.1, 6.8 Hz, 12H) ppm.

^{31}P NMR ($CDCl_3$, 162 MHz) δ 147.91 ppm.

Retro-1-dT$_{10}$ (3.61)

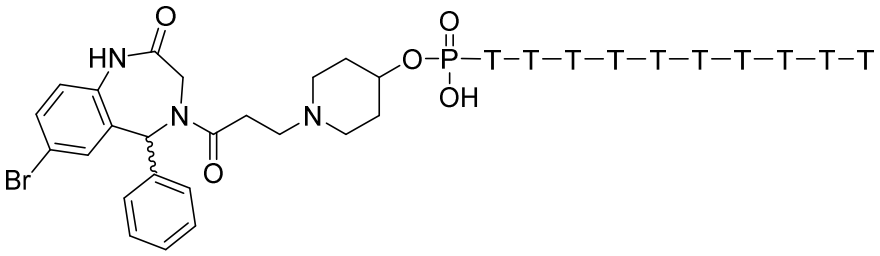

dT$_{10}$-resin was automatically assembled at the 1 µmol-scale using standard phosphoramidite chemistry. Tetrazole-mediated coupling of **3.35** (0.1 M solution in anh. ACN, 10 min coupling time) gave a low incorporation yield (38%) of the Retro-1 derivative as assessed by HPLC analysis after phosphite to phosphate oxidation, deprotection and cleavage of an aliquot with conc. aq. ammonia (the capping step had been omitted to allow coupling to be repeated in case the yield was not good). After a second coupling in the presence of BTT (10 min coupling time), the amount of Retro-1-dT$_{10}$ conjugate rose to 94% (same analysis procedure).

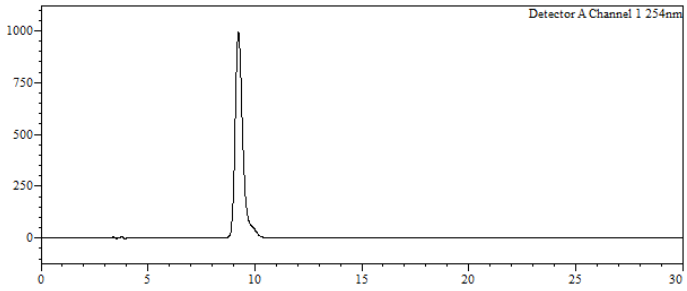

Figure E.3.5 HPLC trace (254 nm) of the purified Retro-1-dT_{10} analogue.

HPLC:
Analysis conditions, 20-60% B, t_R = 9.2 min (**Figure E.3.5**).
Purification gradient: 30-70% B. t_R = 8.5 min Yield: 52%.

MALDI-TOF (negative mode, THAP/CA): *m/z* 3511.4 $[M-H]^-$, calcd. for $C_{123}H_{156}BrN_{23}O_{73}P_{10}$ 3511.5.

PMal[Me_2]-$^{5'}$rGTTATTCTTTAGAATGGTGC$^{3'}$ (3.71)

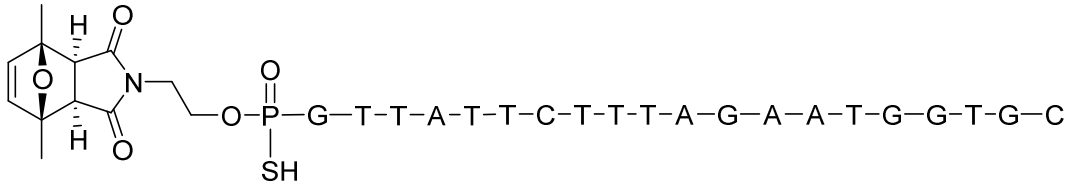

PMal[Me_2]-623-Resin was automatically assembled at the 1 µmol-scale using standard phosphoramidite chemistry using BTT-mediated (0.3 M in anh. ACN) couplings (10 min. couplings) and Beaucage reagent as a sulfurizing agent (0.05 M in anh. ACN; 2 × 4 min). The rT_{OMe} phosphoramidite was dissolved in anh. DCM instead of the usual anh. ACN. For the final incorporation of **3.59** a double coupling of 10 min. (0.1 M solution in anh. ACN) and same sulfurization procedure was employed.

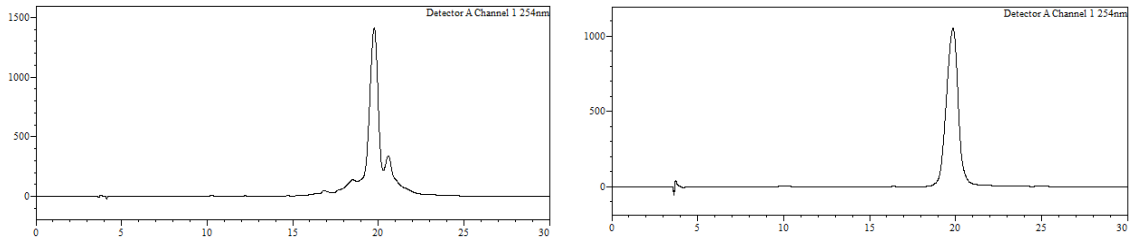

Crude Purified

Figure E.3.6 HPLC traces (254 nm) of crude reaction (left) and purified oligonucleotide derivative (right).

HPLC:
Analysis conditions, 0-50% B, t_R = 19.7 min (**Figure E.3.6**).
Purification gradient: 20-40% B. t_R = 10.7 min Yield: 26%.

MALDI-TOF (negative mode, THAP/CA): *m/z* 7375.1 $[M-H]^-$, M calcd. For $C_{230}H_{304}N_{70}O_{129}P_{20}S_{20}$ 7368.8.

$^{5'}$rTGTGTACTGATGTAGTTATC$^{3'}$ (Scrambled)

Retro1-Scramble-Resin was automatically assembled at the 1 μmol-scale using standard phosphoramidite chemistry. Using BTT-mediated (0.3 M in ACN) couplings (10 min. couplings) and Beaucage reagent as a sulfurizing agent (0.05 M in anh. ACN; 2 × 4 min). The rT_{OMe} phosphoramidite was dissolved in anh. DCM instead of the usual anh. ACN.

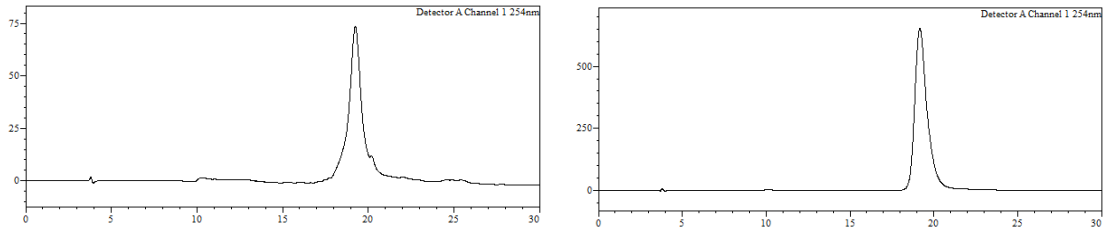

Crude Purified

Figure E.3.7 HPLC traces (254 nm) crude (left) and purified oligonucleotide (right).

HPLC: Analysis conditions, 0-50% B, t_R = 19.2 min (**Figure E.3.7**).

Purification gradient: 20-40% B. t_R = 8.9 min Yield: 43%.

MALDI-TOF (negative mode, THAP/CA): *m/z* 7053.8 $[M-H]^-$, M calcd. for $C_{218}H_{290}N_{69}O_{124}P_{19}S_{19}$ 7053.8.

Retro-1-$^{5'}$rGTTATTCTTTAGAATGGTGC$^{3'}$ (3.72)

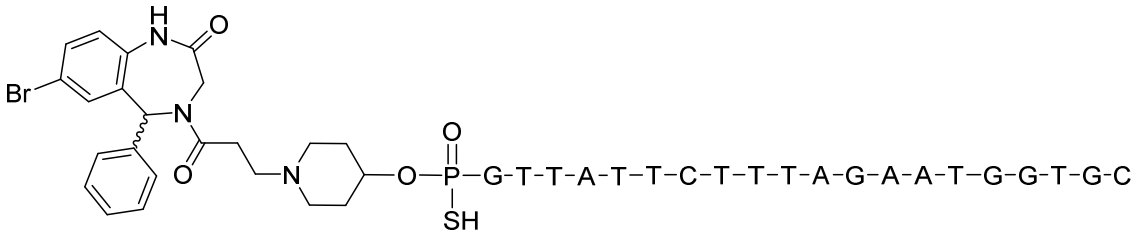

Retro1-623-Resin was automatically assembled at the 1 μmol-scale using standard phosphoramidite chemistry using BTT-mediated (0.3 M in ACN) couplings (10 min. couplings) and Beaucage reagent as a sulfurizing agent (0.05 M in anh. ACN; 2 × 4 min). The rT_{OMe} phosphoramidite was dissolved in anh. DCM instead of the usual anh. ACN. For the final incorporation of **3.35** a double coupling of 10 min. (0.1 M solution in anh. ACN) and the same sulfurization procedure was employed.

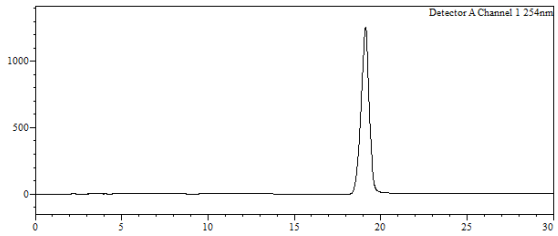

SSO-623

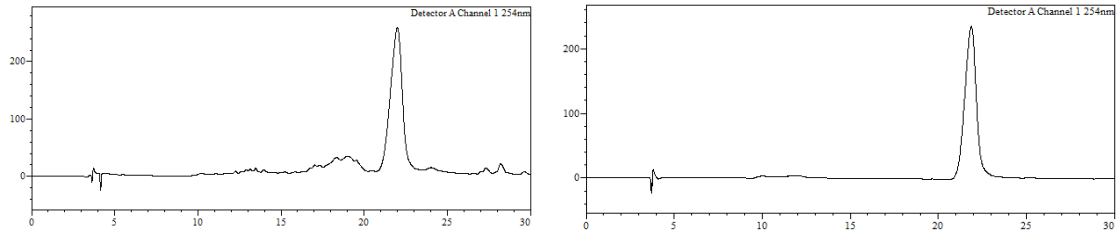

Crude Purified

Figure E.3.8 HPLC traces (254 nm) of the unconjugated 623 (top), **3.35** crude reaction (bottom left) and purified conjugate (bottom right).

HPLC:
Analysis conditions, 0-50% B, t_R = 22.0 min (**Figure E.3.8**).
Purification gradient: 15-40% B. t_R = 19.1 min Yield: 36%.

MALDI-TOF (negative mode, THAP/CA): *m/z* 7610.5 $[M-H]^-$, M calcd. for $C_{241}H_{315}BrN_{72}O_{128}P_{20}S_{20}$ 7602.8.

Retro-1-Lys-(Diene-Mal-$^{5'}$rGTTATTCTTTAGAATGGTGC$^{3'}$)NH (3.74)

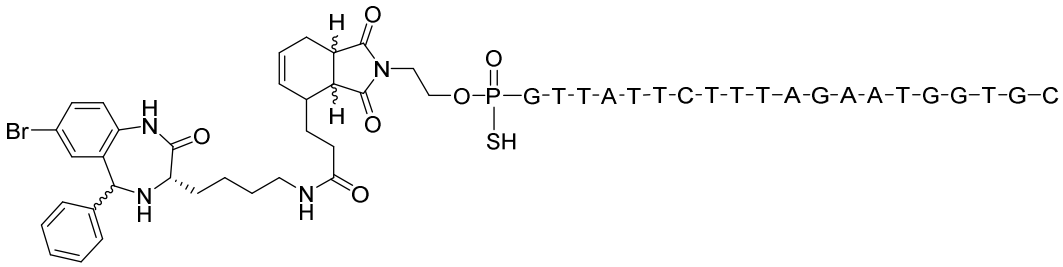

To a solution of **3.71** (800 nm) in MeOH:H_2O (1:1, 20 mL) **3.44** (4000 nmol) was added and the resulting mixture (final oligonucleotide concentration = 40 µM) heated at 90 ºC in a MW oven for 90 min. Afterwards, the MeOH was removed under reduced pressure and the resulting crude purified by HPLC.

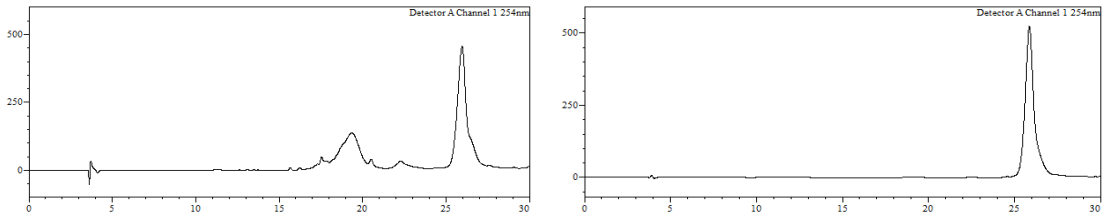

Crude Purified

Figure E.3.9 HPLC traces (254 nm) crude reaction (left) and purified conjugate (right).

HPLC:
Analysis conditions, 0-50% B, t_R = 25.9 min (**Figure E.3.9**).
Purification gradient: 20-40% B. t_R = 21.3 min Yield: 20%.

MALDI-TOF (negative mode, THAP/CA): *m/z* 7772.5 $[M-H]^-$, M calcd. for $C_{250}H_{326}BrN_{73}O_{130}P_{20}S_{20}$ 7767.9.

Retro-1-(S-Mal-$^{5'}$rGTTATTCTTTAGAATGGTGC$^{3'}$) (3.75)

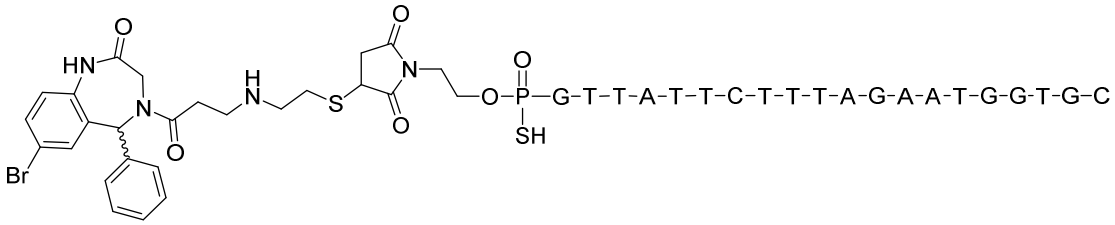

To a solution of **3.71** (260 nmol) in MeOH:H_2O (1:1, 468 µL,) a solution of **3.38** (520 nmol, 52 µL, 10 mM) in MeOH:H_2O (1:1) was added and the resulting mixture (final oligonucleotide concentration = 0.5 mM) heated at 90 ºC in a MW oven for 90 min. Afterwards, MeOH was removed under reduced pressure and the resulting crude purified by HPLC.

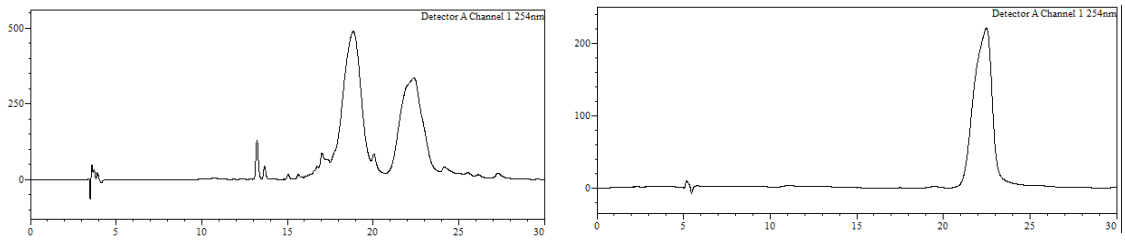

Crude Purified

Figure E.3.10 HPLC traces (254 nm) crude reaction (left) and purified conjugate (right).

HPLC:
Analysis conditions, 0-50% B, t_R = 22.4 min (**Figure E.3.10**).
Purification gradient: 20-40% B. t_R = 14.4 min Yield: 11%.

MALDI-TOF (negative mode, THAP/CA): *m/z* 7720.7 $[M-H]^-$, M calcd. for $C_{244}H_{318}BrN_{73}O_{130}P_{20}S_{21}$ 7719.8.

Retro-1-$^{5'}$rTGTGTACTGATGTAGTTATC$^{3'}$ (3.77)

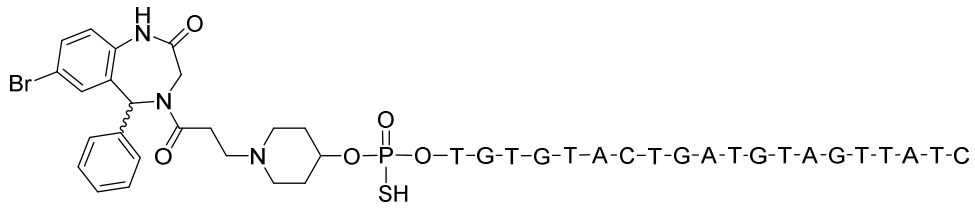

Retro1-Scramble-Resin was automatically assembled at the 1 μmol-scale using standard phophoramidite chemistry using BTT-mediated (0.3 M in ACN) couplings (10 min. couplings) and Beaucage reagent as a sulfurizing agent (0.05 M in anh. ACN; 2 × 4 min). The rT_{OMe} phosphoramidite was dissolved in anh. DCM instead of the usual anh. ACN. For the final incorporation of **3.35** a double coupling of 10 min. (0.1 M solution in anh. ACN) and same sulfurization procedure was employed.

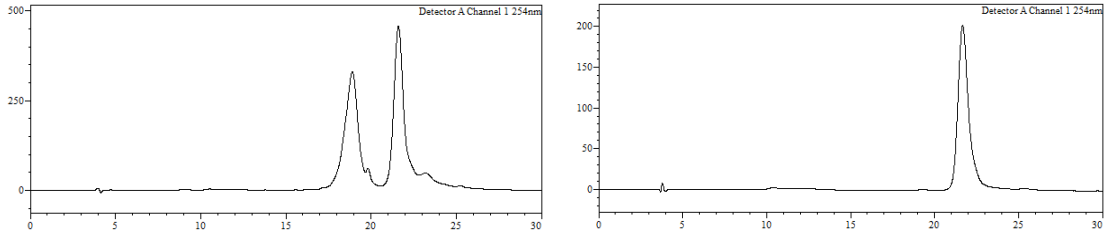

Crude Purified

Figure E.3.11 HPLC traces (254 nm) crude reaction (left) and purified conjugate (right).

HPLC:

Analysis conditions, 0-50% B, t_R = 21.7 min (**Figure E.3.11**).

Purification gradient: 20-40% B. t_R = 13.8 min Yield: 20%.

MALDI-TOF (negative mode, THAP/CA): *m/z* 7602.1 $[M-H]^-$, M calcd. for $C_{241}H_{315}BrN_{72}O_{128}P_{20}S_{20}$ 7602.8.

PMal[Me$_2$]-$^{5'}$rTGTGTACTGATGTAGTTATC$^{3'}$ (3.78)

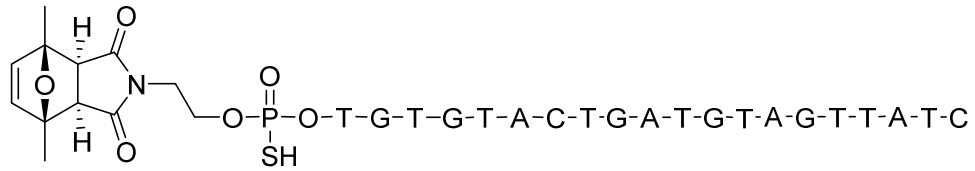

PMal[Me$_2$]-Scrambled-resin was automatically assembled at the 1 μmol-scale using standard phophoramidite chemistry using BTT-mediated (0.3 M in anh. ACN) couplings (10 min. couplings) and Beaucage reagent as a sulfurizing agent (0.05 M in anh. ACN; 2 × 4 min). The rT_{OMe} phosphoramidite was dissolved in anh. DCM instead of the usual anh. ACN. For the final incorporation of **3.59** a double coupling of 10 min. (0.1 M solution in anh. ACN) and same sulfurization procedure was employed.

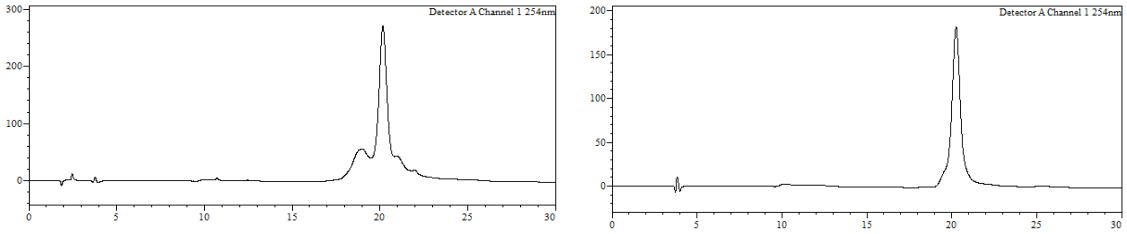

Crude Purified

Figure E.3.12 HPLC traces (254 nm) crude reaction (left) and purified oligonucleotide derivative (right).

HPLC: Analysis conditions, 0-50% B, t_R = 20.2 min (**Figure E.3.12**).

Purification gradient: 20-40% B. t_R = 11.3 min Yield: 20%.

MALDI-TOF (negative mode, THAP/CA): *m/z* 7369.0 $[M-H]^-$, M calcd. For $C_{230}H_{304}N_{70}O_{129}P_{20}S_{20}$ 7368.8.

Retro-1-Lys(Diene-5'rTGTGTACTGATGTAGTTATC3')NH (3.79)

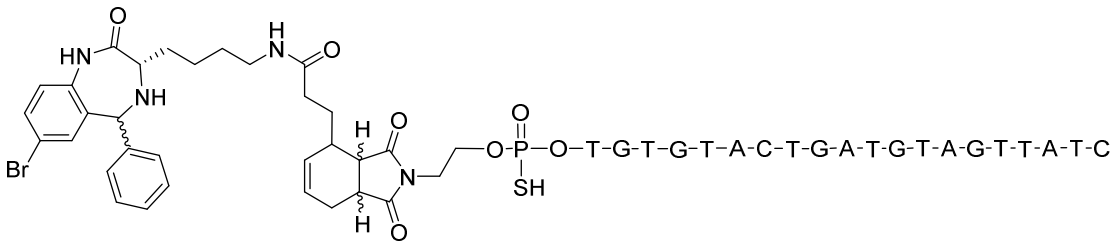

3.78 (800 nm) was dissolved in MeOH:H_2O (1:1, 20 mL) (final oligonucleotide concentration = 40 µM) and heated at 90 ºC in a MW oven for 90 min. Afterwards, a solution of **3.44** (4000 nmol) in H_2O (1 mL) was added and the resulting mixture left stirring for 1 h. Finally, MeOH was removed under reduced pressure and the resulting crude purified by HPLC.

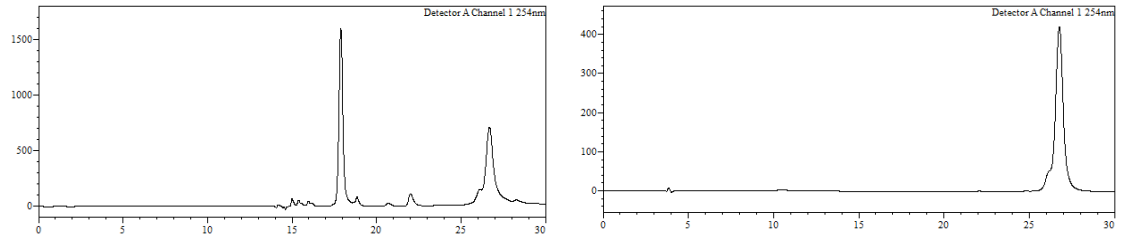

Crude Purified

Figure E.3.13 HPLC traces (254 nm) crude reaction (left) and purified conjugate (right).

HPLC:
Analysis conditions, 0-50% B, t_R = 26.7 min (**Figure E.3.13**).
Purification gradient: 20-40% B. t_R = 8.5 min Yield: 29%.

MALDI-TOF (negative mode, THAP/CA): *m/z* 7758.7 $[M-H]^-$, M calcd. for $C_{250}H_{326}BrN_{73}O_{130}P_{20}S_{20}$ 7767.9.

Experimental section: Chapter 4

3-((*3aR*,4*S*,7*R*,7a*S*)-4,7-Dimethyl-1,3-dioxo-1,3,3a,4,7,7a-hexahydro-2*H*-4,7-epoxyisoindol-2-yl)propanoic acid (4.13)

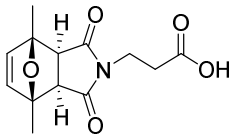

To a solution of maleimidopropionic acid (1.00 g, 5.91 mmol) in ACN (10 mL) was added 2,5-dimethylfuran (1.90 mL, 17.75 mmol) and the mixture left reacting overnight at 65 ºC. Afterwards, the solvent was removed under reduced pressure and the resulting oil was treated with 32 % cc. aq. ammonia (40 mL) and the mixture left overnight at room temperature. Subsequently, ammonia was removed under reduced pressure followed by the addition of aq. HCl 10% (30 mL). The solution was transferred to a separatory funnel and the aqueous layer extracted with DCM (3 × 30 mL). The combined organic phases were dried over $MgSO_4$, filtered and the solvent removed under vacuum. The title compound was obtained as a dark yellow oil (1.15 g, 74%).

^{1}H NMR ($CDCl_3$, 400 MHz) δ 6.30 (s, 2H), 3.78 (t, *J* = 7.3 Hz, 2H), 2.83 (s, 2H), 2.66 (t, *J* = 7.3 Hz, 2H), 1.69 (s, 6H).

^{13}C NMR ($CDCl_3$, 101 MHz) δ 175.0, 140.9, 87.7, 53.8, 15.8 ppm.

HRMS (negative mode): *m/z:* 264.05 $[M-H]^-$ M calcd. for $C_{13}H_{14}NO_5$ 265.09.

3-((3a*R*,4*S*,7*R*,7a*S*)-1,3-Dioxo-1,3,3a,4,7,7a-hexahydro-2*H*-4,7-epoxyisoindol-2-yl)propanoic acid (4.20)

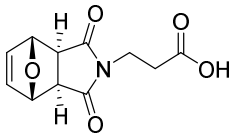

Furan (861 µL, 11.84 mmol) was added to a suspension of 3-maleimidopropanoic acid (**4.18**, 1.04 g, 6.12 mmol) in chloroform (10 mL), and heated under reflux overnight. Afterwards, the solvent was removed under reduced pressure and the residue was redissolved in a mixture of EtOAc and MeOH (5:1, 10 mL) and left to mix for 15 minutes at 45 °C. Subsequently, the mixture was precipitated with hexanes (100 mL) yielding a white solid, which was filtered using a Büchner funnel and washed with additional EtOAc (3 x 15 mL). The filtering process was repeated to ensure that no product was left in the mother liquor to yield the final product as a white solid (939 mg, 65%).

TLC (DCM/EtOAc/AcOH 30:68:2): R_f = 0.50.

mp. 165-168 ºC.

IR (ATR, Solid): ν 2927, 1778, 1692, 1165, 1015, 714 cm^{-1}.

^{1}H NMR (CD_3OD, 400 MHz) δ 6.54 (s, 2H), 5.15 (s, 2H), 3.71 (t, *J* = 7.2 Hz, 2H), 2.92 (s, 2H), 2.53 (t, *J* = 7.6 Hz) ppm.

^{13}C NMR (CD_3OD, 101 MHz): δ 178.17, 174.53, 137.61, 82.24, 48.74, 35.60, 32.83 ppm.

ESI-MS (negative mode): *m/z:* 236.20 $[M-H]^-$ M calcd. for $C_{11}H_{11}NO_5$ 236.05.

(3a*R*,4*S*,7*R*,7a*S*)-3a,4,7,7a-Tetrahydro-4,7-epoxyisobenzofuran-1,3-dione (4.24)

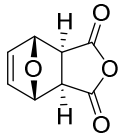

To a suspension of maleic anhydride (5.00 g, 51 mmol) was added furan (20 mL, 275 mmol) and Et_2O (10 mL). The solution was left stirring overnight at rt. Afterwards, the solvent was removed under reduced pressure to afford the title compound as a white solid (8.31 g, 98%).

TLC (DCM/MeOH 95:5): R_f = 0.12.

mp. 134-135 ºC.

IR (ATR, Solid): ν 1857, 1779, 1219, 732 cm^{-1}.

^{1}H NMR ($CDCl_3$, 400 MHz) δ 6.57 (s, 2H), 5.45 (s, 2H), 3.18 (s, 2H) ppm.

^{13}C NMR (CD_3OD, 101 MHz) δ 172.45, 138.01, 85.53, 50.22 ppm.

ESI-MS (positive mode): *m/z:* 167.47 $[M+H]^+$, M calcd. for $C_8H_7O_4$ 167.03.

(3a*R*,4*S*,7*R*,7a*S*)-2-(2-Hydroxyethyl)-3a,4,7,7a-tetrahydro-1*H*-4,7-epoxyisoindole-1,3(2*H*)-dione (4.26)

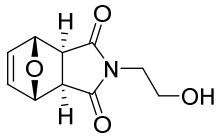

To a solution of **4.24** (1.00 g, 6.02 mmol) in MeOH (10 mL) was added ethanolamine (400 µL, 6.62 mmol) and the mixture left refluxing overnight. Afterwards, the mixture was cooled into a freezer, the precipitate filtered and washed with cold MeOH (3 × 5 mL). The title compound was obtained as a white solid (630 mg, 50%).

^{1}H NMR (DMSO-d_6, 400 MHz): δ 6.54 (s, 2H), 5.12 (s, 2H), 3.45 – 3.38 (m, 4H), 2.92 (s, 2H) ppm.

^{13}C NMR (DMSO-d_6, 101 MHz): δ 176.91, 136.89, 80.72, 57.71, 47.58, 41.05 ppm.

2-Cyanoethyl (2-((3a*R*,4*S*,7*R*,7a*S*)-1,3-dioxo-1,3,3a,4,7,7a-hexahydro-2*H*-4,7-epoxyisoindol-2-yl)ethyl) diisopropylphosphoramidite (4.27)

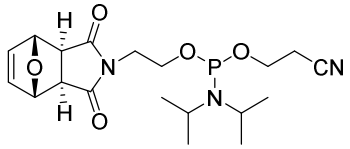

In an ice-cooled round-bottomed flask equipped with a magnet stirrer and an argon balloon was suspended **4.26** (332 mg, 1.58 mmol) in anh. DCM (3 mL). Subsequently anh. DIPEA (550 µL, 3.17 mmol) and a solution of CECP (250 mg, 1.05) in anh. DCM (2 × 1 mL) was added the mixture left reacting at at low temperature 20 min and rt for an additional 2 hours. Afterwards, additional DCM (30 mL) was added and the solution transferred into a separatory funnel, washed with aq. $NaHCO_3$ 5% (2 × 20 mL) and brine (2 × 20 mL). The organic layer was dried over anh. $MgSO_4$, filtered and the solvent

removed under vacuum. The crude was further purified by silica gel column chromatography eluting with DCM:NEt_3 isocratic mixtures 97.5:2.5. The title compound was obtained as a pale yellow oil (360 mg, 83%).

^{1}H NMR ($CDCl_3$, 400 MHz): δ 6.50 (s, 2H), 5.26 (s, 2H), 3.84 – 3.66 (m, 6H), 3.60 – 3.51 (m, 2H), 2.85 (t, *J* = 5.0 Hz, 2H), 2.63 – 2.59 (m, 2H), 1.15 (t, *J* = 7.0 Hz, 12H) ppm.

^{13}C NMR ($CDCl_3$, 101 MHz): δ 176.05, 136.53, 117.77, 80.84, 59.30, 58.57, 47.47, 43.09, 39.93, 24.62, 20.39 ppm.

^{31}P NMR ($CDCl_3$, 162 MHz) δ 147.93 ppm.

PMal[H_2]-dT_{10} (4.28)

dT_{10}-resin was automatically assembled at the 1 μmol-scale using standard phosphoramidite chemistry. For the introduction of **4.27** a BTT-mediated double coupling (0.1 M solution in anh. DCM, 2× 10 min coupling time) was employed.

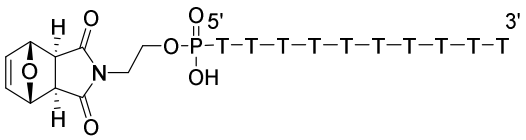

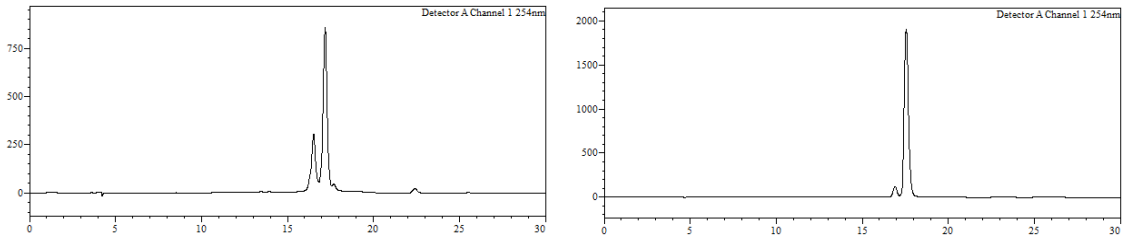

Crude Purified

Figure E.4.1 HPLC traces (254 nm) of crude (left) and purified (right) oxanorbornene-derivatized oligonucleotide.

HPLC: Analysis conditions, 0-50% B, t_R = 17.2 min (**Figure E.4.1**).

Purification gradient: 5-40% B. t_R = 12.3 min Yield: 14%.

MALDI-TOF (negative mode, THAP/CA): *m/z* 3248.3 $[M-H]^-$, M calcd. For $C_{110}H_{140}N_{21}O_{74}P_{10}$ 3248.5.

PMal(H_2)-$^{5'}$dCATGTATCGCATCATCAGT$^{3'}$ (4.30)

Oligonucleotide-resin was automatically assembled at the 1 μmol-scale using standard phosphoramidite chemistry. For the introduction of **4.27** a BTT-mediated double coupling (0.1 M solution in anh. DCM, 2× 10 min coupling time) was employed.

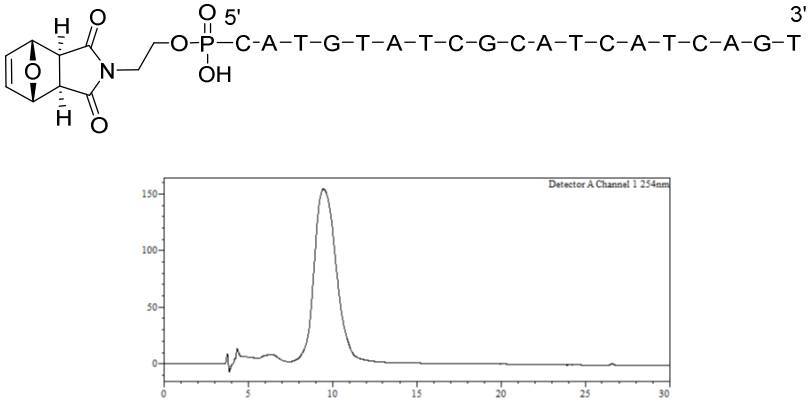

Figure E.4.2 HPLC traces (254 nm) of crude oligonucleotide.

HPLC: Analysis conditions, 10-50% B, t_R = 12.8 min (**Figure E.4.2**).

Yield: 15%.

MALDI-TOF (negative mode, THAP/CA): *m/z* 6033.3 $[M-H]^-$, M calcd. For $C_{195}H_{245}N_{68}O_{119}P_{19}$ 6031.0.

PMal(H_2)-RKKRRQRRR-NH_2 (4.33)

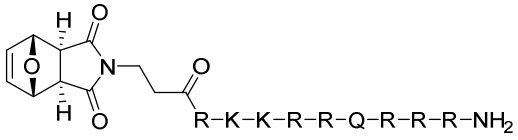

HPLC: Analysis conditions, 0-50% B, t_R = 18.7 min

Purification gradient: 10-50% B. t_R = 11.1 min Yield: 30%.

MALDI-TOF (positive mode, DHB): *m/z* 1558.7 $[M+H]^+$, M calcd. For $C_{64}H_{116}N_{32}O_{14}$ 1556.9.

PMal(H_2)-ctcatactct-NH_2 (4.34)

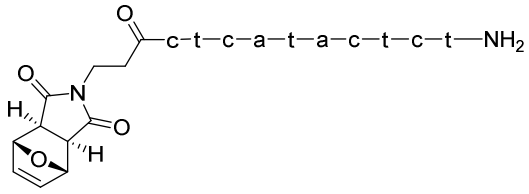

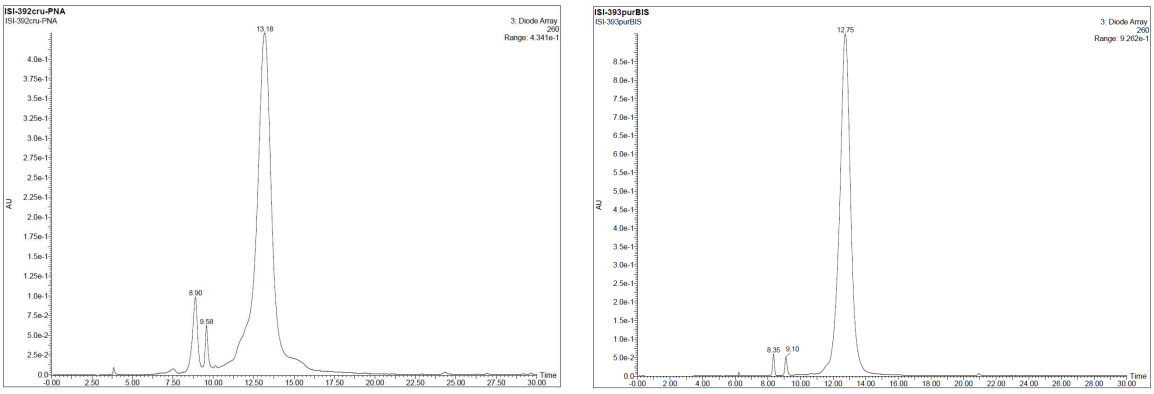

Crude Purified

Figure E.4.3 HPLC traces (254 nm) of crude (left) and purified (right) PNA derivative.

HPLC: Analysis conditions, 0-50% B (0.1% formic acid), t_R = 12.8 min (**Figure E.4.3**).

Purification gradient: 10-50% B (0.1% TFA). t_R = 14.1 min Yield: 24%.

MALDI-TOF (positive mode, DHB): *m/z* 2786.2 $[M\text{-Furan+H}]^+$; 2811.3 $[M\text{-Furan+Na}]^+$; 2827.2 $[M\text{-Furan+K}]^+$ M calcd. For $C_{117}H_{148}N_{52}O_{36}$ 2855.1.

3,6-Diphenyl-1,2,4,5-tetrazine (4.35)

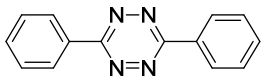

To a solution of sulphur powder (620 mg, 20.0 mmol) in absolute EtOH (25 mL) was added benzonitrile (2.00 mL, 20.0 mmol), acetonitrile (1 mL, 20.0 mmol), hydrazine monohydrate (20 mL, 280 mmol) and the mixture left refluxing for 3 h. Afterwards, the reaction was cooled, filtered and the solid washed with Et_2O (15 mL). The remaining solid was added AcOH (8 mL) followed by an aqueous solution of $NaNO_2$ (1.35 g, 10 mL) and left reacting for an additional hour. Afterwards, the reaction was cooled, neutralized with aq. $NaHCO_{3(sat)}$ and extracted with DCM (3 × 30 mL). The combined organic phases were dried over $MgSO_4$, filtered and the solvent removed *in vacuo*. The crude mixture was purified by flash chromatography eluting with hexanes/DCM 80:20 isocratic mixtures. The title compound was obtained as a purple solid (3.74 g, 80%).

TLC (Hexanes:DCM 80:20): R_f = 0.21

^{1}H NMR ($CDCl_3$, 400 MHz) δ 8.68 – 8.63 (m, 4H), 7.66 – 7.58 (m, 6H) ppm.

^{13}C NMR ($CDCl_3$, 101 MHz) δ 163.94, 132.65, 131.76, 129.28, 127.95 ppm.

ESI-HRMS (positive mode): *m/z* 235.0979 $[M+H]^+$; M calcd for $C_{10}H_{11}N_4$ 234.0978.

3-Methyl-6-phenyl-1,2,4,5-tetrazine (4.36)

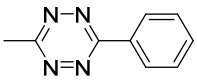

To a suspension of sulphur powder (620 mg, 20.0 mmol) in absolute EtOH (25 mL) was added benzonitrile (2.00 mL, 20.0 mmol), ACN (20 mL, 400.0 mmol) and $N_2H_4 \cdot H_2O$ (20 mL, 280 mmol) and the mixture left refluxing for 3 h. Afterwards, the reaction was cooled, filtered and the solid washed with Et_2O (15 mL). To the filtrate was added AcOH (8 mL) and cooled in an ice bath. Subsequently, an aqueous solution of $NaNO_2$ (1.35 g in 10 mL of H_2O) was added and left reacting for an additional 15 min until bubbling ceased. Afterwards, the reaction was removed from the bath, neutralized with aq. $NaHCO_{3(sat)}$ and extracted with DCM (3 × 30 mL). The combined organic layers were dried over anh. $MgSO_4$, filtered and the solvent removed *in vacuo*. The crude mixture was purified by flash chromatography eluting with hexanes/DCM 80:20 up to 50:50 mixtures. The title compound was obtained as a purple solid (1.46 g, 57%).

TLC (Hexanes:DCM 1:1): R_f = 0.50

^{1}H NMR ($CDCl_3$, 400 MHz) δ 8.59 (dd, *J* = 8.0, 1.8 Hz, 2H), 7.65 – 7.55 (m, 3H), 3.09 (s, 3H) ppm.

^{13}C NMR ($CDCl_3$, 101 MHz) δ 167.23, 164.10, 132.52, 131.77, 129.20, 127.90, 21.14 ppm.

UV-Spectra

1.50 mg weighed and solved in HPLC grade MeOH. The solution was diluted by a factor of 300 and recorded at 25 ºC.

ε_{260} = 23.800 L·mol^{-1}·cm^1; ε_{320} = 1.030 L·mol^{-1}·cm^1; ε_{540} = 320 L·mol^{-1}·cm^1 (25 ºC in MeOH)

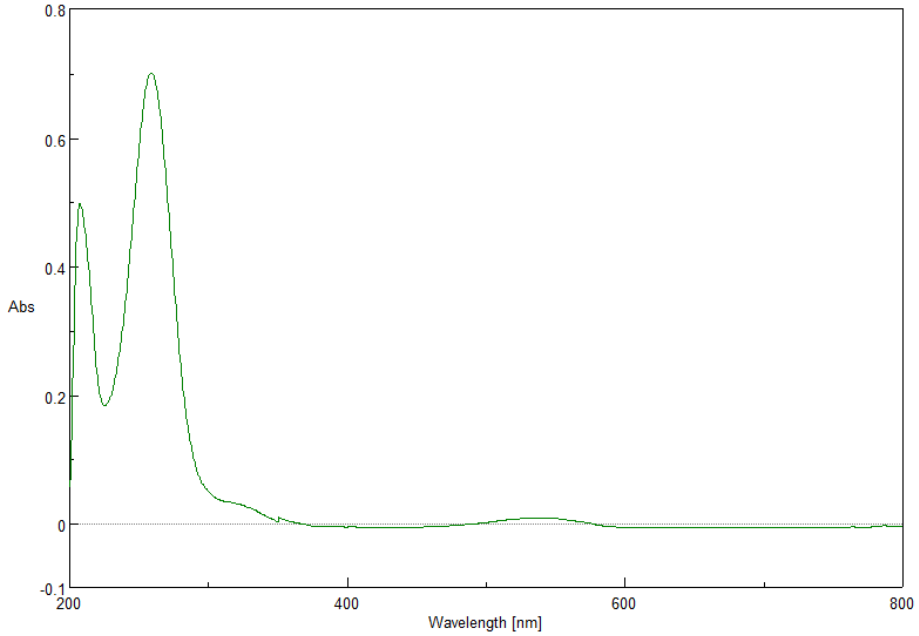

4-(6-(Pyrimidin-2-yl)-1,2,4,5-tetrazin-3-yl)benzoic acid (4.38)

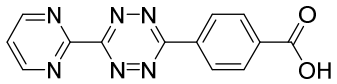

To a solution of 2-pyrimidinecarbonitrile (935 mg, 8.90 mmol) in EtOH (30 mL), 4-cyanobenzoic acid (1.96 g, 13.33 mmol) and $N_2H_4 \cdot H_2O$ 65% (5.5 mL, 70 mmol) and refluxed for overnight. Afterwards, the solution was cooled to room temperature and the precipitate washed with acetone (2 × 50 mL). To the remaining precipitate was added AcOH (10 mL) followed by aq. $NaNO_2$ (2.76 g, 40 mmol, 10 mL) and left stirring at rt for 30 min. The pink precipitate was filtered and washed with H_2O (3 × 10 mL) and transferred into a round-bottomed flask containing boiling DMF (20 mL). The DMF solution was kept at this temperature for 5 min and filtered while it was hot. The filtrate was collected and dried under vacuum. The filtration was repeated 3 times. The title product as a purple solid (357.1 mg, 14%)

^{1}H NMR (DMSO-d_6, 400 MHz) δ 9.21 (d, *J* = 4.8 Hz, 2H), 8.68 (d, *J* = 8.4 Hz, 2H), 8.24 (d, *J* = 8.4 Hz, 2H), 7.84 (t, *J* = 4.9 Hz, 2H) ppm.

^{13}C NMR (DMSO-d_6, 101 MHz) δ 172.47, 163.72, 163.34, 159.51, 158.97, 135.01, 130.65, 128.62, 123.47 ppm.

ESI-HRMS (negative mode): *m/z* 279.0647 $[M-H]^-$; M calcd for $C_{13}H_7N_6O_2$ 279.0636.

tert-Butyl (2-(2-(2-aminoethoxy)ethoxy)ethyl)carbamate (4.41)

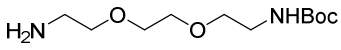

To an ice-cooled solution of 2,2′-(ethylenedioxy)bis(ethylamine) (4.00 mL, 27.49 mmol) in DCM (20 mL) was added dropwise a solution of Boc_2O (2.00 g, 9.16 mmol) in DCM (50 mL) over the course of 1 h. Afterwards, the mixture was allowed to warm at rt and left reacting overnight. Subsequently, the crude was transferred into a separatory funnel with additional DCM (50 mL) and washed with distilled H_2O (40 mL) and the aqueous phase extracted with DCM (2 x 20 mL). The combined organic layers were dried over anh. $MgSO_4$, filtered and the solvent removed under reduced pressure to afford the title compound (1.61 g, 71 % yield) as colorless oil.

^{1}H NMR ($CDCl_3$, 400 MHz) δ 5.34 (br.s, 1H), 3.42 – 3.37 (m, 4H), 3.30 (t, 5.3 Hz, 4H), 3.10 – 3.03 (m, 2H), 2.63 (t, *J* = 5.2 Hz, 2H), 1.41 (br.s, 2H), 1.21 (s, 9H) ppm.

^{13}C NMR ($CDCl_3$, 100 MHz) δ 155.84, 78.65, 73.16, 69.95, 41.47, 40.09, 28.20 ppm.

ESI-HRMS (positive mode): *m/z* 249.1806 $[M+H]^+$; calcd. for $C_{11}H_{25}N_2O_4$ 249.1809

tert-Butyl (2-(2-(2-(4-(6-(pyrimidin-2-yl)-1,2,4,5-tetrazin-3-yl)benzamido)ethoxy)ethoxy)ethyl)carbamate (4.42)

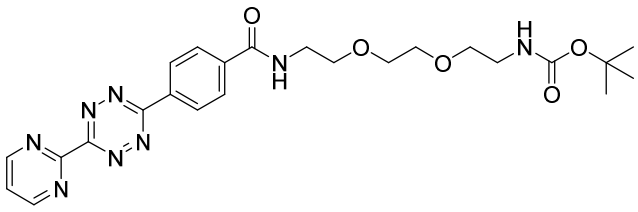

To a 25 mL round-bottomed flask, **4.38** (400.0 mg, 1.43 mmol) and HATU (651.4 mg, 1.71 mmol) were added and dissolved in anh. Pyr (5 mL). The mixture was left stirring for 5 min and a solution of

4.41 (425.3 mg, 1.71 mmol) in anh. Pyr (2 mL) was added. The mixture was left at room temperature for 2 h. Afterwards, to the solvent was removed under vacuum and to the crude was added DCM (20 mL) and washed with aq. HCl 10% (2 × 20 mL). The aqueous phase was extracted with additional DCM (2 × 20 mL). The combined organic layers were dried over anh. $MgSO_4$, filtered and the solvent removed *in vacuo.* The extract was further purified by silica gel flash column chromatography eluting with DCM/MeOH 100:0 up to 97:3 mixtures. The title compound was obtained as a pink solid (405.1 mg, 56%).

TLC (DCM:MeOH 90:10): R_f = 0.50.

^{1}H NMR ($CDCl_3$, 400 MHz) δ 9.15 (d, *J* = 4.9 Hz, 2H), 8.82 (d, *J* = 8.0 Hz, 2H), 8.07 (d, *J* = 7.7 Hz, 2H), 7.60 (t, *J* = 4.9 Hz, 1H), 6.93 (br. s, 1H), 4.98 (br. s, 1H), 3.73 (s, 4H), 3.70 (s, 4H), 3.63 – 3.54 (m, 4H), 1.45 (s, 9H) ppm.

^{13}C NMR ($CDCl_3$, 101 MHz) δ 167.5, 165.4, 164.9, 162.9, 156.1, 155.9, 135.2, 134.2, 130.2, 127.6117.7, 79.5, 73.2, 70.1 41.2, 40.0, 28.4 ppm.

ESI-HRMS (positive mode): *m/z* 511.2409 $[M+H]^+$; M calcd for $C_{24}H_{31}N_8O_5$ 511.2412.

2-(2-(2-(4-(6-(Pyrimidin-2-yl)-1,2,4,5-tetrazin-3-yl)benzamido)ethoxy)ethoxy)ethan-1-aminium chloride (4.43)

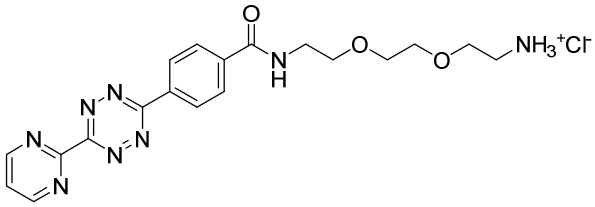

To a 25 mL round-bottomed flask **4.42** (200.0 mg, 0.39 mmol) was dissolved in a 4N HCl in dioxane (5 mL) and the solution stirred for 2 h at room temperature. Afterwards, the mixture was dried under vacuum to yield the title compound as a pink solid (155.1 mg, 96%).

TLC (DCM:MeOH 90:10): R_f = 0.18.

^{1}H NMR (CD_3OD, 400 MHz) δ 9.18 (d, *J* = 4.9 Hz, 2H), 8.81 (d, *J* = 8.7 Hz, 2H), 8.79 (br.s, 1H), 8.14 (d, *J* = 8.7 Hz, 2H), 7.82 (t, *J* = 4.9 Hz, 1H), 3.78 – 3.64 (m, 12H), 3.13 (t, *J* = 5.2 Hz, 2H) ppm.

^{13}C NMR ($CDCl_3$, 101 MHz) δ 167.88, 164.17, 162.62, 158.82, 158.31, 138.36, 134.36, 128.30, 127.90, 123.08, 70.00, 69.93, 69.17, 66.47, 39.45, 39.24 ppm.

ESI-HRMS (positive mode): *m/z* 411.1886 $[M+H]^+$; M calcd for $C_{19}H_{23}N_8O_3$ 411.1888.

UV-Spectra

2.21 mg weighed and solved in HPLC grade MeOH (1 mL). The solution was diluted by a factor of 400 and recorded at 25 ºC.

ε_{260} = 10.210 $L \cdot mol^{-1} \cdot cm^1$; ε_{280} = 18.670 $L \cdot mol^{-1} \cdot cm^1$; ε_{291} (max) = 21.210 $L \cdot mol^{-1} \cdot cm^1$; ε_{550} = 890 $L \cdot mol^{-1} \cdot cm^1$ (25 ºC in MeOH)

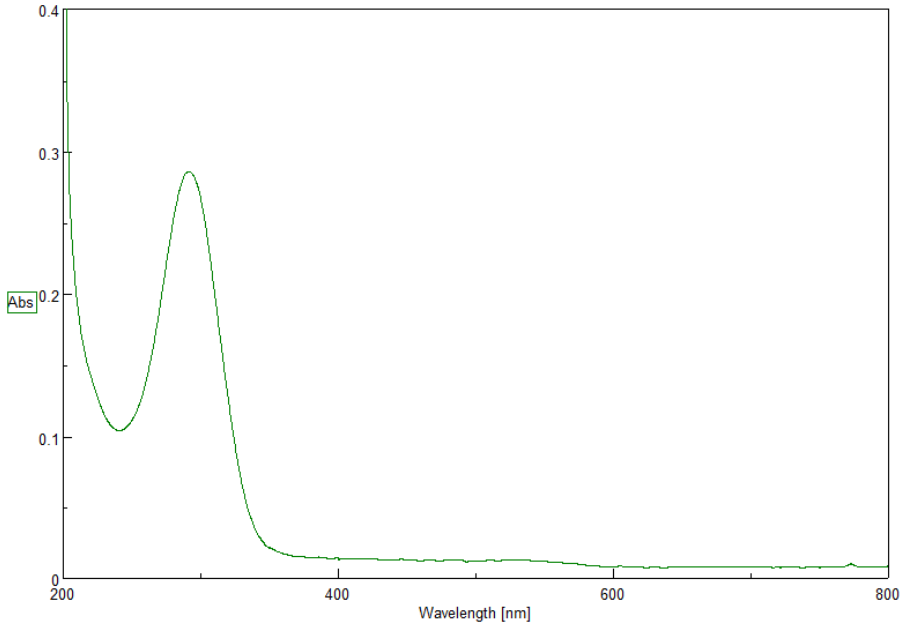

tert-Butyl (4-cyanobenzyl)carbamate (4.51)

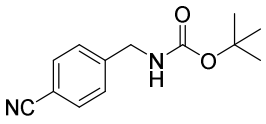

To a solution of 4-(aminoethyl)benzonitrile hydrochloride (**4.50**, 1.00 g, 5.92 mmol) in DCM (20 mL) was added NEt_3 (2.06 mL, 14.80 mmol) and Boc_2O (1.42 g, 6.51 mmol) and the mixture left at room temperature overnight. Subsequently, additional DCM (30 mL) and aq. 10% HCl (20 mL) were added to the mixture and the solution transferred into a separatory funnel. The aqueous layer was extracted with additional DCM (2 × 20 mL). The combined organic layers were dried over anh. $MgSO_4$, filtered and the solvent removed under vacuum. The title product was obtained as a white solid (1.37 g, 99%).

TLC (Hexanes:EtOAc 80:20): R_f = 0.25

^{1}H NMR ($CDCl_3$, 400 MHz) δ 7.62 (d, *J* = 8.2 Hz, 2H), 7.38 (d, *J* = 8.0 Hz, 2H), 4.97 (br. s, 1H), 4.37 (d, *J* = 6.2 Hz, 2H), 1.46 (s, 9H) ppm.

^{13}C NMR ($CDCl_3$, 101 MHz) δ 155.84, 144.61, 132.39, 127.76, 118.74, 111.10, 80.06, 44.18, 28.33 ppm.

tert-Butyl (4-(6-methyl-1,2,4,5-tetrazin-3-yl)benzyl)carbamate (4.52)

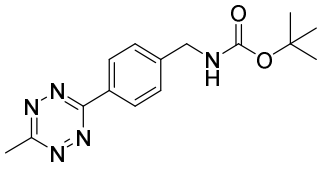

In a high-pressure tube equipped with a stirring bar **4.51** (1.30 g, 5.60 mmol), $NiCl_2 \cdot 6H_2O$ (660.2 mg, 2.80 mmol), ACN (3.0 mL, 55.96 mmol) and $N_2H_4 \cdot H_2O$ (6.8 mL, 139.91 mmol) were added. The mixture was sealed and heated at 60 ºC in an oil bath overnight. Afterwards, to the crude was added H_2O (30 mL), transferred into an Erlenmeyer flask and a solution of $NaNO_2$ (7.72 g, 111.93 mmol) in

H_2O (30 mL) followed by dropwise addition of aq. 10% HCl at 0 ºC until pH ≈ 3. The mixture was transferred into a separatory funnel and the aqueous layer extracted with EtOAc (4 × 50 mL). The combined organic layers were pooled together and washed with brine (50 mL), dried over anh. $MgSO_4$, filtered and the solvent removed under vacuum. The extract were further purified by silica gel column chromatography eluting with hexanes:EtOAc 100:0 up to 80:20 mixtures. The title compound was obtained as a purple solid (1.68 g, 70%).

TLC (Hexanes:EtOAc 80:20): R_f = 0.25

^{1}H NMR ($CDCl_3$, 400 MHz) δ 8.46 (d, *J* = 8.1 Hz, 2H), 7.43 (d, *J* = 8.0 Hz, 2H), 5.21 (br. s, 1H), 4.38 (d, *J* = 5.7 Hz, 2H), 3.03 (s, 3H), 1.43 (s, 9H) ppm.

^{13}C NMR ($CDCl_3$, 101 MHz) δ 167.11, 163.80, 155.96, 144.02, 130.64, 128.06, 127.95, 79.68, 44.29, 28.37, 21.08 ppm.

(4-(6-Methyl-1,2,4,5-tetrazin-3-yl)phenyl)methanamine (4.53)

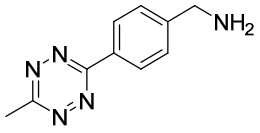

In a 100 mL round-bottomed flask was dissolved **4.52** (1.50 g, 4.98 mmol) was a added a HCl solution (4 M in dioxane, 10 mL) and the mixture was left stirring at room temperature for 2 h. Afterwards, the solvent was removed under vacuum and the mixture solved in sat. aq. $NaHCO_3$ (30 mL). The solution was transferred into a separatory funnel and the aqueous layer was extracted with DCM (4 × 30 mL). The combined organic layers were pooled together, dried over anh. $MgSO_4$ and the solvent removed *in* vacuo. The crude was further purified by silica gel column chromatography eluting with EtOAc:MeOH 100:0 up to 85:15 mixtures. The title compound was obtained as a purple solid (1.00 g, 99 %).

TLC (EtOAc): R_f = 0.20

^{1}H NMR ($CDCl_3$, 400 MHz) δ 8.60 (d, *J* = 8.1 Hz, 2H), 7.44 (d, *J* = 8.1 Hz, 2H), 4.31 (s, 2H), 3.03 (s, 3H) ppm.

^{13}C NMR ($CDCl_3$, 101 MHz) δ 167.40, 165.60, 143.03, 129.54, 127.12, 125.95, 45.91, 20.05 ppm.

Pyrim-Tz-LVPRGSYKGTSKLNYL-NH_2 (4.56)

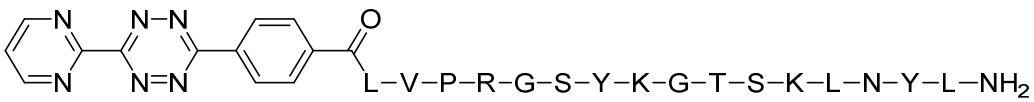

HPLC: purification gradient: 0-40% B; analysis conditions, 0-40% B, t_R = 21.0 min (Figure **E.4.4**).

MALDI-TOF (positive mode, DHB): *m/z* 2057.1 $[M+H]^+$, M calcd. for $C_{95}H_{141}N_{29}O_{23}$ 2056.1.

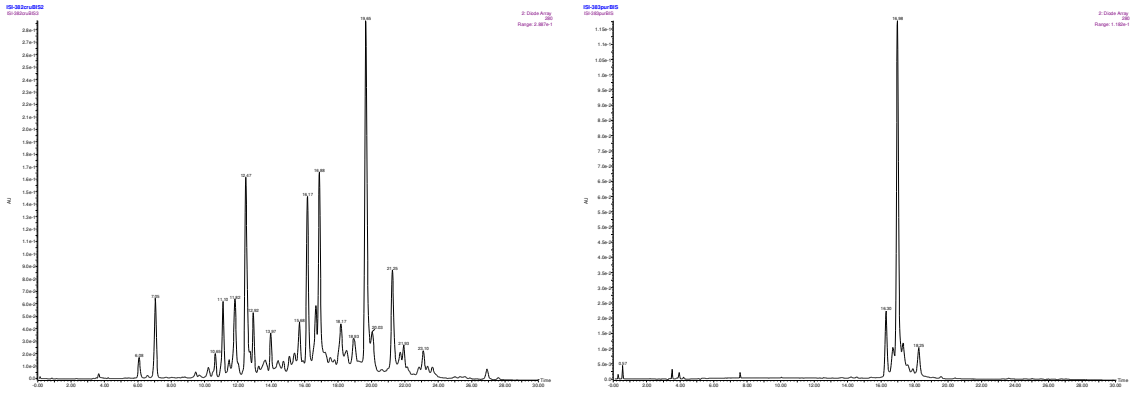

Crude Purified

Figure E.4.4 HPLC traces (254 nm) of crude (left) and purified (right) tetrazine-containing peptide.

(2*R*,3*R*,4*R*,5*R*,6*R*)-3-Acetamido-6-(acetoxymethyl)tetrahydro-2*H*-pyran-2,4,5-triyl triacetate (4.58)

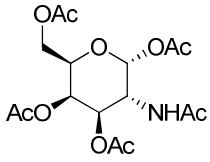

To a 100 mL round-bottomed flask D-(+)-galactosamine hydrochloride (4.00 g, 18.60 mmol) was solved in anh. Pyr (20 mL). Subsequently, Ac_2O (17.6 mL, 186.00 mmol) was added and the reaction mixture was stirred at rt overnight. Afterwards, the mixture was cooled in an ice bath and ice-cold water (100 mL) was added. The white solid precipitate was collected by vacuum filtration washing it with additional ice-cold water (2 × 20 mL). The precipitate was co-evaporated with toluene (30 mL) to remove residual water. The title product was obtained as a white powder (6.60 g, 91 %).

^{1}H NMR ($CDCl_3$, 400 MHz) δ 5.70 (d, *J* = 8.8 Hz, 1H), 5.54 (d, *J* = 9.6 Hz, 1H), 5.37 (d, *J* = 3.2 Hz, 1H), 5.08 (dd, *J* = 11.3, 3.3 Hz, 1H), 4.44 (dt, *J* = 11.3, 9.2 Hz, 1H), 4.14 (qd, *J* = 11.3, 6.5 Hz, 1H), 4.02 (t, *J* = 6.5 Hz, 1H), 2.17 (s, 3H), 2.13 (s, 3H), 2.04 (s, 3H), 2.02 (s, 3H), 1.94 (s, 3H) ppm.

^{13}C NMR ($CDCl_3$, 101 MHz) δ 170.76, 170.40, 170.32, 170.18, 169.59, 93.03, 71.85, 70.31, 66.32, 61.29, 49.76, 23.27, 20.88, 20.65, 20.63 ppm.

ESI-HRMS (positive mode): *m/z* 390.1374 $[M+H]^+$; M calcd for $C_{16}H_{23}NO_{10}$ 389.1322.

(3a*R*,5*R*,6*R*,7*R*,7a*R*)-5-(Acetoxymethyl)-2-methyl-3a,6,7,7a-tetrahydro-5*H*-pyrano[3,2-d]oxazole-6,7-diyl diacetate (4.59)

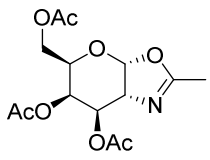

To a solution of **4.58** (500.0 mg, 1.28 mmol) in DCE (30 mL) was added TMSOTf (245 µL, 1.41 mmol) and the mixture heated at 55 ºC for 1 h. Afterwards, the crude was left cooling down and treated with NEt_3 (212 µL, 1.92 mmol) for 10 min. Afterwards, the crude was trespassed into a separatory funnel

and diluted with additional DCM (30 mL). The organic phase was washed with aq. sat. $NaHCO_3$ under vacuum and the residue was purified by silica gel flash column chromatography eluting with EtOAc/NEt_3 (99:1). The title compound was obtained as a pale-yellow oil (420.1 mg, 99 %).

^{1}H NMR ($CDCl_3$, 400 MHz) δ 5.95 (d, *J* = 6.8 Hz, 1H), 5.42 (t, *J* = 3.0 Hz, 1H), 4.87 (dd, *J* = 7.4, 3.4 Hz, 1H), 4.27 – 4.04 (m, 3H), 3.96 (td, *J* = 7.1, 1.4 Hz, 1H), 2.08 (s, 3H), 2.03 (s, 6H), 2.01 (d, *J* = 1.2 Hz, 3H) ppm.

^{13}C NMR ($CDCl_3$, 101 MHz) δ 170.43, 170.09, 169.74, 166.36, 101.44, 71.75, 69.45, 65.25, 63.50, 61.55, 20.74, 20.66, 20.53, 14.39 ppm.

ESI-HRMS (positive mode): *m/z* 330.1180 $[M+H]^+$; M calcd for $C_{14}H_{20}NO_8$ 330.1183.

(2*R*,3*R*,4*R*,5*R*,6*S*)-5-Acetamido-2-(acetoxymethyl)-6-(hex-5-en-1-yloxy)tetrahydro-2*H*-pyran-3,4-diyl diacetate (4.61)

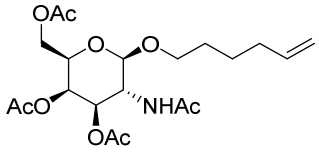

To a solution of **4.59** (300.0 mg, 0.91 mmol) in anh. DCE (20 mL) was added 4Å molecular sieves (1 g) and left stirring for 5 min at rt. Afterwards, 5-hexen-1-ol (**4.60**, 120 µL, 1.00 mmol) was added and stirring continued for 30 min. Subsequently, TMSOTf (79 µL, 0.46 mmol) was added and the mixture stirred for an additional 2 h at rt. The reaction mixture was quenched with aq. sat. $NaHCO_3$ and transferred into a separatory funnel. The aqueous layer was extracted with DCM (3 × 20 mL) and the combined organic layers were dried over anh. $MgSO_4$ and the solvent removed *in vacuo*. The extract was further purified by silica gel column chromatography eluting with DCM:MeoH mixtures from 100:0 up to 95:5. The title compound was obtained as a pale yellow solid (310.0 mg, 79 %).

^{1}H NMR ($CDCl_3$, 400 MHz) δ 5.78 (ddt, *J* = 16.9, 10.1, 6.6 Hz, 1H), 5.46 (t, *J* = 2.9 Hz, 1H), 5.42 (d, *J* = 8.5 Hz, 1H), 5.37 – 5.29 (m, 2H), 5.06 – 4.92 (m, 2H), 4.71 (d, *J* = 8.3 Hz, 1H), 4.20 – 4.07 (m, 3H), 3.96 – 3.85 (m, 3H), 3.49 (dt, *J* = 9.6, 6.7 Hz, 1H), 2.14 (s, 3H), 2.06 (s, 3H), 2.00 (s, 3H), 1.94 (s, 3H), 1.62 – 1.37 (m, 4H) ppm.

Benzyl 4-hydroxybutanoate (4.63)

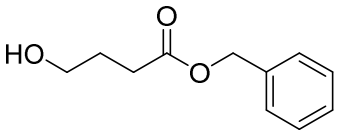

To a solution of NaOH (1.40 g, 34.87 mmol) in H_2O (30 mL) was added γ-butyrolactone (2.67 mL, 34.87 mmol) and the mixture heated to 70 ºC overnight. The crude was concentrated under vacuum, the solid suspended in acetone (30 mL) and TBAB (560 mg, 1.74 mmol) and BnBr (5.0 mL, 41.84 mmol) were added and the mixture left refluxing overnight. Subsequently, the crude was cooled and concentrated *in vacuo*, the residue redissolved in EtOAc (100 mL) and the solution transferred into a separatory funnel. The organic phase was washed with 1 N aqueous $NaHSO_4$ (30 mL), aq. sat. $NaHCO_3$ (30 mL) and brine (30 mL), dried over anh. $MgSO_4$ and concentrated. The crude was further purified using silica gel flash column chromatography eluting with EtOAc:hexane mixtures from 10:90 to 25:75 gradient to afford the title compound (4.30 g, 64%) as colorless oil.

TLC (EtOAc:hexane 40:60): R_f = 0.60.

^{1}H NMR ($CDCl_3$, 400 MHz): δ 7.40 – 7.30 (m, 5H), 5.12 (s, 2H), 3.67 (t, *J* = 6.2 Hz, 2H), 2.49 (t, *J* = 7.2 Hz, 2H), 1.94 – 1.86 (m, 3H) ppm.

^{13}C NMR ($CDCl_3$, 101 MHz): δ 177.81, 140.93, 128.50, 127.55, 126.94, 68.52, 65.24, 30.99, 27.77 ppm.

(2*R*,3*R*,4*R*,5*R*,6*R*)-5-Acetamido-2-(acetoxymethyl)-6-(4-(benzylperoxy)-4-oxobutoxy)tetrahydro-2*H*-pyran-3,4-diyl diacetate (4.64)

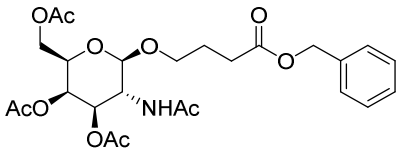

To a 100 mL round-bottomed flask, 4 Å molecular sieves (1 g) and **4.59** (2.23 g, 6.78 mmol) were added in DCE (30 mL) followed by a solution of benzyl 4-hydroxybutanoate (**4.63**, 1.45 g, 7.46 mmol) in DCE (5 mL) and the mixture left 30 min at 50 ºC. Afterwards, TMSOTf (612 µL, 3.39 mmol) was added dropwise and the solution left reacting 2 h at 50 ºC. Subsequently, the solution was transferred into a separatory funnel filtering off the sieves and DCM (30 mL) and aq. sat. $NaHCO_3$ (40 mL) were added. The aqueous phase was extracted with additional DCM until the organic layer was colorless (2 × 30 mL). The combined organic phases were pooled together, dried over anh. $MgSO_4$, filtered and the solvent removed *in vacuo*. The extract was further purified by silica gel column chromatography eluting with DCM:MeoH mixtures from 100:0 up to 95:5. The title compound was obtained as a pale yellow foam (1.48 g, 42 %).

TLC (DCM:MeOH 95:5): R_f = 0.45.

^{1}H NMR ($CDCl_3$, 400 MHz): 7.40 – 7.30 (m, 5H), 5.37 – 5.29 (m, 2H), 5.06 – 4.92 (m, 2H), 4.20 – 4.07 (m, 3H), 3.96 – 3.85 (m, 3H), 3.49 (d, *J* = 6.7 Hz, 2H), 2.14 (s, 3H), 2.06 (s, 3H), 2.00 (s, 3H), 1.94 (s, 3H), 1.62 – 1.37 (m, 4H) ppm.

ESI-HRMS (positive mode): *m/z* 524.2134 $[M+H]^+$; M calcd for $C_{25}H_{34}NO_{11}$ 524.2126.

4-(((2*R*,3*R*,4*R*,5*R*,6*R*)-3-Acetamido-4,5-diacetoxy-6-(acetoxymethyl)tetrahydro-2*H*-pyran-2-yl)oxy)butanoic acid (4.65)

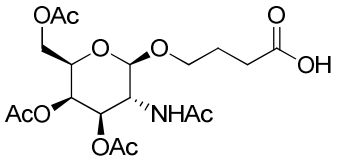

To a 100 mL round-bottomed flask and under an argon atmosphere, **4.64** (700.0 mg, 1.34 mmol) and 10% Pd/C (w/w) (70.0 mg, 0.06 mmol) were added. Subsequently, anh. MeOH (15 mL) was added, through a septum, and the argon was purged by flushing with two balloons full of H_2 (directly bubbling it into the solvent) over the course of 1 h. Afterwards, a new balloon was placed and the mixture stirred at rt for an additional 3 h. Then, the mixture was filtered through a Celite plug washing with additional MeOH (2 × 10 mL). After solvent removal under vacuum, the title compound was obtained as a white foam (520.1 mg, 90 %)

^{1}H NMR (CD_3OD, 400 MHz) δ 4.61 (d, *J* = 12.2 Hz, 1H), 4.37 (d, *J* = 8.4 Hz, 1H), 4.38 (s, 1H), 4.02 – 3.69 (m, 4H), 3.60 – 3.45 (m, 2H), 3.34 (d, *J* = 0.5 Hz, 2H), 2.24 (td, *J* = 7.3, 2.5 Hz, 2H), 2.14 (s, 3H), 2.06 (s, 3H), 2.00 (s, 3H), 1.94 (s, 3H) ppm.

ESI-HRMS (negative mode): *m/z* 432.1510 [M-H]$^-$; M calcd for $C_{18}H_{26}NO_{11}$ 432.1511.

(2*R*,3*R*,4*R*,5*R*,6*R*)-5-acetamido-2-(acetoxymethyl)-6-(4-((4-(6-methyl-1,2,4,5-tetrazin-3-yl)benzyl)amino)-4-oxobutoxy)tetrahydro-2*H*-pyran-3,4-diyl diacetate (4.66)

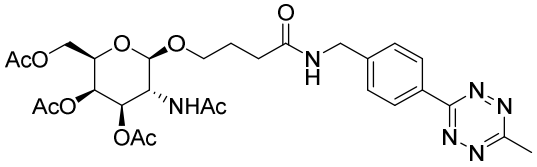

To a 25 mL round-bottomed flask, **4.53** (200.0 mg, 0.63 mmol), EDC·HCl (133.4 mg, 0.70 mmol), HOBt (94.3 mg, 0.70 mmol) and **4.65** (274.9 mg, 0.634 mmol) were weighed. Subsequently, DCM (5 mL) was added and the mixture left at room temperature overnight. Afterwards, the mixture was transferred into a separatory funnel with additional DCM (30 mL) and the organic phase washed with aq. citric acid 10% (2 × 20 mL) and aq. sat. $NaHCO_3$ (2 × 20 mL). The organic phase was driver over anh. $MgSO_4$, filtered and the solvent removed under pressure. The crude was further purified by silica gel flash column chromatography eluting with DCM/MeOH 100:0 up to 97:3 mixtures. The title compound was obtained as a pink solid (131.0 mg, 34%)

TLC (DCM:MeOH 95:5): R_f = 0.23.

^{1}H NMR ($CDCl_3$, 400 MHz) δ 8.54 (d, *J* = 8.3 Hz, 2H), 7.52 (d, *J* = 8.3 Hz, 2H), 6.55 (t, *J* = 6.0 Hz, 1H), 5.74 (d, *J* = 8.6 Hz, 1H), 5.33 (d, *J* = 3.4 Hz, 1H), 5.15 (dd, *J* = 11.3, 3.4 Hz, 1H), 4.61 (d, *J* = 8.3 Hz, 1H), 4.55 (dd, *J* = 6.1, 2.9 Hz, 1H), 4.20 – 3.80 (m, 6H), 3.56 (dt, *J* = 10.0, 6.0 Hz, 1H), 3.09 (s, 3H), 2.45 – 2.26 (m, 2H), 2.12 (s, 3H), 2.03 (s, 3H), 1.99 (s, 3H), 1.92 (s, 3H) ppm.

ESI-HRMS (positive mode): *m/z* 617.2559 [M-H]$^-$; M calcd for $C_{28}H_{37}NO_{10}$ 617.2556.

4-(((2*R*,3*R*,4*R*,5*R*,6*R*)-3-acetamido-4,5-dihydroxy-6-(hydroxymethyl)tetrahydro-2*H*-pyran-2-yl)oxy)-*N*-(4-(6-methyl-1,2,4,5-tetrazin-3-yl)benzyl)butanamide (4.68)

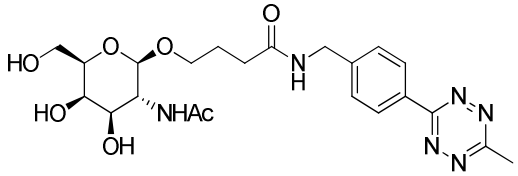

To a 100 mL round-bottomed flask, **4.65** (200 mg, 0.467 mmol) were weighed. Subsequently, 32% conc. aq. ammonia (20 mL) was added and the mixture left stirring at room temperature overnight. Afterwards, the ammonia was removed *in vacuo*, and to the crude added ACN (3 mL), EDC·HCl (133.4 mg, 0.70 mmol), HOBt (94.3 mg, 0.70 mmol) and **4.65** (274.9 mg, 0.634 mmol)**.** The mixture was left reacting for an additional 12 h. The crude was purified by silica gel flash column chromatography eluting with DCM/MeOH 100:0 up to 95:5 mixtures. The title compound was obtained as a pink solid (20.0 mg, 20%).

^{1}H NMR (CD_3OD, 400 MHz): δ 8.61 (d, *J* = 8.3 Hz, 2H), 7.79 (d, *J* = 8.2 Hz, 2H), 4.49 (d, *J* = 4.5 Hz, 1H), 4.35 (d, *J* = 8.4 Hz, 1H), 4.26 (s, 2H), 3.98 – 3.43 (m, 10H), 3.04 (d, *J* = 9.7 Hz, 3H), 2.43 – 2.29 (m, 2H), 1.97 (s, 3H), 1.93 – 1.80 (m, 2H) ppm.

^{13}C NMR (CD_3OD, 101 MHz): δ 174.61, 172.90, 167.43, 165.00, 137.96, 129.83, 127.47, 125.63, 108.70, 78.61, 71.30, 70.66, 62.19, 60.25, 43.63, 32.80, 25.67, 23.55, 20.0 ppm.

ESI-HRMS (positive mode): *m/z* 491.2245 $[M+H]^+$; M calcd for $C_{22}H_{31}N_6O_7$ 491.2249.

N-(2-(2-(2-(5-((3a*S*,4*S*,6a*R*)-2-Oxohexahydro-1*H*-thieno[3,4-*d*]imidazol-4-yl)pentanamido)ethoxy)ethoxy)ethyl)-4-(6-(pyrimidin-2-yl)-1,2,4,5-tetrazin-3-yl)benzamide (4.69)

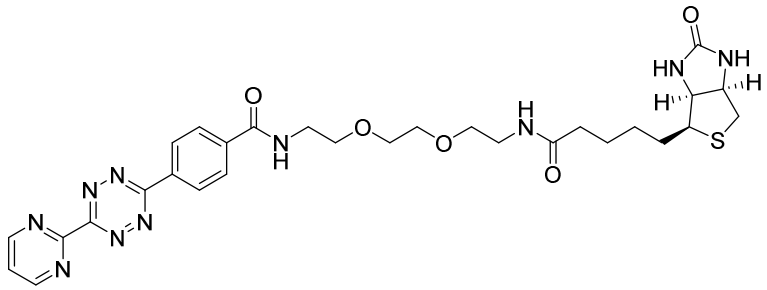

Into a 5 mL round-bottomed flask **4.43** (90.0 mg, 0.22 mmol), HATU (92.0 mg, 0.24 mmol) and D-Biotin (59.0 mg, 0.24 mmol) were dissolved in anh. Pyr (3 mL) and the solution stirred for 2 h at rt. Afterwards, the mixture was purified by silica gel column chromatography eluting with DCM:MeOH mixtures from 95:5 up to 85:15. The title compound was obtained as a pink powder (88.0 mg, 63%).

TLC (DCM:MeOH 90:10): R_f = 0.45.

^{1}H NMR (DMSO-d_6, 400 MHz) δ 9.21 (d, *J* = 5.2 Hz, 2H), 8.82 (t, *J* = 5.6 Hz, 1H), 8.68 (d, *J* = 8.3 Hz, 2H), 8.16 (d, *J* = 8.4 Hz, 1H), 7.87 – 7.80 (m, 2H), 6.40 (s, 1H), 6.34 (s, 1H), 4.29 (dd, *J* = 7.7, 5.0 Hz, 1H), 4.12 (ddd, *J* = 7.7, 4.4, 1.7 Hz, 1H), 3.62 – 3.46 (m, 8H), 3.40 (t, *J* = 5.9 Hz, 2H), 3.18 (q, *J* = 5.8 Hz, 2H), 3.08 (ddd, *J* = 8.5, 6.2, 4.4 Hz, 1H), 2.81 (dd, *J* = 12.4, 5.1 Hz, 1H), 2.56 (d, *J* = 12.4 Hz, 1H), 2.06 (t, *J* = 7.4 Hz, 2H), 1.69 – 1.39 (m, 4H), 1.37 – 1.22 (m, 2H) ppm.

^{13}C NMR (DMSO-d_6, 101 MHz) δ 172.55, 165.99, 163.64, 163.37, 163.12, 159.51, 158.97, 138.60, 134.30, 128.74, 128.58, 123.46, 70.01, 69.62, 69.26, 61.46, 59.62, 55.86, 38.88, 35.54, 28.63, 28.48, 25.70 ppm.

Two signals (CH_2-NHCO) overlap with solvent.

ESI-HRMS (positive mode): *m/z* 637.2659 $[M+H]^+$; M calcd for $C_{29}H_{37}N_{10}O_5S$ 637.2664.

4-Methoxy-4-oxobutanoic acid (4.75)

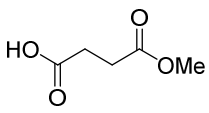

To a 25 mL round-bottomed flask was added succinic anhydride (2.00 g, 19.80 mmol) and MeOH (10 mL). Subsequently, the suspension refluxed for 2 h, cooled down and the solvent removed under reduced pressure to yield the title compound as a white solid (2.63 g, 99 %).

^{1}H NMR (CD_3OD, 400 MHz) δ 3.67 (s, 3H), 2.59 (s, 4H) ppm.

^{13}C NMR ($CDCl_3$, 101 MHz) δ 174.56, 173.34, 50.78, 28.36, 28.30 ppm.

ESI-HRMS (negative mode): *m/z* 131.0347 $[M-H]^-$; M calcd for $C_5H_7NO_4$ 131.0350.

Methyl 4-chloro-4-oxobutanoate (4.76)

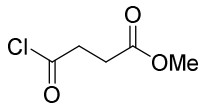

To a 25 mL round-bottomed flask was added 4-methoxy-4-oxobutanoic acid (2.00 g, 19.80 mmol) and thionyl chloride (10 mL) and the suspension refluxed for 2 h. Afterwards, the solvent was removed under reduced pressure to yield the title compound as a yellow oil solid (95%) used without further purification.

^{1}H NMR (CD_3OD, 400 MHz) δ 3.61 (s, 3H), 2.50 (s, 4H) ppm.

^{13}C NMR ($CDCl_3$, 101 MHz) δ 173.10, 172.64, 51.98, 42.20, 29.14 ppm.

3-(4,4-Difluoro-1,3,5,7-tetramethyl-4-bora-3a,4a-diaza-s-indacene-8-yl)-propionic acid methyl ester (4.78)

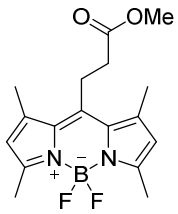

To a 2,4-dimethylpyrrole (5.1 g, 54.0 mmol) solution in anh. DCM (30 mL) was added methyl 4-chloro-4-oxobutanoate (**4.76**, 2.7 g, 18.0 mmol) dissolved in anh. DCM (10 mL). The mixture was left stirring at rt overnight. Afterwards, DIPEA (15.6 mL, 90.0 mmol) were added and left 15 additional min stirring. Then, $BF_3 \cdot OEt_2$ (15 g, 108.0 mmol) was added and the mixture stirred for 1 h at room temperature. Subsequently, the mixture was passed through a small silica plug and the solvent evaporated under reduced pressure. The resulting crude was purified by silica gel flash column chromatography eluting with hexanes:EtOAc mixtures from 95:5 to 90:10. The title compound was obtained as a red solid (940 mg, 15%).

TLC (hexanes:EtOAc 8:2): R_f = 0.33.

^{1}H NMR ($CDCl_3$, 400 MHz) δ 6.06 (s, 2H), 3.74 (s, 3H), 3.34 – 3.28 (m, 2H), 2.64 – 2.57 (m, 2H), 2.51 (s, 6H), 2.43 (s, 6H) ppm.

^{19}F NMR ($CDCl_3$, 376 MHz) δ -146.56 (s, 2F) ppm.

ESI-HRMS (positive mode): *m/z* 334.1768 (^{10}B) / 335.1737 $[M+H]^+$; M calcd for $C_{17}H_{22}BF_2N_2O_2$ 335.1737.

3-(4,4-Difluoro-1,3,5,7-tetramethyl-4-bora-3a,4a-diaza-s-indacene-8-yl)-propionic acid (4.79)

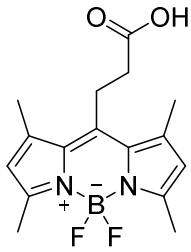

To a solution of **4.78** (400.0 mg, 1.19 mmol) in THF (10 mL) was added a solution of LiOH (143.7 mg, 5.98 mmol) in H_2O (4 mL) and the mixture left stirring for 3 h at rt. Afterwards, the crude was diluted with aq. HCl 10%, (10 mL) transferred into a separatory funnel and extracted with DCM (3 × 30 mL). The combined organic layers were dried over anh. $MgSO_4$ the solvent removed under vacuum and the residue purified by silica gel flash column chromatography eluting with hexanes:EtOAc:AcOH mixture (78:20:2). The title compound was obtained as an orange solid (285.0 mg, 75%)

TLC (hexanes:EtOAc:AcOH 78:20:2): R_f = 0.30.

^{1}H NMR ($CDCl_3$, 400 MHz) δ 6.07 (s, 2H), 3.37 – 3.29 (m, 2H), 2.69 – 2.64 (m, 2H), 2.52 (s, 6H), 2.45 (s, 6H) ppm.

^{13}C NMR ($CDCl_3$, 101 MHz) δ 176.04, 154.85, 142.65, 140.34, 122.04, 109.99, 34.92, 23.35, 16.39, 14.51 ppm.

^{19}F NMR ($CDCl_3$, 376 MHz) δ -146.62 (p, *J* = 33.8 Hz, 2F) ppm.

ESI-HRMS (negative mode): *m/z* 318.1476 (^{10}B) / 319.1439 [M-H]$^-$; M calcd for $C_{16}H_{18}BF_2N_2O_2$ 319.1435.

N-(2-(2-(2-(3-(5,5-Difluoro-1,3,7,9-tetramethyl-5*H*-4λ^4,5λ^4-dipyrrolo[1,2-*c*:2',1'-*f*][1,3,2]diazaborinin-10-yl)propanamido)ethoxy)ethoxy)ethyl)-4-(6-(pyrimidin-2-yl)-1,2,4,5-tetrazin-3-yl)benzamide (4.80)

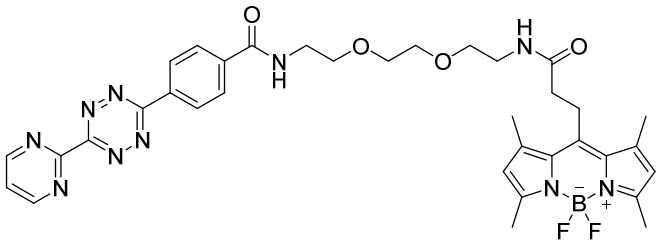

To a 10 mL round-bottomed flask was weighed **4.79 (**78.9 mg, 0.25 mmol), **4.43** (100.0 mg, 0.22 mmol) and HATU (93.7 mg, 0.25 mmol), added anh. Pyr (5 mL) and the mixture left overnight at rt. Afterwards, the solvent was removed under vacuum and the crude was purified by silica gel flash column chromatography eluting with DCM:MeOH mixtures from 100:0 up to 95:5. The title compound was obtained as a bright orange solid (68.0 mg, 38 %)

TLC (DCM:MeOH 95:5): R_f = 0.37.

^{1}H NMR ($CDCl_3$, 400 MHz) δ 9.13 (d, *J* = 4.8 Hz, 2H), 8.74 (d, *J* = 8.5 Hz, 2H), 8.00 (d, *J* = 8.6 Hz, 2H), 7.60 (t, *J* = 4.9 Hz, 1H), 6.96 (br.s, 1H), 6.33 (t, *J* = 5.6 Hz, 1H), 6.00 (s, 2H), 3.74 – 3.59 (m, 8H), 3.53 (t, *J* = 5.1 Hz, 2H), 3.45 (t, *J* = 5.2 Hz, 2H), 3.34 – 3.24 (m, 2H), 2.47 (s, 6H), 2.46 – 2.42 (m, 2H), 2.40 (s, 6H) ppm.

^{13}C NMR ($CDCl_3$, 101 MHz) δ 170.78, 166.65, 163.95, 163.12, 159.37, 158.42, 154.37, 144.43, 140.53, 138.52, 133.92, 131.24, 128.88, 128.16, 127.95, 122.60, 121.81, 120.35, 70.36, 70.24, 69.78, 69.71, 39.95, 39.36, 37.28, 23.76, 16.46, 14.45 ppm.

^{19}F NMR ($CDCl_3$, 376 MHz) δ -145.90 (br.s, F), -146.77 (br.s, F) ppm.

ESI-HRMS (positive mode): *m/z* 735.3111 (^{10}B) / 736.3143 $[M+Na]^+$; M calcd for $C_{35}H_{39}BF_2N_{10}NaO_4$ 735.3109.

PMal(H_2)-TAT + Tz-Biotina (4.82)

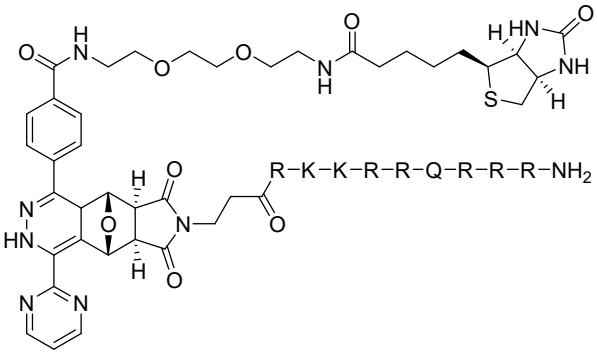

To the lyophilized **4.33** (400 nmol) was added MQ-H_2O (640 µL) followed by a solution of **4.82** (800 nm, 160 µL, 5 mM) in H_2O:MeOH (1:1) to achieve a final peptide concentration of 0.5 mM. The reaction was left stirring overnight at 37 ºC and monitored by HPLC. The conjugate was purified by reversed-phase HPLC.

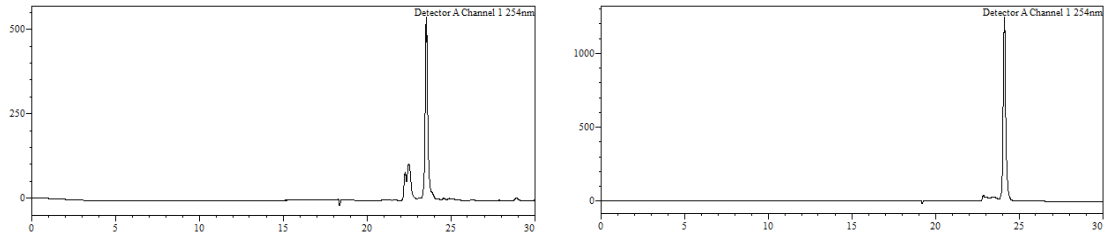

Crude Purified

Figure E.4.5 HPLC traces (254 nm) of crude (left) and purified (right) conjugate.

HPLC: Analysis conditions, 0-50% B, t_R = 23.7 (**Figure E.4.5**).

Purification gradient: 20-50% B. t_R = 10.0 min Yield: 45%.

MALDI-TOF (positive mode, DHB): *m/z* 3585.2 $[M+H]^+$, M calcd. For $C_{159}H_{257}N_{59}O_{37}$ 3585.0.

Tz-Francesos + PMal[H_2]-PNA (4.83)

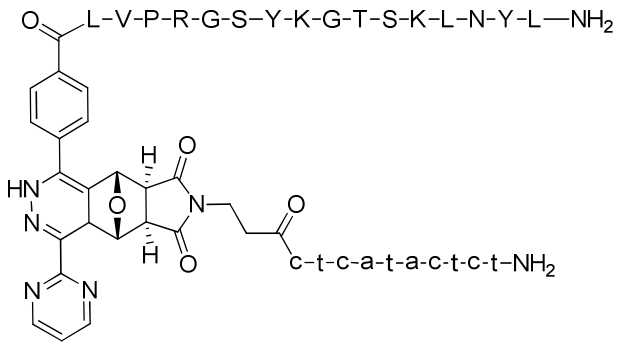

The lyophilized **4.33** (55 nmol) was solved in MQ-H_2O (50 + 50 µL) transferred into a an eppendorf containing 50 nm aliquot of **4.56** to achieve a final peptide concentration of 0.5 mM. The reaction was left stirring overnight at 37 ºC and monitored by HPLC. The conjugate was purified by reversed-phase HPLC.

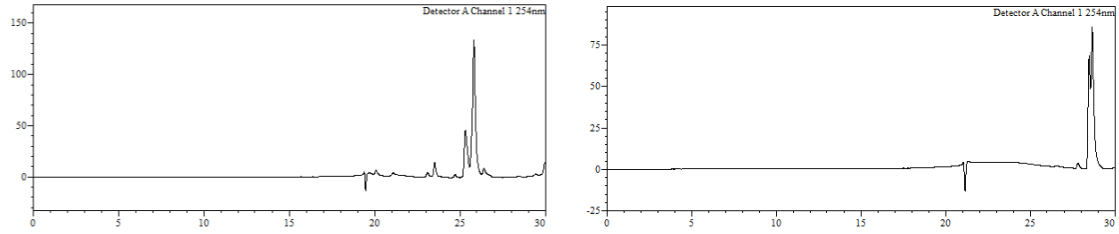

Crude Purified

Figure E.4.6 HPLC traces (254 nm) of crude (left) and purified (right) conjugate.

HPLC: Analysis conditions, 0-50% B, t_R = 25.10 and 25.40 min. (**Figure E.4.6**).

Purification gradient: 0-50% B. t_R = 25.10 and 25.40 min Yield: 35%.

MALDI-TOF (positive mode, DHB): *m/z* 3585.2 $[M+H]^+$, M calcd. For $C_{159}H_{257}N_{59}O_{37}$ 3585.0.

PMal[H_2]-PNA+Tz-GalNAc (4.84)

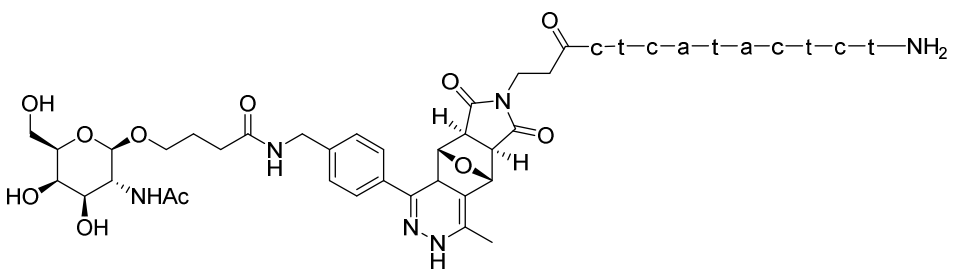

The lyophilized **4.33** (100 nmol) was added a MQ-H_2O:MeOH mixture (1:1, 160 µL) followed by a **4.84** solution (40 µL, 5 mM, 200 nmol) in MQ-H_2O:MeOH (1:1) to achieve a final PNA concentration of 0.5 mM (1:1 H_2O:MeOH). The reaction was left stirring overnight at 37 ºC and monitored by HPLC. The conjugate was purified by reversed-phase HPLC.

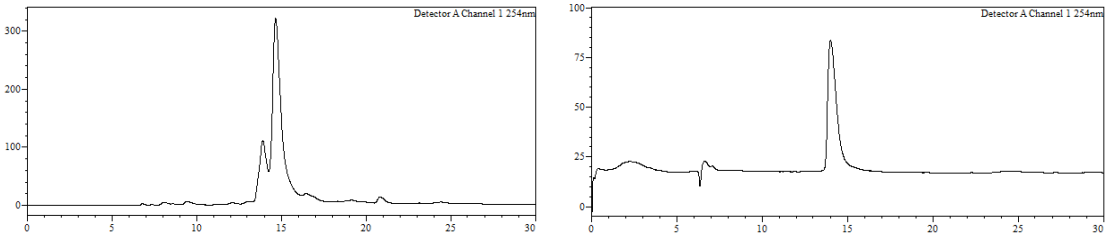

Crude Purified

Figure E.4.7 HPLC traces (254 nm) of crude (left) and purified (right) conjugate.

HPLC: Analysis conditions, 10-50% B, t_R = 14.5 min (Figure **E.4.7**).

A = 0.1M TEAA; B = ACN

Purification gradient: 10-50% B. t_R = 11.5 min Yield: 32%.

MALDI-TOF (positive mode, DHB): *m/z* 3318.5 $[M+H]^+$, M calcd. For $C_{139}H_{176}N_{56}O_{43}$ 3317.3.

PMal[H_2]-PNA+Tz-BODIPY (4.85)

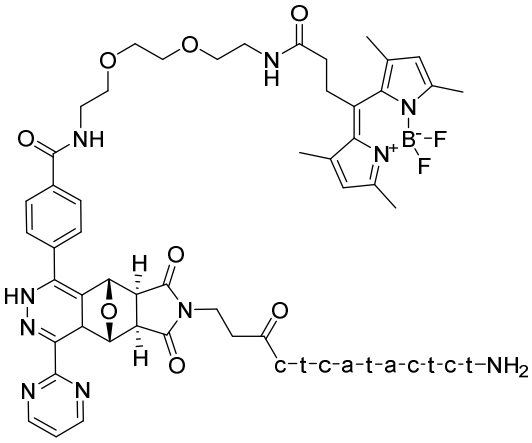

The lyophilized **3434** (100 nmol) was added a MQ-H_2O:MeOH mixture (1:1, 160 µL) followed by a **4.84** solution (40 µL, 5 mM, 200 nmol) in MQ-H_2O:MeOH (1:1) to achieve a final PNA concentration of 0.5 mM (1:1 H_2O:MeOH). The reaction was left stirring overnight at 37 ºC and monitored by HPLC. The conjugate was purified by reversed-phase HPLC.

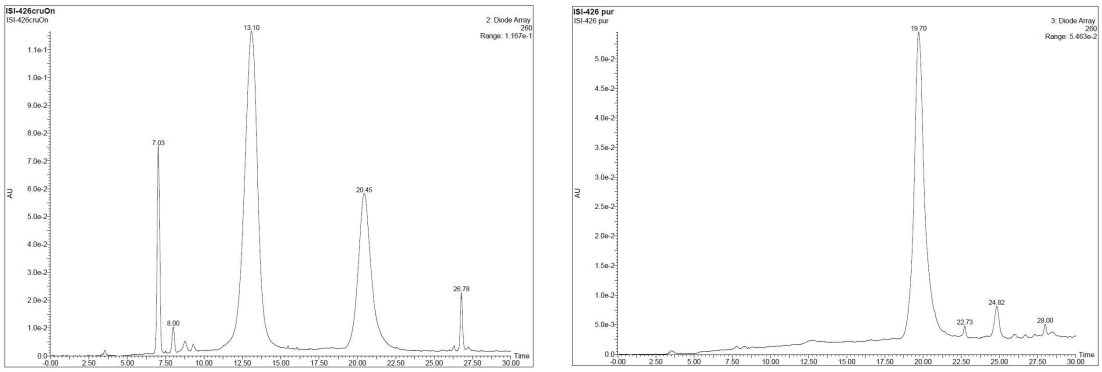

Crude Purified

Figure E.4.8 HPLC traces (254 nm) of crude (left) and purified (right) conjugate.

HPLC: Analysis conditions, 0-50% B, t_R = 19.7 (**Figure E.4.8**).

Purification gradient: 20-50% B. t_R = 11.5 min Yield: 40%.

MALDI-TOF (positive mode, DHB): *m/z* 3539.0 $[M+H]^+$, M calcd. For $C_{152}H_{185}BF_2N_{60}O_{40}$ 3539.4.

Tz Francesos + PMal(H_2)-Oligo (4.86)

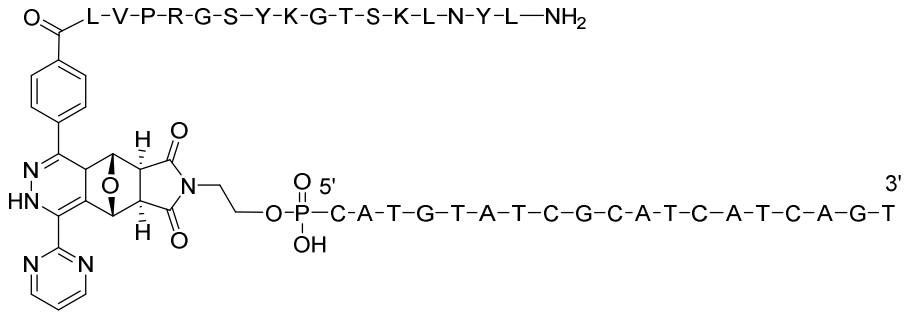

The lyophilized oligonucleotide **4.30** (40 nmol) was solved in MQ-H_2O (40 µL) followed by the addition of **4.82** (80 nmol) in MQ-H_2O (40 µL) to achieve a final oligonucleotide concentration of 0.5 mM. The reaction was left stirring for 5 h at 37 ºC and monitored by HPLC. The conjugate was purified by reversed-phase HPLC.

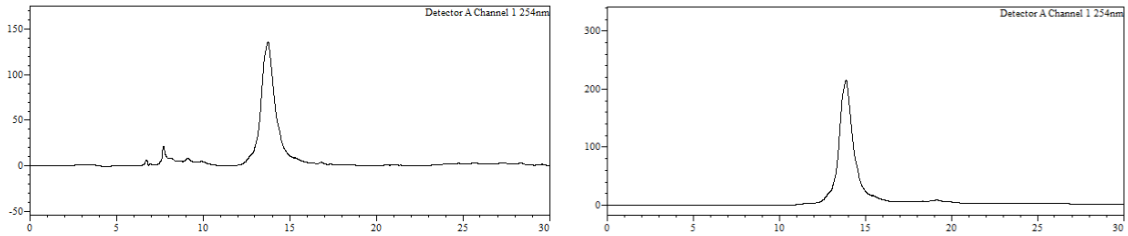

Crude Purified

Figure E.4.9 HPLC traces (254 nm) of crude (left) and purified (right) conjugate.

HPLC: Analysis conditions, 10-40% B, t_R = 13.1 min (**Figure E.4.9**)

Purification gradient: 20-50% B. t_R = 7.5 min Yield: 25%.

MALDI-TOF (negative mode, THAP/CA): *m/z* 8057.0 $[M-H]^-$, M calcd. For $C_{290}H_{386}N_{95}O_{142}P_{19}$ 8058.1.

(GalNAc-Tz-Me)-PMal(H_2)-d$^{5'}$CATGTATCGCATCATCAGT$^{3'}$ (4.87)

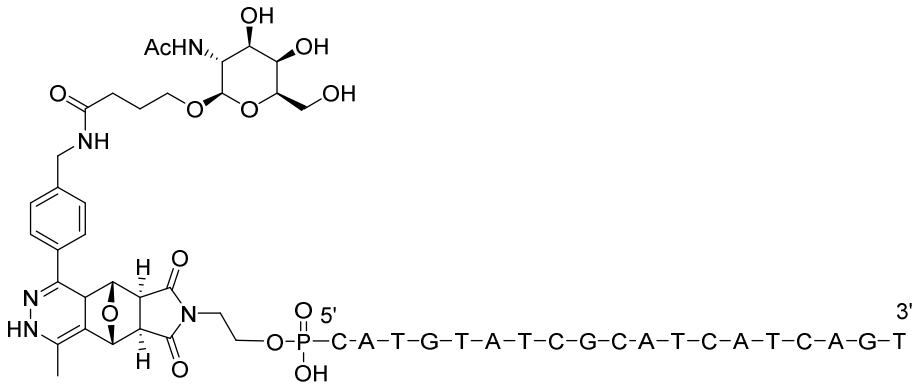

The lyophilized oligonucleotide **4.30** (40 nmol) was solved in MQ-H_2O (64 µL) followed by **4.84** (16 µL, 5 mM in MQ-H_2O:MeOH, 80 nmol) to achieve a final oligonucleotide concentration of 0.5 mM (4:1 H_2O:MeOH). The reaction was left stirring overnight at 37 ºC and monitored by HPLC. The conjugate was purified by reversed-phase HPLC.

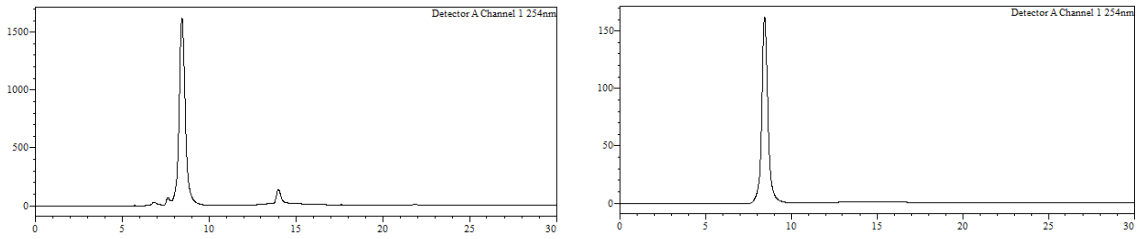

Crude Purified

Figure E.4.10 HPLC traces (254 nm) of crude (left) and purified (right) conjugate.

HPLC: Analysis conditions, 10-40% B, t_R = 8.4 min. (**Figure E.4.10**).

Purification gradient: 10-40% B. t_R = 9.0 min. Yield: 31%.

MALDI-TOF (negative mode, THAP/CA): *m/z* 6490.2 $[M-H]^-$, M calcd. For $C_{217}H_{275}N_{72}O_{126}P_{19}$ 6493.2.

Biotina-Tz-PMal(H_2)-d$^{5'}$CATGTATCGCATCATCAGT$^{3'}$ (4.88)

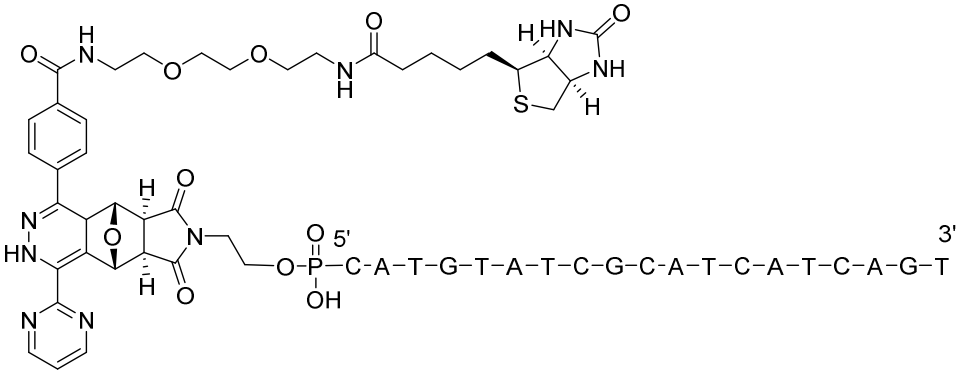

The lyophilized oligonucleotide **4.30** (40 nmol) was solved in MQ-H_2O (64 µL) followed by **4.82** (16 µL, 5 mM in MQ-H_2O:MeOH, 80 nmol) to achieve a final oligonucleotide concentration of 0.5 mM

(4:1 MQ-H_2O:MeOH). The reaction was left stirring for 5 h at 37 ºC and monitored by HPLC. The conjugate was purified by reversed-phase HPLC.

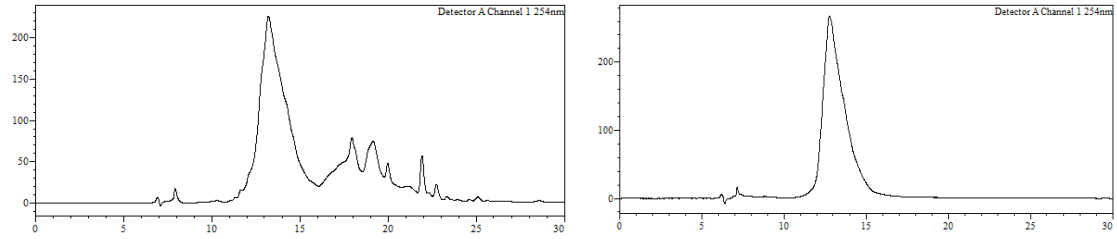

Crude Purified

Figure E.4.11 HPLC traces (254 nm) of crude (left) and purified (right) conjugate.

HPLC: Analysis conditions, 10-40% B, t_R = 13.1 min (**Figure E.4.11**).

Purification gradient: 10-50% B. t_R = 12.7 min Yield: 34%.

MALDI-TOF (negative mode, THAP/CA): *m/z* 6635.1 $[M-H]^-$, M calcd. For $C_{224}H_{281}N_{76}O_{124}P_{19}S$ 6639.2.

BODIPY-Tz-PMal[H_2]-d$^{5'}$CATGTATCGCATCATCAGT$^{3'}$ (4.89)

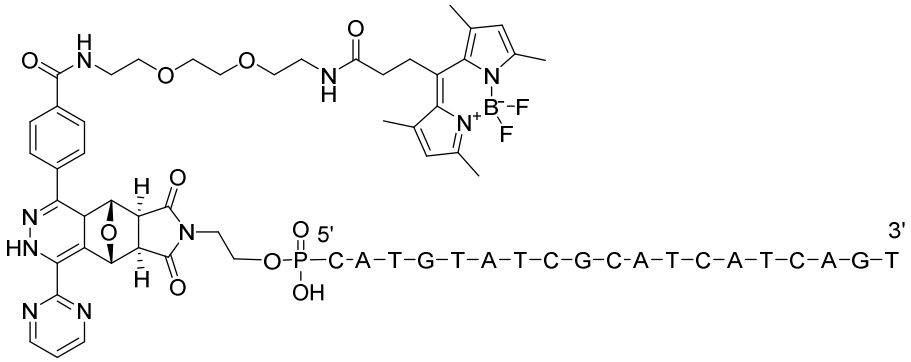

The lyophilized oligonucleotide **4.30** (40 nmol) was solved in MQ-H_2O (64 µL) followed by **4.80** (16 µL, 5 mM, 80 nmol) to achieve a final oligonucleotide concentration of 0.5 mM. The reaction was left stirring for 5 h at 37 ºC and monitored by HPLC. The conjugate was purified by reversed-phase HPLC.

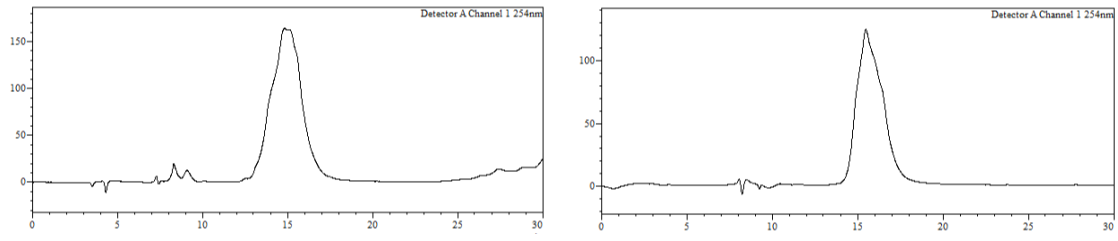

Crude Purified

Figure E.4.12 HPLC traces (254 nm) of crude (left) and purified (right) conjugate.

HPLC: Analysis conditions, 10-40% B, t_R = 15.0 min (**Figure E.4.12**).

Purification gradient: 10-50% B. t_R = 12.7 min Yield: 21%.

MALDI-TOF (negative mode, THAP/CA): *m/z* 6712.0 $[M-H]^-$, M calcd. For $C_{230}H_{284}BF_2N_{76}O_{123}P_{19}$ 6715.3.

(*S*)-2-((((9*H*-Fluoren-9-yl)methoxy)carbonyl)amino)-6-(3-((3a*R*,4*S*,7*R*,7a*S*)-1,3-dioxo-3a,4,7,7a-tetrahydro-1*H*-4,7-epoxyisoindol-2(3*H*)-yl)propanamido)hexanoic acid (4.90)

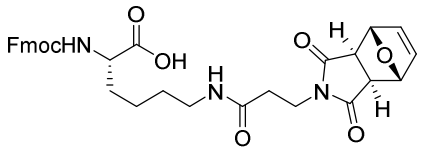

To a suspension of **4.20** (350 mg, 1.47 mmol) in anh. DCM (10 mL) was added NMM (243 µL, 2.21 mmol) and IBCF (284 µL, 2.21 mmol) dropwise and the mixture was left reacting for 10 min. under an argon atmosphere. Afterwards, Fmoc-Lys-OH (815 mg, 2.21 mmol) was added and the mixture left reacting overnight at rt. Subsequently, additional DCM (40 mL) were added and the solution transferred into a separatory funnel and washed with aq. HCl 10% (30 mL). The aqueous phase was further washed with DCM (3 × 20 mL) and the combined organic phases were dried over anh. $MgSO_4$ and the solvent removed *in vacuo.* The resulting crude was purified by silica gel flash column chromatography eluting with DCM/EtOAc/MeOH/AcOH mixtures from 98:0:0:2 to 0:88:10:2. The title compound was obtained as a beige foam (710.1 mg, 82%).

^{1}H NMR ($CDCl_3$, 400 MHz): δ 7.76 (d, *J* = 7.2 Hz, 2H), 7.60 (t, *J* = 5.2 Hz, 2H), 7.39 (t, *J* = 7.6 Hz, 2H), 7.32 (dd, *J* = 7.6 Hz, 0.8 Hz, 2H), 6.46 (s, 2), 5.23 (s, 2H), 4.38 (d, *J* = 7.8Hz, 2H), 4.21 (t, *J* = 6.8 Hz, 2H), 3.77 (t, *J* = 6.8 Hz, 1H), 3.26 (t, *J* = 6.0 Hz, 2H), 2.83 (s, 2H), 2.45 (t, *J* = 7.2 Hz, 2H), 1.93-1.73 (m, 2H), 1.56 (d, *J* = 8.4 Hz, 1H), 1.51 (d, *J* = 8.4 Hz, 2H), 1.26 (t, *J* = 3.2 Hz, 2H) ppm.

^{13}C NMR (101 MHz, $CDCl_3$): δ 143.6, 141.1, 140.3, 127.7, 127.1, 125.3, 120.5, 87.7, 67.0, 52.5, 47.5, 39.4, 35.0, 34.1, 15.6 ppm.

ESI-HRMS (negative mode): *m/z* 578.2266 $[M+H]^+$; M calcd for $C_{32}H_{33}N_3O_8$ 587.2268.

*N*2-(((9*H*-fluoren-9-yl)methoxy)carbonyl)-*N*6-(3-((3aR,4S,7R,7aS)-4,7-dimethyl-1,3-dioxo-1,3,3a,4,7,7a-hexahydro-2H-4,7-epoxyisoindol-2-yl)propanoyl)-*L*-lysine (4.91)

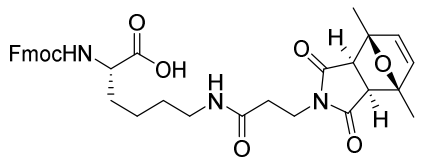

To a suspension of **4.13** (350.0 mg, 1.32 mmol) in anh. DCM (10 mL) was added NMM (234 µL, 2.13 mmol) and IBCF (273 µL, 2.12 mmol) dropwise and the mixture was left reacting for 10 min. under an

argon atmosphere. Afterwards, Fmoc-Lys-OH (785.0 mg, 2.12 mmol) was added and the mixture left reacting overnight at rt. Subsequently, additional DCM (40 mL) were added and the solution transferred into a separatory funnel and washed with aq. HCl 10% (30 mL). The aqueous phase was further washed with DCM (3 × 20 mL) and the combined organic phases were dried over anh. $MgSO_4$ and the solvent removed *in vacuo*. The resulting crude was purified by silica gel flash column chromatography eluting with DCM/EtOAc/MeOH/AcOH mixtures from 98:0:0:2 to 0:88:10:2. The title compound was obtained as a beige foam (649.4 mg, 80%).

^{1}H NMR (400 MHz, $CDCl_3$): δ 7.74 (d, J = 7.54 Hz, 2H), 7.59 (t, J = 6.80 Hz, 2H), 7.38 (t, J = 7.45 Hz, 2H), 7.29 (t, J = 7.43 Hz, 2H), 6.26 (s, 2H), 4.37 (d, J = 7.07 Hz, 2H), 4.20 (t, J = 6.90 Hz, 1H), 3.75 (t, J = 7.06 Hz, 2H), 3.22 (d, J = 5.73 Hz, 2H), 2.81 (s, 2H), 2.48 (t, J = 6.97 Hz, 2H), 1.66 (s, 6H), 2–0.8 (bs, 6H) ppm

^{13}C NMR (101 MHz, $CDCl_3$): δ 143.7, 141.3, 140.8, 127.7, 127.1, 125.1, 120.0, 87.7, 67.0, 52.5, 47.1, 39.0, 35.1, 34.3, 29.7, 28.6, 15.8 ppm.

HRMS (ESI, negative mode): *m/z* 614.2481 $[M-H]^-$, M calcd. for $C_{34}H_{37}N_3O_8$ 615.2581.

PMal(H_2)-NYAK[PMal(Me_2)]ARKV-NH_2 (4.92)

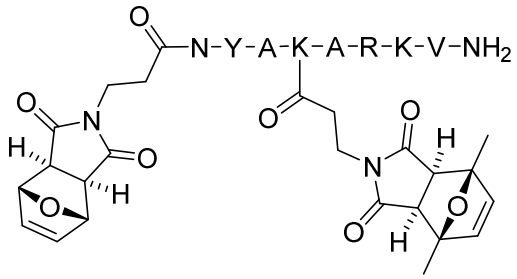

HPLC: purification gradient: 30-70% B (0.1% TFA); analysis conditions, 0-50% B (0.1% Formic acid), t_R = 13.0 min.

HPLC-MS (positive mode): *m/z* 1414.8 $[M+H]^+$, M calcd. for $C_{66}H_{96}N_{17}O_{18}$ 1414.7.

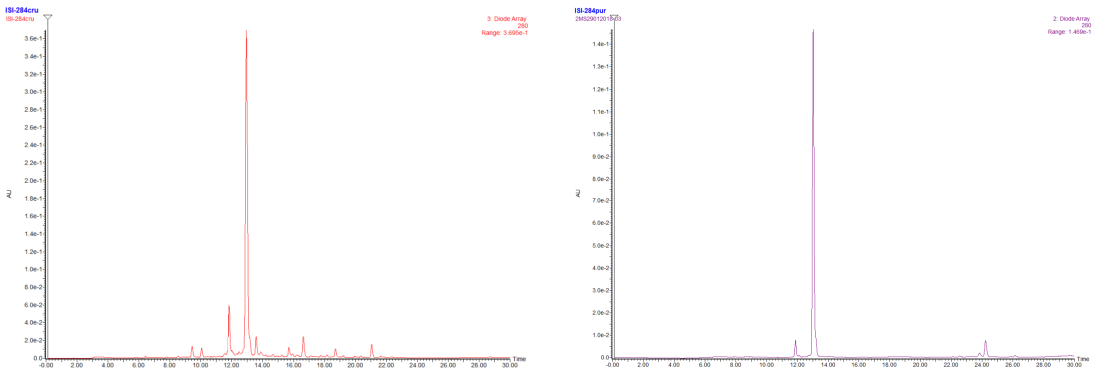

Crude Purified

Figure E.4.13 HPLC traces (254 nm) of crude (left) and purified (right) peptide.

tert-Butyl (2-(5-(dimethylamino)naphthalene-1-sulfonamido)ethyl)carbamate (4.102)

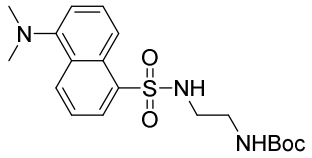

Dansyl chloride (84 mg, 0.31 mmol) was added to a solution of **4.101** (50 mg, 0.31 mmol) in DCM (1 mL) and left under heavy stirring at room temperature for 90 minutes. The crude was diluted with additional DCM (15 mL) and washed with distilled H_2O (3 x 10 mL). The organic layer was dried over anh. $MgSO_4$, filtered and the solvent evaporated under low pressure to afford the title product (101 mg, 82%) as a yellow oil.

TLC (DCM): R_f = 0.50.

IR (Oil): 3285 (w, br), 2974 (w), 1685 (m), 1140 (s) cm^{-1}.

^{1}H NMR ($CDCl_3$, 400 MHz): δ 8.54 (d, *J* = 8.8 Hz, 1H), 8.27 (d, *J* = 8.8 Hz, 1H), 8.23 (d, *J* = 7.6 Hz, 1H), 7.58-7.49 (m, 2H), 7.18 (d, *J* = 7.6 Hz, 1H), 4.81 (br. s, 1H), 3.15 (t, *J* = 5.1 Hz, 2H), 3.00 (t, *J* = 6.0 Hz, 2H), 2.88 (s, 6H), 1.39 (s, 9H) ppm.

^{13}C NMR ($CDCl_3$, 100 MHz): δ 156.35, 151.91, 134.62, 130.42, 129.87, 129.53, 129.43, 128.42, 123.12, 118.74, 115.20, 79.52, 45.37, 43.54, 40.26, 28.28 ppm.

ESI-HRMS (positive mode) *m/z* 394.1839 $[M+H]^+$; calcd for $C_{19}H_{28}N_3O_4S$ 394.1795.

2-(5-(Dimethylamino)naphthalene-1-sulfonamido)ethanaminium chloride (4.103)

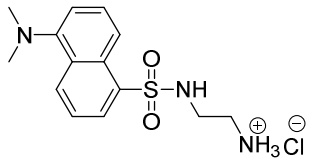

4.102 (80 mg, 0.20 mmol) was added to a round-bottomed flask followed by the addition of HCl (4N in dioxane, 2 mL) and the mixture was left reacting for 2 h at rt. Afterwards, the solvent was removed under reduced pressure to afford the title compound as a pale yellow solid (70.0 mg, 99%).

^{1}H NMR (CD_3OD, 400 MHz) δ 8.92 (d, *J* = 8.8 Hz, 1H), 8.65 (d, *J* = 8.8 Hz, 1H), 8.42 (d, 7.6 Hz, 1H), 8.16 (d, *J* = 7.6 Hz, 1H) 7.93 (dd, *J* = 11.2, 8.7, 7.6 Hz, 2H), 3.50 (s, 6H), 3.14 – 3.03 (m, 4H) ppm.

ESI-HRMS (positive mode): *m/z* 294.1270 $[M+H]^+$ M calcd. for $C_{14}H_{20}N_3O_2S$ 294.1271.

(*E*)-*N*-(2-(5-(Dimethylamino)naphthalene-1-sulfonamido)ethyl)hepta-4,6-dienamide (4.104)

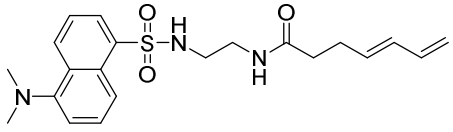

To a solution of **3.48** (47 mg, 0.38 mmol) in DCM (1 mL) was added IBCF (48 µL, 0.375 mmol) and NMM (103 µL, 0.85 mmol) and the mixture left for 10 min at rt. Afterwards, **4.103** (100 mg, 0.34 mmol) was added and the mixture left reacting for 4 h at rt. Afterwards, the crude was transferred into a separatory funnel with additional DCM (50 mL). The organic phase was washed with distilled H_2O (40 mL) and the aqueous phase extracted with DCM (3 x 20 mL). The combined organic layers were dried over anh. $MgSO_4$, filtered and the solvent removed under reduced pressure. The crude was further purified using silica gel flash column chromatography eluting with DCM:EtOAc mixture with a 60:40 isocratic gradient to afford the title compound (112 mg, 82%) as pale yellow solid.

TLC (DCM/EtOAc 30:70): R_f = 0.48.

^{1}H NMR ($CDCl_3$, 400 MHz) δ 8.58 (d, *J* = 8.6 Hz, 1H), 8.28 (d, *J* = 8.6 Hz, 1H), 8.23 (dd, *J* = 7.3, 1.2 Hz, 1H), 7.56 (ddd, *J* = 20.2, 8.6, 7.4 Hz, 2H), 7.21 (d, *J* = 7.6 Hz, 1H), 6.27 (dt, *J* = 17.0, 10.2 Hz, 1H), 6.09 – 5.96 (m, 1H), 5.85 (br. s, 1H), 5.61 (dt, *J* = 14.6, 6.9 Hz, 1H), 5.45 (br s, 1H), 5.10 (dd, *J* = 17.0, 1.6 Hz, 1H), 4.99 (dd, *J* = 10.2, 1.6 Hz, 1H), 3.29 (td, *J* = 7.1, 6.5, 4.7 Hz, 2H), 3.02 (td, *J* = 7.1, 6.5, 4.7 Hz, 2H), 2.91 (s, 6H), 2.35 – 2.25 (m, 2H), 2.08 (m, 2H) ppm.

^{13}C NMR ($CDCl_3$, 100 MHz) δ 173.10, 151.88, 136.81, 134.33, 132.83, 131.90, 130.61, 129.84, 126.67, 129.45, 128.52, 123.26, 118.78, 115.75, 115.34, 45.42, 43.22, 39.17, 35.69, 28.25 ppm.

ESI-HRMS (positive mode): *m/z* 402.1846 $[M+H]^+$; calcd. for $C_{21}H_{28}N_3O_3S$ 402.1846.

Mal-HWSYK[PMal(H_2)]LRPG-NH_2 (4.106)

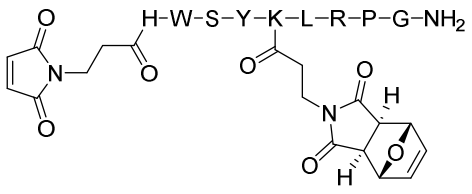

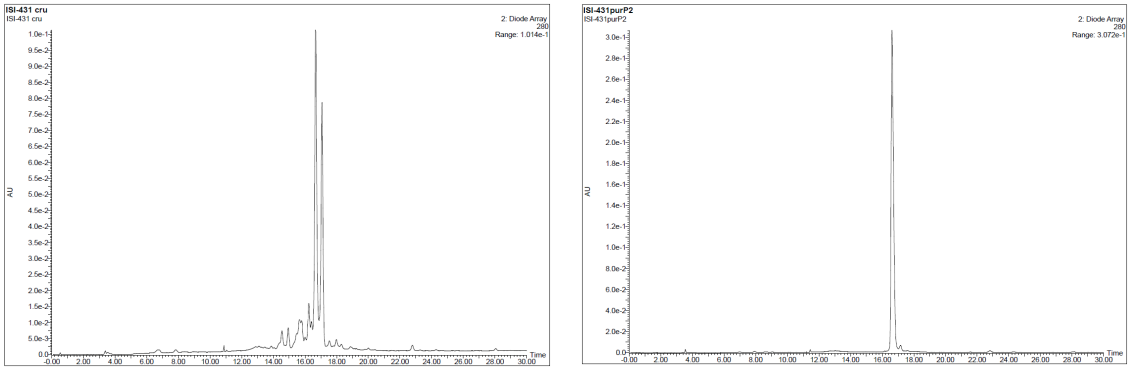

Crude Purified

Figure E.4.14 HPLC traces (254 nm) of crude (left) and purified (right) peptide.

HPLC: Analysis conditions, 0-50% B (0.1% Formic acid), t_R = 16.7 min (**Figure E.4.15**).

Purification gradient: 20-60% B (0.1% TFA) t_R = 16.9 min

HPLC-MS (positive mode): *m/z* 1513.3 $[M+H]^+$, M calcd. for $C_{72}H_{94}N_{19}O_{18}$ 1512.7.

H-CYIQNK[PMal(H$_2$)]PLG-NH$_2$ (4.109)

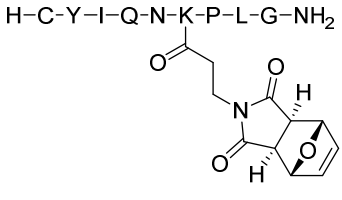

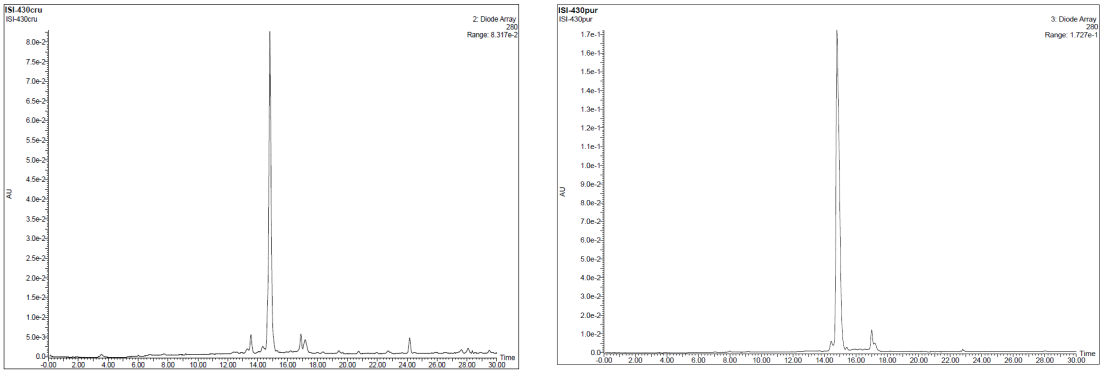

Crude Purified

Figure E.4.15 HPLC traces (254 nm) of crude (left) and purified (right) peptide.

HPLC: Analysis conditions, 0-50% B (0.1% Formic acid), t_R = 14.8 min (**Figure E.4.15**).

Purification gradient: 20-60% B (0.1% TFA) t_R = 13.2 min

HPLC-MS (positive mode): *m/z* 1254.1 $[M+H]^+$, M calcd. for $C_{57}H_{85}N_{14}O_{16}S$ 1253.6.

PMal(H$_2$)-KSWACG-NH$_2$ (4.110)

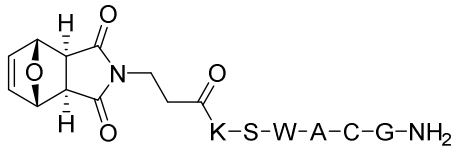

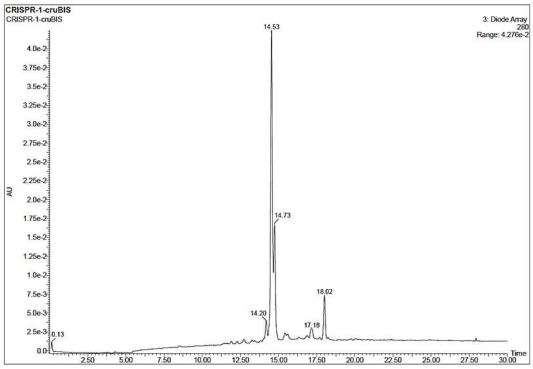

Crude

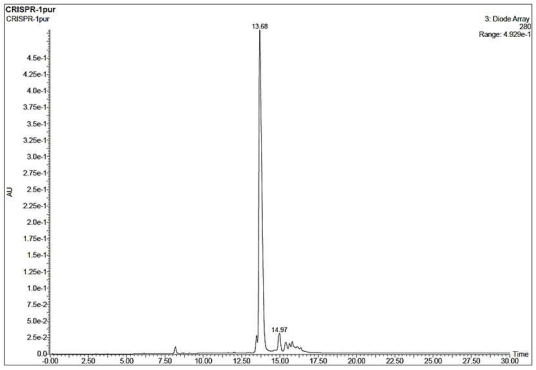

Purified

Figure E.4.16 HPLC traces (254 nm) of crude (left) and purified (right) oxanorbornene-containing peptide.

HPLC: Analysis conditions, 0-50% B (0.1% formic acid), t_R = 13.7 min (**Figure E.4.16**).

Purification gradient: 30-70% B (0.1% TFA). t_R = 6.8 min Yield: 17%.

HPLC-MS (positive mode): *m/z* 869.6 $[M+H]^+$, M calcd. for $C_{39}H_{52}N_{10}O_{11}S$ 868.3.

PMal(H_2)-RYTACG-NH_2 (4.111)

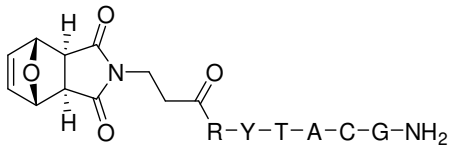

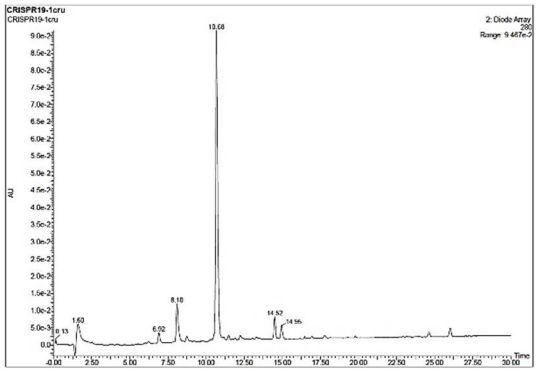

Crude

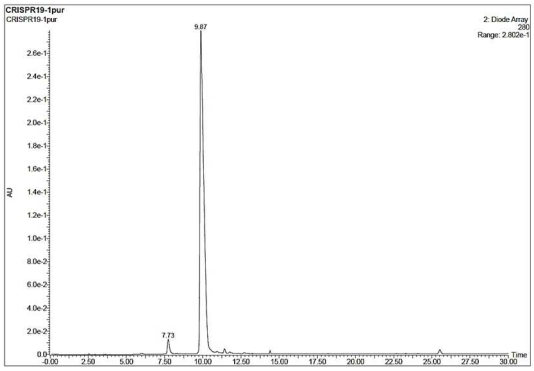

Purified

Figure E.4.17 HPLC traces (254 nm) of crude (left) and purified (right) oxanorbornene-containing peptide.

HPLC: Analysis conditions, 0-50% B (0.1% formic acid), t_R = 10.9 min (**Figure E.4.17**).

Purification gradient: 20-50% B (0.1% TFA). t_R = 7.2 min Yield: 59%.

HPLC-MS (positive mode): *m/z* 888.6 $[M+H]^+$, M calcd. for $C_{38}H_{53}N_{11}O_{12}S$ 887.3.

2-(Tritylthio)ethanamine (4.118)

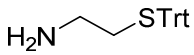

To a solution of 2-aminoethanthiol hydrochloride (1.00 g, 12.98 mmol) in TFA (40 mL) was added trityl chloride (3.61 g, 12.98 mmol) and the mixture stirred for 3 h at rt. Afterwards, the solvent was removed *in vacuo*, the residue diluted in EtOAc (50 mL) and transferred into a separatory funnel. The organic phase was washed with 1 M NaOH (4 × 20 mL), water (20 mL) and aq. sat. $NaHCO_3$ solution (2 × 20 mL). The organic phase was dried over anh. $MgSO_4$, filtered and concentrated under vacuum. The resulting crude was recrystallized with DCM and hexane (1:1, 5 mL) and filtered to give the title compound as a pale yellow solid (1.50 g, 40%).

TLC (hexanes:EtOAc 8:2): R_f = 0.17.

mp. 146─148 ºC.

^{1}H NMR ($CDCl_3$, 400 MHz) δ 7.46 – 7.24 (m, 15H), 2.53 (t, *J* = 6.5 Hz, 2H), 2.31 (t, *J* = 6.5 Hz, 2H)

^{13}C NMR ($CDCl_3$, 101 MHz) δ 144.6, 129.5, 127.9, 126.7, 66.6, 40.4, 34.7 ppm.

ESI-HRMS (positive mode): *m/z* 320.1489 $[M+H]^+$ M calcd. for $C_{21}H_{21}NS$ 320.1467.

5-(dimethylamino)-*N*-(2-(tritylthio)ethyl)naphthalene-1-sulfonamide (4.119)

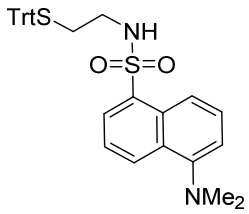

To a solution of dansyl chloride (220 mg, 0.82 mmol) and DIPEA (213 µL, 1.23 mmol) in THF (5 mL) was added **4.118** (521 mg, 1.63 mmol) and the mixture was left at rt for 2 hours. Afterwards, the resulting crude was diluted with DCM (40 mL) and was transferred into a separatory funnel. The organic phase was washed with aq. 5% HCl (2 × 20 mL) and the combined aqueous phases were extracted with additional DCM (20 mL). The combined organic layers were dried with anh. $MgSO_4$, filtered, and concentrated under reduced pressure. The residue was purified in a silica gel column chromatography, eluting with hexane/EtOAc mixtures from 90:10 to 75:25. The title compound was obtained a pale yellow solid (321 mg, 71 % yield).

TLC (hexane/EtOAc 8:2): R_f = 0.30.

^{1}H NMR (400 MHz, $CDCl_3$): δ 8.52 (d, *J* = 8.6 Hz, 1H), 8.17 (d, *J* = 8.6 Hz, 1H), 8.10 (d, *J* = 7.2 Hz, 1H), 7.53 (t, *J* = 8.5, 7.7 Hz, 1H), 7.46 (t, *J* = 8.5, 7.3 Hz, 1H), 7.28 – 7.09 (m, 16H), 4.67 (t, *J* = 6.3 Hz, 1H), 2.88 (s, 6H), 2.54 (q, *J* = 6.5 Hz, 2H), 2.30 (t, *J* = 6.6 Hz, 2H) ppm.

^{13}C NMR (101 MHz, $CDCl_3$): δ 152.00, 144.33, 134.55, 130.45, 129.37, 128.41, 127.91, 127.25, 126.74, 123.14, 118.76, 115.22, 66.87, 45.43, 31.94 ppm.

ESI-HRMS (positive mode): *m/z* 553.1977 $[M+H]^+$; M calcd for $C_{33}H_{32}N_2O_2S_2$ 553.1978.

5-(Dimethylamino)-*N*-(2-mercaptoethyl)naphthalene-1-sulfonamide (4.120)

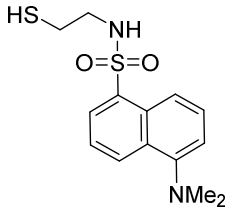

To a round bottom flask containing **4.119** (321 mg, 580 μmol.), was added TFA/TIS (95:5, 4 mL) and the mixture left for 2 hours at rt. Afterwards, the solvent was removed under reduced pressure and the residue was purified using a flash silica gel column chromatography eluting with hexane/EtOAc mixtures from 80:20 to 50:50. The tittle compound was obtained as a white solid (140 mg, 78 % yield).

TLC (hexane/EtOAc 7:3): R_f = 0.46.

^{1}H NMR (400 MHz, $CDCl_3$): δ 8.61 (d, *J* = 8.6 Hz, 1H), 8.53 (d, *J* = 8.7 Hz, 1H), 8.32 (d, *J* = 7.4 Hz, 1H), 7.67 7.70 – 7.63 (m, 2H) 7.44 (d, *J* = 7.6 Hz, 1H), 5.20 (t, *J* = 6.5 Hz, 1H), 3.13 (s, 5H), 3.1015 (q, *J* = 6.0 Hz, 2H), 2.59 – 2.52 (m, 2H) ppm.

^{13}C NMR (101 MHz, $CDCl_3$): δ 147.74, 135.32, 129.80, 129.50, 129.25, 128.68, 128.17, 124.50, 121.57, 116.43, 45.88, 29.67, 24.80 ppm.

ESI-HRMS (positive mode): *m/z* 311.0879 $[M+H]^+$; M calcd for $C_{14}H_{19}N_2O_2S_2$ 311.0882.

***N*-{2-[(6-Chloro-1,2,4,5-tetrazin-3-yl)thio]ethyl}-5-(dimethylamino)naphthalene-1-sulfonamide (4.121)**

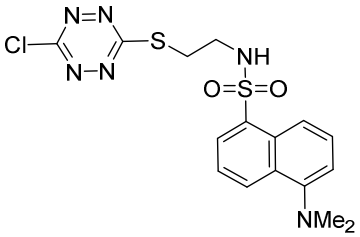

To a solution of **4.120** (70 mg, 0.22 mmol.) in DCM (2 mL) was added 3,6-dichloro-1,2,4,5-tetrazine (52 mg, 0.34 mmol) and the mixture stirred for 3 hours at rt. Afterwards, the solvent was removed under reduced pressure and the residue was purified using a flash silica gel column chromatography eluting with hexane/EtOAc mixtures from 80:20 to 60:40. The title compound was obtained as maroon-coloured solid (52 mg, 55 % yield).

TLC (hexane/EtOAc 8:2): R_f = 0.21.

^{1}H NMR (400 MHz, $CDCl_3$): δ 8.53 (d, *J* = 8.5 Hz, 1H), 8.25 (d, *J* = 7.3 Hz, 1H), 8.18 (d, *J* = 8.6 Hz, 1H), 7.57 – 7.45 (m, 2H), 7.15 (d, *J* = 7.4 Hz, 1H), 3.35 (m, 4H), 2.89 (s, 6H) ppm.

^{13}C NMR (101 MHz, $CDCl_3$): δ 174.86, 165.86, 152.08, 134.19, 130.86, 129.77, 129.33, 128.55, 123.19, 115.29, 45.38, 30.77 ppm.

ESI-HRMS (positive mode): *m/z* 425.0614 $[M+H]^+$; M calcd for $C_{16}H_{18}ClN_6O_2S_2$ 425.0616.

PMal(H_2)-KSWAC(Dansyl-Tz)G-NH_2 (4.122)

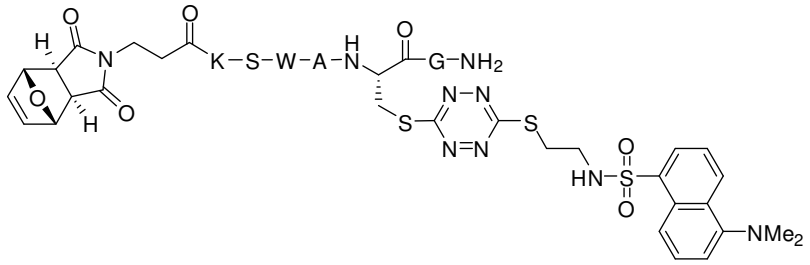

A solution of **4.121** (22 µL, 10 mM, 220 nmol, 1.1 eq.) in MeOH was added into a solution of **4.110** (200 nmol) in H_2O (200 µL) and MeOH (178 µL) and left under stirring at 37 ºC.

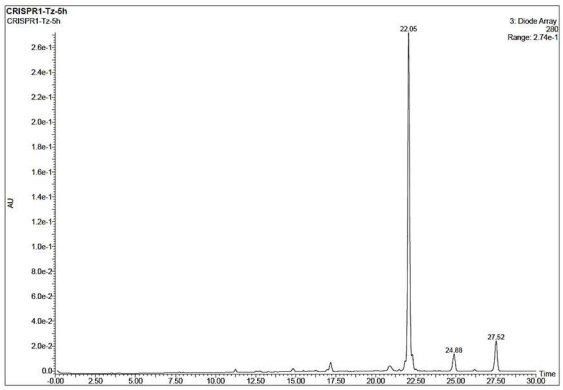

Figure E.4.18 HPLC trace (280 nm) of the crude after 5 hours reacting.

HPLC: Analysis conditions, 0-50% B (0.1% formic acid), t_R = 22.0 min (**Figure E.4.18**).

Purification gradient: 20-50% B (0.1% TFA). t_R = 7.0 min Yield: 53%.

HPLC-MS (positive mode) *m/z* 1257.7 $[M+H]^+$, M calcd. for $C_{55}H_{68}N_{16}O_{13}S_3$ 1256.4.

PMal(H_2)-RYTAC(Dansyl-Tz)G-NH_2 (4.123)

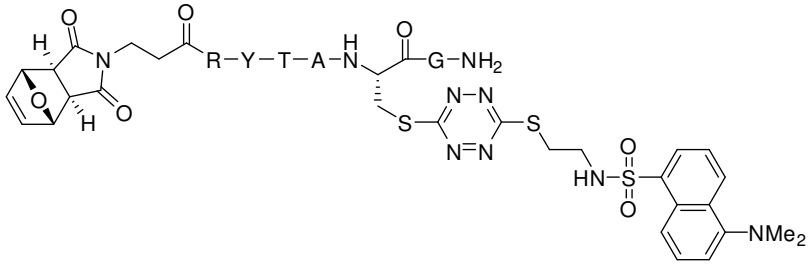

A solution of dansyl-Tz-Cl **4.121** (22 µL, 10 mM, 220 nmol, 1.1 eq.) in MeOH was added into a solution of free **4.111** (200 nmol) in H_2O (200 µL) and MeOH (178 µL) and left under stirring at 37 ºC for 15 min.

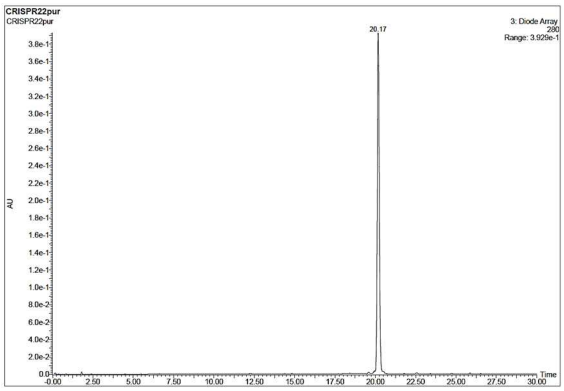

Figure E.4.19 HPLC trace (280 nm) of the purified peptide conjugate.

HPLC: Analysis conditions, 0-50% B (0.1% formic acid), t_R = 20.2 min (**Figure E.4.19**).

Purification gradient: 20-50% B (0.1% TFA). t_R = 6.9 min Yield: 92%.

HPLC-MS (positive mode) *m/z* 1276.7 $[M+H]^+$, M calcd. mass for $C_{54}H_{69}N_{17}O_{14}S_3$ 1275.4.

Dimethyl 2,2'-((1,2,4,5-tetrazine-3,6-diyl)bis(sulfanediyl))diacetate (4.129)

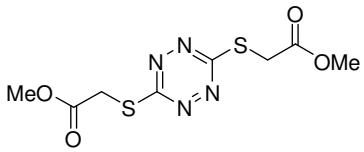

To a solution of Tz-Cl2 (70 mg, 460 µmol, 1 eq.) in DCM, 150 µL of methyl thioglycolate (1.38 mmol, 3 eq.) were added. The mixture was stirred for 1 h at RT. Then, the solvent was removed under reduced pressure. The resulting precipitate was purified by a silica gel column chromatography, eluting with hexane/EtOAc mixtures (85:15). Finally, a maroon-colored precipitate was obtained (46 mg, 35 % yield).

TLC (hexane/EtOAc, 8:2) R*f* = 0.47.

^{1}H NMR ($CDCl_3$, 400 MHz,) δ 4.13 (s, 4H), 3.80 (s, 6H) ppm.

Oligonucleotide STrt-dT10 (4.130)

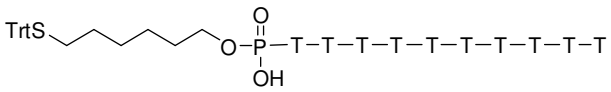

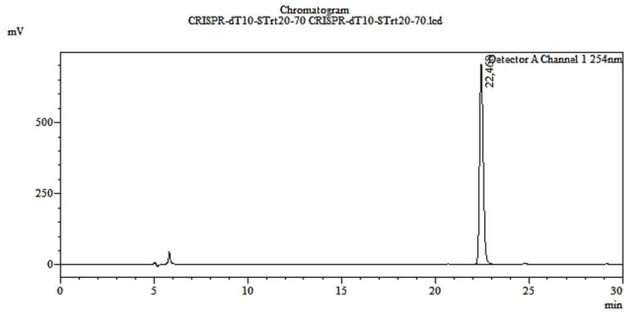

Figure E.4.20 HPLC trace (254 nm) of the crude trityl-protected thiol-oligonucleotide.

Isolation yield**:** 88 %

HPLC analysis conditions**:** 20-70 % B t_R= 22.468 min

MALDI-TOF MS (negative mode, THAP/CA): *m/z* 3417.0 $[M-H]^-$, M calcd. for $C_{125}H_{158}N_{20}O_{70}P_{10}S$ 3416.6.

Oligonucleotide STrt-CAGTCATGTT (4.131)

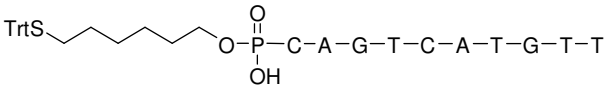

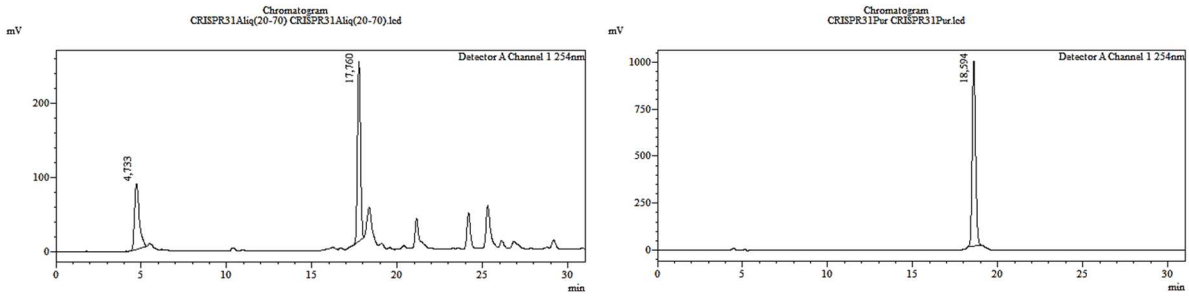

Crude Pure

Figure E.4.21 HPLC trace (254 nm) of the crude (left) and purified (right) trityl-protected thiol-oligonucleotide.

Isolation yield**:** 21 %

HPLC analysis conditions**:** 20-70 % B t_R= 18.6 min

HPLC purification conditions**:** 30-70 % B t_R= 13.4 min

MALDI-TOF MS (negative mode, THAP/CA): *m/z* 3454.5 $[M-H]^-$, M calcd. for $C_{123}H_{152}N_{34}O_{63}P_{10}S$ 3454.7.

Oligonucleotide HS-dT$_{10}$ (4.132)

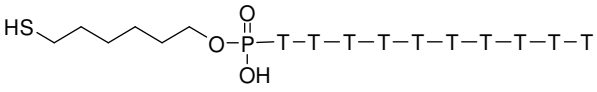

To an eppendorf containing 200 nmol of **4.130** in H_2O (160 µL), $AgNO_3$ (100 µL, 1000 nmol, 10 mM) was added and the mixture stirred at 37 ºC for 45 min. Subsequently, DTT (1400 nmol, 140 µL, 10 mM) was added to the solution and left for an additional 30 min. Finally, the crude was filtered through a hydrophilic PTFE syringe filter and purified by RP-HPLC.

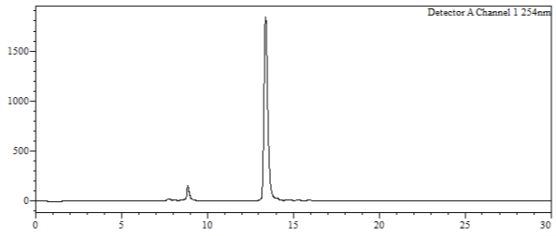

Figure E.4.22 HPLC trace (254 nm) of the crude thiol-oligonucleotide.

Isolation yield: 47 %

HPLC analysis conditions: 20-70 % B t_R= 13.6 min

HPLC purification conditions: 20-70 % B t_R= 6.83 min

MALDI-TOF MS (negative mode, THAP/CA): *m/z* 3175.5 $[M-H]^-$, M calcd. for $C_{106}H_{144}N_{20}O_{71}P_{10}S$ 3174.5.

HS-CAGTCATGTT (4.133)

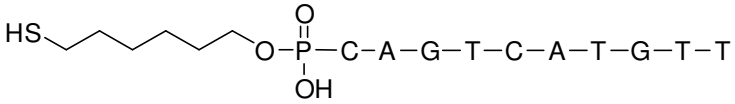

To an eppendorf containing 150 nmol of **4.131** in H_2O (183 µL), $AgNO_3$ (750 µL, 750 nmol, 10 mM) was added and the mixture stirred at 37 ºC for 45 min. Subsequently, DTT (1050 nmol, 42 µL, 25 mM) was added to the solution and left for an additional 30 min. Finally, the crude was filtered through a hydrophilic PTFE syringe filter and purified by RP-HPLC.

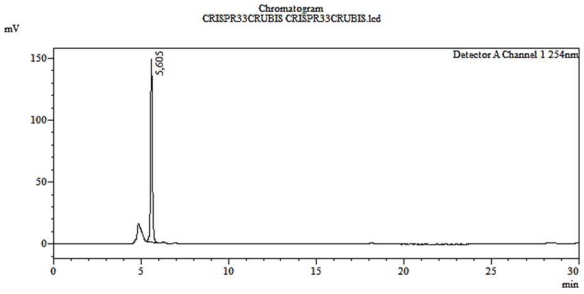

Figure E.4.23 HPLC trace (254 nm) of the crude thiol-oligonucleotide.

Isolation yield: 53 %

HPLC analysis conditions: 20-70 % B t_R= 5.6 min

HPLC purification conditions: 20-60 % B t_R= 6.61 min

MALDI-TOF MS (negative mode, THAP/CA): *m/z* 3212.4 $[M-H]^-$, M calcd. for $C_{104}H_{138}N_{34}O_{63}P_{10}S$ 3212.6.

Cl-Tz-S-d$^{5'}$T$_{10}$

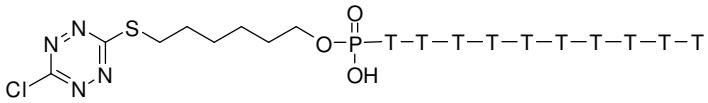

A solution of 3,6-dichloro-1,2,4,5-tetrazine (22 µL, 10 mM in MeOH, 225 nmol) was added to a solution of **4.132** (150 nmol) in H_2O (146 µL) and MeOH (124 µL) and left stirring at 37 ºC for 5 hours.

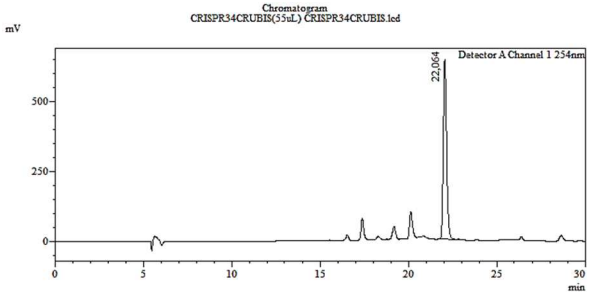

Figure E.4.24 HPLC trace (254 nm) of the crude chlorotetrazine-derivatized oligonucleotide.

Isolation yield: 36 %

HPLC analysis conditions: 20-60 % B t_R= 22.06 min

HPLC purification conditions: 30-70 % B t_R= 20.6 min

MALDI-TOF MS (negative mode, THAP/CA): *m/z* 3285.0 $[M-H]^-$, M calcd. for $C_{108}H_{143}ClN_{24}O_{71}P_{10}S$ 3288.5.

Dansyl-Tz-S-d$^{5'}$T$_{10}$ (4.134)

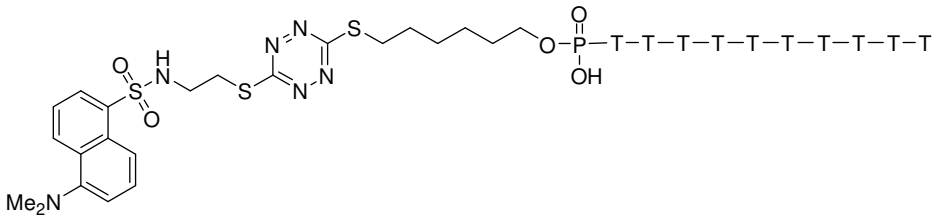

A solution of **4.121** (13,2 µL, 5 mM, 66 nmol, 2.2 eq.) in MeOH was added into a solution of **4.132** (30 nmol) in H_2O (30 µL) and MeOH (16.8 µL) and left under stirring at 37 ºC for 5 hours.

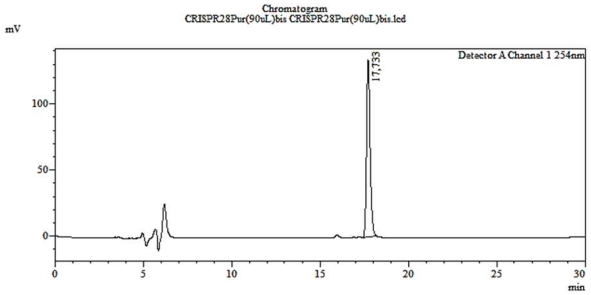

Figure E.4.25 HPLC trace (254 nm) of the crude dansyl-derivatized oligonucleotide.

Isolation yield: 42%

HPLC analysis conditions: 20-70 % B t_R= 17.7 min

HPLC purification conditions: 30-70 % B t_R= 16.0 min

MALDI-TOF MS (negative mode), in CA/THAP as matrix: *m/z* 3562.4 $[M-H]^-$, M calcd. mass for $C_{122}H_{160}N_{26}O_{73}P_{10}S_3$ 3562.6.

Dansyl-Tz-S-d$^{5'}$CAGTCATGTT (4.135)

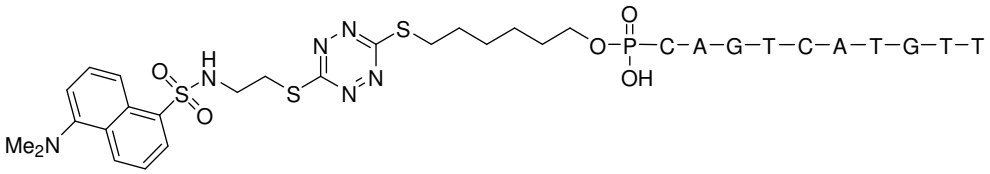

A solution of **4.121** (17.4 µL, 10 mM, 173.8 nmol, 2.2 eq.) in MeOH was added into a solution of **4.133** (79 nmol) in H_2O (80 µL) and MeOH (62.6 µL) and left under stirring at 37 ºC for 5 hours.

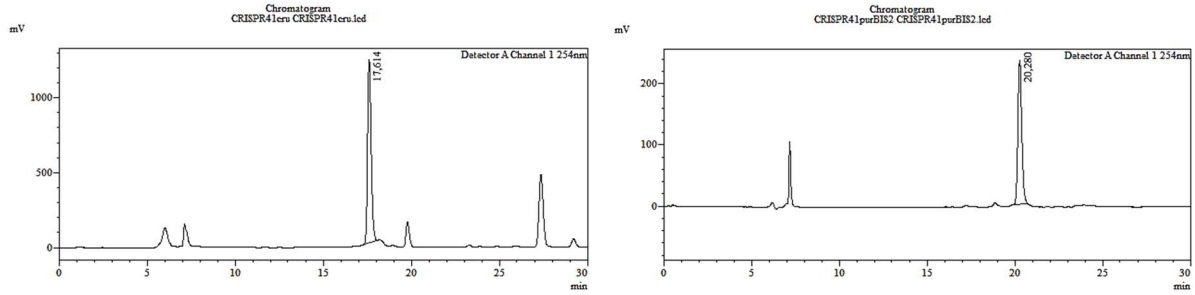

Crude Pure

Figure E.4.26 HPLC trace (254 nm) of the crude (left) and pure (right) dansyl-oligonucleotide conjugate.

Isolation yield: 24%

HPLC analysis conditions: 20-70 % B t_R= 20.3 min

HPLC purification conditions: 30-70 % B t_R= 16.0 min

MALDI-TOF MS (negative mode), in CA/THAP as matrix: *m/z* 3601.1 $[M-H]^-$, M calcd. mass for $C_{120}H_{154}N_{40}O_{65}P_{10}S_3$ 3600.6.

(*R*)-2-Amino-*N*-((1*r*,4*R*)-4-hydroxycyclohexyl)-3-(tritylthio)propenamide (4.138)

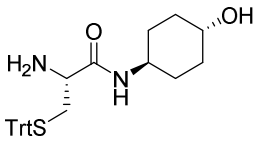

To a round-bottomed flask equipped with a magnetic stirrer, **2.48** (1.65 g, 2.42 mmol) was added 20% piperidine in DCM (20 mL) and the mixture left to mix at room temperature for 1 h. Afterwards, to the mixture was added additional DCM (100 mL) and the organic layer washed with H_2O (3 × 30 mL). The organic layer was dried over anh. $MgSO_4$, filtered and the solvent reduced under vacuum. The extracts were further purified by silica gel column chromatography, eluting with DCM:MeOH mixtures from 100:0 up to 95:5. The title compound was obtained as a white solid (1.08 g, 95%).

TLC (DCM:MeOH 95:5): R_f= 0.13.

MP: 142-145 °C

IR (ATR, Solid): ν 3291, 1644 cm^{-1}.

^{1}H NMR ($CDCl_3$, 400 MHz,): δ: 7.45–7.39 (m, 6H), 7.31–7.27 (t, *J* = 7.5 Hz, 6H), 7.23–7.20 (m, 3H), 3.68–3.55 (m, 2H), 2.98 (dd, *J* = 8.3, 3.9 Hz, 1H), 2.68 (dd, *J* = 12.7, 3.9 Hz 1H), 2.55 (dd, *J* = 12.7, 8.4 Hz, 1H), 1.96–1.89 (m, 4H), 1.42–1.32 (m, 2H), 1.26–11 (m, 2H).

^{13}C NMR ($CDCl_3$, 101 MHz): δ 127.3, 144.8, 129.8, 128.1, 126.9, 69.9, 67.1, 54.2, 47.3, 37.6, 30.8, 30.8 ppm.

ESI-HRMS (positive mode): *m/z*: 461.2269 $[M+H]^+$, M cald. for $C_{28}H_{33}N_2O_2S$ 461.2257.

(*R*)-2-(3-((3a*R*,4*S*,7*R*,7a*S*)-1,3-dioxo-1,3,3a,4,7,7a-hexahydro-2*H*-4,7-Epoxyisoindol-2-yl)propanamido)-*N*-((1r,4*R*)-4-hydroxycyclohexyl)-3-(tritylthio)propenamide (4.139)

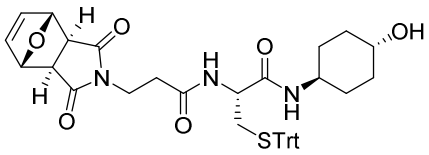

To a solution of **4.20** (310 mg, 1.30 mmol) in DCM (5 mL) was added NMM (117 µL, 1.30 mmol) and ICBF (168 µL, 1.30 mmol) respectively and left 5 min at room temperature. Afterwards, a solution of **4.138** (400 mg, 0.87 mmol) in DCM (2 mL) was added and left reacting at rt for 1 h. Subsequently, to the mixture was added additional DCM (30 mL) and the organic layer washed with aq. HCl 5% (2 × 20 mL). The organic layer was dried over anh. $MgSO_4$, filtered and the solvent removed under vacuum. The extracts were further purified by silica gel column chromatography, eluting with DCM:MeOH mixtures from 100:0 up to 95:5. The title compound was obtained as a pale yellow solid (280.0 mg, 47%).

TLC (DCM:MeOH 98:2): R_f = 0.15.

^{1}H NMR ($CDCl_3$, 400 MHz): δ 7.40 (d, *J* = 7.4 Hz, 6H), 7.29 (t, *J* = 7.7 Hz, 6H), 7.23 (t, *J* = 6.8 Hz, 3H), 6.48 (s, 2H), 5.84 (dd, *J* = 17.0 Hz, 7.6 Hz, 2H), 5.23 (d, *J* = 12.3 Hz, 2H), 3.92–3.79 (m, 2H), 3.72 (t, *J* = 7.6 Hz, 2H), 3.67–3.56 (m, 2H), 2.85–2.81 (m, 1H), 2.77 (s, 2H),

2.72 (dd, *J* = 13.4 Hz, 7.6 Hz, 1H), 2.49–2.44 (m, 1H), 2.43–2.32 (m, 2H, He), 1.93 (m, 4H), 1.40–1.30 (m, 2H), 1.26–1.14 (m, 2H).

ESI-HRMS (positive mode): *m/z* 679.2712 $[M+H]^+$; M calcd for $C_{39}H_{41}N_3O_6S$ 679.2716.

2-Cyanoethyl ((1*R*,4r)-4-((*R*)-2-(3-((3a*R*,4*S*,7*R*,7a*S*)-1,3-dioxo-1,3,3a,4,7,7a-hexahydro-2*H*-4,7-epoxyisoindol-2-yl)propanamido)-3-(tritylthio)propanamido)cyclohexyl) diisopropylphosphoramidite (4.140)

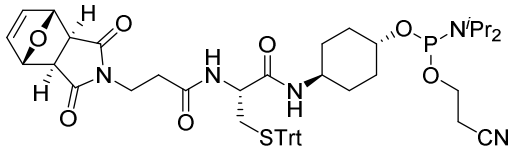

To a solution of **4.139** (531.0 mg, 0.78 mmol) in anh. DCM (5 mL) was added DIPEA (410 µL, 2.34 mmol) and a solution of CECP (250 mg, 1.05 mmol) in anh. DCM (2 mL) under an argon atmosphere and the mixture was left reacting at room temperature for 4 h. Subsequently, the crude was purified by silica gel flash column chromatography eluting with DCM:Hexane:NEt_3 mixtures from 48:50:2 to 98:0:2. The title compound was obtained as a beige foam (504.1 mg, 73%).

TLC (DCM:Hexanes: NEt_3 48:50:2): R_f = 0.29.

^{31}P NMR ($CDCl_3$, 162 MHz,) δ 145.85 ppm.

PMal(H_2)-Cys(Trt)-Cyclhex-$^{5'}$dCAGTCAT$^{3'}$ (4.141)

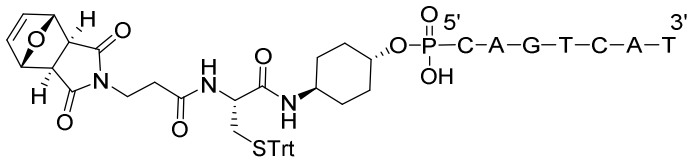

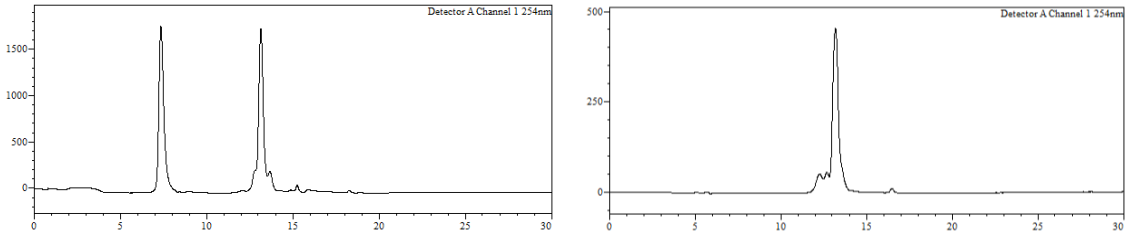

Crude Purified

Figure E.4.27 HPLC traces (254 nm) of crude (left) and purified (right) oligonucleotide.

HPLC: Analysis conditions, 20-70% B, t_R = 13.2 min (**Figure E.4.27**).

Purification gradient: 20-70% B. t_R = 14.0 min Yield: 26%.

MALDI-TOF MS (negative mode, THAP/CA): *m/z* 2826.7 $[M-H]^-$, M calcd. For $C_{107}H_{127}N_{28}O_{48}P_7S$ 2820.6.

PMal(H_2)-Cys-Cyclhex-$^{5'}$dCAGTCAT$^{3'}$ (4.142)

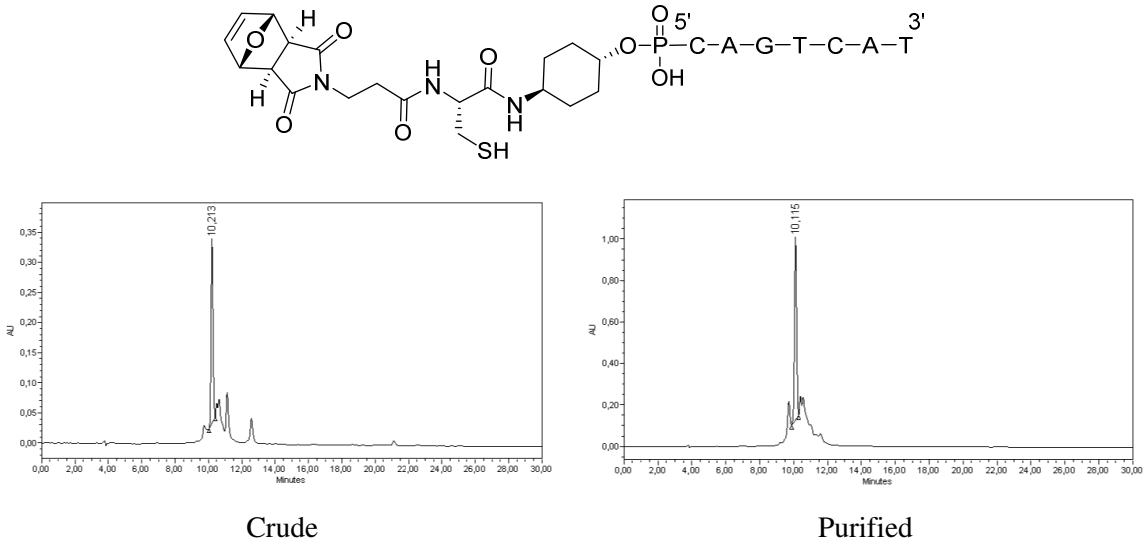

Crude Purified

Figure E.4.28: HPLC traces (254 nm) of crude (left) and purified (right) oligonucleotide.

HPLC: Analysis conditions, 0-50% B, t_R = 10.2 min (**Figure E.4.28**).

Purification gradient: 10-50% B. t_R = 6.0 min Yield: 40%.

MALDI-TOF MS (negative mode, THAP/CA): *m/z* 2576.8 $[M-H]^-$, M calcd. For $C_{88}H_{112}N_{28}O_{48}P_7S$ 2578.5.

Pyrim-Tz-Peptide + Dansly-Tz-Cl + PMal[H_2]-Cys-d$^{5'}$CAGTCAT$^{3'}$. Double conjugate (4.143)

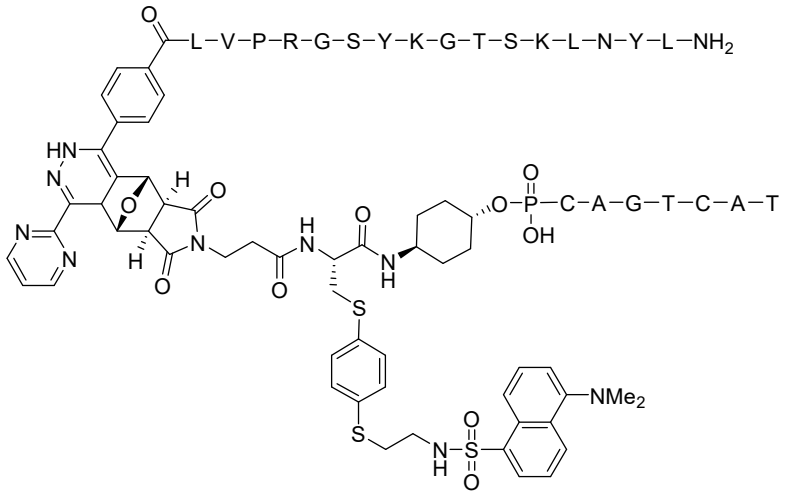

To a solution of oligonucleotide **4.142** (50 nmol) in H_2O (100 µL) was added peptide **4.56** (80 nm) and chlorotetrazine **4.121** (110 nmol in HPLC-grade MeOH) and the reaction left under agitation at 37 ºC overnight.

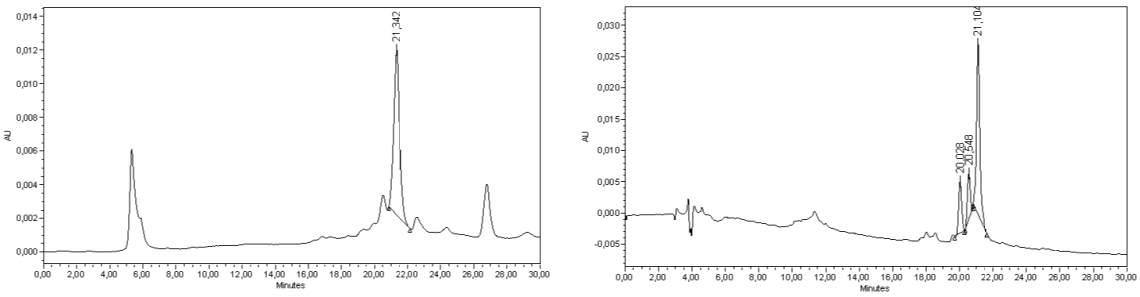

Crude Purified

Figure E.4.29: HPLC traces (254 nm) of crude (left) and purified (right) double conjugate.

HPLC: Analysis conditions, 0-50% B, t_R = 21.1 min (**Figure E.4.29**).

Purification gradient: 10-50% B. t_R = 21.3 min Yield: 40%.

MALDI-TOF MS (negative mode, THAP/CA): *m/z* 4943.3 $[M-H]^-$, M calcd. For $C_{203}H_{274}N_{57}O_8P_7S_3$ 4990.7

N-(1,3-Dihydroxypropan-2-yl)-3-((3*aR*,4*S*,7*R*,7*aS*)-1,3-dioxo-1,3,3*a*,4,7,7*a*-hexahydro-2*H*-4,7-epoxyisoindol-2-yl)propenamide (4.144)

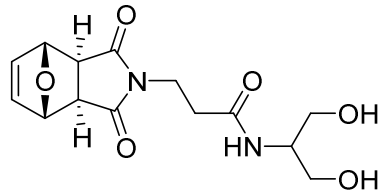

2,3,4,5,6-pentafluorophenol (222 mg, 1.2 mmol, 1.2 eq.) and DIPC (186 µL, 1.2 mmol, 1.2 eq.) were added to a solution of PMal[H_2]-COOH (300 mg, 1.2 mmol, 1.2 eq.) in anh. DMF (6 mL) and the mixture stirred for 30 min. Then, 2-aminopropane-1,3-diol (90 mg, 0.99 mmol, 1 eq.) was added to the solution and left overnight. The solvent was removed under reduced pressure and the resulting crude was purified by silica gel flash column chromatography eluting with DCM:MeOH mixtures from 100:0 to 90:10. The title compound was obtained as a white solid (267 mg, 70 %) was obtained.

TLC (DCM/MeOH 9:1): R_f = 0.39, **Mp.** 167-169 ºC.

IR (ATR, Solid): ν 3310 (w), 1697 (s), 1641 (m), 1154 (m), 1015 (m), 697 (m) cm^{-1}.

^{1}H NMR (400 MHz, CD_3OD): δ 6.55 (s, 2H), 5.16 (s, 2H), 3.87 (p, *J* = 5.6 Hz, 1H), 3.74 (t, *J* = 6.8 Hz, 2H), 3.59 (d, *J* = 4.0 Hz, 4H), 2.92 (s, 2H), 2.47 (t, *J* = 8.0 Hz, 2H) ppm.

^{13}C NMR (101 MHz, CD_3OD): δ 178.20, 172.92, 137.60, 82.21, 61.91, 54.48, 48.76, 36.33, 34.93 ppm.

ESI-HRMS (positive mode): *m/z*: 311.1234 $[M+H]^+$; M calcd for $C_{14}H_{19}N_2O_6$ 311.1238.

_N_-(1-(Bis(4-methoxyphenyl)(phenyl)methoxy)-3-hydroxypropan-2-yl)-3-((3_aR_,4_S_,7_R_,7_aS_)-1,3-dioxo-1,3,3_a_,4,7,7_a_-hexahydro-2_H_-4,7-epoxyisoindol-2-yl)propanamide (4.145)

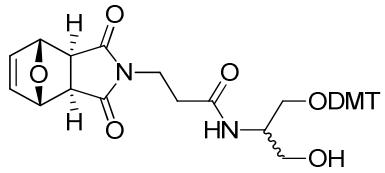

To a 25 mL round-bottomed flask, **4.144** (277.0 mg, 1.17 mmol) and DMT-Cl (271.0 mg, 1.06 mmol) were weighed. Under an argon atmosphere anh. Pyr (10 mL) was added and the resulting mixture was stirred overnight at rt. Afterwards, the solvent was removed under reduced pressure and the resulting crude purified by silica gel flash column chromatography eluting with hexanes:DCM:MeOH:NEt_3 mixtures from 95:0:0:5 to 0:92:3:5. The title compound was obtained as a white solid (144.0 mg, 20%).

TLC (DCM/MeOH 98:2): R_f = 0.18, **Mp** 84-87 ºC.

IR (ATR, Solid): ν 3361 (w), 2931 (w), 1771 (w), 1696 (s), 1605 (m), 1506 (s), 1245 (s), 1172 (s), 1074 (m), 1018 (m), 702 (m) cm^{-1}.

^{1}H NMR (400 MHz, $CDCl_3$): δ 7.54-7.48 (m, 2H), 7.44-7.27 (m, 8H), 6.95 (d, *J* = 8.8 Hz, 1H), 6.46 (s, 2H), 6.25 (d, *J* = 7.6 Hz, 1H), 5.33 (d, *J* = 10 Hz, 2H), 4.23-4.12 (m, 1H), 3.90 (s, 6H), 3.88-3.76 (m, 4H), 3.44-3.30 (m, 2H), 2.92 (s, 2H), 2.57 (t, *J* = 6.8 Hz, 2H) ppm.

^{13}C NMR (101 MHz, $CDCl_3$): δ 175.91, 170.0, 158.6, 158.50, 147.46, 144.93, 139.59, 136.49, 136.04, 135.87, 130.16, 130.09, 129.20, 128.17, 128.09, 128.00, 127.87, 127.84, 127.09, 126.79, 113.22, 113.19 113.20, 86.49, 86.03, 81.49, 80.90, 61.51, 55.29, 55.24, 51.59, 49.02, 47.34, 45.92, 35.37, 35.07, 34.24, 33.82 ppm.

ESI-HRMS (positive mode): *m/z*: 635.2371 $[M+Na]^+$, M calcd for $C_{35}H_{36}N_2NaO_8$ 635.2364.

4-(3-(bis(4-methoxyphenyl)(phenyl)methoxy)-2-(3-((3_aR_,4_S_,7_R_,7_aS_)-1,3-dioxo-1,3,3_a_,4,7,7_a_-hexahydro-2_H_-4,7-epoxyisoindol-2-yl)propanamido)propoxy)-4-oxobutanoic acid (4.146)

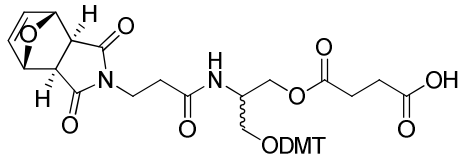

In a 10 mL round-bottomed flask, **4.145** (111 mg, 0.182 mmol, 2 eq.), succinic anhydride (28 mg, 0.28 mmol, 3 eq.) and DMAP (11 mg, 0.09 mmol, 1 eq.) were added under argon atmosphere. Subsequently, anh. Pyr (1.5 mL) was added and the mixture was stirred 72 h at rt. Afterwards, the solvent was removed with ACN co-evaporation under reduced pressure and the resulting crude was dissolved with acid-free

DCM (5 mL). The organic layer was washed with aq. citric acid 10% (3 × 6 mL) and H_2O (5 × 6 mL). The organic phase was dried over anh. $MgSO_4$, filtered and the solvent removed under reduced pressure. The title product was obtained as a white solid (54 mg, 32 %).

^{1}H NMR (400 MHz, $CDCl_3$): δ 7.41-7.34 (m, 2H), 7.31-7.14 (m, 8H), 6.81 (d, *J* = 8.8 Hz, 4H), 6.46 (s, 2H), 6.14-6.06 (m, 1H), 5.20 (t, *J* = 4.0 Hz, 1H), 5.16 (s, 1H), 4.39-4.26 (m, 2H), 3.77 (s, 6H), 3.75-3.68 (m, 3H); 3.31-3.21 (m, 1H), 3.13-3.06 (m, 1H), 2.78 (s, 2H), 2.65-2.37 (m, 6H) ppm.

^{13}C NMR (101 MHz, $CDCl_3$): δ 176.63, 176.50, 174.83, 172.30, 169.55, 158.75, 158.65, 147.45, 144.69, 139.59, 136.64, 135.89, 135.78, 130.20, 130.17, 130.15, 129.27, 128.35, 128.21, 128.00, 127.80, 127.21, 127.01, 113.20, 113.16 113.20, 86.37, 81.03, 63.69, 63.14, 61.92, 55.39, 55.37, 48.54, 47.60, 35.52, 34.11, 29.53, 29.16 ppm.

ESI-HRMS (negative mode): *m/z*: 712.2632 $[M-H]^-$ M calcd for $C_{39}H_{40}N_2O_{11}$ 712.2634.

DMT-*O*-[Protected maleimido]-diol-succinyl-LCAA-CPG (4.147)

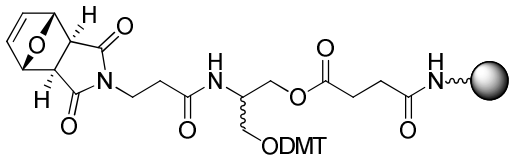

LCAA-CPG resin (156 mg, 71 μmol·g^{-1}) was weighed into a 3 mL polyethylene syringe fitted with a polypropylene filter. The resin was washed with DCM (3 × 3 mL), 3% TCA in DCM (3 × 3 mL), 20% NEt_3 in DCM (5 × 3 mL) and acid-free DCM (5 × 3 mL) and dried under an air stream. The coupling cocktail was prepared dissolving **4.146** (54 mg, 0.103 mmol), DIPC (170 μL, 1.06 mmol) and HOBt (164 mg, 1.06 mmol) in acid-free DCM/DMF 1:1 (500 μL). The mixture was poured into the syringe and it was reacted at room temperature for 6.5 h with occasional stirring. Afterwards, the mixture was filtered; the resin washed with acid-free DCM (5 × 3 mL), ACN (5 × 3 mL) and dried under an air stream.

For quantification, an aliquot was weighed off (3.9 mg) and the DMT group removed to determine the substitution degree. For the DMT removal, the aliquot was treated with 25 mL of 70% $HClO_4$/EtOH (7:1) mixture and the amount of 4,4'-dimethoxytrirtyl cations in solution was determined by absorbance measurement (ε_{495} = 72.000 M^{-1} cm^{-1}) found out to be 24.5 μmol g^{-1}. Possible unreacted amines were capped by acetylation with Ac_2O/Pyr 1:1 (15 min, rt). The glass beads were washed with acid-free DCM (3 × 3 mL), ACN (3 × 3 mL) dried under an air stream and stored under an argon atmosphere at -28 ºC prior to use.

(*E*)-Hepta-4,6-dien-1-ol (4.148)

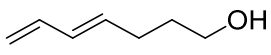

To a suspension of $LiAlH_4$ (666 mg, 17.52 mmol) in anh. Et_2O (5 mL) at 0 ºC was added a solution of **3.47** (900 mg, 5.84 mmol) in Et_2O (10 mL) dropwise. Afterwards, the mixture was allowed to warm to room temperature and was stirred for 1 h. Subsequently, to the mixture was added EtOAc, MeOH, H_2O (1 mL, each) followed by aq. HCl 10% (20 mL) and transferred into a separatory funnel. The aqueous phase was extracted with Et_2O (2 × 20 mL) and the combined extracts washed with aq. 10% $NaHCO_3$ (3 × 20 mL). The organic layer was dried over anh. $MgSO_4$, filtered and the solvent removed under vacuum. The title compound was obtained as a colorless oil (491 mg, 75%).

^{1}H NMR ($CDCl_3$, 400 MHz): δ 6.30 (dt, *J* = 16.9, 10.3 Hz, 1H), 6.12 – 6.04 (m, 1H), 5.71 (dt, *J* = 14.7, 7.0 Hz, 1H), 5.09 (d, *J* = 16.9 Hz, 1H), 4.97 (d, *J* = 10.1 Hz, 1H), 3.65 (t, *J* = 6.5 Hz, 2H), 2.18 (q, *J* = 7.2 Hz, 2H), 1.67 (p ap., *J* = 6.6 Hz, 3H) ppm.

^{13}C NMR ($CDCl_3$, 101 MHz): δ 179.43, 136.73, 132.14, 132.12, 115.92, 33.59, 27.37 ppm.

(*E*)-2-Cyanoethyl hepta-4,6-dien-1-yl diisopropylphosphoramidite (4.149)

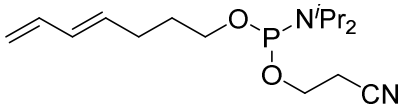

(*E*)-Hepta-4,6-dien-1-ol (**4.148**, 183 mg, 1.17 mmol) was dissolved in anh. DCM (1 mL) under an argon atmosphere. Afterwards, anh. DIPEA (553 µL, 3.18 mmol) and CECP (250.0 mg, 1.06 mmol) dissolved in anh. DCM (2 mL) were added and the mixture was stirred for 6 h. The crude was diluted in acid-free DCM (25 mL), washed with aq. 10% $NaHCO_3$ (3 × 20 mL) and brine (1 × 25 mL) and dried over anh. $MgSO_4$. The solvent was removed under reduced pressure and the resulting crude was purified by silica gel column chromatography (elution with DCM/Hexane/NEt_3 20:80:2). The title compound was obtained as a pale-yellow oil (150 mg, 45 %).

^{1}H NMR (400 MHz, $CDCl_3$): δ 6.37-6.24 (m, 1H), 6.14-6.00 (m, 1H), 5.76-5.64 (m, 1H), 5.09 (d, *J* = 16.0 Hz, 1H), 4.96 (d, *J* = 12.0 Hz, 1H), 3.90-3.76 (m, 2H); 3.72-3.56 (m, 4H); 2.64 (t, *J* = 6.4 Hz, 2H), 2.18 (q, *J* = 7.6 Hz, 2H), 1.72 (p, *J* = 6.4 Hz, 2H), 1.19 (d, *J* = 4.4 Hz, 6H), 1.18 (d, *J* = 4.0 Hz, 6H) ppm.

^{13}C NMR (101 MHz, $CDCl_3$) δ 137.1, 134.3, 131.5, 117.6, 115.0, 63.1, 62.9, 58.4, 58.2, 43.1, 43.0, 30.7, 30.7, 28.9, 24.7, 24.6, 24.6, 24.5, 20.4, 20.3 ppm.

^{31}P NMR (400 MHz, $CDCl_3$): δ 147.38 ppm.

ESI-HRMS (positive mode): *m/z*: 313.2032 $[M+H]^+$; calcd. for $C_{16}H_{30}N_2O_2P$ww 313.2039.

Oligonucleotide diene-dT$_9$-PMal[H$_2$] (4.153)

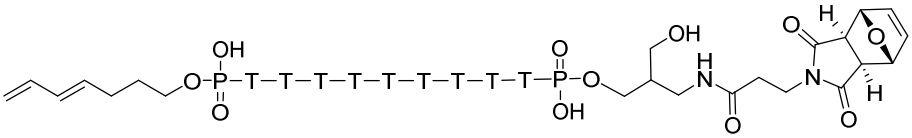

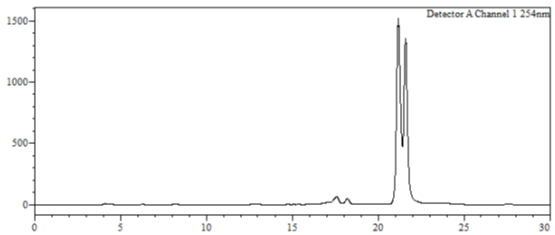

Figure E.4.30 HPLC traces (254 nm) of purified oligonucleotide.

HPLC: Analysis conditions, 0-50% B, t_R = 10.2 min (**Figure E.4.30**).

Purification gradient: 10-50% B. t_R = 14.0 min Yield: 26%.

MALDI-TOF MS (negative mode, THAP/CA): *m/z* 3233.1 $[M-H]^-$, 3168.6 $[M-H]^-$ (Furan loss); M calcd. For $C_{112}H_{148}N_{20}O_{72}P_{10}$ 3234.6

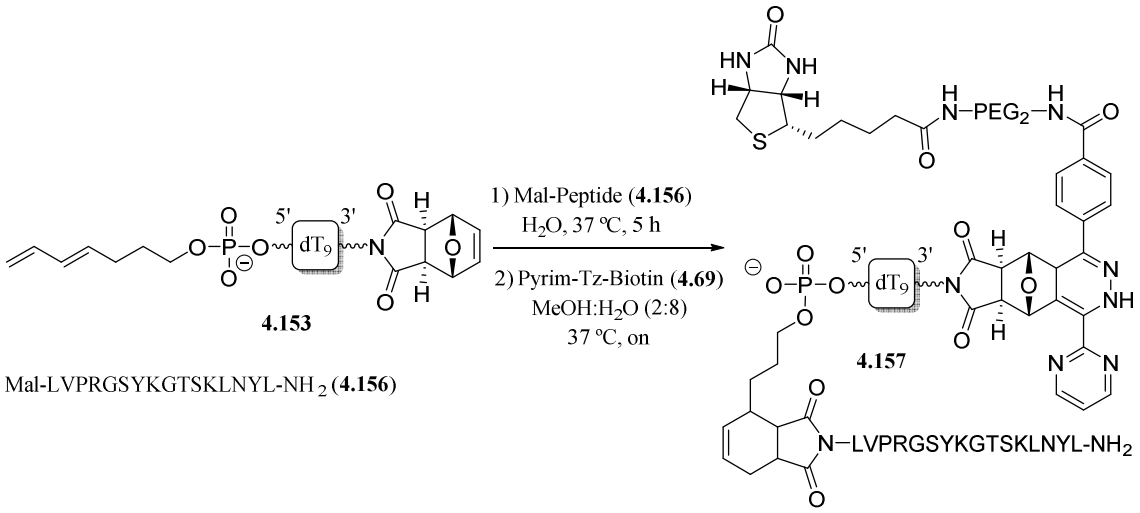

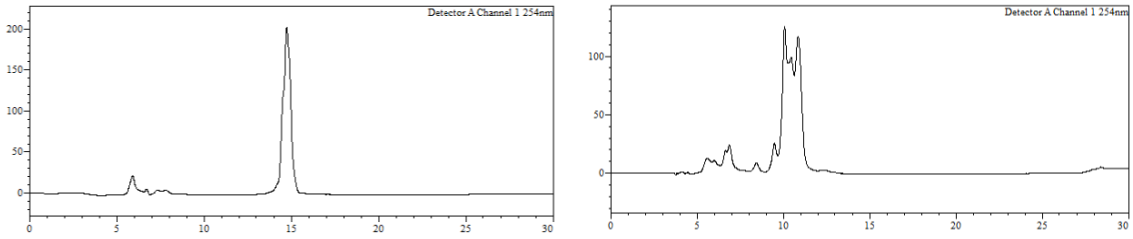

Crude Diels-Alder reaction (5 h) Crude double conjugation (on)

Figure E.4.31: HPLC traces (254 nm) of crude (left) and purified (right) oligonucleotide.

HPLC: Analysis conditions, 0-50% B, t_R = 10.2 min (**Figure E.4.31**).

Purification gradient: 10-50% B. t_R = 9.0 min Yield: 26%.

MALDI-TOF MS (negative mode, THAP/CA): *m/z* 3233.1 $[M-H]^-$, 3168.6 $[M-H]^-$ (Furan loss); M calcd. For $C_{112}H_{148}N_{20}O_{72}P_{10}$ 3234.6

Resum en català

R.C.1 Introducció i objectius

Tant oligonucleòtids com pèptids i proteïnes estan implicats en la majoria dels processos cel·lulars. Aquestes molècules no només fan possible la vida, sinó que algunes d'elles estan directament relacionades amb el desenvolupament de malalties. Per exemple, algunes proteïnes estan implicades en malalties com l'Alzheimer, Parkinson o Huntington.[1,2] Un cas semblant són les repeticions aberrants d'algunes seqüències en el genoma i la seva relació amb una àmplia varietat d'afeccions conegudes com a TRED (de l'anglès *Trinucleotide Repeat Expansion Disorders*).[3,4]

Tot i això, aquestes biomolècules tenen un gran potencial com a possibles medicaments. Fins avui, una multitud de proteïnes han estat aprovades com a fàrmacs o agents de diagnòstic per l'FDA i, tot i que només uns quants oligonucleòtids han arribat al marcat, sí que n'hi ha força que estan en fase d'assajos clínics.[5,6] Els pèptids també tenen un lloc important en el camp de la medicina: les ciclosporines actuen com a immunosupressors,[7] els anàlegs de somatostatina s'usen per al tractament de tumors nueroendocrins,[8] etc.

Tot i això, tant oligonucleòtids com pèptids i proteïnes necessiten, normalment, ser modificats químicament per millorar les seves propietats farmacocinètiques i farmacodinàmiques. D'entre les modificacions normalment practicades, en aquesta tesi doctoral s'ha treballat amb la conjugació posant especial èmfasi en la seva aplicació tant en pèptids, àcids nucleics peptídics (PNAs) i oligonucleòtids.

La conjugació s'utilitza normalment per a conferir propietat noves o millorar-ne d'intrínseques de la biomolècula. Des de millorar la biodistribució, estabilitat o internalització cel·lular passant per dotar biomolècules amb marques radioactives o fluorescent per a proveir un mètode de seguiment dins l'organisme o dins la cèl·lula.

Malgrat l'ampli ventall de reaccions útils en bioconjugació, cada una d'elles presenta algun inconvenient o limitació, instigant el desenvolupament de noves metodologies per a tal de minimitzar aquestes mancances. Factors com la formació de més d'un estèreo- o regioisòmer en la generació de nous enllaços o l'estabilitat dels conjugats encara són limitacions a l'hora de generar conjugats de biomolècules.

D'altra banda, en certs contextos, hi ha la necessitat de no només derivatitzar la biomolècula només un cop sinó més d'un. Degut a aquest necessitat, les múltiples conjugacions estan essent explorades recentment com un nou vehicle per a adreçar més adequadament algunes mancances associades amb l'ús de biomolècules abans mencionades. Tot i això, l'ús de dues o més reaccions de bioconjugació simultàniament no es trivial degut no només a la selectivitat i compatibilitat dels reactius qüestió però a les substàncies addicionals que poden necessitar certes metodologies de conjugació. Essent així, en certes instàncies, un problema difícil d'abordar.

En base als fets exposats ens vàrem plantejar

1- Explorar l'ús de ciclopent-4-en-1,3-diones 2,2-disbustituïdes (CPDs) com a anàlegs de maleimides en reaccions de tipus Michael amb tiols per a la conjugació i ciclació de pèptids, PNAs i oligonucleòtids.
2- Explorar la possibilitat d'emprar la reacció de conjugació exhibida per les CPDs amb cisteïnes per a preparar dobles conjugats, combinant-la amb les reaccions de Michael amb tiols, la cicloaddició azida-alquí catalitzada per Cu(I) o la formació d'oximes.
3- Explorar si el resultat de la unió covalent entre una molècula (Retro-1) amb propietats d'internalització d'oligonucleòtids i una cadena oligonucleotídica amb potencial terapèutic té un efecte superior a la utilització dels dos components per separat.

4- Explorar l'ús de 7-oxanorbornenes com a dienòfils de la reacció de Diels-Alder de demanda electrònica inversa amb 1,2,4,5-tetrazines 3.6-disbustituïdes per a la producció de conjugats de pèptids, PNAs i oligonucleòtids.
5- Avaluar les diverses possibilitats per a la preparació de dobles conjugats combinant la reacció de Diels-Alder de demanda electrònica inversa amb la reacció de Michael entre una maleimida i un tiol, la reacció de CPD-cisteïna, la reacció de Diels-Alder i la substitució nucleòfila aromàtica entre un tiol i una clorotetrazina.

R.C.2 Ciclopent-4-en-1,3-diones 2,2-disbustituïdes: conjugacions simples i dobles

Tot i que la reacció entre tiols i maleimides s'havia considerat sempre exempta de problemes, en els últims anys s'ha posat de manifest que les 4-alquilsulfonilsuccinimides generades després de la reacció de tipus Michael no gaudeixen de l'estabilitat que se'ls havia atribuït. Per una banda el tiol unit a la succinimida pot intercanviar-se per d'altres coexistint al medi,[9] les succinimides poden experimentar també reaccions d'hidròlisi en medis aquosos (**Figura R.C.1**).[10,11] Aquesta segona reacció genera dos nous regioisòmers que poden tenir propietats diferents, cosa que pot acabar essent un problema tant del punt de vista purament química com també del biològic.

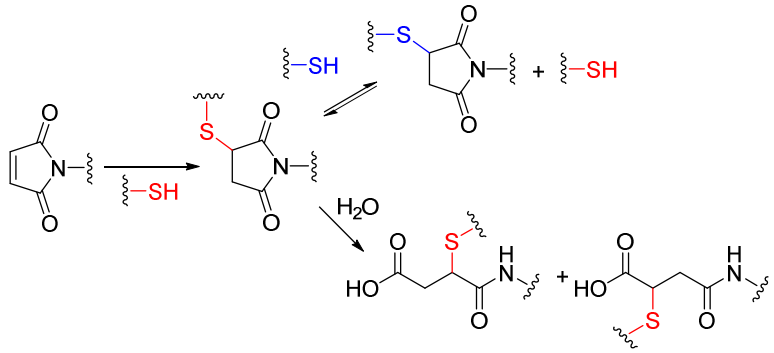

Figura R.C.1 Possibles reaccions secundàries experimentades per una 4-alquilsulfonilsuccinimida en medi aquós.

Degut al fet que la reacció de tipus Michael entre tiols i maleimides és una eina molt útil com a mètode de conjugació i alguns conjugats sintetitzats seguint aquest procediment han arribat al mercat o estan en fases avançades en assajos clínics, ens vam plantejar la possibilitat de treballar amb un anàleg de maleimida que no fos hidrolitzable.

En aquesta línia de treball es va proposar emprar les ciclopent-4-en-1,3-diones 2,2-disbustituides (CPDs), unes molècules que, en comparació amb la maleimida, s'ha substituït el grup imido per una dicetona. Aquest canvi comporta, conseqüentment, la impossibilitat d'hidròlisi ja sigui abans o després de l'addició d'un tiol.

Quan el Dr. Brun va procedir a avaluar la reacció d'aquest tipus de compostos amb pèptids que contenien cisteïnes en posicions internes va comprovar que el seu comportament es diferenciava al de les maleimides. Contràriament a la reacció que experimenten les maleimides amb tiols (amb qualsevol tipus de tiol i de forma quantitativa per general adductes de tipus Michael que no reverteixen a menys que hi hagi altres tiols presents al medi de reacció), la reacció entre una CPD i un tiol que no posseeixi una amina lliure en la posició 2 no es va produir mai de manera quantitativa. Tot i que la primer addició de Michael era ràpida, va poder comprovar que els adductes formats a partir de les CPDs eren reversibles a temperatura ambient i que l'equilibri estava desplaçat cap a la formació dels reactius de partida.

D'altre banda, aquells pèptids on la cisteïna ocupava la posició *N*-terminal van reaccionar completament quan es van mesclar amb CPDs. Sorprenentment, però, l'adducte generat no va ser l'esperat tipus Michael, sinó un amb una massa 20 Da inferior (M-20). Diferents experiments li van permetre postular una possible estructura per aquest nou producte, així com un camí de reacció plausible per explicar la seva formació representat a l'**Esquema R.C.1**

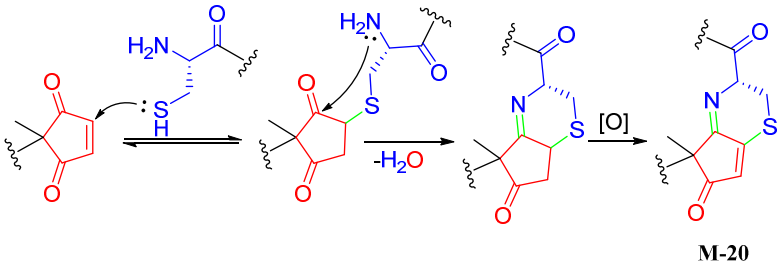

Esquema R.C.1 Camí de reacció proposat per la formació de l'adducte final M-20.

Breument, després de la reacció de tipus Michael inicial entre la CPD i el tiol, l'amina de la posició *N*-terminal i un dels grups cetona de la CPD condensen per formar una imina, donant lloc a un producte cíclic de sis baules que presenta una massa 18 unitats menor que l'esperat. Aquest producte intermedi generat per deshidratació s'oxida, en una etapa més lenta, per donar l'adducte estable final M-20, que posseeix un sistema conjugat amb un màxim d'absorció al voltant de 330 nm.

Un cop es va avaluar la característica reacció entre les CPDs i les cisteïnes *N*-terminals, i degut a que les nostres intencions eren utilitzar les CPDs per a conjugacions de pèptids un derivat que contingués un àcid carboxílic era molt útil. Es van sintetitzar dos derivats de CPD, un incorporant el fluoròfor dansil i l'altre, la biotina. Totes dues CPDs es van fer reaccionar amb cisteïnat de metil i es va comprovar que seguint el mateix camí de reacció i que formaven el mateix tipus d'adducte que les CPDs anteriorment emprades. Anàlogament, es va comprovar la viabilitat d'introduir CPDs a la posició *N*-terminal d'una cadena peptídica utilitzant mètodes estàndard de síntesi de pèptids en fase sòlida. Tant la introducció de CPDs com la seva resistència a la mescla àcida emprada per al desancoratge i desprotecció de poliamides van quedar clares, podent-se obtenir poliamides (pèptids i PNAs) amb aquest tipus d'estructures (**Esquema R.C.2**). Tot i això es va comprovar la descomposició de la CPD a condicions bàsiques emprades per a la desprotecció del grup Fmoc.

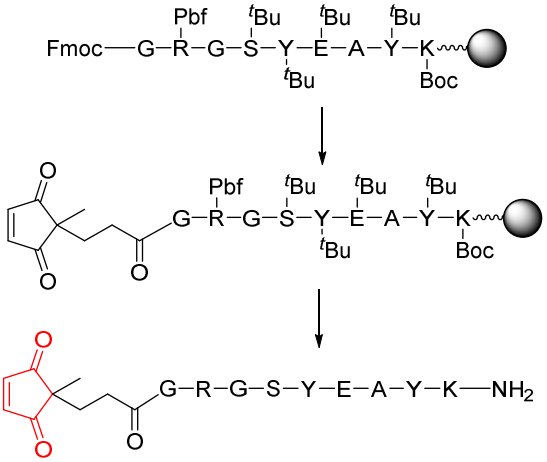

Esquema R.C.2 Introducció d'una CPD a una cadena peptídica usant mètodes estàndard de síntesi en fase sòlida.

Seguint aquest procediment es van sintetitzar 2 poliamides més contenint la CPD a la posició *N*-terminal i es van conjugar amb altres pèptids (contenint cisteïnes a la posició *N*-terminal) de forma satisfactòria.

Tot seguit, veient els bons resultats obtinguts amb pèptids i PNAs, ens vàrem plantejar produir conjugats de oligonucleòtids. Tenint en compte les posicions on es solen modificar els oligonucleòtids (les nucleobases, als grups fosfat i les posicions 3' i 5', respectivament) vam proposar-nos modificar la posició 5' degut al fet que és la més fàcilment derivatitzable per medis químics de la llista anterior.

En aquest cas, tenim dos opcions per a la modificació en la posició 5' d'un oligonucleòtid completament protegit: acoblar la CPD o la cisteïna. La primera opció es va descartar ràpidament degut a la ràpida degradació de la CPD al tractament final amb amoníac aquós concentrat. D'altra banda, a la literatura ja hi havia descrits procediments per tal d'obtenir cisteïnes en aquesta posició.[12,13]

Així doncs, veien que la segona opció era la més factible, es van sintetitzar dos fosforamidits de cisteïna amb el tiol protegit amb el grup tritil o *tert*-butiltio, tal com es descriu a la literatura, i es van acoblar satisfactòriament a tres oligonucleòtids. Tot seguit, tal com es mostra a l'**Esquema R.C.3** després de la respectiva desprotecció del grups protectors del tiol, emprant les condicions adients (Ag^+ per el tritil i TCEP per el *tert*-butiltio)[14,15] es va aconseguir H-Cys-oligonucleòtids i es van utilitzar per a reaccions de conjugació amb CPDs.

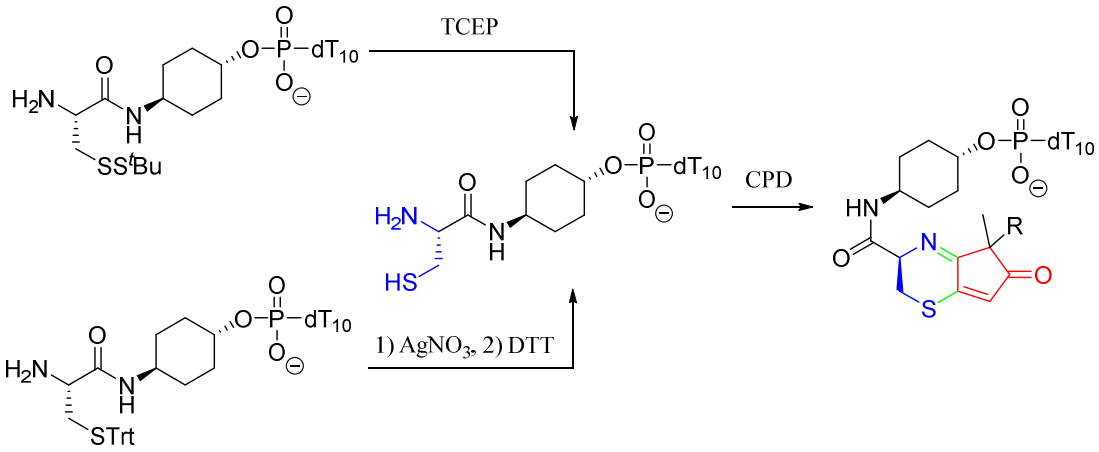

Esquema R.C.3 Condicions de desprotecció i conjugació amb una CPD d'un oligonucleòtid derivatitzat amb una cisteïna a la posició 5'.

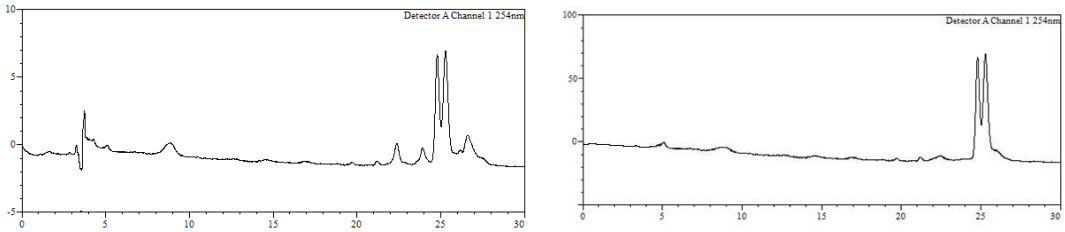

Cru Pur

Figura R.C.2 Cru de reacció per a la síntesi del conjugat oligonucleòtid-CPD-pèptid (esquerra) i producte purificat.

A continuació es va procedir a realitzar dobles conjugats utilitzant almenys una reacció de CPD-Cys. Basant-se en resultats obtinguts per el Dr. Brun en la seva tesi doctoral on, va marcar selectivament un pèptid que contenia un cisteïna en la posició *N*-terminal en presència d'un altre pèptid que la tenia en una posició interna. L'ús de CPDs va permetre marcar selectivament només aquell que contenia la cisteïna en la posició *N*-terminal, una diferència important respecte la maleimida, que seria incapaç de diferenciar-los.

Observant aquest resultats, vam proposar aprofitar aquesta diferent reactivitat de les CPDs en front de 1,2-aminotiols respecte a altres tipus de tiols, utilitzant un pèptid que contenia dues cisteïnes: una en posició *N*-terminal i l'altre en una posició interna. Per aconseguir-ho es va procedir incubant el pèptid amb 1.1 equivalents de CPD fins a la formació de l'adducte bicíclic i, tot seguit, es fa afegir 3

equivalents de maleimida. Al cap de una hora ja es va obtenir, amb bon rendiment, el producte desitjat tal com s'indica a l'**Esquema R.C.4**.

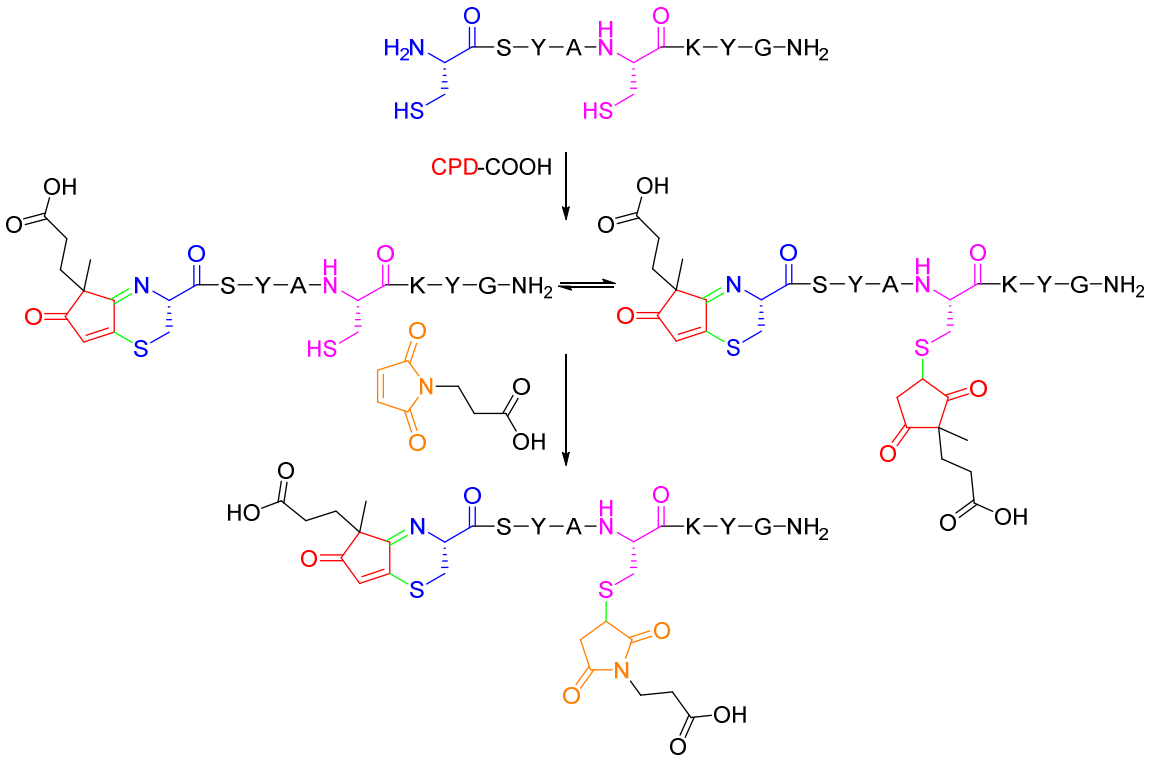

Esquema R.C.4 Doble derivatització regioselectiva d'un pèptid que conté dues cisteïnes, una en la posició *N*-terminal i l'altre en una posició amb una CPD i una maleimida.

Addicionalment es va combinar la reacció de cicloaddició 1,3-dipolar entre una azida i un alquí catalitzada per Cu(I) (CuAAC)i la reacció de CPD-Cys. Per tal d'aconseguir-ho es van derivatitzar pèptids amb un alquí incorporat a la cadena lateral d'una lisina conjuntament amb la CPD o una cisteïna *N*-terminal. Es va comprovar la viabilitat de dur a terme la reacció de CPD-Cys i la satisfactòriament sense afectar la funció alquí. Seguidament, es va comprovar que l'adducte M-20 aguantava les condicions de reacció de CuAAC aïllant el producte desitjat de doble conjugació en diversos pèptids contenint cisteïnes *N*-terminals o CPDs independentment amb diverses azides.

D'altre banda, es va comprovar l'ordre de les reaccions era de primordial importància. Si es realitzava la reacció de CuAAC en presència de la CPD s'obtenien crus complexes indicant possibles interaccions entre la CPD i les azides utilitzades. D'altre banda si es realitzava la reacció sobre pèptids amb tiols lliures s'obtenien productes de cicloaddició juntament amb subproductes d'oxidació dels tiols, tal com s'havia indicat a la literatura.[16]

Veient l'èxit de les dobles conjugacions, encara que s'haguessin de realitzar en un ordre estricte, es va decidir explorar si les CPDs i les azides reaccionaven per tal de donar una explicació als resultats negatius s'havien obtingut prèviament.

Per aquest objectiu es va fer reaccionar un model de CPD i azida i es va observar al formació de dos sets de productes resultants de la reacció d'ambdós (**Figura R.C.3**).

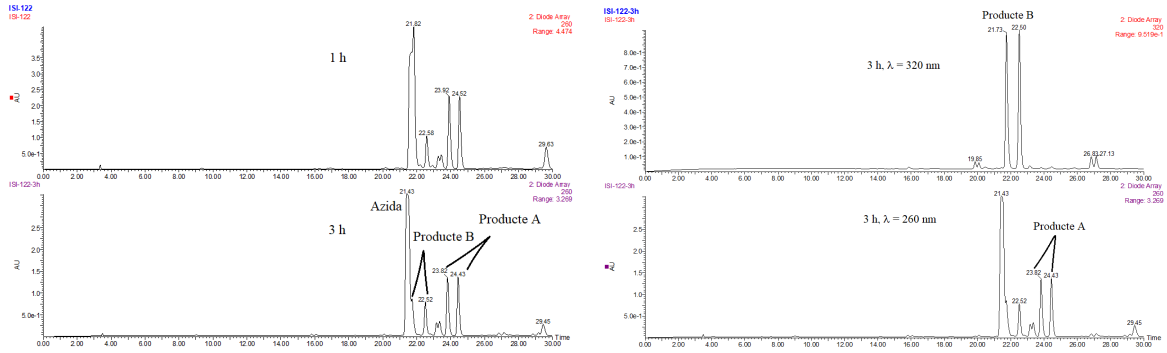

Figura R.C.3 Perfils de HPLC-MS (260 nm, esquerra) de la reacció entre CPD-COOH i AZT a una i tres hores i perfils de HPLC (320 nm o 260 nm, dret) a les tres hores.

Vista aquesta primera aproximació es va procedir a realitzar un procés d'optimització de la reacció per tal d'aconseguir afavorir un dels dos compostos. Els resultats van ser un parcial afavoriment d'un compost respecte l'altre però mai es va poder aconseguir promoure suficient la reacció per tal de consumir la totalitat dels reactius.

Tot i això, es van aïllar ambdós compostos i caracteritzar completament per ressonància magnètica nuclear i mètodes espectroscòpics per tal d'elucidar les dues estructures (**Figura R.C.4**).

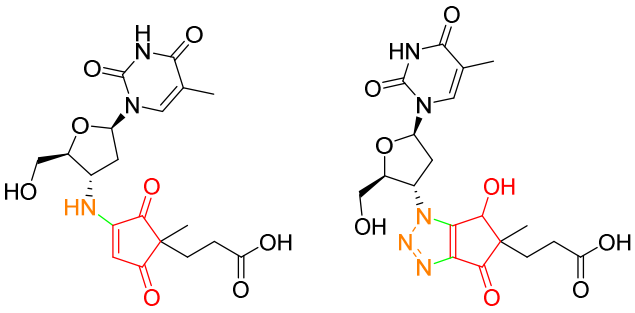

Figura R.C.4 Productes aïllats de la cicloaddició 1,3-dipolar entre AZT i la CPD-COOH

Breument, en ambdós casos, l'espectre bidimensional heteronuclear de correlació de múltiples enllaços (HMBC) ens va donar la informació necessària per concloure ens les estructures proposades a dalt. Tal com s'indica a la **Figura R.C.5**, en el cas de la molècula desnitrogenada, la correlació clau (marcada en verd) és entre el carboni quaternari enamínic i el protó del carboni 3' de l'anell de 2'-deoxiribosa.

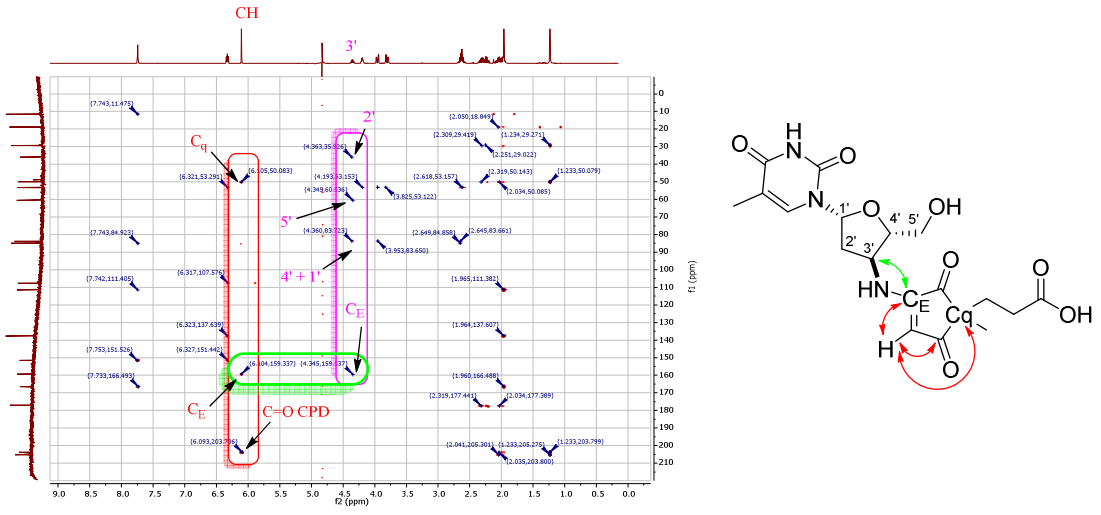

Figura R.C.5 Espectre de HBMC i correlacions clau (esquerra) per la identificació de l'estructura desnitrogenada. A la dreta es mostra l'estructura amb les correlacions.

Respecte a l'estructura bicíclica, el procediment va ser quelcom semblant. En aquesta instància, però les correlacions claus per identificar el compost va ser un altre cop entre el protó a la posició 3' de l'anel de 2'-desoxiribosa i el carboni quaternari de la triazole formada per la reacció de cicloaddició 1,3-dipolar, com s'indica a la **Figura R.C.6**.

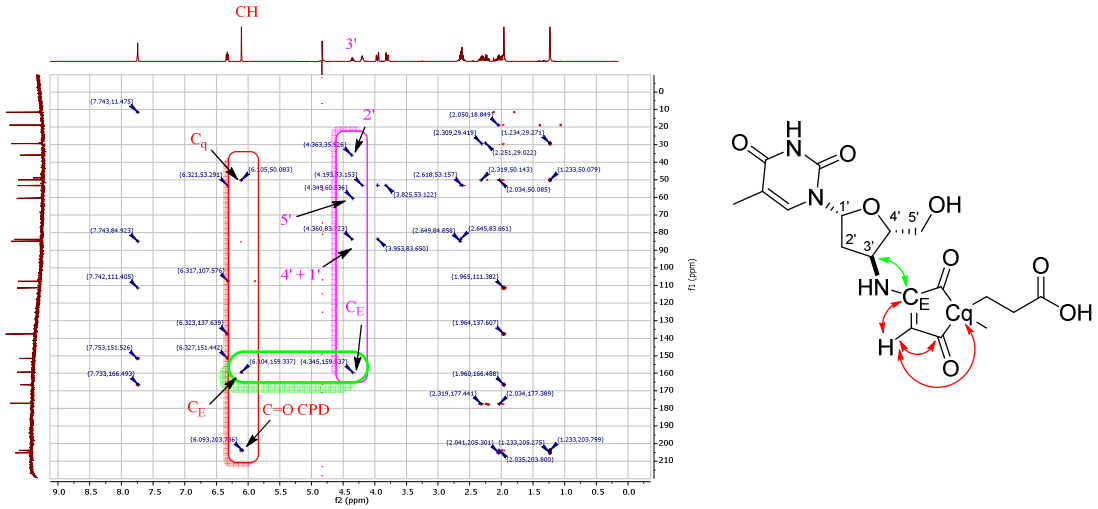

Figura R.C.6 Correlacions clau observades a l'espectre de HMBC de l'adducte bicíclic (esquerra) i estructura proposada (dreta).

A continuació es va procedir a realitzar estudies de dobles conjugacions amb una altre reacció de bioconjugació. En aquest cas es va decidir utilitzar la reacció de formació d'oximes per tal d'aprofitar el carbonil restant de l'adducte M-20 i utilitzar-lo en una subseqüent reacció amb una alkoxiamina tal com s'indica a l'**Esquema R.C.5**.

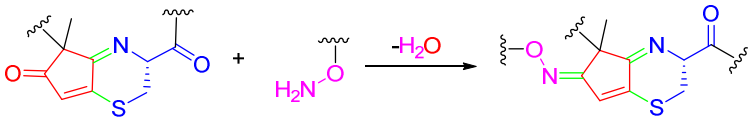

Esquema R.C.5 Primer concepte de dobles conjugacions utilitzant les reaccions de CPD-Cys i la formació d'oximes.

Primerament, es va observar amb molècules models que l'adducte M-20 no reaccionava amb clorhidrat d'hidroxilamina en cap de les condicions testades, donant indicacions que aquest grup carbonil no era suficientment electròfil. Tot i això, a continuació es va testar si la CPD podia formar oximes i es va arribar a la conclusió que, efectivament, si es podia donar la formació d'oximes per ambdós carbonils de la CPD.

Observada aquestes dues reactivitats d'ambdós molècules es va procedir a sintetitzar pèptids contenint la CPD o cisteïna en la posició *N*-terminal i la funció alkoxiamina incorporada a la cadena lateral d'una lisina utilitzant procediments estàndards de fase sòlida de pèptids sense cap problemàtica.

Respecte al pèptid contenint la CPD i la alkoxiamina, es va observar com dos contratemps. En primer lloc, el grup alkoxiamina reaccionava amb traces d'acetaldehid en l'acetonitril emprat per a l'anàlisi i purificació dels pèptids per HPLC tal com estava descrit a la literatura.[17] A més a més, també es va poder observar l'alkoxiamina i la CPD reaccionaven, tal com s'havia vist amb molècules model, per donar l'anàleg cíclic, tot i que no amb gaire èxit degut a al fet que s'obtenien crus complexes.

D'altra banda, quan es va utilitzar el pèptid amb la cisteïna *N*-terminal, es va observar la mateixa problemàtica de l'acetaldehid. Tot i això, va poder utilitzar aquest pèptid per tal de fer primer una conjugació amb vanil·lina (sense purificar el cru original) i, després de la formació d'oxima procedir a general l'adducte M-20 per tal d'obtenir el doble conjugat, tal com s'indica a l'**Esquema R.C.6**.

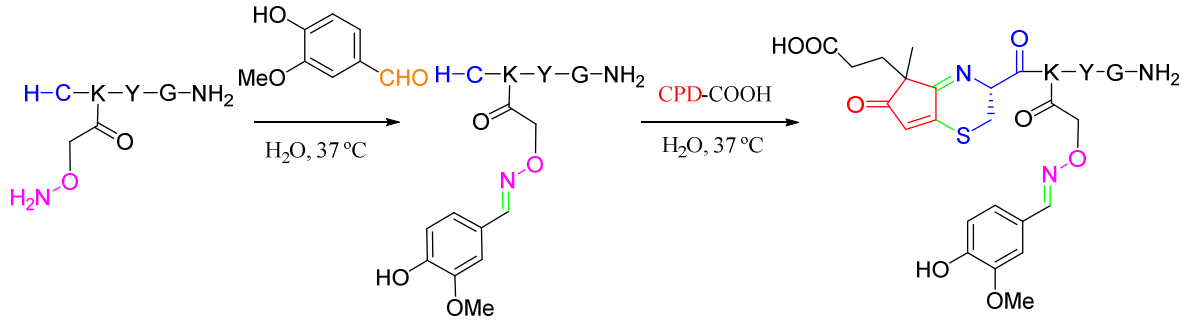

Esquema R.C.6 Ús de les reaccions de formació d'oxima i CPD-Cys per a la producció de dobles conjugats de pèptids.

Donada la importància dels pèptids cíclics així com l'interès en trobar metodologies que permetin ciclar i derivatitzar pèptids en una sola etapa, el Dr. Brun duran la seva tesi doctoral, va posar apunt una metodologia per a la conjugació i ciclació utilitzant les CPDs, en un sol pas, en pèptids que contenien dues cisteïnes una d'elles en la posició *N*-terminal.

En el nostre cas, com a continuació d'aquests estudis, ens vàrem proposar explorar la possibilitat de derivatitzar i ciclar oligonucleòtids contenint una cisteïna en la posició 5', tal com s'ha explicat anteriorment, i un tiol lliure en la posició 3', fàcilment obtenible degut al fet que la resina necessària és comercial. Així doncs, amb aquest objectiu en ment vam emprar un fosforamidit de cisteïna semblant als anteriorment usat per a la derivatització de la posició 5' d'oligonucleòtids. En aquest cas, però en comptes de l'enantiòmer natural "L" es va emprar el "D" degut a observacions experimentals d'epimerització pel Dr. Brun.

Seguint la metodologia anterior comentada i fent ús de la resina adequada es va obtenir un oligonucleòtid model derivatitzat en la posició 5' amb una cisteïna i en la posició 3' un tiol. Tot seguit, es va fer reaccionar amb una CPD en les condicions de ciclació i es va observar s'obtenia un oligonucleòtid cíclic tal com es representa a l'**Esquema R.C.7**.

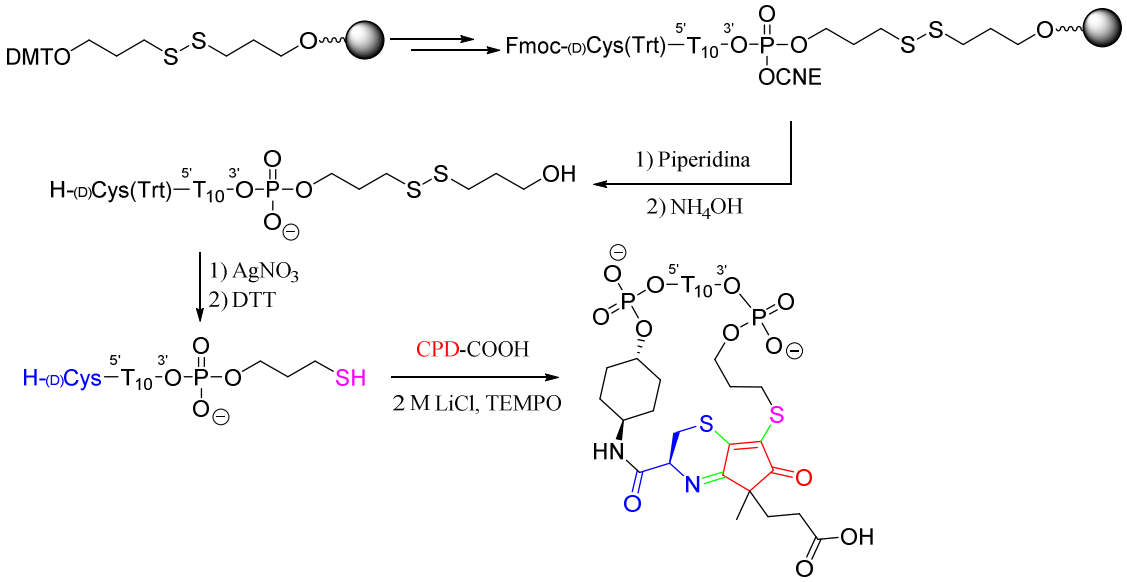

Esquema R.C.7 Pla per a la obtenció d'oligonucleòtids cíclics per mitjà de una reacció de CPD-Cys en oligonucleòtids incorporant un tiol en 3' i una cisteïna en 5'.

Tot i això, aquest resultat només es va obtenir un cop i no es va poder reproduir en cap dels subseqüents experiments que es van dur a terme. Concloent, doncs, en la infectivitat del sistema per ciclar i derivatitzar oligonucleòtids.

R.C.3 Conjugats de Retro-1 i oligonucleòtids

Un dels processos cel·lulars en qualsevol organisme viu es el dogma central de la biologia. Més específicament, postula que, amb l'excepció dels retrovirus, el flux d'informació és del DNA cap al RNA i, finalment, a les proteïnes mitjançant dues etapes seqüencials nombrades transcripció i traducció, respectivament.[18] La transcripció és el procés pel qual la informació en una copia de DNA és copiada en una nova molècula de RNA que és immediatament processada en RNA missatger (mRNA). L'objectiu del DNA és l'emmagatzematge de la informació genètica al nucli cel·lular, comparable a una plantilla. D'altre banda, el mRNA és pot comparar a una copia d'un llibre de referència perquè conté la mateixa informació però pot sortir lliurement del nucli.

En contrast, la traducció és el procés pel qual es sintetitza una proteïna a partir de la informació continguda dins mRNA. Durant la translació es llegeix una molècula de mRNA utilitzant un conjunt de normes que defineixen com un mRNA es traduirà en els 20 aminoàcids proteïnògens naturals. La traducció es duu a terme als ribosomes, llegint una combinació de tres oligonucleòtids alhora anomenada codó. Inicialment, es creia que la seqüència codificant era contigua, es a dir, el codó per un aminoàcid es situava immediatament adjacent al codó per el següent aminoàcid expressat a la proteïna final. Aquest fet és cert per la gran majoria de bactèries i els seus fags, però rarament és el cas per eucariotes.

Molts eucariòtic gens són doncs, arranjaments de tipus mosaic que consisteixen en seqüències codificants, exons, separades per blocs que no productius, anomenats introns. Un dels processos que converteix el pre-mRNA en mRNA madur s'anomena empalmament i ha de produir-se amb molta precisió per tal d'evitar l'addició, pèrdua o substitució fins i tot d'un sol oligonucleòtid. Falta de precisió en l'empalmament podria produir errors en la lectura d'exons i, aleshores, els codons serien seleccionats erròniament i, per tant, aminoàcids diferents serien incorporats a la proteïna final.

Tractar malalties controlant el flux d'informació genètica segueix sent un problema. Tot i que la teràpia genètica es pot emprar per substituir gens mutats, no és lliure de problemes (el nou DNA ha d'arribar al cromosoma precisament, inserit i expressat correctament). En aquest context, l'ús d'oligonucleòtids com a medicina consisteix en una alternativa atractiva a la teràpia genètica. Entre els diverses teràpies basades en oligonucleòtids diverses s'han establert com les preferides. Els siRNAs (per l'anglès *small interfering RNAs*),[19] els oligonucleòtids antisentit (ASOs)[20] i aptamers.[21]

Tot i això, en totes aquestes categories d'oligonucleòtids aptes per a ser usats com a medicament, una problemàtica clau existeix encara: la pobre internalització d'aquests compostos altament polars per la membrana cel·lular. Per tal d'intentar alleujar o eliminar aquest problema, s'han plantejat alternatives que es basen en la modificació química de l'esquelet d'aquestes molècules o la bioconjugació amb molècules capaces de travessar amb facilitat aquesta barrera per tal de promoure internalització.

Dins aquest ventall de possibilitats fa uns anys es va descriure un conjunt de molècules anomenat "Retro" que afectava profunda i selectivament el tràfic intracel·lular. Específicament es va descriure dos compostos nombrats "Retro-1" i "Retro-2" (**Figura R.C.7**).

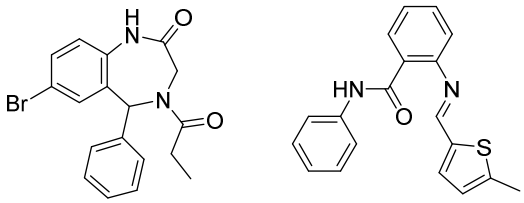

Figura R.C.7 Estructures químiques de les molècules Retro-1 i Retro-2 respectivament.

En un estudi posterior, el Prof. R. L. Juliano i col·laboradors van decidir investigar els compostos Retro com a possibles beneficiaris del tràfic intracel·lular d'oligonucleòtids per tal de potenciar el seu efecte farmacològic. En aquest estudi es va poder observar que quantitats creixents de Retro-1 progressivament potenciaven l'afecte d'un oligonucleòtid antisentit a un reportador de luciferasa transfectat a cèl·lules HeLa.

Així doncs, veien aquests resultats experimentals ens vam plantejar si el fet d'unir covalentment la molècula de Retro-1 a l'oligonucleòtid en qüestió podria tenir un afecte beneficiós per a l'afecte farmacològic observat. Per tal objectiu ens vam decidir derivatitzar la molècula de Retro-1 per dues posicions diferents, el metilè en posició α al carbonil dins l'anell de 7 baules i per el grup propanoil.

Amb aquest objectiu en ment, doncs, primer de tot vam reproduir la síntesi de la Retro-1 descrita a la literatura[22] satisfactòriament emprant un esquema sintètic de 5 passos amb un 36% de rendiment global, tal com es mostra a l'**Esquema R.C.8**.

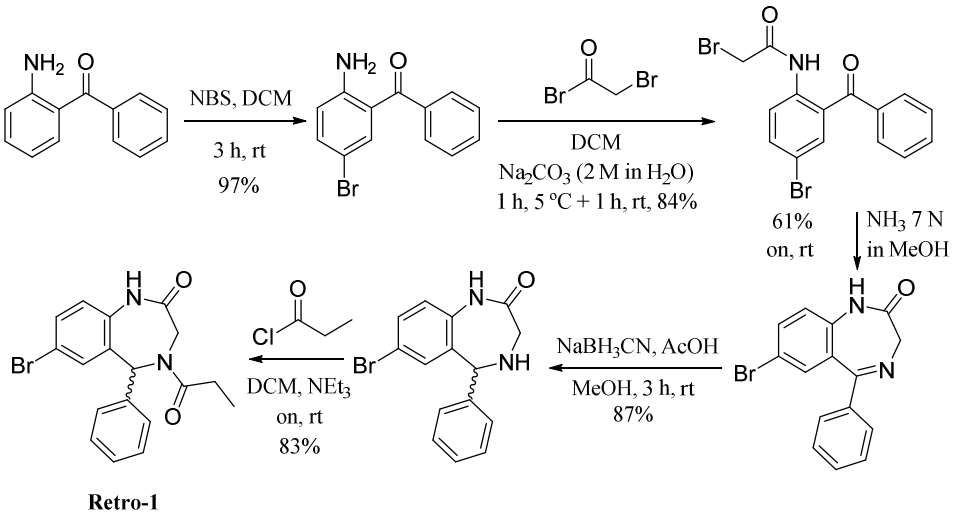

Esquema R.C.8 Esquema sintètic seguit per l'obtenció de la molècula Retro-1 descrit per Abdelkafi *et al.*[22]

A continuació, es va procedir a sintetitzar derivats que continguessin un grup hidroxil per tal de poder fosfitilar-lo. Es va utilitzar com a material de partida el precursor de la Retro-1 contenint una amina secundària incorporat a l'anell de 7 baules i es va fer reaccionar, en primera instància, amb lactones per tal d'obtenir la hidroxilamida en un sol pas de reacció tal com s'indica a l'**Esquema R.C.9**.

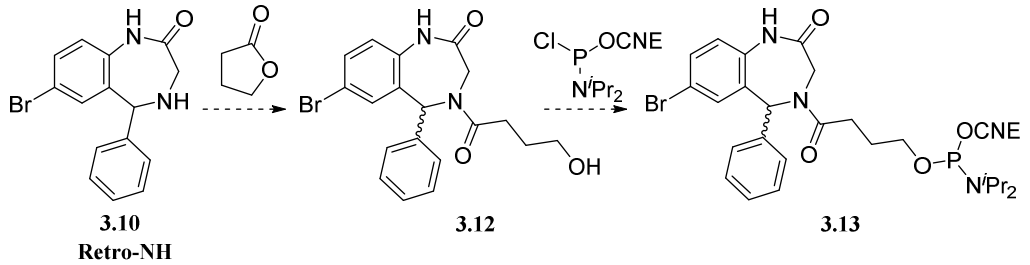

Esquema R.C.9 Primera alternativa per al síntesi de *N*-acil Retro-1 fosforamidits *via* la obertura de lactones promoguda per amines.

Aquesta alternativa es va provar amb diferents lactones i diferents mètodes d'activació (àcids de Lewis, bases nucleofíliques) obtenint sempre productes de partida. Seguidament, es va derivatitzar amb un funció carboxílica i es van intentar diverses opcions. Tant la reducció selectiva de l'àcid carboxílic com la formació d'amides amb diverses aminoalcohols foren en tots els casos infructuoses recuperant o bé curs complexes o productes de partida.

Tot i això, vista aquestes dificultats, vam optar per utilitzar una addició de Michael amb un derivat acrílic i una hidroxilamina com a pas clau per tal d'obtenir el grup alcohol desitjat que, subseqüentment, va ser fosfitilat satisfactòriament tal com es mostra a l'**Esquema R.C.10**.

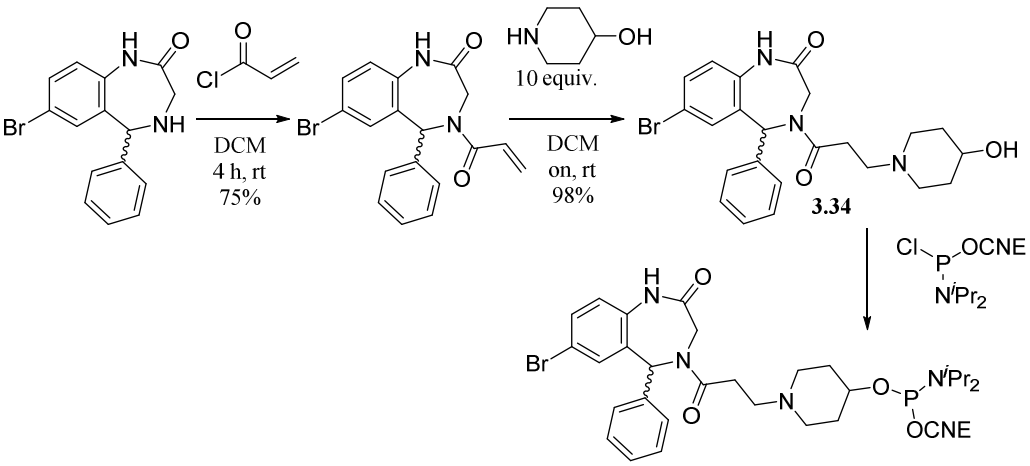

Esquema R.C.10 Pla sintètic per a l'obtenció d'un derivat de Retro-1 incorporant un grup hidroxil i posterior fosfitilació.

Un cop es va aconseguir el fosforamidit, es va utilitzar la mateixa metodologia per aconseguir, a través d'una addició de Michael al derivat acrílic amb *S*-tritil cisteamina i, el tiol corresponent després de la desprotecció del tritil.

D'altra banda, ens vam proposar sintetitzar altres derivats de Retro-1 amb grups tiols i diè per altres punts d'unió a l'oligonucleòtid, com s'ha comentat abans. En aquest cas, l'esquema sintètic es semblant a l'emprat per a la síntesi de la Retro-1, però en comptes d'acilar l'anilina amb bromur de bromo acetil, en aquesta instància empràvem un derivat de lisina, protegida amb els grup Fmoc i Boc, tal com s'indica a l'**Esquema R.C.11**.

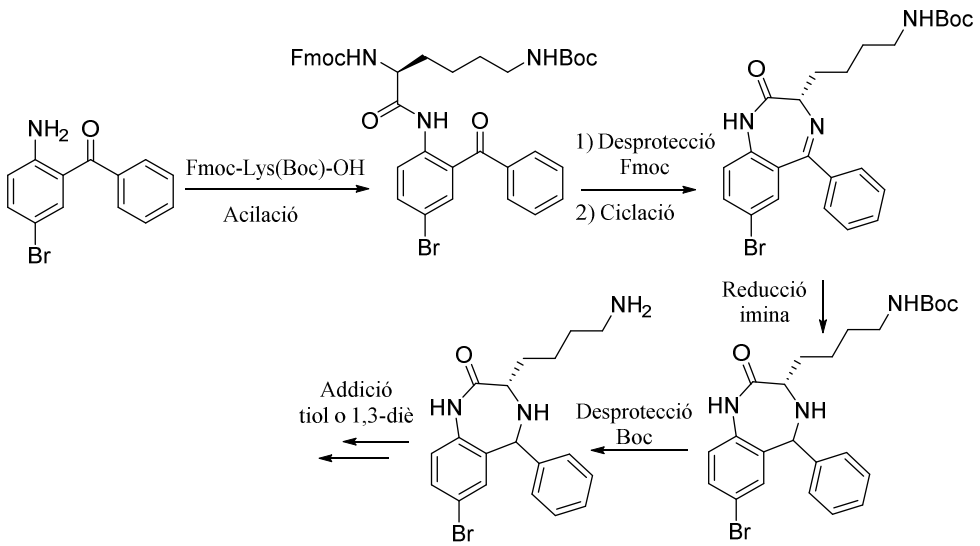

Esquema R.C.11 Ruta sintètica per a la obtenció de derivats Retro-1 incorporant un grup tiol o 1,3-diè.

Un cop es va obtenir tots els derivats de Retro-1 es va procedir a sintetitzar oligonucleòtids. Es van sintetitzar oligonucleòtids (amb la seqüència 623 i *scrambled*) i se'ls va incorporar el fosforamidit de Retro-1 o el de la maleimida 1,4-dimetilfura protegida exitosament.

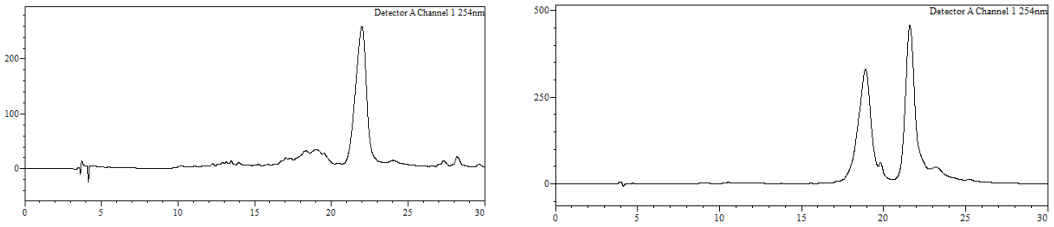

Cru Retro-1-623

Cru Retro-1-*scrambled (*1r es oligonucleòtid sense derivatitzar)

Figura R.C.8 Crus de conjugat dels oligonucleòtids Retro-1-623 (esquerra) i Retro-1-*scrambled* (dreta)

A més a més, amb els derivats contenint maleimida protegida es va poder sintetitzar (tant del 623 com de l'*scrambled*, en solució i mitjançant una reacció de *retro*-Diels-Alder (de 1,4-dimetilfurà per desprotegit la maleimida de l'oligonucleòtid). Tot seguit una cicloaddició de Diels-Alder amb el derivat contenint el diè o una addició tipus Michael amb el derivat de Retro-1 contenint el tiol donaria els conjugats objectiu.

Amb tots aquestes molècules es van dur a terme assajos biològics al laboratori del Prof. Rudolph L. Juliano. Per aquests experiments es va utilitzar dos línies cel·lulars, la HeLa Luc 705 i cèl·lules traqueals de ratolí modificades amb EGFP654. L'experiment es basava en l'observació de fluorescència degut a la correcció de l'expressió en l'empalmament d'una seqüència genòmica cel·lular per expressar una Luciferasa o proteïna verda fluorescent, respectivament.

En aquests es va comprovar per una banda que, en la línia cel·lular HeLa, els conjugats de Retro-1-623 obtinguts no mostraven una millora respecte la coadministració de la molècula de Retro-1 i

l'oligonucleòtid nu, obtenint nivells de fluorescència iguals o lleugerament inferiors als obtinguts en estudis previs. D'altra banda, quan es van emprar cèl·lules traqueals de ratolí, una millora substancial es va poder observar tal com es mostra a la figura

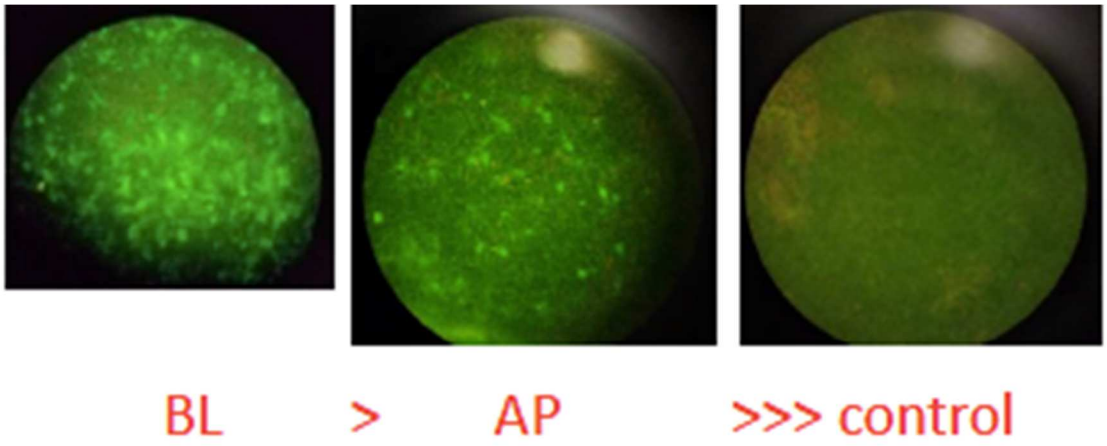

Figura R.C.9 Efecte del conjugat Retro-1-623 en la inducció de la EGFP654 en cèl·lules traqueals de ratolí. La imatge mostra expressió de la EGFP als 7 dies per administració basolateral (esquerra), apical (centre) i el control 623 nu.

R.C.4 Oxanorbornens com dienòfil en la reacció de Diels-Alder de demanda electrònica inversa amb 1,2,4,5-tetrazines

La cicloaddició de Diels-Alder de demanda electrònica inversa (IEDDA) és una de les reaccions de bioconjugació més utilitzades en la actualitat. La seva utilitat es basa en uns punts claus, més específicament, la cinètica extremadament ràpida (fins a 2000 M s^{-1}), gran quimioselectivitat, i compatibilitat amb medi aquós.

La reacció de IEDDA és formalment una cicloaddició de Diels-Alder [4+2] entre un diè, en general una tetrazina, i un dienòfil, normalment un alquè, per formar un anell de sis baules. La diferència clau respecte la reacció estàndard de Diels-Alder és la necessitat del diè a ser electrònicament empobrit i el dienòfil, enriquit.

Degut al fet que la gran majoria de reaccions IEDDA emprades per bioconjugació utilitzen les tetrazines com a diè, ens vam focalitzar en l'altre reactiu, el dienòfil. En aquest cas, a la literatura hi ha descrites varis dienòfils, essent els més populars els norbornens, els ciclopropens i els *trans*-ciclooctens (**Figura R.C.10**)

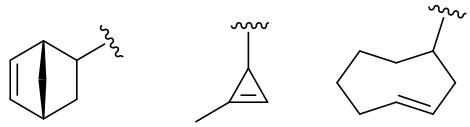

Figura R.C.10 Estructura química del norborne (esquerra), metilciclopropè (centre) i *trans*-ciclopropè (dreta).

Tot i que aquest tres dienòfils són els més emprats, pateixen de dos problemes fonamentals. En primer lloc, són difícils d'aconseguir sintèticament (especialment el ciclopropè i el *trans*-ciclooctè). El segon és el fet que, un cop es dona la reacció de bioconjugació amb la tetrazine, es forma un nombre elevat de isòmers finals (fins a un total de 8) degut a la naturalesa asimètrica dels compostos.

Degut a aquestes problemàtiques en vam plantejar la cerca d'altres dienòfils que fossin suficientment reactius i alleugessin el problema de la generació elevada d'isòmers finals. Per aquest objectiu ens vam plantejar utilitzar un anàleg de norbornè, l'oxanorbornè (PMal[H_2]) per a reaccions de IEDDA.

En estudis previs al grup de recerca s'havia observat com 1,4-dimetil-7-oxanorbornens no reaccionaven amb 1,2,3,4-tetrazines (Tz) a temperatura ambient. Aquest resultat es va racionalitzar amb l'efecte estèric proporcionat per els dos metils addicionals, reduint dràsticament les constant de reacció i, per tant, Tot i això, quan es va incubar un 7-oxanorbornè que contenia un carboxil (PMal[H_2]-COOH) d'altres estudies anteriors del grup, amb una tetrazine electrònicament menys idònia (amb metil i fenil com a substituents), observant completa conversió als productes desitjats en una nit en agitació a tempera ambient (**Figura R.C.11**).

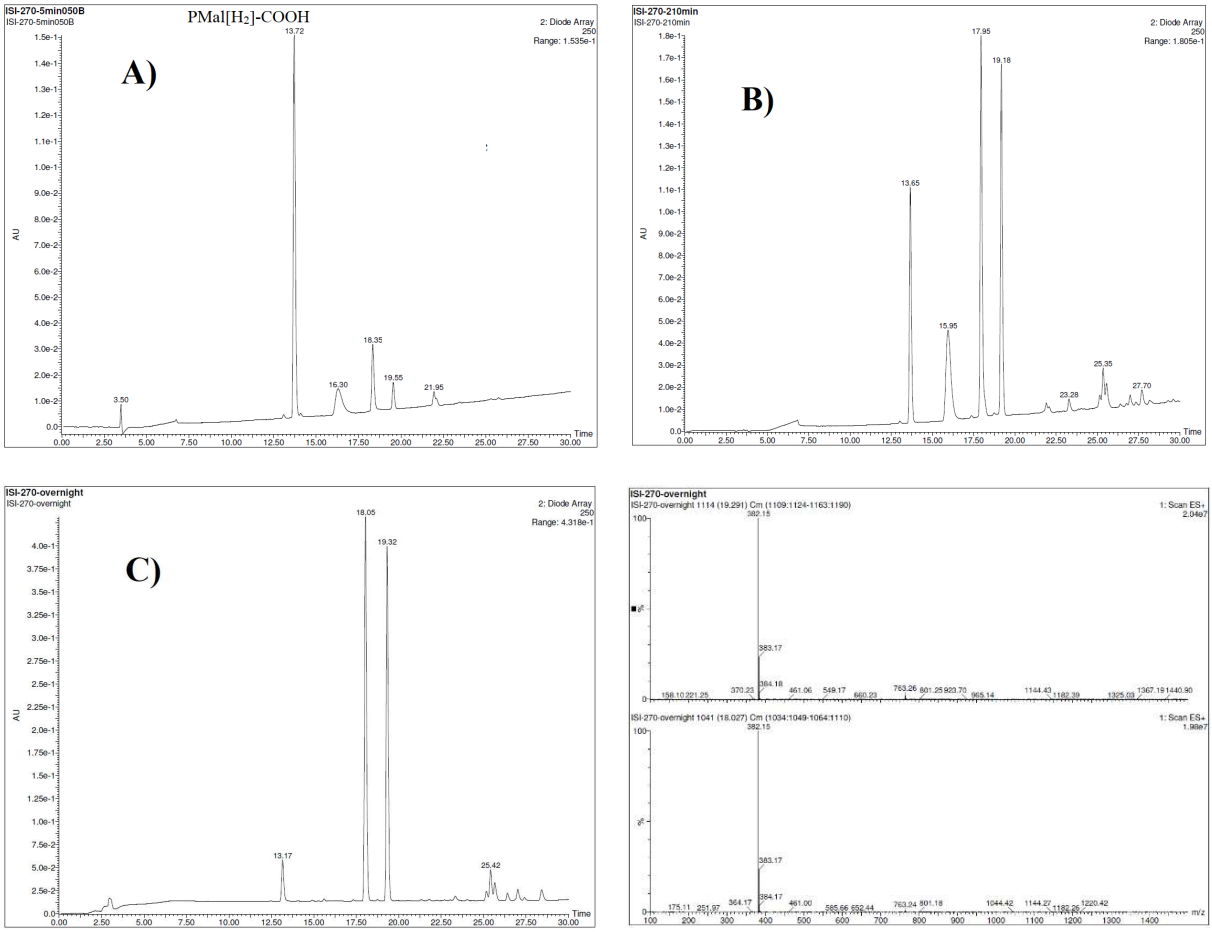

Figura R.C.11 Cromatogrames (250 nm) de la reacció entre PMal[H_2]-COOH i fenil-metil-Tz

Veient aquest resultat positiu, vam sintetitzar anàlegs contenint un fosforamidit i carboxil seguint procediments experimentals descrits a la literatura.[23,24] En ambdós casos, l'etapa clau es una reacció de Diels-Alder entre un dienòfil (anhídrid maleic o maleimida) i el fura per tal d'obtenir l'esquelet d'oxanorborne tal com s'indica a l'esquema

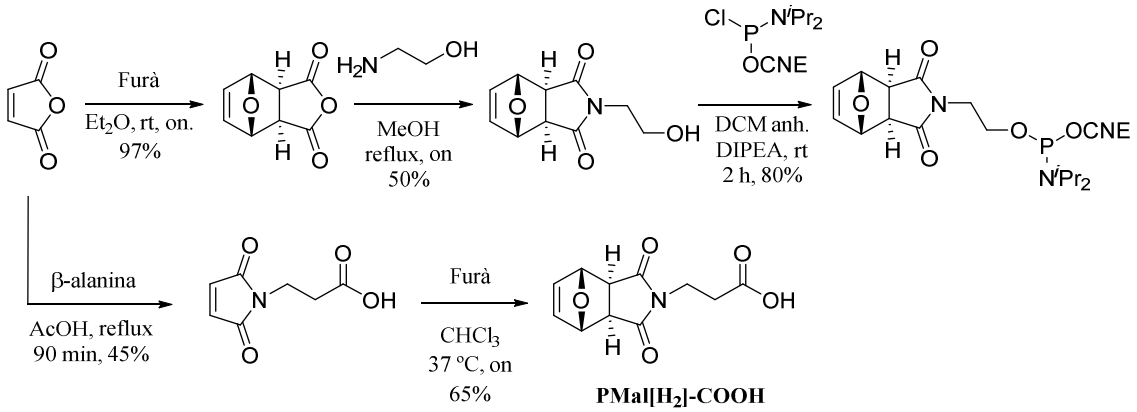

Esquema R.C.12 Pla per la síntesi de derivats d'oxanorbornè contenint els grups carboxil o fosforamidit.

Tot seguit, es van emprar ambdós derivats per incorporar-los a la posició 5' o *N*-terminal d'oligonucleòtids o poliamides (pèptids i PNAs), respectivament utilitzant metodologies estàndard de fase sòlida.

Respecte als oligonucleòtids se'n van sintetitzar dos, un amb 10 timidines (dT_{10}) i un altre contenint tots els nucleòsids ($d^{5'}$CATGTATTCGCATCATCAGT$^{3'}$, 20mer) satisfactòriament tal com s'observen als crus de síntesi representats a la **Figura R.C.12**.

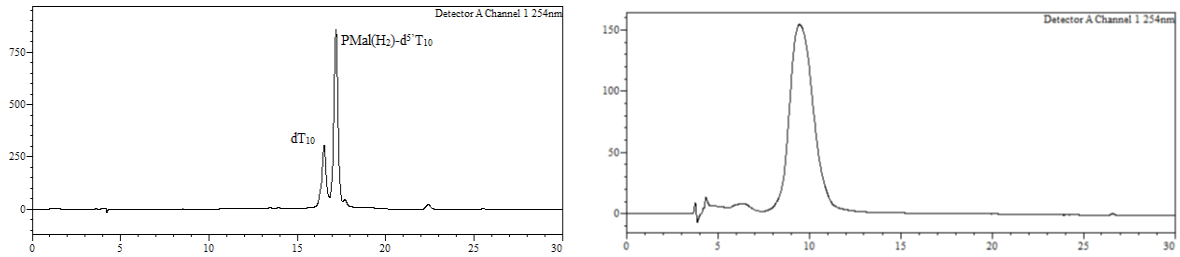

Cru PMal[H_2]-dT_{10} Cru PMal[H_2]-20mer

Figura R.C.12 Cromatogrames (254 nm) dels crus de síntesi d'oligonucleòtids contenint el grup oxanorbornè en la posició 5'.

Un cop es van aconseguir els dienòfils corresponents, es va procedir a preparar diferents tetrazines per tal de tenir un ventall més ampli amb el qual produir conjugats.

En primera instància es ver una cerca de condicions de síntesi de tetrazines, concloent amb el mètode clàssic d'ús de nitrils arílics o alquílics. Emprant aquestes condicions es van confeccionar dos tetrazines diferents, una amb un grup amina i metil, i la segona amb un àcid carboxílic i 2-pirimidil tal com es mostra a la **Figura R.C.13**.

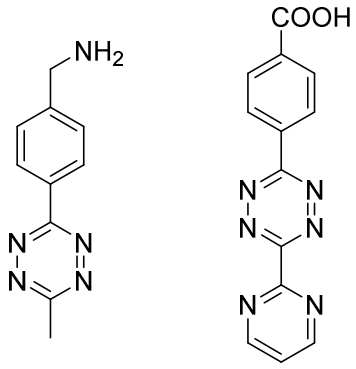

Figura R.C.13 Estructures químiques de les dues tetrazines emprades per a la síntesi de marques útils en reacció de conjugació IEDDA.

Un cop es van obtenir aquestes dues tetrazines intermèdies es van derivatitzar diverses molècules d'interès biològic. Per aquest objectiu es va triar, la D-*N*-acetilgalactosamina (GalNAc) i el fluoròfor BODIPY la biotina. Breument, es van seleccionar aquestes tres molècules per les següents raons. En primer lloc, es conegut que la GalNAc és un lligant extremadament eficient del receptor expressat en asialoglicoproteines expressat en hepatòcits i facilitador de la internalització cel·lular. Sintèticament es va procedir amb química descrita prèviament amb petites modificacions (**Esquema R.C.13**).[25]

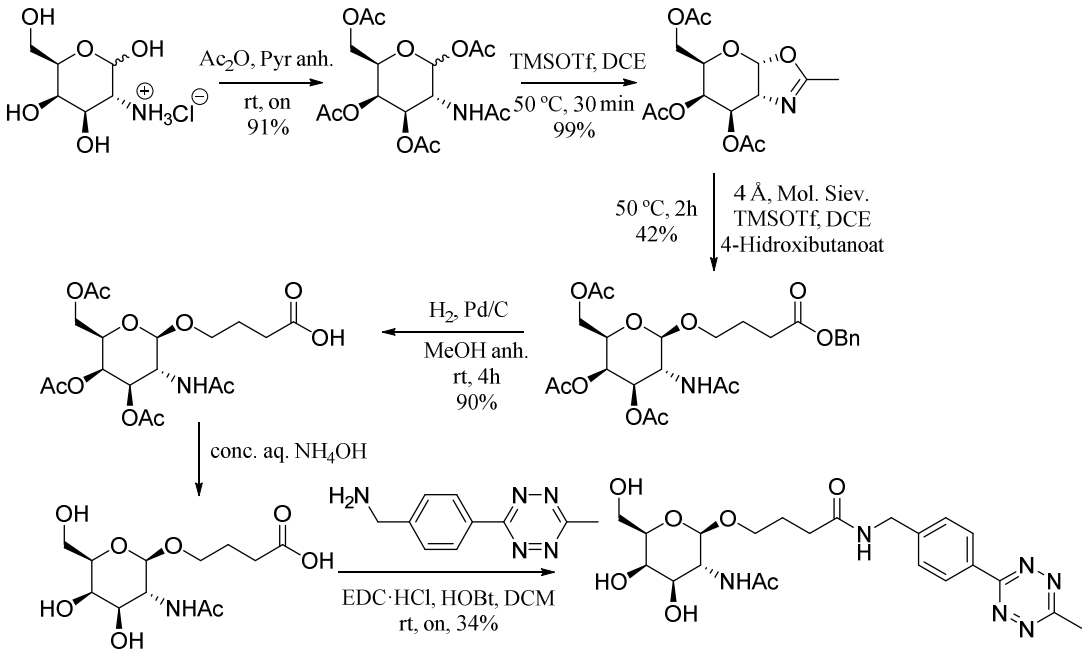

Esquema R.C.13 Pla sintètic per la obtenció d'un derivat de GalNAc incorporant una tetrazina.

El 4,4-difluoro-4-bora-3a,4a-diaza-*s*-indacè (BODIPY) és un tint que absorbeix fortament el rang UV i emet pics de fluorescència relativament aguts amb grans rendiments quàntics. Els anàlegs de BODIPY son relativament insensibles a canvis de pH, polaritat i la seva estabilitat en medis fisiològics és raonablement adequada. Per aconseguir el derivat de BODIPY adient, es van seguir procediments descrits a la literatura.[26] Tal com s'indica a l'**Esquema R.C.14**, utilitzant 2 equivalents del corresponent pirrole i un clorur d'àcid, s'obté el corresponent esquelet de BODIPY que, després de transformar-lo, es pot reaccionar amb una tetrazina.

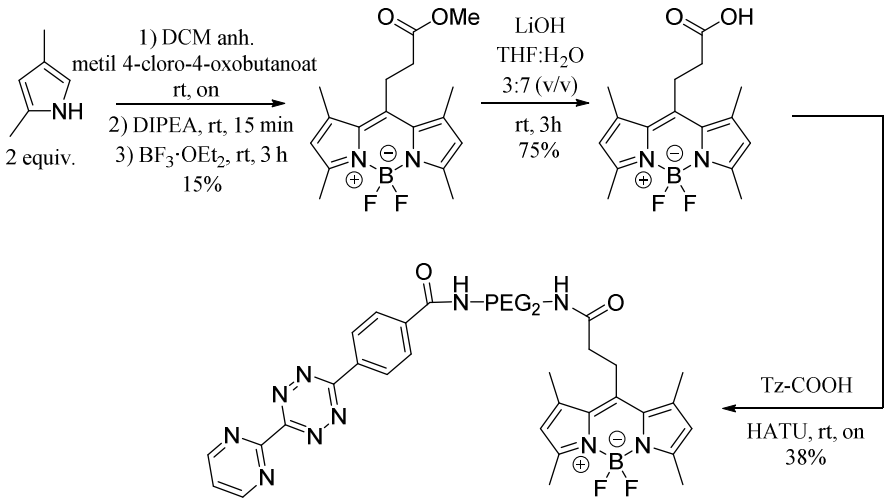

Esquema R.C.14 Síntesi d'un anàleg de BODIPY que conté una tetrazina apta per conjugacions.

Finalment, es va sintetitzar un derivat de tetrazine amb la biotina. La biotina és biològicament rellevant per la seva forta interacció amb streptavidina/avidina facilitant enormement purificació de compostos biotinilats.

En aquest cas, degut al fet que la D-biotina natural ja conté un grup carboxil apte per a realitzar-hi una amida, no es va haver de fer cap transformació addicional. La tetrazine contenint una amina es va reaccionar directament amb la biotina tal com s'indica a l'**Esquema R.C.15**.

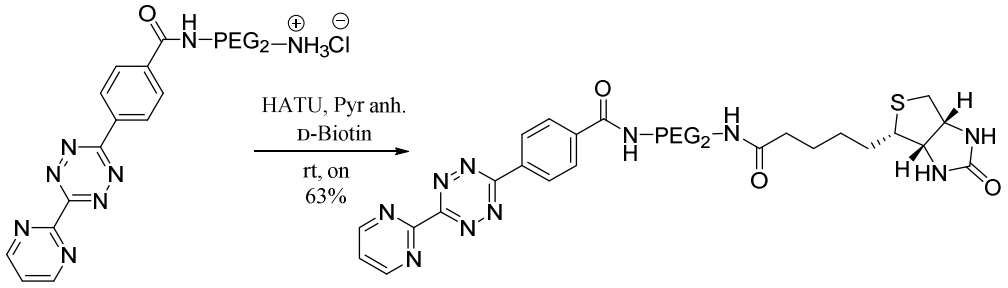

Esquema R.C.15 Síntesi de una tetrazine derivatitzada amb biotina.

Finalment, es va derivatitzar també un pèptid en posició *N*-terminal amb una tetrazine contenint un grup carboxil per metodologies en fase sòlida optimitzades i mostrades a l'**Esquema R.C.16**. Resumidament, aquestes optimitzacions van ser necessàries per la poca solubilitat de la tetrazine en qüestió.

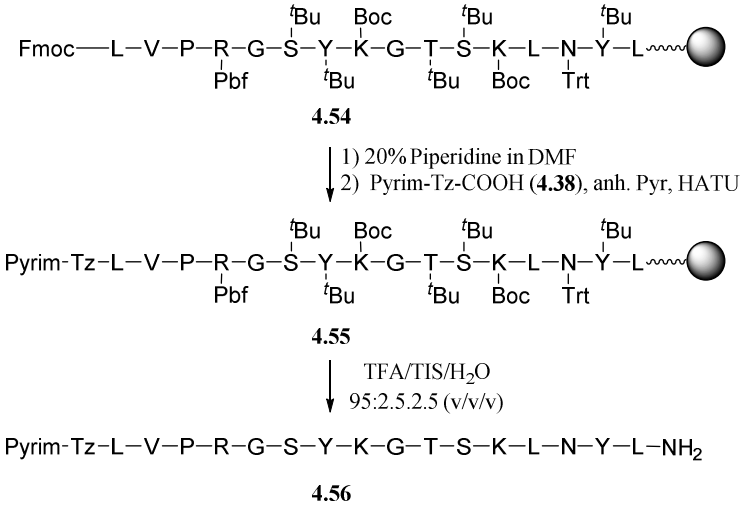

Esquema R.C.16 Pla per la preparació d'un pèptid derivatitzat a la posició *N*-terminal amb una tetrazina.

Un cop es va obtenir tots els reactius, tant biomolècules derivatitzades amb oxanorbornè com molècules petites amb tetrazines, es va procedir a realitzar conjugats simples emprant combinacions dels oligonucleòtids i poliamides (pèptids o PNAs) amb les diverses tetrazines tal com s'indica a continuació a l'**Esquema R.C.17** i una selecció de cromatogrames de crus de reacció (**Figura R.C.14**).

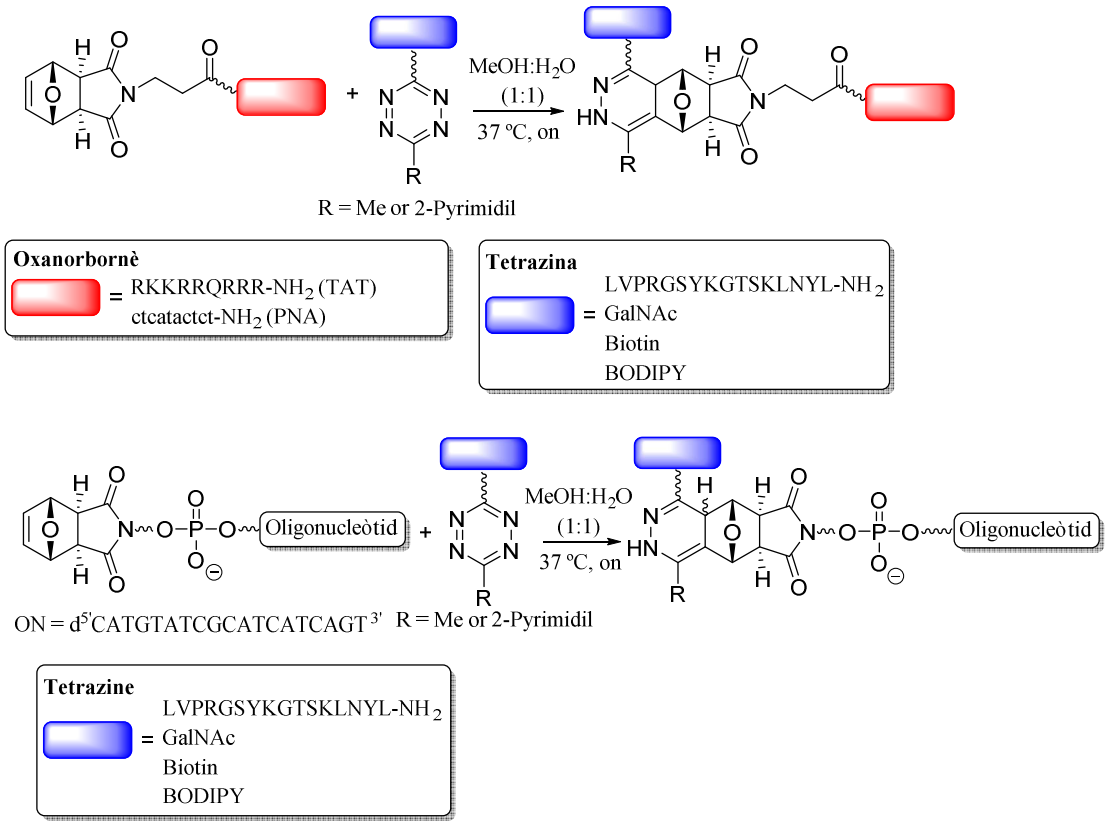

Esquema R.C.17 Conjugacions simples aconseguides utilitzant la cicloaddició IEDDA emprant poliamides (a dalt) o oligonucleòtids (a baix) derivatitzats amb 7-oxanorbornens com a dienòfils i tetrazines com a diè.

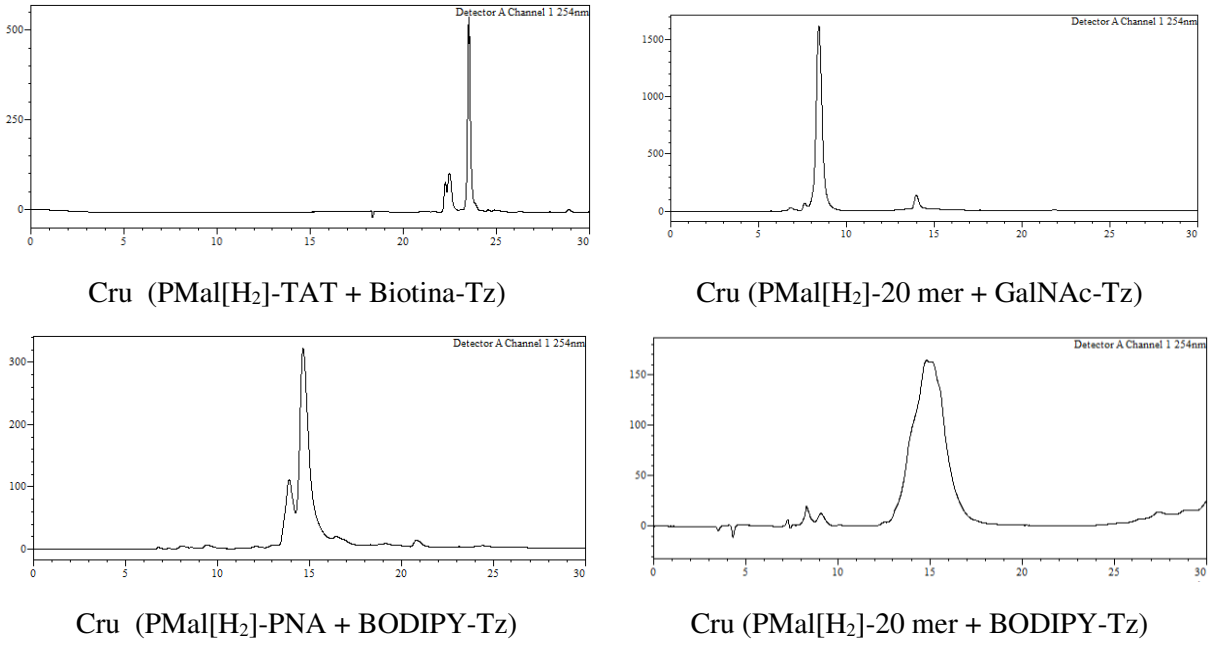

Cru (PMal[H_2]-TAT + Biotina-Tz)

Cru (PMal[H_2]-20 mer + GalNAc-Tz)

Cru (PMal[H_2]-PNA + BODIPY-Tz)

Cru (PMal[H_2]-20 mer + BODIPY-Tz)

Figura R.C.14 Crus de reacció de varies reaccions de conjugació entre poliamides i oligonucleòtids derivatitzats amb oxanorbornens i tetrazines.

Veient els bons resultats obtinguts en conjugacions simples, ens vam plantejar passar a fer dobles conjugats utilitzant, almenys, una reacció de cicloaddició IEDDA, tal com s'havia fet anteriorment amb les CPDs.

En primer lloc, es va intentar aprofitar la naturalesa no reactiva exhibida per part del derivat dimetílic en reaccions IEDDA. Per investigar aquesta possibilitat, es va sintetitzar primerament un derivat de lisina el qual contenia la 1,4-dimetil-7-oxanorbornè. Tot seguit, es fa sintetitzar un pèptid amb aquest derivat i amb l'oxanorbornè en la posició *N*-terminal tal com s'havia descrit anteriorment (**Figura R.C.15**).[27]

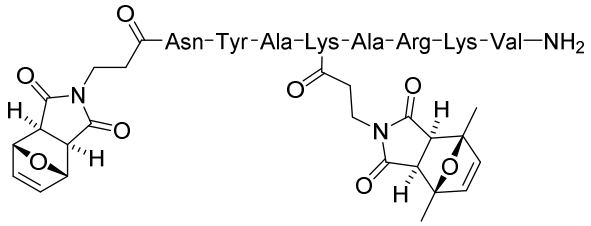

Figura R.C.15 Pèptid contenint un grup oxanorbornè en posició *N*-terminal i un 1,4-dimetil-7-oxanorbornè penjant d'una residu de lisina.

Tot seguit es van fer estudis de la eliminació de 2,5-dimetifurà (per tal d'obtenir la corresponent maleimida), sense afectar el furà el qual forma part de l'oxanorbornè. Aquest estudi va concloure que en cap de les condicions testades es va aconseguir suprimir la eliminació parcial del fura respecte el 2,5-dimetilfurà. Tot i això, es va procedir a realitzar experiments de dobles conjugacions combinant tetrazines i tiols o diens, respectivament. Una altre conclusió d'aquests estudis preliminars va ser la incompatibilitat dels diens d'estar en el mateix medi de reacció que les tetrazines, ja que reaccionen entre ells. Degut a aquestes problemàtiques, entre d'altres, es va concloure que aquest aproximació per a l'obtenció de dobles conjugats no era l'òptima.

Com un següent pas a aquesta opció, es va utilitzar un altre pèptid que contenia anàleg de lisina contenint l'oxanorbornè i una maleimida en posició *N*-terminal (**Figura R.C.16**).

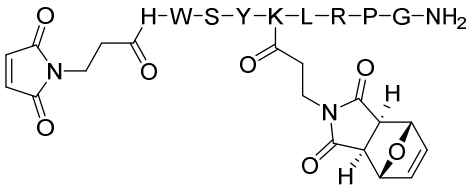

Amb aquest pèptid, en primer lloc es va comprovar que les tetrazines no reaccionaven amb maleimides. Seguidament, es va provar de fer la doble conjugació observant com el producte de doble conjugació s'aconseguia satisfactòriament. Tot i això, en aquest cas, es va procedir no de forma seqüencial sinó per passos. Primer es va reaccionar la maleimida amb un diè per donar l'adducte de Diels-Alder i, seguidament i després de purificar, es va reaccionar amb una tetrazine per donar el doble conjugat objectiu tal com es pot observar a la **Figura R.C.16**.

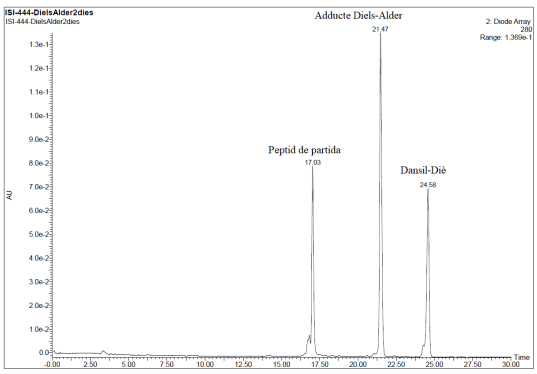

Cru de Diels-Alder (48 h, 280 nm)

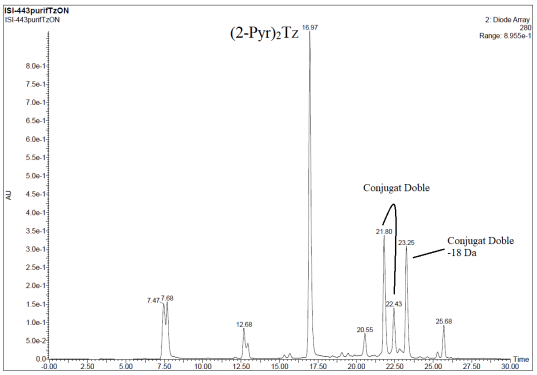

Cru reacció IEDDA (24 h, 280 nm)

Figura R.C.16 Cromatogrames (280 nm) dels crus de reacció entre el maleimido-pèptid i un anàleg de dansil que conté un 1,3-diè (esquerra) i l'adducte corresponent de Diels-Alder amb $(2\text{-Pyr})_2$Tz.

Veient els bons resultats obtinguts amb pèptids que contenien maleimides, ens vam decidir sintetitzar pèptids amb tiols en aquest casi. Per aquest raó vam sintetitzar tres pèptids diferents, un contenint una cisteïna en posició *N*-terminal i dos més amb cisteïnes internes tal com s'indica a la **Figura R.C.17**.

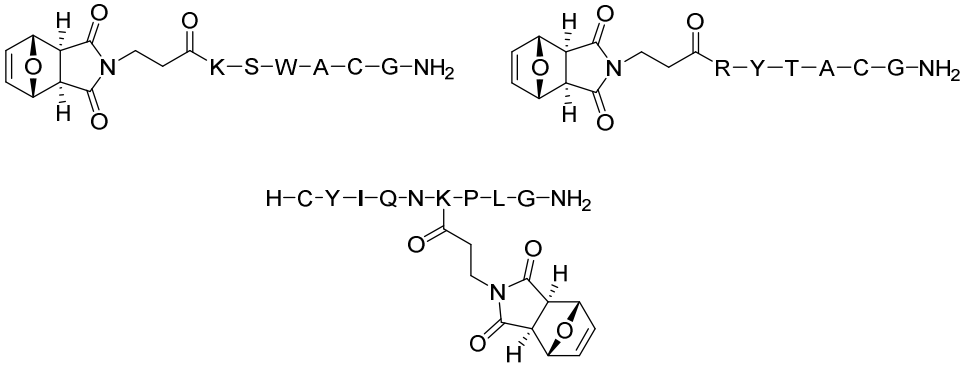

Figura R.C.17 Estructura química dels tres pèptids contenint un oxanorbornè I un tiol emprats en aquest treball.

Com que un dels objectius era explorar la possibilitat d'utilitzar la CPD o una maleimida en les dobles conjugacions (aprofitant el pèptid amb cisteïna *N*-terminal, per més informació mirar el primer capítol) s'havia de verificar que la CPD no reaccionava amb la tetrazina. Satisfactòriament, es va observar com no es donava cap tipus de reacció a les condicions de reacció IEDDA emprades fins al moment i es va procedir a fer les dobles conjugacions. Per a tal objectiu, es van incubar models, és a dir CPD-COOH i $(2\text{-Pyr})_2$Tz amb el pèptid contenint la cisteïna *N*-terminal i es va observar, deixant una nit a temperatura ambient sota agitació com es formava el doble conjugat esperat tal com s'indica a la **Figura R.C.18**.

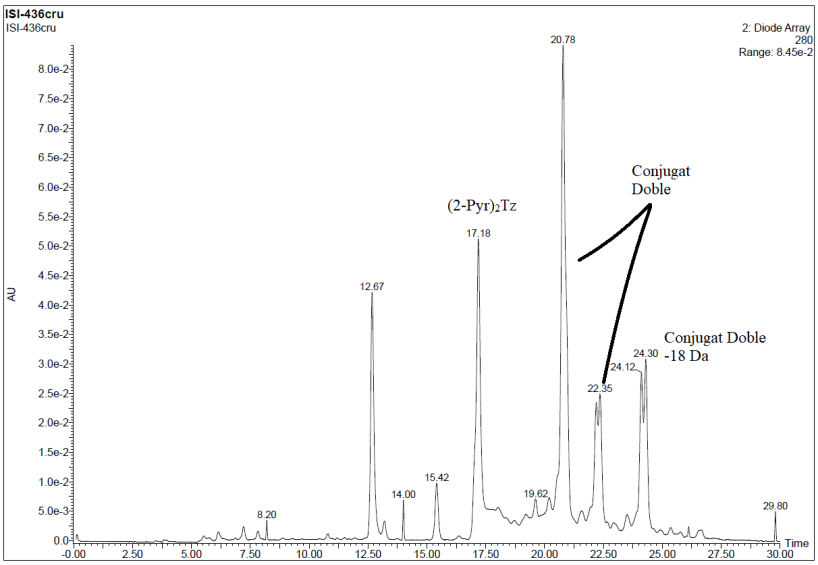

Figura R.C.17 Cromatograma (280 nm) del cru de doble conjugació utilitzant una reacció de CPD-Cys i una IEDDA.

Anàlogament, quan l'acceptor de Michael era una maleimida, en comptes d'una CPD, la reacció s'aconseguia amb resultats semblants, s'obtenien producte majoritaris desitjats i, minoritàriament, l'adducte -18 Da.

D'altra banda, mentre s'estaven realitzant aquests experiments es van veure a la literatura grups que utilitzaven 3,6-dicloro-1,2,4,5-tetrazines (Cl_2Tz) com agents de bioconjugació *via* dues successives substitucions nucleofíliques aromàtiques amb diversos nucleòfils com ara tiols, amines i alcohols. Aquesta química es va utilitzar per a general dobles conjugats de carbohidrat-pèptid i per el marcatge de proteïnes en condicions suaus, entre d'altres.[28,29]

Pel que fa el nostre cas, es va sintetitzar un derivat del fluoròfor dansil contenint el grup cloro-tetrazina (Cl-Tz-dansil) seguint l'**Esquema R.C.18** que es mostra a continuació.

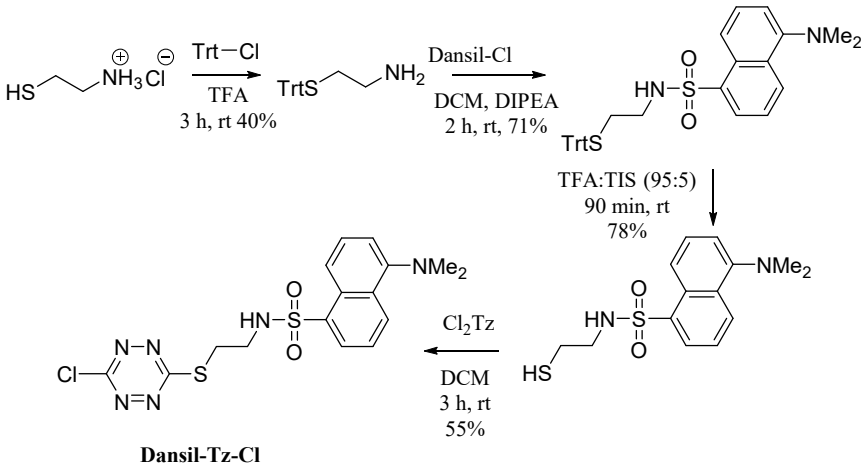

Esquema R.C.18 Síntesi d'un anàleg de dansil que conté una clorotetrazina.

Amb aquest anàleg es van fer probes de reactivitat amb els tres pèptids anteriors i es va poder observar com es donava una S_NAr extremadament ràpida en els tres casos. Tot i així, en el cas del pèptid amb la cisteïna *N*-terminal, s'observava un producte de segona addició, segurament causat per una migració del tiol *via* un intermedi de 5 baules per donar el tiol lliure i la aza-tetrazina (més estable) que,

subseqüentment podria tornar a reaccionar amb una altre clorotetrazina donant el producte observat de doble addició.

A més a més, es va traslladar aquesta química als oligonucleòtids emprant un fosforamidit comercial per tal d'introduir la funció tiol a l'extrem 5'. Després de la corresponen desprotecció, es va conjugar satisfactòriament al derivat de dansil, completant, així els conjugats simples amb cloroterazines.

Un altre punt important que es va observar durant aquest experiments amb chlorotetrazines es la seva baixa, o inexistent, reactivitat amb l'oxanorbornè que havíem estat utilitzant en altre conjugacions simples i dobles. El fe que la tetrazina ditiosubstituda fos inert a l'oxanorbornè suposava un avantatge perquè, d'aquesta manera, es podria utilitzar en tàndem amb una tetrazina "convencional" que havíem estat fent servir fins ara per obtenir dobles conjugats combinant les reacció de SNAr de la clorotetrazina amb un tiol i la IEDDA d'una aril o alquil tetrazine amb un oxanorbornè.

Basant-nos doncs en aquesta hipòtesi, vam incubar els pèptids amb el tiol intern que s'havien emprat per a conjugacions simples anteriorment amb una tetrazine i la dansil-Tz-Cl.

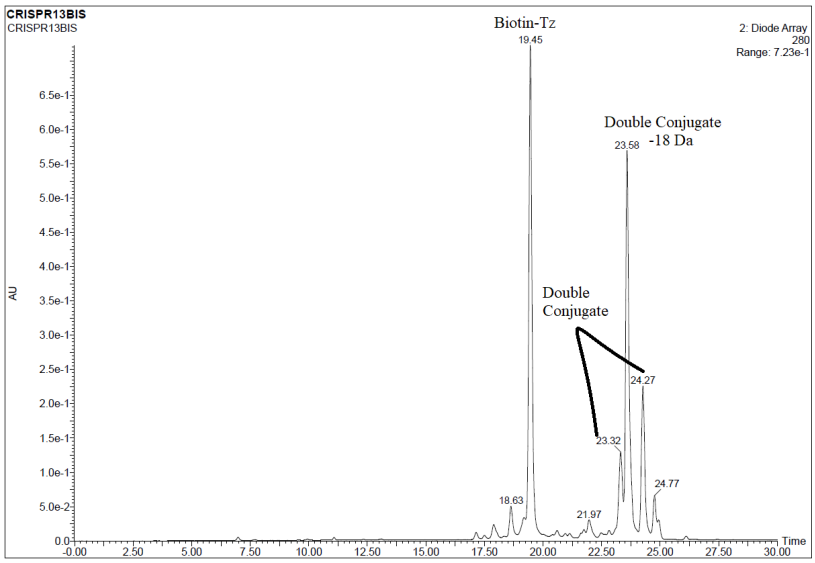

Figura R.C.18 Cromatograma (280 nm) del cru de reacció entre pèptid PMal[H_2]-KSWACG-NH_2, la biotina-tetrazina i la dansil-clorotetrazina.

Per tal d'aprofitar aquesta possibilitats en el camp d'oligonucleòtids, es va sintetitzar un anàleg de cisteïna contenint l'oxanorbornè, el tiol protegit amb tritil i el grup fosformadit per tal d'utilitzar química en fase sòlida tal com s'indica a l'**Esquema R.C.19**.

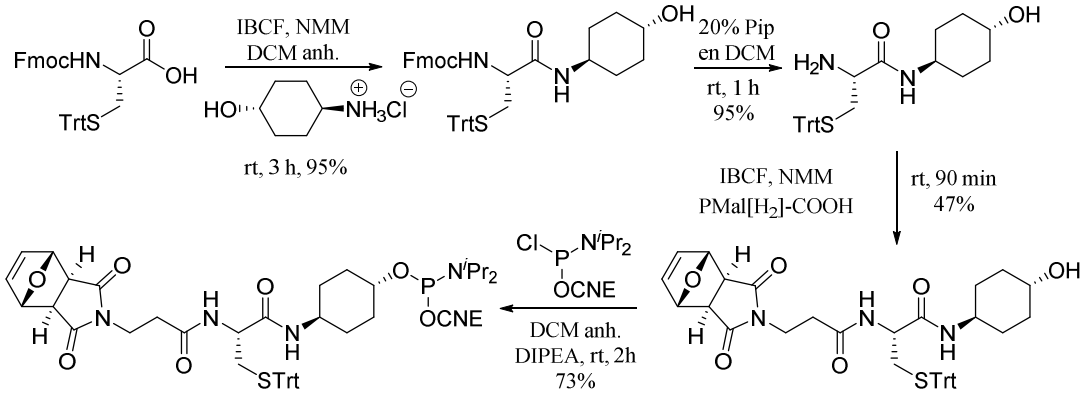

Esquema R.C. 19 Pla per a la preparació d'un anàleg de cisteïna que conté un oxanorbornè i el grup fosforamidit.

Amb aquest fosforamidit es fa sintetitzar un oligonucleòtid amb i es va acoblar a l'extrem 5' i, després de la desprotecció corresponent del tritil (amb Ag^+, tal com s'ha comentat al 1r capítol) s'ha aconseguit realitzar dobles conjugats de pèptids amb un pèptid derivatitzat amb una tetrazina i la anterior dansil-clorotetrazina satisfactòriament demostrant que aquesta metodologia és aplicable, també, al camp d'oligonucleòtids.

Finalment, ens vam proposar combinar les reaccions de Diels-Alder i IEDDA amb un oligonucleòtid que fos derivatitzat amb un diè i un oxanorbornè. Per tal d'aconseguir-ho, es va haver de sintetitzar una suport polimèric adequat que contingués l'oxanorbornè per tal de fer créixer l'oligonucleòtid tal com es mostra a l'**Esquema R.C.20**.

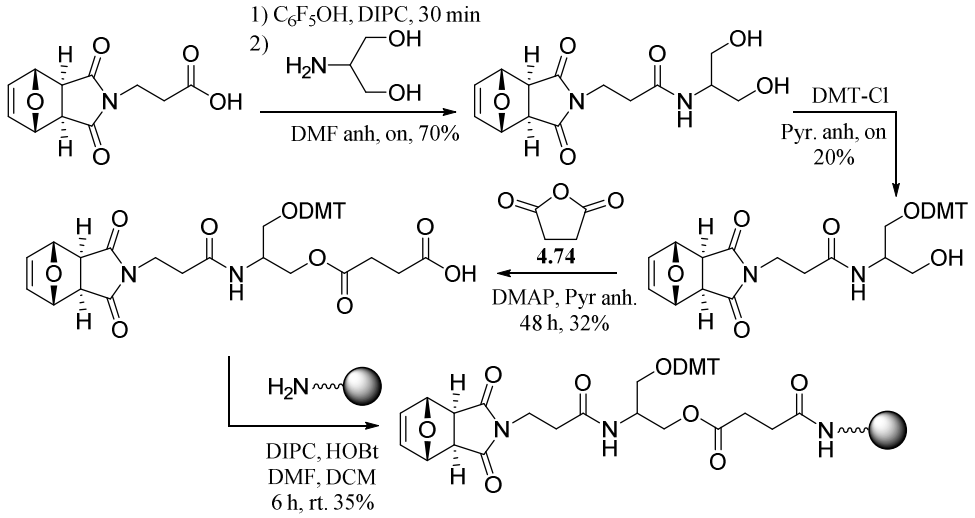

Esquema R.C. 20 Esquema sintètics per a la obtenció d'un suport polimèric útil per a la síntesi d'oligonucleòtids contenint la molècula d'oxanorbornè a la posició 3'.

Finalment, es va sintetitzar un oligonucleòtid (dT_{10}) i es va afegir a l'extrem 5' un fosforamidit sintètic de 1,3-diè. Tot seguit, es va desprotegir i desancorar l'oligonucleòtid amb amoníac concertat aquós i es va fer reaccionar amb un pèptid que contenia una maleimida en la posició *N*-terminal i la tetraizna derivatitzada amb biotina per aconseguir satisfactòriament el conjugat sense purificació intermèdia.

R.C.5 Conclusions

1) Els experiments duts a terme en aquest treball han confirmat que les reacció entre ciclopent-4-en-1,3-diones (CPDs), que poden ser considerades com anàlegs no hidrolitzable de maleimides, i cisteïnes proporcionen adductes bicíclics estables resultants d'una addició de tia-Michael, posterior ciclació i oxidació. Derivats de CPD que contenen grups carboxílics es poden incorporar a pèptids units sobre un suport polimèric (pèptid o PNA) per proporcionar CPD-poliamides. D'altre banda, també es pot emprar els mateixos derivats carboxílics per la síntesi d'altres molècules que continguin grups biotina o dansil per a la preparació de conjugats. Tots aquets compostos han produït l'adducte esperat de conjugació reaccionant-los amb poliamides incorporant una cisteïna *N*-terminal.

2) No és possible preparar CPD-oligonucleòtids perquè la CPD no aguanta el tractament amb amoníac concentrat aquós necessari per al desancoratge i desprotecció d'oligonucleòtids després de l'elongació. Tot i això, conjugats d'oligonucleòtids utilitzant la reacció de CPD-Cys

es poden preparar usant oligonucleòtids derivatitzats amb cisteïnes. Per aquesta raó, es van preparar dos fosforamidits de cisteïna amb els grups protectors *S*-tritil o *S*-S-*terc*-butil respectivament per acoblar-los a la posició 5' d'un oligonucleòtid unit a un suport polimèric.

3) Pèptids contenint dues residus de cisteïna, un d'ells a la posició *N*-terminal, es pot emprar per a dobles derivatitzacions en síntesis d'una sola etapa reaccionant primer el pèptid amb un compost que contingui una CPD, per tal de selectivament etiquetar la cisteïna *N*-terminal i, a continuació, utilitzar una maleimida per donar una reacció de tia-Michael amb el tiol intern.

4) També es poden preparar dobles conjugats amb pèptids que continguin una CPD o cisteïna a la posició *N*-terminal i un grup alquí penjant del residu d'una lisina. In aquest cas es obligatori fer la reacció de CPD-Cys en primera instància seguit de la cicloaddició 1,3-dipolar entre una azida i un alquí catalitzada per Cu(I). En estudis posteriors, es va concloure que les CPDs reaccionen amb azides per donar dos adductes estables als quals la seva estructura es va elucidar. Tot i això, no va ser possible trobar un set de condicions per ajudar a completar la reacció per a qualsevol d'ambdós.

5) Els dos grups carbonils de la CPD reaccionen amb alkoxiamines per donar oximes, mentre que el carbonil de l'adducte CPD-Cys no. La possibilitat de preparar dobles conjugats de pèptids incorporant ja sigui una cisteïna o una CPD a la posició *N*-terminal i una oxiamina d'un residu de lisina s'ha explorar amb poc èxit. A més de la formació de crus complexes en les reaccions de conjugació, s'ha trobat que les alkoxiamines reaccionen amb traces d'acetaldehid present en l'acetonitril emprat en l'anàlisi i aïllament dels conjugats en qüestió.

6) Pèptids contenint una cisteïna en posició *N*-terminal i interna poden ser ciclats amb CPDs. En el cas que la CPD incorpori una biotina o fluorfor la ciclació i marcatge són complerts simultàniament. La formació de l'adducte CPD-Cys es seguit de la formació d'una segona addició de Michael del tiol intern amb aquest adducte i, finalment, per una oxidació, per aconseguir un sistema conjugat amb un màxim d'absorció al voltant de 370 nm. Intents de traslladar aquesta metodologia a la química d'oligonucleòtids ha sigut exitosos un cop, però sent irreproduïble en tots els intents subseqüents.

7) El compost Retro-1 s'ha obtingut satisfactòriament seguint protocols descrits. Introduint petits canvis a l'esquema sintètic, derivats incorporant tant un grup tiol, die o fosforamidit s'han aconseguit i utilitzat per a la preparació de conjugats de Retro-1-oligonucleòtids. El fosforamidit s'ha adjuntat directament a dos tipus d'oligonucleòtids sobre el suport polimèric, un contenint una seqüència capaç d'alterar l'empalmament (referida com a 623) i una altre amb els mateixos nucleòsid en diferent ordre (*scrambled*). També s'han derivatitzat els mateixos oligonucleòtids amb una maleimida en la posició 5' i s'han usat per a reacció de tia-Micahel i Diels-Alder amb derivats de Retro-1.

8) Assajos de correcció d'empalmament s'ha dut a terme al laboratori del Prof. R. L. Juliano utilitzant la línia cel·lular HeLa Luc 705 o cèl·lules traqueals de ratolí induïts amb la EGFP654. En primera instància, assajos amb els conjugats de 623 no van mostrar una millora substancial en comparació amb la versió nua de l'oligonucleòtid 623 amb coadministració de Retro-1. D'altra banda, utilitzant les cèl·lules traqueals de ratolí, un benefici important es va observar un benefici important en el conjugat de Retro-1-623 en comparació amb la versió nua.

9) Els 7-oxanorbornens (adductes *exo*, obtinguts de la reacció entre furans i maleimides) han demostrat ser dienòfils útils per a la reacció de cicloaddició de Diels-Alder de demanda electrònica inversa (IEDDA) en conjunt amb 1,2,4,5-tetrazine 3,6-disbustituides. La reacció es dona a condicions suaus a 37 ºC en medi aquós emprant un excés molar de tetrazine (2 equivalents) i en general finalitza en agitació durant tota la nit.

10) S'han preparat derivats d'oxanorbornè adients per a ser incorporats a la posició *N*-terminal o interna de poliamides (pèptids i PNAs) i a les posicions 5' i 3' d'oligonucleòtids. S'han sintetitzat satisfactòriament tetrazines incorporant marcadors com ara BODIPY, biotina o GalNAc. Addicionalment, el grup tetrazine s'ha incorporat a la posició *N*-terminal d'una cadena peptídica creient utilitzant metodologies de fase sòlida optimitzades. Amb tots aquests compostos s'han aconseguit conjugats simples de pèptids, PNAs i oligonucleòtids.

11) Diferents alternatives per a la dobles conjugacions involucrant almenys una reacció de IEDDA entre un oxanorborne-Tz s'han examinat. Apart de la seva idoneïtat per dobles derivatitzacions de pèptids i oligonucleòtids (comentades a continuació), aquests assajos han mostrat que 1,2,4,5-tetrazines 3,6-disbustituides amb grups alquil o aril no reacciones amb 1,4-dimetil-7-oxanorbornens (és a dir, maleimides protegides amb 2,5-dimetilfurà), CPDs ni maleimides. D'altre banda, reaccionen amb 1,3-diens. A més a més, també s'ha observat que 1,2,4,5-tetrazines substituïdes amb grups alquilsufanil en les posicions 3 i 6 no reaccionen amb 7-oxanorbornens.

12) Intents de derivatitzar pèptids incorporant 1,4-dimetil-7-oxanorbornens i 7-oxanorbornes han mostrat que no és possible eliminar el grup protector més làbil de la maleimida (2,5-dimetilfurà) deixant inalterat el 7-oxanorbornè (o maleimida protegida amb furà), ja que sempre s'ha observat eliminació del furà fins a cert punt. Assajos amb l'objectiu d'aconseguir dobles conjugats primer fent ús d'una reacció de IEDDA i, a continuació, desprotecció de la maleimida i reacció amb un tiol o diè, han produït crus complexes o poc èxit.

13) En el cas que el pèptid incorpori un oxanorbornè i una maleimida lliure, les dobles conjugacions s'han assolit satisfactòriament si es fa reaccionar primer el pèptid amb un 1,3-diè, seguit de l'aïllament del conjugat simple i, finalment reaccionar-lo amb una tetrazine. La substitució de la reacció de Diels-Alder per una addició tipus tia-Michael és una opció factible.

14) Pèptids que contenen un tiol (a la posició *N*-terminal o interna) i un oxanorbornè s'han combinat amb tetrazines en una reacció de IEDDA i amb una CPD o maleimida per una reacció de tia-Michael (la primera necessita una cisteïna a la posició *N*-terminal). És interessant remarcar que en ambdós casos les dues reaccions de conjugació es poden dur a terme simultàniament.

15) El mateix tipus de pèptid s'ha utilitzat per combinar la reacció de cicloaddició IEDDA amb la S_NAr. In aquest cas, la S_NAr s'ha dut a terme primer, reaccionant el tiol amb una chloro-1,2,4,5-tetrazine unida a un dansil o a un oligonucleòtid. Aquest reacció és extremadament ràpida, tant que el segon reactiu (una tetrazine substituïda amb grups arils o alquils) es pot afegir gairebé immediatament. Tot i això, s'ha de tenir en compte que en el cas que el tiol sigui la cadena lateral d'una cisteïna *N*-terminal, la reacció amb una clorotetrazina és precedida per una reorganització que acaba donant la tetrazine *N*-substituïda, alliberant el tiol, que pot patir una segona reacció de S_NAr.

16) La combinació de S_NAr-IEDDA s'ha transportat a la química d'oligonucleòtids satisfactòriament. Per tal d'aconseguir-ho, s'ha hagut de sintetitzar un derivat de cisteïna protegida amb *S*-tritil, l'oxanorbornè enllaçat per l'amina, i el carboxil derivatitzat per tal d'incorporar el grup fosforamidit. Les dobles conjugacion emprant Cys-oligonucleòtids requereixen temps de reacció mes llarg per la S_NAr (*ca.* 4 h).

17) Finalment, s'ha explorat la combinació DA-IEDDA amb un oligonucleòtid derivatitzat amb un oxanorbornè a l'extrem 3' i un 1,3-diè al 5', respectivament. Un procediment en un sol pas sense purificació, en el qual una cicloaddició de DA amb una maleimida, seguit per una IEDDA amb una tetrazine ha produït el doble conjugat objectiu satisfactòriament.

R.C.5 Acrònims

Ac	Acetil
Ac_2O	Anhídrid acètic
AcOH	Àcid acètic
Anh	Anhidre
AoA	Aminoxiacetil
ASOs	Oligonucleòtids antisentit
AZT	Azidotimidina
Bn	Benzil
Boc	*340erç*-Butoxicarbonil
CNE	2-Cyanoetil
CPD	Ciclopten-4-en-1,3-diona
CuAAC	Cicloaddició 1,3-dipolar entre una azida I un alquí catalitzada per Cu(I)
Cys	Cisteïna

DA	Cicloaddició de Diels-Alder
Dansil-Cl	Clorur de dansil
DCE	Dicloroetà
DCM	Diclorometà
DIPC	Diisopropilcarbodiimida
DIPEA	Diisopropiletilamina
DMF	*N,N*-Dimetilformamida
DMT	4,4'-Dimethoxytrityl
DNA	Àcid desoxiribonucleic
DTT	Ditiotreitol
EDC·HCl	Clorhidrat de etil-3-(3-dimetilaminopropil)carbodiimida
Et_2O	Èter etílic
FDA	*Food and Drug Administration* (USA)
Fmoc	Fluorenilmethiloxicarbonil
GalNAc	*N*-Acetilgalactosamina
HATU	1-[Bis(dimetilamino)metilè]-1*H*-1,2,3-triazolo[4,5-*b*]pyridini 3-òxid hexafluorofosfat
HMBC	Correlació bidimensional heteronuclear de múltiples enllaços
HOBt	Hidroxibenzotriazole
IBCF	Cloroformiat d'isobutil
IEDDA	Cicloaddició de Diels-Alder de demanda electrònica inversa
^{i}Pr	Isopropil
Me	Metil
MeOH	Metanol
Mol. Siev.	Tamís molecular
mRNA	RNA missatger
NBS	*N*-Bromo succinimida
Net_3	Trietilamina
NMM	*N*-Metilmorfolina
PBf	2,2,4,6,7-Pentametildihidrobenzofurà-5-sulfonil
PEG	Polietilenglicol
Pip	Piperidina
Pmal[H_2]	7-Oxanorbornè
PNA	Àcid nucleic peptídic
Pyr	Piridina
RNA	Àcid ribonucleic
siRNAs	*Small 341erç341ferint RNAs*
S_NAr	Substitució nucleòfila aromàtica
SS^{t}Bu	*341erç*-Butiltio
^{t}Bu	*341erç*-Butoxi
TCEP	*tris*-(2-Carboxietil)fosfina
TEMPO	Radical (2,2,6,6-tetrametilpiperidin-1-il)oxil
TFA	Àcid trifluoroacètic
THF	Tetrahidrofurà

TIS	Triisopropilsilà
TMSOTf	Trimetilsilil trifluormetansulfonat
Trt	Tritil
Trt-Cl	Clorur de tritil
Tz	1,2,4,5-Tetrazina

R.C.6 Bibliografia

(1) Iqbal, K.; del C. Alonso, A.; Chen, S.; Chohan, M. O.; El-Akkad, E.; Gong, C.-X.; Khatoon, S.; Li, B.; Liu, F.; Rahman, A.; et al. *Biochim. Biophys. Acta - Mol. Basis Dis.* **2005**, *1739* (2–3), 198–210.

(2) Rubinsztein, D. C. *Nature* **2006**, *443* (7113), 780–786.

(3) Ranum, L. P. W.; Cooper, T. A. *Annu. Rev. Neurosci.* **2006**, *29* (1), 259–277.

(4) Orr, H. T.; Zoghbi, H. Y. *Annu. Rev. Neurosci.* **2007**, *30*, 575–623.

(5) Drugs - DrugBank https://www.drugbank.ca/biotech_drugs?utf8=âœ“&approved=0&approved=1&nutraceutical=0&illicit=0&investigational=0&withdrawn=0&experimental=0&us=0&ca=0&eu=0&Protein+Based+Therapies=0&Nucleic+Acid+Based+Therapies=0&Nucleic+Acid+Based+Therap (accessed Sep 20, 2019).

(6) Drugs - DrugBank https://www.drugbank.ca/biotech_drugs?utf8=✓&approved=0&approved=1&nutraceutical=0&illicit=0&investigational=0&withdrawn=0&experimental=0&us=0&ca=0&eu=0&Protein+Based+Therapies=0&Protein+Based+Therapies=1&Nucleic+Acid+Based+Therapies=0&Gene+Therap (accessed Sep 20, 2019).

(7) Hebert, M. F. *Adv. Drug Deliv. Rev.* **1997**, *27* (2–3), 201–214.

(8) Wolin, E. M. *Gastrointest. Cancer Res.* **2012**, *5* (5), 161–168.

(9) Baldwin, A. D.; Kiick, K. L. *Bioconjug. Chem.* **2011**, *22* (10), 1946–1953.

(10) Lyon, R. P.; Setter, J. R.; Bovee, T. D.; Doronina, S. O.; Hunter, J. H.; Anderson, M. E.; Balasubramanian, C. L.; Duniho, S. M.; Leiske, C. I.; Li, F.; et al. *Nat. Biotechnol.* **2014**, *32* (10), 1059–1062.

(11) Kalia, J.; Raines, R. T. *Bioorganic Med. Chem. Lett.* **2007**, *17* (22), 6286–6289.

(12) Stetsenko, D. A.; Gait, M. J. *Nucleosides, Nucleotides and Nucleic Acids* **2000**, *19* (10–12), 1751–1764.

(13) Stetsenko, D. A.; Gait, M. J. *J. Org. Chem.* **2000**, *65* (16), 4900–4908.

(14) Isidro-Llobet, A.; Álvarez, M.; Albericio, F. *Chem. Rev.* **2009**, *109* (6), 2455–2504.

(15) Burns, J. A.; Butler, J. C.; Moran, J.; Whitesides, G. M. *J. Org. Chem.* **1991**, *56* (8), 2648–2650.

(16) Meyer, A.; Vasseur, J.-J.; Morvan, F. *European J. Org. Chem.* **2013**, *2013* (3), 465–473.

(17) Forget, D.; Boturyn, D.; Defrancq, E.; Lhomme, J.; Dumy, P. *Chem. - A Eur. J.* **2001**, *7* (18), 3976–3984.

(18) Crick, F. *Nature* **1970**, *227* (5258), 561–563.

(19) Suhr, O. B.; Coelho, T.; Buades, J.; Pouget, J.; Conceicao, I.; Berk, J.; Schmidt, H.; Waddington-Cruz, M.; Campistol, J. M.; Bettencourt, B. R.; et al. *Orphanet J. Rare Dis.* **2015**, *10* (1), 109.

(20) Mendell, J. R.; Rodino-Klapac, L. R.; Sahenk, Z.; Roush, K.; Bird, L.; Lowes, L. P.; Alfano, L.; Gomez, A. M.; Lewis, S.; Kota, J.; et al. *Ann. Neurol.* **2013**, *74* (5), 637–647.

(21) Zhang, H.; Ma, Y.; Xie, Y.; An, Y.; Huang, Y.; Zhu, Z.; Yang, C. J. *Sci. Rep.* **2015**, *5* (1), 10099.

(22) Abdelkafi, H.; Michau, A.; Clerget, A.; Buisson, D. A.; Johannes, L.; Gillet, D.; Barbier, J.; Cintrat, J. C. *ChemMedChem* **2015**, *10* (7), 1153–1156.

(23) Sánchez, A.; Pedroso, E.; Grandas, A. *Org. Lett.* **2011**, *13* (16), 4364–4367.

(24) Discekici, E. H.; St. Amant, A. H.; Nguyen, S. N.; Lee, I. H.; Hawker, C. J.; Read De Alaniz, J. *J. Am. Chem. Soc.* **2018**, *140* (15), 5009–5013.

(25) Nair, J. K.; Willoughby, J. L. S.; Chan, A.; Charisse, K.; Alam, M. R.; Wang, Q.; Hoekstra, M.; Kandasamy, P.; Kelin, A. V.; Milstein, S.; et al. *J. Am. Chem. Soc.* **2014**, *136* (49), 16958–16961.

(26) Pakhomov, A. A.; Kononevich, Y. N.; Stukalova, M. V.; Svidchenko, E. A.; Surin, N. M.; Cherkaev, G. V.; Shchegolikhina, O. I.; Martynov, V. I.; Muzafarov, A. M. *Tetrahedron Lett.* **2016**, *57* (9), 979–982.

(27) Elduque, X.; Sánchez, A.; Sharma, K.; Pedroso, E.; Grandas, A. *Bioconjug. Chem.* **2013**, *24* (5), 832–839.

(28) Venkateswara Rao, B.; Dhokale, S.; Rajamohanan, P. R.; Hotha, S. *Chem. Commun.* **2013**, *49* (92), 10808–10810.

(29) Canovas, C.; Moreau, M.; Bernhard, C.; Oudot, A.; Guillemin, M.; Denat, F.; Goncalves, V. *Angew. Chemie - Int. Ed.* **2018**, *57* (33), 10646–10650.